COGNITIVE DYSFUNCTIONS IN PSYCHIATRIC DISORDERS: BRAIN-IMMUNE INTERACTION MECHANISMS AND INTEGRATIVE THERAPEUTIC APPROACHES

EDITED BY: Weiwen Wang, Bart Ellenbroek, Haiyun Xu and Zili You

PUBLISHED IN: Frontiers in Psychiatry, Frontiers in Pharmacology, Frontiers in Integrative Neuroscience and Frontiers in Molecular Neuroscience

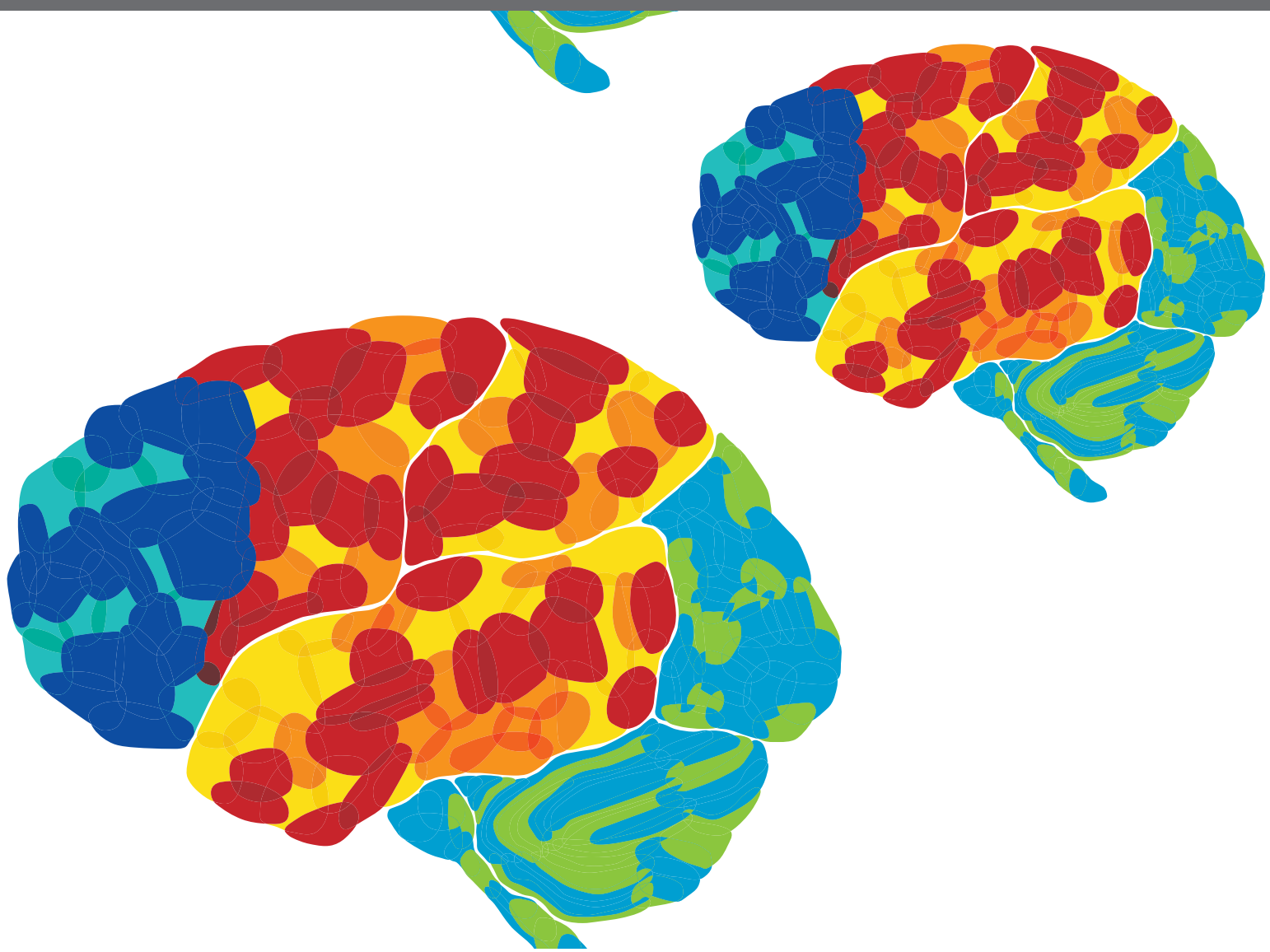

frontiers Research Topics

frontiers

ISSN 1664-8714
ISBN 978-2-88966-627-0
DOI 10.3389/978-2-88966-627-0

About Frontiers

Frontiers is more than just an open-access publisher of scholarly articles: it is a pioneering approach to the world of academia, radically improving the way scholarly research is managed. The grand vision of Frontiers is a world where all people have an equal opportunity to seek, share and generate knowledge. Frontiers provides immediate and permanent online open access to all its publications, but this alone is not enough to realize our grand goals.

Frontiers Journal Series

The Frontiers Journal Series is a multi-tier and interdisciplinary set of open-access, online journals, promising a paradigm shift from the current review, selection and dissemination processes in academic publishing. All Frontiers journals are driven by researchers for researchers; therefore, they constitute a service to the scholarly community. At the same time, the Frontiers Journal Series operates on a revolutionary invention, the tiered publishing system, initially addressing specific communities of scholars, and gradually climbing up to broader public understanding, thus serving the interests of the lay society, too.

Dedication to Quality

Each Frontiers article is a landmark of the highest quality, thanks to genuinely collaborative interactions between authors and review editors, who include some of the world's best academicians. Research must be certified by peers before entering a stream of knowledge that may eventually reach the public - and shape society; therefore, Frontiers only applies the most rigorous and unbiased reviews.
Frontiers revolutionizes research publishing by freely delivering the most outstanding research, evaluated with no bias from both the academic and social point of view. By applying the most advanced information technologies, Frontiers is catapulting scholarly publishing into a new generation.

What are Frontiers Research Topics?

Frontiers Research Topics are very popular trademarks of the Frontiers Journals Series: they are collections of at least ten articles, all centered on a particular subject. With their unique mix of varied contributions from Original Research to Review Articles, Frontiers Research Topics unify the most influential researchers, the latest key findings and historical advances in a hot research area! Find out more on how to host your own Frontiers Research Topic or contribute to one as an author by contacting the Frontiers Editorial Office: frontiersin.org/about/contact

COGNITIVE DYSFUNCTIONS IN PSYCHIATRIC DISORDERS: BRAIN-IMMUNE INTERACTION MECHANISMS AND INTEGRATIVE THERAPEUTIC APPROACHES

Topic Editors:
Weiwen Wang, Institute of Psychology, Chinese Academy of Sciences, China
Bart Ellenbroek, Victoria University of Wellington, New Zealand
Haiyun Xu, Wenzhou Medical University, China
Zili You, University of Electronic Science and Technology of China, China

Citation: Wang, W., Ellenbroek, B., Xu, H., You, Z., eds. (2021). Cognitive Dysfunctions in Psychiatric Disorders: Brain-Immune Interaction Mechanisms and Integrative Therapeutic Approaches. Lausanne: Frontiers Media SA.
doi: 10.3389/978-2-88966-627-0

Table of Contents

frontiers in Integrative Neuroscience

EDITORIAL
published: 18 February 2021
doi: 10.3389/fnint.2021.649425

Editorial: Cognitive Dysfunctions in Psychiatric Disorders: Brain-Immune Interaction Mechanisms and Integrative Therapeutic Approaches

Haiyun Xu[1], *Weiwen Wang*[2,3]*, *Bart Ellenbroek*[4] *and Zili You*[5]

[1] School of Mental Health, Wenzhou Medical University, Wenzhou, China, [2] CAS Key Laboratory of Mental Health, Institute of Psychology, Beijing, China, [3] Department of Psychology, University of Chinese Academy of Sciences, Beijing, China, [4] School of Psychology, Victoria University of Wellington, Wellington, New Zealand, [5] School of Life Science and Technology, Center for Informational Biology, University of Electronic Science and Technology of China, Chengdu, China

Keywords: brain, cognitive dysfunction, immune regulation, mental disorder, neuroinflammation

Editorial on the Research Topic

Cognitive Dysfunctions in Psychiatric Disorders: Brain-Immune Interaction Mechanisms and Integrative Therapeutic Approaches

This Research Topic, consisting of 13 research and review articles, aimed to deepen our understanding of the brain-immune interaction mechanisms underlying cognitive dysfunction in psychiatric disorders and help to develop better integrative therapeutic approaches of the five human research articles, the study by Yang Z. et al. reported that patients with schizophrenia performed poorly compared to healthy controls in all the cognitive tasks in the repeatable battery for the assessment of neuropsychological status, which consists of 12 subtests measuring the cognitive domains of immediate memory, visuospatial/constructional, language, attention, and delayed memory (Randolph et al., 1998). In addition, patients with schizophrenia showed lower plasma GDF-11 (growth differentiation factor 11) relative to that in healthy controls. Moreover, there were significant negative correlations between GDF-11 level and the PANSS total score, positive symptoms score, negative symptoms score, or general psychopathological score in the patients, whereas plasma GDF-11 level was positively associated with the immediate memory and delayed memory. The results of this study added evidence associating GDF-11 to the cognitive impairments (CI) in schizophrenia patients thus linking this TGF-ß superfamily member to the pathophysiology of schizophrenia.

Numerous neuropsychological studies demonstrate a broad range of measurable cognitive deficits in patients with schizophrenia, including impairments in attention, working memory (WM), episodic memory, processing speed, and executive functions (Xu et al., 2011; Kahn and Keefe, 2013). Here Xin et al. investigated how acute stress influences human WM functions using a well-validated neural measure of visual–spatial WM storage. They found: (1) the participants performed the visual WM task better after the control treatment than after the CPS (cold pressor stress) treatment, (2) the subjects showed a late CDA (contralateral delay activity) amplitude in the two-red-items condition after the CPS treatment, which was significantly larger than that after the control treatment, and (3) N2pc components showed significant disparity across three types of stimuli arrays after control treatment, which disappeared in the CPS session. These results demonstrate that acute stress impaired individuals' cognition processes of object individuation and maintenance in visual–spatial WM, as well as in task performance.

Edited and reviewed by:
Elizabeth B. Torres, Rutgers, The State University of New Jersey, United States

***Correspondence:**
Weiwen Wang
wangww@psych.ac.cn

Received: *04 January 2021*
Accepted: *25 January 2021*
Published: *18 February 2021*

Citation:
Xu H, Wang W, Ellenbroek B and You Z (2021) Editorial: Cognitive Dysfunctions in Psychiatric Disorders: Brain-Immune Interaction Mechanisms and Integrative Therapeutic Approaches. Front. Integr. Neurosci. 15:649425. doi: 10.3389/fnint.2021.649425

There is increasing evidence supporting the association of depression with overall CI among people living with HIV (PLWH), and in the cognitive domains of processing speed, executive function, as well as learning and memory (Rubin and Maki, 2019). Moreover, CI has been linked to incomplete HIV suppression in the CNS despite effective antiretroviral therapy (Zayyad and Spudich, 2015; Saylor et al., 2016). Here Rubin et al. examined the contribution of early immune signatures to cognitive performance among HIV-infected, virally suppressed women (HIV+VS) and in HIV-uninfected (HIV–) women. They showed that leukocyte influx into brain was a major contributor to CI in HIV+VS women, while T cell exhaustion, microglial activity, and cytokine signaling predicted both global and domain-specific performance for HIV– women.

Non-invasive neuromodulatory techniques such as rTMS (repeated transcranial magnetic stimulation) and tDCS (transcranial direct current stimulation) have been demonstrated to help prevent and ameliorate stress, with effects on emotion, cognition, behavior, as well as autonomic nervous system (Schestatsky et al., 2013). Here Castelo-Branco and Fregni provided a comment on the potential tDCS application on preventing and treating stress-related symptoms during social isolation, while addressing the feasibility and efficacy of home-based tDCS. Furthermore, Carvalho et al. designed a study protocol for a parallel, randomized, triple-blind, sham-controlled clinical trial in which a total of 90 drug-naïve, first-episode MDD patients (45 per arm) will receive a 6-weeks of CBT combined with either active or sham tDCS applied to DLPFC. The primary outcome is depressive symptoms improvement while the secondary aim is to test whether CBT combined with tDCS can engage the proposed mechanistic target of restoring the prefrontal imbalance and connectivity through the bilateral neuro-modulation of the DLPFC.

High validity disease-related animal model is a powerful tool to explore the immune regulation of cognitive dysfunction and underlying brain mechanism. Using a classic animal model of schizophrenia induced by social isolation, Zhou et al. reported prepulse inhibition (PPI) deficits in C57BL/6J mice after social isolation for 5 weeks during PND21-56. And the CX3CR1 protein level was increased in the medial prefrontal cortex, nucleus accumbens and hippocampus of the isolated C57BL/6J mice. But the same protocol had no effect on PPI in the CX3CR1$^{-/-}$ mice, which were stress resistant as shown in a previous study (Winkler et al., 2017). CX3CR1 and its ligand CX3CL1 directly modulate the function of microglia (Wolf et al., 2013). Therefore, the authors suggested that the social isolation-induced PPI deficit in mice is CX3CR1-dependent.

Relevant to the above animal study, Zhang et al. used a mouse model of MIA (maternal immune activation) by the viral dsRNA analog poly(I:C) to mimic the effects of inflammation during pregnancy. They found that mRNA expression of the genes SRY-related HMG-box 10, myelin-associated glycoprotein, and transferrin were generally reduced in the limbic system of the hemispheres of prenatal poly(I:C)-exposed mouse offspring. The results provided evidence that prenatal exposure to poly(I:C) elicits profound and long-term changes in transcript level and spatial distribution of myelin-related genes in multiple neocortical and limbic regions, which play prominent roles in learning, memory, and social interaction.

The evidence for the involvement of microglia and oligodendrocytes (OLs) in the pathogenesis of psychiatric disorders also came from another animal model, the cuprizone-exposed mouse. Cuprizone (CPZ) is a chemical chelator toxic to mitochondria (Pasquini et al., 2007; Acs et al., 2013). In comparison to the other animal models of schizophrenia, the brain neuropathology of CPZ-exposed mice involves mitochondrial dysfunction, neuroinflammation, and white matter damage, three essential components in the pathogenesis of schizophrenia (Najjar and Pearlman, 2015; Xu et al., 2016). Here Yang L. et al. reported that deep rTMS for 4 weeks during the CPZ-exposure period effectively blocked the behavioral changes, myelin breakdown, and OL loss in CPZ-fed mice while inhibited microglia activation in the lesion sites and regulated the expression of inflammatory cytokines of IL-1ß, IL-6, and IL-10 in the same brain regions. These data added experimental evidence for the beneficial effects of deep rTMS in treating behavioral abnormalities such as working memory and improving the associated neuropathologic damage like microglia activation and OL loss in the brain.

The senescence accelerated mouse prone strain-8 (SAMP8) is an established and widely used model that features accelerated aging (Takeda, 1999) and shows spatial learning impairments from 12 weeks of age and spatial memory deficits commencing from 16 weeks of age (Flood and Morley, 1998; Cheng et al., 2008). Here, Lam et al. compared from a young age of 6 weeks cognitive and motor performance of SAMP8 in an olfactory-visual spatial water maze task administered longitudinally. In classic MWM (Morris-Water-Maze), it took much more time for SAMP8 to reach a rescue platform compared to age-matched SAMR1 (senescence accelerated mouse resistant-strain 1) mice. And this strain difference was apparent from as young as 6 weeks of age. In the olfactory-visual water maze, this strain difference in latency time to reach the rescue platform was markedly greater compared to the classic MWM, indicating a significant olfactory processing deficit in the SAMP8 strain. The findings complement the extant literature in SAMP8 mice that demonstrate CNS physiological aberrations preceding loss of spatial and associative memory.

The last, but not least, an animal study by Wang et al. reported that Notoginsenoside R1 (NR1, the main component with cardiovascular activity in Panax notoginseng) effectively blocked the spatial and cognitive impairment in C57BL/6 mice exposed to acrylamide, a common chemical having chronic neurotoxic effects. Moreover, NR1 protected against the acrylamide-induced neurotoxicity by upregulating thioredoxin-1 in PC12 cells and mice. In the meanwhile, the autophagy-related proteins-like Cathepsin D, LC3 II, lysosomal-associated membrane protein 2a, and integrin alpha V were restored to normal levels by NR1 in both PC12 cells and mice. The results suggest a potential application of NR1 in treating acrylamide-induced neurotoxicity.

As mentioned above, inflammatory responses and immunity are important players in the development and onset of depression. Therefore, modulation of inflammation may mitigate depressive behavior in depressive patients. Here Kim et al.

reviewed the therapeutic effects of GLP-1 (glucagon-like peptide-1) on depression from a variety of perspectives. They summarized evidence showing that GLP-1 attenuates the process of neuroinflammation and protects neurons and glia under oxidative stress conditions in the depressive brain, described the role of GLP-1 in neurotransmitter homeostasis in the depressive brain in which GLP-1 improves neurotransmitter balance, reviewed the role GLP-1 in promoting neuronal differentiation and neural stem cell proliferation in the depressive brain, and summarized studies showing the improvement of impaired cognitive function in subjects by GLP-1.

The over-activation of microglia has been posited to contribute to suicidal behavior (Calcia et al., 2016; Mondelli et al., 2017). Therefore, chronic microglial activation may influence the interaction between the stress and diathesis components of the stress diathesis model of suicidal behavior by contributing to an increased vulnerability to suicidal tendencies. Here Baharikhoob and Kolla reviewed the findings from human post-mortem and neuroimaging studies reporting a relationship between microglial activation and suicidal behavior and updated the clinical model of suicidal behavior to integrate the role of microglia.

Another category of psychiatric disorders is dementia. Of the conditions leading to dementia, the most common one is Alzheimer's disease (AD, 50–75%) followed by vascular dementia (20%), dementia with Lewy bodies (5%), and frontotemporal lobar dementia (5%) (Prince et al., 2013). In addition, patients with amyotrophic lateral sclerosis (ALS) may also experience cognitive impairment (Beeldman et al., 2016). Therefore, this Research Topic included a review article by Guan and Han summarizing recent research developments regarding the NLRP3 inflammasome and its role in AD, PD, and ALS. In AD, Aß induces NLRP3 activation followed by ever-increasing production of IL-1ß and the other proinflammatory cytokines from microglia. In this manner, the neurotoxic effects of Aß on brain neurons are amplified (Heneka et al., 2013). In patients with PD, fibrillar a-syn induces NLRP3-caspase-1 complex activation which in turn causes the truncation and aggregation of a-syn. Then a-syn enters microglial cells in an endocytosis-dependent manner and subsequently activates two innate receptors in the TLR2 (TLR4)/NF-kB and NLRP3/caspase-1 pathways (Gustot et al., 2015; Fan et al., 2016). In ALS, microglia and astrocytes switch from a neuroprotective to a proinflammatory phenotype by releasing potentially neurotoxic cytokines. Importantly, inhibition of NLRP3 in animal models reduces the inflammatory response, decreases abnormal protein deposition, and corrects behavioral abnormalities associated with neurodegenerative diseases, suggesting that targeting NLRP3 inflammasome is a plausible therapeutic approach to treating such psychiatric disorders.

In sum, the collection highlights the wide range of technological strategies and research models available, each with its own advantages. These studies not only advance our understanding of the brain-immune interaction mechanisms underlying cognitive dysfunction in psychiatric disorders, but also help develop promising avenues to improve cognitive impairments in patients with psychiatric disorders.

AUTHOR CONTRIBUTIONS

HX wrote the draft. WW, BE, and ZY read and revised the draft. All authors approved the publication of this editorial.

REFERENCES

Acs, P., Selak, M. A., Komoly, S., and Kalman, B. (2013). Distribution of oligodendrocyte loss and mitochondrial toxicity in the cuprizone induced experimental demyelination model. *J. Neuroimmunol.* 262, 128–131. doi: 10.1016/j.jneuroim.2013.06.012

Beeldman, E., Raaphorst, J., Klein Twennaar, M., de Visser, M., Schmand, B. A., and de Haan, R. J. (2016). The cognitive profile of ALS: a systematic review and meta-analysis update. *J. Neurol. Neurosurg. Psychiatry* 87: 611–619. doi: 10.1136/jnnp-2015-310734

Calcia, M. A., Bonsall, D. R., Bloomfield, P. S., Selvaraj, S., Barichello, T., and Howes, O. D. (2016). Stress and neuro-inflammation: a systematic review of the effects of stress on microglia and the implications for mental illness. *Psychopharmacology (Berl).* 233, 1637–1650. doi: 10.1007/s00213-016-4218-9

Cheng, H., Yu, J., Jiang, Z., Zhang, X., Liu, C., Peng, Y., et al. (2008). Acupuncture improves cognitive deficits and regulates the brain cell proliferation of SAMP8 mice. *Neurosci. Lett.* 432, 111–116. doi: 10.1016/j.neulet.2007.12.009

Fan, Z., Lu, M., Qiao, C., Zhou, Y., Ding, J. H., and Hu, G. (2016). MicroRNA-7 enhances subventricular zone neurogenesis by inhibiting NLRP3/caspase-1 Axis in adult neural stem cells. *Mol. Neurobiol.* 53, 7057–7069. doi: 10.1007/s12035-015-9620-5

Flood, J. F., and Morley, J. E. (1998). Learning and memory in the SAMP8 mouse. *Neurosci. Biobehav. Rev.* 22, 1–20. doi: 10.1016/S0149-7634(96)00063-2

Gustot, A., Gallea, J. I., Sarroukh, R., Celej, M. S., Ruysschaert, J. M., and Raussens, V. (2015). Amyloid fibrils are the molecular trigger of inflammation in Parkinson's disease. *Biochem. J.* 471, 323–333. doi: 10.1042/BJ20150617

Heneka, M. T., Kummer, M. P., Stutz, A., Delekate, A., Schwartz, S., Vieira-Saecker, A., et al. (2013). NLRP3 is activated in Alzheimer's disease and contributes to pathology in APP/PS1 mice. *Nature* 493, 74–678. doi: 10.1038/nature11729

Kahn, R. S., and Keefe, R. S. (2013). Schizophrenia is a cognitive illness: time for a change in focus. *JAMA Psychiatry* 70, 1107–1112. doi: 10.1001/jamapsychiatry.2013.155

Mondelli, V., Vernon, A. C., Turkheimer, F., Dazzan, P., and Pariante, C. M. (2017). Brain microglia in psychiatric disorders. *Lancet Psychiatry* 4, 563–572. doi: 10.1016/S2215-0366(17)30101-3

Najjar, S., and Pearlman, D. M. (2015). Neuroinflammation and white matter pathology in schizophrenia: systematic review. *Schizophr. Res.* 161, 102–112. doi: 10.1016/j.schres.2014.04.041

Pasquini, L. A., Calatayud, C. A., Bertone Uña, A. L., Millet, V., Pasquini, J. M., and Soto, E. F. (2007). The neurotoxic effect of cuprizone on oligodendrocytes depends on the presence of pro-inflammatory cytokines secreted by microglia. *Neurochem. Res.* 32, 279–292. doi: 10.1007/s11064-006-9165-0

Prince, M., Bryce, R., Albanese, E., Wimo, A., Ribeiro, W., and Ferri, C. P. (2013). The global prevalence of dementia: a systematic review and meta analysis. *Alzheimers Dement.* 9, 63–75. doi: 10.1016/j.jalz.2012.11.007

Randolph, C., Tierney, M. C., Mohr, E., and Chase, T. N. (1998). The repeatable battery for the assessment of neuro- psychological status (RBANS): preliminary clinical validity. *J. Clin. Exp. Neuropsychol.* 20, 310–319. doi: 10.1076/jcen.20.3.310.823

Rubin, L. H., and Maki, P. M. (2019). HIV, depression, and cognitive impairment in the era of effective antiretroviral therapy. *Curr. Hiv. Aids Rep.* 16, 82–95. doi: 10.1007/s11904-019-00421-0

Saylor, D., Dickens, A. M., Sacktor, N., Haughey, N., Slusher, B., Pletnikov, M., et al. (2016). HIV-associated neuro-cognitive disorder—pathogenesis and prospects for treatment. *Nat. Rev. Neurol.* 12, 234–248. doi: 10.1038/nrneurol.2016.27

Schestatsky, P., Simis, M., Freeman, R., Pascual-Leone, A., and Fregni, F. (2013). Non-invasive brain stimulation and the autonomic nervous system. *Clin. Neurophysiol.* 124, 1716–1728. doi: 10.1016/j.clinph.2013.03.020

Takeda, T. (1999). Senescence-accelerated mouse (SAM): a biogerontological resource in aging research. *Neurobiol. Aging* 20, 105–110. doi: 10.1016/S0197-4580(99)00008-1

Winkler, Z., Kuti, D., Ferenczi, S., Gulyás, K., Polyák, Á., and Kovács, K. J. (2017). Impaired microglia fractalkine signaling affects stress reaction and coping style in mice. *Behav. Brain Res.* 334, 119–128. doi: 10.1016/j.bbr.2017.07.023

Wolf, Y., Yona, S., Kim, K. W., and Jung, S. (2013). Microglia, seen from the CX3CR1 angle. *Front. Cell Neurosci.* 7:26. doi: 10.3389/fncel.2013.00026

Xu, H., Yang, H., and Rose, G. M. (2011). "Working memory deficits in schizophrenia: neurobiological correlates and treatment," in *Working Memory: Capacity, Developments and Improvement Techniques*, ed E. S. Levin (New York, NY: Nova Science Publishers), 313–344.

Xu, H., Zhang, H., Zhang, J., Huang, Q., Shen, Z., and Wu, R. (2016). Evaluation of neuron-glia integrity by *in vivo* proton magnetic resonance spectroscopy: implications for psychiatric disorders. *Neurosci. Biobehav. Rev.* 71, 563–577. doi: 10.1016/j.neubiorev.2016.09.027

Zayyad, Z., and Spudich, S. (2015). Neuropathogenesis of HIV: from initial neuroinvasion to HIV-associated neurocognitive disorder (HAND). *Curr. Hiv. Aids Rep.* 12, 16–24. doi: 10.1007/s11904-014-0255-3

Conflict of Interest: The authors declare that the research was conducted in the absence of any commercial or financial relationships that could be construed as a potential conflict of interest.

frontiers in Integrative Neuroscience

ORIGINAL RESEARCH
published: 24 April 2020
doi: 10.3389/fnint.2020.00020

Early Inflammatory Signatures Predict Subsequent Cognition in Long-Term Virally Suppressed Women With HIV

Leah H. Rubin[1,2,3†], Yanxun Xu[4,5†], Philip J. Norris[6], Xuzhi Wang[4], Raha Dastgheyb[1], Kathryn C. Fitzgerald[1], Sheila M. Keating[6], Robert C. Kaplan[7], Pauline M. Maki[8,9], Kathryn Anastos[7,10,11], Gayle Springer[3], Lorie Benning[3], Seble Kassaye[12], Deborah R. Gustafson[13], Victor G. Valcour[14] and Dionna W. Williams[15,16†]*

[1] Department of Neurology, Johns Hopkins University, Baltimore, MD, United States, [2] Department of Psychiatry, Johns Hopkins University, Baltimore, MD, United States, [3] Department of Epidemiology, Johns Hopkins University Bloomberg School of Public Health, Baltimore, MD, United States, [4] Department of Applied Mathematics and Statistics, Johns Hopkins University, Baltimore, MD, United States, [5] Division of Biostatistics and Bioinformatics, Sidney Kimmel Comprehensive Cancer Center, Johns Hopkins University, Baltimore, MD, United States, [6] Department of Laboratory Medicine, Vitalant Research Institute, University of California, San Francisco, San Francisco, CA, United States, [7] Department of Epidemiology and Population Health, Albert Einstein College of Medicine, Bronx, NY, United States, [8] Department of Psychiatry, University of Illinois at Chicago, Chicago, IL, United States, [9] Department of Psychology, University of Illinois at Chicago, Chicago, IL, United States, [10] Department of General Internal Medicine, Albert Einstein College of Medicine, Bronx, NY, United States, [11] Department of Obstetrics and Gynecology and Women's Health, Albert Einstein College of Medicine, Bronx, NY, United States, [12] Department of Medicine, Georgetown University, Washington, DC, United States, [13] Department of Neurology, SUNY Downstate Health Sciences University, Brooklyn, NY, United States, [14] Department of Neurology, University of California, San Francisco, San Francisco, CA, United States, [15] Department of Molecular and Comparative Pathobiology, Johns Hopkins University, Baltimore, MD, United States, [16] Division of Clinical Pharmacology, Johns Hopkins University School of Medicine, Baltimore, MD, United States

OPEN ACCESS

Edited by:
Bart Ellenbroek,
Victoria University of Wellington, New Zealand

Reviewed by:
Min Wang,
The First Hospital of Changsha, China
Ferdinand W. N. M. Wit,
Amsterdam University Medical Center, Netherlands

***Correspondence:**
Leah H. Rubin
lrubin@jhu.edu

[†] These authors have contributed equally to this work

Received: 11 November 2019
Accepted: 23 March 2020
Published: 24 April 2020

Citation:
Rubin LH, Xu Y, Norris PJ, Wang X, Dastgheyb R, Fitzgerald KC, Keating SM, Kaplan RC, Maki PM, Anastos K, Springer G, Benning L, Kassaye S, Gustafson DR, Valcour VG and Williams DW (2020) Early Inflammatory Signatures Predict Subsequent Cognition in Long-Term Virally Suppressed Women With HIV. Front. Integr. Neurosci. 14:20. doi: 10.3389/fnint.2020.00020

Immunologic function is an important determinant of cognition. Here we examined the contribution of early immune signatures to cognitive performance among HIV-infected, virally suppressed women (HIV+VS) and in HIV-uninfected (HIV-) women. Specifically, we measured serum inflammatory markers, developed combinatory immune signatures, and evaluated their associations with cognition. Forty-nine HIV+VS women in the Women's Interagency HIV Study (WIHS) who achieved viral suppression shortly after effective antiretroviral therapy (ART) initiation, and 56 matched HIV− women were selected. Forty-two serum inflammatory markers were measured within 2 years of effective ART initiation for HIV+VS women, and at an initial timepoint for HIV− women. The same inflammatory markers were also measured approximately 1, 7, and 12 years later for all women. Of the 105 women with complete immune data, 83 (34 HIV+VS, 49 HIV−) also had cognitive data available 12 years later at ≥1 time points (median = 3.1). We searched for combinatory immune signatures by adapting a dynamic matrix factorization analytic method that builds upon Tucker decomposition followed by Ingenuity® Pathway Analysis to facilitate data interpretation. Seven combinatory immune signatures emerged based on the Frobenius residual. Three signatures were common between HIV+VS and HIV− women, while four signatures were unique. These inflammatory signatures predicted subsequent cognitive performance in both groups using mixed-effects modeling, but more domain-specific

associations were significant in HIV+VS than HIV− women. Leukocyte influx into brain was a major contributor to cognitive function in HIV+VS women, while T cell exhaustion, inflammatory response indicative of depressive/psychiatric disorders, microglial activity, and cytokine signaling predicted both global and domain-specific performance for HIV− women. Our findings suggest that immune signatures may be useful diagnostic, prognostic, and immunotherapeutic targets predictive of subsequent cognitive performance. Importantly, they also provide insight into common and distinct inflammatory mechanisms underlying cognition in HIV− and HIV+VS women.

Keywords: HIV, viral suppression, immune, cognition, women

INTRODUCTION

Central nervous system (CNS) complications persist during HIV infection despite effective antiretroviral therapy (ART) and impact HIV care, including ART adherence (Thames et al., 2011). A common CNS complication in the current ART era is cognitive impairment (CI). While the incidence of HIV-associated cognitive complications has markedly decreased, less severe forms of CI remain prevalent, affecting 30–60% of people with HIV (PWH) during their lifetime (Grant, 2008; Heaton et al., 2011; Cysique et al., 2014). Even in PWH who do not have dementia, CI is associated with poorer daily functioning, including financial and medication management, driving, multitasking, and vocational functioning (Heaton et al., 1996; Heaton et al., 2004; Marcotte et al., 2006; Waldrop-Valverde et al., 2010; Scott et al., 2011).

Despite the persistence and severity of CI in PWH, the underlying pathophysiology remains elusive and the underlying mechanisms are complex and multifactorial. CI has been linked to incomplete HIV suppression in the CNS despite ART (Bingham et al., 2011; Tamarit Mdel et al., 2012; Chen et al., 2014; Zayyad and Spudich, 2015; Saylor et al., 2016), compartmentalization of HIV RNA (Ritola et al., 2005), CNS escape (Joseph et al., 2018), viral rebound in the CSF (Gianella et al., 2016), viral persistence in peripheral tissues (Chun et al., 2008, 2015; Fletcher et al., 2014; Martinez-Picado and Deeks, 2016), and genetic factors leading to a persistent HIV CNS reservoir (Anuurad et al., 2009; Mavigner et al., 2009; Joska et al., 2011). Despite the heterogeneity of these mechanisms of viral persistence, immune activation and inflammation arise as a common thread that both promote and result from the CNS viral reservoir (Brouillette et al., 2016; Rubin et al., 2017; Gomez et al., 2018). However, the neuroinflammatory processes that promote CI in the context of HIV are not completely understood. While many studies have focused on individual inflammatory markers, it is unlikely that any single immune factor will serve as the sole predictor of cognition for all people. Rather, it is much more likely that a combination of multiple immune factors work in tandem to promote CI. Furthermore, it is expected that many combinatory inflammatory signatures exist that reflect unique mechanisms of CI for specific populations. To date, combinatory neuroinflammatory signatures that specifically identify CI in HIV+VS, but not HIV-uninfected (HIV-) individuals, have not been identified. As such, our goal was to identify peripheral immune signatures, in both HIV− and HIV+VS women, that were predictive of subsequent cognitive function.

Using a novel statistical analytic approach, we evaluated peripheral soluble and cellular biomarkers of immune activation and inflammation, including cytokines, chemoattractants, soluble forms of cell surface receptors, as well as growth and metabolic factors, and their prospective (median = 3.1 years post-measurement of immune markers) associations with cognitive function in a sample of women with HIV who remained virally suppressed for over a decade after initiating effective ART and a well-matched sample of HIV− women.

MATERIALS AND METHODS

Participants

A limited number of Women's Interagency HIV Study (WIHS) participants (Barkan et al., 1998; Bacon et al., 2005) were tested for biomarkers, based on key characteristics of interest for the WIHS. The initial selection of women was based on a nested case-control study, with the cases being women who were effective ART-initiators while on study, at least 20 HIV RNA-suppressed visits (at least 10 years), with viral suppression at the 2nd or 3rd ART visit (where each visit is approximately 6 months apart) and viral suppression at the 4th or 5th ART visit (n = 84). These 84 cases were matched with 84 HIV-uninfected controls using propensity scores based on race (African-American or not), HCV Ab and RNA status at study baseline visit, age (±5 years), BMI, current smoking status at index visit, and CD4 cell count at the stop of phenotype period (±150). From the 168 (84 HIV+VS; 84 HIV-), we selected 49 women with HIV who achieved and maintained viral suppression shortly after effective ART initiation (within 2 years) and a matched sample of 56 HIV- women from the WIHS. Sixteen HIV+VS cases were removed as there was more than a 4 year gap between effective ART initiation and the date of collection for the first immune visit. An additional 21 women were removed in order to maintain an approximate 1 year gap between the initial and second visit with immune data available. Of the remaining 131 women, 28 were removed for not having 4 visits with immune data.

Serum levels of 42 inflammatory markers (see below) were measured using stored samples from within 2 years of effective ART initiation and 1, 7, and 12 years later for

HIV+VS women. Among HIV− women, the same serum inflammatory markers were run at an initial time point, 1, 7, and 12 years later. Of the 105 women with complete immune data, 83 women (34 HIV+VS, 49 HIV−) had prospective neuropsychological test data (median = 3.1 years post inflammatory marker assessment) available at ≥1 time points. Specifically, 17 women contributed only one visit (7 HIV+VS, 10 HIV−), 12 women contributed two visits (5 HIV+VS, 7 HIV−), 12 contributed three visits (6 HIV+VS, 6 HIV−), and 42 contributed four visits (16 HIV+VS, 26 HIV−). Of the 22 women without cognitive data, fifteen (68%) were Spanish speakers and therefore not administered the neuropsychological test battery (normed for English speakers), five (23%) refused to participate in neuropsychological testing, one (4.5%) participant died before neuropsychological testing began in the WIHS, and one (4.5%) participant was deemed unable to complete neuropsychological testing. The 83 women with prospective neuropsychological test data were similar to the 105 women in terms of sociodemographic and behavioral characteristics **Supplementary Table S1**).

Multiplex Serum Analyses

All luminex kits were purchased from Millipore (Billerica, MA, United States) and ELISAs were purchased from R&D systems (Minneapolis, MN, United States). Interleukin (IL)-6, IL-10, and TNF-α were assayed using the High Sensitivity MILLIPLEX kit. Fibroblast growth factor (FGF)-2, fractalkine, GRO, IL-17, interferon induced protein (IP)-10, monocyte chemotactic protein (MCP)-1, monocyte derived chemokine (MDC), and macrophage inflammatory protein (MIP)-1α were measured using the Standard Sensitivity MILLIPLEX Map kit. CXCL13/B-cell attracting chemokine (BCA)-1, CCL27/cutaneous T-cell attracting chemokine (CTACK), SDF-1 a + b, TRAIL, MIG, ITAC/CXCL11, and MIP-3b/CCL19 were measured using the Standard Sensitivity Panel II kit. Macrophage colony stimulating factor (M-CSF), CXCL9/monokine induced by gamma (MIG), CXCL11/Interferon-inducible T cell alpha chemoattractant (I-TAC), and CXCL19/MIP-3β were measured using the Standard Sensitivity Panel III kit. Soluble (s) TNFRII, sTNFRI, sVEGFRI, sVEGFR2, sIL-2Rα, and sgp130 were measured using the Soluble Receptors kit. Adiponectin, MMP-9, MPO, sE-selectin, sICAM, sVCAM, total Plasminogen Activation Inhibitor, CRP, SAA, and SAP were measured using CVD Panel 1. KIM-1, osteopontin, and renin were measured using Kidney Toxicity Panel 1. Beta2 microglobulin, Cystatin, and Clusterin were measured using Kidney Tox Panel 2. CD14 and CD163 were measured using ELISA. Standards and samples were tested in duplicate. Beads were acquired on a Labscan analyzer (Luminex) using Bio-Plex manager 6.1 software (Bio-Rad). Values that were determined to be out of range (OOR) low were assigned 1/2 the lowest value in the data set. Values that were determined to be OOR high were assigned 2 times the highest standard. Values that were extrapolated beyond the standard curve were assigned the determined value (**Supplementary Table S2**). **Supplementary Table S3** provides the descriptive statistics for each analyte. All immune markers were log transformed and winsorized (<1% of values changed to be equal to the highest or lowest value that was within 2.5 standard deviations of the interquartile range) to normalize distributions.

Cognitive Outcomes

The following cognitive domains and related neuropsychological tests were used: *learning and memory*, Hopkins Verbal Learning Test-Revised (HVLT-R; learning outcomes: trial 1 and total learning; memory = delay free recall); *attention/working memory*, Letter-Number sequencing (outcomes = control and experimental conditions total correct); *executive function*, Trail Making Test Part B (mental flexibility) and Stroop Test color-word trial (behavioral inhibition) (outcomes = time to completion); *psychomotor speed*, Symbol Digit Modalities Test (outcome = total correct) and Stroop Test color-naming trial (outcome = time to completion); *fluency*, letter (outcome = total correct) and semantic (outcome = total correct); and *motor function*, Grooved Pegboard (outcome time to completion, dominant and non-dominant hand). Timed outcomes were log transformed to normalize distributions and reverse scored so that better performance equaled higher values. Demographically adjusted T-scores were calculated for each outcome and T-scores were used to create domain scores consistent with previous large-scale WIHS-wide studies (Rubin et al., 2017, 2018). For each domain, a composite T-score was derived by averaging the T-scores for domains with ≥2 outcomes. If only one test in a domain was completed, the T-score for that test was used. A global neuropsychological score was derived for individuals who had T-scores for at least 4 out of 7 cognitive domains (higher values = poorer cognition). Given that cognitive performance was relatively stable over time post-immune data, our primary outcomes were the global and domain-specific T-scores itself rather than computing rate of change (slope outcomes).

Statistical Analyses

We searched for latent immune signatures (underlying patterns of immune markers) among HIV+VS and HIV− women by adapting a dynamic matrix factorization analytic method building upon Tucker decomposition (**Supplementary Material S1**). We developed this method given the small sample size per group. With 42 immune markers at four time points for 49 HIV+VS and 56 HIV− women, the developed method can adequately reduce a high dimension of markers (42 immune markers) to a small number of immune signatures per group. As shown in previous studies, when data are well conditioned with a small number of factors compared to a large number of variables (42 in our case), matrix factorization can yield reliable results for sample sizes below 50 (de Winter et al., 2009). We calculated the Frobenius residual to choose the number of signatures (**Supplementary Material S2**). Based on these results, we subsequently used Ingenuity® Pathway Analysis (IPA®, Qiagen, Redwood City, CA, United States), a web-based software application, to facilitate interpretation of data derived from the dynamic matrix factorization analytic method. Gene Pathways identified for each immune profile are included as **Supplementary Material** (**Supplementary Figures S1–S13**). Names for each immune profile were given based on the markers contributing to each profile combined with IPA results. Immune

profile scores derived from the dynamic matrix factorization analytic method were then used as outcomes in a subsequent series of mixed-effects regression models (MRMs). The MRMs were used to examine whether the immune profile scores were stable or changing across the time course of study (12 years). Given that changes in immune profile scores over time were stable in the overall sample but individual differences were noted, our primary predictors were the average level and variability (standard deviation) of immune profile scores (**Supplementary Figure S14**). The average and variability in immune profile scores were then examined in relation to cognitive performance (domain-specific and global T-scores) at a given point in time (median = 3.1 years later) using MRMs to account for the number of visits each woman contributed to the analysis. MRMs were not corrected for multiple comparisons because the goal was to examine the potential clinical significance of these associations for future larger-scale studies.

RESULTS

Participants

Table 1 provides sociodemographic, behavioral, and clinical factors for HIV+VS and HIV− women. The two groups were similar in all factors except for recent heavy alcohol and marijuana use (*P*'s < 0.05). Specifically, HIV- women were more likely to be recent heavy alcohol and marijuana users than HIV+VS women. Among the HIV+VS women, the mean number of years on ART was less than 1 year (range: 0.35–6.49).

Identification of Combinatory Immune Signatures

A panel of immune factors, rather than individual immune markers, are the most accurate reflection of the neuroinflammatory processes that contribute to cognition in PWH (Marcotte et al., 2013; Bandera et al., 2019). However, it is unclear which inflammatory signatures are directly related to HIV, and which serve as general inflammatory processes that promote CI, but are not specific to HIV. To ascertain this, we evaluated 42 soluble plasma inflammatory markers in 49 HIV+VS women within 2 years of ART initiation, and again 1, 7, and 12 years later. Similarly, we also performed this same longitudinal analysis in 56 demographically matched HIV-women. To identify mutual and distinct inflammatory signatures that existed between HIV+VS and HIV− women, we developed a novel statistical approach by adapting a dynamic matrix factorization analytic method. Utilizing this technique, we identified seven latent immune profiles, which we termed "combinatory inflammatory signatures," in the HIV+VS and HIV- groups. This statistical method is based on the interrelated network of inflammatory processes that occur as a result of how the immune markers cooperate together, rather than individual analytes. This was achieved, in part, by evaluating the directionality of the association between each immune marker and their respective combinatory immune signature. In conjunction with IPA analysis, we assigned categorical names to each of these seven combinatory inflammatory signatures to provide an accurate description of how the networks of soluble markers interconnected to promote neuroinflammation. As our analyses focused on how the interrelated networks of inflammatory markers cooperated together, the same categorical description could have been used despite having a non-identical composition of individual immune markers. Inflammatory gene pathways identified through IPA analysis for each combinatory immune signature are included as (**Supplementary Figures S1–S13**).

Using our novel statistical approach and IPA analysis, we identified three combinatory inflammatory signatures implicated in neuroinflammation that were shared between HIV- and HIV+VS women: *Immune Activation & Vascular Dysfunction* (Signature 1); *T Cell-Dependent Antiviral Response* (Signature 2);

TABLE 1 | Demographic, behavioral, and clinical characteristics at the initial visit when immune makers were assessed among HIV-uninfected (HIV-) women and virally suppressed women with HIV (HIV+VS).

Variable	HIV− (*n* = 56) *n* (%)	HIV+VS (*n* = 49) *n* (%)	*P*-value
Age, M (SD)	38.0 (9.3)	38.9 (8.5)	0.62
Years of education, M (SD)	3.9 (1.0)	3.9 (1.2)	0.75
Race/ethnicity			0.27
Black, non-hispanic	31 (55)	21 (43)	
Hispanic	20 (36)	19 (39)	
Other	5 (9)	9 (18)	
Annual household income ≤12,000/year	33 (59)	23 (47)	0.22
Currently employed	23 (41)	15 (31)	0.27
Clinically relevant depressive symptoms†	17 (30)	19 (39)	0.36
Currently smoking	22 (39)	17 (35)	0.63
Recent use			
Heavy alcohol	6 (11)	0 (0)	0.02
Marijuana	11 (20)	3 (6)	0.04
Crack, cocaine, and/or heroin use	5 (9)	2 (4)	0.32
Hepatitis C RNA positive	14 (25)	12 (24)	0.95
Body mass index	28.6 (6.9)	28.9 (5.9)	0.81
Hypertension	10 (18)	14 (28)	0.19
Diabetes	3 (5)	6 (12)	0.21
ART treated	–	49 (100)	
CD4 count, median (IQR) Current Nadir	–	426 (242) 212 (213)	
Effective ART duration, mean (SD), years	–	0.72 (0.42)	
ART duration, mean (SD), years		2.45 (1.35)	
Prior AIDS diagnosis	–	13 (26)	

WRAT-3, wide range achievement test standard score; Years of Education: 1, no schooling; 2, grades 1–6; 3, grades 7–11; 4, completed high school, 5, some college, 6, completed 4 years of college, and 7, attended/completed graduate school. †CES-D, Center for Epidemiological Studies Depression scale ≥16 cutoff; current, refers to within the past week; recent, refers to within 6 months of the most recent WIHS visit; heavy alcohol use reflects >7 drinks/week or ≥4 drinks in one sitting; ART, antiretroviral therapy. Variables reported as n (%) were analyzed with Chi–square tests. Variables reported as M (SD) were analyzed t2with independent t-tests. Variables reported as median/IQR were analyzed with Wilcoxon–Mann–Whitney test.

TABLE 2 | Strongest network of inflammatory markers contributing to Combinatory Immune Signature that were common between HIV-uninfected (HIV-) women and virally suppressed women with HIV (HIV+VS).

Combinatory immune signature	HIV-serostatus	
	HIV- (*n* = 56)	**HIV+VS (*n* = 49)**
1	**Immune activation & vascular dysfunction**	**Immune activation & vascular dysfunction**
	Beta-2 microglobulin, Clusterin, Cystatin C, sCD14, sVEGFR2	*Beta-2 microglobulin*, *Clusterin*, *Cystatin C, sCD14, sVEGFR2*
2	**T Cell-dependent antiviral response**	**T Cell-dependent antiviral response**
	TRAIL/CD253, *IL-10*, *FGF-2, Fractalkine/CX3CL1,* SDF-1a + b/CXCL12, ITAC/CXCL11	TRAIL/CD253, IL-10, BCA-1/CXCL13, 6CKINE/CCL21
3	**Neuroinflammatory signaling**	**Neuroinflammatory signaling**
	Fractalkine/CX3CL1, FGF-2, serum amyloid A, CRP	TRAIL/CD253, serum amyloid A, CRP, *IL-10, Adiponectin*

Markers in italics were negatively associated with the profile; otherwise, the markers were positively associated with the profile. Our analyses focused on how the interrelated networks of inflammatory mediators cooperated together. As such, the same categorical description could be assigned for Combinatory Immune Signatures, despite having non-identical composition of individual immune markers.

TABLE 3 | Strongest network of inflammatory markers contributing to Combinatory Immune Signatures that were specific to HIV-uninfected (HIV−) women.

Combinatory immune signature	HIV- (*n* = 56)
4^{HIV-}	**Depressive/Psychiatric disorder inflammatory response**
	IL-10, FGF-2, *Fractalkine/CX3CL1,* IL-6
5^{HIV-}	**Anti-inflammatory microglial activity**
	Myeloperoxidase, MIP-1α/CCL3, IL-6
6^{HIV-}	**Cytokine mediated inflammatory response**
	IL-6, IL-10
7^{HIV-}	**T Cell exhaustion**
	Fractalkine/CX3CL1, IL-10, *CRP*, sVEGFR2, *serum amyloid A*

Markers in italics were negatively associated with the profile; otherwise, the markers were positively associated with the profile.

TABLE 4 | Strongest network of inflammatory markers contributing to Combinatory Immune Signatures that were specific to virally suppressed women with HIV (HIV+VS).

Combinatory immune signature	HIV+VS (*n* = 49)
4^{HIV+VS}	**Myeloid, T Cell, and Endothelial Cell Communication**
	IL-10, FGF-2, Fractalkine/CX3CL1, IL-17
5^{HIV+VS}	**Microglial chemokine-mediated T Cell recruitment to brain**
	Fractalkine/CX3CL1, IL-10, CRP, *sVEGFR2, MIP3b/CCL19, MIG/CXCL9, ITAC/CXCL11*
6^{HIV+VS}	**Leukocyte recruitment to brain**
	IL-6, serum amyloid A, MIP3b/CCL19, MIG/CXCL9, ITAC/CXCL11, FGF-2, Fractalkine/CX3CL1
7^{HIV+VS}	**Oxidative stress**
	Myeloperoxidase, IL-6, sVEGFR1, *IL-17, IL-10*

Markers in italics were negatively associated with the profile; otherwise, the markers were positively associated with the profile.

and *Neuroinflammatory Signaling* (Signature 3) (**Table 2**). The immune markers identified in Signature 1 (*Immune Activation & Vascular Dysfunction*), as well as the directionality of their associations within this signature, were identical between HIV- and HIV+VS women. Signature 1 was defined by the neuroinflammatory profile that existed by the interrelated network of Beta-2 microgloblin, Clusterin, Cystatin c, sCD14, and sVEGFR2, which were all negatively associated with this immune signature. In contrast, this was not the case for the remaining signatures that were in common between HIV− and HIV+VS women. Because our analyses focused on *how* the interrelated networks of inflammatory mediators cooperated together, the same categorical description was assigned to Signature 2 (*T Cell-Dependent Antiviral Response*) and Signature 3 (*Neuroinflammatory Signaling*), for HIV- and HIV+VS women despite having a different composition of individual immune markers. However, the signatures were not completely distinct. In fact, two immune markers were consistent between HIV− and HIV+VS women for Signature 2 (TRAIL/CD253 and IL-10) and Signature 3 (serum amyloid A and CRP 3).

In contrast to the first three signatures, the remaining four combinatory immune signatures were unique and stratified according to HIV-serostatus. For HIV- women, each of the remaining signatures reflected distinct inflammatory processes and included: *Depressive/Psychiatric Disorder Inflammatory Response* (Signature 4^{HIV-}); *Anti-Inflammatory Microglial Activity* (Signature 5^{HIV-}); *Cytokine-Mediated Inflammatory Response* (Signature 6^{HIV-}); and *T Cell Exhaustion* (Signature 7^{HIV-}) (**Table 3**). This was not the case for HIV+VS women (**Table 4**). Notably, three of the four signatures specific to HIV+VS women were indicative of a single inflammatory process: leukocyte influx into the CNS. These signatures were assigned the categorical descriptions of *Myeloid, T Cell, and Endothelial Cell Communication* (Signature 4^{HIV+VS}), *Microglial Chemokine-Mediated T cell Recruitment to Brain* (Signature 5^{HIV+VS}), and *Leukocyte Recruitment to Brain* (Signature 6^{HIV+VS}). While these three signatures reflected a single inflammatory process, the individual immune markers comprising the immune network were not identical. There were

both conserved (IL-10, Fractalkine/CX3CL1, and ITAC/CXCL11) and unique markers (CRP, IL-17, sVEGFR2, Il-6, serum amyloid A, MIP3b/CCL19, MIG/CXCL9, and FGF-2) represented within these three immune networks. The final combinatory immune signature that was uniquely present in HIV+VS women was *Oxidative Stress* (Signature 7^{HIV+VS}).

Predictive Associations Between Combinatory Immune Signatures and Cognition

We were interested in determining the contribution of peripheral immune responses implicated in neuroinflammatory processes to cognitive function. Therefore, we next evaluated the predictive abilities of the combinatory immune signatures to prospectively identify cognition in 49 HIV- and 34 HIV+VS women. To do this, we used mixed-effects regression models to identify associations between the combinatory immune signatures and global and domain-specific cognition, for both groups of women. We were particularly interested in identifying combinatory immune signatures that distinguished between HIV-related and HIV-unrelated mechanisms underlying CI. Only average (not variability) immune signatures were associated with cognition. **Table 5** provides descriptive statistics for the average factor loadings for the immune signatures and average neuropsychological test performance by HIV-serostatus.

Combinatory immune signatures were equally predictive of global neuropsychological performance for both the HIV- and HIV+VS women, as four associations with global cognition were identified for both groups. Signatures 4-7^{HIV-} (Signature 4^{HIV-}, *Depressive/Psychiatric Disorder Inflammatory Response*; Signature 5^{HIV-}, *Anti-Inflammatory Microglial Activity*; Signature 6^{HIV-}, *Cytokine-Mediated Inflammatory Response*; Signature 7^{HIV-}, *T Cell Exhaustion*) were the only immune profiles significantly predicted with global cognition for HIV- women (**Figure 1**). That is, for HIV- women, the combinatory immune signatures that were unique to this group were significantly associated with global cognition, while those in common with HIV+VS women had no such associations. In contrast, both unique and common combinatory immune signatures were predictive of global cognition for HIV+VS women. Signatures 1^{HIV+VS} (*Immune Activation & Vascular Dysfunction*), 2^{HIV+VS} (*T Cell-Dependent Antiviral Response*), 4^{HIV+VS} (*Myeloid, T Cell, and Endothelial Cell Communication*), and 5^{HIV+VS} (*Microglial Chemokine-Mediated T cell Recruitment to Brain*) were significantly associated with global cognition for HIV+VS women. For both HIV- and HIV+VS women, some combinatory immune signatures were predictive of better global cognition (HIV-: Signatures 5^{HIV-} and 7^{HIV-}; HIV+VS: Signatures 4^{HIV+VS} and 5^{HIV+VS}) while other were predictive of poorer global cognition (HIV-: Signatures 4^{HIV-} and 6^{HIV-}; HIV+VS: Signatures 1^{HIV+VS} and 2^{HIV+VS}). Adding marijuana and heavy alcohol use to the model did not change the pattern of associations.

While our primary interest was in the combination of immune signatures, we are still able to interpret associations between each marker and cognition. To this end, we need to multiple the sign (+ or −) of the marker (W) relating to the immune

TABLE 5 | Descriptive statistics for immune signature loadings and cognitive function for the subset of participants with neuropsychological (NP) test performance data available.

	Variable	HIV− (*n* = 49) M (SD)	HIV+VS (*n* = 34) M (SD)
Immune signature loadings			
1	Immune activation & vascular dysfunction	−22.5 (0.4)	−22.7 (0.4)
2	T Cell-dependent antiviral response	0.07 (1.0)	0.02 (1.0)
3	Neuroinflammatory signaling	0.09 (0.8)	0.07 (0.7)
4^{HIV-}	Depressive/Psychiatric disorder infammatory response	0.02 (0.82)	–
5^{HIV-}	Anti-inflammatory microglial activity	−0.05 (0.7)	–
6^{HIV-}	Cytokine mediated inflammatory response	−0.04 (0.4)	–
7^{HIV-}	T Cell exhaustion	−0.02 (0.4)	–
4^{HIV+VS}	Myeloid, T Cell, and Endothelial Cell communication	–	−0.02 (0.7)
5^{HIV+VS}	Microglial chemokine-mediated T Cell recruitment to brain	–	0.06 (0.6)
6^{HIV+VS}	Leukocyte recruitment to brain	–	0.00 (0.5)
7^{HIV+VS}	Oxidative stress	–	0.04 (0.5)
Neuropsychological test performance			
Global NP function		3.5 (2.1)	3.2 (1.7)
Learning		48.4 (8.9)	50.7 (9.9)
Memory		48.4 (9.9)	51.6 (9.7)
Attention/WM		50.2 (9.5)	48.1 (11.2)
Executive Function		48.9 (9.8)	48.4 (9.3)
Speed		49.6 (10.5)	50.5 (9.9)
Fluency		48.5 (9.3)	50.5 (9.6)
Motor		47.6 (12.9)	50.2 (8.9)

M, mean; SD, standard deviation; WM, working memory; global NP function, higher values equal poorer cognition.

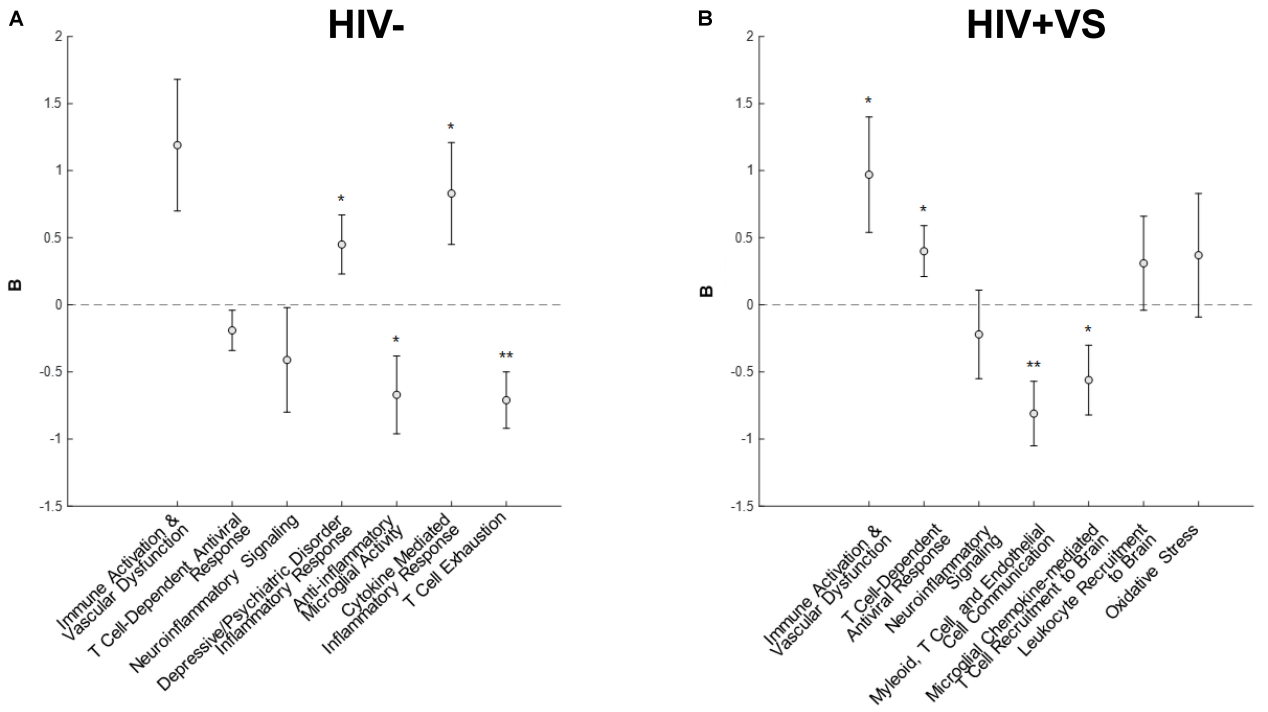

FIGURE 1 | Associations between inflammatory profile scores and global cognitive performance at a subsequent point in time among **(A)** HIV- uninfected (HIV-) woman and **(B)** virally suppressed women with HIV (HIV + VS). $*p < 0.05$; $**p < 0.01$. Circles denote the unstandardized beta weights **(B)** and standard errors of **(B)**. Circles above 0 indicate positive associations whereas circles below 0 indicate negative associations. Inflammatory signatures highlighted in gray are common to both HIV– and HIV+ VS women whereas inflammatory signatures not highlighted in gray are specific to either HIV– or HIV+ VS women.

profile to the sign of the beta coefficient (B) from the mixed-effects regression models. For example, the markers (W) listed in signature 1^{HIV+VS} (*Immune Activation & Vascular Dysfunction*) include five markers negatively associated with the signature (Beta-2 microglobulin, clusterin, cystatin C, sCD14, sVEGFR2). The beta coefficient (B) between the average factor loading for signature 1^{HIV+VS} and global cognition is positive. So the negative sign for the marker (−W) multiplied times the positive sign for global cognition (+B) equals a negative sign between the marker-global cognition association. Since higher scores on global cognition means poorer function, higher levels of each of these markers predict better global cognition (see **Supplementary Figure S15** for an implemented example).

To more completely characterize the predictive abilities of the combinatory immune signatures, we also evaluated their associations with domain-specific cognition (**Figure 2** and **Supplementary Figure S16**). In contrast to that which occurred for global cognition, the combinatory immune signatures were more predictive of domain-specific neuropsychological performance for HIV+VS women. Furthermore, the majority of combinatory immune signatures were predictive of worsening domain-level neuropsychological function in HIV+VS women. Signatures reflecting leukocyte influx into the brain (Signatures 4^{HIV+VS}, 5^{HIV+VS}, 6^{HIV+VS}) and immune activation/vascular dysfunction (Signature 1) were highly predictive of domain-specific cognition for HIV+VS women. Each of these combinatory immune signatures were predictive of worsening speed, fluency, motor function, attention and working memory, and executive function. Notably, Myeloid, T Cell, and Endothelial Cell Communication (Signature 4^{HIV+VS}) and Microglial Chemokine-Mediated T Cell Recruitment to Brain (Signature 5^{HIV+VS}) were predictive of worsening cognition in 6/7 and 3/7 domains, respectively. Combinatory immune signatures reflecting T Cell-Dependent Antiviral Response (Signature 2) and Neuroinflammatory Signaling (Signature 3) were more specific, and predictive of only one and two domains: improved speed and worsening executive function and speed, respectively, in HIV+VS women. Interestingly, Immune Activation and Vascular Dysfunction (Signature 1) was predictive of improved attention/working memory, speed, and motor function, while also being predictive of worsening executive function. It is important to note that Oxidative Stress (Signature 7^{HIV+VS}) was the only combinatory immune signature for HIV+VS women that was not predictive of neuropsychological function, both globally and at the domain-level. See **Supplementary Figure S17** for an implemented example of marker and domain-specific cognition. Adding marijuana and heavy alcohol use to the model did not change the pattern of associations.

For HIV- women, half of the combinatory immune signatures were predictive of improved domain-level neuropsychological function, while the remainder were predictive of worsening cognition. Combinatory immune signatures reflecting Immune Activation & Vascular Dysfunction (Signature 1; executive function, speed, and motor function), Depressive/Psychiatric

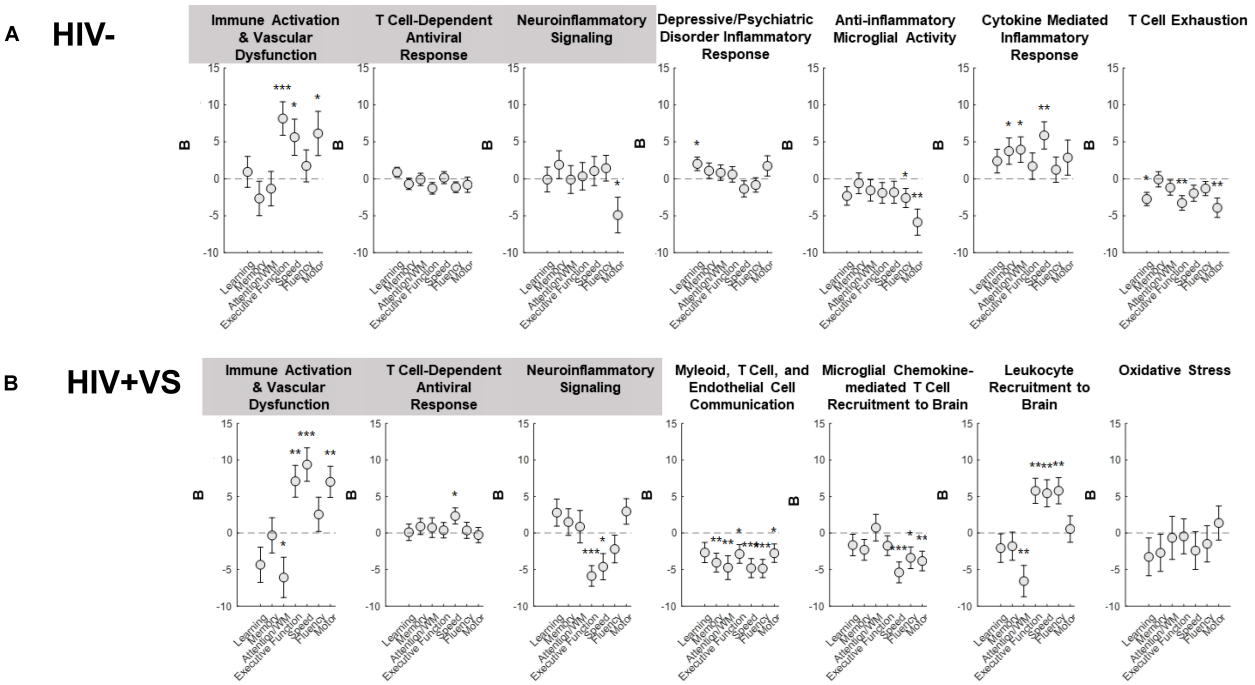

FIGURE 2 | Associations between inflammatory profile scores and domain-specific cognitive performance at a subsequent point in time among **(A)** HIV- uninfected (HIV-) woman and **(B)** virally suppressed women with HIV (HIV + VS). WM, working memory; $^{*}p < 0.05$; $^{**}p < 0.01$; $^{***}p < 0.001$. Circles denote the unstandardized beta weights **(B)** and standard errors of **(B)**. Circles above 0 indicate positive associations whereas circles below 0 indicate negative associations. Inflammatory signatures highlighted in gray are common to both HIV– and HIV+ VS women whereas inflammatory signatures not highlighted in gray are specific to either HIV– or HIV+ VS women.

Disorder Inflammatory Response (Signature 4^{HIV-}; learning), and Cytokine Mediated Inflammatory Response (Signature 6^{HIV-}; memory, attention/working memory, and speed), were predictive of improved cognition. In contrast, Neuroinflammatory signaling (Signature 3; motor function), Anti-inflammatory Microglial Activity (Signature 5^{HIV-}; fluency and motor function) and T Cell Exhaustion (Signature 7^{HIV-}; learning, executive function, and motor function) were predictive of worsening domain-level cognitive function. Notably, the T Cell-Dependent Antiviral Response (Signature 2^{HIV-}) was the only combinatory immune signature for HIV- women that was not predictive of neuropsychological function, both globally and at the domain-level. Adding marijuana and heavy alcohol use to the model did not change the pattern of associations.

DISCUSSION

We performed a prospective study to identify combinatory immune signatures indicative of neuroinflammatory processes in HIV+VS and HIV- women that predicted subsequent cognitive performance at a given point in time up to 12 years later (median ∼3 years). Forty-two immune markers were evaluated to identify combinatory immune signatures based on underlying patterns of inflammatory processes. We identified seven combinatory immune signatures: three that were common across groups (Immune Activation and Vascular Dysfunction, T Cell-Dependent Antiviral Responses, and Neuroinflammatory Signaling), while four signatures were distinct. Combinatory immune signatures were predictive of global and domain-level cognitive function for both HIV- and HIV+VS women, though differences existed between the groups. There was a greater predictive ability for the combinatory immune signatures with domain-level cognition in HIV+VS women, while the immune signatures were equally predictive of global cognitive performance for both HIV- and HIV+VS women. The predictive abilities of combinatory immune signatures were nuanced, where some were associated with worsening cognition, while others indicated improving cognitive performance. These findings are among the first to provide critical insight into the mechanisms that contribute to the heterogeneity underlying cognitive function of effective ART-treated, HIV+VS women and of demographically similar HIV- women.

Signatures reflective of *Immune Activation and Vascular Dysfunction* (Signature 1) were identical in HIV- and HIV+VS women. These mechanisms are not specific to HIV, and it is not surprising this immune signature emerged for both groups of women. Immune activation and vascular dysfunction can occur for many non-viral reasons, including metabolic disease (Jansson, 2007; Hameed et al., 2015), cardiovascular insults (Hadi et al., 2005; Frostegard, 2013), and stroke (Roquer et al., 2009; Iadecola and Anrather, 2011). Furthermore, the predictive relationship between *Immune Activation and Vascular Dysfunction* with cognition is also not surprising. Persistent immune activation

may occur within the CNS and peripherally (Tchessalova et al., 2018), and is associated with CI in many psychiatric and neurological disorders (Kipnis et al., 2004; Onore et al., 2012; Krukowski et al., 2018). Vascular dysfunction is also well known to contribute to CI, which can occur through three distinct mechanisms: altered endothelial function, dysregulation of vessel tone, and altered cerebral flow (De Silva and Faraci, 2016). Each of these mechanisms affects the brain's energy reserve and greatly contributes to cognitive decline (de Haan et al., 2006; Snyder et al., 2015; Toth et al., 2017). Similarly, the associations between the immune signature reflecting *Neuroinflammatory Signaling* (Signature 3) and cognition were expected., as the production of cytokines, innate immune and cholinergic signaling responses, and inflammatory proteins is well implicated in CI (Passos et al., 2009; Terrando et al., 2011; Griffin, 2013; Li et al., 2013; Wang et al., 2013; Peixoto et al., 2015; Reardon et al., 2018; Tchessalova et al., 2018).

Surprisingly, immune signatures implicating *T-Cell Dependent Antiviral Responses* (Signature 3) were observed in both groups of women. While an antiviral response is anticipated for the HIV+VS women, unexpectedly, this phenotype also emerged in the HIV- group. The antiviral response may have occurred in some HIV- women as a result of Hepatitis C infection. However, unlike the name suggests, antiviral responses are not restricted to viral pathogens. Instead, they may also be elicited during non-infectious insults, including metabolic disease (Li et al., 2012; Zhao et al., 2015), cancer (Zaidi and Merlino, 2011; Snell et al., 2017), cardiovascular disorders (Voloshyna et al., 2014; King et al., 2017), and autoimmune disease (Ronnblom and Eloranta, 2013; Crow et al., 2015). Therefore, the antiviral response in HIV- women may have occurred to infection with a virus other than HIV, general inflammation, or another immune stressor (Trinchieri, 2010). Over-reactive antiviral responses, particularly those associated in the Type I Interferon pathway, are associated with CI, as well as neurologic and psychiatric disease (Bonaccorso et al., 2002; Baruch et al., 2014; Sarkar et al., 2015). In PWH, a monocyte-derived type I interferon response was associated with cognitive decline (Pulliam, 2014). Our present study identified a lymphocytic, rather than myeloid, derived response that contributed to cognitive performance in only HIV+VS women.

The remaining combinatory immune signatures were specific to each group of women. Those for HIV+VS women were highly concordant with each other, where 3/4 signatures reflected a single immune response: leukocyte influx into the CNS (Signatures 4-6^{HIV+VS}). As this myeloid-dependent leukocyte migration immune profile was identified in multiple clusters for HIV+VS, suggesting that this pathway is a major contributor to immune dysfunction during HIV infection. Leukocyte influx is reliably associated with viral seeding of the brain, maintaining viral reservoir in the brain, and perpetuating low level, chronic neuroinflammation during HIV infection (Nottet, 1999; Fischer-Smith et al., 2001; Grovit-Ferbas and Harris-White, 2010; Williams et al., 2014, 2015). Of note, one of the combinatory immune signatures reflective of this immune response (Signature 4^{HIV+VS}) was predictive of worsening cognition in 6/7 domains, with the exception of learning, and was also significantly associated with global function. These findings indicate that sustained leukocyte infiltration into the brain occurs, despite successful viral suppression with ART, and is a major mechanism by which CI occurs for HIV+VS individuals. Oxidative stress was the other profile that occurred specifically in HIV+VS. Although oxidative stress is a well-known contributor to cognitive decline (Pratico et al., 2002; Wu et al., 2004; Droge and Schipper, 2007), for the HIV+VS women, oxidative stress was not associated with cognitive performance. While oxidative stress may contribute to other comorbidities in HIV+VS women, it does not appear to be an additional contributor to cognitive function in PWH.

We also identified a number of distinct combinatory immune signatures in HIV- women that were associated with subsequent cognitive function. Specifically, there were four immune signatures specific to HIV- women that implicated (1) *Depressive/Psychiatric Inflammatory Responses* (Signature 4^{HIV-}), (2) *Anti-Inflammatory Microglial Activity* (Signature 5^{HIV-}), (3) *Cytokine-Mediated Inflammatory Responses* (Signature 6^{HIV-}) and (4) *T Cell Exhaustion* (Signature 7^{HIV-}). Two of these were of particular interest: Signatures 4 and 7^{HIV-}. Persistent CI occurs in individuals with depressive and psychiatric disorders, particularly in the domains of attention, verbal/working memory, executive function, processing speed, and visuospatial/problem solving (Gotlib and Joormann, 2010; Millan et al., 2012; Masson et al., 2016; Bernhardt et al., 2019). These CI are multifactorial and occur as a result of genetic, developmental, and environmental factors (Millan et al., 2012). We identified an inflammatory response signature associated with depressive and psychiatric disorders that predicted subsequent learning, as well as global cognition in HIV- women. There was no significant difference in the rates of clinically relevant depressive symptoms between HIV- and HIV+VS women, yet an immune profile related to the disorder was identified solely in HIV− women. This may have occurred as a result of a "masking" effect in HIV+VS women, wherein the immune response during HIV infection was driven so strongly by viral-mediated responses that it makes it difficult to assess those that are attributed to depressive and psychiatric diseases.

The identification of an immune profile related to T cell exhaustion in HIV- women was among the most interesting findings. T cell exhaustion refers to the state of dysfunction where the T cell is unable to elicit appropriate effector functions due to a transcriptional state that permits the sustained expression of inhibitory receptors. T cell exhaustion is most commonly associated with cancer and chronic infections (Wherry, 2011). Therefore, T cell exhaustion rarely occurs in a purely "healthy" population. The HIV- women involved in this study were well matched to the HIV+VS group, and while they were HIV seronegative, they had comorbidities that may contribute to a state of T cell exhaustion (Sumida et al., 2013; Massanella et al., 2015). T cell exhaustion is often implicated in CI associated with viral infections (Enose-Akahata et al., 2009; Ndhlovu et al., 2011; Grauer et al., 2015). However, the contribution of T cell exhaustion to cognitive function in the absence of pathogenic infection has not been extensively evaluated. Our finding that early plasma markers of T cell exhaustion were predictive of worsening learning, executive function, motor function and

global cognition may reflect the specific comorbidities among this group of HIV- women, and may not be reflective of cognitive function in a "healthier" population of seronegative individuals. This provides insight into the importance of having a well-matched, HIV seronegative, control population when evaluating HIV and cognitive function. While it may be interesting that the T cell exhaustion cluster was not identified in HIV+VS, it is not particularly unexpected as all of the women were receiving ART and were completely virally suppressed. While not completely reversible, ART does decrease T cell exhaustion (Serrano-Villar et al., 2014). ART decreases the heightened state of immune activation, which leads to T cell exhaustion, as indicated by CD38 + HLA-DR + expression (Pallikkuth et al., 2013). Further, ART increases functionality of both CD4 and CD8 T cells, as indicated by IL-2 production upon stimulation – something which exhausted lympocytes are unable to do (Harari et al., 2004; Rehr et al., 2008).

There were a number of study limitations. This was secondary data analysis of prospective data that included a limited sample size. Furthermore, only 80% of women had subsequent neuropsychological test data available; however, the subset of women with neuropsychological test data were similar to the larger group of women in terms of sociodemographic, behavioral, and clinical characteristics. Another limitation is that comprehensive neuropsychological test data was not collected in the WIHS until 2009 thus limiting our ability to comment on the prevalence and severity of CI in our sample initially. Additionally, a targeted approach was used to evaluate the 42 immune markers. While this is a powerful methodology that allows for multiplexed analyses of pathways known to be associated with cognitive function, our results were limited as unbiased, untargeted discovery was not feasible. Additionally, interpreting directionality of the pattern of immune profile-cognition associations (e.g., higher markers, lower cognition) is difficult but possible with our analytic approach as we were interested in the combined effects of markers (signatures) rather than any one marker which has not been sufficient for understanding cognitive function. As we are the first to our knowledge to identify these exact combinatorial immune profiles, there is no precedent among immunologists as to the nomenclature of the profiles. Further, as many proteins are involved in multiple pathways, the understanding of their biological function can be context dependent (i.e., cancer vs. HIV). As such, it is difficult to ensure that our nomenclature status will satisfy all immunologists. However, there is a general consensus agreement among immunologists as to the function of the individual immune mediators that comprise the profile - which is represented in the published work of others. The nomenclature designation for the combined immune profiles was first derived in consultation with the literature to ensure we ascribed an accurate title to each group. Further, to ensure that our results were unbiased and as extensive as possible, we next used Ingenuity® Pathway Analysis (IPA®, Qiagen, Redwood City, CA, United States), a web-based software application, to facilitate interpretation of data derived from the dynamic matrix factorization analytic method. As such, our nomenclature system is sound and strongly supported by existing ideas within the literature. Finally, our findings may not necessarily be generalizable to long-term virally suppressed men with HIV. There is a growing body of evidence demonstrating the importance of considering sex as a biological variables in studies of inflammatory biomarkers in HIV (Ticona et al., 2015; Scully, 2018; Scully et al., 2019) and in studies focusing on inflammatory contributors to cognitive function in HIV (Rubin et al., 2019). Future larger, scale studies are necessary to examine the reproducibility of these findings. Extending this work to CSF markers and brain structure and function would also further our understanding of the effects of dynamic immune signaling (peripherally and centrally) and brain health in PWH.

In sum, we identified early plasma immune signatures in HIV+VS and HIV− women that were predictive of subsequent cognitive function up to 12 years later. Importantly, our findings identified HIV-related, as well as HIV-unrelated, immune mechanisms that were associated with global and domain-specific cognitive function. Broadly, the results indicate that the underlying mechanisms that contribute to CI in these groups are both overlapping and distinct.

DATA AVAILABILITY STATEMENT

Women's Interagency HIV Study de-identified data can be obtained by submitting a request to the Data Analysis and Coordination Center (DACC) for the Multicenter AIDS Cohort Study (MACS) and the Women's Interagency HIV Study (WIHS) Combined Cohort Study (MACS/WIHS-CCS).

ETHICS STATEMENT

The studies involving human participants were reviewed and approved by the Institutional Review Boards of University of Mississippi Medical Center, University of North Carolina at Chapel Hill, University of Alabama at Birmingham, University of Miami, Emory University, SUNY Downstate Medical Center, Kings County Medical Center, Montefiore Medical Center, Beth Israel Medical Center, Mount Sinai School of Medicine, Cook County Health and Hospitals System, Northwestern University, Rush University Medical Center, University of Illinois at Chicago, University of California, San Francisco, Alameda Health System, Sutter Health, Santa Clara Valley Medical Center, San Mateo Medical Center, Georgetown University, Montgomery County Department of Health and Human Services, Inova, Howard University, Whitman-Walker Clinic, University of Southern California Medical Center, Santa Barbara Neighborhood Clinics, and University of Hawai'i at Mânoa. The patients/participants provided their written informed consent to participate in this study.

AUTHOR CONTRIBUTIONS

LR conceived the study idea, took responsibility for the integrity of the analyses linking the immune to cognitive data, and wrote

the first draft of the manuscript with DW. YX and XW took responsibility for the integrity of the statistical analyses. PN took responsibility for the Ingenuity Pathway Analyses. PN and SK conducted all of the immune analyses. All authors contributed to the writing of the manuscript and approved the final version of the manuscript.

FUNDING

This research was funded by the Johns Hopkins University NIMH Center for novel therapeutics for HIV-associated cognitive disorders (P30MH075773) 2018 pilot award to LR. DW's effort was supported by R00DA044838. Data in this manuscript were collected by the Women's Interagency HIV Study, now the MACS/WIHS Combined Cohort Study (MWCCS). The contents of this publication are solely the responsibility of the authors and do not represent the official views of the National Institutes of Health (NIH). MWCCS (Principal Investigators): Atlanta CRS (Ighovwerha Ofotokun, Anandi Sheth, and Gina Wingood), U01-HL146241; Baltimore CRS (Todd Brown and Joseph Margolick), U01-HL146201; Bronx CRS (Kathryn Anastos and Anjali Sharma), U01-HL146204; Brooklyn CRS (Deborah Gustafson and Tracey Wilson), U01-HL146202; Data Analysis and Coordination Center (Gypsyamber D'Souza, Stephen Gange and Elizabeth Golub), U01-HL146193; Chicago-Cook County CRS (Mardge Cohen and Audrey French), U01-HL146245; Chicago-Northwestern CRS (Steven Wolinsky), U01-HL146240; Connie Wofsy Women's HIV Study, Northern California CRS (Bradley Aouizerat and Phyllis Tien), U01-HL146242; Los Angeles CRS (Roger Detels), U01-HL146333; Metropolitan Washington CRS (Seble Kassaye and Daniel Merenstein), U01-HL146205; Miami CRS (Maria Alcaide, Margaret Fischl, and Deborah Jones), U01-HL146203; Pittsburgh CRS (Jeremy Martinson and Charles Rinaldo), U01-HL146208; UAB-MS CRS (Mirjam-Colette Kempf and Deborah Konkle-Parker), U01-HL146192; UNC CRS (Adaora Adimora), U01-HL146194. The MWCCS is funded primarily by the National Heart, Lung, and Blood Institute (NHLBI), with additional co-funding from the Eunice Kennedy Shriver National Institute Of Child Health & Human Development (NICHD), National Human Genome Research Institute (NHGRI), National Institute On Aging (NIA), National Institute Of Dental & Craniofacial Research (NIDCR), National Institute Of Allergy And Infectious Diseases (NIAID), National Institute Of Neurological Disorders And Stroke (NINDS), National Institute Of Mental Health (NIMH), National Institute On Drug Abuse (NIDA), National Institute Of Nursing Research (NINR), National Cancer Institute (NCI), National Institute on Alcohol Abuse and Alcoholism (NIAAA), National Institute on Deafness and Other Communication Disorders (NIDCD), National Institute of Diabetes and Digestive and Kidney Diseases (NIDDK). MWCCS data collection is also supported by UL1-TR000004 (UCSF CTSA), P30-AI-050409 (Atlanta CFAR), P30-AI-050410 (UNC CFAR), and P30-AI-027767 (UAB CFAR).

ACKNOWLEDGMENTS

We would like to thank all the WIHS participants for their continued involvement in the study. Without you this work would not be possible.

SUPPLEMENTARY MATERIAL

The Supplementary Material for this article can be found online at: https://www.frontiersin.org/articles/10.3389/fnint.2020.00020/full#supplementary-material

REFERENCES

Anuurad, E., Semrad, A., and Berglund, L. (2009). Human immunodeficiency virus and highly active antiretroviral therapy-associated metabolic disorders and risk factors for cardiovascular disease. *Metab. Syndr. Relat. Disord.* 7, 401–410.

Bacon, M. C., Von Wyl, V., Alden, C., Sharp, G., Robison, E., Hessol, N., et al. (2005). The Women's interagency HIV study: an observational cohort brings clinical sciences to the bench. *Clin. Diagn. Lab Immunol.* 12, 1013–1019.

Bandera, A., Taramasso, L., Bozzi, G., Muscatello, A., Robinson, J. A., Burdo, T. H., et al. (2019). HIV-associated neurocognitive impairment in the modern ART era: are we close to discovering reliable biomarkers in the setting of virological suppression? *Front. Aging Neurosci.* 11:187. doi: 10.3389/fnagi.2019.00187

Barkan, S. E., Melnick, S. L., Preston-Martin, S., Weber, K., Kalish, L. A., Miotti, P., et al. (1998). The Women's interagency HIV Study. WIHS collaborative study group. *Epidemiology* 9, 117–125.

Baruch, K., Deczkowska, A., David, E., Castellano, J. M., Miller, O., Kertser, A., et al. (2014). Aging. Aging-induced type I interferon response at the choroid plexus negatively affects brain function. *Science* 346, 89–93.

Bernhardt, M., Klauke, S., and Schroder, A. (2019). Longitudinal course of cognitive function across treatment in patients with MDD: a meta-analysis. *J. Affect. Disord.* 249, 52–62.

Bingham, R., Ahmed, N., Rangi, P., Johnson, M., Tyrer, M., and Green, J. (2011). HIV encephalitis despite suppressed viraemia: a case of compartmentalized viral escape. *Int. J. Std. Aids* 22, 608–609.

Bonaccorso, S., Marino, V., Puzella, A., Pasquini, M., Biondi, M., Artini, M., et al. (2002). Increased depressive ratings in patients with hepatitis C receiving interferon-alpha-based immunotherapy are related to interferon-alpha-induced changes in the serotonergic system. *J. Clin. Psychopharmacol.* 22, 86–90.

Brouillette, M. J., Yuen, T., Fellows, L. K., Cysique, L. A., Heaton, R. K., and Mayo, N. E. (2016). Identifying neurocognitive decline at 36 months among HIV-positive participants in the CHARTER Cohort Using group-based trajectory analysis. *PLoS One* 11:e0155766. doi: 10.1371/journal.pone.0155766

Chen, M. F., Gill, A. J., and Kolson, D. L. (2014). Neuropathogenesis of HIV-associated neurocognitive disorders: roles for immune activation, HIV blipping and viral tropism. *Curr. Opin. Hiv Aids* 9, 559–564.

Chun, T. W., Moir, S., and Fauci, A. S. (2015). HIV reservoirs as obstacles and opportunities for an HIV cure. *Nat. Immunol.* 16, 584–589.

Chun, T. W., Nickle, D. C., Justement, J. S., Meyers, J. H., Roby, G., Hallahan, C. W., et al. (2008). Persistence of HIV in gut-associated lymphoid tissue despite long-term antiretroviral therapy. *J. Infect. Dis.* 197, 714–720.

Crow, M. K., Olferiev, M., and Kirou, K. A. (2015). Targeting of type I interferon in systemic autoimmune diseases. *Transl. Res.* 165, 296–305.

Cysique, L. A., Heaton, R. K., Kamminga, J., Lane, T., Gates, T. M., Moore, D. M., et al. (2014). HIV-associated neurocognitive disorder in Australia: a case of a high-functioning and optimally treated cohort and implications for international neuroHIV research. *J. Neurovirol.* 20, 258–268.

de Haan, E. H., Nys, G. M., and Van Zandvoort, M. J. (2006). Cognitive function following stroke and vascular cognitive impairment. *Curr. Opin. Neurol.* 19, 559–564.

De Silva, T. M., and Faraci, F. M. (2016). Microvascular dysfunction and cognitive impairment. *Cell Mol. Neurobiol.* 36, 241–258.

de Winter, J. C., Dodou, D., and Wieringa, P. A. (2009). Exploratory factor analysis with small sample sizes. *Multivariate Behav. Res.* 44, 147–181.

Droge, W., and Schipper, H. M. (2007). Oxidative stress and aberrant signaling in aging and cognitive decline. *Aging Cell* 6, 361–370.

Enose-Akahata, Y., Matsuura, E., Oh, U., and Jacobson, S. (2009). High expression of CD244 and SAP regulated CD8 T cell responses of patients with HTLV-I associated neurologic disease. *PLoS Pathog.* 5:e1000682. doi: 10.1371/journal.ppat.1000682

Fischer-Smith, T., Croul, S., Sverstiuk, A. E., Capini, C., L'heureux, D., Regulier, E. G., et al. (2001). CNS invasion by CD14+/CD16+ peripheral blood-derived monocytes in HIV dementia: perivascular accumulation and reservoir of HIV infection. *J. Neurovirol.* 7, 528–541.

Fletcher, C. V., Staskus, K., Wietgrefe, S. W., Rothenberger, M., Reilly, C., Chipman, J. G., et al. (2014). Persistent HIV-1 replication is associated with lower antiretroviral drug concentrations in lymphatic tissues. *Proc. Natl. Acad. Sci. U.S.A.* 111, 2307–2312.

Frostegard, J. (2013). Immunity, atherosclerosis and cardiovascular disease. *BMC Med.* 11:117. doi: 10.1016/s1471-4906(00)01848-2

Gianella, S., Kosakovsky Pond, S. L., Oliveira, M. F., Scheffler, K., Strain, M. C., De La Torre, A., et al. (2016). Compartmentalized HIV rebound in the central nervous system after interruption of antiretroviral therapy. *Virus Evol.* 2:vew020.

Gomez, D., Power, C., Gill, M. J., Koenig, N., Vega, R., and Fujiwara, E. (2018). Empiric neurocognitive performance profile discovery and interpretation in HIV infection. *J. Neurovirol.* 25, 72–84.

Gotlib, I. H., and Joormann, J. (2010). Cognition and depression: current status and future directions. *Annu. Rev. Clin. Psychol.* 6, 285–312.

Grant, I. (2008). Neurocognitive disturbances in HIV. *Int. Rev. Psychiatry* 20, 33–47.

Grauer, O. M., Reichelt, D., Gruneberg, U., Lohmann, H., Schneider-Hohendorf, T., Schulte-Mecklenbeck, A., et al. (2015). Neurocognitive decline in HIV patients is associated with ongoing T-cell activation in the cerebrospinal fluid. *Ann. Clin. Transl. Neurol.* 2, 906–919.

Griffin, W. S. (2013). Neuroinflammatory cytokine signaling and Alzheimer's disease. *N. Engl. J. Med.* 368, 770–771.

Grovit-Ferbas, K., and Harris-White, M. E. (2010). Thinking about HIV: the intersection of virus, neuroinflammation and cognitive dysfunction. *Immunol. Res.* 48, 40–58.

Hadi, H. A., Carr, C. S., and Al Suwaidi, J. (2005). Endothelial dysfunction: cardiovascular risk factors, therapy, and outcome. *Vasc Health Risk Manag.* 1, 183–198.

Hameed, I., Masoodi, S. R., Mir, S. A., Nabi, M., Ghazanfar, K., and Ganai, B. A. (2015). Type 2 diabetes mellitus: from a metabolic disorder to an inflammatory condition. *World J. Diabetes* 6, 598–612.

Harari, A., Petitpierre, S., Vallelian, F., and Pantaleo, G. (2004). Skewed representation of functionally distinct populations of virus-specific CD4 T cells in HIV-1-infected subjects with progressive disease: changes after antiretroviral therapy. *Blood* 103, 966–972.

Heaton, R. K., Franklin, D. R., Ellis, R. J., Mccutchan, J. A., Letendre, S. L., Leblanc, S., et al. (2011). HIV-associated neurocognitive disorders before and during the era of combination antiretroviral therapy: differences in rates, nature, and predictors. *J. Neurovirol.* 17, 3–16.

Heaton, R. K., Marcotte, T. D., Mindt, M. R., Sadek, J., Moore, D. J., Bentley, H., et al. (2004). The impact of HIV-associated neuropsychological impairment on everyday functioning. *J. Int. Neuropsychol. Soc.* 10, 317–331.

Heaton, R. K., Marcotte, T. D., White, D. A., Ross, D., Meredith, K., Taylor, M. J., et al. (1996). Nature and vocational significance of neuropsychological impairment associated with HIV infection. *Clin. Neuropsychol.* 10, 1–14.

Iadecola, C., and Anrather, J. (2011). The immunology of stroke: from mechanisms to translation. *Nat. Med.* 17, 796–808.

Jansson, P. A. (2007). Endothelial dysfunction in insulin resistance and type 2 diabetes. *J. Intern. Med.* 262, 173–183.

Joseph, S. B., Kincer, L. P., Bowman, N. M., Evans, C., Vinikoor, M. J., Lippincott, C. K., et al. (2018). HIV-1 RNA detected in the CNS after years of suppressive antiretroviral therapy can originate from a replicating CNS reservoir or clonally expanded cells. *Clin. Infect. Dis.* 69, 1345–1352.

Joska, J. A., Westgarth-Taylor, J., Myer, L., Hoare, J., Thomas, K. G., Combrinck, M., et al. (2011). Characterization of HIV-associated neurocognitive disorders among individuals starting antiretroviral therapy in South Africa. *AIDS Behav.* 15, 1197–1203.

King, K. R., Aguirre, A. D., Ye, Y. X., Sun, Y., Roh, J. D., Ng, R. P., et al. (2017). IRF3 and type I interferons fuel a fatal response to myocardial infarction. *Nat. Med.* 23, 1481–1487.

Kipnis, J., Cohen, H., Cardon, M., Ziv, Y., and Schwartz, M. (2004). T cell deficiency leads to cognitive dysfunction: implications for therapeutic vaccination for schizophrenia and other psychiatric conditions. *Proc. Natl. Acad. Sci. U.S.A.* 101, 8180–8185.

Krukowski, K., Chou, A., Feng, X., Tiret, B., Paladini, M. S., Riparip, L. K., et al. (2018). . Traumatic brain injury in aged mice induces Chronic microglia activation, synapse loss, and complement-dependent memory deficits. *Int. J. Mol. Sci.* 19:3753.

Li, P., Zhao, Y., Wu, X., Xia, M., Fang, M., Iwasaki, Y., et al. (2012). Interferon gamma (IFN-gamma) disrupts energy expenditure and metabolic homeostasis by suppressing SIRT1 transcription. *Nucleic Acids Res.* 40, 1609–1620.

Li, R. L., Zhang, Z. Z., Peng, M., Wu, Y., Zhang, J. J., Wang, C. Y., et al. (2013). Postoperative impairment of cognitive function in old mice: a possible role for neuroinflammation mediated by HMGB1. S100B, and RAGE. *J. Surg. Res.* 185, 815–824.

Marcotte, T. D., Deutsch, R., Michael, B. D., Franklin, D., Cookson, D. R., Bharti, A. R., et al. (2013). A concise panel of biomarkers identifies neurocognitive functioning changes in HIV-infected individuals. *J. Neuroimmune Pharmacol.* 8, 1123–1135.

Marcotte, T. D., Lazzaretto, D., Scott, J. C., Roberts, E., Woods, S. P., Letendre, S., et al. (2006). Visual attention deficits are associated with driving accidents in cognitively-impaired HIV-infected individuals. *J. Clin. Exp. Neuropsychol.* 28, 13–28.

Martinez-Picado, J., and Deeks, S. G. (2016). Persistent HIV-1 replication during antiretroviral therapy. *Curr. Opin. Hiv Aids* 11, 417–423.

Massanella, M., Gianella, S., Schrier, R., Dan, J. M., Perez-Santiago, J., Oliveira, M. F., et al. (2015). Methamphetamine Use in HIV-infected individuals affects T-cell function and viral outcome during suppressive antiretroviral therapy. *Sci. Rep.* 5:13179.

Masson, M., East-Richard, C., and Cellard, C. (2016). A meta-analysis on the impact of psychiatric disorders and maltreatment on cognition. *Neuropsychology* 30, 143–156.

Mavigner, M., Delobel, P., Cazabat, M., Dubois, M., L'faqihi-Olive, F. E., Raymond, S., et al. (2009). HIV-1 residual viremia correlates with persistent T-cell activation in poor immunological responders to combination antiretroviral therapy. *PLoS One* 4:e7658. doi: 10.1371/journal.pone.0007658

Millan, M. J., Agid, Y., Brune, M., Bullmore, E. T., Carter, C. S., Clayton, N. S., et al. (2012). Cognitive dysfunction in psychiatric disorders: characteristics, causes and the quest for improved therapy. *Nat. Rev. Drug Discov.* 11, 141–168.

Ndhlovu, L. C., Leal, F. E., Hasenkrug, A. M., Jha, A. R., Carvalho, K. I., Eccles-James, I. G., et al. (2011). HTLV-1 tax specific CD8+ T cells express low levels of Tim-3 in HTLV-1 infection: implications for progression to neurological complications. *PLoS Negl. Trop. Dis.* 5:e1030. doi: 10.1371/journal.pntd.0001030

Nottet, H. S. (1999). Interactions between macrophages and brain microvascular endothelial cells: role in pathogenesis of HIV-1 infection and blood - brain barrier function. *J. Neurovirol.* 5, 659–669.

Onore, C., Careaga, M., and Ashwood, P. (2012). The role of immune dysfunction in the pathophysiology of autism. *Brain Behav. Immun.* 26, 383–392.

Pallikkuth, S., Fischl, M. A., and Pahwa, S. (2013). Combination antiretroviral therapy with raltegravir leads to rapid immunologic reconstitution in treatment-naive patients with chronic HIV infection. *J. Infect. Dis.* 208, 1613–1623.

Passos, G. F., Figueiredo, C. P., Prediger, R. D., Pandolfo, P., Duarte, F. S., Medeiros, R., et al. (2009). Role of the macrophage inflammatory protein-1alpha/CC chemokine receptor 5 signaling pathway in the neuroinflammatory response

and cognitive deficits induced by beta-amyloid peptide. *Am. J. Pathol.* 175, 1586–1597.

Peixoto, C. A., Nunes, A. K., and Garcia-Osta, A. (2015). Phosphodiesterase-5 Inhibitors: action on the signaling pathways of neuroinflammation, neurodegeneration, and cognition. *Mediators Inflamm* 2015:940207.

Pratico, D., Clark, C. M., Liun, F., Rokach, J., Lee, V. Y., and Trojanowski, J. Q. (2002). Increase of brain oxidative stress in mild cognitive impairment: a possible predictor of Alzheimer disease. *Arch. Neurol.* 59, 972–976.

Pulliam, L. (2014). Cognitive consequences of a sustained monocyte type 1 IFN response in HIV-1 infection. *Curr. HIV Res.* 12, 77–84.

Reardon, C., Murray, K., and Lomax, A. E. (2018). Neuroimmune communication in health and disease. *Physiol. Rev.* 98, 2287–2316.

Rehr, M., Cahenzli, J., Haas, A., Price, D. A., Gostick, E., Huber, M., et al. (2008). Emergence of polyfunctional CD8+ T cells after prolonged suppression of human immunodeficiency virus replication by antiretroviral therapy. *J. Virol.* 82, 3391–3404.

Ritola, K., Robertson, K., Fiscus, S. A., Hall, C., and Swanstrom, R. (2005). Increased human immunodeficiency virus type 1 (HIV-1) env compartmentalization in the presence of HIV-1-associated dementia. *J. Virol.* 79, 10830–10834.

Ronnblom, L., and Eloranta, M. L. (2013). The interferon signature in autoimmune diseases. *Curr. Opin. Rheumatol.* 25, 248–253.

Roquer, J., Segura, T., Serena, J., and Castillo, J. (2009). Endothelial dysfunction, vascular disease and stroke: the ARTICO study. *Cerebrovasc. Dis.* 27(Suppl. 1), 25–37.

Rubin, L. H., Maki, P. M., Springer, G., Benning, L., Anastos, K., Gustafson, D., et al. (2017). Cognitive trajectories over 4 years among HIV-infected women with optimal viral suppression. *Neurology* 89, 1594–1603.

Rubin, L. H., Neigh, G. N., Sundermann, E. E., Xu, Y., Scully, E. P., and Maki, P. M. (2019). Sex differences in neurocognitive function in adults with HIV: patterns, predictors, and mechanisms. *Curr. Psychiatry Rep.* 21:94.

Rubin, L. H., Radtke, K. K., Eum, S., Tamraz, B., Kumanan, K. N., Springer, G., et al. (2018). Cognitive burden of common non-antiretroviral medications in HIV-infected women. *J. Acquir. Immune Defic. Syndr.* 79, 83–91.

Sarkar, S., Sarkar, R., Berg, T., and Schaefer, M. (2015). Sadness and mild cognitive impairment as predictors for interferon-alpha-induced depression in patients with hepatitis C. *Br. J. Psychiatry* 206, 45–51.

Saylor, D., Dickens, A. M., Sacktor, N., Haughey, N., Slusher, B., Pletnikov, M., et al. (2016). HIV-associated neurocognitive disorder - pathogenesis and prospects for treatment. *Nat. Rev. Neurol.* 12, 234–248.

Scott, J. C., Woods, S. P., Vigil, O., Heaton, R. K., Schweinsburg, B. C., Ellis, R. J., et al. (2011). A neuropsychological investigation of multitasking in HIV infection: implications for everyday functioning. *Neuropsychology* 25, 511–519.

Scully, E. P. (2018). Sex differences in HIV infection. *Curr. Hiv Aids Rep.* 15, 136–146.

Scully, E. P., Gandhi, M., Johnston, R., Hoh, R., Lockhart, A., Dobrowolski, C., et al. (2019). Sex-based differences in human immunodeficiency virus type 1 reservoir activity and residual immune activation. *J. Infect. Dis.* 219, 1084–1094.

Serrano-Villar, S., Sainz, T., Lee, S. A., Hunt, P. W., Sinclair, E., Shacklett, B. L., et al. (2014). HIV-infected individuals with low CD4/CD8 ratio despite effective antiretroviral therapy exhibit altered T cell subsets, heightened CD8+ T cell activation, and increased risk of non-AIDS morbidity and mortality. *PLoS Pathog.* 10:e1004078. doi: 10.1371/journal.ppat.1004078

Snell, L. M., Mcgaha, T. L., and Brooks, D. G. (2017). Type I interferon in chronic virus infection and cancer. *Trends Immunol.* 38, 542–557.

Snyder, H. M., Corriveau, R. A., Craft, S., Faber, J. E., Greenberg, S. M., Knopman, D., et al. (2015). Vascular contributions to cognitive impairment and dementia including Alzheimer's disease. *Alzheimers Dement.* 11, 710–717.

Sumida, K., Shimoda, S., Iwasaka, S., Hisamoto, S., Kawanaka, H., Akahoshi, T., et al. (2013). Characteristics of splenic CD8+ T cell exhaustion in patients with hepatitis C. *Clin. Exp. Immunol.* 174, 172–178.

Tamarit Mdel, P., Quereda, C., Gonzalez-Rozas, M., Corral, I., and Casado, J. L. (2012). HIV type 1 viral encephalitis after development of viral resistance to plasma suppressive antiretroviral therapy. *AIDS Res. Hum. Retroviruses* 28, 83–86.

Tchessalova, D., Posillico, C. K., and Tronson, N. C. (2018). Neuroimmune activation drives multiple brain states. *Front. Syst. Neurosci.* 12:39. doi: 10.3389/fnsys.2018.00039

Terrando, N., Eriksson, L. I., Ryu, J. K., Yang, T., Monaco, C., Feldmann, M., et al. (2011). Resolving postoperative neuroinflammation and cognitive decline. *Ann. Neurol.* 70, 986–995.

Thames, A. D., Kim, M. S., Becker, B. W., Foley, J. M., Hines, L. J., Singer, E. J., et al. (2011). Medication and finance management among HIV-infected adults: the impact of age and cognition. *J. Clin. Exp. Neuropsychol.* 33, 200–209.

Ticona, E., Bull, M. E., Soria, J., Tapia, K., Legard, J., Styrchak, S. M., et al. (2015). Biomarkers of inflammation in HIV-infected Peruvian men and women before and during suppressive antiretroviral therapy. *AIDS* 29, 1617–1622.

Toth, P., Tarantini, S., Csiszar, A., and Ungvari, Z. (2017). Functional vascular contributions to cognitive impairment and dementia: mechanisms and consequences of cerebral autoregulatory dysfunction, endothelial impairment, and neurovascular uncoupling in aging. *Am. J. Physiol. Heart Circ. Physiol.* 312, H1–H20.

Trinchieri, G. (2010). Type I interferon: friend or foe? *J. Exp. Med.* 207, 2053–2063.

Voloshyna, I., Littlefield, M. J., and Reiss, A. B. (2014). Atherosclerosis and interferon-gamma: new insights and therapeutic targets. *Trends Cardiovasc. Med.* 24, 45–51.

Waldrop-Valverde, D., Jones, D. L., Gould, F., Kumar, M., and Ownby, R. L. (2010). Neurocognition, health-related reading literacy, and numeracy in medication management for HIV infection. *AIDS Patient Care STDS* 24, 477–484.

Wang, Y., He, H., Li, D., Zhu, W., Duan, K., Le, Y., et al. (2013). The role of the TLR4 signaling pathway in cognitive deficits following surgery in aged rats. *Mol. Med. Rep.* 7, 1137–1142.

Wherry, E. J. (2011). T cell exhaustion. *Nat. Immunol.* 12, 492–499.

Williams, D. W., Anastos, K., Morgello, S., and Berman, J. W. (2015). JAM-A and ALCAM are therapeutic targets to inhibit diapedesis across the BBB of CD14+CD16+ monocytes in HIV-infected individuals. *J. Leukoc Biol.* 97, 401–412.

Williams, D. W., Byrd, D., Rubin, L. H., Anastos, K., Morgello, S., and Berman, J. W. (2014). CCR2 on CD14(+)CD16(+) monocytes is a biomarker of HIV-associated neurocognitive disorders. *Neurol. Neuroimmunol. Neuroinflamm.* 1:e36.

Wu, A., Ying, Z., and Gomez-Pinilla, F. (2004). The interplay between oxidative stress and brain-derived neurotrophic factor modulates the outcome of a saturated fat diet on synaptic plasticity and cognition. *Eur. J. Neurosci.* 19, 1699–1707.

Zaidi, M. R., and Merlino, G. (2011). The two faces of interferon-gamma in cancer. *Clin. Cancer Res.* 17, 6118–6124.

Zayyad, Z., and Spudich, S. (2015). Neuropathogenesis of HIV: from initial neuroinvasion to HIV-associated neurocognitive disorder (HAND). *Curr. Hiv Aids Rep.* 12, 16–24.

Zhao, G. N., Jiang, D. S., and Li, H. (2015). Interferon regulatory factors: at the crossroads of immunity, metabolism, and disease. *Biochim. Biophys. Acta* 1852, 365–378.

Conflict of Interest: The authors declare that the research was conducted in the absence of any commercial or financial relationships that could be construed as a potential conflict of interest.

frontiers in Molecular Neuroscience

ORIGINAL RESEARCH
published: 30 June 2020
doi: 10.3389/fnmol.2020.00115

Poly(I:C) Challenge Alters Brain Expression of Oligodendroglia-Related Genes of Adult Progeny in a Mouse Model of Maternal Immune Activation

Xiao-Fan Zhang[1,2†], Ting Chen[3†], Aifen Yan[4], Jia Xiao[5,6], Yong-Li Xie[6], Jing Yuan[6], Pin Chen[5], Anderson On-Lam Wong[7], Yang Zhang[3] and Nai-Kei Wong[2,6]**

[1]Department of Psychiatry, Tongji Hospital, Tongji Medical College, Huazhong University of Science and Technology, Wuhan, China, [2]Department of Psychiatry, The University of Hong Kong, Hong Kong, China, [3]CAS Key Laboratory of Tropical Marine Bio-resources and Ecology (LMB), Key Laboratory of Applied Marine Biology of Guangdong Province and Chinese Academy of Sciences (LAMB), South China Sea Institute of Oceanology, Chinese Academy of Sciences, Guangzhou, China, [4]School of Stomatology and Medicine, Foshan University, Foshan, China, [5]School of Biomedical Sciences, Li Ka Shing Faculty of Medicine, The University of Hong Kong, Hong Kong, China, [6]National Clinical Research Center for Infectious Diseases, Shenzhen Third People's Hospital, The Second Hospital Affiliated to Southern University of Science and Technology, Shenzhen, China, [7]School of Biological Sciences, The University of Hong Kong, Hong Kong, China

OPEN ACCESS

Edited by:
Haiyun Xu,
Shantou University, China

Reviewed by:
Weiwen Wang,
Institute of Psychology (CAS), China
Li-Jin Chew,
Children's National Hospital, United States

***Correspondence:**
Nai-Kei Wong
wongnksz@163.com
Yang Zhang
yzhang@scsio.ac.cn

†These authors have contributed equally to this work

Received: *02 February 2020*
Accepted: *03 June 2020*
Published: *30 June 2020*

Citation:
Zhang X-F, Chen T, Yan A, Xiao J, Xie Y-L, Yuan J, Chen P, Wong AO-L, Zhang Y and Wong N-K (2020) Poly(I:C) Challenge Alters Brain Expression of Oligodendroglia-Related Genes of Adult Progeny in a Mouse Model of Maternal Immune Activation. Front. Mol. Neurosci. 13:115. doi: 10.3389/fnmol.2020.00115

Background: Altered white matter connectivity, as evidenced by pervasive microstructural changes in myelination and axonal integrity in neuroimaging studies, has been implicated in the development of autism spectrum disorder (ASD) and related neurodevelopmental conditions such as schizophrenia. Despite an increasing appreciation that such white matter disconnectivity is linked to social behavior deficits, virtually no etiologically meaningful myelin-related genes have been identified in oligodendrocytes, the key myelinating cells in the CNS, to furnish an account on the causes. The impact of neurodevelopmental perturbations during pregnancy such as maternal immune activation (MIA) on these genes in memory-related neural networks has not been experimentally scrutinized.

Methods: In this study, a mouse model of MIA by the viral dsRNA analog poly(I:C) was employed to mimic the effects of inflammation during pregnancy. Transcriptional expression levels of selected myelin- or oligodendroglia-related genes implicated in schizophrenia or ASD development were analyzed by *in situ* hybridization (ISH) and quantitative real-time PCR (qRT-PCR) with brain samples from MIA and control groups.

Abbreviations: ASD, autism spectrum disorder; MIA, maternal immune activation; poly(I:C), polyriboinosinic-polyribocytidylic acid; ISH, *in situ* hybridization (ISH); qRT-PCR, quantitative real-time polymerase chain reaction; *MAG*, myelin associated glycoprotein; *L-MAG*, long-form *MAG*; *SOX-10*, SRY-related HMG-box 10; *Tf*, transferrin; GD9, gestation day 9; CDS, coding sequences; RSG, retrosplenial granular cortex; RSD, retrosplenial dysgranular cortex; GrDG, granular layer of dentate gyrus; CPu, caudate putamen; SC, somatosensory cortex; AC, auditory cortex; PC, piriform cortex; pRh, perirhinal cortex.

The analysis focused on *SOX-10* (SRY-related HMG-box 10), *MAG* (myelin-associated glycoprotein), and *Tf* (transferrin) expression in the hippocampus and the surrounding memory-related cortical regions in either hemisphere.

Results: Specifically, ISH reveals that in the brain of prenatal poly(I:C)-exposed mouse offspring in the MIA model (gestation day 9), mRNA expression of the genes *SOX10*, *MAG* and *Tf* were generally reduced in the limbic system including the hippocampus, retrosplenial cortex and parahippocampal gyrus on either side of the hemispheres. qRT-PCR further confirms the reduction of *SOX10*, *MAG*, and *Tf* expression in the medial prefrontal cortex, sensory cortex, amygdala, and hippocampus.

Conclusions: Our present results provide direct evidence that prenatal exposure to poly(I:C) elicits profound and long-term changes in transcript level and spatial distribution of myelin-related genes in multiple neocortical and limbic regions, notably the hippocampus and its surrounding memory-related neural networks. Our work demonstrates the potential utility of oligodendroglia-related genes as biomarkers for modeling neurodevelopmental disorders, in agreement with the hypothesis that MIA during pregnancy could lead to compromised white matter connectivity in ASD.

Keywords: maternal immune activation (MIA), poly(I:C), *SOX10*, myelin-associated glycoprotein (*MAG*), transferrin (*Tf*), schizophrenia, autistic spectrum disorder, white matter

BACKGROUND

Growing evidence suggests that functional disconnectivity within and across large-scale neural networks is a central hallmark of clinically overlapping neurodevelopmental disorders such as autism spectrum disorder (ASD) and schizophrenia (Sharma et al., 2017; van den Heuvel et al., 2017). Indeed, numerous studies by diffusion tensor imaging (DTI; Cheung et al., 2008; Nickel et al., 2017; Boets et al., 2018; d'Albis et al., 2018) and histopathology (Drakesmith et al., 2016; Aoki et al., 2017) have demonstrated regional deficits in the white matter volume, microstructural alterations in white matter tracts, and aberrant oligodendroglial features in patients with schizophrenia or ASD. Post-mortem microarray and quantitative real-time PCR (qRT-PCR) analysis have revealed a reduction in the expression of oligodendroglia-related genes in multiple brain regions of schizophrenic patients (Tkachev et al., 2003; Aberg et al., 2006; Sokolov, 2007) and children with ASD (Broek et al., 2014; Tian et al., 2017). In particular, altered expression patterns of myelin- or oligodendroglia-related genes reported in schizophrenia patients include the oligodendrocyte markers SRY-related HMG-box 10 (*SOX10*, Iwamoto et al., 2005; Jones et al., 2007; Maeno et al., 2007; Kato and Iwamoto, 2014), myelin-associated glycoprotein (*MAG*, Fujita et al., 1998; Yin et al., 1998; Felsky et al., 2012) and transferrin (Escobar Cabrera et al., 1994; Guardia Clausi et al., 2010), which are critically involved in myelination and oligodendrocyte progenitor differentiation (Baumann and Pham-Dinh, 2001). Previously, both clinical and experimental studies have proposed a variety of potential diagnostic or prognostic biomarkers for ASD based on biological samples from peripheral tissues or body fluids such as serum and urine (Bridgemohan et al., 2019; Salloum-Asfar et al., 2019; Swanson and Hazlett, 2019; Shen et al., 2020). In contrast, information on the clinical profiles of myelin- or oligodendroglia-related genes in patients with ASD is virtually wanting, necessitating an urgent need to address this important gap. It is being increasingly appreciated that dysfunction of oligodendrocytes contributes at least in part to abnormal synaptic communication and uncoupled white matter connection reported in schizophrenia (Olney et al., 1999; McGlashan and Hoffman, 2000; Najjar and Pearlman, 2015; Vikhreva et al., 2016; Yuan et al., 2016) and ASD studies (Zoghbi and Bear, 2012; Hahamy et al., 2015). However, the causal mechanisms of oligodendroglial abnormality have remained poorly understood and particularly difficult to clarify in human subjects. Also, there has been no consensus as to which of the molecular markers should be profiled toward a systematic understanding of oligodendroglial abnormality in animal models for ASD or schizophrenia, including the MIA (maternal immune activation) models (Estes and McAllister, 2016).

Modeling MIA by polyriboinosinic-polyribocytidylic acid [poly(I:C)] induction in animals is a robust method for investigating neurodevelopmental disorders (Careaga et al., 2017; Mueller et al., 2018). In this study, we employed a poly(I:C)-induced MIA model in mice to study any changes in the oligodendroglia-related genes of interest in the brain of adult progeny. Specifically, we exposed pregnant mice to poly(I:C), a synthetic mimetic of viral dsRNA analog, a well-documented mouse model of MIA. We and others have reported that poly(I:C)-induced MIA precipitates altered brain and behavioral phenotypes in offspring that mirror abnormalities observed in ASD and related neurodevelopmental conditions such as schizophrenia (Meyer et al., 2006; Li et al., 2015; Wei et al., 2016; Wu et al., 2018).

Another objective of this study was to identify which of the myelin-rich neural substrates are potentially affected by inflammation during pregnancy concerning the expression of the oligodendroglia-related genes. To this end, we performed *in situ* hybridization to directly assess the effects of MIA on the transcriptional expression of the oligodendroglia-related genes including *SOX10*, *MAG*, and transferrin (*Tf*) in the brain of adult mouse offspring. Based on the literature on white matter disconnectivity associated with the hippocampus-amygdala complex or temporal lobes in schizophrenia and ASD (Sigmundsson et al., 2001; Herbert et al., 2003; Ha et al., 2015; Sforazzini et al., 2016; van den Heuvel et al., 2016), we anticipated that a loss of oligodendroglia-related gene markers would be detected in the corresponding brain regions in prenatal MIA-exposed mice. Also, based on initial histological observations in our *in situ* hybridization analysis that bilateral hemispheric differences may exist for *SOX10*, *MAG*, and *Tf* among certain sub-cortical regions of the mouse brain, we employed an experimental design in quantitative real-time PCR that permits left-right brain comparison of the genes. This design helps to validate *in situ* hybridization observations, and complement knowledge gained from whole-brain approaches to the study of white matter changes in MIA models.

MATERIALS AND METHODS

Animals

Breeding and mating of female and male C57BL6/N mice were performed in compliance with the guidelines of the Laboratory Animal Unit (LAU), the University of Hong Kong. Timed-pregnant mice were kept in a 12:12-h reversed light-dark cycle (light onset at 19:00), and temperature and humidity-controlled (21 ± 1°C, 55 ± 5%) animal vivarium. Animals had access ad libitum to food and water supplied by the LAU. All experiments had been approved by the Committee on the Use of Live Animals in Teaching and Research at the University of Hong Kong, and every effort had been made to minimize the number of animals used and their suffering.

Prenatal Treatment

Prenatal treatment was performed as previously reported by our group (Li et al., 2015). Briefly, poly(I:C; potassium salt, Sigma Aldrich) with a dosage of 5 mg/kg in an injection volume of 5 ml/kg was freshly prepared on the day of injection and administered to pregnant dams on GD9 (gestation day 9) *via* the tail vein under mild physical constraint. Control animals were similarly administered with 5 ml/kg saline *via* tail vein on GD9. The animals were returned to their home cages after injection. The resulting offspring from six litters [poly(I:C) $n = 3$; control $n = 3$] were weaned and sexed at postnatal day (PND) 21. Pups were weighed and littermates of the same sex were caged separately (3–4 per cage). Only adult male offspring were used in subsequent experiments.

Molecular Cloning

Murine brain tissues were collected from stock adult mice, which were then immediately frozen in liquid nitrogen and stored at −80°C until use for total RNA isolation. Total RNA was extracted from mouse brains by using TRIzol (Invitrogen, San Diego, CA, USA) and reverse-transcribed with SuperScript II (Invitrogen). Based on the cDNAs from reverse transcription, gene-specific primers for *SOX10*, *L-MAG* (long-form *MAG*), and *Tf* (**Supplementary Table S1**) were used to clone the coding sequences (CDS) of the oligodendroglia-related genes. The PCR products were purified by using a BigDye Sequencing Kit (Applied Biosystems, Forster City, CA, USA). The purified cDNAs were then subcloned into a pGEM-T Easy cloning vector (Promega, Madison, WI, USA), and subjected to DNA sequencing for confirmation of the identity of oligodendroglia-related genes. The resulting cDNA plasmids were used in subsequent experiments for DIG-labeled probe synthesis.

DIG-Labeled Probe Synthesis

Double-strand (ds) DIG (digoxygenin)-labeled DNA probes were prepared with a PCR DIG Probe Synthesis Kit (Roche) by using specific PCR primers (**Supplementary Table S2**) according to the instructions of the manufacturer. Labeled probes were analyzed by gel electrophoresis to check for "size shift" after DIG-labeling. The performance of labeled probes in terms of hybridization selectivity and titering of probes used in hybridization reaction was confirmed in spot tests. Storage of DIG-labeled probe stock solutions was done in small aliquots (2–4 μl volume) at –80°C for future use.

Tissue Sectioning and *in situ* Hybridization

In situ hybridization was performed on several selected regions of the mouse brain, based on methods previously reported by our group (Jiang et al., 2008). Brains ($n = 3$ per group) from adult offspring of different pregnant mice ($n = 3$ per group) either exposed to poly(I:C)- or saline at GD9 were collected. The brains were perfused under terminal anesthesia, fixed in 4% paraformaldehyde, and embedded in paraffin wax. Brain sections of 5 μm in thickness were prepared on a Leica RM2135 microtome (Leica Microsystems, Wetzlar, Germany) and mounted onto pre-coated Superfrost Plus glass slides (Thermo Scientific, Waltham, MA, United States). The tissue sections were stored at −80°C for subsequent experiments. For *in situ* hybridization, brain sections were dewaxed with xylene, rehydrated with decreasing levels of ethanol, and post-fixed briefly in 4% paraformaldehyde. After that, the sections were digested with proteinase K (Roche), washed, and incubated at 37°C for 10 min with hybridization solution [4× saline sodium citrate (SSC), 1× Denhardt's solution, 10% dextran sulfate, 10 mM DTT, 40% formamide, 1 mg/ml salmon sperm DNA, 500 μg/ml yeast tRNA, 5 μg/ml poly deoxy adenylic acid, and 100 μg/ml polyadenylic acid]. For *in situ* hybridization, DIG-labeled DNA probes for mouse *SOX10, L-MAG*, and *Tf* were added to brain sections, followed by incubation at 42°C overnight in a humidified chamber. On the following day, post-hybridization washing was performed in decreasing concentrations of SSC solution at 42°C. Signal development was conducted with an anti-DIG antibody (1:500, Roche) by using NBT and BCIP as the substrates. In these experiments,

TABLE 1 | Primers and amplification conditions for quantitative PCR in this study.

Gene target/Accession no. (Primer sequences, 5′-3′)	PCR conditions						Amplif. efficiency	Product size
	Denaturing	Annealing	Extension	Detection	Cycle no.	Tm		
***SOX10*/NM_011437.1** AACGGTGCCAGCAAGAGCAA CGAGGTTGGTACTTGTAGTC	94°C 30 s	60°C 30 s	72°C 30 s	87°C 20 s	35	91°C	1.98	245 bp
***Transferrin*/AF440692.1** GGCCTGACTCCGAACAACCTGAAGC CTGCCCGAGAAGAAACTGGACACAG	94°C 30 s	60°C 30 s	72°C 30 s	87°C 20 s	35	91°C	1.98	260 bp
***L-MAG*/NM_010758** AGTGAGAAGCAGCGCCTGGGATCTG TCACTTGACTCGGATTTCTGCATACTC	94°C 30 s	62°C 30 s	72°C 30 s	87°C 20 s	35	88°C	1.86	168 bp
***T-MAG*/NM_010758** GATGCCCTCGACCATCTCAGCCTTC GGAAATAGTATTTGCCTCCCAGCTC	94°C 30 s	50°C 30 s	72°C 30 s	87°C 20 s	35	91°C	1.76	278 bp
***GAPDH*/M32599.1** GTGGAGCCAAACGGGTCATCATCT GGTCATGAGCCCTTCCACAAT	94°C 30 s	62°C 30 s	72°C 30 s	85°C 20 s	30	89°C	1.84	188 bp

hybridization with coronal sections of the saline-challenged mouse brain was used as a control.

RNA Preparation and Gene Expression Studies

Total RNA from individual mouse (n = 3 per group) brain regions including mPFC, hippocampus, amygdala, neocortex, and thalamus from an independent batch of the samples used by *in situ* experiments, was isolated with TRIzol reagent (Invitrogen). Next, 4 μg of each total RNA sample was digested with DNase I (Invitrogen) and reverse-transcribed into cDNA (RT) with SuperScript II (Invitrogen). Gene-specific primers for real-time PCR were designed based on the sequences of mouse *SOX10, L-MAG, T-MAG* (total *MAG*), *Tf*, and GAPDH. The RT samples obtained were then subjected to quantitative PCR in a RotorGene 6,000 Real-time PCR System (Corbett Research, Eight Mile Plains, New South Wales, Australia) and PCR reactions were conducted with a Light-cycler DNA Master SYBR Green I Kit (Roche). The primer sequences and real-time PCR reactions for gene expression studies are as shown in **Table 1**.

Data Transformation and Statistical Analysis

For quantitative real-time PCR for transcript expression of *SOX10, L-MAG, T-MAG*, and *Tf*, standard curves were constructed with serial dilutions of plasmids carrying the ORF of the respective gene targets, as described previously (Wong et al., 2013). After linear regression of threshold cycle values, standard curves within the dynamic range and with a correlation coefficient of ≥0.95 were used for data calibration. The raw data for the respective gene targets were quantified in terms of femtomole transcript detected per microgram of total RNA. There was no significant difference for *GAPDH* mRNA expression in our experiments, thus *SOX10, L-MAG, T-MAG*, and *Tf* mRNA expression were normalized as a ratio of *GAPDH* mRNA detected in the same sample for statistical analysis. Data expressed as mean ± SEM. were analyzed by using Student's *t*-test; significance was determined at $^{*}p < 0.05$, $^{**}p < 0.01$, or $^{***}p < 0.001$ by using SPSS (IBM Software).

RESULTS

In situ Hybridization

SOX10, L-MAG, and *Tf* transcript expression was generally reduced in several brain regions (both right and left sides) including the hippocampus, retrosplenial granular cortex (RSG), and retrosplenial dysgranular cortex (RSD), in the prenatal poly(I:C)-exposed group relative to saline-exposed control.

Within the hippocampus, the granular layer of the dentate gyrus (GrDG) showed the highest density of *SOX10* signals, while the CA1 and CA3 regions showed mild to moderate expression in saline control mice (**Figure 1**). Besides, *SOX10* signals were also observed in the left caudate-putamen (CPu; **Figure 1G**), but no *SOX10* signals were detected on the right side of CPu (**Figure 1H**) in saline control mice. In the neocortex of saline-exposed control, *SOX10* signals were abundantly detected in the medial part of the RSD and RSG (**Figure 4A**), the somatosensory cortex (SC), auditory cortex (AC) and the piriform cortex (PC; **Supplementary Figure S1**). However, in the prenatal poly(I:C)-exposed group, *SOX10* signals were either very weak in the hippocampus (GrDG, CA1, and CA3), left CPu, RSG and RSD, or SC, AC or PC (**Figures 1**, **4A** and **Supplementary Figure S1**) compared to that of the saline control mice or virtually undetectable in the right CPu, which was similar to the case of the control group (**Figure 1H**).

For *L-MAG* expression in saline-exposed control, the hippocampal regions (i.e., GrDG, CA1, CA3; **Figure 2**) again showed the strongest signals in terms of intensity and density compared to poly(I:C)-challenged mice. *L-MAG* signals were abundantly detected in an area encompassing the perirhinal cortex (PRh) and the lateral amygdaloid nucleus dorsolateral part

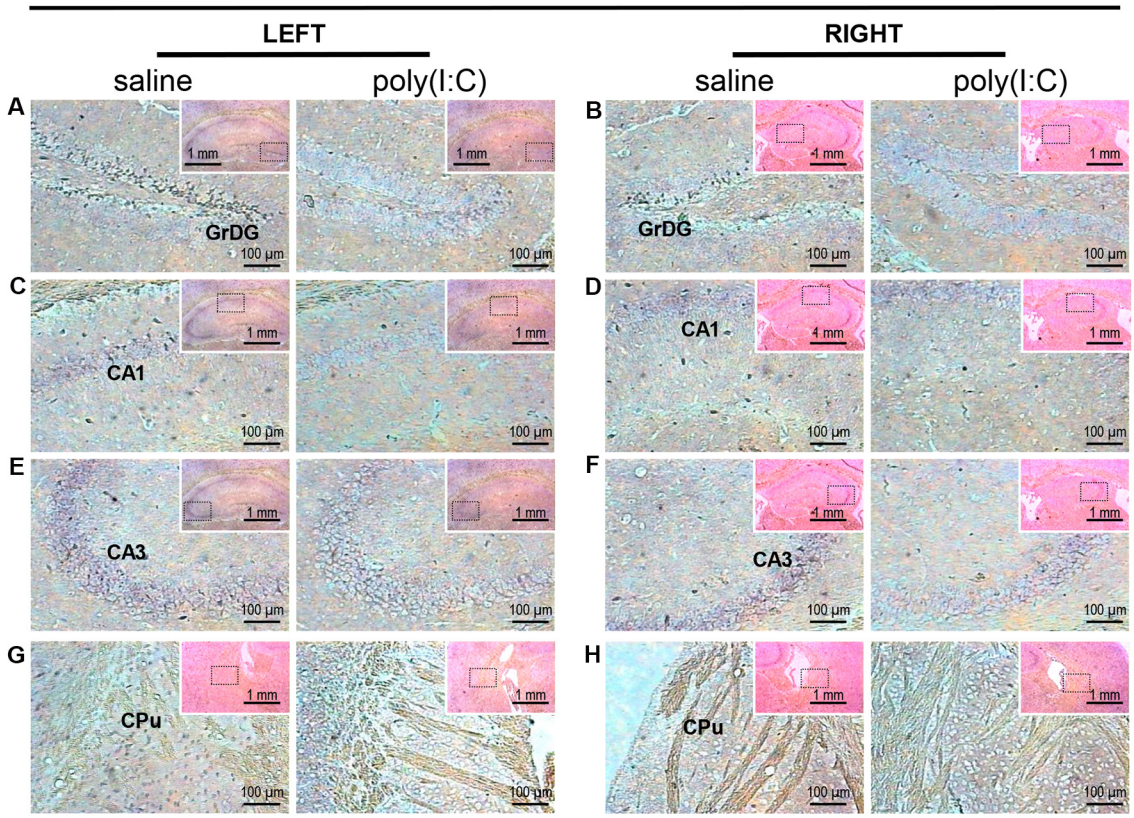

FIGURE 1 | *In situ* hybridization with a SRY-related HMG-box 10 (*SOX10*)-specific probe in the left and right hippocampi and striatums of adult mouse offspring. *SOX10* was detected as dark blue puncta. Four ROIs (regions of interest) in the brain of poly(I:C)- or saline-exposed mice were examined, namely, granular layer of the dentate gyrus (GrDG; panels **A,B**), CA1 (panels **C,D**), CA3 panels **(E,F)** and CPu (caudate-putamen; panels **G,H**) in a coronal section. Results are representative of two independent experiments. Insets show the approximate location of the ROIs in each panel relative to a larger area of the tissue. Representative images in detail were acquired at 100× magnification, and those in the inset (top right of each detailed image) at 25× magnification.

(LaDL; **Figures 2G,H**) in either hemisphere of the saline-exposed control. When viewed as a larger anatomical neighborhood, the ectorhinal cortex (Ect), PRh, and dorsolateral entorhinal (DLEnt) in the left brain seemed to have marginally stronger *L-MAG* signals than their counterparts in the right brain (**Figure 5**). Also, *L-MAG* expressing cells were abundantly found in the medial retrosplenial cortex (RSD and RSG; **Figure 4B**; **Supplementary Figures S2A,B**). In contrast, *L-MAG* mRNA expression of the prenatal poly(I:C)-exposed group was conspicuously absent or dramatically reduced in the same brain regions examined above when compared with that of the saline-exposed control (**Figures 2**, **4**, **5**).

Transcript expression patterns of *Tf* strikingly resembled that of *SOX10* and *L-MAG* in the hippocampus (**Figure 3**) of saline-exposed control. Again, the left GrGD showed the highest density and intensity of *Tf* signals among the hippocampal ROIs examined. In both the left and right parahippocampal regions, moderately strong *Tf* signals could be found (**Figures 3G,H**). *Tf* signals were also abundantly detected in the retrosplenial cortex (**Figure 4C**) and various sensory cortical regions (**Supplementary Figure S3**). In contrast, in the prenatal poly(I:C)-exposed mouse brain, there was a prevalent and remarkable reduction in *Tf* signals in the same brain regions examined above (**Figures 3**, **4**, **Supplementary Figure S3**).

Lastly, in the thalamus (Th), *SOX10, L-MAG* and *Tf* signals were undetectable in both the prenatal poly(I:C)- and saline-exposed groups (**Supplementary Figures S4A**, **S5A**, **S6A**), whereas in the ventral hypothalamus (VH), *SOX10, L-MAG*, and *Tf* ignals were moderate in the saline-exposed control, but again undetectable in the prenatal poly(I:C)-exposed group (**Supplementary Figures S4B**, **S5B**, **S6B**).

qRT-PCR Analysis on *SOX10*, *MAG*, and *Tf* mRNA Expression

To clarify whether poly(I:C) induced MIA would give rise to nonspecific modulatory effects on global gene expression in the mouse brain, we included the housekeeping gene *GAPDH* as a reference gene. Also, the qRT-PCR results reveal that there was no significant difference between the prenatal poly(I:C)- and saline-exposed groups in all the brain regions compared (**Figure 9**), which is consistent with the oligodendroglia-related

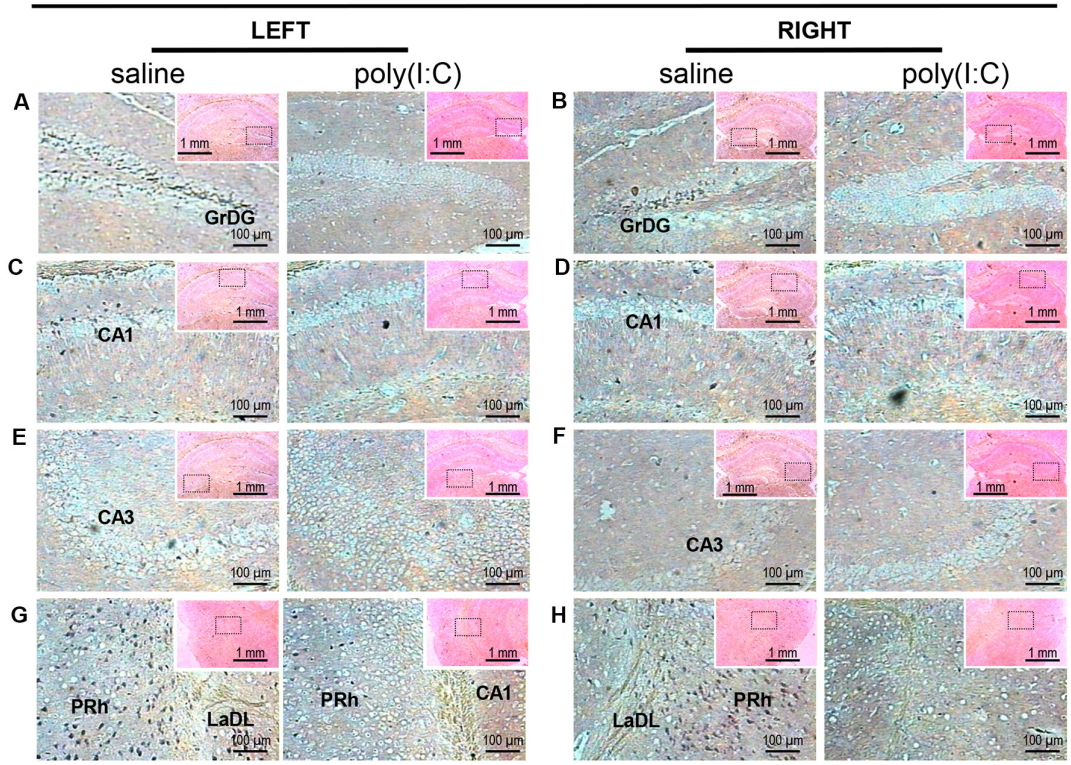

FIGURE 2 | *In situ* hybridization with an long-form myelin-associated glycoprotein (*L-MAG*)-specific probe in the left and right hippocampi and parahippocampal regions of adult mouse offspring. *L-MAG* was detected as dark blue puncta. Five ROIs in the brain of poly(I:C)- or saline-exposed mice were examined, namely, granular layer of the dentate gyrus (GrDG; panels **A,B**), CA1 (panels **C,D**), CA3 panels **(E,F)**, perirhinal cortex (PRh) and lateral amygdaloid nucleus dorsolateral part (LaDL; panels **G,H**) in a coronal section. Results are representative of two independent experiments. Insets show the approximate location of the ROIs in each panel relative to a larger area of the tissue. Representative images in detail were acquired at 100× magnification, and those in the inset (top right of each detailed image) at 25× magnification.

genes results for *in situ* hybridization for these regions (**Supplementary Figures S1**–**S6**).

In the mPFC, hippocampus, amygdala, and parts of the neocortex in both hemispheres, the transcript levels of *SOX10* in prenatal poly(I:C)-exposed group were significantly lower (by at least one-fold difference) than that of saline-exposed control (**Figure 6**). In contrast, in the thalamus, there was a marginal but nonsignificant difference in *SOX10* mRNA expression between prenatal poly(I:C)- and saline-exposed groups (**Figure 6E**). In both right and left mPFC, mRNA expression of *L-MAG* and *T-MAG* in prenatal poly(I:C)-exposed group was significantly lower ($p < 0.05$; **Figure 7A**). In the hippocampus, prenatal poly(I:C) challenge induced marked reduction in *L-MAG* mRNA expression in either hemisphere, while a reduction in *T-MAG* expression was found only on the right side ($p < 0.05$; **Figure 7B**). In the amygdala, poly(I:C)-exposed group showed decreased expression of *L-MAG* and *T-MAG* on the right but not the left side (**Figure 7C**). In the neocortex of poly(I:C)-exposed mice, significantly lower *T-MAG* mRNA expression appeared on the right side, while decreased *L-MAG* mRNA expression appeared on the left side (**Figure 7D**). Additionally, in the thalamus, poly(I:C) treatment induced a moderate but significant effect in lowering mRNA levels of *L-MAG* and *T-MAG* (**Figure 7E**). Consistent with *in situ* hybridization results, prevalent and marked reduction of *Tf* mRNA was found in all brain regions examined in either hemisphere of prenatal poly(I:C)-exposed mice (**Figure 8**). Among these, the mPFC, amygdala, and neocortex showed about two-fold decrease of *Tf* signals (**Figures 8A,C,D**), while the hippocampus and thalamus showed at least four-fold difference (**Figures 8B,E**).

DISCUSSION

In this study, a remarkable reduction of *SOX10, MAG*, and *Tf* transcript expression were seen in nearly all neocortical and limbic structures in prenatal poly(I:C)-exposed mice. Specifically, we found that several brain regions with prominent functions in learning, memory and social interaction (including the hippocampus, amygdaloid nuclei, entorhinal cortex, and retrosplenial cortex) showed markedly reduced *SOX10, MAG*, and *Tf* mRNA expression, suggesting that they may be high-risk regions susceptible to the effects of poly(I:C)-

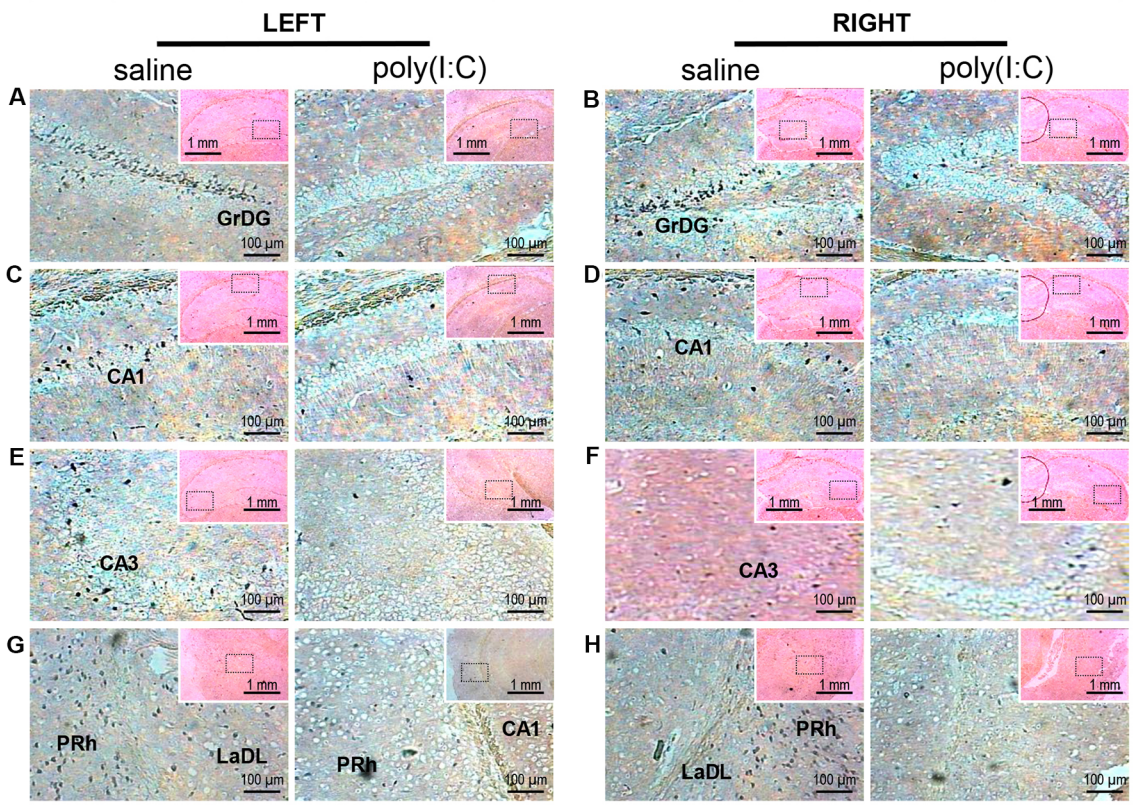

FIGURE 3 | *In situ* hybridization with a transferrin (*Tf*)-specific probe in the left and right hippocampi and parahippocampal regions of adult mouse offspring. *Tf* was detected as dark blue puncta. Five ROIs in the brain of poly(I:C)- or saline-exposed mice were examined, namely, granular layer of the dentate gyrus (GrDG; panels **A,B**), CA1 (panels **C,D**), CA3 panels **(E,F)**, perirhinal cortex (PRh) and lateral amygdaloid nucleus dorsolateral part (LaDL; panels **G,H**) in a coronal section. Results are representative of two independent experiments. Insets show the approximate location of the ROIs in each panel relative to a larger area of the tissue. Representative images in detail were acquired at 100× magnification, and those in the inset (top right of each detailed image) at 25× magnification.

induced MIA during pregnancy. This disruption of the normal course of development could result in a compromised capacity to maintain synchrony of widely distributed neural networks, which is ultimately manifested in the heterogeneity of symptoms and cognitive deficits of schizophrenia and autism (Bartzokis, 2002; Uhlhaas and Singer, 2010; French et al., 2015; Zalesky et al., 2015).

The transcriptional deficits of oligodendroglia-related genes in the different brain regions that we have found in this study are in agreement with the anatomical substrates reported in structural MRI studies (Bauman and Kemper, 1985; Aylward et al., 1999; Rojas et al., 2004; Honea et al., 2005; Nacewicz et al., 2006; Ellison-Wright and Bullmore, 2009). Abnormalities of the fronto-temporoparietal cortex network, hippocampus, and cerebellum and white matter connecting these regions seem to underscore the pathology of ASD and, that such changes could result from abnormal brain development during early life (Brambilla et al., 2003; Barnea-Goraly et al., 2004).

Myelin deficits shared by the hippocampal formation and the entorhinal cortex support the idea that white matter disconnectivity affects interconnected components of neural networks, rather than isolated brain loci. Within the hippocampus, the GrDG consistently showed the greatest intensity and density of *SOX10, L-MAG*, and *Tf* signals in saline-exposed control (**Figures 1–3**). Accordingly, the qualitative differences observed between the poly(I:C)- and saline-exposed groups were also greatest in this subregion of the hippocampus. The entorhinal cortex (layer II) is physically adjacent to the hippocampal formation and provides primary projections to both the dentate gyrus and CA3 (Tamminga et al., 2010). The dentate gyrus has been deemed a gateway structure receiving and transmitting neural inputs into the hippocampus. It is interesting to note that the apparent reduction in oligodendroglia-related gene expression in the GrDG of prenatal poly(I:C)-exposed brain (**Figures 1A,B**, **2A,B**, **3A,B**) parallels the well-documented reduction in dentate gyrus glutamatergic output (Tamminga et al., 2010), an abnormality traditionally attributed to neuronal dysfunction.

Apart from the hippocampus and entorhinal cortex, a memory-related brain region that showed clear transcriptional alterations was the retrosplenial cortex (RSD and RSG; **Figure 4**). The retrosplenial cortex is known to be reciprocally

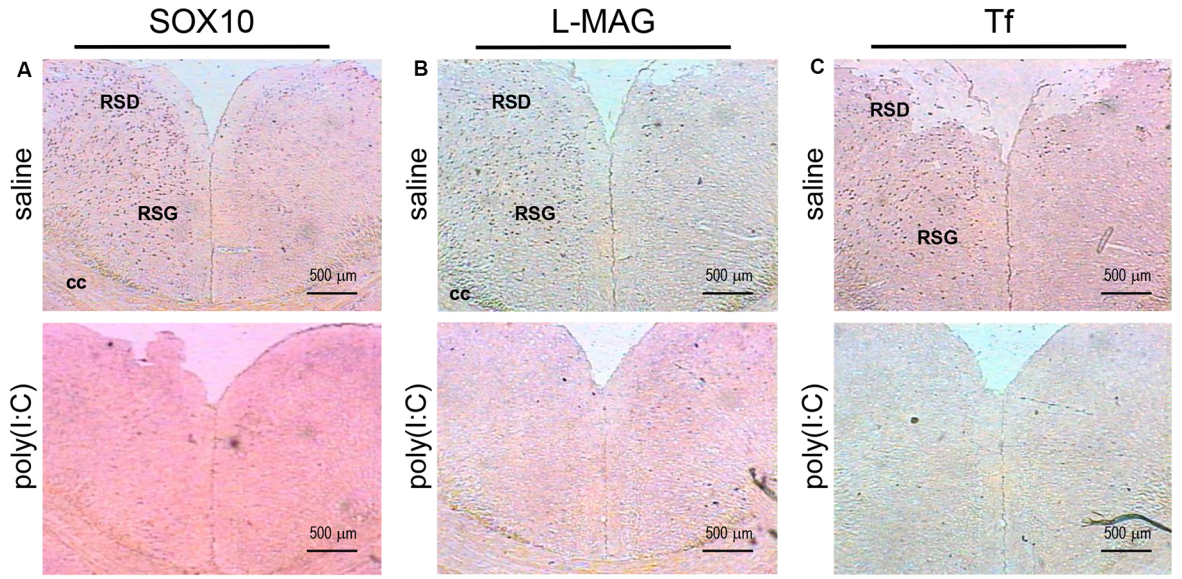

FIGURE 4 | *In situ* hybridization with a *SOX10*-, *L-MAG*- or *Tf*-specific probe in the medial part of the retrosplenial cortex of adult mouse offspring. *SOX10* mRNA was detected as dark blue puncta in panel **(A)**, *L-MAG* mRNA in panel **(B)**, and *Tf* mRNA in panel **(C)**. Two ROIs in the brain of poly(I:C)- or saline-exposed mice were examined, namely, the retrosplenial dysgranular cortex (RSD) and retrosplenial granular cortex (RSG) in a coronal section. Results are representative of two independent experiments. cc, corpus callosum. Representative images were acquired at 40× magnification.

interconnected with both the hippocampus and the prefrontal cortex and is involved in a range of cognitive functions including episodic memory, spatial working memory, and even emotion (Maddock, 1999; Vann et al., 2009). Indeed, schizophrenic and ASD patients have been shown to have major deficits in spatial working memory, previously thought to stem from prefrontal cortical dysfunction (Park and Holzman, 1992; Demetriou et al., 2018). For *SOX10, L-MAG*, and *Tf* in our study, transcript expression patterns in the RSD/RSG showed a discernible interhemispheric difference, with signals being preferentially stronger on the left brain of saline-exposed control. Due to the generally very low *SOX10, L-MAG*, and *Tf* signals being detected in prenatal poly(I:C)-exposed brain, this interhemispheric difference was not observed in *in situ* hybridization. In qRT-PCR, *SOX10, L-MAG/T-MAG*, and *Tf* transcript levels were reduced by over three folds (**Figure 6A**), one fold (**Figure 7A**), and two folds (**Figure 8A**), respectively, in the mPFC, an observation consistent with hypoactivity of executive-control in schizophrenia. Likewise, there was a clear trend of reduction in *SOX10, L-MAG/T-MAG*, and *Tf* transcript levels in the amygdala (**Figures 6C**, **7C**, **8C**), a center that modifies plasticity of fear memories and projects into the hippocampus and other limbic structures. Of note, *SOX10* mRNA levels were reduced by close to three folds in the right and left amygdala in mice prenatal exposed to poly(I:C), whereas only about one-fold difference was observed for *L-MAG/T-MAG* mRNA in the right but not left amygdala. As a structural protein with cell signaling functions mediated by its additional cytoplasmic domain, *L-MAG* contributes to most functions of total *T-MAG* in the CNS. The proportionally more significant reduction in *SOX10* mRNA expression could mean that *SOX10* as a transcription factor contributes significant weight to altered myelination or oligodendrocyte function in the postnatal offspring.

The relationship between poly(I:C) exposure induced MIA during pregnancy and selected oligodendroglia-related genes involved in myelination are as delineated in **Figure 10**. As posited in previous research, in humans, the temporal extent of brain plasticity can extend into the middle age, when maximal white matter volume and myelination are reached in frontal lobes and association areas (Bartzokis, 2002; Insel, 2010). However, the expression of certain genes critical to myelination is linearly driven and activatable only at early developmental stages. For example, *SOX10* expression is possible in embryonic neurons but becomes exclusively restricted to oligodendrocytes in postnatal life. Disruption of normal gene expression patterns (especially *SOX10*, which interacts with other transactivators, e.g., Olig1, Olig2, etc.) early in brain development could well have a more profound effect than the case of later stage disturbances. Consistent with our findings, reduced *SOX10* expression was found in the hippocampus and anterior cingulate cortex (ACC) of subjects with schizophrenia (Dracheva et al., 2006). Also, *SOX10* is a key regulator of oligodendrocyte differentiation by directly controlling the transcription of genes implicated in this process (Stolt et al., 2002). *Tf* acts as trophic and survival factors for neurons and astrocytes, with important implications for oligodendrocyte functions (Baumann and Pham-Dinh, 2001; **Figure 10**). *MAG* is selectively located in periaxonal Schwann cells and oligodendroglia membranes of myelin sheaths. It promotes the differentiation, maintenance, and survival of oligodendrocytes (Quarles, 2007). Also, *MAG* helps structure

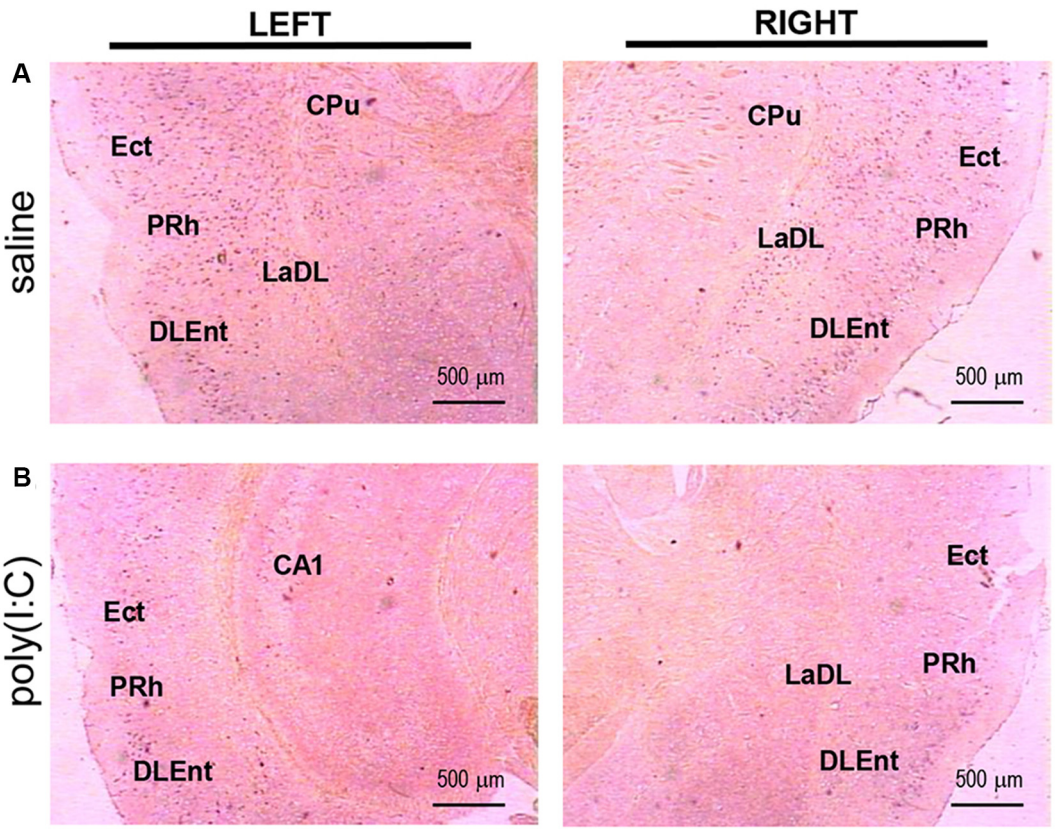

FIGURE 5 | *In situ* hybridization with an *L-MAG*-specific probe in the left and right parahippocampal regions of adult mouse offspring. *L-MAG* mRNA was detected as dark blue puncta in panel **(A)** for prenatal saline-exposed control, and in panel **(B)** for prenatal poly(I:C)-exposed group. Several ROIs in the brain of poly(I:C)- or saline-exposed mice were examined, namely, the ectorhinal cortex (Ect), perirhinal cortex (PRh), and dorsolateral entorhinal cortex (DLEnt) in a coronal section. Results are representative of two independent experiments. CPu, caudate putamen; LaDL, lateral amygdaloid nucleus dorsolateral part. Representative images were acquired at 25× magnification.

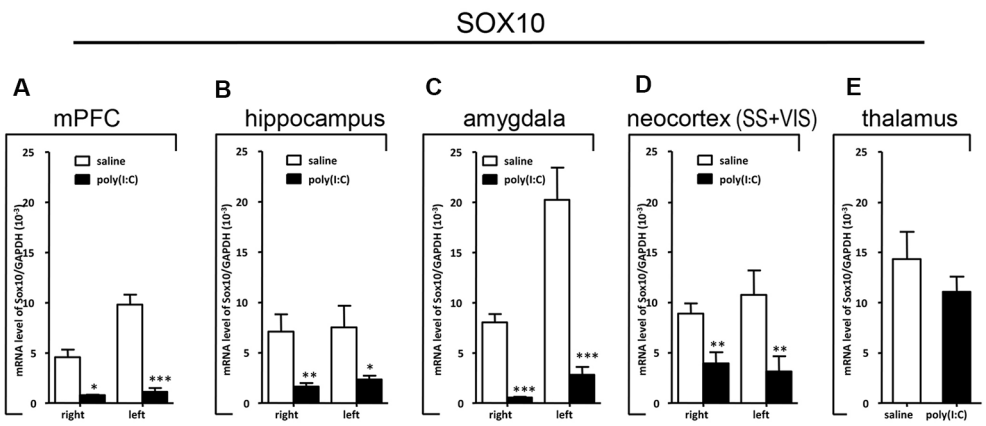

FIGURE 6 | Quantitative real-time polymerase chain reaction (qRT-PCR) evaluation of effects of poly(I:C)-induced maternal immune activation (MIA) on *SOX10* mRNA expression in selected brain regions (panels **A–E**: mPFC, hippocampus, amygdala, neocortex (SS+VIS) and thalamus). Tissues from the left and right hemispheres of adult mouse offspring [$n = 3$ for prenatal poly(I:C) or saline-exposed groups] were analyzed. Each bar represents mean ± SEM. Significance was determined at $^{*}p < 0.05$, $^{**}p < 0.01$, and $^{***}p < 0.001$ between treatments. SS + VIS: sensory and visual cortices; mPFC: the medial prefrontal cortex.

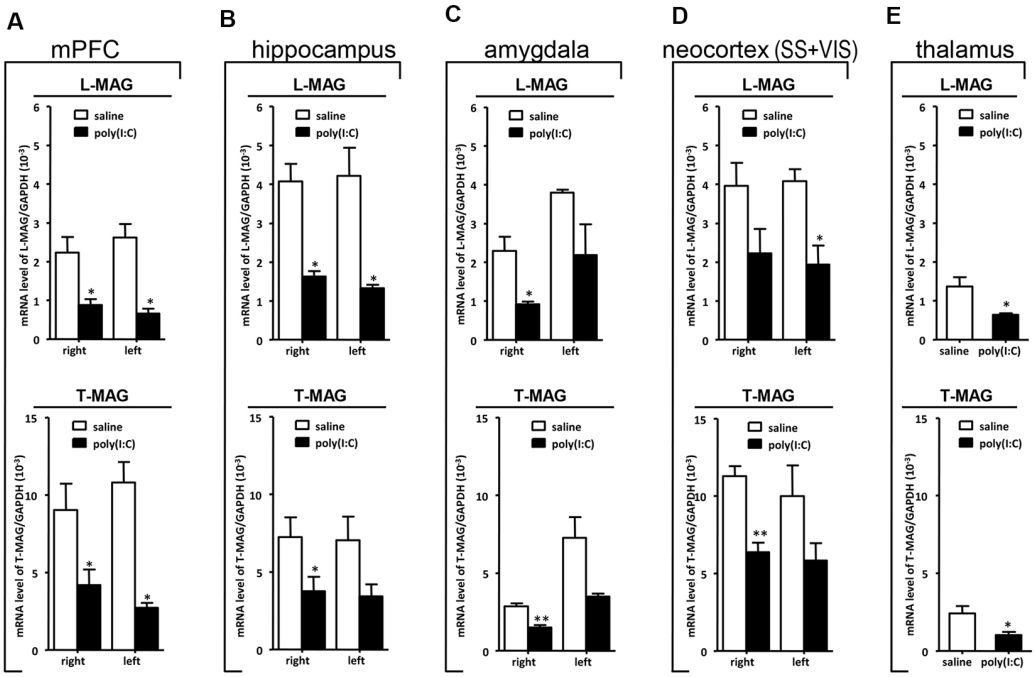

FIGURE 7 | qRT-PCR evaluation of effects of poly(I:C)-induced MIA on *L-MAG* and *T-MAG* mRNA expression in selected brain regions (panels **A–E**: mPFC, hippocampus, amygdala, neocortex (SS+VIS) and thalamus). Tissues from the left and right hemispheres of adult mouse offspring [$n = 3$ for prenatal poly(I:C) or saline-exposed groups] were analyzed. Each bar represents mean ± SEM. Significance was determined at $^{*}p < 0.05$ and $^{**}p < 0.01$ between treatments. SS + VIS: sensory and visual cortices; mPFC: the medial prefrontal cortex.

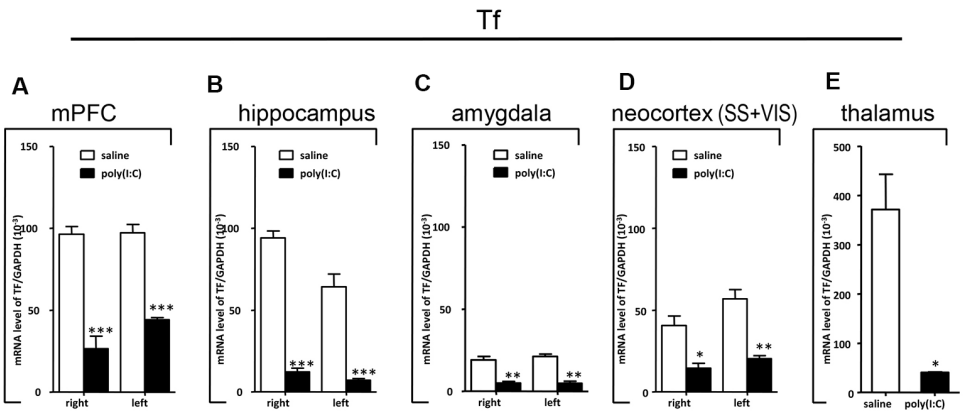

FIGURE 8 | qRT-PCR evaluation of effects of poly(I:C)-induced MIA on *Tf* mRNA expression in selected brain regions (panels **A–E**: mPFC, hippocampus, amygdala, neocortex (SS+VIS) and thalamus). Tissues from the left and right hemispheres of adult mouse offspring ($n = 3$ for prenatal poly(I:C) or saline-exposed groups) were analyzed. Each bar represents mean ± SEM. Significance was determined at $^{*}p < 0.05$, $^{**}p < 0.01$, and $^{***}p < 0.001$ between treatments. SS + VIS: sensory and visual cortices; mPFC: the medial prefrontal cortex.

nodes of Ranvier and inhibits neurite regeneration after injury (Schnaar and Lopez, 2009; **Figure 10**). Decreased transcript expression of *Tf* and *MAG* in the white matter of the ACC has been reported in subjects with schizophrenia (McCullumsmith et al., 2007). Furthermore, expression of these oligodendrocyte-related genes is disrupted in ASD-related animal models. For example, Fatemi et al. (2009) demonstrated that middle second (E16) and late second (E18) trimester infections of pregnant mice with human influenza virus reduced the expression of myelin basic protein (*MBP*) and *MAG* in

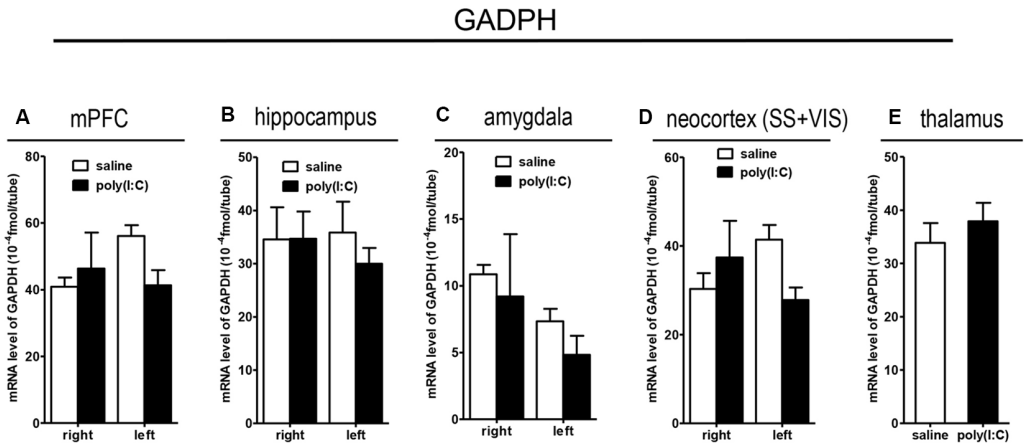

FIGURE 9 | qRT-PCR evaluation of effects of poly(I:C)-induced MIA on *GAPDH* mRNA expression in selected brain regions (panels **A–E**: mPFC, hippocampus, amygdala, neocortex (SS+VIS) and thalamus). Tissues from the left and right hemispheres of adult mouse offspring [n = 3 for prenatal poly(I:C) or saline-exposed groups] were analyzed. Each bar represents mean ± SEM. SS + VIS: sensory and visual cortices; mPFC: the medial prefrontal cortex.

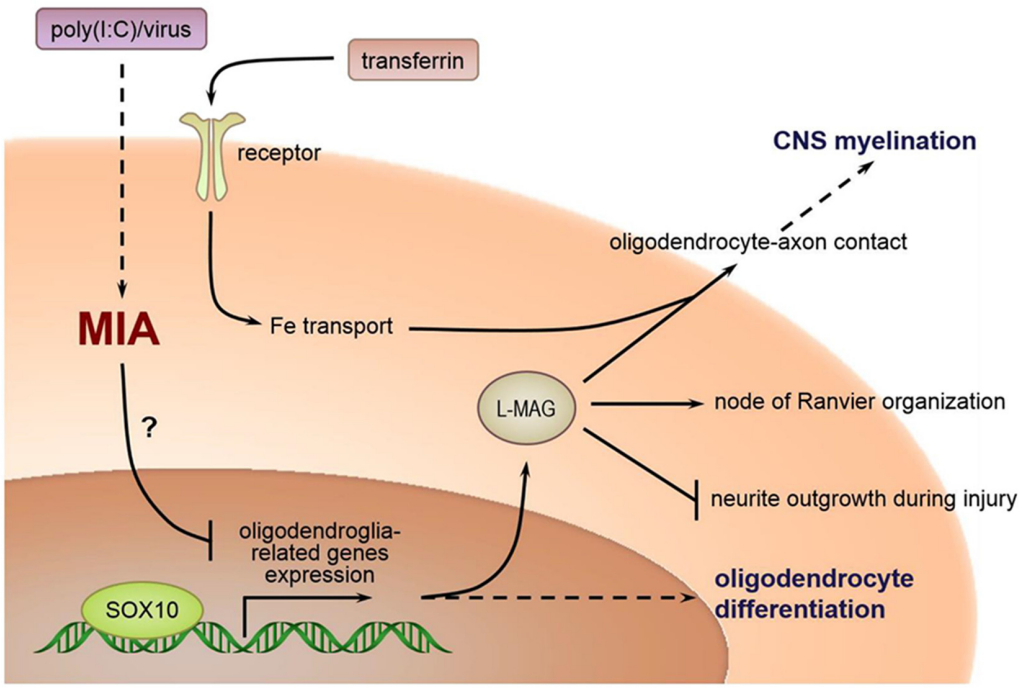

FIGURE 10 | Relations between MIA during pregnancy and selected oligodendroglia-related genes involved in myelination.

the cerebella of mouse offspring (Fatemi et al., 2009), and compromised their white matter integrity as measured by diffusion tensor MRI, respectively (Fatemi et al., 2008). To our best knowledge, our present study presents the first evidence that prenatal poly(I:C) challenge precipitates profoundly reduced transcriptional expression of the oligodendroglia-related genes including *SOX10, MAG* and *Tf* in memory-related neural networks in either brain hemisphere of the adult mouse offspring. These molecular changes may underscore the white matter alterations reported in MIA models elsewhere. It is tempting to suggest identification of these molecular markers may provide opportunities for better understanding ASD pathogenesis in the clinical and experimental settings, for which further interrogation is warranted.

The prevalent nature of gene expression changes seen in many brain regions has unexpectedly stretched the scope of this study. As a result, we only chose to focus on describing the effects of poly(I:C)-induced MIA on a few ROIs known

to be involved in learning, memory, and social interaction. For *in situ* hybridization, we examined a typical coronal section (Bregma –1.70 mm) revealing the hippocampus but did not explore some other brain regions deemed important in canonical schizophrenia or autism pathophysiology such as the prefrontal cortex. Similarly, a sagittal section would reveal more information on oligodendroglial markers in anatomical structures relevant to autism, such as the cerebellum. In qRT-PCR, we chose to examine transcript expression patterns separately in the left and right brains, but our findings were restricted by relatively small sample sizes. Differences in tissue sampling methods used in *in situ* hybridization and qRT-PCR mean that their results are coupled to differential spatial resolution and variability. Therefore, qualitative differences seen in histology (e.g., subregions of the hippocampus) may not always be reflected in quantitative differences in qRT-PCR (e.g., whole hippocampus).

Overall, our work is relatively exploratory. It attempted to address the need for specific molecular biomarkers relevant to myelin- or oligodendroglia-related changes in murine MIA models, in particular, that of poly(I:C)-induced MIA in pregnant mice. While previously some of our works supported the utility of C57BL/6N mice in evaluating behavior on social-affective functions (Zhang et al., 2015a,b), we did not include a behavioral assessment component in the current study. For future investigations involving interventional measures, more in-depth behavioral and histological characterization in conjunction with quantitation of new molecular markers related to myelination changes could be an interesting approach.

CONCLUSION

In the current study, prenatal poly(I:C) exposure dramatically altered the spatial distribution and transcript level of oligodendroglial molecular signatures including *SOX10, MAG*, and *Tf* in memory and social interaction-related brain regions including mPFC, hippocampus, amygdala, neocortex, and thalamus, which lends support to the notion that white matter abnormalities have their anatomical substrates at the molecular level in neurodevelopmental disorders such as ASD and schizophrenia. Given that myelination and oligodendroglial function are coupled to synaptic communication, altered expression patterns of oligodendroglia-related genes seem a useful molecular indicator for evaluating myelination status or oligodendroglial function concerning certain cognitive deficits found in schizophrenia or ASD patients. The extensive spatial scope of neural substrates showing altered oligodendroglia-related gene expression agrees with the observation that schizophrenia and ASD are heterogeneous disorders where inter-gray matter miscommunication and white matter disconnectivity co-occur. We believe that further study of prophylactic medicine at the perinatal or postnatal stages to ameliorate or rescue oligodendrocyte dysfunction is warranted, as it may open up new avenues for the prevention of neurodevelopmental or psychiatric disorders.

DATA AVAILABILITY STATEMENT

The datasets analyzed in this article are not publicly available. Requests to access the datasets should be directed to wongnksz@163.com.

ETHICS STATEMENT

The experiments had been reviewed and approved by the Committee on the Use of Live Animals in Teaching and Research at the University of Hong Kong, and every effort had been made to minimize the number of animals used and their suffering.

AUTHOR CONTRIBUTIONS

N-KW, YZ, and AW conceived and designed the experiments. X-FZ, TC, AY, PC, and Y-LX performed the experiments. N-KW, Y-LX, JY, and JX analyzed the imaging data. X-FZ, YZ, and TC performed the statistical analysis. N-KW, X-FZ, YZ, and TC wrote the article. All authors read and approved the final manuscript.

FUNDING

This work was supported in part by an National Natural Science Foundation of China (NSFC) grant (81801318) and a National Key R&D Program grant (2017YFC1310000) of China (X-FZ). Work by N-KW has been supported in part by Special Support Funds of Shenzhen for Introduced High-Level Medical Team grants (ZDSYS201504301534057 and SZSM201512005).

ACKNOWLEDGMENTS

We are thankful to Prof. Grainne M. McAlonan for her valuable insights and comments during this study, and Dr. Qi Li for her support in animal modeling.

SUPPLEMENTARY MATERIAL

The Supplementary Material for this article can be found online at: https://www.frontiersin.org/articles/10.3389/fnmol.2020.00115/full#supplementary-material.

FIGURE S1 | *In situ* hybridization with a *SOX10*-specific probe in the left and right cortical regions of adult mouse offspring. *SOX10* mRNA was detected as dark blue puncta. Several ROIs in the brain of poly(I:C)- or saline-exposed mice were examined, namely, retrosplenial granular cortex (RSG) and retrosplenial dysgranular cortex (RSD; panels **A,B**), the somatosensory cortex (SC; panels **C,D**), auditory cortex (AC; panels **E,F**), and the piriform cortex (PC; panels **G,H**). Results are representative of two independent experiments. cc: corpus callosum. Representative images were acquired at 25× magnification.

FIGURE S2 | *In situ* hybridization with an *L-MAG*-specific probe in the left and right cortical regions of adult mouse offspring. *L-MAG* mRNA was detected as dark blue puncta. Several ROIs in the brain of poly(I:C)- or saline-exposed mice were examined, namely, retrosplenial granular cortex (RSG) and retrosplenial dysgranular cortex (RSD; panels **A,B**), the somatosensory cortex (SC; panels **C,D**), auditory cortex (AC; panels **E,F**), and the piriform cortex (PC; panels **G,H**).

Results are representative of two independent experiments. cc: corpus callosum. Representative images were acquired at 25× magnification.

FIGURE S3 | *In situ* hybridization with a *Tf*-specific probe in the left and right cortical regions of adult mouse offspring. *Tf* mRNA was detected as dark blue puncta. Several ROIs in the brain of poly(I:C)- or saline-exposed mice were examined, namely, retrosplenial granular cortex (RSG) and retrosplenial dysgranular cortex (RSD; panels **A,B**), the somatosensory cortex (SC; panels **C,D**), auditory cortex (AC; panels **E,F**), and the piriform cortex (PC; panels **G,H**). Results are representative of two independent experiments. cc: corpus callosum. Representative images were acquired at 25× magnification.

FIGURE S4 | *In situ* hybridization with a *SOX10*-specific probe in the thalamus and ventral hypothalamus of adult mouse offspring. *SOX10* mRNA was detected as dark blue puncta. Several ROIs in the brain of poly(I:C)- or saline-exposed mice were examined, namely, thalamus (Th; panel **A**), and ventral hypothalamus (VH; panel **B**). Results are representative of two independent experiments. Representative images were acquired at 25× magnification.

FIGURE S5 | *In situ* hybridization with an *L-MAG*-specific probe in the thalamus and ventral hypothalamus of adult mouse offspring. *L-MAG* mRNA was detected as dark blue puncta. Several ROIs in the brain of poly(I:C)- or saline-exposed mice were examined, namely, thalamus (Th; panel **A**), and ventral hypothalamus (VH; panel **B**). Results are representative of two independent experiments. Representative images were acquired at 25× magnification.

FIGURE S6 | *In situ* hybridization with a *Tf*-specific probe in the thalamus and ventral hypothalamus of adult mouse offspring. *Tf* mRNA was detected as dark blue puncta. Several ROIs in the brain of poly(I:C)- or saline-exposed mice were examined, namely, thalamus (Th; panel **A**), and ventral hypothalamus (VH; panel **B**). Results are representative of two independent experiments. Representative images were acquired at 25× magnification.

TABLE S1 | TABLE S1 Primers for generating cDNA templates in molecular cloning.

TABLE S2 | Primers for gene-specific DIG-labeled probes used in in situ hybridization.

REFERENCES

Aberg, K., Saetre, P., Jareborg, N., and Jazin, E. (2006). Human QKI, a potential regulator of mRNA expression of human oligodendrocyte-related genes involved in schizophrenia. *Proc. Natl. Acad. Sci. U S A* 103, 7482–7487. doi: 10.1073/pnas.0601213103

Aoki, Y., Yoncheva, Y. N., Chen, B., Nath, T., Sharp, D., Lazar, M., et al. (2017). Association of white matter structure with autism spectrum disorder and attention-deficit/hyperactivity disorder. *JAMA Psychiatry* 74, 1120–1128. doi: 10.1001/jamapsychiatry.2017.2573

Aylward, E. H., Minshew, N. J., Goldstein, G., Honeycutt, N. A., Augustine, A. M., Yates, K. O., et al. (1999). MRI volumes of amygdala and hippocampus in non-mentally retarded autistic adolescents and adults. *Neurology* 53, 2145–2150. doi: 10.1212/wnl.53.9.2145

Barnea-Goraly, N., Kwon, H., Menon, V., Eliez, S., Lotspeich, L., and Reiss, A. L. (2004). White matter structure in autism: preliminary evidence from diffusion tensor imaging. *Biol. Psychiatry* 55, 323–326. doi: 10.1016/j.biopsych.2003.10.022

Bartzokis, G. (2002). Schizophrenia: breakdown in the well-regulated lifelong process of brain development and maturation. *Neuropsychopharmacology* 27, 672–683. doi: 10.1016/s0893-133x(02)00364-0

Bauman, M., and Kemper, T. L. (1985). Histoanatomic observations of the brain in early infantile autism. *Neurology* 35, 866–874. doi: 10.1212/wnl.35.6.866

Baumann, N., and Pham-Dinh, D. (2001). Biology of oligodendrocyte and myelin in the mammalian central nervous system. *Physiol. Rev.* 81, 871–927. doi: 10.1152/physrev.2001.81.2.871

Boets, B., Van Eylen, L., Sitek, K., Moors, P., Noens, I., Steyaert, J., et al. (2018). Alterations in the inferior longitudinal fasciculus in autism and associations with visual processing: a diffusion-weighted MRI study. *Mol. Autism* 9:10. doi: 10.1186/s13229-018-0188-6

Brambilla, P., Hardan, A., di Nemi, S. U., Perez, J., Soares, J. C., and Barale, F. (2003). Brain anatomy and development in autism: review of structural MRI studies. *Brain Res. Bull.* 61, 557–569. doi: 10.1016/j.brainresbull.2003.06.001

Bridgemohan, C., Cochran, D. M., Howe, Y. J., Pawlowski, K., Zimmerman, A. W., Anderson, G. M., et al. (2019). Investigating potential biomarkers in autism spectrum disorder. *Front. Integr. Neurosci.* 13:31. doi: 10.3389/fnint.2019.00031

Broek, J. A., Guest, P. C., Rahmoune, H., and Bahn, S. (2014). Proteomic analysis of post mortem brain tissue from autism patients: evidence for opposite changes in prefrontal cortex and cerebellum in synaptic connectivity-related proteins. *Mol. Autism* 5:41. doi: 10.1186/2040-2392-5-41

Careaga, M., Murai, T., and Bauman, M. D. (2017). Maternal immune activation and autism spectrum disorder: from rodents to nonhuman and human primates. *Biol. Psychiatry* 81, 391–401. doi: 10.1016/j.biopsych.2016.10.020

Cheung, V., Cheung, C., McAlonan, G. M., Deng, Y., Wong, J. G., Yip, L., et al. (2008). A diffusion tensor imaging study of structural dysconnectivity in never-medicated, first-episode schizophrenia. *Psychol. Med.* 38, 877–885. doi: 10.1017/S0033291707001808

d'Albis, M. A., Guevara, P., Guevara, M., Laidi, C., Boisgontier, J., Sarrazin, S., et al. (2018). Local structural connectivity is associated with social cognition in autism spectrum disorder. *Brain* 141, 3472–3481. doi: 10.1093/brain/awy275

Demetriou, E. A., Lampit, A., Quintana, D. S., Naismith, S. L., Song, Y. J. C., Pye, J. E., et al. (2018). Autism spectrum disorders: a meta-analysis of executive function. *Mol. Psychiatry* 23, 1198–1204. doi: 10.1038/mp.2017.75

Dracheva, S., Davis, K. L., Chin, B., Woo, D. A., Schmeidler, J., and Haroutunian, V. (2006). Myelin-associated mRNA and protein expression deficits in the anterior cingulate cortex and hippocampus in elderly schizophrenia patients. *Neurobiol. Dis.* 21, 531–540. doi: 10.1016/j.nbd.2005.08.012

Drakesmith, M., Dutt, A., Fonville, L., Zammit, S., Reichenberg, A., Evans, C. J., et al. (2016). Mediation of developmental risk factors for psychosis by white matter microstructure in young adults with psychotic experiences. *JAMA Psychiatry* 73, 396–406. doi: 10.1001/jamapsychiatry.2015.3375

Ellison-Wright, I., and Bullmore, E. (2009). Meta-analysis of diffusion tensor imaging studies in schizophrenia. *Schizophr. Res.* 108, 3–10. doi: 10.1016/j.schres.2008.11.021

Escobar Cabrera, O. E., Bongarzone, E. R., Soto, E. F., and Pasquini, J. M. (1994). Single intracerebral injection of apotransferrin in young rats induces increased myelination. *Dev. Neurosci.* 16, 248–254. doi: 10.1159/000112116

Estes, M. L., and McAllister, A. K. (2016). Maternal immune activation: implications for neuropsychiatric disorders. *Science* 353, 772–777. doi: 10.1126/science.aag3194

Fatemi, S. H., Folsom, T. D., Reutiman, T. J., Abu-Odeh, D., Mori, S., Huang, H., et al. (2009). Abnormal expression of myelination genes and alterations in white matter fractional anisotropy following prenatal viral influenza infection at E16 in mice. *Schizophr. Res.* 112, 46–53. doi: 10.1016/j.schres.2009.04.014

Fatemi, S. H., Reutiman, T. J., Folsom, T. D., Huang, H., Oishi, K., Mori, S., et al. (2008). Maternal infection leads to abnormal gene regulation and brain atrophy in mouse offspring: implications for genesis of neurodevelopmental disorders. *Schizophr. Res.* 99, 56–70. doi: 10.1016/j.schres.2007.11.018

Felsky, D., Voineskos, A. N., Lerch, J. P., Nazeri, A., Shaikh, S. A., Rajji, T. K., et al. (2012). Myelin-associated glycoprotein gene and brain morphometry in schizophrenia. *Front. Psychiatry* 3:40. doi: 10.3389/fpsyt.2012.00040

French, L., Gray, C., Leonard, G., Perron, M., Pike, G. B., Richer, L., et al. (2015). Early cannabis use, polygenic risk score for schizophrenia and brain maturation in adolescence. *JAMA Psychiatry* 72, 1002–1011. doi: 10.1001/jamapsychiatry.2015.1131

Fujita, N., Kemper, A., Dupree, J., Nakayasu, H., Bartsch, U., Schachner, M., et al. (1998). The cytoplasmic domain of the large myelin-associated glycoprotein isoform is needed for proper CNS but not peripheral nervous system myelination. *J. Neurosci.* 18, 1970–1978. doi: 10.1523/jneurosci.18-06-01970.1998

Guardia Clausi, M., Pasquini, L. A., Soto, E. F., and Pasquini, J. M. (2010). Apotransferrin-induced recovery after hypoxic/ischaemic injury on myelination. *ASN Neuro* 2:e00048. doi: 10.1042/an20100020

Ha, S., Sohn, I. J., Kim, N., Sim, H. J., and Cheon, K. A. (2015). Characteristics of brains in autism spectrum disorder: structure, function and connectivity across the lifespan. *Exp. Neurobiol.* 24, 273–284. doi: 10.5607/en.2015.24.4.273

Hahamy, A., Behrmann, M., and Malach, R. (2015). The idiosyncratic brain: distortion of spontaneous connectivity patterns in autism spectrum disorder. *Nat. Neurosci.* 18, 302–309. doi: 10.1038/nn.3919

Herbert, M. R., Ziegler, D. A., Deutsch, C. K., O'Brien, L. M., Lange, N., Bakardjiev, A., et al. (2003). Dissociations of cerebral cortex, subcortical and cerebral white matter volumes in autistic boys. *Brain* 126, 1182–1192. doi: 10.1093/brain/awg110

Honea, R., Crow, T. J., Passingham, D., and Mackay, C. E. (2005). Regional deficits in brain volume in schizophrenia: a meta-analysis of voxel-based morphometry studies. *Am. J. Psychiatry* 162, 2233–2245. doi: 10.1176/appi.ajp.162.12.2233

Insel, T. R. (2010). Rethinking schizophrenia. *Nature.* 468, 187–193. doi: 10.1038/nature09552

Iwamoto, K., Bundo, M., Yamada, K., Takao, H., Iwayama-Shigeno, Y., Yoshikawa, T., et al. (2005). DNA methylation status of SOX10 correlates with its downregulation and oligodendrocyte dysfunction in schizophrenia. *J. Neurosci.* 25, 5376–5381. doi: 10.1523/jneurosci.0766-05.2005

Jiang, Q., Ko, W. K. W., Lerner, E. A., Chan, K. M., and Wong, A. O. L. (2008). Grass carp somatolactin: I. Evidence for PACAP induction of somatolactin-α and -β gene expression *via* activation of pituitary PAC-I receptors. *Am. J. Physiol. Endocrinol. Metab.* 295, E463–E476. doi: 10.1152/ajpendo.90385.2008

Jones, E. A., Jang, S. W., Mager, G. M., Chang, L. W., Srinivasan, R., Gokey, N. G., et al. (2007). Interactions of Sox10 and Egr2 in myelin gene regulation. *Neuron Glia Biol.* 3, 377–387. doi: 10.1017/s1740925x08000173

Kato, T., and Iwamoto, K. (2014). Comprehensive DNA methylation and hydroxymethylation analysis in the human brain and its implication in mental disorders. *Neuropharmacology* 8, 133–139. doi: 10.1016/j.neuropharm.2013.12.019

Li, Q., Leung, Y. O., Zhou, I., Ho, L. C., Kong, W., Basil, P., et al. (2015). Dietary supplementation with n-3 fatty acids from weaning limits brain biochemistry and behavioural changes elicited by prenatal exposure to maternal inflammation in the mouse model. *Transl. Psychiatry* 5:e641. doi: 10.1038/tp.2015.126

Maddock, R. J. (1999). The retrosplenial cortex and emotion: new insights from functional neuroimaging of the human brain. *Trends Neurosci.* 22, 310–316. doi: 10.1016/s0166-2236(98)01374-5

Maeno, N., Takahashi, N., Saito, S., Ji, X., Ishihara, R., Aoyama, N., et al. (2007). Association of SOX10 with schizophrenia in the Japanese population. *Psychiatr. Genet.* 17, 227–231. doi: 10.1097/ypg.0b013e3280ae6cd8

McCullumsmith, R. E., Gupta, D., Beneyto, M., Kreger, E., Haroutunian, V., Davis, K. L., et al. (2007). Expression of transcripts for myelination-related genes in the anterior cingulate cortex in schizophrenia. *Schizophr. Res.* 90, 15–27. doi: 10.1016/j.schres.2006.11.017

McGlashan, T. H., and Hoffman, R. E. (2000). Schizophrenia as a disorder of developmentally reduced synaptic connectivity. *Arch. Gen. Psychiatry* 57, 637–648. doi: 10.1001/archpsyc.57.7.637

Meyer, U., Nyffeler, M., Engler, A., Urwyler, A., Schedlowski, M., Knuesel, I., et al. (2006). The time of prenatal immune challenge determines the specificity of inflammation-mediated brain and behavioral pathology. *J. Neurosci.* 26, 4752–4762. doi: 10.1523/jneurosci.0099-06.2006

Mueller, F. S., Polesel, M., Richetto, J., Meyer, U., and Weber-Stadlbauer, U. (2018). Mouse models of maternal immune activation: mind your caging system! *Brain Behav. Immun.* 7, 643–660. doi: 10.1016/j.bbi.2018.07.014

Nacewicz, B. M., Dalton, K. M., Johnstone, T., Long, M. T., McAuliff, E. M., Oakes, T. R., et al. (2006). Amygdala volume and nonverbal social impairment in adolescent and adult males with autism. *Arch. Gen. Psychiatry* 63, 1417–1428. doi: 10.1001/archpsyc.63.12.1417

Najjar, S., and Pearlman, D. M. (2015). Neuroinflammation and white matter pathology in schizophrenia: systematic review. *Schizophr. Res.* 161, 102–112. doi: 10.1016/j.schres.2014.04.041

Nickel, K., Tebartz van Elst, L., Perlov, E., Endres, D., Muller, G. T., Riedel, A., et al. (2017). Altered white matter integrity in adults with autism spectrum disorder and an IQ >100: a diffusion tensor imaging study. *Acta Psychiatr. Scand.* 135, 573–583. doi: 10.1111/acps.12731

Olney, J. W., Newcomer, J. W., and Farber, N. B. (1999). NMDA receptor hypofunction model of schizophrenia. *J. Psychiatr. Res.* 33, 523–533. doi: 10.1016/s0022-3956(99)00029-1

Park, S., and Holzman, P. S. (1992). Schizophrenics show spatial working memory deficits. *Arch. Gen. Psychiatry* 49, 975–982. doi: 10.1001/archpsyc.1992.01820120063009

Quarles, R. H. (2007). Myelin-associated glycoprotein (MAG): past, present and beyond. *J. Neurochem.* 100, 1431–1448. doi: 10.1111/j.1471-4159.2006.04319.x

Rojas, D. C., Smith, J. A., Benkers, T. L., Camou, S. L., Reite, M. L., and Rogers, S. J. (2004). Hippocampus and amygdala volumes in parents of children with autistic disorder. *Am. J. Psychiatry* 161, 2038–2044. doi: 10.1176/appi.ajp.161.11.2038

Salloum-Asfar, S., Satheesh, N. J., and Abdulla, S. A. (2019). Circulating miRNAs, small but promising biomarkers for autism spectrum disorder. *Front. Mol. Neurosci.* 12:253. doi: 10.3389/fnmol.2019.00253

Schnaar, R. L., and Lopez, P. H. (2009). Myelin-associated glycoprotein and its axonal receptors. *J. Neurosci. Res.* 87, 3267–3276. doi: 10.1002/jnr.21992

Sforazzini, F., Bertero, A., Dodero, L., David, G., Galbusera, A., Scattoni, M. L., et al. (2016). Altered functional connectivity networks in acallosal and socially impaired BTBR mice. *Brain Struct. Funct.* 221, 941–954. doi: 10.1007/s00429-014-0948-9

Sharma, A., Wolf, D. H., Ciric, R., Kable, J. W., Moore, T. M., Vandekar, S. N., et al. (2017). Common dimensional reward deficits across mood and psychotic disorders: a connectome-wide association study. *Am. J. Psychiatry* 174, 657–666. doi: 10.1176/appi.ajp.2016.16070774

Shen, L., Liu, X., Zhang, H., Lin, J., Feng, C., and Iqbal, J. (2020). Biomarkers in autism spectrum disorders: current progress. *Clin. Chim. Acta* 50, 41–54. doi: 10.1016/j.cca.2019.12.009

Sigmundsson, T., Suckling, J., Maier, M., Williams, S., Bullmore, E., Greenwood, K., et al. (2001). Structural abnormalities in frontal, temporal, and limbic regions and interconnecting white matter tracts in schizophrenic patients with prominent negative symptoms. *Am. J. Psychiatry* 158, 234–243. doi: 10.1176/appi.ajp.158.2.234

Sokolov, B. P. (2007). Oligodendroglial abnormalities in schizophrenia, mood disorders and substance abuse. Comorbidity, shared traits, or molecular phenocopies? *Int. J. Neuropsychopharmacol.* 10, 547–555. doi: 10.1017/s1461145706007322

Stolt, C. C., Rehberg, S., Ader, M., Lommes, P., Riethmacher, D., Schachner, M., et al. (2002). Terminal differentiation of myelin-forming oligodendrocytes depends on the transcription factor Sox10. *Genes Dev.* 16, 165–170. doi: 10.1101/gad.215802

Swanson, M. R., and Hazlett, H. C. (2019). White matter as a monitoring biomarker for neurodevelopmental disorder intervention studies. *J. Neurodev. Disord.* 11:33. doi: 10.1186/s11689-019-9295-8

Tamminga, C. A., Stan, A. D., and Wagner, A. D. (2010). The hippocampal formation in schizophrenia. *Am. J. Psychiatry* 167, 1178–1193. doi: 10.1176/appi.ajp.2010.09081187

Tian, Y., Wang, L., Jia, M., Lu, T., Ruan, Y., Wu, Z., et al. (2017). Association of oligodendrocytes differentiation regulator gene DUSP15 with autism. *World J. Biol. Psychiatry* 18, 143–150. doi: 10.1080/15622975.2016.1178395

Tkachev, D., Mimmack, M. L., Ryan, M. M., Wayland, M., Freeman, T., Jones, P. B., et al. (2003). Oligodendrocyte dysfunction in schizophrenia and bipolar disorder. *Lancet* 362, 798–805. doi: 10.1016/S0140-6736(03)14289-4

Uhlhaas, P. J., and Singer, W. (2010). Abnormal neural oscillations and synchrony in schizophrenia. *Nat. Rev. Neurosci.* 11, 100–113. doi: 10.1038/nrn2774

van den Heuvel, M. P., de Lange, S. C., Zalesky, A., Seguin, C., Yeo, B. T. T., and Schmidt, R. (2017). Proportional thresholding in resting-state fMRI functional connectivity networks and consequences for patient-control connectome studies: issues and recommendations. *NeuroImage* 15, 437–449. doi: 10.1016/j.neuroimage.2017.02.005

van den Heuvel, M. P., Scholtens, L. H., de Reus, M. A., and Kahn, R. S. (2016). Associated microscale spine density and macroscale connectivity disruptions in schizophrenia. *Biol. Psychiatry* 80, 293–301. doi: 10.1016/j.biopsych.2015.10.005

Vann, S. D., Aggleton, J. P., and Maguire, E. A. (2009). What does the retrosplenial cortex do? *Nat. Rev. Neurosci.* 10, 792–802. doi: 10.1038/nrn2733

Vikhreva, O. V., Rakhmanova, V. I., Orlovskaya, D. D., and Uranova, N. A. (2016). Ultrastructural alterations of oligodendrocytes in prefrontal white matter in schizophrenia: a post-mortem morphometric study. *Schizophr. Res.* 177, 28–36. doi: 10.1016/j.schres.2016.04.023

Wei, R., Li, Q., Lam, S., Leung, J., Cheung, C., Zhang, X., et al. (2016). A single low dose of valproic acid in late prenatal life alters postnatal behavior and glutamic acid decarboxylase levels in the mouse. *Behav. Brain Res.* 31, 190–198. doi: 10.1016/j.bbr.2016.08.006

Wong, M. K. H., Sze, K. H., Chen, T., Cho, C. K., Law, H. C. H., Chu, I. K., et al. (2013). Goldfish spexin: solution structure and novel function as a satiety factor in feeding control. *Am. J. Physiol. Endocrinol. Metab.* 305, E348–E366. doi: 10.1152/ajpendo.00141.2013

Wu, Y., Qi, F., Song, D., He, Z., Zuo, Z., Yang, Y., et al. (2018). Prenatal influenza vaccination rescues impairments of social behavior and lamination in a mouse model of autism. *J. Neuroinflammation* 15:228. doi: 10.1186/s12974-018-1252-z

Yin, X., Crawford, T. O., Griffin, J. W., Tu, P., Lee, V. M., Li, C., et al. (1998). Myelin-associated glycoprotein is a myelin signal that modulates the caliber of myelinated axons. *J. Neurosci.* 18, 1953–1962. doi: 10.1523/jneurosci.18-06-01953.1998

Yuan, Q., Yang, F., Xiao, Y., Tan, S., Husain, N., Ren, M., et al. (2016). Regulation of brain-derived neurotrophic factor exocytosis and γ-aminobutyric acidergic interneuron synapse by the schizophrenia susceptibility gene dysbindin-1. *Biol. Psychiatry* 80, 312–322. doi: 10.1016/j.biopsych.2015.08.019

Zalesky, A., Pantelis, C., Cropley, V., Fornito, A., Cocchi, L., McAdams, H., et al. (2015). Delayed development of brain connectivity in adolescents with schizophrenia and their unaffected siblings. *JAMA Psychiatry* 72, 900–908. doi: 10.1001/jamapsychiatry.2015.0226

Zhang, X., Li, Q., Wong, N.-K., Zhang, M., Wang, W., Bu, B., et al. (2015a). Behaviour and prefrontal protein differences in C57BL/6N and 129 X1/SvJ mice. *Brain Res. Bull.* 116, 16–24. doi: 10.1016/j.brainresbull.2015.05.003

Zhang, X., Li, Q., Zhang, M., Lam, S., Sham, P. C., Bu, B., et al. (2015b). The effect of oxytocin on social and non-social behaviour and striatal protein expression in C57BL/6N mice. *PLoS One* 10:e0145638. doi: 10.1371/journal.pone.0145638

Zoghbi, H. Y., and Bear, M. F. (2012). Synaptic dysfunction in neurodevelopmental disorders associated with autism and intellectual disabilities. *Cold Spring Harb. Perspect. Biol.* 4:a009886. doi: 10.1101/cshperspect.a009886

Conflict of Interest: The authors declare that the research was conducted in the absence of any commercial or financial relationships that could be construed as a potential conflict of interest.

frontiers in Integrative Neuroscience

REVIEW
published: 24 July 2020
doi: 10.3389/fnint.2020.00037

Key Mechanisms and Potential Targets of the NLRP3 Inflammasome in Neurodegenerative Diseases

Yadi Guan[1,2] *and Fang Han*[1]*

[1]PTSD Laboratory, Department of Histology and Embryology, Basic Medical University, China Medical University, Shenyang, China, [2]Department of Gastroenterology, Shengjing Hospital of China Medical University, Shenyang, China

Neurodegenerative diseases are neuronal disorders characterized by the loss of a large number of neurons in the human brain. Innate immunity-mediated neuroinflammation actively contributes to the onset and progression of neurodegenerative diseases. Inflammasomes are involved in the progression of the innate immune response and are responsible for the maturation of caspase-1 and inflammatory cytokines during neuroinflammation. The nucleotide-binding oligomerization domain leucine-rich repeat and pyrin domain-containing protein 3 (NLRP3) inflammasome, which is one of the most intensively investigated inflammasomes, has been reported to play a key role in neurodegenerative diseases. Here, we reviewed the mechanisms, role, and latest developments regarding the NLRP3 inflammasome with respect to three neurodegenerative diseases: Alzheimer's disease (AD), Parkinson's disease (PD), and amyotrophic lateral sclerosis (ALS). Patient and animal model studies have found that abnormal protein aggregation of Aβ, synuclein, or copper–zinc superoxide dismutase-1 (SOD1), which are the main proteins expressed in the three diseases, respectively, can activate microglial cells, induce increased interleukin-1β (IL-1β) release, and activate the NLRP3 pathway, leading to neurodegeneration. In contrast, a deficiency of the components of the NLRP3 pathway may inhibit Aβ, synuclein, or SOD1-induced microglial activation. These studies indicate a positive correlation between NLRP3 levels and abnormal protein aggregation. However, in the case of ALS, not only microglia but also

OPEN ACCESS

Edited by:
Weiwen Wang,
Institute of Psychology (CAS), China

Reviewed by:
Zili You,
University of Electronic Science and Technology of China, China
Sa Li,
University of Manitoba, Canada
Zhang Weining,
Jiangsu University, China

***Correspondence:**
Fang Han
fhan@cmu.edu.cn

Received: *14 April 2020*
Accepted: *08 June 2020*
Published: *24 July 2020*

Citation:
Guan Y and Han F (2020) Key Mechanisms and Potential Targets of the NLRP3 Inflammasome in Neurodegenerative Diseases. Front. Integr. Neurosci. 14:37. doi: 10.3389/fnint.2020.00037

Abbreviations: NLRP3, nucleotide-binding oligomerization domain leucine-rich repeat and pyrin domain-containing protein 3; AD, Alzheimer's disease; PD, Parkinson's disease; ALS, amyotrophic lateral sclerosis; α-syn, α-synuclein; SOD1, superoxide dismutase-1; IL-1β, interleukin-1β; CNS, central nervous system; PAMPs, pathogen-associated molecular patterns; DAMPs, danger-associated molecular patterns; ASC, apoptosis-associated speck-like protein containing a caspase recruitment domain; NLRs, nucleotide-binding domain and leucine-rich repeat containing receptors; ALRs, absent in melanoma-like receptors; PYD, pyrin domain; CARD, caspase recruitment domain; AIM2, absent in melanoma 2; NACHT, nucleotide-binding and oligomerization domain; LRR, leucine-rich repeat domain; TLRs, toll-like receptors; PRR, pattern recognition receptor; GSDMD, gasdermin D; LPS, lipopolysaccharide; Aβ, amyloid-β; NFTs, neurofibrillary tangles; TXNIP, thioredoxin-interacting protein; SN, substantia nigra; UPDRS, Unified Parkinson's Disease Rating Scale; MPTP, 1-methyl-4-phenyl-1,2,3,6-tetrahydropyridine; 6-OHDA, 6-hydroxydopamine; PPARβ/δ, peroxisome proliferator-activated receptor β/δ; ROS, reactive oxygen species.

astrocytes express increased NLRP3 levels and contribute to activation of the NLRP3 pathway. In addition, in this review article, we also focus on the therapeutic implications of targeting novel inhibitors of the NLRP3 inflammasome or of novel drugs that mediate the NLRP3 pathway, which could play a role *via* NLRP3 in the treatment of neurodegenerative diseases.

Keywords: NLRP3 inflammasome, Alzheimer's disease, Parkinson's disease, amyotrophic lateral sclerosis, neurodegenerative disease

INTRODUCTION

Neurodegenerative diseases are neuronal disorders characterized by the loss of a large number of neurons in the human brain, for example, Alzheimer's disease (AD), Parkinson's disease (PD), amyotrophic lateral sclerosis (ALS), and Huntington's disease. Although the location and etiology of these diseases differ, they share the common characteristic of neurodegeneration. AD and PD mainly occur in middle and old ages, so as the population ages, the incidences of AD and PD are increasing. It is generally believed that the prevalence of dementia in the population over 65 years old is 4% and that the annual incidence rate is 0.6% to 1.2%. The prevalence of PD is second only to that of AD, with PD mainly occurring in those of middle age or older at a prevalence of 2% in the population over 65 years old. However, Huntington's disease and ALS can occur in patients of different ages, and there is no cure available for these diseases. One of the pathological hallmarks of neurodegenerative diseases is the aggregation of abnormal protein in the central nervous system (CNS). However, innate immunity-mediated neuroinflammation actively contributes to the onset and progression of neurodegenerative diseases (Labzin et al., 2018). Furthermore, inflammasomes have an important role to play in neuroinflammation and in neurodegenerative diseases (Heneka et al., 2013).

Inflammasomes are multiprotein complexes mainly located in the CNS, where they are found in immune cells, neural cells, microglia, and astrocytes (Freeman et al., 2017; Heneka et al., 2018; Song et al., 2018). They are integral parts of the innate immune response and are responsible for detecting and eliminating pathogen-associated molecular patterns (PAMPs), as well as danger-associated molecular patterns (DAMPs), subsequently secreting proinflammatory cytokines (Martinon et al., 2002). Various inflammasomes play critical roles in neurodegenerative diseases, especially the nucleotide-binding oligomerization domain leucine-rich repeat and pyrin domain-containing (NLRP) 3 inflammasome. The NLRP3 inflammasome can be activated by the abnormal protein aggregation that occurs in neurodegenerative diseases (Heneka et al., 2013; Wang et al., 2020). The resulting overexpression of proinflammatory cytokines can aggravate the chronic inflammatory response and pyroptosis in the CNS (Voet et al., 2019; Haque et al., 2020).

In this review article, we discuss the latest research developments regarding the NLRP3 inflammasome; its role in AD, PD, and ALS; and the therapeutic implications of targeting the NLRP3 inflammasome.

STRUCTURES AND ACTIVATION OF THE NLRP3 INFLAMMASOME

The components of inflammasomes consist of sensors, the apoptosis-associated speck-like protein containing a caspase recruitment domain (ASC) protein, and procaspase-1. The sensors, which can detect PAMPs, DAMPs, and cytosolic double-stranded DNA, are classified into three types: nucleotide-binding domain and leucine-rich repeat-containing receptors (NLRs); absent in melanoma-like receptors (ALRs); and pyrin (Dubois et al., 2016). ASC links the pyrin domain (PYD) of the NLR, ALR, or pyrin to the caspase recruitment domain (CARD) of procaspase-1 (Lang et al., 2018; Voet et al., 2019). NLRP1, NLRP2, NLRP3, NLRP6, NLRP7, NLRP12, and NLR family CARD domain-containing 4 (NLRC4) all belong to the NLR family (Lamkanfi and Dixit, 2014; Lenart et al., 2016), while absent in melanoma 2 (AIM2) is a well-characterized ALR from a protein family containing four members in humans (Wang and Yin, 2017).

The NLRP3 inflammasome is one of the most intensively investigated inflammasomes and plays a vital role in innate immunity. It consists of an amino-terminal PYD, a central nucleotide-binding and oligomerization domain (NACHT), and a C-terminal leucine-rich repeat domain (LRR; Franchi et al., 2009). After the PYD of NLRP3 interacts with the PYD of ASC, the NLRP3 inflammasome is assembled and attracts caspase-1. The activation of the NLRP3 inflammasome requires a two-step process, comprising priming and then activation. Firstly, cells need to activate the nuclear factor-kappa B (NF-κB) pathway to upregulate the expression of NLRP3, caspase-1, and pro-interleukin-1β (pro-IL-1β), through the stimulation of toll-like receptors (TLRs; Toma et al., 2010; Qiao et al., 2012). Once primed, the NLRP3 complex is activated by multiple stimuli, including ionic flux, extracellular ATP, reactive oxygen species (ROS), and lysosomal rupture (Muñoz-Planillo et al., 2013; Minutoli et al., 2016; Li R. et al., 2018; Kelley et al., 2019).

There are two types of signaling pathways that activate the NLRP3 inflammasome: the canonical and noncanonical signaling pathways (Xiang et al., 2020). The canonical signaling pathway depends on caspase-1 and involves inflammasome complexes detecting pattern recognition receptor (PRR) proteins and inducing recruitment of procaspase-1. Procaspase-1 recruitment causes proximity-induced oligomerization and autoactivation, and release of active caspase-1 fragments (Voet et al., 2019). Consequently, caspase-1 cleaves biologically inactive pro-IL-1β and pro-IL-18 into the mature inflammatory

cytokines IL-1β and IL-18, respectively (Akita et al., 1997; Rano et al., 1997). Caspase-1 also activates gasdermin D (GSDMD), which translocates to the plasma membrane and forms pores. Then IL-1β and IL-18 are transferred from the cytoplasm to the extracellular space through these pores, inducing a proinflammatory form of cell death known as pyroptosis, which exerts an inflammatory effect to cause further damage (Haque et al., 2020; Liang et al., 2020).

The noncanonical signal pathway is mainly dependent on mouse caspase-11 (of which caspase-4 and caspase-5 are the human counterparts). The noncanonical inflammasome is activated by lipopolysaccharide (LPS) in the cytosol released from gram-negative bacteria, such as *Escherichia coli*, *Citrobacter rodentium*, and *Vibrio cholera* (Hagar et al., 2013). The CARD motif of pro-caspase-11 (pro-caspase-4/-5) directly interacts with the lipid A tail of intracellular LPS (Yi, 2017), whereas the mature caspase-11 can induce pyroptosis and secretion of proinflammatory cytokines. Activation of caspase-11 in the noncanonical inflammasome can also induce activation of the canonical NLRP3 inflammasome, a process that is termed "noncanonical NLRP3 inflammasome activation" (Pellegrini et al., 2017).

ROLE OF NLRP3 IN ALZHEIMER'S DISEASE

AD is mainly caused by the accumulation of amyloid-β (Aβ) plaques and neurofibrillary tangles (NFTs) in the brain, involving the increased production, oligomerization, and aggregation of Aβ peptides cleaved from the amyloid β-precursor protein (APP) by the β- and γ-secretase complexes. Aβ is the main component of extracellular senile plaques, which can cause neurotoxicity in AD (Hardy and Selkoe, 2002), triggering neurodegeneration and apoptosis, and leading to memory loss. In the past 15 years, numerous studies have focused on the role of the NLRP3 inflammasome in mediating neuroinflammation during the pathogenesis of AD. During this time spent studying the association between the NLRP3 inflammasome and AD, there have been two clear phases of research. Before 2013, most articles examined the role and regulatory pathway of NLRP3 in AD. From 2013 onwards, published articles have focused more on the therapeutic implication of targets and inhibitors of NLRP3 in AD.

Studies based on clinical data and animal experiments have both found that Aβ deposits can cause inflammasome activation in AD. Aβ activates microglial cells to produce IL-1β, which is a major outcome of NLRP3 inflammasome activation (Lamkanfi and Dixit, 2010; Lamkanfi, 2011). Levels of IL-1β level are significantly increased in the brain tissue, cerebrospinal fluid, and peripheral blood of AD patients (Tschopp and Schroder, 2010). Results from AD transgenic mice with Aβ treatment show that they also express high levels of caspase-1 and IL-1β in their brain tissue (Lue et al., 2001; Halle et al., 2008; Heneka et al., 2013). Microglia express higher levels of IL-1β especially around Aβ plaques (Apelt and Schliebs, 2001; Martinon et al., 2006). This overexpression of IL-1β can aggravate the chronic inflammatory response in the CNS (Meyer-Luehmann et al., 2008). Some additional elements such as particulate matter (PM) 2.5 or chronic cerebral hypoperfusion can accelerate the activation of the NLRP3 inflammasome and enhance inflammatory responses and neuronal damage in an AD model (Wang et al., 2018; Shang et al., 2019). Conversely, in an AD mouse model, inhibitors of NLRP3 or caspase-1 have been shown to significantly enhance the ability of microglia to clear Aβ deposits, reduce Aβ deposition, and improve cognitive impairment and hyperactive behavior (Heneka et al., 2013; Dempsey et al., 2017).

Furthermore, some studies have found that IL-1β can induce tau protein phosphorylation in the cortex of AD rats (Murakami et al., 2012). Thioredoxin-interacting protein (TXNIP) is an endogenous regulator of redox/glucose-induced stress and inflammation. Overexpression of TXNIP and its colocalization with IL-1β have been found near Aβ plaques and p-tau in the brains of AD patients (Li et al., 2019). The effects of inhibitors of caspase-1 or NLRP3 on Aβ deposits and behaviors in an AD model are reduced by decreasing the level of microglial pyroptosis. These findings suggest that NLRP3 and IL-1β play important roles in the pathophysiology of AD by regulating the pyroptosis, tau, or TXNIP pathways.

In general, in the AD brain, microglia phagocytose the increased amounts of Aβ and cause lysosomal damage. Disruption of lysosomes causes cytosolic release of cathepsin B, which is an endogenous signal for the NLRP3 inflammasome (Halle et al., 2008). NLRP3 activated by Aβ can induce ever-increasing production of IL-1β, promote "downstream" microglial synthesis, and release proinflammatory cytokines, and potentially neurotoxic factors, into the surrounding brain tissue (Heneka et al., 2013). These cytokines and cytotoxins further influence surrounding tissues and amplify the neurotoxic effects of Aβ.

Recently, studies have found that a number of drugs, such as donepezil, rivastigmine, and memantine, only partially improve cognitive and memory decline in patients with AD but do not fundamentally block or reverse the pathological changes resulting from the disease. Therefore, finding drugs that can reverse the development of AD is key to its treatment, with anti-inflammatory drugs potentially providing new possibilities for the treatment of AD. Although nonsteroidal anti-inflammatory drugs are effective in the treatment of AD model rats, their clinic application is limited owing to obvious side effects on the digestive system during the clinical treatment of AD (Wang et al., 2015). However, a large number of studies have clearly and uniformly concluded that the expression of Aβ deposits causes inflammasome activation, including activation of NLRPs and release of IL-1β in AD. Moreover, inhibition of NLRP3 can significantly inhibit amyloidosis and neuropathy and ameliorate cognitive behavior impairment in AD (Heneka et al., 2013; Dempsey et al., 2017). These studies reveal the possible roles of the NLRP3 inflammasome in the pathogenesis of AD and offer the possibility that an NLRP3 inhibitor could become a potential molecular target for improving AD-related symptoms and slowing AD progression at the neuroinflammatory level.

A few NLRP3 inhibitors have already been produced, and their roles in AD have been investigated in disease models. MCC950 is a novel type of NLRP3 inhibitor that specifically inhibits the activation of NLRP3 in macrophages by inhibiting NLRP3-induced ASC oligomerization. *In vivo* experiments have shown that MCC950 significantly reduces the production of IL-1β/IL-18 and reduces the severity of disease in experimental autoimmune encephalomyelitis mice. MCC950 reduces the accumulation of Aβ in brain tissue and reduces the behavioral abnormalities of amyloid precursor protein (APP)/presenilin-1 (PS-1) transgenic mice (Dempsey et al., 2017; Mao et al., 2017). JC-124, a rationally designed NLRP3 inflammasome inhibitor, decreases levels of Aβ deposition and of soluble and insoluble Aβ1–42 in the brains of CRND8 transgenic mice with AD-related deficits. The purinergic 2 × 7 (P2 × 7) receptor antagonist, which is an inhibitor of the P2 × 7/NLRP3/caspase-1 pathway in microglia, might exert an anti-neuroinflammatory effect and be applicable for treating early-stage AD (Thawkar and Kaur, 2019).

Besides NLRP3 inhibitors, a number of novel anti-inflammatory and anti-allergy drugs might contribute to the treatment of AD *via* the NLRP3 pathway. OLT1177 is a novel drug for treating arthritis, which reduces neutrophil infiltration into the peripheral blood, reduces joint swelling, and inhibits IL-1 secretion in animal models of arthritis (Marchetti et al., 2018b). *In vitro* experiments suggest that OLT1177 inhibits the activation of NLRP3-mediated inflammation. Results from *in vivo* tests suggest that OLT1177 reduces the activity of caspase-1 and inhibits the production of IL-1 by direct binding to NLRP3 and inhibiting ATPase activity (Marchetti et al., 2018a,b). Meanwhile, tranilast is an anti-allergy drug that also has an anti-inflammatory effect and inhibits IgE-induced histamine secretion from mast cells (Darakhshan and Pour, 2015). Tranilast is a specific NLRP3 inhibitor that directly binds to the intermediate domain of NLRP3 and inhibits the oligomerization of ASC (Huang et al., 2018). *In vivo* experiments have also corroborated the preventive and therapeutic effects of tranilast on NLRP3 inflammation-related diseases (Huang et al., 2018).

Recently, some studies have shown that Chinese traditional medicines have advantages for the treatment of AD because of their multitarget pharmacological activities. Among these medicines for AD treatment, a number play immunomodulative or anti-inflammatory roles in treating AD, including icariin, rhodiola, poria cocos, total glycosides of Radix Paeoniae Alba, atractylodes, ginseng, and yuanzhi. Recent studies have found that the effects of these medicine are mediated through NLRP3; for example, the protective effect of *Epimedii folium* and Curculiginis Rhizoma on AD has been regulated by the inhibitions of the NF-κB/mitogen-activated protein kinase (MAPK) pathway and the NLRP3 inflammasome (Lan et al., 2017). Meanwhile, high-dose modified buwang-san ameliorates learning and memory deficits and attenuates neuroinflammation in the hippocampus of an AD mouse model by inhibiting the expression of NLRP3, caspase-1, and IL-1 (HE Ling-Ling et al., 2020). In addition, electroacupuncture, on the basis of the theory of traditional Chinese medicine, may improve spatial learning/memory and inhibit the inflammatory reaction in an animal model of AD by reducing the expression of IL-1β and NLRP3 inflammasome-related proteins (Jiang et al., 2018).

ROLE OF NLRP3 IN PARKINSON'S DISEASE

PD is an age-related neurodegenerative disorder characterized by progressive degeneration of dopaminergic (DA) neurons in the substantia nigra (SN) and accumulation of Lewy bodies, which are constituted of fibrillar α-synuclein (α-syn; Codolo et al., 2013; Petrucci et al., 2014). Numerous recent studies have indicated that inflammasomes play an important role in the progression of PD.

Research indicates that NLRP3, ASC, caspase-1, and IL-1β are increased in the peripheral blood mononuclear cells and plasma of PD patients compared with those of age-matched healthy controls (Zhou et al., 2016; Chatterjee et al., 2020; Fan et al., 2020). Levels of IL-1β in plasma have a positive correlation with the Hoehn and Yahr staging scale and Unified Parkinson's disease Rating Scale (UPDRS) part III scores (Fan et al., 2020). Both IL-1β and IL-18 levels were found to be higher in the cerebrospinal fluid of PD patients than in that of control subjects (Zhang et al., 2016). Concentrations of IL-1β in the striatal regions, of cleaved caspase-1 and ASC in the SN, and of caspase-1 in mesencephalon were significantly higher in parkinsonian patients compared with normal group (Mogi et al., 1994; Gordon et al., 2018; von Herrmann et al., 2018). High mRNA and protein expression levels of NLRP3 inflammasome components were observed in LPS-, 6-hydroxydopamine- (6-OHDA), MPTP-, and MPTP/p-induced PD rats (Mao et al., 2017; Qiao et al., 2018). NLRP3 deficiency has been shown to alleviate motor dysfunction and loss of DA neurons in MPTP-treated mice (Lee et al., 2019). MPTP/p treatment elevates expression of caspase-1 in the mouse midbrain, whereas caspase-1 knockout ameliorates DA neuronal loss and dyskinesia induced by MPTP/p (Qiao et al., 2017). Inhibiting the downstream pathway of the NLRP3/caspase-1/IL-1β axis using Ac-YVAD-CMK, a caspase-1 inhibitor, improves the number of DA neurons in the SN and alleviates symptoms in both LPS- and 6-OHDA-induced PD rats (Mao et al., 2017). Furthermore, administration of IL-1 receptor antagonist (IL-1Ra) attenuates MPTP-induced PD phenotypes in mice (Lee et al., 2019). Therefore, these studies show that NLRP3 inflammasome activation is involved in the pathogenesis of PD.

The histopathological hallmark of PD is Lewy bodies, which are mainly composed of fibrillar aggregates of α-syn, is a presynaptic protein, which plays a crucial role in the pathogenesis of PD. Both oligomers and phosphorylated α-syn in the peripheral blood of PD patients have been shown to be significantly elevated (Fan et al., 2020). A number of studies have revealed a strong association between α-syn and the NLRP3 pathway. Plasma α-syn levels show a positive correlation with both UPDRS part III scores, and plasma NLRP3 and IL-1β levels (Chatterjee et al., 2020; Fan et al., 2020). Briefly, fibrillar α-syn induces NLRP3-caspase-1 complex activation followed by secretion of IL-1β in peripheral blood mononuclear cells, monocytes, microglia,

and astrocytes (Chatterjee et al., 2020; Wang et al., 2020), with this proinflammatory cytokine further influencing brain tissue and increasing the inflammatory response. Caspase-1 then causes the truncation and aggregation of α-syn, and α-syn enters microglial cells in an endocytosis-dependent manner and subsequently activates two important innate receptors in the TLR2 (TLR4)/NF-κB and NLRP3/caspase-1 pathways (Gustot et al., 2015; Fan et al., 2016; Zhou et al., 2016). The truncation-induced aggregation of α-syn has been shown to be toxic to neuronal cultures (Wang et al., 2016). Caspase-1 deficiency significantly inhibits α-syn-induced microglial activation and IL-1β production (Zhou et al., 2016).

Other elements and factors also affect the activation of α-syn by the inflammasome: (1) fyn, a nonreceptor Src family tyrosine kinase, contributes to α-syn-induced NLRP3 inflammasome priming *via* PKCδ-mediated NF-κB activation (Panicker et al., 2019); (2) autophagy also participates in α-syn-induced neuroinflammation, with α-syn significantly increasing the autophagy-associated molecule Atg5, and the autophagy inhibitor 3-MA inhibiting α-syn-mediated activation of NLRP3/caspase-1/IL-1β (Wang et al., 2020); and (3) microRNAs, which have been recently recognized as crucial regulators of inflammasomes in PD models. MicroRNA-30e (miR-30e) ameliorates neuroinflammation in the MPTP model of PD by directly targeting NLRP3 and inhibiting the activation of the NLRP3 inflammasome (Li D. et al., 2018). MicroRNA-135b (miR-135b) plays a protective role in the MPP+-induced PD model *in vitro via* the inhibition of forkhead Box 1 (FOXO1)/NLRP3/caspase-1-mediated pyroptosis (Zeng et al., 2019). NLRP3 is a target gene of microRNA-7 (miR-7), with injection of miR-7 mimics into mouse striatum notably suppressing NLRP3 inflammasome activation and attenuating DA neuron degeneration in MPTP-induced PD model mice (Zhou et al., 2016). These microRNAs might therefore be effective therapeutic targets for PD.

A number of exogenous compounds have been shown to alleviative NLRP3 inflammasome-mediated neuroinflammation in PD models. Peroxisome proliferator-activated receptor β/δ (PPARβ/δ) agonists have been shown to suppress the inflammatory reaction and NLRP3 inflammasome activation. Administration of GW501516, a selective PPARβ/δ agonist, *via* intracerebroventricular infusion reduces movement impairment and attenuates DA neurodegeneration in the midbrain of PD mice (Chen et al., 2019). The potent sphingosine-1-phosphate receptor antagonist fingolimod (FTY720) significantly attenuates MPTP-induced PD progression and reduces the loss of DA neurons by inhibiting NLRP3 inflammasome activation (Yao et al., 2019). Traditional Chinese medicines have been proved to possess anti-inflammatory properties in relation to PD. Tenuigenin (a component of *Polygala tenuifolia*), Astragaloside IV (a component of *Astragalus membranaceus*), and bushen-yizhi formula (composed of common Cnidium fruit, tree peony bark, ginseng root, Radix Polygoni Multiflori preparata, Barbary wolfberry fruit, and Fructus Ligustri Lucidi) were shown to significantly ameliorate DA neuron degeneration and alleviate motor impairment by suppressing NLRP3 inflammasome activation in the MPTP mouse model (Fan et al., 2017; Mo et al., 2018; Leng et al., 2019). Based on these findings, medicines and exogenous compounds that target the NLRP3 inflammasome may offer novel therapeutic directions for treating PD.

ROLE OF NLRP3 IN AMYOTROPHIC LATERAL SCLEROSIS

ALS is a progressive neurodegenerative disease caused by the deterioration of motor neurons in the brain and spinal cord. Among the cases of ALS, more than 90% are sporadic ALS (sALS) patients, and 5–10% are familial ALS (fALS) patients. Most fALS cases involve autosomal genetic diseases, such as superoxide dismutase-1 (SOD1) and nerve microfilament defects. Neuroinflammation is believed to significantly contribute to ALS disease progression (Byrne et al., 2011; Hardiman et al., 2011; Morgan and Orrell, 2016). Inflammation-induced neurotoxicity causes the activation of glial cells, including microglia and astrocytes (Philips and Robberecht, 2011), the activation of which leads to IL-1β production, causing further motor neuron death (Meissner et al., 2010). Inflammasome activation and upregulation of NLRP3 and its inflammasome components, caspase-1 and IL-1β, have been observed in ALS patients and in mouse models of ALS (Bellezza et al., 2018), suggesting that the NLRP3 complex plays key roles in ALS pathology (Meissner et al., 2010).

The SOD1G93A mutation was used to create the SOD1G93A mouse (Ince et al., 2011), which is the most widely used model of fALS. This mutation decreases the folding stability of SOD1, inducing the formation of protein aggregates (Philips and Robberecht, 2011) that play an important role in SOD1-mediated pathogenesis of ALS (Alexianu et al., 2001). High levels of caspase-1 and IL-1β in microglia contribute to disease progression in the mouse SOD1G93A model, suggesting a role for microglial NLRP3 in ALS (Alexianu et al., 2001; Philips and Robberecht, 2011). LPS activates caspase-1, leading to an increase in IL-1β release in SOD1G93A mice (Meissner et al., 2010). LPS also increases levels of ROS and nitric oxide, which forms peroxynitrite, leading to protein nitration, and concomitantly increasing protein nitrify in the spinal cord of pre-symptomatic SOD1G93A mice (Sargsyan et al., 2011; Bellezza et al., 2018). The reduction in peroxynitrite levels results in a decrease in caspase-1 activity. These studies indicate that peroxynitrite formation induced by oxidative/nitrosative stress may play a critical role in inflammasome activation and might be exploited as potential therapeutic target for ALS (Zhao et al., 2010; Jo et al., 2016)

However, other results from ALS patients and from SOD1G93A mice indicate that microglia do not express NLRP3. Caspase-1 activation and IL-1β production in microglia have been shown to occur independently of NLRP3 (Meissner et al., 2010). However, microglial NLRP3 upregulation has been observed in another ALS model, the tar DNA-binding protein 43 (TDP-43) mouse, suggesting that the TDP-43 mutant might activate microglial inflammasomes in an NLRP3-dependent manner (Ince et al., 2011). TDP-43 is a major hallmark of the protein aggregates induced by SOD1 in ALS patients (Neumann et al., 2006) and translocates from the nucleus to the cytoplasm as part of the pathogenesis of the disease (Barmada et al., 2010).

Mutations in TDP-43 (e.g., TDP-43Q331K) also lead to fALS (Sreedharan et al., 2008). Transgenic TDP-43Q331K mice have increased microglial activation and motor neuron degeneration (Lee et al., 2018). These studies indicate that pathological ALS proteins activate the microglial NLRP3 inflammasome.

In addition, besides microglia, astrocytes are also capable of contributing to innate immune signaling by increasing their release of cytokines, including IL-1β and IL-18 (Dong and Benveniste, 2001; Kipp et al., 2007; van Neerven et al., 2010). Gene expression profiling of astrocytes suggests that inflammatory mechanisms are activated early in ALS. Spinal cord astrocytes have been identified as the major cell type expressing NLRP3 components. In human ALS tissue, increased levels of NLRP3, ASC, IL-18, and active caspase-1 have been found in astrocytes (Haidet-Phillips et al., 2011; Johann et al., 2015).

In general, these findings suggest that astroglial NLRP3 inflammasome complexes are critically involved in neuroinflammation in ALS. In ALS, microglia and astrocytes switch from a neuroprotective to a proinflammatory phenotype by releasing potentially neurotoxic cytokines.

CONCLUSION AND FUTURE RESEARCH DIRECTION

A number of studies have been focused on understanding the role of the inflammasome in neurodegenerative diseases. Increasing evidence indicates a link between NLRP3 and neurodegenerative diseases, although the exact roles and mechanisms by which the NLRP3 inflammasome regulates neurodegenerative diseases remain unclear and require further confirmation. Most importantly, inhibition of NLRP3 in animal models reduces the inflammatory response, decreases abnormal protein deposition, and corrects behavioral abnormalities associated with neurodegenerative diseases, suggesting the possibility of targeting NLRP3 inflammasome to treat such diseases. However, many important topics still need to be explored, such as how the activation or inhibition of the NLRP3 inflammasome influences neurodegenerative diseases. The solution of such questions is important for studying the pathogenesis of neurodegenerative diseases and for providing more evidence and targets for exploring novel treatments. Despite the fact that inhibition of NLRP3 inflammasome activation has been shown exert beneficial effects in animal models of neurodegenerative diseases, the effectiveness and safety of specific NLRP3 inflammasome inhibitors in patients have yet to be verified in clinical trials.

AUTHOR CONTRIBUTIONS

FH and YG contributed to the conception and organization and wrote the first draft of the manuscript. FH contributed to manuscript revision. All authors approved the submitted version.

FUNDING

This research was supported by grants from the National Natural Science Foundation of China (no. 81571324) and the Science and Technology Plan Project of Liaoning Province, China (no. 2017225011) to FH.

REFERENCES

Akita, K., Ohtsuki, T., Nukada, Y., Tanimoto, T., Namba, M., Okura, T., et al. (1997). Involvement of caspase-1 and caspase-3 in the production and processing of mature human interleukin 18 in monocytic THP.1 cells. *J. Biol. Chem.* 272, 26595–26603. doi: 10.1074/jbc.272.42.26595

Alexianu, M. E., Kozovska, M., and Appel, S. H. (2001). Immune reactivity in a mouse model of familial ALS correlates with disease progression. *Neurology* 57, 1282–1289. doi: 10.1212/wnl.57.7.1282

Apelt, J., and Schliebs, R. (2001). Beta-amyloid-induced glial expression of both pro- and anti-inflammatory cytokines in cerebral cortex of aged transgenic Tg2576 mice with Alzheimer plaque pathology. *Brain Res.* 894, 21–30. doi: 10.1016/s0006-8993(00)03176-0

Barmada, S. J., Skibinski, G., Korb, E., Rao, E. J., Wu, J. Y., and Finkbeiner, S. (2010). Cytoplasmic mislocalization of TDP-43 is toxic to neurons and enhanced by a mutation associated with familial amyotrophic lateral sclerosis. *J. Neurosci.* 30, 639–649. doi: 10.1523/jneurosci.4988-09.2010

Bellezza, I., Grottelli, S., Costanzi, E., Scarpelli, P., Pigna, E., Morozzi, G., et al. (2018). Peroxynitrite activates the NLRP3 inflammasome cascade in SOD1(G93A) mouse model of amyotrophic lateral sclerosis. *Mol. Neurobiol.* 55, 2350–2361. doi: 10.1007/s12035-017-0502-x

Byrne, S., Walsh, C., Lynch, C., Bede, P., Elamin, M., Kenna, K., et al. (2011). Rate of familial amyotrophic lateral sclerosis: a systematic review and meta-analysis. *J. Neurol. Neurosurg. Psychiatry* 82, 623–627. doi: 10.1136/jnnp.2010.224501

Chatterjee, K., Roy, A., Banerjee, R., Choudhury, S., Mondal, B., Halder, S., et al. (2020). Inflammasome and α-synuclein in Parkinson's disease: a cross-sectional study. *J. Neuroimmunol.* 338:577089. doi: 10.1016/j.jneuroim.2019.577089

Chen, L., Xue, L., Zheng, J., Tian, X., Zhang, Y., and Tong, Q. (2019). PPARss/delta agonist alleviates NLRP3 inflammasome-mediated neuroinflammation in the MPTP mouse model of Parkinson's disease. *Behav. Brain Res.* 356, 483–489. doi: 10.1016/j.bbr.2018.06.005

Codolo, G., Plotegher, N., Pozzobon, T., Brucale, M., Tessari, I., Bubacco, L., et al. (2013). Triggering of inflammasome by aggregated α-synuclein, an inflammatory response in synucleinopathies. *PLoS One* 8:e55375. doi: 10.1371/journal.pone.0055375

Darakhshan, S., and Pour, A. B. (2015). Tranilast: a review of its therapeutic applications. *Pharmacol. Res.* 91, 15–28. doi: 10.1016/j.phrs.2014.10.009

Dempsey, C., Rubio Araiz, A., Bryson, K. J., Finucane, O., Larkin, C., Mills, E. L., et al. (2017). Inhibiting the NLRP3 inflammasome with MCC950 promotes non-phlogistic clearance of amyloid-β and cognitive function in APP/PS1 mice. *Brain Behav. Immun.* 61, 306–316. doi: 10.1016/j.bbi.2016.12.014

Dong, Y., and Benveniste, E. N. (2001). Immune function of astrocytes. *Glia* 36, 180–190. doi: 10.1002/glia.1107

Dubois, H., Wullaert, A., and Lamkanfi, M. (2016). General strategies in inflammasome biology. *Curr. Top. Microbiol. Immunol.* 397, 1–22. doi: 10.1007/978-3-319-41171-2_1

Fan, Z., Liang, Z., Yang, H., Pan, Y., Zheng, Y., and Wang, X. (2017). Tenuigenin protects dopaminergic neurons from inflammation *via* suppressing NLRP3 inflammasome activation in microglia. *J. Neuroinflammation* 14:256. doi: 10.1186/s12974-017-1036-x

Fan, Z., Lu, M., Qiao, C., Zhou, Y., Ding, J. H., and Hu, G. (2016). MicroRNA-7 enhances subventricular zone neurogenesis by inhibiting NLRP3/caspase-1 Axis in adult neural stem cells. *Mol. Neurobiol.* 53, 7057–7069. doi: 10.1007/s12035-015-9620-5

Fan, Z., Pan, Y. T., Zhang, Z. Y., Yang, H., Yu, S. Y., Zheng, Y., et al. (2020). Systemic activation of NLRP3 inflammasome and plasma α-synuclein levels

are correlated with motor severity and progression in Parkinson's disease. *J. Neuroinflammation* 17:11. doi: 10.1186/s12974-019-1670-6

Franchi, L., Warner, N., Viani, K., and Nunez, G. (2009). Function of Nod-like receptors in microbial recognition and host defense. *Immunol. Rev.* 227, 106–128. doi: 10.1111/j.1600-065x.2008.00734.x

Freeman, L., Guo, H., David, C. N., Brickey, W. J., Jha, S., and Ting, J. P. (2017). NLR members NLRC4 and NLRP3 mediate sterile inflammasome activation in microglia and astrocytes. *J. Exp. Med.* 214, 1351–1370. doi: 10.1084/jem.20150237

Gordon, R., Albornoz, E. A., Christie, D. C., Langley, M. R., Kumar, V., Mantovani, S., et al. (2018). Inflammasome inhibition prevents α-synuclein pathology and dopaminergic neurodegeneration in mice. *Sci. Transl. Med.* 10:eaah4066. doi: 10.1126/scitranslmed.aah4066

Gustot, A., Gallea, J. I., Sarroukh, R., Celej, M. S., Ruysschaert, J. M., and Raussens, V. (2015). Amyloid fibrils are the molecular trigger of inflammation in Parkinson's disease. *Biochem. J.* 471, 323–333. doi: 10.1042/bj20150617

Hagar, J. A., Powell, D. A., Aachoui, Y., Ernst, R. K., and Miao, E. A. (2013). Cytoplasmic LPS activates caspase-11: implications in TLR4-independent endotoxic shock. *Science* 341, 1250–1253. doi: 10.3410/f.718106716.793488210

Haidet-Phillips, A. M., Hester, M. E., Miranda, C. J., Meyer, K., Braun, L., Frakes, A., et al. (2011). Astrocytes from familial and sporadic ALS patients are toxic to motor neurons. *Nat. Biotechnol.* 29, 824–828. doi: 10.1038/nm.2484

Halle, A., Hornung, V., Petzold, G. C., Stewart, C. R., Monks, B. G., Reinheckel, T., et al. (2008). The NALP3 inflammasome is involved in the innate immune response to amyloid-β. *Nat. Immunol.* 9, 857–865. doi: 10.3410/f.1116856.572943

Haque, M. E., Akther, M., Jakaria, M., Kim, I. S., Azam, S., and Choi, D. K. (2020). Targeting the microglial NLRP3 inflammasome and its role in Parkinson's disease. *Mov. Disord.* 35, 20–33. doi: 10.1002/mds.27874

Hardiman, O., van den Berg, L. H., and Kiernan, M. C. (2011). Clinical diagnosis and management of amyotrophic lateral sclerosis. *Nat. Rev. Neurol.* 7, 639–649. doi: 10.1038/nrneurol.2011.153

Hardy, J., and Selkoe, D. J. (2002). The amyloid hypothesis of Alzheimer's disease: progress and problems on the road to therapeutics. *Science* 297, 353–356. doi: 10.1126/science.1072994

HE Ling-Ling, L. X.-Q., LIU Xiao-Lei, H. O. U., and LI Xin-Yi, M.-M. (2020). Effect of modified Buwanggsan on expression of relayted molecules in NLRP3 inflam-matory signaling pathway in hippocmpaus of AD rats. *Chinese J. Exp. Tradit. Med. Formul.* 26, 35–41.

Heneka, M. T., Kummer, M. P., Stutz, A., Delekate, A., Schwartz, S., Vieira-Saecker, A., et al. (2013). NLRP3 is activated in Alzheimer's disease and contributes to pathology in APP/PS1 mice. *Nature* 493, 674–678. doi: 10.1038/nature11729

Heneka, M. T., McManus, R. M., and Latz, E. (2018). Inflammasome signalling in brain function and neurodegenerative disease. *Nat. Rev. Neurosci.* 19, 610–621. doi: 10.1038/s41583-018-0055-7

Huang, Y., Jiang, H., Chen, Y., Wang, X., Yang, Y., Tao, J., et al. (2018). Tranilast directly targets NLRP3 to treat inflammasome-driven diseases. *EMBO Mol. Med.* 10:e8689. doi: 10.15252/emmm.201708689

Ince, P. G., Highley, J. R., Kirby, J., Wharton, S. B., Takahashi, H., Strong, M. J., et al. (2011). Molecular pathology and genetic advances in amyotrophic lateral sclerosis: an emerging molecular pathway and the significance of glial pathology. *Acta Neuropathol.* 122, 657–671. doi: 10.1007/s00401-011-0913-0

Jiang, J., Ding, N., Wang, K., and Li, Z. (2018). Electroacupuncture could influence the expression of IL-1β and NLRP3 inflammasome in hippocampus of Alzheimer's disease animal model. *Evid. Based Complement. Alternat. Med.* 2018:8296824. doi: 10.1155/2018/8296824

Jo, E. K., Kim, J. K., Shin, D. M., and Sasakawa, C. (2016). Molecular mechanisms regulating NLRP3 inflammasome activation. *Cell. Mol. Immunol.* 13, 148–159. doi: 10.1038/cmi.2015.95

Johann, S., Heitzer, M., Kanagaratnam, M., Goswami, A., Rizo, T., Weis, J., et al. (2015). NLRP3 inflammasome is expressed by astrocytes in the SOD1 mouse model of ALS and in human sporadic ALS patients. *Glia* 63, 2260–2273. doi: 10.1002/glia.22891

Kelley, N., Jeltema, D., Duan, Y., and He, Y. (2019). The NLRP3 inflammasome: an overview of mechanisms of activation and regulation. *Int. J. Mol. Sci.* 20:3328. doi: 10.17077/etd.sjblxfjh

Kipp, M., Karakaya, S., Johann, S., Kampmann, E., Mey, J., and Beyer, C. (2007). Oestrogen and progesterone reduce lipopolysaccharide-induced expression of tumour necrosis factor-α and interleukin-18 in midbrain astrocytes. *J. Neuroendocrinol.* 19, 819–822. doi: 10.1111/j.1365-2826.2007.01588.x

Labzin, L. I., Heneka, M. T., and Latz, E. (2018). Innate Immunity and Neurodegeneration. *Annu. Rev. Med.* 69, 437–449. doi: 10.1146/annurev-med-050715-104343

Lamkanfi, M. (2011). Emerging inflammasome effector mechanisms. *Nat. Rev. Immunol.* 11, 213–220. doi: 10.1038/nri2936

Lamkanfi, M., and Dixit, V. M. (2010). Manipulation of host cell death pathways during microbial infections. *Cell Host Microbe* 8, 44–54. doi: 10.1016/j.chom.2010.06.007

Lamkanfi, M., and Dixit, V. M. (2014). Mechanisms and functions of inflammasomes. *Cell* 157, 1013–1022. doi: 10.1016/j.cell.2014.04.007

Lang, Y., Chu, F., Shen, D., Zhang, W., Zheng, C., Zhu, J., et al. (2018). Role of inflammasomes in neuroimmune and neurodegenerative diseases: a systematic review. *Mediators Inflamm.* 2018:1549549. doi: 10.1155/2018/1549549

Lan, Z., Xie, G., Wei, M., Wang, P., and Chen, L. (2017). The protective effect of epimedii folium and curculiginis rhizoma on Alzheimer's disease by the inhibitions of NF-κB/MAPK pathway and NLRP3 inflammasome. *Oncotarget* 8, 43709–43720. doi: 10.18632/oncotarget.12574

Lee, E., Hwang, I., Park, S., Hong, S., Hwang, B., Cho, Y., et al. (2019). MPTP-driven NLRP3 inflammasome activation in microglia plays a central role in dopaminergic neurodegeneration. *Cell Death Differ.* 26, 213–228. doi: 10.1038/s41418-018-0124-5

Lee, J. D., Levin, S. C., Willis, E. F., Li, R., Woodruff, T. M., and Noakes, P. G. (2018). Complement components are upregulated and correlate with disease progression in the TDP-43(Q331K) mouse model of amyotrophic lateral sclerosis. *J. Neuroinflammation* 15:171. doi: 10.1186/s12974-018-1217-2

Lenart, N., Brough, D., and Denes, A. (2016). Inflammasomes link vascular disease with neuroinflammation and brain disorders. *J. Cereb. Blood Flow Metab.* 36, 1668–1685. doi: 10.1177/0271678x16662043

Leng, B., Zhang, Y., Liu, X., Zhang, Z., Liu, Y., Wang, H., et al. (2019). Astragaloside IV suppresses high glucose-induced NLRP3 inflammasome activation by inhibiting TLR4/NF-κB and CaSR. *Mediators Inflamm.* 2019:1082497. doi: 10.1155/2019/1082497

Li, L., Ismael, S., Nasoohi, S., Sakata, K., Liao, F. F., McDonald, M. P., et al. (2019). Thioredoxin-Interacting protein (TXNIP) associated NLRP3 inflammasome activation in human Alzheimer's disease brain. *J. Alzheimers Dis.* 68, 255–265. doi: 10.3233/jad-180814

Li, D., Yang, H., Ma, J., Luo, S., Chen, S., and Gu, Q. (2018). MicroRNA-30e regulates neuroinflammation in MPTP model of Parkinson's disease by targeting Nlrp3. *Hum. Cell* 31, 106–115. doi: 10.1007/s13577-017-0187-5

Li, R., Wang, J., Li, R., Zhu, F., Xu, W., Zha, G., et al. (2018). ATP/P2X7-NLRP3 axis of dendritic cells participates in the regulation of airway inflammation and hyper-responsiveness in asthma by mediating HMGB1 expression and secretion. *Exp. Cell Res.* 366, 1–15. doi: 10.1016/j.yexcr.2018.03.002

Liang, F., Zhang, F., Zhang, L., and Wei, W. (2020). The advances in pyroptosis initiated by inflammasome in inflammatory and immune diseases. *Inflamm. Res.* 69, 159–166. doi: 10.1007/s00011-020-01315-3

Lue, L. F., Rydel, R., Brigham, E. F., Yang, L. B., Hampel, H., Murphy, G. M., et al. (2001). Inflammatory repertoire of Alzheimer's disease and nondemented elderly microglia *in vitro*. *Glia* 35, 72–79. doi: 10.1002/glia.1072

Mao, Z., Liu, C., Ji, S., Yang, Q., Ye, H., Han, H., et al. (2017). The NLRP3 inflammasome is involved in the pathogenesis of Parkinson's disease in rats. *Neurochem. Res.* 42, 1104–1115. doi: 10.1007/s11064-017-2185-0

Marchetti, C., Swartzwelter, B., Gamboni, F., Neff, C. P., Richter, K., Azam, T., et al. (2018a). OLT1177, a β-sulfonyl nitrile compound, safe in humans, inhibits the NLRP3 inflammasome and reverses the metabolic cost of inflammation. *Proc. Natl. Acad. Sci. U S A* 115, E1530–E1539. doi: 10.1073/pnas.1716095115

Marchetti, C., Swartzwelter, B., Koenders, M. I., Azam, T., Tengesdal, I. W., Powers, N., et al. (2018b). NLRP3 inflammasome inhibitor OLT1177 suppresses joint inflammation in murine models of acute arthritis. *Arthritis Res. Ther.* 20:169. doi: 10.1186/s13075-018-1664-2

Martinon, F., Burns, K., and Tschopp, J. (2002). The inflammasome: a molecular platform triggering activation of inflammatory caspases and processing of proIL-β. *Mol. Cell* 10, 417–426. doi: 10.3410/f.1008963.128907

Martinon, F., Petrilli, V., Mayor, A., Tardivel, A., and Tschopp, J. (2006). Gout-associated uric acid crystals activate the NALP3 inflammasome. *Nature* 440, 237–241. doi: 10.1038/nature04516

Meissner, F., Molawi, K., and Zychlinsky, A. (2010). Mutant superoxide dismutase 1-induced IL-1β accelerates ALS pathogenesis. *Proc. Natl. Acad. Sci. U S A* 107, 13046–13050. doi: 10.1073/pnas.1002396107

Meyer-Luehmann, M., Spires-Jones, T. L., Prada, C., Garcia-Alloza, M., de Calignon, A., Rozkalne, A., et al. (2008). Rapid appearance and local toxicity of amyloid-β plaques in a mouse model of Alzheimer's disease. *Nature* 451, 720–724. doi: 10.1038/nature06616

Minutoli, L., Puzzolo, D., Rinaldi, M., Irrera, N., Marini, H., Arcoraci, V., et al. (2016). ROS-mediated NLRP3 inflammasome activation in brain, heart, kidney, and testis ischemia/reperfusion injury. *Oxid. Med. Cell. Longev.* 2016:2183026. doi: 10.1155/2016/2183026

Mo, Y., Xu, E., Wei, R., Le, B., Song, L., Li, D., et al. (2018). Bushen-yizhi formula alleviates neuroinflammation *via* inhibiting NLRP3 inflammasome activation in a mouse model of Parkinson's disease. *Evid. Based Complement. Alternat. Med.* 2018:3571604. doi: 10.1155/2018/3571604

Mogi, M., Harada, M., Kondo, T., Riederer, P., Inagaki, H., Minami, M., et al. (1994). Interleukin-1 β, interleukin-6, epidermal growth factor and transforming growth factor-α are elevated in the brain from parkinsonian patients. *Neurosci. Lett.* 180, 147–150. doi: 10.1016/0304-3940(94)90508-8

Morgan, S., and Orrell, R. W. (2016). Pathogenesis of amyotrophic lateral sclerosis. *Br. Med. Bull.* 119, 87–98. doi: 10.1093/bmb/ldw026

Muñoz-Planillo, R., Kuffa, P., Martínez-Colón, G., Smith, B. L., Rajendiran, T. M., and Nunez, G. (2013). K^+ efflux is the common trigger of NLRP3 inflammasome activation by bacterial toxins and particulate matter. *Immunity* 38, 1142–1153. doi: 10.1016/j.immuni.2013.05.016

Murakami, T., Ockinger, J., Yu, J., Byles, V., McColl, A., Hofer, A. M., et al. (2012). Critical role for calcium mobilization in activation of the NLRP3 inflammasome. *Proc. Natl. Acad. Sci. U S A* 109, 11282–11287. doi: 10.1073/pnas.1117765109

Neumann, M., Sampathu, D. M., Kwong, L. K., Truax, A. C., Micsenyi, M. C., Chou, T. T., et al. (2006). Ubiquitinated TDP-43 in frontotemporal lobar degeneration and amyotrophic lateral sclerosis. *Science* 314, 130–133. doi: 10.1126/science.1134108

Panicker, N., Sarkar, S., Harischandra, D. S., Neal, M., Kam, T. I., Jin, H., et al. (2019). Fyn kinase regulates misfolded α-synuclein uptake and NLRP3 inflammasome activation in microglia. *J. Exp. Med.* 216, 1411–1430. doi: 10.1084/jem.20182191

Pellegrini, C., Antonioli, L., Lopez-Castejon, G., Blandizzi, C., and Fornai, M. (2017). Canonical and non-canonical activation of NLRP3 inflammasome at the crossroad between immune tolerance and intestinal inflammation. *Front. Immunol.* 8:36. doi: 10.3389/fimmu.2017.00036

Petrucci, S., Consoli, F., and Valente, E. M. (2014). Parkinson disease genetics: a "continuum" from mendelian to multifactorial Inheritance. *Curr. Mol. Med.* 14, 1079–1088. doi: 10.2174/1566524014666141010155509

Philips, T., and Robberecht, W. (2011). Neuroinflammation in amyotrophic lateral sclerosis: role of glial activation in motor neuron disease. *Lancet Neurol.* 10, 253–263. doi: 10.1016/s1474-4422(11)70015-1

Qiao, Y., Wang, P., Qi, J., Zhang, L., and Gao, C. (2012). TLR-induced NF-κB activation regulates NLRP3 expression in murine macrophages. *FEBS Lett.* 586, 1022–1026. doi: 10.1016/j.febslet.2012.02.045

Qiao, C., Zhang, Q., Jiang, Q., Zhang, T., Chen, M., Fan, Y., et al. (2018). Inhibition of the hepatic Nlrp3 protects dopaminergic neurons *via* attenuating systemic inflammation in a MPTP/p mouse model of Parkinson's disease. *J. Neuroinflammation* 15:193. doi: 10.1186/s12974-018-1236-z

Qiao, C., Zhang, L. X., Sun, X. Y., Ding, J. H., Lu, M., and Hu, G. (2017). Caspase-1 deficiency alleviates dopaminergic neuronal death *via* inhibiting caspase-7/AIF pathway in MPTP/p mouse model of Parkinson's disease. *Mol. Neurobiol.* 54, 4292–4302. doi: 10.1007/s12035-016-9980-5

Rano, T. A., Timkey, T., Peterson, E. P., Rotonda, J., Nicholson, D. W., Becker, J. W., et al. (1997). A combinatorial approach for determining protease specificities: application to interleukin-1β converting enzyme (ICE). *Chem. Biol.* 4, 149–155. doi: 10.1016/s1074-5521(97)90258-1

Sargsyan, S. A., Blackburn, D. J., Barber, S. C., Grosskreutz, J., De Vos, K. J., Monk, P. N., et al. (2011). A comparison of *in vitro* properties of resting SOD1 transgenic microglia reveals evidence of reduced neuroprotective function. *BMC Neurosci.* 12:91. doi: 10.1186/1471-2202-12-91

Shang, J., Yamashita, T., Zhai, Y., Nakano, Y., Morihara, R., Li, X., et al. (2019). Acceleration of NLRP3 inflammasome by chronic cerebral hypoperfusion in Alzheimer's disease model mouse. *Neurosci. Res.* 143, 61–70. doi: 10.1016/j.neures.2018.06.002

Song, Y., Na, H. S., Park, E., Park, M. H., Lee, H. A., and Chung, J. (2018). Streptococcus mutans activates the AIM2, NLRP3 and NLRC4 inflammasomes in human THP-1 macrophages. *Int. J. Oral. Sci.* 10:23. doi: 10.1038/s41368-018-0024-z

Sreedharan, J., Blair, I. P., Tripathi, V. B., Hu, X., Vance, C., Rogelj, B., et al. (2008). TDP-43 mutations in familial and sporadic amyotrophic lateral sclerosis. *Science* 319, 1668–1672. doi: 10.1126/science.1154584

Thawkar, B. S., and Kaur, G. (2019). Inhibitors of NF-κB and P2X7/NLRP3/Caspase 1 pathway in microglia: novel therapeutic opportunities in neuroinflammation induced early-stage Alzheimer's disease. *J. Neuroimmunol.* 326, 62–74. doi: 10.1016/j.jneuroim.2018.11.010

Toma, C., Higa, N., Koizumi, Y., Nakasone, N., Ogura, Y., McCoy, A. J., et al. (2010). Pathogenic Vibrio activate NLRP3 inflammasome *via* cytotoxins and TLR/nucleotide-binding oligomerization domain-mediated NF-κ B signaling. *J. Immunol.* 184, 5287–5297. doi: 10.4049/jimmunol.0903536

Tschopp, J., and Schroder, K. (2010). NLRP3 inflammasome activation: the convergence of multiple signalling pathways on ROS production? *Nat. Rev. Immunol.* 10, 210–215. doi: 10.1038/nri2725

van Neerven, S., Nemes, A., Imholz, P., Regen, T., Denecke, B., Johann, S., et al. (2010). Inflammatory cytokine release of astrocytes *in vitro* is reduced by all-trans retinoic acid. *J. Neuroimmunol.* 229, 169–179. doi: 10.1016/j.jneuroim.2010.08.005

Voet, S., Srinivasan, S., Lamkanfi, M., and van Loo, G. (2019). Inflammasomes in neuroinflammatory and neurodegenerative diseases. *EMBO Mol. Med.* 11:e10248. doi: 10.15252/emmm.201810248

von Herrmann, K. M., Salas, L. A., Martinez, E. M., Young, A. L., Howard, J. M., Feldman, M. S., et al. (2018). NLRP3 expression in mesencephalic neurons and characterization of a rare NLRP3 polymorphism associated with decreased risk of Parkinson's disease. *NPJ Parkinsons Dis.* 4:24. doi: 10.1038/s41531-018-0061-5

Wang, X., Chi, J., Huang, D., Ding, L., Zhao, X., Jiang, L., et al. (2020). α-synuclein promotes progression of Parkinson's disease by upregulating autophagy signaling pathway to activate NLRP3 inflammasome. *Exp. Ther. Med.* 19, 931–938. doi: 10.3892/etm.2019.8297

Wang, W., Nguyen, L. T., Burlak, C., Chegini, F., Guo, F., Chataway, T., et al. (2016). Caspase-1 causes truncation and aggregation of the Parkinson's disease-associated protein α-synuclein. *Proc. Natl. Acad. Sci. U S A* 113, 9587–9592. doi: 10.1073/pnas.1610099113

Wang, B. R., Shi, J. Q., Ge, N. N., Ou, Z., Tian, Y. Y., Jiang, T., et al. (2018). PM2.5 exposure aggravates oligomeric amyloid β-induced neuronal injury and promotes NLRP3 inflammasome activation in an *in vitro* model of Alzheimer's disease. *J. Neuroinflammation* 15:132. doi: 10.1186/s12974-018-1178-5

Wang, J., Tan, L., Wang, H. F., Tan, C. C., Meng, X. F., Wang, C., et al. (2015). Anti-inflammatory drugs and risk of Alzheimer's disease: an updated systematic review and meta-analysis. *J. Alzheimers Dis.* 44, 385–396. doi: 10.3233/JAD-141506

Wang, B., and Yin, Q. (2017). AIM2 inflammasome activation and regulation: a structural perspective. *J. Struct. Biol.* 200, 279–282. doi: 10.1016/j.jsb.2017.08.001

Xiang, H., Zhu, F., Xu, Z., and Xiong, J. (2020). Role of inflammasomes in kidney diseases *via* both canonical and non-canonical pathways. *Front. Cell Dev. Biol.* 8:106. doi: 10.3389/fcell.2020.00106

Yao, S., Li, L., Sun, X., Hua, J., Zhang, K., Hao, L., et al. (2019). FTY720 inhibits MPP(+)-induced microglial activation by affecting NLRP3 inflammasome activation. *J. Neuroimmune Pharmacol.* 14, 478–492. doi: 10.1007/s11481-019-09843-4

Yi, Y. S. (2017). Caspase-11 non-canonical inflammasome: a critical sensor of intracellular lipopolysaccharide in macrophage-mediated inflammatory responses. *Immunology* 152, 207–217. doi: 10.1111/imm.12787

Zeng, R., Luo, D. X., Li, H. P., Zhang, Q. S., Lei, S. S., and Chen, J. H. (2019). MicroRNA-135b alleviates MPP^+-mediated Parkinson's disease in *in vitro* model through suppressing FoxO1-induced NLRP3 inflammasome and pyroptosis. *J. Clin. Neurosci.* 65, 125–133. doi: 10.1016/j.jocn.2019.04.004

Zhang, P., Shao, X. Y., Qi, G. J., Chen, Q., Bu, L. L., Chen, L. J., et al. (2016). Cdk5-dependent activation of neuronal inflammasomes in Parkinson's disease. *Mov. Disord.* 31, 366–376. doi: 10.1002/mds.26488

Zhao, W., Beers, D. R., Henkel, J. S., Zhang, W., Urushitani, M., Julien, J. P., et al. (2010). Extracellular mutant SOD1 induces microglial-mediated motoneuron injury. *Glia* 58, 231–243. doi: 10.1002/glia.20919

Zhou, Y., Lu, M., Du, R. H., Qiao, C., Jiang, C. Y., Zhang, K. Z., et al. (2016). MicroRNA-7 targets Nod-like receptor protein 3 inflammasome to modulate neuroinflammation in the pathogenesis of Parkinson's disease. *Mol. Neurodegener.* 11:28. doi: 10.1186/s13024-016-0094-3

Conflict of Interest: The authors declare that the research was conducted in the absence of any commercial or financial relationships that could be construed as a potential conflict of interest.

frontiers in Psychiatry

REVIEW
published: 11 August 2020
doi: 10.3389/fpsyt.2020.00781

Microglial Dysregulation and Suicidality: A Stress-Diathesis Perspective

Paria Baharikhoob[1,2,3] *and Nathan J. Kolla*[1,2,3,4,5]*

[1] Institute of Medical Science, University of Toronto, Toronto, ON, Canada, [2] Centre for Addiction and Mental Health (CAMH) Research Imaging Centre and Campbell Family Mental Health Research Institute, Toronto, ON, Canada, [3] Violence Prevention Neurobiological Research Unit, CAMH, Toronto, ON, Canada, [4] Department of Psychiatry, University of Toronto, Toronto, ON, Canada, [5] Waypoint Centre for Mental Health Care, Waypoint Research Institute, Penetanguishene, ON, Canada

According to the stress-diathesis model of suicidal behavior, completed suicide depends on the interaction between psychosocial stressors and a trait-like susceptibility. While there are likely multiple biological processes at play in suicidal behavior, recent findings point to over-activation of microglia, the resident macrophages of the central nervous system, as implicated in stress-induced suicidal behavior. However, it remains unclear how microglial dysregulation can be integrated into a clinical model of suicidal behavior. Therefore, this narrative review aims to (1) examine the findings from human post-mortem and neuroimaging studies that report a relationship between microglial activation and suicidal behavior, and (2) update the clinical model of suicidal behavior to integrate the role of microglia. A systematic search of SCOPUS, PubMed, PsycINFO, and Embase databases revealed evidence of morphological alterations in microglia and increased translocator protein density in the brains of individuals with suicidality, pointing to a positive relationship between microglial dysregulation and suicidal behavior. The studies also suggested several pathological mechanisms leading to suicidal behavior that may involve microglial dysregulation, namely (1) enhanced metabolism of tryptophan to quinolinic acid through the kynurenine pathway and associated serotonin depletion; (2) increased quinolinic acid leading to excessive N-methyl-D-aspartate-signaling, resulting in potential disruption of the blood brain barrier; (3) increased quinolinic acid resulting in higher neurotoxicity, and; (4) elevated interleukin 6 contributing to loss of inhibition of glutamatergic neurons, causing heightened glutamate release and excitotoxicity. Based on these pathways, we reconceptualized the stress-diathesis theory of suicidal behavior to incorporate the role of microglial activity.

Keywords: suicide, stress-diathesis model, microglia, neuroinflammation, post-mortem, positron emission tomography

OPEN ACCESS

Edited by:
Bart Ellenbroek,
Victoria University of Wellington, New Zealand

Reviewed by:
Gilles J. Guillemin,
Macquarie University, Australia
Seth Davin Norrholm,
Wayne State University, United States
Chai K. Lim,
Macquarie University, Australia

***Correspondence:**
Nathan J. Kolla
nathan.kolla@camh.ca

Specialty section:
This article was submitted to Molecular Psychiatry, a section of the journal Frontiers in Psychiatry

Received: *04 May 2020*
Accepted: *22 July 2020*
Published: *11 August 2020*

Citation:
Baharikhoob P and Kolla NJ (2020) Microglial Dysregulation and Suicidality: A Stress-Diathesis Perspective. Front. Psychiatry 11:781. doi: 10.3389/fpsyt.2020.00781

INTRODUCTION

Understanding the complex, multifactorial phenomena of suicidal behavior (SB) has long been a research priority. In 1999, Mann and colleagues were the first to introduce a stress-diathesis approach to suicide risk, which they denoted as the clinical model of SB. This model postulates that state-dependent "stress" in the form of psychosocial stressors and psychiatric illness(es) in

combination with a trait-like "diathesis" to suicidal tendencies could result in SB (1). The stress component refers to the proximal risk factors that affect the timing and probability of suicidal acts, while the diathesis component describes distal risk factors influencing SB and may be considered independent of a psychiatric illness (2). This model is highly influential and has formed the framework for much of the contemporary research in suicidology; however, the model is not without limitations. Most importantly, it is difficult to discern the neurobiological or molecular underpinnings that influence the stress component and its interactions with the diathesis component.

The clinical model of SB has since been modified by the fields of neurobiology and genetics in order to incorporate a neurobiological basis. For example, studies have demonstrated that early life stressors or trauma, such as physical or sexual abuse, decrease serotonergic neurotransmission (3–6), which is associated with increased impulsivity and aggressive behavior in adults (7). Epigenetic regulation of genes involved with hypothalamic pituitary adrenal (HPA) axis responsiveness have also been implicated in the model, which results in a blunted cortisol response and reduced resilience in managing stress (8–15). These changes likely contribute to emotion dysregulation, high anxiety, impulsive/aggressive behavior, as well as impaired problem-solving and decision-making. Furthermore, early life stressors are also found to be associated with reduced cerebrospinal fluid (CSF) oxytocin levels (16). Neuropeptides, such as opioids, oxytocin, and vasopressin, play an important role in emotion regulation and are disrupted in individuals with borderline personality disorder, who are highly prone to engaging in SB (17).

Though the aforementioned findings regarding the neurobiological and genetic dimensions of suicide risk have undoubtedly been useful in improving the clinical model of SB, the most updated stress-diathesis orientated model that integrates and illustrates these findings (18) is by no means exhaustive. This is because there have been other molecular abnormalities described in relation to the risk of suicide that have not yet been incorporated in the model. In particular, several studies have recently suggested a relationship between microglial activation and SB. Specifically, the over-activation of microglia, which are the resident immune cells of the central nervous system (CNS), is posited to contribute to SB. In addition to traumatic and immune stimuli, microglia can be activated as a result of psychosocial stress (19–21). Chronic microglial activation may, therefore, also influence the interaction between the stress and diathesis components of the stress-diathesis model of SB, including contributing to an increased vulnerability to suicidal tendencies. The role of microglial dysregulation has not been discussed within the context of a stress-diathesis model. In this paper, we review the results from the original immunohistochemistry and neuroimaging studies that discuss microglial activity in relation to SB. We then incorporate the role of microglial activity in an updated stress-diathesis theory of SB.

PHENOTYPE AND FUNCTION OF MICROGLIA

Microglia are the resident tissue macrophages of the CNS, representing 5 to 20% of the total glial cell population (22). In a healthy brain, "resting" or "quiescent" microglia have a small cell body with fine, ramified, and highly dynamic processes. This increased surface area allows microglia to continually scan their local environment for signs of potential threats. Upon recognition of harmful stimuli or infectious agents within the micro-environment, microglia rapidly become activated. This leads to a retraction of microglia protrusions and hypertrophy of their soma, giving the microglia an amoeboid-like shape (20). When activated, microglia release different inflammatory mediators depending on the state of activation.

Activated microglia can be divided into two states, the pro-inflammatory (M1) and anti-inflammatory (M2) pathways. The M1 pathway is triggered after neuronal injury has occurred and results in the release of a number of pro-inflammatory cytokines by microglia, including interleukin (IL)-1β, IL-6, tumor necrosis factor (TNF)-α, and nitric oxide (NO) (23). This is followed by the secondary response of the M2 pathway, which leads to the release of anti-inflammatory signals by microglia, namely IL-10, insulin-like growth factor 1, transforming growth factor beta, as well as various neurotrophic factors. The anti-inflammatory response of the M2 pathway is meant to restore homeostasis through the clearing of debris, reconstruction of the extracellular matrix, tissue repair, and angiogenesis. In a healthy immune system, both the M1 and M2 pathways are necessary, and the balance between the two states is part of a functional immune response (19, 23).

The nomenclature of the M1 and M2 pathways has, nevertheless, been challenged. This is because the states were defined based on the exposure of macrophages to stimuli *in vitro* and not *in vivo*. Thus, several scholars argue that the differentiation of the two states for activated microglia may be

Abbreviations: ACC, Anterior Cingulate Cortex; AD, affective disorder; AS, Asphyctic Suicide; BD, Bipolar Disorder or Bipolar Depression; BBB, Blood Brain Barrier; CSF, Cerebrospinal Fluid; CD45, Cluster of Differentiation 45; CD68, Cluster of Differentiation 68; CNS, Central Nervous System; dACC, Dorsal Anterior Cingulate Cortex; DBCBB, Douglas-Bell Canada Brain Bank; DCEM, Department of Clinical and Experimental Medicine; DLPFC, Dorsolateral Prefrontal Cortex; D-NOS, Depression Not Otherwise Specified; DPFWM, Dorsal Prefrontal White Matter; DRN, Dorsal Raphe Nucleus; HC, Healthy Control; HLA-DR, Human Leukocyte Antigen–DR isotype; HPA, Hypothalamic Pituitary Adrenal; Iba-IR, Ionized Calcium-binding Adaptor Molecule 1-immunoreactive; Iba-1, Ionized Calcium-binding Adaptor Molecule 1; IDO1, Indoleamine 2,3-dioxygenase; IFN-γ, Interferon Gamma; IL-1β, Interleukin-1β; IL-6, Interleukin-6; IL-10, Interleukin-10; IL-18, Interleukin-18; KYN, Kynurenine; KYNA, Kynurenic Acid; M1, Pro-inflammatory Pathway; M2, Anti-inflammatory Pathway; MBB, Magdeburg Brain Bank; MDT, Mediodorsal Thalamus; MDD, Major Depressive Disorder; NMDA, N-methyl-D-aspartic Acid; NO, Nitric Oxide; NOX2/MAC387, NADPH Oxidase and Macrophage Marker Antibody; NYSPIBC, New York State Psychiatric Institute Brain Collection; pACC, Pregenual Anterior Cingulate Cortex; PET, Positron Emission Tomography; PIC, Picolinic Acid; QUIN, Quinolinic acid; ROS, Reactive Oxygen Species; SB, Suicidal Behavior; SCZ, Schizophrenia; TNF-α, Tumor Necrosis Factor-α; TRY, Tryptophan; TSPO, Translocator Protein; UD, Unipolar Disorder; UF, University of Foggia; VPFWM, Ventral Prefrontal White Matter.

too reductionistic and instead hypothesize that microglial activation exists along a continuum (20, 24). With this point in mind, we will refer to microglial activation in general terms rather than specifying the M1 or M2 pathways for the purposes of this review.

PSYCHOSOCIAL STRESS, MICROGLIA AND DEPRESSIVE-LIKE BEHAVIOR IN ANIMAL MODELS

According to several studies involving animal models, prolonged psychosocial stress can activate microglia (19). In fact, as evident in **Table 1**, at least 16 animal studies have shown that in the prefrontal cortex, exposure to different psychosocial stressors gives rise to increases in ionized calcium-binding adaptor molecule 1 (Iba-1) immunoreactivity, a specific marker for the morphological changes and expansion of microglia. These psychosocial stressors involve repeated social defeat (SD), varying unpredictable stress, prenatal stress, social isolation, and chronic restraint (25–37). Similar effects from psychosocial stressors were also evident in other areas of the brain, including the amygdala (25, 26), hippocampus (25–28, 30, 36, 38, 39, 41–47), nucleus accumbens (36, 37) and paraventricular nucleus (25, 26). The SD paradigm, which is described below, appears to have the most marked effect on Iba-1 immunoreactivity.

SD is considered an animal model of depression as it induces depressive-like behavior in animals following prolonged psychosocial stress. The paradigm is typically initiated when a male rodent is presented to the domicile of an older, more dominant and aggressive male. The less dominant intruder rodent is rapidly attacked and forced into submission, consistently exhibiting signs of distress. These signs involve elevated glucocorticoid activity, hyperthermia, and tachycardia (48). Chronic psychosocial stress induced by repeated exposure to this situation has also been shown to impose long-term, depressive-like behavioral changes in the intruder, including sensitivity to other stressors and signs of social avoidance, anhedonia, locomotor hypomotility, and metabolic changes (49–51).

Unlike in other animal models of depression, chronic, but not acute, administration of anti-inflammatory medications to rodents can be effective in reducing depressive-like manifestations. Four-week treatment with minocycline, a tetracycline antibiotic which inhibits the increase and activation of microglia, successfully reduces the depressive-like behavior of rats exposed to chronic stress. Minocycline normalizes Iba-1 immunoreactivity in the hippocampus and reduces the increase of mRNA levels of pro-inflammatory cytokines, such as IL-1β, IL-18, and IL-6 (34, 52). These results suggest that microglial activation may play a crucial role in the regulation of stress-induced depressive-like behavior.

These findings are supported by a number of other animal studies, which have shown that stress-induced depressive-like outcomes by SD may, in part, be mediated by microglial activation (40, 47, 53–56). Stein and colleagues, who reviewed these studies in depth, posit that chronic stress contributes to the over-activated states of microglia. The over-activation of microglia, as a result, leads to highly increased levels of pro-inflammatory mediators, cytotoxins, and reactive oxygen species (ROS), which may produce excessively pruned synaptic connections, causing cellular dystrophy and loss or reduced functioning of neuronal activity. The cellular damage as well as impaired neuronal activity may subsequently induce the development of depressive-like outcomes (57).

Depressive-like behavior, which is part of the stress component of the clinical model of SB, can be emulated by animal models, such as the aforementioned SD paradigm; however, the outcome, SB, *cannot* be reproduced by animals as there are no convincing animal models of SB. This is partially due to the notion that animals cannot arguably execute SB due to their inability to possess a will to die, to perceive the ultimate consequences of their suicidal acts, or to consider the emotional reactions of those who would survive their conceivable death (58, 59). Therefore, for this review, we turn our attention to microglial dysregulation in relation to suicidality in human studies.

Interestingly, in human post-mortem studies, microglial over-activation also appears to be implicated in the pathophysiology of SB. According to Steiner and colleagues, suicide victims with a prior history of either major depressive disorder (MDD) or paranoid schizophrenia (SCZ) have elevated levels of microglial activity in the dorsolateral prefrontal cortex (DLPFC), anterior cingulate cortex (ACC) and mediodorsal thalamus (MDT) (60). Moreover, in a study that measured Iba-1 immunoreactivity similar to the animal models above, the results demonstrated a significantly higher degree of microglial priming in the dorsal ACC white matter of depressed suicide victims (61). Other studies have theorized, likewise to Stein and investigators (57), that microglial dysregulation results in elevated levels of pro-inflammatory cytokines, such as IL-1β, IL-6, TNF-α, cytotoxins, and NOX2-derived ROS. These studies also propose that such mechanisms

TABLE 1 | Effect of psychosocial stress on microglial activity in prefrontal cortex.

Reference	Stress Type	Species	Effect on Iba-1[1]
(25–28)	Chronic social defeat, chronic unpredictable stress	Mice, rats	↑↑↑
(29, 30)	Chronic unpredictable stress, prenatal stress	Mice, rats	↑↑
(31–37)	Chronic unpredictable stress, chronic restraint, social isolation	Mice, rats	↑
(32, 38–40)	Chronic social defeat, chronic unpredictable stress, chronic restraint	Mice, rats	↔

[1]*Microglial activity as measured by Iba-1 immunoreactivity. A ↑↑↑ effect represents a >70% increase in Iba-1 activity, a ↑↑ effect represents a 30-70% increase, a ↑ effect represents a 5-30% increase, and a ↔ represents no significant differences.*

contribute to neurotoxicity, excitotoxicity, and heightened glutamate release, alterations of which may then lead to depressive-like behavior apposite to suicidality (62–64). The aforementioned literature, alongside other human studies evaluating microglial dysregulation in SB, will be described in detail later in this review.

METHODS

Information Sources and Search Strategy

Potentially relevant studies were identified using the four electronic databases, SCOPUS, PubMed, PsycINFO, and Embase. Studies eligible for review included those concerning microglial activation and suicidal and self-harming acts in humans. They included human post-mortem and neuroimaging studies. Searches were performed between January 2006 and December 2019. We chose 2006 as the lower limit because it marked the year that the first paper addressing a possible relationship between microglial dysregulation and suicidality in humans was published (65). The following keywords were used for searches for each database: "microglia", "microglial activation", "microglial dysregulation", "suicidality", "suicidal behavior", "suicide", "suicide attempt", "suicidal ideation", "parasuicidal behavior", "self-harming behavior", and "self-harm".

Eligibility Criteria

Considering the different databases used for identifying studies, the abstracts and titles identified from the database searches were initially screened for eligibility using the following inclusion criteria: (1) original articles published between January 1, 2006, and December 31, 2019. Following this step, 44 were excluded from an initial 277 studies. This led to a remaining 233 studies, which were then screened using the following inclusion criteria: (1) studies that involved human subjects, (2) studies that were in English, and (3) studies that were not review articles. 121 studies were eliminated after this stage of screening, resulting in 112 articles.

The remaining 112 articles that met the aforementioned eligibility criteria were extracted to the reference management software, Zotero (Version 5.0.79). The full text of these articles was reviewed and included if they reported microglial dysregulation in the context of SB. All duplicate articles were subsequently deleted. This step in the screening process eliminated 103 articles, constituting a total of 9 studies that were included in this review.

Study Selection

The lead author was responsible for reviewing titles and abstracts following the database searches. The full text of articles that passed the first set of eligibility criteria were also reviewed by the lead author. If the relevance of an article was deemed questionable by the lead author, then the second author was responsible for reviewing the full text of the article and concluding its appropriateness for inclusion. The study selection process is summarized in **Figure 1**.

RESULTS

Post-Mortem or Immunohistochemistry Studies Implicating Microglia and SB

Performing immunohistochemical analyses from post-mortem brain samples is an important technique for furthering our understanding of the neurochemical dimensions of complex psychiatric phenomena, including SB (67). Eight separate post-mortem studies utilized this technique to investigate potentially dysregulated microglial activity in SB, which can be observed in **Table 2**. Findings from four studies pointed to significant microglial activity in the brains of suicide victims compared with healthy control (HC) subjects (60–62, 65); two studies observed no significant differences in activated microglia between suicide victims and HC subjects or found a minor percentage of microglia changes (63, 64); one study observed decreased microglial activity in their non-suicide group (69); and, a final study found decreased microglial activity in suicide victims compared to HC subjects (68).

Positive Studies

The results from four studies point to a positive association between increased microglial activity and SB. To begin, in 2006, Steiner et al. published the first study with an incidental observation of increased microglial densities in the ACC and MDT of 2 paranoid SCZ suicide victims (65). A similar group followed up on this finding and went on to provide the first significant evidence, using HLA-DR staining, of higher microglial density in the DLPFC, ACC, and MDT of suicide victims who had MDD or paranoid SCZ (60). This positive relationship was similarly replicated in a later study using the endogenous modulator, quinolinic acid (QUIN), as an immunoreactivity signature. The authors from this study observed significantly increased density of QUIN-positive cells in the subgenual ACC and anterior midcingulate cortex of suicide victims with MDD (62). Furthermore, another paper observed increased microglial priming in the dorsal ACC white matter of depressed suicide victims through the use of Iba-1–immunoreactive and Cluster of Differentiation (CD45) staining (61). Altogether, these results suggest that increased microglial activity may be correlated with death by suicide and that mechanisms relating to increased QUIN production by activated microglia may underlie this association.

Mixed Studies

Two studies presented unclear conclusions that neither support nor refute the *a priori* hypothesis of a positive relationship between the degree of microglial over-activation and SB. A team examining Iba-1 with CD68 discovered no significant differences in the ventral prefrontal white matter or dorsal prefrontal white matter between suicide victims and non-suicidal victims after adjusting for multiple statistical tests. There was an effect of suicide on the density of activated phagocytes in the ventral prefrontal white matter compared with the dorsal prefrontal white matter. Nevertheless, considering that activated phagocytes in their study comprised both activated microglia and macrophages, making any conclusions about the exclusivity

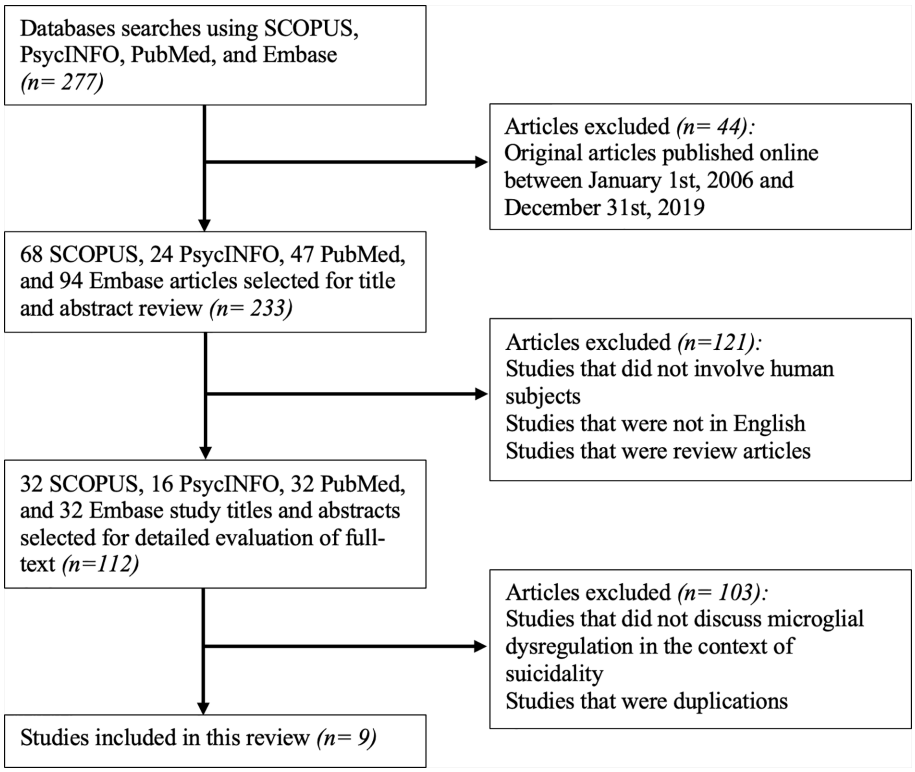

FIGURE 1 | Flowchart for the inclusion of appropriate original articles. This flowchart showcases the selection process for the inclusion of articles for review according to the PRISMA statement (66).

of microglial activity is difficult (63). Comparatively, a study utilizing NADPH oxidase and macrophage marker antibody (NOX2/MAC387) co-staining found a small percentage of this staining in the cortex of victims of asphyxia suicide. It remains unclear, however, whether this percentage was significantly different from the percentage of those who died by non-suicidal asphyxia or in HC subjects (64). These results preclude firm conclusions; however, the authors speculated that disruption of the blood brain barrier (BBB) due to higher QUIN levels as well as increased IL-6 production could be mechanisms associated with SB.

Finally, two studies found evidence of unchanged or reduced microglial activity in suicide cases compared to HC subjects. A paper from 2017 identified significantly decreased microglial activity, using HLA-DR staining, in the dorsal raphe nucleus of the non-suicidal depressed group in comparison to suicide victims with either MDD or bipolar disorder (BD), as well as HC subjects (69). Similarly, a study by Busse and colleagues revealed decreased microglial QUIN-immunoreactivity after *post hoc* tests in the right hippocampal CA1 field of suicidal patients with MDD or BD. These subjects, nevertheless, had an unchanged hippocampal volume size (68). The findings of these studies suggest that local anti-inflammatory and/or neuroprotective responses in these subjects may have influenced the extent of the microglial activation.

In summary, four of the eight post-mortem studies described above provided evidence of morphological alterations, predominantly increased cell density, in the microglia of the brains of suicide victims. These results support the theory of a positive relationship between microglial dysregulation and SB regardless of psychiatric diagnosis, implying that microglial-induced SB may be independent of psychiatric illness(es). However, the remaining four post-mortem studies had inconclusive findings, for example, unchanged or reduced microglial activity in subjects with SB. With this information in mind, more extensive post-mortem or immunohistochemistry investigations are required to make any definitive statements regarding neuroinflammation, specifically activated microglia, in suicide victims.

Limitations

There are some limitations to the post-mortem studies reviewed that must be mentioned. First, the microglial markers HLA-DR, Iba-1, and NOX2/MAC387 were limiting in that there was no suggestion of a molecular mechanism for which increased microglial activity may be related to SB. Moreover, with regards to the microglial marker, QUIN, the presence of released or secreted QUIN in the extracellular space and/or of protein expression or activity of the kynurenine (KYN) pathway enzyme QUIN phosphoribosyltransferase may have also

TABLE 2 | Post-mortem studies of microglial activity in SB.

Reference	Brain bank	Study Population	Death from Suicide	Mean Age (years)	Immunoreactivity marker(s) for microglial activity	Brain region	Findings
(65)	MBB	9 SCZ (paranoid) 7 SCZ (residual) 16 HC	2 SCZ (paranoid)	SCZ suicide: 50 SCZ non-suicide: 51 HC: 58	HLA-DR	DLPFC, ACC, MDT, and hippocampus	Highly elevated microglial activity in ACC and MDT of suicide victims.
(60)	MBB	9 MDD 5 BD 12 SCZ (paranoid) 4 SCZ (residual) 10 HC	7 MDD 6 SCZ (paranoid)	SCZ suicide: 50 SCZ non-suicide: 55 AD suicide: 41 AD non-suicide: 51 HC: 54	HLA-DR	DLPFC, ACC, MDT, and hippocampus	Significant microglial activity observed in DLPFC (p=0.004), ACC (p=0.012), and MDT (p=0.004) of suicide victims.
(62)	MBB	7 MDD 5 BD 10 HC	7 MDD 5 BD	Suicide: 51 HC: 56	QUIN	sACC, aMCC, pACC	Significant microglial activity evident in sACC (p=0.003) and aMCC (p=0.015) of suicide victims with MDD.
(61)	DBCBB	20 UD 4 D-NOS	20 UD 4 D-NOS	Suicide: 46 HC: 39	IBA-IR, CD45	dACC white matter	Significantly increased microglial priming in dACC white matter of depressed suicide victims (p=0.030).
(63)	NYSPIBC	10 SCZ 8 AD 18 No Illness	3 SCZ 5 AD 3 No Illness	Suicide: 56 Non-suicide: 55	IBA-1, CD68	VPFWM, DPFWM	No difference in microglial activity between suicide victims and non-suicide victims in VPFWM or DPFWM.
(68)	MBB	6 UD 6 BD 10 HC	6 UD 6 BD	Suicide: 49 HC: 56	QUIN	Hippocampus subregions (CA1 and CA2/3)	Significantly decreased microglial activity in right CA1 subregion of both UD (p=0.048) and BD (p=0.031) suicide victims.
(69)	MBB	15 MDD 12 BD 9 SCZ (paranoid) 9 SCZ (residual) 22 HC	9 MDD 7 BD 7 SCZ (paranoid) 1 SCZ (residual)	Suicide: 48 Non-suicide: 54 HC: 52	HLA-DR	DRN	Significantly decreased microglial activity in DRN depressed in non-suicide group compared to suicide victims with MDD or BD and controls (p=0.039).
(64)	DCEM, UF	26 AS 6 NSA 10 HC	26 AS	Not available	NOX2/MAC387	Cortex	Minor percentage of NOX2/MAC387 co-staining in cortex of AS victims.

AD, affective disorder; aMCC, anterior midcingulate cortex; AS, asphyctic suicide; BD, bipolar disorder or bipolar depression; CD45, cluster of differentiation 45; CD68, cluster of differentiation 68; dACC, dorsal anterior cingulate cortex; DBCBB, Douglas-Bell Canada Brain Bank; DCEM, Department of Clinical and Experimental Medicine; DLPFC, dorsolateral prefrontal cortex; D-NOS, depression not otherwise specified; DPFWM, dorsal prefrontal white matter; DRN, dorsal raphe nucleus; HC, healthy control; HLA-DR, human leukocyte antigen– DR isotype; IBA-IR, ionized calcium-binding adaptor molecule 1-immunoreactive; IBA-1, ionized calcium-binding adaptor molecule 1; MBB, Magdeburg Brain Bank; MDT, mediodorsal thalamus; MDD, major depressive disorder; NOX2/MAC387, NADPH oxidase and macrophage marker antibody; NYSPIBC, New York State Psychiatric Institute Brain Collection; pACC, pregenual anterior cingulate cortex; QUIN, quinolinic acid; sACC, subgenual anterior cingulate cortex; SCZ, schizophrenia; UD, unipolar disorder; UF, University of Foggia; VPFWM, ventral prefrontal white matter.

influenced glutamatergic neurotransmission. These other sources of QUIN thereby eliminate our ability to conclude that strictly microglial QUIN influences neuromodulation and ultimately behavioral manifestations. Second, all of the studies had small sample sizes, especially with consideration to the number of suicide victims. Third, for many of the studies, brain samples were obtained from different brain banks and comprised patients who had differing lengths of psychiatric illnesses, causes of death, exposure to psychopharmacological interventions, and potentially other age-related brain pathologies.

Positron Emission Tomography Study Discussing Microglial Activation in Relation to SB

The imaging modality positron emission tomography (PET) with the radioligand, [^{11}C]-(R)-PK11195, is another useful tool for visualizing microglial activity in the CNS in various psychiatric disorders. This is because [^{11}C]-(R)-PK11195 binds selectively to the translocator protein (TSPO) 18 kDa, a protein that is upregulated in the mitochondria of activated microglia. Binding of [^{11}C]-(R)-PK11195 or similar tracers may, therefore, be a biomarker of microglial activation as it is expected to be higher in areas of the brain with significant inflammation or neuronal damage (70).

Using [^{11}C]-(R)-PK11195 PET imaging, Holmes and colleagues (71) published the first *in vivo* study examining microglial activation and suicidal thinking. The authors observed increased TSPO density in the individuals with MDD compared to HC subjects, with the most pronounced finding in the ACC. They also found that TSPO expression was significantly elevated in the ACC and insula in patients with suicidal thoughts compared to patients without suicidal thoughts. The authors concluded that the greater TSPO binding in people with MDD and suicidal thoughts supported what four of the eight post-mortem studies had observed regarding a positive relationship between microglial activation and SB. It was also postulated that there was a

higher specificity of microglial activation for suicide over psychiatric diagnoses.

Limitations

The authors, however, were unable to distinguish between the resting and activated phenotypes of microglia and, therefore, could not infer any underlying mechanisms. Currently, TSPO PET imaging is considered the only valid modality for examining microglial activity *in vivo*; however, there are some additional drawbacks to this imaging technique that must be discussed. Though TSPO binding is thought to exclusively reflect microglial activation (72), some argue that under certain circumstances, it can be expressed when astrocytes are activated as well (73). Moreover, the radioligand, [^{11}C]-(R)-PK11195, used in the above PET study is limited due to the short half-life of carbon-11, high nonspecific binding, high plasma protein binding, and low brain penetration (74). [^{11}C]-(R)-PK11195 PET imaging, in addition, requires a brain region with no specific binding of TSPO as a reference region in order to quantify the *in vivo* binding. Nevertheless, no region is completely devoid of TSPO expression, as it is thought to be present throughout the entire brain (70, 75).

Due to these problems, second generation TSPO radiotracers have been synthesized to offer a superior quality for quantifying *in vivo* TSPO expression. These second-generation radioligands include [^{18}F]-FEPPA (76), [^{18}F]-PBR06 (77), [^{18}F]-FEDAA1106 (78), [^{11}C]-DAA1106 (79), [^{11}C]-DPA-713 (80), [^{18}F]-PBR111 (81), [^{18}F]-DPA-714 (82), and [^{11}C]-PBR28 (83). [^{18}F]-FEPPA is promising, for example, given that it displays an appropriate metabolic profile, a high affinity for TSPO, good pharmacokinetics, and high brain penetration (74). However, given the sensitivity of second-generation tracers to a single nucleotide polymorphism in the TSPO gene, third-generation TSPO radiotracers are also being developed that would be insensitive to this polymorphism. Examples of third-generation radioligands are [^{18}F]-GE180 and [^{11}C]-ER176; nonetheless, the safety and efficacy of these compounds in humans have not yet been established (84, 85).

In sum, TSPO PET imaging, specifically [^{11}C]-(R)-PK11195 PET, has several limitations that may affect the findings of studies using this modality, including the aforementioned study. More recent TSPO second-generation radiotracers are recommended for future studies investigating microglial activity *in vivo*.

Mechanisms Connecting Psychosocial Stress, Microglia, and SB in Human Studies

The most recent neurobiologically inclined stress-diathesis model proposed that life stressors or trauma lead to neurobiological alternations, such as deceased serotonergic neurotransmission, dysregulated HPA axis responsiveness, and reduced CSF oxytocin levels that may then result in behavioral alterations (18). This reconceptualized model is undoubtedly helpful in shedding additional light on the mechanisms by which early stressors contribute to the vulnerability to SB in later adolescence and adulthood. The model does not, however, include the growing evidence regarding the association between microglial dysregulation and SB. To address this, we evaluated eight immunohistochemistry studies and one TSPO PET imaging study that directly discuss microglial over-activation in relation to SB. Now, for this section, we further explore the neurobiological mechanisms that were proposed by some of these studies and also provide an updated stress-diathesis model of SB.

In 1969, a study introduced the "serotonin hypothesis", a theory which proposes that dysregulation in the metabolic pathway of the essential amino acid, tryptophan (TRY), is a significant risk factor for depression. Specifically, this theory suggests that there is a dysregulated shift, using TRY as a precursor, from serotonin synthesis to KYN synthesis (86). The dysregulated shift is theorized to occur due to the up-regulation of indoleamine 2,3-dioxygenase (IDO1). This enzyme becomes activated due to increased hormones and/or proinflammatory cytokines, including IL-1β, IL-6, TNF-α, and interferon gamma (IFN-γ) (87–89). By consistently stimulating the shift from serotonin synthesis to increased KYN synthesis *via* the KYN pathway, systematic IDO1 activation ultimately leads to depressive-like behavior (87). Nevertheless, the exact mechanisms that underlie how this dysregulation leads to depressive-like outcomes and/or SB remain unclear.

Steiner and collaborators (62) primarily tackle this conundrum by proposing that increased KYN contributes to serotonin depletion and a higher production of the excitotoxic metabolite QUIN, both of which result in behavioral changes. Both this team and others (63) suggest that depleted serotonin levels may be caused by activated microglia that have enhanced metabolism of TRY to QUIN through the KYN pathway (62, 63). Given that previous literature has found low serotonergic functioning to be associated with increased impulsivity and aggressive behaviors in adults (6), the finding that activated microglia decrease serotonin levels provides some understanding as to how microglial activation influences depressive-like behavior pertinent to SB. Moreover, a recent study has shown that reduced serotonin level is associated with an increased risk for SB despite adjustments for depression severity, further suggesting that serotonin depletion *via* KYN dysregulation may impact suicidality directly, regardless of a depression diagnosis (90).

Beyond serotonin reduction, the shift from TRY to QUIN is also posited to detrimentally affect the metabolism of kynurenic acid (KYNA), an N-methyl-D-aspartic acid (NMDA) receptor antagonist that is considered neuroprotective due to its inhibitory effect on glutamate neurotransmission (91, 92). In fact, reduced concentrations of KYNA have been correlated with excitotoxicity by QUIN (93). QUIN is considered excitotoxic because it is an agonist of the NMDA receptor; therefore, an increase in QUIN can lead to excessive NMDA signaling or glutamatergic dysregulation (94, 95). These mechanisms, as postulated by Schnieder and colleagues (63), can potentially disrupt the BBB. As a result, QUIN can heighten the stimulation of glutamatergic neurons, particularly in the ventral prefrontal cortex, causing a decrease in normal neuron connectivity within the limbic system and, subsequently, reduced

impulse control. In addition to being a direct NMDA receptor agonist, QUIN has pro-oxidant properties that worsen the neurotoxic effects by corticosterone and pro-inflammatory cytokines, as well as pro-inflammatory capabilities due to enhancement of the IFN-γ/IL-10 ratio (68). The adverse consequences of elevated QUIN are theorized to result in depressive features and/or SB. While astrocytes appear to predominantly catabolize KYNA from KYN, microglia instead transform KYN into 3-hydroxy kynurenine and QUIN (96, 97). This suggests that the above-mentioned mechanisms by which QUIN negatively affect the CNS may primarily be attributed to activated microglia.

Furthermore, an increase in IL-6, which is produced by microglia, is predicted by Schiavone and investigators (64) to enhance expression of NOX2 and NOX2-derived ROS production in GABAergic neurons. This subsequently causes altered GABAergic neurotransmission and thereby a loss of inhibition of glutamatergic neurons. The loss of inhibitory tone on the glutamatergic neurons contributes to excitotoxicity from increased glutamate release. This mechanism is hypothesized to also result in behavioral manifestations corresponding with SB; however, the authors do not specify which behavioral alterations may be affected.

Potential Role of Microglial Cells in Reconceptualized Model of SB

Based on the aforementioned mechanisms, we propose that psychosocial stress, one of the stress components of the stress-diathesis theory, induces microglial activation, which increases the release of pro-inflammatory cytokines, shifting from serotonin to KYN synthesis through the induction of IDO1 (62). Subsequently, the catalyzation of TRY by IDO1 produces QUIN, which disrupts glutamatergic neurotransmission, disrupting the BBB and ultimately leading to reduced impulse control through reduced neuronal connectivity within the limbic system (63). Production of QUIN by activated microglia has pro-inflammatory and pro-oxidant properties that additionally contribute to increased neurotoxicity (68). Microglial activation also, in part, leads to enhanced IL-6 release, which causes elevated NOX2 expression and NOX2-derived ROS production, resulting in a loss of inhibition in glutamatergic neurons. These series of reactions affect glutamatergic neurotransmission by increasing glutamate release. The increased excitotoxicity due to the higher glutamate release then contribute to the altered behavior that is associated with SB (64). Thus, the changes in serotonergic and glutamatergic neurotransmission mentioned above lead to

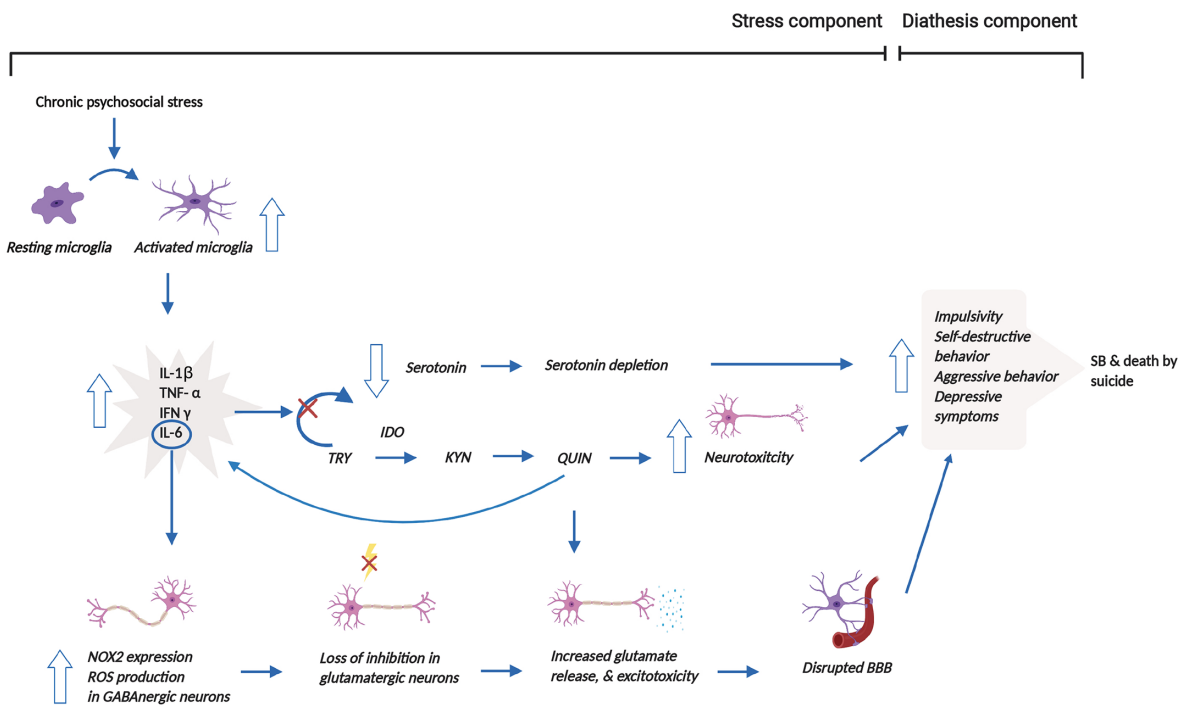

FIGURE 2 | Reconceptualized clinical model of SB incorporating microglial dysregulation. This model proposes that prolonged psychosocial stress leads to the over-activation of microglia and associated release of pro-inflammatory cytokines. The release of pro-inflammatory cytokines stimulates the shift from serotonin to KYN synthesis through the induction of IDO1. This shift results in the depletion of serotonin. The production of QUIN from KYN synthesis, in addition, increases neurotoxicity. Moreover, increased QUIN production directly leads to heightened glutamate release and associated excitotoxicity but also indirectly causes this elevation by increasing IL-6 levels. Increased glutamate release and excitotoxicity contribute to the disruption of the BBB. Altogether, all these mechanisms contribute to behavioral manifestations, which may then result in SB and/or death by suicide. This figure was created with BioRender.com. BBB, blood brain barrier; IDO1, indoleamine 2,3-dioxygenase; IFN-γ, interferon gamma; IL-1β, interleukin-1β; IL-6, interleukin-6; NOX2, NADPH oxidase; KYN, kynurenine; QUIN, quinolinic acid; ROS, reactive oxygen species; SB, suicidal behavior; TNF-α, tumor necrosis factor-α; TRY, tryptophan.

behavioral changes. These altered behavioral traits in suicide victims do not appear to be diagnosis specific (64, 68), thereby constituting a diagnosis-independent diathesis for SB. **Figure 2** illuminates these mechanisms and the interactions between the stress and diathesis components of the clinical model of SB.

Blood and Cerebrospinal Fluid Markers, Depressive Outcomes, and SB

A number of human studies have also investigated the relationship between metabolites of the KYN pathway and depressive features and/or SB by measuring these metabolites in the blood or CSF. Eleven studies of the KYN pathway metabolite, KYN, provided no convincing evidence of differences in blood KYN levels between depressed patients without SB relative to healthy controls (91, 98–107). On the other hand, seven studies reported lower blood KYN concentrations in the depressed group (108–114). A meta-analysis, which evaluated these studies, similarly concluded that blood KYN levels were lower in depressed patients compared to HC (115). Moreover, the study by the Setoyama group found that blood KYN levels were negatively correlated with suicidal ideation in depressed patients (114). By contrast, Sublette and colleagues demonstrated that blood KYN concentrations were elevated in suicide attempters compared to non-suicidal patients (107). Another study reported a higher blood KYN/TRP ratio in MDD subjects with SB versus MDD subjects without SB or HC. Results indicated that the KYN/TRP ratio was positively correlated with the severity of suicidality in patients with histories of SB (116). Brundin et al. (117) additionally identified a higher ratio of CSF KYN/TRP in patients with prior suicide attempts relative to HC. Altogether, these results suggest that higher concentrations of KYN have a greater association with SB compared to the relationship with depression.

Twelve studies examining KYNA, another metabolite of the KYN pathway, found no significant differences in blood KYNA concentrations between patients with depression without SB and HC (91, 99, 100–102, 105, 106, 108–110, 118, 119). One study, in addition, reported no differences in levels of CSF KYNA among depressed patients and HC (120). Four studies, however, provided evidence of reduced levels of KYNA concentrations in depressed patients relative to HC, with three studies reporting the result based on KYNA levels in blood (98, 111, 121) and one from KYNA levels in the CSF (120). Also, a meta-analysis that reviewed the above-mentioned studies measuring blood and CSF KYNA likewise concluded that concentrations of this metabolite were reduced in patients with depression in comparison to HC (115). On the other hand, one study reported that psychiatric patients who made previous suicide attempts rather than simply endorsing an MDD diagnosis had reduced levels of KYNA in the CSF when compared to HC (122). These studies evaluating KYNA showed largely no differences between study and control groups for either depressive-like behaviors or SB.

Several studies have also measured levels of the KYN pathway metabolite, QUIN, in the blood or CSF in patients with depression. Among these investigations, six studies identified no group differences in blood QUIN concentrations between depressed patients and HC (99, 100, 102, 105, 106, 115), while three found elevated levels of QUIN in patients with depression, with two reporting the finding after measuring QUIN levels in blood (91, 98) and another from measuring QUIN levels in CSF (120). A meta-analysis, which also reviewed the above studies, additionally revealed that blood QUIN levels were higher in the depressed group, although the effect size was small (115). Moreover, Bay-Richter and colleagues reported greater concentrations of CSF QUIN in patients with prior histories of suicide attempts compared to HC (122). A more recent study found a decreased ratio of CSF picolinic acid (PIC), an additional neuroprotective metabolite of the KYN pathway, to QUIN in subjects who attempted suicide relative to HC (117). These results indicate that a lower PIC/QUIN ratio could potentially represent a marker of suicidality; however, these results remain preliminary and await further research. Although the majority of investigations examining QUIN relevant to depression found no significant results, the studies that analyzed QUIN in relation to SB conversely reported findings that were significant when compared with HC.

To summarize, there have been many studies of blood or CSF markers of the KYN pathway that may relate to depression and/or SB. Of these studies, a number of them investigated metabolites of the KYN pathway (e.g., KYN, KYNA, QUIN) in relation to depression; however, most studies did not find significant results. Among studies that sampled patients with SB, results predominantly showed significant results, such as elevated levels of blood or CSF KYN/TRP ratio and CSF QUIN, indicating perhaps that the upregulation of the KYN pathway may be associated with suicidality. However, the number of studies evaluating this relationship was limited and more research is needed.

CONCLUSIONS

In the past decades, several theories have been proposed to conceptualize the etiology of SB; particularly, in recent years, many studies have focused on investigating the neurobiological aspects of this complex, multifactorial phenomenon. Through this review, we examined the original immunohistochemistry and neuroimaging studies that analyzed the relationship between microglial dysregulation and SB. Based on their results and proposed mechanisms, we were then able to construct a reconceptualized stress-diathesis theory of SB that incorporates the role of microglial activity. In our updated model, we suggest that chronic microglial activation may play a mediating role in the etiology of SB. That is, microglial dysregulation may be triggered by environmental challenges, namely psychosocial stressors, and then mediate several pathological neurobiological pathways that lead to behavioral changes and ultimately the outcome of SB.

The neurobiological pathways illustrated in this model predominantly involve dysfunction in the KYN pathway. As previously discussed, the results from studies, which evaluated the

concentrations and/or ratios of various metabolites of the KYN pathway, also showed that SB may be associated with KYN dysregulation. Such findings are consistent with the results and hypothesized mechanisms from studies of microglial over-activation in suicidality that were examined in this review; nevertheless, it should be noted that the number of studies measuring peripheral blood and/or CSF metabolite levels of the KYN pathway in patients with SB are highly limited at this time. Research that further investigates these metabolites in suicidal patients is, therefore, necessary. It would also behoove investigators to test the efficacy of currently available pharmacotherapeutics in normalizing KYN dysregulation in suicidal individuals.

We synthesized our updated clinical model of SB by evaluating the specific hypothesized neurobiological pathways discussed in the studies that were included in this review. However, advances in the fields of neurobiology and epigenetics have revealed that other mediating factors, namely HPA axis responsiveness, blunted cortisol, and oxytocin are also related to the outcome of SB (9, 11–14, 16, 17). These factors were not incorporated in our reconceptualized model but may be related to microglial dysregulation as well, thereby representing another area for which to conduct original research.

Also, it remains unclear whether microglial cells become primed due to early adverse experiences, thus making them more susceptible to prolonged activation in response to subsequent stressors later in life. In this case, we may speculate that chronic microglial activation would not only assume a role in instigating the diathesis for SB, which we outlined in **Figure 1**, but might provoke, later in time, the outcome of SB. In this case, future research, ideally from prospective or longitudinal study designs, is needed to definitively establish whether microglial dysregulation exclusively impacts the risk for developing the diathesis traits leading to SB or whether it also perpetuates SB at a later time in life.

All studies that were included in this review consisted of subjects who were either victims of suicide or participants who had suicidal thinking. None of the papers discussed the over-activation of microglia in relation to self-harming behavior, despite our inclusion of the keywords, "parasuicidal behavior", "self-harming behavior", and "self-harm". Considering this paucity of information, it would be interesting to determine, likely through neuroimaging research, whether there is also a positive relationship between microglial activity and self-harm, as well as to inform through an updated stress-diathesis model how self-harm subsequently relates to the risk for death by suicide.

In this review, we observed an overarching number of immunohistochemistry studies in comparison to the singular neuroimaging study. It appears that PET studies that can detect microglial activity, such as the aforementioned TSPO PET imaging, are in their infancy and require further research and refinements. The field of suicidology would benefit greatly by enhanced radioligands that have improved signal-to-noise ratio and lower nonspecific binding. Second- and third-generation radiotracers show promise for future research investigations as they do display these favorable properties. Accordingly, using such radiotracers can allow for more definitive conclusions to be made from studies that evaluate microglial cells through TSPO PET imaging. It would also enable scientists to perform clinical trials that test anti-inflammatory psychopharmacological medications, such as minocycline, on humans with SB *in vivo*. This work would be valuable for elucidating the role of neuroinflammation in SB as well as prospectively providing an accessible treatment option to individuals who are at high risk of death by suicide. To reiterate, however, as SB is a highly complex phenomenon, extensive future research is warranted to further refine our understanding of the neurobiology of these behaviors before a targeted psychopharmacological intervention may be established.

AUTHOR CONTRIBUTIONS

NJK conceived and designed the study, reviewed the full-text of three articles that were deemed questionable for eligibility by PB, and made revisions to the manuscript drafts. PB reviewed the titles and abstracts of studies following database searches as well as the full-text of select articles, drafted the manuscript, and made edits to the manuscript drafts. All authors contributed to the article and approved the submitted version.

FUNDING

This review article was funded by a Canadian Institutes of Health Research Clinician Scientist Salary Award and the Centre for Addiction and Mental Health Alternative Funding Plan, both awarded to NJK.

REFERENCES

1. Mann JJ, Waternaux C, Haas GL, Malone KM. Toward a clinical model of suicidal behavior in psychiatric patients. *Am J Psychiatry* (1999) 156(2):181–9. doi: 10.1176/ajp.156.2.181
2. Mann JJ. Neurobiology of suicidal behaviour. *Nat Rev Neurosci* (2003) 4 (10):819–28. doi: 10.1038/nrn1220
3. Benedetti F, Riccaboni R, Poletti S, Radaelli D, Locatelli C, Lorenzi C, et al. The serotonin transporter genotype modulates the relationship between early stress and adult suicidality in bipolar disorder. *Bipolar Disord* (2014) 16 (8):857–66. doi: 10.1111/bdi.12250
4. Gibb BE, McGeary JE, Beevers CG, Miller IW. Serotonin transporter (5-HTTLPR) genotype, childhood abuse, and suicide attempts in adult psychiatric inpatients. *Suicide Life Threat Behav* (2006) 36(6):687–93. doi: 10.1521/suli.2006.36.6.687
5. Roy A, Hu X-Z, Janal MN, Goldman D. Interaction between childhood trauma and serotonin transporter gene variation in suicide. *Neuropsychopharmacology* (2007) 32(9):2046–52. doi: 10.1038/sj.npp.1301331

6. Stanley M, Mann JJ. Increased serotonin-2 binding sites in frontal cortex of suicide victims. *Lancet* (1983) 321(8318):214–6. doi: 10.1016/S0140-6736(83)92590-4
7. Brodsky BS, Oquendo M, Ellis SP, Haas GL, Malone KM, Mann JJ. The relationship of childhood abuse to impulsivity and suicidal behavior in adults with major depression. *Am J Psychiatry* (2001) 158(11):1871–7. doi: 10.1176/appi.ajp.158.11.1871
8. Steinberg LJ, Mann JJ. Abnormal stress responsiveness and suicidal behavior: A risk phenotype. *Biomark Neuropsychiat* (2020) 10:100011. doi: 10.1016/j.bionps.2020.100011
9. O'Connor DB, Green JA, Ferguson E, O'Carroll RE, O'Connor RC. Effects of childhood trauma on cortisol levels in suicide attempters and ideators. *Psychoneuroendocrinology* (2018) 88:9–16. doi: 10.1016/j.psyneuen.2017.11.004
10. O'Connor DB, Green JA, Ferguson E, O'Carroll RE, O'Connor RC. Cortisol reactivity and suicidal behavior: Investigating the role of hypothalamic-pituitary-adrenal axis responses to stress in suicide attempters and ideators. *Psychoneuroendocrinology* (2017) 75:183–91. doi: 10.1016/j.psyneuen.2016.10.019
11. Melhem NM, Keilp JG, Porta G, Oquendo MA, Burke A, Stanley B, et al. Blunted HPA axis activity in suicide attempters compared to those at high risk for suicidal behavior. *Neuropsychopharmacology* (2016) 41(6):1447–56. doi: 10.1038/npp.2015.309
12. Roy A, Gorodetsky E, Yuan Q, Goldman D, Enoch M-A. Interaction of FKBP5, a stress-related gene, with childhood trauma increases the risk for attempting suicide. *Neuropsychopharmacology* (2010) 35(8):1674–83. doi: 10.1038/npp.2009.236
13. McGirr A, Diaconu G, Berlim MT, Pruessner JC, Sablé R, Cabot S, et al. Dysregulation of the sympathetic nervous system, hypothalamic–pituitary–adrenal axis and executive function in individuals at risk for suicide. *J Psychiatry Neurosci Jpn* (2010) 35(6):399–408. doi: 10.1503/jpn.090121
14. Pfennig A, Kunzel HE, Kern N, Ising M, Majer M, Fuchs B, et al. Hypothalamus-pituitary-adrenal system regulation and suicidal behavior in depression. *Biol Psychiatry* (2005) 57(4):336–42. doi: 10.1016/j.biopsych.2004.11.017
15. Turecki G, Ota VK, Belangero SI, Jackowski A, Kaufman J. Early life adversity, genomic plasticity, and psychopathology. *Lancet Psychiatry* (2014) 1(6):461–6. doi: 10.1016/S2215-0366(14)00022-4
16. Chatzittofis A, Nordström P, Uvnäs-Moberg K, Asberg M, Jokinen J. CSF and plasma oxytocin levels in suicide attempters, the role of childhood trauma and revictimization. *Neuro Endocrinol Lett* (2014) 35(3):213–7.
17. Stanley B, Siever LJ. The interpersonal dimension of borderline personality disorder: Toward a neuropeptide model. *Am J Psychiatry* (2010) 167(1):24–39. doi: 10.1176/appi.ajp.2009.09050744
18. Brodsky BS. Early childhood environment and genetic interactions: the diathesis for suicidal behavior. *Curr Psychiatry Rep* (2016) 18(9):86. doi: 10.1007/s11920-016-0716-z
19. Calcia MA, Bonsall DR, Bloomfield PS, Selvaraj S, Barichello T, Howes OD. Stress and neuroinflammation: a systematic review of the effects of stress on microglia and the implications for mental illness. *Psychopharmacol (Berl)* (2016) 233(9):1637–50. doi: 10.1007/s00213-016-4218-9
20. Mondelli V, Vernon AC, Turkheimer F, Dazzan P, Pariante CM. Brain microglia in psychiatric disorders. *Lancet Psychiatry* (2017) 4(7):563–72. doi: 10.1016/S2215-0366(17)30101-3
21. Tay TL, Béchade C, D'Andrea I, St-Pierre M-K, Henry MS, Roumier A, et al. Microglia gone rogue: Impacts on psychiatric disorders across the lifespan. *Front Mol Neurosci* (2017) 10:421. doi: 10.3389/fnmol.2017.00421
22. Yang I, Han SJ, Kaur G, Crane C, Parsa AT. The role of microglia in central nervous system immunity and glioma immunology. *J Clin Neurosci Off J Neurosurg Soc Australas* (2010) 17(1):6–10. doi: 10.1016/j.jocn.2009.05.006
23. Howes OD, McCutcheon R. Inflammation and the neural diathesis-stress hypothesis of schizophrenia: a reconceptualization. *Transl Psychiatry* (2017) 7(2):e1024–4. doi: 10.1038/tp.2016.278
24. Ransohoff RM. A polarizing question: do M1 and M2 microglia exist? *Nat Neurosci* (2016) 19(8):987–91. doi: 10.1038/nn.4338
25. Wohleb ES, Hanke ML, Corona AW, Powell ND, Stiner LM, Bailey MT, et al. β-Adrenergic receptor antagonism prevents anxiety-like behavior and microglial reactivity induced by repeated social defeat. *J Neurosci* (2011) 31(17):6277–88. doi: 10.1523/JNEUROSCI.0450-11.2011
26. Wohleb ES, Fenn AM, Pacenta AM, Powell ND, Sheridan JF, Godbout JP. Peripheral innate immune challenge exaggerated microglia activation, increased the number of inflammatory CNS macrophages, and prolonged social withdrawal in socially defeated mice. *Psychoneuroendocrinology* (2012) 37(9):1491–505. doi: 10.1016/j.psyneuen.2012.02.003
27. Ferle V, Repouskou A, Aspiotis G, Raftogianni A, Chrousos G, Stylianopoulou F, et al. Synergistic effects of early life mild adversity and chronic social defeat on rat brain microglia and cytokines. *Physiol Behav* (2020) 215:112791. doi: 10.1016/j.physbeh.2019.112791
28. Bian Y, Pan Z, Hou Z, Huang C, Li W, Zhao B. Learning, memory, and glial cell changes following recovery from chronic unpredictable stress. *Brain Res Bull* (2012) 88(5):471–6. doi: 10.1016/j.brainresbull.2012.04.008
29. Horchar MJ, Wohleb ES. Glucocorticoid receptor antagonism prevents microglia-mediated neuronal remodeling and behavioral despair following chronic unpredictable stress. *Brain Behav Immun* (2019) 81:329–40. doi: 10.1016/j.bbi.2019.06.030
30. Ślusarczyk J, Trojan E, Głombik K, Budziszewska B, Kubera M, Lasoń W, et al. Prenatal stress is a vulnerability factor for altered morphology and biological activity of microglia cells. *Front Cell Neurosci* (2015) 9:82. doi: 10.3389/fncel.2015.00082
31. Couch Y, Anthony DC, Dolgov O, Revischin A, Festoff B, Santos AI, et al. Microglial activation, increased TNF and SERT expression in the prefrontal cortex define stress-altered behaviour in mice susceptible to anhedonia. *Brain Behav Immun* (2013) 29:136–46. doi: 10.1016/j.bbi.2012.12.017
32. Kopp BL, Wick D, Herman JP. Differential effects of homotypic vs. heterotypic chronic stress regimens on microglial activation in the prefrontal cortex. *Physiol Behav* (2013) 122:246–52. doi: 10.1016/j.physbeh.2013.05.030
33. Wohleb ES, Terwilliger R, Duman CH, Duman RS. Stress-induced neuronal colony stimulating factor 1 provokes microglia-mediated neuronal remodeling and depressive-like behavior. *Biol Psychiatry* (2018) 83(1):38–49. doi: 10.1016/j.biopsych.2017.05.026
34. Hinwood M, Morandini J, Day TA, Walker FR. Evidence that microglia mediate the neurobiological effects of chronic psychological stress on the medial prefrontal cortex. *Cereb Cortex* (2012) 22(6):1442–54. doi: 10.1093/cercor/bhr229
35. Hinwood M, Tynan RJ, Charnley JL, Beynon SB, Day TA, Walker FR. Chronic stress induced remodeling of the prefrontal cortex: Structural re-organization of microglia and the inhibitory effect of minocycline. *Cereb Cortex* (2013) 23(8):1784–97. doi: 10.1093/cercor/bhs151
36. Tynan RJ, Naicker S, Hinwood M, Nalivaiko E, Buller KM, Pow DV, et al. Chronic stress alters the density and morphology of microglia in a subset of stress-responsive brain regions. *Brain Behav Immun* (2010) 24(7):1058–68. doi: 10.1016/j.bbi.2010.02.001
37. Schiavone S, Sorce S, Dubois-Dauphin M, Jaquet V, Colaianna M, Zotti M, et al. Involvement of NOX2 in the development of behavioral and pathologic alterations in isolated rats. *Biol Psychiatry* (2009) 66(4):384–92. doi: 10.1016/j.biopsych.2009.04.033
38. Giovanoli S, Engler H, Engler A, Richetto J, Voget M, Willi R, et al. Stress in puberty unmasks latent neuropathological consequences of prenatal immune activation in mice. *Science* (2013) 339(6123):1095–9. doi: 10.1126/science.1228261
39. Kreisel T, Frank MG, Licht T, Reshef R, Ben-Menachem-Zidon O, Baratta MV, et al. Dynamic microglial alterations underlie stress-induced depressive-like behavior and suppressed neurogenesis. *Mol Psychiatry* (2014) 19(6):699–709. doi: 10.1038/mp.2013.155
40. Tong L, Gong Y, Wang P, Hu W, Wang J, Chen Z, et al. Microglia loss contributes to the development of major depression induced by different types of chronic stresses. *Neurochem Res* (2017) 42(10):2698–711. doi: 10.1007/s11064-017-2270-4
41. Brevet M, Kojima H, Asakawa A, Atsuchi K, Ushikai M, Ataka K, et al. Chronic foot-shock stress potentiates the influx of bone marrow-derived microglia into hippocampus. *J Neurosci Res* (2010) 88(9):1890–7. doi: 10.1002/jnr.22362
42. Diz-Chaves Y, Astiz M, Bellini MJ, Garcia-Segura LM. Prenatal stress increases the expression of proinflammatory cytokines and exacerbates the inflammatory response to LPS in the hippocampal formation of adult male mice. *Brain Behav Immun* (2013) 28:196–206. doi: 10.1016/j.bbi.2012.11.013

43. Diz-Chaves Y, Pernía O, Carrero P, Garcia-Segura LM. Prenatal stress causes alterations in the morphology of microglia and the inflammatory response of the hippocampus of adult female mice. *J Neuroinflamm* (2012) 9(1):71. doi: 10.1186/1742-2094-9-71
44. Kojo A, Yamada K, Kubo K-Y, Yamashita A, Yamamoto T. Occlusal disharmony in mice transiently activates microglia in hippocampal CA1 region but not in dentate gyrus. *Tohoku J Exp Med* (2010) 221(3):237–43. doi: 10.1620/tjem.221.237
45. Park JH, Yoo K-Y, Lee CH, Kim IH, Shin BN, Choi JH, et al. Comparison of glucocorticoid receptor and ionized calcium-binding adapter molecule 1 immunoreactivity in the adult and aged gerbil hippocampus following repeated restraint stress. *Neurochem Res* (2011) 36(6):1037–45. doi: 10.1007/s11064-011-0444-z
46. Yoo K-Y, Lee CH, Park JH, Hwang IK, Park OK, Kwon S-H, et al. Antioxidant enzymes are differently changed in experimental ischemic hippocampal CA1 region following repeated restraint stress. *J Neurol Sci* (2011) 302(1):33–42. doi: 10.1016/j.jns.2010.12.006
47. McKim DB, Niraula A, Tarr AJ, Wohleb ES, Sheridan JF, Godbout JP. Neuroinflammatory dynamics underlie memory impairments after repeated social defeat. *J Neurosci* (2016) 36(9):2590–604. doi: 10.1523/JNEUROSCI.2394-15.2016
48. Hollis F, Kabbaj M. Social defeat as an animal model for depression. *ILAR J* (2014) 55(2):221–32. doi: 10.1093/ilar/ilu002
49. Hollis F, Wang H, Dietz D, Gunjan A, Kabbaj M. The effects of repeated social defeat on long-term depressive-like behavior and short-term histone modifications in the hippocampus in male Sprague–Dawley rats. *Psychopharmacol (Berl)* (2010) 211(1):69–77. doi: 10.1007/s00213-010-1869-9
50. Rygula R, Abumaria N, Flügge G, Fuchs E, Rüther E, Havemann-Reinecke U. Anhedonia and motivational deficits in rats: Impact of chronic social stress. *Behav Brain Res* (2005) 162(1):127–34. doi: 10.1016/j.bbr.2005.03.009
51. Toyoda A. Social defeat models in animal science: What we have learned from rodent models. *Anim Sci J* (2017) 88(7):944–52. doi: 10.1111/asj.12809
52. Wang Y-L, Han Q-Q, Gong W-Q, Pan D-H, Wang L-Z, Hu W, et al. Microglial activation mediates chronic mild stress-induced depressive- and anxiety-like behavior in adult rats. *J Neuroinflamm* (2018) 15(1):21. doi: 10.1186/s12974-018-1054-3
53. Lehmann ML, Cooper HA, Maric D, Herkenham M. Social defeat induces depressive-like states and microglial activation without involvement of peripheral macrophages. *J Neuroinflamm* (2016) 13(1):224. doi: 10.1186/s12974-016-0672-x
54. Ramirez K, Niraula A, Sheridan JF. GABAergic modulation with classical benzodiazepines prevent stress-induced neuro-immune dysregulation and behavioral alterations. *Brain Behav Immun* (2016) 51:154–68. doi: 10.1016/j.bbi.2015.08.011
55. Ramirez K, Sheridan JF. Antidepressant imipramine diminishes stress-induced inflammation in the periphery and central nervous system and related anxiety- and depressive- like behaviors. *Brain Behav Immun* (2016) 57:293–303. doi: 10.1016/j.bbi.2016.05.008
56. Brachman RA, Lehmann ML, Maric D, Herkenham M. Lymphocytes from chronically stressed mice confer antidepressant-like effects to naive mice. *J Neurosci* (2015) 35(4):1530–8. doi: 10.1523/JNEUROSCI.2278-14.2015
57. Stein DJ, Vasconcelos MF, Albrechet-Souza L, Ceresér KMM, de Almeida RMM. Microglial over-activation by social defeat stress contributes to anxiety- and depressive-like behaviors. *Front Behav Neurosci* (2017) 11:207. doi: 10.3389/fnbeh.2017.00207
58. Preti A. Suicide among animals: A review of evidence. *Psychol Rep* (2007) 101(3):831–48. doi: 10.2466/pr0.101.3.831-848
59. Preti A. Animal model and neurobiology of suicide. *Prog Neuropsychopharmacol Biol Psychiatry* (2011) 35(4):818–30. doi: 10.1016/j.pnpbp.2010.10.027
60. Steiner J, Bielau H, Brisch R, Danos P, Ullrich O, Mawrin C, et al. Immunological aspects in the neurobiology of suicide: Elevated microglial density in schizophrenia and depression is associated with suicide. *J Psychiatr Res* (2008) 42(2):151–7. doi: 10.1016/j.jpsychires.2006.10.013
61. Torres-Platas SG, Cruceanu C, Chen GG, Turecki G, Mechawar N. Evidence for increased microglial priming and macrophage recruitment in the dorsal anterior cingulate white matter of depressed suicides. *Brain Behav Immun* (2014) 42:50–9. doi: 10.1016/j.bbi.2014.05.007
62. Steiner J, Walter M, Gos T, Guillemin GJ, Bernstein H-G, Sarnyai Z, et al. Severe depression is associated with increased microglial quinolinic acid in subregions of the anterior cingulate gyrus: Evidence for an immune-modulated glutamatergic neurotransmission? *J Neuroinflamm* (2011) 8(1):1–9. doi: 10.1016/j.npbr.2012.02.043
63. Schnieder TP, Trencevska I, Rosoklija G, Stankov A, Mann JJ, Smiley J, et al. Microglia of prefrontal white matter in suicide. *J Neuropathol Exp Neurol* (2014) 73(9):880–90. doi: 10.1097/NEN.0000000000000107
64. Schiavone S, Neri M, Mhillaj E, Morgese MG, Cantatore S, Bove M, et al. The NADPH oxidase NOX2 as a novel biomarker for suicidality: Evidence from human post mortem brain samples. *Transl Psychiatry* (2016) 6(5):e813. doi: 10.1038/tp.2016.76
65. Steiner J, Mawrin C, Ziegeler A, Bielau H, Ullrich O, Bernstein H-G, et al. Distribution of HLA-DR-positive microglia in schizophrenia reflects impaired cerebral lateralization. *Acta Neuropathol (Berl)* (2006) 112(3):305–16. doi: 10.1007/s00401-006-0090-8
66. Moher D. Preferred reporting items for systematic reviews and meta-analyses: The PRISMA statement. *Ann Intern Med* (2009) 151(4):264. doi: 10.7326/0003-4819-151-4-200908180-00135
67. Ferrer I, Martinez A, Boluda S, Parchi P, Barrachina M. Brain banks: benefits, limitations and cautions concerning the use of post-mortem brain tissue for molecular studies. *Cell Tissue Bank* (2008) 9(3):181. doi: 10.1007/s10561-008-9077-0
68. Busse M, Busse S, Myint AM, Gos T, Dobrowolny H, Müller UJ, et al. Decreased quinolinic acid in the hippocampus of depressive patients: evidence for local anti-inflammatory and neuroprotective responses? *Eur Arch Psychiatry Clin Neurosci* (2015) 265(4):321–9. doi: 10.1007/s00406-014-0562-0
69. Brisch R, Steiner J, Mawrin C, Krzyżanowska M, Jankowski Z, Gos T. Microglia in the dorsal raphe nucleus plays a potential role in both suicide facilitation and prevention in affective disorders. *Eur Arch Psychiatry Clin Neurosci* (2017) 267(5):403–15. doi: 10.1007/s00406-017-0774-1
70. Turkheimer FE, Rizzo G, Bloomfield PS, Howes O, Zanotti-Fregonara P, Bertoldo A, et al. The methodology of TSPO imaging with positron emission tomography. *Biochem Soc Trans* (2015) 43(4):586–92. doi: 10.1042/BST20150058
71. Holmes SE, Hinz R, Conen S, Gregory CJ, Matthews JC, Anton-Rodriguez JM, et al. Elevated translocator protein in anterior cingulate in major depression and a role for inflammation in suicidal thinking: A positron emission tomography study. *Biol Psychiatry* (2018) 83(1):61–9. doi: 10.1016/j.biopsych.2017.08.005
72. Rupprecht R, Papadopoulos V, Rammes G, Baghai TC, Fan J, Akula N, et al. Translocator protein (18 kDa) (TSPO) as a therapeutic target for neurological and psychiatric disorders. *Nat Rev Drug Discovery* (2010) 9(12):971–88. doi: 10.1038/nrd3295
73. Lavisse S, Guillermier M, Herard A-S, Petit F, Delahaye M, Van Camp N, et al. Reactive astrocytes overexpress TSPO and are detected by TSPO positron emission tomography imaging. *J Neurosci* (2012) 32(32):10809–18. doi: 10.1523/JNEUROSCI.1487-12.2012
74. Mizrahi R, Rusjan PM, Kennedy J, Pollock B, Mulsant B, Suridjan I, et al. Translocator protein (18 kDa) polymorphism (rs6971) explains in-vivo brain binding affinity of the PET radioligand [18F]-FEPPA. *J Cereb Blood Flow Metab* (2012) 32(6):968–72. doi: 10.1038/jcbfm.2012.46
75. Chauveau F, Boutin H, Van Camp N, Dollé F, Tavitian B. Nuclear imaging of neuroinflammation: a comprehensive review of [11C]PK11195 challengers. *Eur J Nucl Med Mol Imag* (2008) 35(12):2304–19. doi: 10.1007/s00259-008-0908-9
76. Wilson AA, Garcia A, Parkes J, McCormick P, Stephenson KA, Houle S, et al. Radiosynthesis and initial evaluation of [18F]-FEPPA for PET imaging of peripheral benzodiazepine receptors. *Nucl Med Biol* (2008) 35(3):305–14. doi: 10.1016/j.nucmedbio.2007.12.009
77. Fujimura Y, Zoghbi SS, Simèon FG, Taku A, Pike VW, Innis RB, et al. Quantification of translocator protein (18 kDa) in the human brain with PET and a novel radioligand, 18F-PBR06. *J Nucl Med* (2009) 50(7):1047–53. doi: 10.2967/jnumed.108.060186

78. Fujimura Y, Ikoma Y, Yasuno F, Suhara T, Ota M, Matsumoto R, et al. Quantitative analyses of 18F-FEDAA1106 binding to peripheral benzodiazepine receptors in living human brain. *J Nucl Med* (2006) 47(1):43–50.
79. Ikoma Y, Yasuno F, Ito H, Suhara T, Ota M, Toyama H, et al. Quantitative analysis for estimating binding potential of the peripheral benzodiazepine receptor with [11C]DAA1106. *J Cereb Blood Flow Metab* (2007) 27(1):173–84. doi: 10.1038/sj.jcbfm.9600325
80. Boutin H, Chauveau F, Thominiaux C, Grégoire M-C, James ML, Trebossen R, et al. 11C-DPA-713: A novel peripheral benzodiazepine receptor PET ligand for in vivo imaging of neuroinflammation. *J Nucl Med* (2007) 48 (4):573–81. doi: 10.2967/jnumed.106.036764
81. Fookes CJR, Pham TQ, Mattner F, Greguric I, Loc'h C, Liu X, et al. Synthesis and biological evaluation of substituted [18F]Imidazo[1,2-a]pyridines and [18F]Pyrazolo[1,5-a]pyrimidines for the study of the peripheral benzodiazepine receptor using positron emission tomography. *J Med Chem* (2008) 51(13):3700–12. doi: 10.1021/jm7014556
82. Arlicot N, Vercouillie J, Ribeiro M-J, Tauber C, Venel Y, Baulieu J-L, et al. Initial evaluation in healthy humans of [18F]DPA-714, a potential PET biomarker for neuroinflammation. *Nucl Med Biol* (2012) 39(4):570–8. doi: 10.1016/j.nucmedbio.2011.10.012
83. Fujita M, Imaizumi M, Zoghbi SS, Fujimura Y, Farris AG, Suhara T, et al. Kinetic analysis in healthy humans of a novel positron emission tomography radioligand to image the peripheral benzodiazepine receptor, a potential biomarker for inflammation. *NeuroImage* (2008) 40(1):43–52. doi: 10.1016/j.neuroimage.2007.11.011
84. Best L, Ghadery C, Pavese N, Tai YF, Strafella AP. New and old TSPO PET radioligands for imaging brain microglial activation in neurodegenerative Disease. *Curr Neurol Neurosci Rep* (2019) 19(5):24. doi: 10.1007/s11910-019-0934-y
85. Dupont A-C, Largeau B, Santiago Ribeiro MJ, Guilloteau D, Tronel C, Arlicot N. Translocator protein-18 kDa (TSPO) positron emission tomography (PET) imaging and its clinical impact in neurodegenerative diseases. *Int J Mol Sci* (2017) 18(4):785. doi: 10.3390/ijms18040785
86. Lapin IP, Oxenkrug GF. Intensification of the central serotonergic processes as a possible determinant of the thymoleptic effect. *Lancet* (1969) 18293 (7586):132–6. doi: 10.1016/S0140-6736(69)91140-4
87. Oxenkrug GF. Tryptophan–kynurenine metabolism as a common mediator of genetic and environmental impacts in major depressive disorder: the serotonin hypothesis revisited 40 years later. *Isr J Psychiatry Relat Sci* (2010) 47(1):56–63 doi: 10.3410/f.13356987.14726252
88. Bryleva EY, Brundin L. Kynurenine pathway metabolites and suicidality. *Neuropharmacology* (2017) 112:324–30. doi: 10.1016/j.neuropharm.2016.01.034
89. Dantzer R, Walker AK. Is there a role for glutamate-mediated excitotoxicity in inflammation-induced depression? *J Neural Transm* (2014) 121(8):925–32. doi: 10.1007/s00702-014-1187-1
90. Achtyes E, Keaton SA, Smart L, Burmeister AR, Heilman PL, Krzyzanowski S, et al. Inflammation and kynurenine pathway dysregulation in post-partum women with severe and suicidal depression. *Brain Behav Immun* (2020) 83:239–47. doi: 10.1016/j.bbi.2019.10.017
91. Savitz J, Drevets WC, Wurfel BE, Ford BN, Bellgowan PSF, Victor TA, et al. Reduction of kynurenic acid to quinolinic acid ratio in both the depressed and remitted phases of major depressive disorder. *Brain Behav Immun* (2015) 46:55–9. doi: 10.1016/j.bbi.2015.02.007
92. Brundin L, Bryleva EY, Thirtamara Rajamani K. Role of inflammation in suicide: From mechanisms to treatment. *Neuropsychopharmacology* (2017) 42(1):271–83. doi: 10.1038/npp.2016.116
93. Schwarcz R, Guidetti P, Sathyasaikumar KV, Muchowski PJ. Of mice, rats and men: Revisiting the quinolinic acid hypothesis of Huntington's disease. *Prog Neurobiol* (2010) 90(2):230–45. doi: 10.1016/j.pneurobio.2009.04.005
94. Guillemin GJ. Quinolinic acid, the inescapable neurotoxin. *FEBS J* (2012), 279(8):1356–65. doi: 10.1111/j.1742-4658.2012.08485.x
95. Brundin L, Erhardt S, Bryleva EY, Achtyes ED, Postolache TT. The role of inflammation in suicidal behaviour. *Acta Psychiatr Scand* (2015) 132 (3):192–203. doi: 10.1111/acps.12458
96. Dantzer R, O'Connor JC, Lawson MA, Kelley KW. Inflammation-associated depression: From serotonin to kynurenine. *Psychoneuroendocrinology* (2011) 36(3):426–36. doi: 10.1016/j.psyneuen.2010.09.012
97. Stone TW, Forrest CM, Darlington LG. Kynurenine pathway inhibition as a therapeutic strategy for neuroprotection. *FEBS J* (2012) 279(8):1386–97. doi: 10.1111/j.1742-4658.2012.08487.x
98. Young KD, Drevets WC, Dantzer R, Teague TK, Bodurka J, Savitz J. Kynurenine pathway metabolites are associated with hippocampal activity during autobiographical memory recall in patients with depression. *Brain Behav Immun* (2016) 56:335–42. doi: 10.1016/j.bbi.2016.04.007
99. Cho HJ, Savitz J, Dantzer R, Teague TK, Drevets WC, Irwin MR. Sleep disturbance and kynurenine metabolism in depression. *J Psychosom Res* (2017) 99:1–7. doi: 10.1016/j.jpsychores.2017.05.016
100. Dahl J, Andreassen OA, Verkerk R, Malt UF, Sandvik L, Brundin L, et al. Ongoing episode of major depressive disorder is not associated with elevated plasma levels of kynurenine pathway markers. *Psychoneuroendocrinology* (2015) 56:12–22. doi: 10.1016/j.psyneuen.2015.02.011
101. Maes M, Galecki P, Verkerk R, Rief W. Somatization, but not depression, is characterized by disorders in the tryptophan catabolite (TRYCAT) pathway, indicating increased indoleamine 2,3-dioxygenase and lowered kynurenine aminotransferase activity. *Neuroendocrinol Lett* (2011) 32 (3):264–73.
102. Meier TB, Drevets WC, Wurfel BE, Ford BN, Morris HM, Victor TA, et al. Relationship between neurotoxic kynurenine metabolites and reductions in right medial prefrontal cortical thickness in major depressive disorder. *Brain Behav Immun* (2016) 53:39–48. doi: 10.1016/j.bbi.2015.11.003
103. Møller SE, Kirk L, Honoré P. Tryptophan tolerance and metabolism in endogenous depression. *Psychopharmacol (Berl)* (1982) 76(1):79–83. doi: 10.1007/BF00430761
104. Myint A-M, Kim YK, Verkerk R, Scharpé S, Steinbusch H, Leonard B. Kynurenine pathway in major depression: Evidence of impaired neuroprotection. *J Affect Disord* (2007) 98(1):143–51. doi: 10.1016/j.jad.2006.07.013
105. Savitz J, Dantzer R, Meier TB, Wurfel BE, Victor TA, McIntosh SA, et al. Activation of the kynurenine pathway is associated with striatal volume in major depressive disorder. *Psychoneuroendocrinology* (2015) 62:54–8. doi: 10.1016/j.psyneuen.2015.07.609
106. Savitz J, Drevets WC, Smith CM, Victor TA, Wurfel BE, Bellgowan PS, et al. Putative neuroprotective and neurotoxic kynurenine pathway metabolites are associated with hippocampal and amygdalar volumes in subjects with major depressive disorderr. *Neuropsychopharmacology* (2015) 40(2):463–71. doi: 10.1038/npp.2014.194
107. Sublette ME, Galfalvy HC, Fuchs D, Lapidus M, Grunebaum MF, Oquendo MA, et al. Plasma kynurenine levels are elevated in suicide attempters with major depressive disorder. *Brain Behav Immun* (2011) 25(6):1272–8. doi: 10.1016/j.bbi.2011.05.002
108. Hu L-J, Li X-F, Hu J-Q, Ni X-J, Lu H-Y, Wang J-J, et al. A simple HPLC–MS/MS method for determination of tryptophan, kynurenine and kynurenic acid in human serum and its potential for monitoring antidepressant therapy. *J Anal Toxicol* (2017) 41(1):37–44. doi: 10.1093/jat/bkw071
109. Krause D, Myint A-M, Schuett C, Musil R, Dehning S, Cerovecki A, et al. High kynurenine (a tryptophan metabolite) predicts remission in patients with major depression to add-on treatment with celecoxib. *Front Psychiatry* (2017) 8:16. doi: 10.3389/fpsyt.2017.00016
110. Veen C, Myint AM, Burgerhout KM, Schwarz MJ, Schütze G, Kushner SA, et al. Tryptophan pathway alterations in the postpartum period and in acute postpartum psychosis and depression. *J Affect Disord* (2016) 189:298–305. doi: 10.1016/j.jad.2015.09.064
111. Nikkheslat N, Zunszain PA, Horowitz MA, Barbosa IG, Parker JA, Myint A-M, et al. Insufficient glucocorticoid signaling and elevated inflammation in coronary heart disease patients with comorbid depression. *Brain Behav Immun* (2015) 48:8–18. doi: 10.1016/j.bbi.2015.02.002
112. Hennings A, Schwarz MJ, Riemer S, Stapf TM, Selberdinger VB, Rief W. Exercise affects symptom severity but not biological measures in depression and somatization – Results on IL-6, neopterin, tryptophan, kynurenine and 5-HIAA. *Psychiatry Res* (2013) 210(3):925–33. doi: 10.1016/j.psychres.2013.09.018
113. Quak J, Doornbos B, Roest AM, Duivis HE, Vogelzangs N, Nolen WA, et al. Does tryptophan degradation along the kynurenine pathway mediate the association between pro-inflammatory immune activity and depressive symptoms? *Psychoneuroendocrinology* (2014) 45:202–10. doi: 10.1016/j.psyneuen.2014.03.013

114. Setoyama D, Kato TA, Hashimoto R, Kunugi H, Hattori K, Hayakawa K, et al. Plasma metabolites predict severity of depression and suicidal ideation in psychiatric patients-a multicenter pilot analysis. *PloS One* (2016) 11(12): e0165267. doi: 10.1371/journal.pone.0165267
115. Ogyu K, Kubo K, Noda Y, Iwata Y, Tsugawa S, Omura Y, et al. Kynurenine pathway in depression: A systematic review and meta-analysis. *Neurosci Biobehav Rev* (2018) 90:16–25. doi: 10.1016/j.neubiorev.2018.03.023
116. Bradley KAL, Case JAC, Khan O, Ricart T, Hanna A, Alonso CM, et al. The role of the kynurenine pathway in suicidality in adolescent major depressive disorder. *Psychiatry Res* (2015) 227(2):206–12. doi: 10.1016/j.psychres.2015.03.031
117. Brundin L, Sellgren CM, Lim CK, Grit J, Pålsson E, Landén M, et al. An enzyme in the kynurenine pathway that governs vulnerability to suicidal behavior by regulating excitotoxicity and neuroinflammation. *Transl Psychiatry* (2016) 6(8):e865–5. doi: 10.1038/tp.2016.133
118. Clark SM, Pocivavsek A, Nicholson JD, Notarangelo FM, Langenberg P, McMahon RP, et al. Reduced kynurenine pathway metabolism and cytokine expression in the prefrontal cortex of depressed individuals. *J Psychiatry Neurosci* (2016) 41(6):386–94. doi: 10.1503/jpn.150226
119. Krause DL, Riedel M, Müller N, Weidinger E, Schwarz MJ, Myint A-M. Effects of antidepressants and cyclooxygenase-2 inhibitor on cytokines and kynurenines in stimulated in vitro blood culture from depressed patients. *Inflammopharmacology* (2012) 20(3):169–76. doi: 10.1007/s10787-011-0112-6
120. Erhardt S, Lim CK, Linderholm KR, Janelidze S, Lindqvist D, Samuelsson M, et al. Connecting inflammation with glutamate agonism in suicidality. *Neuropsychopharmacology* (2013) 38(5):743–52. doi: 10.1038/npp.2012.248
121. Schwieler L, Samuelsson M, Frye MA, Bhat M, Schuppe-Koistinen I, Jungholm O, et al. Electroconvulsive therapy suppresses the neurotoxic branch of the kynurenine pathway in treatment-resistant depressed patients. *J Neuroinflamm* (2016) 13(1):51. doi: 10.1186/s12974-016-0517-7
122. Bay-Richter C, Linderholm KR, Lim CK, Samuelsson M, Träskman-Bendz L, Guillemin GJ, et al. A role for inflammatory metabolites as modulators of the glutamate N-methyl-d-aspartate receptor in depression and suicidality. *Brain Behav Immun* (2015) 43:110–7. doi: 10.1016/j.bbi.2014.07.012

Conflict of Interest: The authors declare that the research was conducted in the absence of any commercial or financial relationships that could be construed as a potential conflict of interest.

frontiers in Pharmacology

REVIEW
published: 14 August 2020
doi: 10.3389/fphar.2020.01270

Alleviation of Depression by Glucagon-Like Peptide 1 Through the Regulation of Neuroinflammation, Neurotransmitters, Neurogenesis, and Synaptic Function

Young-Kook Kim[1], *Oh Yoen Kim*[2,3]* *and Juhyun Song*[4]*

[1] Department of Biochemistry, Chonnam National University Medical School, Hwasun, South Korea, [2] Department of Food Science and Nutrition, Dong-A University, Busan, South Korea, [3] Center for Silver-targeted Biomaterials, Brain Busan 21 Plus Program, Graduate School, Dong-A University, Busan, South Korea, [4] Department of Anatomy, Chonnam National University Medical School, Hwasun, South Korea

OPEN ACCESS

Edited by:
Bart Ellenbroek,
Victoria University of Wellington,
New Zealand

Reviewed by:
Victor Gault,
Ulster University, United Kingdom
Cesare Patrone,
Karolinska Institutet (KI), Sweden

***Correspondence:**
Oh Yoen Kim
oykim@dau.ac.kr
Juhyun Song
juhyunsong@chonnam.ac.kr

Specialty section:
This article was submitted to Neuropharmacology, a section of the journal Frontiers in Pharmacology

Received: 08 May 2020
Accepted: 31 July 2020
Published: 14 August 2020

Citation:
Kim Y-K, Kim OY and Song J (2020) Alleviation of Depression by Glucagon-Like Peptide 1 Through the Regulation of Neuroinflammation, Neurotransmitters, Neurogenesis, and Synaptic Function. Front. Pharmacol. 11:1270. doi: 10.3389/fphar.2020.01270

Depression has emerged as a major cause of mortality globally. Many studies have reported risk factors and mechanisms associated with depression, but it is as yet unclear how these findings can be applied to the treatment and prevention of this disorder. The onset and recurrence of depression have been linked to diverse metabolic factors, including hyperglycemia, dyslipidemia, and insulin resistance. Recent studies have suggested that depression is accompanied by memory loss as well as depressive mood. Thus, many researchers have highlighted the relationship between depressive behavior and metabolic alterations from various perspectives. Glucagon-like peptide-1 (GLP-1), which is secreted from gut cells and hindbrain areas, has been studied in metabolic diseases such as obesity and diabetes, and was shown to control glucose metabolism and insulin resistance. Recently, GLP-1 was highlighted as a regulator of diverse pathways, but its potential as the therapeutic target of depressive disorder was not described comprehensively. Therefore, in this review, we focused on the potential of GLP-1 modulation in depression.

Keywords: depression, glucagon-like peptide-1 (GLP-1), neuroinflammation, neurogenesis, synaptic plasticity

INTRODUCTION

Depression is emerging as one of the main causes of morbidity and mortality globally, and the number of individuals reported to be afflicted with the disorder continues to increase (Ledford, 2014; Gerhard et al., 2016). Even though extensive research has been conducted, depression remains incompletely understood owing to the scarcity of biomarkers and the heterogeneity of precipitating causes, such as chronic stress (Kessler et al., 2005; Krishnan and Nestler, 2008). A recent study investigated the relationship between depression and metabolism, and found that metabolites, such as advanced glycation end products, in patients with depression are altered compared to those in controls (Setoyama et al., 2016; Akimoto et al., 2019).

Glucagon-like peptide-1 (GLP-1) is a peptide hormone primarily synthesized in the gut that circulates through the blood, and plays a critical role in the regulation of glucose metabolism in the gut-brain axis. GLP-1 is also secreted by a small population of neurons in the hindbrain (Richard et al., 2015). GLP-1 receptors (GLP-1Rs) are distributed across various organs including the pancreas, lung, stomach, intestine, kidney, heart, and diverse brain regions (Bullock et al., 1996; Li et al., 2009; Campbell and Drucker, 2013; Heppner et al., 2015a).

In the central nervous system (CNS), GLP-1 and GLP-1R agonists are diffused into the cerebrospinal fluid (CSF) and the brain as demonstrated in rodent models (Wang et al., 2015), and increased GLP-1 concentration in the brain is thought to influence brain function in the hippocampus (Kastin et al., 2002; Kastin and Akerstrom, 2003; McClean et al., 2010; Hunter and Holscher, 2012). Glucose-insulin metabolic homeostasis is important for the gut-brain axis because glucose is used as the main source of energy in the brain (Weber, 2016). Major incretins such as GLP-1 and GIP can control appetite by reducing feelings of hunger and by increasing satiety and have a regulatory effect on glucose homeostasis through the reduction of blood glucose levels and insulin release (**Figure 1**) (Edholm et al., 2010; Duarte et al., 2013).

Although previous studies have demonstrated that GLP-1 has positive effects on attenuating neuropathology, its function and specific actions in CNS diseases have not been reviewed comprehensively. Here, we review the therapeutic effects of GLP-1 on depression from a variety of perspectives and highlight the promising, beneficial roles of GLP-1 as the therapeutic regulator of impaired neurogenesis, neuroinflammation, imbalance of neurotransmitter secretion, and synaptic dysfunction in the depressive brain.

WHAT IS GLP-1?

GLP-1 is a 30 amino acid-long peptide hormone mainly produced in the intestinal L-cells of the gut that is secreted into the blood (**Figure 1**) (Habib et al., 2013; Richard et al., 2015). GLP-1 is also secreted from microglia (Kappe et al., 2012) and specific neurons of the nucleus tractus solitarius (NTS)

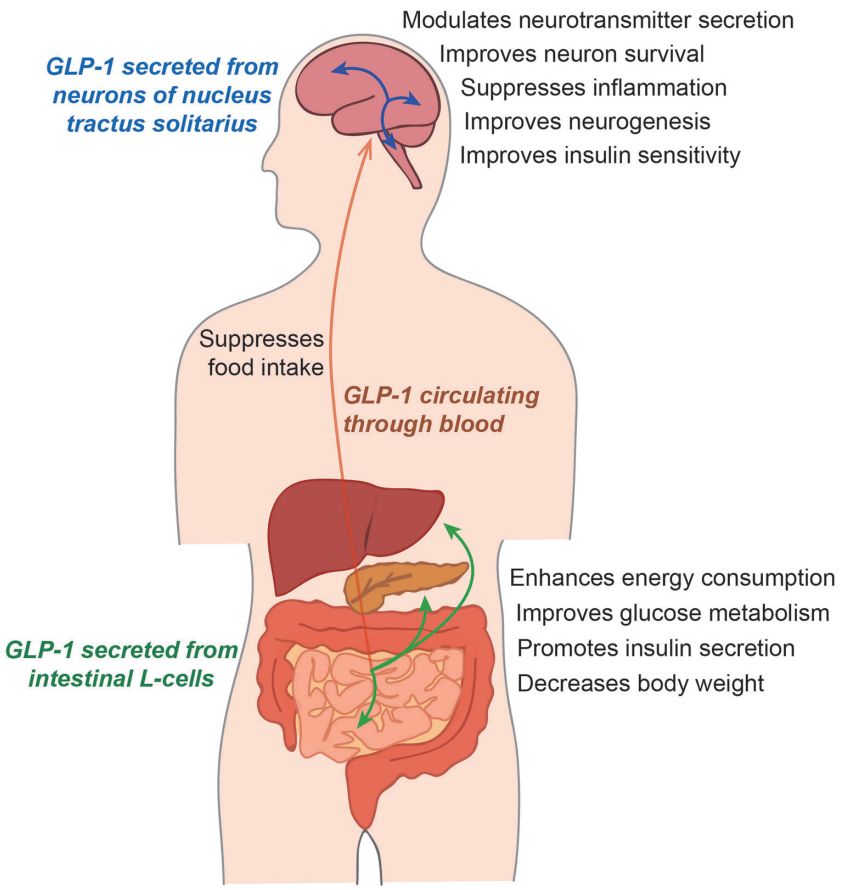

FIGURE 1 | The function of glucagon-like peptide 1 (GLP-1) in humans. GLP-1, secreted from the intestinal L-cells, circulates the whole body through the blood. GLP-1 influences energy metabolism and glucose metabolism by regulating the insulin level. In the brain, GLP-1 secreted from intestinal cells can be absorbed into the brain, and the GLP-1 secreted from neurons remains in the cerebrospinal fluid. GLP-1 can control the secretion of various neurotransmitters and the progression of neuroinflammation, and can regulate insulin sensitivity in the brain.

(Alhadeff et al., 2012). Activation of these GLP-1-secreting neurons is regulated by the glucose level. The neurons innervate several brain regions including the hypothalamus, thalamus, paraventricular nucleus, cortex, and arcuate nucleus (Cork et al., 2015), and convey vagal motor information to the pancreas (Parker et al., 2010; Kappe et al., 2013; Calsolaro and Edison, 2015; Richard et al., 2015). GLP-1 has been reported to improve glucose-dependent insulin action through the G-protein-coupled receptor, GLP-1R (Drucker and Nauck, 2006).

GLP-1 is involved in the regulation of energy balance (Holst, 2007), and its activation and subsequent binding to the GLP-1R reduces food intake and, consequently, body weight (Turton et al., 1996). In the CNS, GLP-1Rs are expressed by neurons in the hippocampus, which is known to be a cognition-related brain region, and have been observed in neocortical pyramidal neurons (Hamilton and Holscher, 2009). In the brain, GLP-1 secreted from intestinal cells can be absorbed into the brain, and GLP-1 secreted from neurons remains in the CSF (Cabou and Burcelin, 2011). GLP-1 can control the secretion of various neurotransmitters, the progression of neuroinflammation, and the increase in insulin sensitivity in the brain (Athauda and Foltynie, 2016). GLP-1 is also thought to play an important role in glucose metabolism and neuronal function, including synaptic plasticity and neuronal metabolism, in the brain (Holscher, 2012). One study demonstrated that overexpression of GLP-1R in the hippocampus leads to an improvement in memory function (McClean and Holscher, 2014; Hansen et al., 2015). Microglia are also known to secrete GLP-1 (Kappe et al., 2012). Furthermore, the activity of GLP-1 secreting neurons is regulated by the glucose level (Parker et al., 2010; Kappe et al., 2013).

A recent study demonstrated that GLP-1 has a neurotrophic effect and promotes neurotrophic processes in the brain (Mainardi et al., 2015). Robinson et al. demonstrated that a mixture of GLP-1 agonists boosts memory and improves insulin action in the brain (Robinson et al., 2019). Exendin-4, a stable synthetic form of GLP-1, is commonly used clinically for diabetes treatment because GLP-1 has a short half-life (Drucker and Nauck, 2006; Heppner et al., 2015b). Furthermore, exendin-4 can cross the blood-brain barrier (Kastin and Akerstrom, 2003) and has a neuroprotective role in some neurological disorders (Holscher, 2010; Candeias et al., 2015). Clinically, GLP-1 analogs have been developed to treat diabetes and obesity, given that they have beneficial effects on blood glucose control and on the cardiovascular system. Liraglutide is a GLP-1 analog used in clinically obese patients for reducing body weight (Crane and McGowan, 2016). The effects of weight loss were observed upon daily liraglutide injection (Mora and Johnson, 2017), oral administration of liraglutide (3 mg) (Manigault and Thurston, 2016), and subcutaneous treatment of liraglutide for 20 weeks (1.2 to 3 mg) (Astrup et al., 2009). An interesting study also showed that oral administration of GLP-1 could reduce depression risk caused by hyperglycemia in a patient with type 2 diabetes (Onoviran et al., 2019).

In the next part of this review, the diverse roles of GLP-1 in the depressive brain will be discussed. Moreover, in each section, we will describe the various anti-depressive effects of GLP-1 in the CNS based on recent evidence.

OVERVIEW OF DEPRESSION

Major depressive disorder (MDD) is a highly prevalent mood disorder characterized by ruminative thoughts, impaired cognition and anhedonia, and attentional control deficits (Marchetti et al., 2012; Disease et al., 2016). Depression is thought to arise from a combination of genetic background and environmental stressors (Belmaker and Agam, 2008). Depression is considered a severe disorder because the features of depression negatively influence the quality of life of patients and their families, and are associated with increased economic and mental health burden (Hamilton et al., 2015).

Some reports have demonstrated that more than 50% of patients with depression experience chronic and recurrent problems throughout their lifetime, and that depressive symptoms can gradually aggravate and lead to suicide if patients are not treated with proper drugs or counseling (Monroe and Harkness, 2005; Rush et al., 2006). For these reasons, patients with depression must be accurately treated, and research aimed at preventing the onset of depression is therefore critical.

Depression is a disease that is highly related to neuroinflammation, neurotransmitter imbalance, blood-brain barrier hyperpermeability, deficits in neurogenesis, and synaptic dysfunction (Najjar et al., 2013; Felger and Treadway, 2017). One study observed that patients with depression showed impaired neurogenesis, neural growth retardation, and synaptic plasticity reduction (Serafini, 2012). In particular, the prefrontal cortex (PFC), amygdala, and hippocampus are crucial for regulating emotion, stress responses, and motivation. In patients with depression, the function of the PFC and hippocampus is disrupted, whereas the amygdala is hyperactivated (Serafini, 2012).

Although numerous anti-depressive treatments are available, 30% of patients diagnosed with depression do not experience positive therapeutic effects with these therapies (Al-Harbi, 2012). Hence, the mechanism of depression must be elucidated to facilitate the discovery of novel and effective anti-depressive therapies.

The gut is a key member of the gut-brain axis owing to its own enteric nervous system and its independent responses to the exterior environment and stress (Rao and Gershon, 2016). In recent years, the gut-brain axis has been increasingly considered a promising topic for the study of CNS-related diseases because the gut microbiota and gut hormones have been shown to interact with other organs including the brain (Knight et al., 2017), although the mechanisms involved in gut homeostasis and brain function are as yet uncharacterized (Collins and Bercik, 2009; Neufeld and Foster, 2009). Previous studies have demonstrated that the regulation of the immune system, endocrine system, and nervous system is strongly involved in the connection between the gut and the brain (Forsythe et al., 2010).

Several studies have shown that depressed patients have impaired gut-brain axis metabolism, appetite disturbances, and gut hormone abnormality (Collins and Bercik, 2009; Evrensel and Ceylan, 2015; Jiang et al., 2015). For these reasons, the current view of depression as an exclusively neurological

disorder was expanded to consider it a systemic disease, given that depression involves the impairment of the hypothalamic–pituitary–adrenal (HPA) axis, immune dysregulation, and disturbance of the gut-brain axis (Maes et al., 2011; O'Mahony et al., 2015). Various factors and signaling pathways are linked to gut-brain axis dysfunction that putatively leads to depression (Scott et al., 2013).

Although there is evidence associating depression with the gut, the action of the gut hormone GLP-1 is still not fully understood in the depressive brain. In the next section, we will focus on the diverse roles of GLP-1 in depression (**Table 1**).

Neuroinflammation in Depression and Its Relation to GLP-1

The immune system in the CNS has been shown to regulate brain development, neurogenesis, mood, and behavior (do Prado et al., 2016; Zheng et al., 2016; de Miranda et al., 2017). Over the past two decades, several studies have indicated that neuroinflammation is a critical reason for the onset, deterioration, relapse, and maintenance of depression (**Figure 2**) (Kopschina Feltes et al., 2017; Paudel et al., 2018; Woelfer et al., 2019). A recent study demonstrated that neuroinflammation could evoke depressive symptoms such as anhedonia and motor retardation (Felger and Treadway, 2017). Chronic neuroinflammation has been reported to contribute to serotonergic, dopaminergic, and noradrenergic dysfunction in the brain (Song and Wang, 2011) and to lead to chronic immune dysregulation (Carvalho et al., 2013).

Previous studies found that pro-inflammatory cytokines, including tumor necrosis factor-α (TNF-α) and interleukin (IL)-6, IL-1β, and C-reactive protein (CRP), are markedly increased in the blood and CSF of patients with depression (Hestad et al., 2016; Smith et al., 2018). IL-1, IL-6, IL-1β, TNF-α, and CRP are considered markers of the initiation, relapse, and progression of depression (**Figure 2**) (Haapakoski et al., 2016). Clinically, elevated levels of CRP and IL-6 were observed in patients with depression when compared to healthy subjects (Goldsmith et al., 2016) and were associated with cognitive symptoms in such patients (Gimeno et al., 2009). Furthermore, these increased levels of pro-inflammatory cytokines resulted in an increase of corticotropin-releasing hormone activity and hyperactivity of the HPA axis in most patients with depression (Kopschina Feltes et al., 2017). Excessive pro-inflammatory cytokines suppress the negative feedback of the HPA axis, boost the permeability of the blood-brain barrier, decrease the synthesis of neurotransmitters such as serotonin (5-HT), and ultimately lead to the onset of depression (Haroon and Miller, 2017; Leonard, 2018). Moreover, higher concentrations of several chemokines, such as CCL2 and CXCL8, were detected in the serum and CSF of depressed patients (Sutcigil et al., 2007; Piletz et al., 2009; Black and Miller, 2015; Khandaker et al., 2015; Slusarczyk et al., 2016). Previous studies have demonstrated that the proliferation of mononuclear cells is suppressed and T cell mitogens in the blood are decreased in patients with severe depression (Nunes et al., 2002; Irwin and Miller, 2007), and that impaired cell-mediated immunity is involved in the pathophysiology of depression (Kohler et al., 2017). Other studies have demonstrated a strong correlation between Th_{17} immune cells and the progression of depression (Korn et al., 2009; Slyepchenko et al., 2016).

As mentioned above, inflammatory responses and immunity are involved in the development and onset of depression (**Figure 2**). Modulation of inflammation may thus mitigate depressive behavior in patients with depression.

GLP-1 has been reported to promote the production of anti-inflammatory cytokines in various organs including the adipose tissue and pancreas, and the brain (Dobrian et al., 2011; Lee et al.,

TABLE 1 | Possible association between glucagon-like peptide 1 (GLP-1) and depression based on previous studies.

Experiment target	Result	Reference
GLP-1 or exendin-4	Influenced the dopamine system and reduced food reward behavior	(Richard et al., 2015)
Liraglutide	Exerted antipsychotic effect	(Dixit et al., 2013)
Exendin-4	Reduced cocaine self-administration	(Sorensen et al., 2015)
Exendin-4	Elevated turnover of dopamine through dopamine receptor 2 signaling	(Anderberg et al., 2014)
GLP-1R activation	Stimulated the release of GABA, glutamate, serotonin, and dopamine	(Rebosio et al., 2018)
Liraglutide or exendin-4	Enhanced neurogenesis and neural proliferation	(Bertilsson et al., 2008; Li et al., 2009; Isacson et al., 2011; Darsalia et al., 2012; McGovern et al., 2012; Porter et al., 2013; Parthsarathy and Holscher, 2013a; Holscher, 2014; Darsalia et al., 2014b; Sango and Utsunomiya, 2015)
(Val(8))GLP-1-Glu-PAL	Increased hippocampal neurogenesis and cell proliferation	(Lennox et al., 2013)
P7C3 (aminopropyl carbazole compound)	Activation of cAMP/PKA and Akt/GSK3 signaling	(Wang et al., 2018)
Liraglutide	Promoted neurite outgrowth through Wnt signaling	(He et al., 2018)
Liraglutide	Enhanced synaptic plasticity and attenuated depressive behavior	(Weina et al., 2018)
Liraglutide	Improved cognitive function and depressive symptoms in patients	(Cuomo et al., 2018)
Sitagliptin	Enhanced cognitive function and protected neurons against oxidative stress	(Gault et al., 2015)
Liraglutide	Activated LTP and improved cognitive dysfunction	(McClean et al., 2011)
GLP-1R knockout mouse	Impaired synaptic plasticity and memory formation	(Abbas et al., 2009)
GLP-1R overexpression mouse	Enhanced learning and neuroprotection	(During et al., 2003)
GLP-1 or exendin-4	Chronic administration reduced depression-like behavior	(Anderberg et al., 2016)

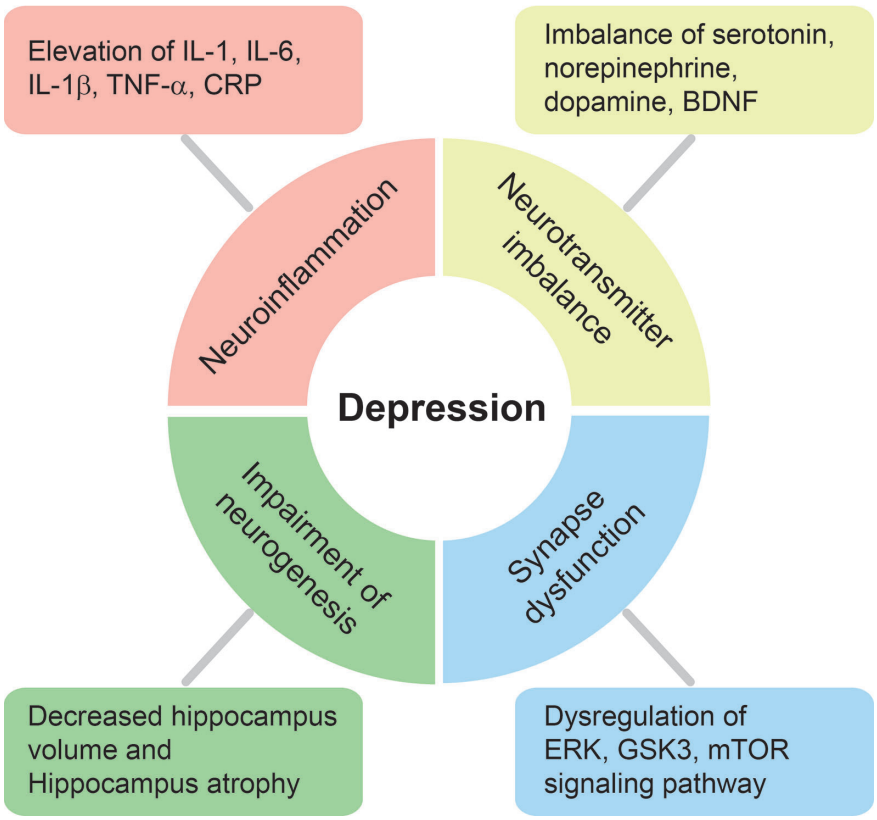

FIGURE 2 | Schematic diagram of physiological and molecular changes in the brain of patients with depression. We have summarized several physiological and molecular alterations in the brain of patients with depression. The depressive brain exhibits severe neuroinflammation involving higher pro-inflammatory cytokine production, neurotransmitter imbalance, and synaptic dysfunction through the dysregulation of ERK, Glycogen synthase kinase 3β (GSK-3β), and mammalian target of the rapamycin (mTOR) pathways, and these ultimately lead to the loss of hippocampal volume and cognitive decline.

2012; Darsalia et al., 2014a; Augestad et al., 2020; Reed et al., 2020). In addition, GLP-1 can boost immune cell infiltration as well as the production of pro-inflammatory cytokines under inflammatory conditions (Liu et al., 2009; Parthsarathy and Holscher, 2013b). One study demonstrated that exendin-4 (50 nM) treatment reduces the expression of pro-inflammatory genes such as NF-κB p65 and the TNF receptor superfamily member 1A in human pancreatic islet cells (Velmurugan et al., 2012). In addition, treatment of a DPP-4 inhibitor in diabetic mice increased the levels of anti-inflammatory cytokines, and increased the activation of regulatory T cells, indicating an involvement in the pathology of diabetes (Tian et al., 2010). Another study has reported that treatment of the DPP-4 inhibitor vildagliptin (10 mg/kg) in STZ-induced diabetic rats suppresses plasma TNF-α concentrations and inhibits nitric oxide concentrations in the serum (Akarte et al., 2012). Exendin-4 (10 nM) promotes the expression of serine protease inhibitor-9, thus underlying the survival capability of cells against the attack of immune cells such as natural killer cells and cytotoxic T cells in human islets (Cechin et al., 2012).

In the brain, GLP-1 treatment has a preventive effect on the progression of Alzheimer's disease pathology in rats (Iwai et al., 2014; Solmaz et al., 2015). Exenatide-4 (20 μg/kg/day). GLP-1 treatment suppressed the level of TNF-α in an Alzheimer's disease animal model brain induced by injection of STZ (Solmaz et al., 2015). Additionally, GLP-1 (50 nM) protected against synaptic dysfunction in the rat hippocampus induced by injection of lipopolysaccharide (LPS) (Iwai et al., 2014). In an Alzheimer's disease mouse model, liraglutide (25 nmol/kg/day) treatment attenuated the neuroinflammation response in the cortex (McClean et al., 2011). In addition, the Alzheimer's disease APPSWE/PS1ΔE9 mouse model showed a reduction of neuroinflammation upon liraglutide treatment (Holscher, 2014). Exendin-4 treatment (0.5 μg/kg) resulted in a reduction of pro-inflammatory cytokines such as TNF-α and IL-1β in CSF and in hippocampal and cortical brain areas (Ventorp et al., 2017).

Thus, GLP-1 can improve responses to neuroinflammation, and controls the production of cytokines in the brain. This function of GLP-1 under an inflammatory condition shows the therapeutic possibility of GLP-1 in the depressive brain accompanied by neuroinflammation.

Neurotransmitter Imbalance in Depression and Its Relation to GLP-1

Neurotransmitters play a cardinal role in the brain and contribute to the regulation of behavior (Lener et al., 2017).

Depression is typically thought to arise from a neurotransmitter imbalance (**Figure 2**) (Lener et al., 2017). Previous studies have demonstrated that the deficiency of monoaminergic neurotransmitters, such as 5-HT, norepinephrine (NE), and dopamine (DA), aggravates depressive behaviors and can be used as a diagnostic index for depression (Massart et al., 2012; Hamon and Blier, 2013). Serotonin is critical for mood processing and emotional regulation in brain areas such as the amygdala and hippocampus (Hervas et al., 2000; McKie et al., 2005), and may be essential for ameliorating depressive behaviors. Clinically depressed patients reportedly have impaired glutamatergic and hyperactive acetylcholine systems, whereas they have a dramatically suppressed gamma-aminobutyric acid (GABA) system (Pytka et al., 2016; Murrough et al., 2017). A previous brain magnetic resonance spectroscopy imaging study demonstrated that the levels of GABA and glutamate cycling was abnormal in patients with depression when compared to those in the normal brain (Sanacora et al., 2008). Yuen et al. demonstrated that chronic stress disrupts glutamate transmission in the PFC and cognition-related brain regions (Yuen et al., 2012). A number of other studies have also suggested that chronic stress causes atrophy of the PFC and hippocampus owing to glucocorticoid imbalance (Eisch and Petrik, 2012; McEwen et al., 2012).

Brain-derived neurotrophic factor (BDNF) is important for neurogenesis, and various depressive symptoms arise from decreased BDNF levels (Sahay and Hen, 2007). A previous study reported that anti-depressant therapy can increase the level of BDNF and subsequently boost neurogenesis, attenuate neuronal apoptosis in the depressive brain, and ultimately improve depressive mood (Sahay and Hen, 2007). Furthermore, recovery of BDNF levels results in the improvement of neuroplasticity and reduction of neuronal apoptosis (Alves et al., 2017; Kraus et al., 2017). Decreased BDNF in the hippocampus and PFC has been noted in depressed patients (Krishnan and Nestler, 2008; Duman and Voleti, 2012). Anti-depressants, which increase BDNF levels, lead to improvements in depressive behavior in BDNF-deletion mutant mice (Taliaz et al., 2010; Duman and Voleti, 2012; Yu et al., 2012). Some studies have reported that depression caused by chronic stress disrupts the BDNF–tropomyosin related kinase B (TrkB) receptor signaling pathway in the PFC and hippocampus, and ultimately contributes to impaired synaptic maturation, synaptic protein synthesis, and glutamate receptor cycling (Collingridge et al., 2010; Duric et al., 2010; Hoeffer and Klann, 2010; Christoffel et al., 2011; Duman and Voleti, 2012).

Therefore, because neurotransmitter imbalance contributes to depressive behaviors in patients with depression as described above, the appropriate modulation of neurotransmitters in the brain is key to treating depression (**Figure 2**).

A previous study reported that GLP-1Rs are observed in brain regions related to energy balance and regulation of moods, such as the amygdala, hippocampus, and dorsal raphe nucleus (Merchenthaler et al., 1999). Some studies have also shown the presence of GLP-1Rs in mood-related brain regions and demonstrated its powerful role in emotional processing within the CNS (Merchenthaler et al., 1999; Sharma et al., 2015).

Serotonin is produced by specific neurons localized in raphe nuclei in the brainstem (Llewellyn-Smith et al., 2013). These neurons innervate the amygdala (Vertes, 1991) and the hippocampus (McQuade and Sharp, 1997). The endogenous ligands of GLP-1-producing neurons were found to innervate the brainstem raphe nuclei (Llewellyn-Smith et al., 2013). Another study reported that injection of the GLP-1 agonist exendin-4 influenced the dopamine system and reduced food-related reward behavior in rats (Hayes and Schmidt, 2016). In patients with depression, the reward learning process is disrupted, and impaired reward learning is thought to lead to depressive mood and behavior (Fletcher and Reback, 2015). Dopamine regulates the reward learning system by stimulating the mesolimbic circle (Steinberg et al., 2013; Lietzau et al., 2020).

The exendin-4 treatment has been shown to reduce cocaine self-administration, suggesting that the GLP-1 system may be a novel target of drug addiction (Sorensen et al., 2015). Dopamine as a neurotransmitter has also been shown to reduce depressive-like behaviors such as anxiety (Dunlop and Nemeroff, 2007; Tye et al., 2013; Mohammadi et al., 2015; Lietzau et al., 2020). Recent studies have demonstrated that the GLP-1 agonist, liraglutide, exerts an antipsychotic effect in a mouse model of psychosis (Dixit et al., 2013). GLP-1 can elevate the turnover of dopamine in the brain amygdala through dopamine receptor 2 signaling (Anderberg et al., 2014; Lietzau et al., 2020). Furthermore, GLP-1Rs have been shown to be able to stimulate the depolarization-evoked release of other neurotransmitters, such as GABA and glutamate, as well as of serotonin and dopamine, in the cortex and hippocampus (Rebosio et al., 2018).

These studies indicate that GLP-1 modulates the release of several neurotransmitters including serotonin, dopamine, GABA, and glutamate, which may regulate depressive-like behaviors. Modulation of neurotransmitter secretion by GLP-1 may be another effective solution for alleviating the effects of depression.

Neurogenesis in Depression and Its Relation to GLP-1

In the brain, neurogenesis is a critical repair response against stress and age (Dranovsky et al., 2011). New neurons generated through the neurogenesis process are produced from neural progenitors mainly located in the subgranular zone of the dentate gyrus (Dranovsky et al., 2011). Neurogenesis repairs the damaged brain and improves cognition (Schmidt-Hieber et al., 2004). The depressive brain has been shown to exhibit a decrease in hippocampal neurogenesis, and this reduction is recovered by antidepressant drug treatment (Tanti and Belzung, 2013). Some brain imaging studies have demonstrated that depressed patients show neuronal atrophy and decreased volume of the cortex and limbic lobe regions, including the PFC and hippocampus. These regions are known to regulate emotion and cognition, and pathological problems and impaired

cognitive function are observed in depressive conditions (Price and Drevets, 2010; MacQueen and Frodl, 2011).

Patients with recurrent depression exhibit reduced hippocampal volume and hippocampal atrophy in the brain when compared to healthy controls (**Figure 2**) (Bremner et al., 2000). Moreover, the decrease in hippocampal volume is significantly related to the total duration of depressive episodes (Sheline et al., 1999). Other studies have reported that a reduction in hippocampal neurogenesis leads to an increase in anxiety symptoms and the onset of depression (Hanson et al., 2011; Eisch and Petrik, 2012; Moylan et al., 2013; Smitha et al., 2014). Increased hippocampal neurogenesis influences anxiety and depressive behavior through the HPA axis and is considered a promising strategy to promote antidepressant-like effects (Hill et al., 2015).

Calcium signaling resulting from GABA receptor activation has been found to promote neuronal differentiation and control the synaptic integration of neuronal precursor cells (Ge et al., 2006). A serotonin 5-HT_{2A} receptor antagonist was shown to reduce neuronal proliferation, and chronic administration of a 5-HT_{1A} receptor agonist increased neuronal proliferation (Jha et al., 2008). With this perspective, the regulation of neurotransmitter secretion may be considerably linked with the activation of neurogenesis in the depressive brain. Moreover, chemokines are important regulators of neuronal proliferation and neural progenitor cell differentiation (Tran et al., 2007; Miller et al., 2008). As such, cytokine and chemokine dysregulation likely contribute to impaired neurogenesis in the depressive brain. Thus, we expect that the promotion of neurogenesis in the brain may be a key strategy to cure depression.

The GLP-1R agonist exendin-4 was shown to promote neurogenesis in the subventricular zone region in a neurodegenerative disease rodent model (Bertilsson et al., 2008). Interestingly, several studies have demonstrated that exendin-4 has neurotrophic and neuroprotective effects and that it enhances neurogenesis and neural proliferation (Li et al., 2009; Holscher, 2014; Sango and Utsunomiya, 2015). Furthermore, Isacson et al. demonstrated that GLP-1 agonist administration could lead to an increase in neurogenesis in the hippocampus dentate gyrus region, and demonstrated an improvement in mood and cognitive function through the swim test in adult rodents (Isacson et al., 2011). Moreover, GLP-1 has been reported to enhance synaptic plasticity and synaptic formation in the hippocampus (Cai et al., 2014). The increase of hippocampal neurogenesis is essential for improved cognitive function induced by environmental factors such as exercise (Petrik et al., 2012; Klempin et al., 2013).

Previous studies have demonstrated that neurogenesis influences emotional regulation in adult mice (Deng et al., 2009), and that enhanced neurogenesis in the hippocampus acts as an antidepressant for increasing serotonin receptor activity (Wang et al., 2008; David et al., 2009; Kondo et al., 2015). Moreover, hippocampal neurogenesis reduces neuronal damage by replacing lost neurons, which appears to improve depressive-like behavior (Zhang et al., 2008). It has been demonstrated that the administration of GLP-1 analogs, including liraglutide and exendin-4, promotes neurogenesis and neural progenitor cell proliferation in the hippocampus of rodent models (Darsalia et al., 2012; McGovern et al., 2012; Porter et al., 2013). It has also been reported that liraglutide increases neural stem cell proliferation and neuronal differentiation in the APP/PS1 neurodegenerative disease model (Parthsarathy and Holscher, 2013a). Moreover, a GLP-1 analog, (Val(8))GLP-1-Glu-PAL, increased hippocampal neurogenesis and cell proliferation in obese mice fed a high-fat diet (Lennox et al., 2013). Further, the expression of neurogenesis-related proteins was promoted by the activation of the cAMP/PKA and Akt/GSK3 signaling pathways through the stimulation of GLP-1R in mice (Wang et al., 2018). From *in vitro* studies using human SH-SY5Y neuronal cells, it was demonstrated that cell proliferation is increased with GLP-1 treatment (Li et al., 2010; Salcedo et al., 2012).

Some studies demonstrated that the administration of antidepressants leads to an improvement in depressive mood through the increase of hippocampal neurogenesis and the enhancement of synaptic connectivity (Duman et al., 2001; Toni et al., 2007; Boldrini et al., 2009; Denny et al., 2012). Several studies have demonstrated that increasing neurogenesis in the brain is an effective therapeutic approach for reducing depressive-like behaviors (Anacker et al., 2011; Mendez-David et al., 2013; Weina et al., 2018). A previous study indicated that treatment with the GLP-1 agonist liraglutide (subcutaneously at a dose gradually titrated from 0.6 to 3 mg) in bipolar and mood disorder depression patients could result in an improvement in cognitive function and an alleviation of depressive pathological symptoms (Cuomo et al., 2018).

Considering this evidence, increasing neurogenesis in the brain through the GLP-1 pathway may provide a novel approach for improving depressive-like behavior in patients with depression.

Synaptic Dysfunction and Memory Loss in Depression and Its Relation to GLP-1

In patients with depression, neural circuits are impaired as a result of aberrant communication between neurons (Williams, 2016). Functional brain imaging studies have reported a decrease in synaptic connectivity and neuronal circuitry in the PFC and hippocampus in depressed patients (Perlman et al., 2012; Zeng et al., 2012). Moreover, postmortem brains of depressed patients are reduced in size and show loss of pyramidal neurons (Rajkowska et al., 1999), GABAergic interneurons, and glia in the PFC (Rajkowska et al., 2007). Several neuronal morphological studies also reported a reduction in synapse number and synaptic signaling proteins in the PFC of depressed patients through electron microscopy (Kang et al., 2012). Reduced glutamate receptors, presynaptic neurotransmitter proteins, and postsynaptic functional proteins in the PFC and hippocampus were also observed (**Figure 2**) (Zhao et al., 2012; Duric et al., 2013).

Chronic unpredictable stress, considered a model of depression, results in a reduction in dendritic lengths and

branching of apical dendrites, the loss of functional synaptic spines, and the reduction of dendritic complexity in PFC neurons and in the hippocampal CA3 pyramidal neuronal cell layer (McEwen et al., 2012; Morrison and Baxter, 2012). Furthermore, chronic stress aggravates neuronal damage in the amygdala and nucleus accumbens and subsequently disrupts the motivation and reward system (Duman and Voleti, 2012). Another study reported that depression caused by chronic stress blocks glutamate signaling and synaptic transmission, and this ultimately leads to cognitive dysfunction (Yuen et al., 2012). Moreover, depressed patients show a reduction in synaptic density proteins in response to stress (Kang et al., 2012). Depression reportedly increases the negative regulation of ERK signaling associated with synaptic plasticity (Duric et al., 2010) and inhibits downstream signaling of BDNF and neuritin that are essential for normal synaptic function (Son et al., 2012).

Glycogen synthase kinase 3 (GSK3) has been shown to regulate synaptic homeostasis in the brain (Collingridge et al., 2010). Many researchers have demonstrated that depressed patients have excessive activation of GSK3-deconsolidation, which leads to a reduction in synaptic spines (Li and Jope, 2010; Wilkinson et al., 2011). Previous studies have shown that synaptic plasticity, synaptic transmission, and long-term potentiation (LTP) are dramatically attenuated in the depressive brain (Karpova et al., 2011; Bath et al., 2012). In dendrites and cell bodies of the neuron, activation of the mammalian target of the rapamycin (mTOR) signaling pathway accelerates long-term synaptogenesis (Hoeffer and Klann, 2010). In the depressive brain, activation of mTOR is reduced, which subsequently decreases the release of BDNF and the synthesis of synaptic proteins (Jourdi et al., 2009).

Most patients with depression show mood disturbances, as well as general cognitive impairment, which may explain the two-fold greater risk of dementia development seen in such patients (Bulbena and Berrios, 1986; Kohler et al., 2010; Byers et al., 2012; Tsai and Rosenheck, 2016). A neuroimaging study suggested that depression strongly leads to memory dysfunction given that morphological changes in the brain of depressed patients, such as atrophy and abnormal alteration of the frontal cortex, thalamus, and hippocampus, is related to cognitive impairment (Zhang et al., 2016).

Based on these reports, the impairment of synaptic function and synaptic transmission and the loss of synaptic density proteins are widely observed in the depressive brain (**Figure 2**). Synaptic dysfunction may lead to memory dysfunction in patients with depression. Therefore, improving synaptic function is an important component for treating depressive neuropathology.

One study reported that GLP-1 is negatively correlated with body mass index (BMI) and that it appears to increase dentate gyrus neurogenesis based on immunostaining images (Coplan et al., 2014). Recent research has demonstrated that liraglutide promotes neurite outgrowth of cortical neurons in severe oxidative stress conditions through Wnt signaling (He et al., 2018). Furthermore, another study has highlighted the role of liraglutide in preventing depressive-like behaviors by enhancing hippocampal neuron synaptic plasticity (Weina et al., 2018). Gault et al. demonstrated that oral administration of the DPP inhibitor sitagliptin (50 mg/kg) can enhance cognitive function and protects neurons against oxidative stress in high fat-fed mice (Gault et al., 2015). One *in vitro* study reported that exendin-4 increases the number of neurites, promotes neuronal outgrowth, and considerably increases neurite length (Luciani et al., 2010).

It was previously shown that the GLP-1 receptor can control neuronal function in the rat hippocampus by enhancing GABAA signaling through presynaptic and postsynaptic mechanisms (Korol et al., 2015). Previous studies reported that the administration of the GLP-1R agonist exendin-4 (25 nmol/kg, twice daily) inhibits learning and memory formation through the suppression of synaptic plasticity in the hippocampus of a high fat diet mouse model (Gault et al., 2010; Lennox et al., 2014).

LTP results from the synchronous activity of neurons and is widely considered an indicator of memory formation. One study demonstrated that GLP-1 can activate LTP in the brain and ameliorate cognitive dysfunction in a neurodegenerative disorder model (McClean et al., 2011). Another study showed that GLP-1R knockout mice have impaired LTP when compared to control animals (Abbas et al., 2009). Overexpression of GLP-1Rs in the mouse brain leads to enhanced learning, as measured with the Morris water maze and learning performance tests (During et al., 2003). Interestingly, a recent study showed that GLP-1 and exendin-4 induced anxiety-like behaviors in mice (Anderberg et al., 2016). The stimulation of GLP-1Rs alters serotonin signaling in the amygdala (Anderberg et al., 2016). Importantly, chronic administration of exendin-4 significantly reduces depression-like behavior (Anderberg et al., 2016).

These previous studies together suggest that GLP-1 may improve memory and cognitive function in patients with depression by enhancing synaptic function and neuronal signal transmission in the brain.

CONCLUSIONS

In this review, we have presented four cardinal points about the roles of GLP-1 in the depressive brain. First, we summarized significant evidence pointing to the relationship between neuroinflammation and GLP-1 administration. GLP-1 appears to attenuate the process of neuroinflammation and protects neurons and glia under oxidative stress conditions in the depressive brain. Second, we described the role of GLP-1 in neurotransmitter homeostasis in the depressive brain in which GLP-1 can improve neurotransmitter balance. In the depressive brain, the secretion of diverse neurotransmitters is not stable compared to that in the normal brain. GLP-1 is a useful therapeutic modulator of depression, suggesting that abnormal alteration of neurotransmitter levels in the depressive brain results in mood impairment and cognitive decline. Third, we reviewed the role GLP-1 in promoting neuronal differentiation and neural stem cell proliferation in the depressive brain. GLP-1 is a promising target for the treatment of depression because

impaired neurogenesis ability and the reduction of neuronal differentiation leads to multiple depressive pathological symptoms. Finally, we summarized studies showing that GLP-1 can enhance cognitive decline by improving synaptic function in the depressive brain. GLP-1 ameliorates synaptic dysfunction in the depressive brain and subsequently leads to the enhancement of cognitive function. Hence, GLP-1 may be key to improving cognitive decline in patients with depression.

Taken together, we have highlighted GLP-1 as a novel therapeutic marker for identifying and treating the neuropathology of depression. Furthermore, we emphasize the necessity of further studies concerning the mechanisms and function of GLP-1 in the depressive brain. Similar to the use of GLP-1 analogs in diabetic patients, we believe that GLP-1 may be used for patients with depression in the near future.

AUTHOR CONTRIBUTIONS

Y-KK contributed to the writing of the text and provided the table and figures. OK and JS wrote and revised the manuscript. OK provided financial support for the study. JS finalized the revised manuscript.

FUNDING

This research was supported by the Basic Science Research Program through the National Research Foundation of Korea (NRF) funded by the Ministry of Education (grant number: NRF-2019R1F1A1054111 (JS), NRF-2019R1I1A3A01058861 (OK), and NRF-2018R1A2B6001104 (Y-KK).

REFERENCES

Abbas, T., Faivre, E., and Holscher, C. (2009). Impairment of synaptic plasticity and memory formation in GLP-1 receptor KO mice: Interaction between type 2 diabetes and Alzheimer's disease. *Behav. Brain Res.* 205, 265–271. doi: 10.1016/j.bbr.2009.06.035

Akarte, A. S., Srinivasan, B. P., Gandhi, S., and Sole, S. (2012). Chronic DPP-IV inhibition with PKF-275-055 attenuates inflammation and improves gene expressions responsible for insulin secretion in streptozotocin induced diabetic rats. *Eur. J. Pharm. Sci.* 47, 456–463. doi: 10.1016/j.ejps.2012.07.003

Akimoto, H., Tezuka, K., Nishida, Y., Nakayama, T., Takahashi, Y., and Asai, S. (2019). Association between use of oral hypoglycemic agents in Japanese patients with type 2 diabetes mellitus and risk of depression: A retrospective cohort study. *Pharmacol. Res. Perspect.* 7, e00536. doi: 10.1002/prp2.536

Alhadeff, A. L., Rupprecht, L. E., and Hayes, M. R. (2012). GLP-1 neurons in the nucleus of the solitary tract project directly to the ventral tegmental area and nucleus accumbens to control for food intake. *Endocrinology* 153, 647–658. doi: 10.1210/en.2011-1443

Al-Harbi, K. S. (2012). Treatment-resistant depression: therapeutic trends, challenges, and future directions. *Patient Prefer. Adherence* 6, 369–388. doi: 10.2147/PPA.S29716

Alves, N. D., Correia, J. S., Patricio, P., Mateus-Pinheiro, A., Machado-Santos, A. R., Loureiro-Campos, E., et al. (2017). Adult hippocampal neuroplasticity triggers susceptibility to recurrent depression. *Transl. Psychiatry* 7, e1058. doi: 10.1038/tp.2017.29

Anacker, C., Zunszain, P. A., Cattaneo, A., Carvalho, L. A., Garabedian, M. J., Thuret, S., et al. (2011). Antidepressants increase human hippocampal neurogenesis by activating the glucocorticoid receptor. *Mol. Psychiatry* 16, 738–750. doi: 10.1038/mp.2011.26

Anderberg, R. H., Anefors, C., Bergquist, F., Nissbrandt, H., and Skibicka, K. P. (2014). Dopamine signaling in the amygdala, increased by food ingestion and GLP-1, regulates feeding behavior. *Physiol. Behav.* 136, 135–144. doi: 10.1016/j.physbeh.2014.02.026

Anderberg, R. H., Richard, J. E., Hansson, C., Nissbrandt, H., Bergquist, F., and Skibicka, K. P. (2016). GLP-1 is both anxiogenic and antidepressant; divergent effects of acute and chronic GLP-1 on emotionality. *Psychoneuroendocrinology* 65, 54–66. doi: 10.1016/j.psyneuen.2015.11.021

Astrup, A., Rossner, S., Van Gaal, L., Rissanen, A., Niskanen, L., Al Hakim, M., et al. (2009). Effects of liraglutide in the treatment of obesity: a randomised, double-blind, placebo-controlled study. *Lancet* 374, 1606–1616. doi: 10.1016/S0140-6736(09)61375-1

Athauda, D., and Foltynie, T. (2016). The glucagon-like peptide 1 (GLP) receptor as a therapeutic target in Parkinson's disease: mechanisms of action. *Drug Discov. Today* 21, 802–818. doi: 10.1016/j.drudis.2016.01.013

Augestad, I. L., Pintana, H., Larsson, M., Krizhanovskii, C., Nystrom, T., Klein, T., et al. (2020). The Regulation of Glycemia in the Recovery Phase After Stroke Counteracts the Detrimental Effect of Obesity-Induced Type 2 Diabetes on Neurological Recovery. *Diabetes* db200095. doi: 10.2337/db20-0095

Bath, K. G., Jing, D. Q., Dincheva, I., Neeb, C. C., Pattwell, S. S., Chao, M. V., et al. (2012). BDNF Val66Met impairs fluoxetine-induced enhancement of adult hippocampus plasticity. *Neuropsychopharmacology* 37, 1297–1304. doi: 10.1038/npp.2011.318

Belmaker, R. H., and Agam, G. (2008). Major depressive disorder. *N Engl. J. Med.* 358, 55–68. doi: 10.1056/NEJMra073096

Bertilsson, G., Patrone, C., Zachrisson, O., Andersson, A., Dannaeus, K., Heidrich, J., et al. (2008). Peptide hormone exendin-4 stimulates subventricular zone neurogenesis in the adult rodent brain and induces recovery in an animal model of Parkinson's disease. *J. Neurosci. Res.* 86, 326–338. doi: 10.1002/jnr.21483

Black, C., and Miller, B. J. (2015). Meta-Analysis of Cytokines and Chemokines in Suicidality: Distinguishing Suicidal Versus Nonsuicidal Patients. *Biol. Psychiatry* 78, 28–37. doi: 10.1016/j.biopsych.2014.10.014

Boldrini, M., Underwood, M. D., Hen, R., Rosoklija, G. B., Dwork, A. J., John Mann, J., et al. (2009). Antidepressants increase neural progenitor cells in the human hippocampus. *Neuropsychopharmacology* 34, 2376–2389. doi: 10.1038/npp.2009.75

Bremner, J. D., Narayan, M., Anderson, E. R., Staib, L. H., Miller, H. L., and Charney, D. S. (2000). Hippocampal volume reduction in major depression. *Am. J. Psychiatry* 157, 115–118. doi: 10.1176/ajp.157.1.115

Bulbena, A., and Berrios, G. E. (1986). Pseudodementia: facts and figures. *Br. J. Psychiatry* 148, 87–94. doi: 10.1192/bjp.148.1.87

Bullock, B. P., Heller, R. S., and Habener, J. F. (1996). Tissue distribution of messenger ribonucleic acid encoding the rat glucagon-like peptide-1 receptor. *Endocrinology* 137, 2968–2978. doi: 10.1210/endo.137.7.8770921

Byers, A. L., Covinsky, K. E., Barnes, D. E., and Yaffe, K. (2012). Dysthymia and depression increase risk of dementia and mortality among older veterans. *Am. J. Geriatr. Psychiatry* 20, 664–672. doi: 10.1097/JGP.0b013e31822001c1

Cabou, C., and Burcelin, R. (2011). GLP-1, the gut-brain, and brain-periphery axes. *Rev. Diabetes Stud.* 8, 418–431. doi: 10.1900/RDS.2011.8.418

Cai, H. Y., Holscher, C., Yue, X. H., Zhang, S. X., Wang, X. H., Qiao, F., et al. (2014). Lixisenatide rescues spatial memory and synaptic plasticity from amyloid beta protein-induced impairments in rats. *Neuroscience* 277, 6–13. doi: 10.1016/j.neuroscience.2014.02.022

Calsolaro, V., and Edison, P. (2015). Novel GLP-1 (Glucagon-Like Peptide-1) Analogues and Insulin in the Treatment for Alzheimer's Disease and Other Neurodegenerative Diseases. *CNS Drugs* 29, 1023–1039. doi: 10.1007/s40263-015-0301-8

Campbell, J. E., and Drucker, D. J. (2013). Pharmacology, physiology, and mechanisms of incretin hormone action. *Cell Metab.* 17, 819–837. doi: 10.1016/j.cmet.2013.04.008

Candeias, E. M., Sebastiao, I. C., Cardoso, S. M., Correia, S. C., Carvalho, C. I., Placido, A. I., et al. (2015). Gut-brain connection: The neuroprotective effects

of the anti-diabetic drug liraglutide. *World J. Diabetes* 6, 807–827. doi: 10.4239/wjd.v6.i6.807

Carvalho, L. A., Torre, J. P., Papadopoulos, A. S., Poon, L., Juruena, M. F., Markopoulou, K., et al. (2013). Lack of clinical therapeutic benefit of antidepressants is associated overall activation of the inflammatory system. *J. Affect. Disord.* 148, 136–140. doi: 10.1016/j.jad.2012.10.036

Cechin, S. R., Perez-Alvarez, I., Fenjves, E., Molano, R. D., Pileggi, A., Berggren, P. O., et al. (2012). Anti-inflammatory properties of exenatide in human pancreatic islets. *Cell Transplant.* 21, 633–648. doi: 10.3727/096368911X576027

Christoffel, D. J., Golden, S. A., and Russo, S. J. (2011). Structural and synaptic plasticity in stress-related disorders. *Rev. Neurosci.* 22, 535–549. doi: 10.1515/RNS.2011.044

Collingridge, G. L., Peineau, S., Howland, J. G., and Wang, Y. T. (2010). Long-term depression in the CNS. *Nat. Rev. Neurosci.* 11, 459–473. doi: 10.1038/nrn2867

Collins, S. M., and Bercik, P. (2009). The relationship between intestinal microbiota and the central nervous system in normal gastrointestinal function and disease. *Gastroenterology* 136, 2003–2014. doi: 10.1053/j.gastro.2009.01.075

Coplan, J. D., Syed, S., Perera, T. D., Fulton, S. L., Banerji, M. A., Dwork, A. J., et al. (2014). Glucagon-like peptide-1 as predictor of body mass index and dentate gyrus neurogenesis: neuroplasticity and the metabolic milieu. *Neural Plast.* 2014, 917981. doi: 10.1155/2014/917981

Cork, S. C., Richards, J. E., Holt, M. K., Gribble, F. M., Reimann, F., and Trapp, S. (2015). Distribution and characterisation of Glucagon-like peptide-1 receptor expressing cells in the mouse brain. *Mol. Metab.* 4, 718–731. doi: 10.1016/j.molmet.2015.07.008

Crane, J., and McGowan, B. (2016). The GLP-1 agonist, liraglutide, as a pharmacotherapy for obesity. *Ther. Adv. Chronic Dis.* 7, 92–107. doi: 10.1177/2040622315620180

Cuomo, A., Bolognesi, S., Goracci, A., Ciuoli, C., Beccarini Crescenzi, B., Maina, G., et al. (2018). Feasibility, Adherence and Efficacy of Liraglutide Treatment in a Sample of Individuals With Mood Disorders and Obesity. *Front. Psychiatry* 9, 784. doi: 10.3389/fpsyt.2018.00784

Darsalia, V., Mansouri, S., Ortsater, H., Olverling, A., Nozadze, N., Kappe, C., et al. (2012). Glucagon-like peptide-1 receptor activation reduces ischaemic brain damage following stroke in Type 2 diabetic rats. *Clin. Sci. (Lond.)* 122, 473–483. doi: 10.1042/CS20110374

Darsalia, V., Hua, S., Larsson, M., Mallard, C., Nathanson, D., Nystrom, T., et al. (2014a). Exendin-4 reduces ischemic brain injury in normal and aged type 2 diabetic mice and promotes microglial M2 polarization. *PLoS One* 9, e103114. doi: 10.1371/journal.pone.0103114

Darsalia, V., Olverling, A., Larsson, M., Mansouri, S., Nathanson, D., Nystrom, T., et al. (2014b). Linagliptin enhances neural stem cell proliferation after stroke in type 2 diabetic mice. *Regul. Pept.* 190-191, 25–31. doi: 10.1016/j.regpep.2014.05.001

David, D. J., Samuels, B. A., Rainer, Q., Wang, J. W., Marsteller, D., Mendez, I., et al. (2009). Neurogenesis-dependent and -independent effects of fluoxetine in an animal model of anxiety/depression. *Neuron* 62, 479–493. doi: 10.1016/j.neuron.2009.04.017

de Miranda, A. S., Zhang, C. J., Katsumoto, A., and Teixeira, A. L. (2017). Hippocampal adult neurogenesis: Does the immune system matter? *J. Neurol. Sci.* 372, 482–495. doi: 10.1016/j.jns.2016.10.052

Deng, W., Saxe, M. D., Gallina, I. S., and Gage, F. H. (2009). Adult-born hippocampal dentate granule cells undergoing maturation modulate learning and memory in the brain. *J. Neurosci.* 29, 13532–13542. doi: 10.1523/JNEUROSCI.3362-09.2009

Denny, C. A., Burghardt, N. S., Schachter, D. M., Hen, R., and Drew, M. R. (2012). 4- to 6-week-old adult-born hippocampal neurons influence novelty-evoked exploration and contextual fear conditioning. *Hippocampus* 22, 1188–1201. doi: 10.1002/hipo.20964

Disease, G. B. D., Injury, I., and Prevalence, C. (2016). Global, regional, and national incidence, prevalence, and years lived with disability for 310 diseases and injuries 1990-2015: a systematic analysis for the Global Burden of Disease Study 2015. *Lancet* 388, 1545–1602. doi: 10.1016/S0140-6736(16)31678-6

Dixit, T. S., Sharma, A. N., Lucot, J. B., and Elased, K. M. (2013). Antipsychotic-like effect of GLP-1 agonist liraglutide but not DPP-IV inhibitor sitagliptin in mouse model for psychosis. *Physiol. Behav.* 114-115, 38–41. doi: 10.1016/j.physbeh.2013.03.008

do Prado, C. H., Narahari, T., Holland, F. H., Lee, H. N., Murthy, S. K., and Brenhouse, H. C. (2016). Effects of early adolescent environmental enrichment on cognitive dysfunction, prefrontal cortex development, and inflammatory cytokines after early life stress. *Dev. Psychobiol.* 58, 482–491. doi: 10.1002/dev.21390

Dobrian, A. D., Ma, Q., Lindsay, J. W., Leone, K. A., Ma, K., Coben, J., et al. (2011). Dipeptidyl peptidase IV inhibitor sitagliptin reduces local inflammation in adipose tissue and in pancreatic islets of obese mice. *Am. J. Physiol. Endocrinol. Metab.* 300, E410–E421. doi: 10.1152/ajpendo.00463.2010

Dranovsky, A., Picchini, A. M., Moadel, T., Sisti, A. C., Yamada, A., Kimura, S., et al. (2011). Experience dictates stem cell fate in the adult hippocampus. *Neuron* 70, 908–923. doi: 10.1016/j.neuron.2011.05.022

Drucker, D. J., and Nauck, M. A. (2006). The incretin system: glucagon-like peptide-1 receptor agonists and dipeptidyl peptidase-4 inhibitors in type 2 diabetes. *Lancet* 368, 1696–1705. doi: 10.1016/S0140-6736(06)69705-5

Duarte, A. I., Candeias, E., Correia, S. C., Santos, R. X., Carvalho, C., Cardoso, S., et al. (2013). Crosstalk between diabetes and brain: glucagon-like peptide-1 mimetics as a promising therapy against neurodegeneration. *Biochim. Biophys. Acta* 1832, 527–541. doi: 10.1016/j.bbadis.2013.01.008

Duman, R. S., and Voleti, B. (2012). Signaling pathways underlying the pathophysiology and treatment of depression: novel mechanisms for rapid-acting agents. *Trends Neurosci.* 35, 47–56. doi: 10.1016/j.tins.2011.11.004

Duman, R. S., Nakagawa, S., and Malberg, J. (2001). Regulation of adult neurogenesis by antidepressant treatment. *Neuropsychopharmacology* 25, 836–844. doi: 10.1016/S0893-133X(01)00358-X

Dunlop, B. W., and Nemeroff, C. B. (2007). The role of dopamine in the pathophysiology of depression. *Arch. Gen. Psychiatry* 64, 327–337. doi: 10.1001/archpsyc.64.3.327

Duric, V., Banasr, M., Licznerski, P., Schmidt, H. D., Stockmeier, C. A., Simen, A. A., et al. (2010). A negative regulator of MAP kinase causes depressive behavior. *Nat. Med.* 16, 1328–1332. doi: 10.1038/nm.2219

Duric, V., Banasr, M., Stockmeier, C. A., Simen, A. A., Newton, S. S., Overholser, J. C., et al. (2013). Altered expression of synapse and glutamate related genes in post-mortem hippocampus of depressed subjects. *Int. J. Neuropsychopharmacol.* 16, 69–82. doi: 10.1017/S1461145712000016

During, M. J., Cao, L., Zuzga, D. S., Francis, J. S., Fitzsimons, H. L., Jiao, X., et al. (2003). Glucagon-like peptide-1 receptor is involved in learning and neuroprotection. *Nat. Med.* 9, 1173–1179. doi: 10.1038/nm919

Edholm, T., Degerblad, M., Gryback, P., Hilsted, L., Holst, J. J., Jacobsson, H., et al. (2010). Differential incretin effects of GIP and GLP-1 on gastric emptying, appetite, and insulin-glucose homeostasis. *Neurogastroenterol. Motil.* 22, 1191–1200, e1315. doi: 10.1111/j.1365-2982.2010.01554.x

Eisch, A. J., and Petrik, D. (2012). Depression and hippocampal neurogenesis: a road to remission? *Science* 338, 72–75. doi: 10.1126/science.1222941

Evrensel, A., and Ceylan, M. E. (2015). The Gut-Brain Axis: The Missing Link in Depression. *Clin. Psychopharmacol. Neurosci.* 13, 239–244. doi: 10.9758/cpn.2015.13.3.239

Felger, J. C., and Treadway, M. T. (2017). Inflammation Effects on Motivation and Motor Activity: Role of Dopamine. *Neuropsychopharmacology* 42, 216–241. doi: 10.1038/npp.2016.143

Fletcher, J. B., and Reback, C. J. (2015). Depression mediates and moderates effects of methamphetamine use on sexual risk taking among treatment-seeking gay and bisexual men. *Health Psychol.* 34, 865–869. doi: 10.1037/hea0000207

Forsythe, P., Sudo, N., Dinan, T., Taylor, V. H., and Bienenstock, J. (2010). Mood and gut feelings. *Brain Behav. Immun.* 24, 9–16. doi: 10.1016/j.bbi.2009.05.058

Gault, V. A., Porter, W. D., Flatt, P. R., and Holscher, C. (2010). Actions of exendin-4 therapy on cognitive function and hippocampal synaptic plasticity in mice fed a high-fat diet. *Int. J. Obes. (Lond.)* 34, 1341–1344. doi: 10.1038/ijo.2010.59

Gault, V. A., Lennox, R., and Flatt, P. R. (2015). Sitagliptin, a dipeptidyl peptidase-4 inhibitor, improves recognition memory, oxidative stress and hippocampal neurogenesis and upregulates key genes involved in cognitive decline. *Diabetes Obes. Metab.* 17, 403–413. doi: 10.1111/dom.12432

Ge, S., Goh, E. L., Sailor, K. A., Kitabatake, Y., Ming, G. L., and Song, H. (2006). GABA regulates synaptic integration of newly generated neurons in the adult brain. *Nature* 439, 589–593. doi: 10.1038/nature04404

Gerhard, D. M., Wohleb, E. S., and Duman, R. S. (2016). Emerging treatment mechanisms for depression: focus on glutamate and synaptic plasticity. *Drug Discovery Today* 21, 454–464. doi: 10.1016/j.drudis.2016.01.016

Gimeno, D., Kivimaki, M., Brunner, E. J., Elovainio, M., De Vogli, R., Steptoe, A., et al. (2009). Associations of C-reactive protein and interleukin-6 with

cognitive symptoms of depression: 12-year follow-up of the Whitehall II study. *Psychol. Med.* 39, 413–423. doi: 10.1017/S0033291708003723

Goldsmith, D. R., Rapaport, M. H., and Miller, B. J. (2016). A meta-analysis of blood cytokine network alterations in psychiatric patients: comparisons between schizophrenia, bipolar disorder and depression. *Mol. Psychiatry* 21, 1696–1709. doi: 10.1038/mp.2016.3

Haapakoski, R., Ebmeier, K. P., Alenius, H., and Kivimaki, M. (2016). Innate and adaptive immunity in the development of depression: An update on current knowledge and technological advances. *Prog. Neuropsychopharmacol. Biol. Psychiatry* 66, 63–72. doi: 10.1016/j.pnpbp.2015.11.012

Habib, A. M., Richards, P., Rogers, G. J., Reimann, F., and Gribble, F. M. (2013). Co-localisation and secretion of glucagon-like peptide 1 and peptide YY from primary cultured human L cells. *Diabetologia* 56, 1413–1416. doi: 10.1007/s00125-013-2887-z

Hamilton, A., and Holscher, C. (2009). Receptors for the incretin glucagon-like peptide-1 are expressed on neurons in the central nervous system. *Neuroreport* 20, 1161–1166. doi: 10.1097/WNR.0b013e32832fbf14

Hamilton, J. P., Farmer, M., Fogelman, P., and Gotlib, I. H. (2015). Depressive Rumination, the Default-Mode Network, and the Dark Matter of Clinical Neuroscience. *Biol. Psychiatry* 78, 224–230. doi: 10.1016/j.biopsych.2015.02.020

Hamon, M., and Blier, P. (2013). Monoamine neurocircuitry in depression and strategies for new treatments. *Prog. Neuropsychopharmacol. Biol. Psychiatry* 45, 54–63. doi: 10.1016/j.pnpbp.2013.04.009

Hansen, H. H., Fabricius, K., Barkholt, P., Niehoff, M. L., Morley, J. E., Jelsing, J., et al. (2015). The GLP-1 Receptor Agonist Liraglutide Improves Memory Function and Increases Hippocampal CA1 Neuronal Numbers in a Senescence-Accelerated Mouse Model of Alzheimer's Disease. *J. Alzheimers Dis.* 46, 877–888. doi: 10.3233/JAD-143090

Hanson, N. D., Owens, M. J., and Nemeroff, C. B. (2011). Depression, antidepressants, and neurogenesis: a critical reappraisal. *Neuropsychopharmacology* 36, 2589–2602. doi: 10.1038/npp.2011.220

Haroon, E., and Miller, A. H. (2017). Inflammation Effects on Brain Glutamate in Depression: Mechanistic Considerations and Treatment Implications. *Curr. Top. Behav. Neurosci.* 31, 173–198. doi: 10.1007/7854_2016_40

Hayes, M. R., and Schmidt, H. D. (2016). GLP-1 influences food and drug reward. *Curr. Opin. Behav. Sci.* 9, 66–70. doi: 10.1016/j.cobeha.2016.02.005

He, W., Tian, X., Lv, M., and Wang, H. (2018). Liraglutide Protects Neurite Outgrowth of Cortical Neurons Under Oxidative Stress though Activating the Wnt Pathway. *J. Stroke Cerebrovasc. Dis.* 27, 2696–2702. doi: 10.1016/j.jstrokecerebrovasdis.2018.05.039

Heppner, K. M., Kirigiti, M., Secher, A., Paulsen, S. J., Buckingham, R., Pyke, C., et al. (2015a). Expression and distribution of glucagon-like peptide-1 receptor mRNA, protein and binding in the male nonhuman primate (Macaca mulatta) brain. *Endocrinology* 156, 255–267. doi: 10.1210/en.2014-1675

Heppner, K. M., Marks, S., Holland, J., Ottaway, N., Smiley, D., Dimarchi, R., et al. (2015b). Contribution of brown adipose tissue activity to the control of energy balance by GLP-1 receptor signalling in mice. *Diabetologia* 58, 2124–2132. doi: 10.1007/s00125-015-3651-3

Hervas, I., Queiroz, C. M., Adell, A., and Artigas, F. (2000). Role of uptake inhibition and autoreceptor activation in the control of 5-HT release in the frontal cortex and dorsal hippocampus of the rat. *Br. J. Pharmacol.* 130, 160–166. doi: 10.1038/sj.bjp.0703297

Hestad, K. A., Engedal, K., Whist, J. E., Aukrust, P., Farup, P. G., Mollnes, T. E., et al. (2016). Patients with depression display cytokine levels in serum and cerebrospinal fluid similar to patients with diffuse neurological symptoms without a defined diagnosis. *Neuropsychiatr. Dis. Treat* 12, 817–822. doi: 10.2147/NDT.S101925

Hill, A. S., Sahay, A., and Hen, R. (2015). Increasing Adult Hippocampal Neurogenesis is Sufficient to Reduce Anxiety and Depression-Like Behaviors. *Neuropsychopharmacology* 40, 2368–2378. doi: 10.1038/npp.2015.85

Hoeffer, C. A., and Klann, E. (2010). mTOR signaling: at the crossroads of plasticity, memory and disease. *Trends Neurosci.* 33, 67–75. doi: 10.1016/j.tins.2009.11.003

Holscher, C. (2010). Incretin analogues that have been developed to treat type 2 diabetes hold promise as a novel treatment strategy for Alzheimer's disease. *Recent Pat. CNS Drug Discov.* 5, 109–117. doi: 10.2174/157488910791213130

Holscher, C. (2012). Potential role of glucagon-like peptide-1 (GLP-1) in neuroprotection. *CNS Drugs* 26, 871–882. doi: 10.2165/11635890-000000000-00000

Holscher, C. (2014). Central effects of GLP-1: new opportunities for treatments of neurodegenerative diseases. *J. Endocrinol.* 221, T31–T41. doi: 10.1530/JOE-13-0221

Holst, J. J. (2007). The physiology of glucagon-like peptide 1. *Physiol. Rev.* 87, 1409–1439. doi: 10.1152/physrev.00034.2006

Hunter, K., and Holscher, C. (2012). Drugs developed to treat diabetes, liraglutide and lixisenatide, cross the blood brain barrier and enhance neurogenesis. *BMC Neurosci.* 13, 33. doi: 10.1186/1471-2202-13-33

Irwin, M. R., and Miller, A. H. (2007). Depressive disorders and immunity: 20 years of progress and discovery. *Brain Behav. Immun.* 21, 374–383. doi: 10.1016/j.bbi.2007.01.010

Isacson, R., Nielsen, E., Dannaeus, K., Bertilsson, G., Patrone, C., Zachrisson, O., et al. (2011). The glucagon-like peptide 1 receptor agonist exendin-4 improves reference memory performance and decreases immobility in the forced swim test. *Eur. J. Pharmacol.* 650, 249–255. doi: 10.1016/j.ejphar.2010.10.008

Iwai, T., Sawabe, T., Tanimitsu, K., Suzuki, M., Sasaki-Hamada, S., and Oka, J. (2014). Glucagon-like peptide-1 protects synaptic and learning functions from neuroinflammation in rodents. *J. Neurosci. Res.* 92, 446–454. doi: 10.1002/jnr.23335

Jha, S., Rajendran, R., Fernandes, K. A., and Vaidya, V. A. (2008). 5-HT2A/2C receptor blockade regulates progenitor cell proliferation in the adult rat hippocampus. *Neurosci. Lett.* 441, 210–214. doi: 10.1016/j.neulet.2008.06.028

Jiang, H., Ling, Z., Zhang, Y., Mao, H., Ma, Z., Yin, Y., et al. (2015). Altered fecal microbiota composition in patients with major depressive disorder. *Brain Behav. Immun.* 48, 186–194. doi: 10.1016/j.bbi.2015.03.016

Jourdi, H., Hsu, Y. T., Zhou, M., Qin, Q., Bi, X., and Baudry, M. (2009). Positive AMPA receptor modulation rapidly stimulates BDNF release and increases dendritic mRNA translation. *J. Neurosci.* 29, 8688–8697. doi: 10.1523/JNEUROSCI.6078-08.2009

Kang, H. J., Voleti, B., Hajszan, T., Rajkowska, G., Stockmeier, C. A., Licznerski, P., et al. (2012). Decreased expression of synapse-related genes and loss of synapses in major depressive disorder. *Nat. Med.* 18, 1413–1417. doi: 10.1038/nm.2886

Kappe, C., Tracy, L. M., Patrone, C., Iverfeldt, K., and Sjoholm, A. (2012). GLP-1 secretion by microglial cells and decreased CNS expression in obesity. *J. Neuroinflammation* 9, 276. doi: 10.1186/1742-2094-9-276

Kappe, C., Patrone, C., Holst, J. J., Zhang, Q., and Sjoholm, A. (2013). Metformin protects against lipoapoptosis and enhances GLP-1 secretion from GLP-1-producing cells. *J. Gastroenterol.* 48, 322–332. doi: 10.1007/s00535-012-0637-5

Karpova, N. N., Pickenhagen, A., Lindholm, J., Tiraboschi, E., Kulesskaya, N., Agustsdottir, A., et al. (2011). Fear erasure in mice requires synergy between antidepressant drugs and extinction training. *Science* 334, 1731–1734. doi: 10.1126/science.1214592

Kastin, A. J., and Akerstrom, V. (2003). Entry of exendin-4 into brain is rapid but may be limited at high doses. *Int. J. Obes. Relat. Metab. Disord.* 27, 313–318. doi: 10.1038/sj.ijo.0802206

Kastin, A. J., Akerstrom, V., and Pan, W. (2002). Interactions of glucagon-like peptide-1 (GLP-1) with the blood-brain barrier. *J. Mol. Neurosci.* 18, 7–14. doi: 10.1385/JMN:18:1-2:07

Kessler, R. C., Chiu, W. T., Demler, O., Merikangas, K. R., and Walters, E. E. (2005). Prevalence, severity, and comorbidity of 12-month DSM-IV disorders in the National Comorbidity Survey Replication. *Arch. Gen. Psychiatry* 62, 617–627. doi: 10.1001/archpsyc.62.6.617

Khandaker, G. M., Cousins, L., Deakin, J., Lennox, B. R., Yolken, R., and Jones, P. B. (2015). Inflammation and immunity in schizophrenia: implications for pathophysiology and treatment. *Lancet Psychiatry* 2, 258–270. doi: 10.1016/S2215-0366(14)00122-9

Klempin, F., Beis, D., Mosienko, V., Kempermann, G., Bader, M., and Alenina, N. (2013). Serotonin is required for exercise-induced adult hippocampal neurogenesis. *J. Neurosci.* 33, 8270–8275. doi: 10.1523/JNEUROSCI.5855-12.2013

Knight, R., Callewaert, C., Marotz, C., Hyde, E. R., Debelius, J. W., Mcdonald, D., et al. (2017). The Microbiome and Human Biology. *Annu. Rev. Genomics Hum. Genet.* 18, 65–86. doi: 10.1146/annurev-genom-083115-022438

Kohler, S., Thomas, A. J., Barnett, N. A., and O'brien, J. T. (2010). The pattern and course of cognitive impairment in late-life depression. *Psychol. Med.* 40, 591–602. doi: 10.1017/S0033291709990833

Kohler, C. A., Freitas, T. H., Maes, M., De Andrade, N. Q., Liu, C. S., Fernandes, B. S., et al. (2017). Peripheral cytokine and chemokine alterations in depression: a

meta-analysis of 82 studies. *Acta Psychiatr. Scand.* 135, 373–387. doi: 10.1111/acps.12698

Kondo, M., Nakamura, Y., Ishida, Y., and Shimada, S. (2015). The 5-HT3 receptor is essential for exercise-induced hippocampal neurogenesis and antidepressant effects. *Mol. Psychiatry* 20, 1428–1437. doi: 10.1038/mp.2014.153

Kopschina Feltes, P., Doorduin, J., Klein, H. C., Juarez-Orozco, L. E., Dierckx, R. A., Moriguchi-Jeckel, C. M., et al. (2017). Anti-inflammatory treatment for major depressive disorder: implications for patients with an elevated immune profile and non-responders to standard antidepressant therapy. *J. Psychopharmacol.* 31, 1149–1165. doi: 10.1177/0269881117711708

Korn, T., Bettelli, E., Oukka, M., and Kuchroo, V. K. (2009). IL-17 and Th17 Cells. *Annu. Rev. Immunol.* 27, 485–517. doi: 10.1146/annurev.immunol.021908.132710

Korol, S. V., Jin, Z., Babateen, O., and Birnir, B. (2015). GLP-1 and exendin-4 transiently enhance GABAA receptor-mediated synaptic and tonic currents in rat hippocampal CA3 pyramidal neurons. *Diabetes* 64, 79–89. doi: 10.2337/db14-0668

Kraus, C., Castren, E., Kasper, S., and Lanzenberger, R. (2017). Serotonin and neuroplasticity - Links between molecular, functional and structural pathophysiology in depression. *Neurosci. Biobehav. Rev.* 77, 317–326. doi: 10.1016/j.neubiorev.2017.03.007

Krishnan, V., and Nestler, E. J. (2008). The molecular neurobiology of depression. *Nature* 455, 894–902. doi: 10.1038/nature07455

Ledford, H. (2014). Medical research: if depression were cancer. *Nature* 515, 182–184. doi: 10.1038/515182a

Lee, Y. S., Park, M. S., Choung, J. S., Kim, S. S., Oh, H. H., Choi, C. S., et al. (2012). Glucagon-like peptide-1 inhibits adipose tissue macrophage infiltration and inflammation in an obese mouse model of diabetes. *Diabetologia* 55, 2456–2468. doi: 10.1007/s00125-012-2592-3

Lener, M. S., Niciu, M. J., Ballard, E. D., Park, M., Park, L. T., Nugent, A. C., et al. (2017). Glutamate and Gamma-Aminobutyric Acid Systems in the Pathophysiology of Major Depression and Antidepressant Response to Ketamine. *Biol. Psychiatry* 81, 886–897. doi: 10.1016/j.biopsych.2016.05.005

Lennox, R., Porter, D. W., Flatt, P. R., and Gault, V. A. (2013). (Val(8))GLP-1-Glu-PAL: a GLP-1 agonist that improves hippocampal neurogenesis, glucose homeostasis, and beta-cell function in high-fat-fed mice. *ChemMedChem* 8, 595–602. doi: 10.1002/cmdc.201200409

Lennox, R., Porter, D. W., Flatt, P. R., Holscher, C., Irwin, N., and Gault, V. A. (2014). Comparison of the independent and combined effects of sub-chronic therapy with metformin and a stable GLP-1 receptor agonist on cognitive function, hippocampal synaptic plasticity and metabolic control in high-fat fed mice. *Neuropharmacology* 86, 22–30. doi: 10.1016/j.neuropharm.2014.06.026

Leonard, B. E. (2018). Inflammation and depression: a causal or coincidental link to the pathophysiology? *Acta Neuropsychiatr.* 30, 1–16. doi: 10.1017/neu.2016.69

Li, X., and Jope, R. S. (2010). Is glycogen synthase kinase-3 a central modulator in mood regulation? *Neuropsychopharmacology* 35, 2143–2154. doi: 10.1038/npp.2010.105

Li, Y., Perry, T., Kindy, M. S., Harvey, B. K., Tweedie, D., Holloway, H. W., et al. (2009). GLP-1 receptor stimulation preserves primary cortical and dopaminergic neurons in cellular and rodent models of stroke and Parkinsonism. *Proc. Natl. Acad. Sci. U. S. A.* 106, 1285–1290. doi: 10.1073/pnas.0806720106

Li, Y., Tweedie, D., Mattson, M. P., Holloway, H. W., and Greig, N. H. (2010). Enhancing the GLP-1 receptor signaling pathway leads to proliferation and neuroprotection in human neuroblastoma cells. *J. Neurochem.* 113, 1621–1631. doi: 10.1111/j.1471-4159.2010.06731.x

Lietzau, G., Magni, G., Kehr, J., Yoshitake, T., Candeias, E., Duarte, A. I., et al. (2020). Dipeptidyl peptidase-4 inhibitors and sulfonylureas prevent the progressive impairment of the nigrostriatal dopaminergic system induced by diabetes during aging. *Neurobiol. Aging* 89, 12–23. doi: 10.1016/j.neurobiolaging.2020.01.004

Liu, H., Dear, A. E., Knudsen, L. B., and Simpson, R. W. (2009). A long-acting glucagon-like peptide-1 analogue attenuates induction of plasminogen activator inhibitor type-1 and vascular adhesion molecules. *J. Endocrinol.* 201, 59–66. doi: 10.1677/JOE-08-0468

Llewellyn-Smith, I. J., Gnanamanickam, G. J., Reimann, F., Gribble, F. M., and Trapp, S. (2013). Preproglucagon (PPG) neurons innervate neurochemically identified autonomic neurons in the mouse brainstem. *Neuroscience* 229, 130–143. doi: 10.1016/j.neuroscience.2012.09.071

Luciani, P., Deledda, C., Benvenuti, S., Cellai, I., Squecco, R., Monici, M., et al. (2010). Differentiating effects of the glucagon-like peptide-1 analogue exendin-4 in a human neuronal cell model. *Cell Mol. Life Sci.* 67, 3711–3723. doi: 10.1007/s00018-010-0398-3

MacQueen, G., and Frodl, T. (2011). The hippocampus in major depression: evidence for the convergence of the bench and bedside in psychiatric research? *Mol. Psychiatry* 16, 252–264. doi: 10.1038/mp.2010.80

Maes, M., Leonard, B. E., Myint, A. M., Kubera, M., and Verkerk, R. (2011). The new '5-HT' hypothesis of depression: cell-mediated immune activation induces indoleamine 2,3-dioxygenase, which leads to lower plasma tryptophan and an increased synthesis of detrimental tryptophan catabolites (TRYCATs), both of which contribute to the onset of depression. *Prog. Neuropsychopharmacol. Biol. Psychiatry* 35, 702–721. doi: 10.1016/j.pnpbp.2010.12.017

Mainardi, M., Fusco, S., and Grassi, C. (2015). Modulation of hippocampal neural plasticity by glucose-related signaling. *Neural Plast.* 2015, 657928. doi: 10.1155/2015/657928

Manigault, K. R., and Thurston, M. M. (2016). Liraglutide: A Glucagon-Like Peptide-1 Agonist for Chronic Weight Management. *Consult Pharm.* 31, 685–697. doi: 10.4140/TCP.n.2016.685

Marchetti, I., Koster, E. H., Sonuga-Barke, E. J., and De Raedt, R. (2012). The default mode network and recurrent depression: a neurobiological model of cognitive risk factors. *Neuropsychol. Rev.* 22, 229–251. doi: 10.1007/s11065-012-9199-9

Massart, R., Mongeau, R., and Lanfumey, L. (2012). Beyond the monoaminergic hypothesis: neuroplasticity and epigenetic changes in a transgenic mouse model of depression. *Philos. Trans. R. Soc. Lond. B. Biol. Sci.* 367, 2485–2494. doi: 10.1098/rstb.2012.0212

McClean, P. L., and Holscher, C. (2014). Liraglutide can reverse memory impairment, synaptic loss and reduce plaque load in aged APP/PS1 mice, a model of Alzheimer's disease. *Neuropharmacology* 76 (Pt A), 57–67. doi: 10.1016/j.neuropharm.2013.08.005

McClean, P. L., Gault, V. A., Harriott, P., and Holscher, C. (2010). Glucagon-like peptide-1 analogues enhance synaptic plasticity in the brain: a link between diabetes and Alzheimer's disease. *Eur. J. Pharmacol.* 630, 158–162. doi: 10.1016/j.ejphar.2009.12.023

McClean, P. L., Parthsarathy, V., Faivre, E., and Holscher, C. (2011). The diabetes drug liraglutide prevents degenerative processes in a mouse model of Alzheimer's disease. *J. Neurosci.* 31, 6587–6594. doi: 10.1523/JNEUROSCI.0529-11.2011

McEwen, B. S., Eiland, L., Hunter, R. G., and Miller, M. M. (2012). Stress and anxiety: structural plasticity and epigenetic regulation as a consequence of stress. *Neuropharmacology* 62, 3–12. doi: 10.1016/j.neuropharm.2011.07.014

McGovern, S. F., Hunter, K., and Holscher, C. (2012). Effects of the glucagon-like polypeptide-1 analogue (Val8)GLP-1 on learning, progenitor cell proliferation and neurogenesis in the C57B/16 mouse brain. *Brain Res.* 1473, 204–213. doi: 10.1016/j.brainres.2012.07.029

McKie, S., Del-Ben, C., Elliott, R., Williams, S., Del Vai, N., Anderson, I., et al. (2005). Neuronal effects of acute citalopram detected by pharmacoMRI. *Psychopharmacol. (Berl)* 180, 680–686. doi: 10.1007/s00213-005-2270-y

McQuade, R., and Sharp, T. (1997). Functional mapping of dorsal and median raphe 5-hydroxytryptamine pathways in forebrain of the rat using microdialysis. *J. Neurochem.* 69, 791–796. doi: 10.1046/j.1471-4159.1997.69020791.x

Mendez-David, I., Hen, R., Gardier, A. M., and David, D. J. (2013). Adult hippocampal neurogenesis: an actor in the antidepressant-like action. *Ann. Pharm. Fr.* 71, 143–149. doi: 10.1016/j.pharma.2013.02.006

Merchenthaler, I., Lane, M., and Shughrue, P. (1999). Distribution of pre-pro-glucagon and glucagon-like peptide-1 receptor messenger RNAs in the rat central nervous system. *J. Comp. Neurol.* 403, 261–280. doi: 10.1002/(SICI)1096-9861(19990111)403:2<261::AID-CNE8>3.0.CO;2-5

Miller, R. J., Rostene, W., Apartis, E., Banisadr, G., Biber, K., Milligan, E. D., et al. (2008). Chemokine action in the nervous system. *J. Neurosci.* 28, 11792–11795. doi: 10.1523/JNEUROSCI.3588-08.2008

Mohammadi, M., Nasehi, M., and Zarrindast, M. R. (2015). Modulation of the effects of the cannabinoid agonist, ACPA, on spatial and non-spatial novelty detection in mice by dopamine D1 receptor drugs infused into the basolateral amygdala. *Behav. Brain Res.* 280, 36–44. doi: 10.1016/j.bbr.2014.11.003

Monroe, S. M., and Harkness, K. L. (2005). Life stress, the "kindling" hypothesis, and the recurrence of depression: considerations from a life stress perspective. *Psychol. Rev.* 112, 417–445. doi: 10.1037/0033-295X.112.2.417

Mora, P. F., and Johnson, E. L. (2017). Cardiovascular Outcome Trials of the Incretin-Based Therapies: What Do We Know So Far? *Endocr. Pract.* 23, 89–99. doi: 10.4158/EP161481.RA

Morrison, J. H., and Baxter, M. G. (2012). The ageing cortical synapse: hallmarks and implications for cognitive decline. *Nat. Rev. Neurosci.* 13, 240–250. doi: 10.1038/nrn3200

Moylan, S., Maes, M., Wray, N. R., and Berk, M. (2013). The neuroprogressive nature of major depressive disorder: pathways to disease evolution and resistance, and therapeutic implications. *Mol. Psychiatry* 18, 595–606. doi: 10.1038/mp.2012.33

Murrough, J. W., Abdallah, C. G., and Mathew, S. J. (2017). Targeting glutamate signalling in depression: progress and prospects. *Nat. Rev. Drug Discov.* 16, 472–486. doi: 10.1038/nrd.2017.16

Najjar, S., Pearlman, D. M., Devinsky, O., Najjar, A., and Zagzag, D. (2013). Neurovascular unit dysfunction with blood-brain barrier hyperpermeability contributes to major depressive disorder: a review of clinical and experimental evidence. *J. Neuroinflammation* 10, 142. doi: 10.1186/1742-2094-10-142

Neufeld, K. A., and Foster, J. A. (2009). Effects of gut microbiota on the brain: implications for psychiatry. *J. Psychiatry Neurosci.* 34, 230–231.

Nunes, S. O., Reiche, E. M., Morimoto, H. K., Matsuo, T., Itano, E. N., Xavier, E. C., et al. (2002). Immune and hormonal activity in adults suffering from depression. *Braz. J. Med. Biol. Res.* 35, 581–587. doi: 10.1590/S0100-879X2002000500011

Onoviran, O. F., Li, D., Toombs Smith, S., and Raji, M. A. (2019). Effects of glucagon-like peptide 1 receptor agonists on comorbidities in older patients with diabetes mellitus. *Ther. Adv. Chronic Dis.* 10, 2040622319862691. doi: 10.1177/2040622319862691

O'Mahony, S. M., Clarke, G., Borre, Y. E., Dinan, T. G., and Cryan, J. F. (2015). Serotonin, tryptophan metabolism and the brain-gut-microbiome axis. *Behav. Brain Res.* 277, 32–48. doi: 10.1016/j.bbr.2014.07.027

Parker, H. E., Reimann, F., and Gribble, F. M. (2010). Molecular mechanisms underlying nutrient-stimulated incretin secretion. *Expert Rev. Mol. Med.* 12, e1. doi: 10.1017/S146239940900132X

Parthsarathy, V., and Holscher, C. (2013a). Chronic treatment with the GLP1 analogue liraglutide increases cell proliferation and differentiation into neurons in an AD mouse model. *PLoS One* 8, e58784. doi: 10.1371/journal.pone.0058784

Parthsarathy, V., and Holscher, C. (2013b). The type 2 diabetes drug liraglutide reduces chronic inflammation induced by irradiation in the mouse brain. *Eur. J. Pharmacol.* 700, 42–50. doi: 10.1016/j.ejphar.2012.12.012

Paudel, Y. N., Shaikh, M. F., Shah, S., Kumari, Y., and Othman, I. (2018). Role of inflammation in epilepsy and neurobehavioral comorbidities: Implication for therapy. *Eur. J. Pharmacol.* 837, 145–155. doi: 10.1016/j.ejphar.2018.08.020

Perlman, G., Simmons, A. N., Wu, J., Hahn, K. S., Tapert, S. F., Max, J. E., et al. (2012). Amygdala response and functional connectivity during emotion regulation: a study of 14 depressed adolescents. *J. Affect. Disord.* 139, 75–84. doi: 10.1016/j.jad.2012.01.044

Petrik, D., Jiang, Y., Birnbaum, S. G., Powell, C. M., Kim, M. S., Hsieh, J., et al. (2012). Functional and mechanistic exploration of an adult neurogenesis-promoting small molecule. *FASEB J.* 26, 3148–3162. doi: 10.1096/fj.11-201426

Piletz, J. E., Halaris, A., Iqbal, O., Hoppensteadt, D., Fareed, J., Zhu, H., et al. (2009). Pro-inflammatory biomakers in depression: treatment with venlafaxine. *World J. Biol. Psychiatry* 10, 313–323. doi: 10.3109/15622970802573246

Porter, W. D., Flatt, P. R., Holscher, C., and Gault, V. A. (2013). Liraglutide improves hippocampal synaptic plasticity associated with increased expression of Mash1 in ob/ob mice. *Int. J. Obes. (Lond.)* 37, 678–684. doi: 10.1038/ijo.2012.91

Price, J. L., and Drevets, W. C. (2010). Neurocircuitry of mood disorders. *Neuropsychopharmacology* 35, 192–216. doi: 10.1038/npp.2009.104

Pytka, K., Dziubina, A., Mlyniec, K., Dziedziczak, A., Zmudzka, E., Furgala, A., et al. (2016). The role of glutamatergic, GABA-ergic, and cholinergic receptors in depression and antidepressant-like effect. *Pharmacol. Rep.* 68, 443–450. doi: 10.1016/j.pharep.2015.10.006

Rajkowska, G., Miguel-Hidalgo, J. J., Wei, J., Dilley, G., Pittman, S. D., Meltzer, H. Y., et al. (1999). Morphometric evidence for neuronal and glial prefrontal cell pathology in major depression. *Biol. Psychiatry* 45, 1085–1098. doi: 10.1016/S0006-3223(99)00041-4

Rajkowska, G., O'dwyer, G., Teleki, Z., Stockmeier, C. A., and Miguel-Hidalgo, J. J. (2007). GABAergic neurons immunoreactive for calcium binding proteins are reduced in the prefrontal cortex in major depression. *Neuropsychopharmacology* 32, 471–482. doi: 10.1038/sj.npp.1301234

Rao, M., and Gershon, M. D. (2016). The bowel and beyond: the enteric nervous system in neurological disorders. *Nat. Rev. Gastroenterol. Hepatol.* 13, 517–528. doi: 10.1038/nrgastro.2016.107

Rebosio, C., Balbi, M., Passalacqua, M., Ricciarelli, R., and Fedele, E. (2018). Presynaptic GLP-1 receptors enhance the depolarization-evoked release of glutamate and GABA in the mouse cortex and hippocampus. *Biofactors* 44, 148–157. doi: 10.1002/biof.1406

Reed, J., Bain, S., and Kanamarlapudi, V. (2020). Recent advances in understanding the role of glucagon-like peptide 1. *F1000Res* 9, 239. doi: 10.12688/f1000research.20602.1

Richard, J. E., Anderberg, R. H., Goteson, A., Gribble, F. M., Reimann, F., and Skibicka, K. P. (2015). Activation of the GLP-1 receptors in the nucleus of the solitary tract reduces food reward behavior and targets the mesolimbic system. *PLoS One* 10, e0119034. doi: 10.1371/journal.pone.0119034

Robinson, A., Lubitz, I., Atrakchi-Baranes, D., Licht-Murava, A., Katsel, P., Leroith, D., et al. (2019). Combination of Insulin with a GLP1 Agonist Is Associated with Better Memory and Normal Expression of Insulin Receptor Pathway Genes in a Mouse Model of Alzheimer's Disease. *J. Mol. Neurosci.* 67, 504–510. doi: 10.1007/s12031-019-1257-9

Rush, A. J., Trivedi, M. H., Wisniewski, S. R., Nierenberg, A. A., Stewart, J. W., Warden, D., et al. (2006). Acute and longer-term outcomes in depressed outpatients requiring one or several treatment steps: a STAR*D report. *Am. J. Psychiatry* 163, 1905–1917. doi: 10.1176/ajp.2006.163.11.1905

Sahay, A., and Hen, R. (2007). Adult hippocampal neurogenesis in depression. *Nat. Neurosci.* 10, 1110–1115. doi: 10.1038/nn1969

Salcedo, I., Tweedie, D., Li, Y., and Greig, N. H. (2012). Neuroprotective and neurotrophic actions of glucagon-like peptide-1: an emerging opportunity to treat neurodegenerative and cerebrovascular disorders. *Br. J. Pharmacol.* 166, 1586–1599. doi: 10.1111/j.1476-5381.2012.01971.x

Sanacora, G., Zarate, C. A., Krystal, J. H., and Manji, H. K. (2008). Targeting the glutamatergic system to develop novel, improved therapeutics for mood disorders. *Nat. Rev. Drug Discov.* 7, 426–437. doi: 10.1038/nrd2462

Sango, K., and Utsunomiya, K. (2015). Efficacy of glucagon-like peptide-1 mimetics for neural regeneration. *Neural Regener. Res.* 10, 1723–1724. doi: 10.4103/1673-5374.169611

Schmidt-Hieber, C., Jonas, P., and Bischofberger, J. (2004). Enhanced synaptic plasticity in newly generated granule cells of the adult hippocampus. *Nature* 429, 184–187. doi: 10.1038/nature02553

Scott, L. V., Clarke, G., and Dinan, T. G. (2013). The brain-gut axis: a target for treating stress-related disorders. *Mod. Trends Pharmacopsychiatry* 28, 90–99. doi: 10.1159/000343971

Serafini, G. (2012). Neuroplasticity and major depression, the role of modern antidepressant drugs. *World J. Psychiatry* 2, 49–57. doi: 10.5498/wjp.v2.i3.49

Setoyama, D., Kato, T. A., Hashimoto, R., Kunugi, H., Hattori, K., Hayakawa, K., et al. (2016). Plasma Metabolites Predict Severity of Depression and Suicidal Ideation in Psychiatric Patients-A Multicenter Pilot Analysis. *PLoS One* 11, e0165267. doi: 10.1371/journal.pone.0165267

Sharma, A. N., Ligade, S. S., Sharma, J. N., Shukla, P., Elased, K. M., and Lucot, J. B. (2015). GLP-1 receptor agonist liraglutide reverses long-term atypical antipsychotic treatment associated behavioral depression and metabolic abnormalities in rats. *Metab. Brain Dis.* 30, 519–527. doi: 10.1007/s11011-014-9591-7

Sheline, Y. I., Sanghavi, M., Mintun, M. A., and Gado, M. H. (1999). Depression duration but not age predicts hippocampal volume loss in medically healthy women with recurrent major depression. *J. Neurosci.* 19, 5034–5043. doi: 10.1523/JNEUROSCI.19-12-05034.1999

Slusarczyk, J., Trojan, E., Chwastek, J., Glombik, K., and Basta-Kaim, A. (2016). A Potential Contribution of Chemokine Network Dysfunction to the Depressive Disorders. *Curr. Neuropharmacol.* 14, 705–720. doi: 10.2174/1570159X14666160219131357

Slyepchenko, A., Maes, M., Kohler, C. A., Anderson, G., Quevedo, J., Alves, G. S., et al. (2016). T helper 17 cells may drive neuroprogression in major depressive

disorder: Proposal of an integrative model. *Neurosci. Biobehav. Rev.* 64, 83–100. doi: 10.1016/j.neubiorev.2016.02.002

Smith, K. J., Au, B., Ollis, L., and Schmitz, N. (2018). The association between C-reactive protein, Interleukin-6 and depression among older adults in the community: A systematic review and meta-analysis. *Exp. Gerontol.* 102, 109–132. doi: 10.1016/j.exger.2017.12.005

Smitha, J. S., Roopa, R., Sagar, B. K., Kutty, B. M., and Andrade, C. (2014). Images in electroconvulsive therapy: ECS dose-dependently increases cell proliferation in the subgranular region of the rat hippocampus. *J. ECT* 30, 193–194. doi: 10.1097/YCT.0000000000000076

Solmaz, V., Cinar, B. P., Yigitturk, G., Cavusoglu, T., Taskiran, D., and Erbas, O. (2015). Exenatide reduces TNF-alpha expression and improves hippocampal neuron numbers and memory in streptozotocin treated rats. *Eur. J. Pharmacol.* 765, 482–487. doi: 10.1016/j.ejphar.2015.09.024

Son, H., Banasr, M., Choi, M., Chae, S. Y., Licznerski, P., Lee, B., et al. (2012). Neuritin produces antidepressant actions and blocks the neuronal and behavioral deficits caused by chronic stress. *Proc. Natl. Acad. Sci. U. S. A.* 109, 11378–11383. doi: 10.1073/pnas.1201191109

Song, C., and Wang, H. (2011). Cytokines mediated inflammation and decreased neurogenesis in animal models of depression. *Prog. Neuropsychopharmacol. Biol. Psychiatry* 35, 760–768. doi: 10.1016/j.pnpbp.2010.06.020

Sorensen, G., Reddy, I. A., Weikop, P., Graham, D. L., Stanwood, G. D., Wortwein, G., et al. (2015). The glucagon-like peptide 1 (GLP-1) receptor agonist exendin-4 reduces cocaine self-administration in mice. *Physiol. Behav.* 149, 262–268. doi: 10.1016/j.physbeh.2015.06.013

Steinberg, E. E., Keiflin, R., Boivin, J. R., Witten, I. B., Deisseroth, K., and Janak, P. H. (2013). A causal link between prediction errors, dopamine neurons and learning. *Nat. Neurosci.* 16, 966–973. doi: 10.1038/nn.3413

Sutcigil, L., Oktenli, C., Musabak, U., Bozkurt, A., Cansever, A., Uzun, O., et al. (2007). Pro- and anti-inflammatory cytokine balance in major depression: effect of sertraline therapy. *Clin. Dev. Immunol.* 2007, 76396. doi: 10.1155/2007/76396

Taliaz, D., Stall, N., Dar, D. E., and Zangen, A. (2010). Knockdown of brain-derived neurotrophic factor in specific brain sites precipitates behaviors associated with depression and reduces neurogenesis. *Mol. Psychiatry* 15, 80–92. doi: 10.1038/mp.2009.67

Tanti, A., and Belzung, C. (2013). Hippocampal neurogenesis: a biomarker for depression or antidepressant effects? Methodological considerations and perspectives for future research. *Cell Tissue Res.* 354, 203–219. doi: 10.1007/s00441-013-1612-z

Tian, L., Gao, J., Hao, J., Zhang, Y., Yi, H., O'brien, T. D., et al. (2010). Reversal of new-onset diabetes through modulating inflammation and stimulating beta-cell replication in nonobese diabetic mice by a dipeptidyl peptidase IV inhibitor. *Endocrinology* 151, 3049–3060. doi: 10.1210/en.2010-0068

Toni, N., Teng, E. M., Bushong, E. A., Aimone, J. B., Zhao, C., Consiglio, A., et al. (2007). Synapse formation on neurons born in the adult hippocampus. *Nat. Neurosci.* 10, 727–734. doi: 10.1038/nn1908

Tran, P. B., Banisadr, G., Ren, D., Chenn, A., and Miller, R. J. (2007). Chemokine receptor expression by neural progenitor cells in neurogenic regions of mouse brain. *J. Comp. Neurol.* 500, 1007–1033. doi: 10.1002/cne.21229

Tsai, J., and Rosenheck, R. A. (2016). US Veterans' Use Of VA Mental Health Services And Disability Compensation Increased From 2001 To 2010. *Health Aff. (Millwood)* 35, 966–973. doi: 10.1377/hlthaff.2015.1555

Turton, M. D., O'shea, D., Gunn, I., Beak, S. A., Edwards, C. M., Meeran, K., et al. (1996). A role for glucagon-like peptide-1 in the central regulation of feeding. *Nature* 379, 69–72. doi: 10.1038/379069a0

Tye, K. M., Mirzabekov, J. J., Warden, M. R., Ferenczi, E. A., Tsai, H. C., Finkelstein, J., et al. (2013). Dopamine neurons modulate neural encoding and expression of depression-related behaviour. *Nature* 493, 537–541. doi: 10.1038/nature11740

Velmurugan, K., Balamurugan, A. N., Loganathan, G., Ahmad, A., Hering, B. J., and Pugazhenthi, S. (2012). Antiapoptotic actions of exendin-4 against hypoxia and cytokines are augmented by CREB. *Endocrinology* 153, 1116–1128. doi: 10.1210/en.2011-1895

Ventorp, F., Bay-Richter, C., Nagendra, A. S., Janelidze, S., Matsson, V. S., Lipton, J., et al. (2017). Exendin-4 Treatment Improves LPS-Induced Depressive-Like Behavior Without Affecting Pro-Inflammatory Cytokines. *J. Parkinsons. Dis.* 7, 263–273. doi: 10.3233/JPD-171068

Vertes, R. P. (1991). A PHA-L analysis of ascending projections of the dorsal raphe nucleus in the rat. *J. Comp. Neurol.* 313, 643–668. doi: 10.1002/cne.903130409

Wang, J. W., David, D. J., Monckton, J. E., Battaglia, F., and Hen, R. (2008). Chronic fluoxetine stimulates maturation and synaptic plasticity of adult-born hippocampal granule cells. *J. Neurosci.* 28, 1374–1384. doi: 10.1523/JNEUROSCI.3632-07.2008

Wang, X. F., Liu, J. J., Xia, J., Liu, J., Mirabella, V., and Pang, Z. P. (2015). Endogenous Glucagon-like Peptide-1 Suppresses High-Fat Food Intake by Reducing Synaptic Drive onto Mesolimbic Dopamine Neurons. *Cell Rep.* 12, 726–733. doi: 10.1016/j.celrep.2015.06.062

Wang, Y. H., Liou, K. T., Tsai, K. C., Liu, H. K., Yang, L. M., Chern, C. M., et al. (2018). GSK-3 inhibition through GLP-1R allosteric activation mediates the neurogenesis promoting effect of P7C3 after cerebral ischemic/reperfusional injury in mice. *Toxicol. Appl. Pharmacol.* 357, 88–105. doi: 10.1016/j.taap.2018.08.023

Weber, C. (2016). Neurogastroenterology: Improving glucose tolerance via the gut-brain axis. *Nat. Rev. Gastroenterol. Hepatol.* 13, 4. doi: 10.1038/nrgastro.2015.204

Weina, H., Yuhu, N., Christian, H., Birong, L., Feiyu, S., and Le, W. (2018). Liraglutide attenuates the depressive- and anxiety-like behaviour in the corticosterone induced depression model via improving hippocampal neural plasticity. *Brain Res.* 1694, 55–62. doi: 10.1016/j.brainres.2018.04.031

Wilkinson, M. B., Dias, C., Magida, J., Mazei-Robison, M., Lobo, M., Kennedy, P., et al. (2011). A novel role of the WNT-dishevelled-GSK3beta signaling cascade in the mouse nucleus accumbens in a social defeat model of depression. *J. Neurosci.* 31, 9084–9092. doi: 10.1523/JNEUROSCI.0039-11.2011

Williams, L. M. (2016). Precision psychiatry: a neural circuit taxonomy for depression and anxiety. *Lancet Psychiatry* 3, 472–480. doi: 10.1016/S2215-0366(15)00579-9

Woelfer, M., Kasties, V., Kahlfuss, S., and Walter, M. (2019). The Role of Depressive Subtypes within the Neuroinflammation Hypothesis of Major Depressive Disorder. *Neuroscience* 403, 93–110. doi: 10.1016/j.neuroscience.2018.03.034

Yu, H., Wang, D. D., Wang, Y., Liu, T., Lee, F. S., and Chen, Z. Y. (2012). Variant brain-derived neurotrophic factor Val66Met polymorphism alters vulnerability to stress and response to antidepressants. *J. Neurosci.* 32, 4092–4101. doi: 10.1523/JNEUROSCI.5048-11.2012

Yuen, E. Y., Wei, J., Liu, W., Zhong, P., Li, X., and Yan, Z. (2012). Repeated stress causes cognitive impairment by suppressing glutamate receptor expression and function in prefrontal cortex. *Neuron* 73, 962–977. doi: 10.1016/j.neuron.2011.12.033

Zeng, L. L., Shen, H., Liu, L., Wang, L., Li, B., Fang, P., et al. (2012). Identifying major depression using whole-brain functional connectivity: a multivariate pattern analysis. *Brain* 135, 1498–1507. doi: 10.1093/brain/aws059

Zhang, R. L., Zhang, Z. G., and Chopp, M. (2008). Ischemic stroke and neurogenesis in the subventricular zone. *Neuropharmacology* 55, 345–352. doi: 10.1016/j.neuropharm.2008.05.027

Zhang, K., Zhu, Y., Zhu, Y., Wu, S., Liu, H., Zhang, W., et al. (2016). Molecular, Functional, and Structural Imaging of Major Depressive Disorder. *Neurosci. Bull.* 32, 273–285. doi: 10.1007/s12264-016-0030-0

Zhao, J., Bao, A. M., Qi, X. R., Kamphuis, W., Luchetti, S., Lou, J. S., et al. (2012). Gene expression of GABA and glutamate pathway markers in the prefrontal cortex of non-suicidal elderly depressed patients. *J. Affect. Disord.* 138, 494–502. doi: 10.1016/j.jad.2012.01.013

Zheng, P., Zeng, B., Zhou, C., Liu, M., Fang, Z., Xu, X., et al. (2016). Gut microbiome remodeling induces depressive-like behaviors through a pathway mediated by the host's metabolism. *Mol. Psychiatry* 21, 786–796. doi: 10.1038/mp.2016.44

Conflict of Interest: The authors declare that the research was conducted in the absence of any commercial or financial relationships that could be construed as a potential conflict of interest.

frontiers in Pharmacology

ORIGINAL RESEARCH
published: 02 September 2020
doi: 10.3389/fphar.2020.559046

Notoginsenoside R1 Protects Against the Acrylamide-Induced Neurotoxicity *via* Upregulating Trx-1-Mediated ITGAV Expression: Involvement of Autophagy

Wenjun Wang[1,2†], *Lu Huang*[1†], *Elizabeth Rosalind Thomas*[3], *Yingying Hu*[1], *Fancai Zeng*[1*] *and Xiang Li*[1*]

[1] Department of Biochemistry and Molecular Biology, School of Basic Medical Science, Southwest Medical University, Luzhou, China, [2] Institute for Cancer Medicine and School of Basic Medical Sciences, Southwest Medical University, Luzhou, China, [3] Department of Biotechnology and Bioinformatics, North Eastern Hill University, Shillong, India

OPEN ACCESS

Edited by:
Haiyun Xu,
Shantou University, China

Reviewed by:
Zhang Pengyue,
Yunnan University of Traditional Chinese Medicine, China
Lianwei Li,
Chinese Academy of Sciences, China

***Correspondence:**
Xiang Li
lix2009@126.com
Fancai Zeng
zfcai@swmu.edu.cn

[†]These authors have contributed equally to this work

Specialty section:
This article was submitted to Neuropharmacology, a section of the journal Frontiers in Pharmacology

Received: 05 May 2020
Accepted: 17 August 2020
Published: 02 September 2020

Citation:
Wang W, Huang L, Thomas ER, Hu Y, Zeng F and Li X (2020) Notoginsenoside R1 Protects Against the Acrylamide-Induced Neurotoxicity via Upregulating Trx-1-Mediated ITGAV Expression: Involvement of Autophagy. Front. Pharmacol. 11:559046. doi: 10.3389/fphar.2020.559046

Acrylamide (ACR) is a common chemical used in various industries and it said to have chronic neurotoxic effects. It is produced during tobacco smoking and is also generated in high-starch foods during heat processing. Notoginsenoside R1 (NR1) is a traditional Chinese medicine, which is used to improve the blood circulation and clotting. The objective of this study was to investigate the mechanism of ACR-triggered neurotoxicity and to identify the protective role of NR1 by upregulating thioredoxin-1 (Trx-1). Our results have shown that NR1 could block the spatial and cognitive impairment caused by ACR administration. Bioinformatics analysis revealed that Trx-1 regulated autophagy *via* Integrin alpha V (ITGAV). NR1 could resist the ACR-induced neurotoxicity by upregulating thioredoxin-1 in PC12 cells and mice. The autophagy-related proteins like autophagy-related gene (ATG) 4B, Cathepsin D, LC3 II, lysosomal-associated membrane protein 2a (LAMP2a), and ITGAV were restored to normal levels by NR1 treatment in both PC12 cells and mice. Besides, we also found that overexpression of Trx-1 resisted ACR-induced autophagy in PC12 cells and downregulation of Trx-1 triggered autophagy induced by ACR in PC12 cells. Therefore, it could be concluded that Trx-1 was involved in the autophagy pathway. Besides, we also found that ITGAV was an intermediate node linking Trx-1 and the autophagy pathway.

Keywords: acrylamide, notoginsenoside r1, thioredoxin-1, autophagy, integrin alpha V

INTRODUCTION

Acrylamide (ACR), a well-known water-soluble chemical, is extensively used in various industries. It is also an important reagent that is commonly used for laboratory research, for example, while performing gel electrophoretic separation of molecules. Because of its wide application, human beings are exposed to high levels of ACR (Adewale et al., 2015). Neurotoxicity is a typical phenomenon of ACR toxicity in animal and cell models. Some studies have proven that ACR

toxicity could induce cogitative deficits by influencing the autophagic function of the neurons in the hippocampus (Hip) (Tan et al., 2019). Recently, it was found that ACR-induced cellular toxicity in neurons could lead to apoptosis (He et al., 2017), mitochondrial dysfunction (Zamani et al., 2017), and downregulate antioxidant signaling pathway (Pan et al., 2017). However, the relationship between ACR and autophagy in PC12 cells still remains unmapped.

Notoginsenoside R1 (NR1) is an efficient free radical scavenger. It has been known to possess antioxidant properties and can repress adhesion molecules and chemokines (Dou et al., 2012). NR1 is a conventional Chinese medicine used in the treatment of cardiovascular diseases (Chan et al., 2002; Chen et al., 2011) and acute ischemic stroke (Chen et al., 2008; He et al., 2011). Recent studies have shown that NR1 could reduce myocardial ischemia-reperfusion injury by the autophagy pathway (Liu X. W. et al., 2019), however, the detailed mechanism is not clear.

The responses of cells to reactive oxygen species (ROS) and nitric oxide synthase (NOS) can be changed through various mechanisms. ROS and autophagy are the key players that regulate cellular homeostasis in neural cells. Autophagy can be stimulated by ROS through different kinds of signaling pathways, and conversely, inhibit ROS-induced damage to cells and tissues. Li et al. (2015) proved that ROS can induce autophagy, however, it is also known that autophagy functions as a buffer system to maintain the ROS levels in the cells and reduce toxicity. Some studies have revealed that exposure to cadmium (2 μM) could extensively increase ROS production and induce autophagy. Autophagy induction was further proved by the upregulation of autophagy-related gene (ATG) 4 (Lv et al., 2018). In the other pathways, ATG4 could proteolyze pro-LC3 to form LC3 I. Later, LC3 I forms a conjugate with phosphatidylethanolamine (PE) by the transforming action of ATG7 and ATG3, thereby generating LC3 II. LC3 II then attaches to the autophagosome membrane triggering its elongation (Mondaca-Ruff et al., 2018). The lysosomal proteolytic enzyme Cathepsin D is the only aspartic-type protease that is ubiquitously found in every cell of the human body. It is expressed at high levels in the brain. Normally, Cathepsin D mediates proteolysis and is required for the neuronal cell homeostasis. This is acquired by the degeneration of the unfolded or oxidized protein compounds, which are moved to the lysosomes by the process of autophagy or endocytosis. Besides, previous studies have also reported that lysosomal-associated membrane protein 2 (LAMP2) was involved in the binding of phagosomes with lysosomes (Tanaka et al., 2000; Huynh et al., 2007) and thus it could contribute to the autophagy regulation.

Thioredoxin-1 (Trx-1) is known to have numerous biological applications, such as regulation of the cellular redox balance, activation of the different transcription factors, and protecting the neurons (Bai et al., 2003; Burkegaffney et al., 2005). Previous *in vivo* studies have shown that NR1 could enhance the expression of Trx-1 (Luo et al., 2011).

Integrin alpha V (ITGAV) heterodimers has been known to promote or suppress cancer development in epithelial tissues (Lee et al., 2018). Recent studies have proven that ITGAV was associated with epithelial-mesenchymal transition and cell migration (van der Horst et al., 2011; Shidal et al., 2018). However, there are very few studies which report the potential role of ITGAV in autophagy.

Although NR1 was said to possess protective properties against various neurological diseases, the mechanism behind this hypothesis remains unclear. Our previous study had shown that NR1 played a neuroprotective role in ACR-induced neurotoxicity by suppressing mitochondrial apoptosis (Wang et al., 2020). However, it is still unclear how Trx-1 affects apoptosis. In this study, by using bioinformatics analysis, our results have proven the neuroprotective properties of NR1 on ACR-induced autophagy in PC12 cells. More importantly, this study has revealed that NR1 could inhibit ACR-induced autophagy by increasing the expression of Trx-1 *via* regulation of ITGAV and suppression of autophagy. Therefore, our results showed that ITGAV was an intermediate node linking Trx-1 and autophagy pathway.

MATERIALS AND METHODS

Animals

Male C57BL/6 mice (wild-type, weight 22–25 g, 8 weeks of age) were purchased from Chengdu Dossy Experimental Animals CO., LTD, China. All the mice were housed in plastic cages under controlled conditions: average temperature 23°C, 12 h light/dark cycles, and it had free access to food and water. The mice were randomly divided into four groups: control group (n=8), ACR group (n=8), NR1 group (n=8), and ACR+NR1 group (n=8). In the control group, the mice were administrated with saline (0.9%) once a day for 4 consecutive weeks. In the ACR group, the mice were administrated with ACR (20 mg/kg) once a day for 4 consecutive weeks. The dosage of ACR used in the experiment was based on previous reports (Santhanasabapathy et al., 2015). In the NR1 group, the mice were administrated with NR1 (25 mg/kg) once a day for 4 consecutive weeks. In the ACR+NR1 group, the mice were pretreated with NR1 for 30 min prior to ACR administration. After the behavioral test, the mice were sacrificed by cervical vertebra dislocation. The Hip was immediately dissected, frozen, and stored in a deep freezer at −80°C until the assays were performed. All procedures and protocols had been approved by the animal ethics council of Southwest Medical University and were in accordance with the National Institutes of Health Guide for the Care and Use of Animals.

Morris Water Maze (MWM) Test

MWM was performed to evaluate the spatial learning and memory of the mice after ACR administration. This was performed according to previously published methods (Sharma et al., 2010). MWM consisted of a black circular pool (Height: 50 cm, Diameter: 120 cm) filled with water (Depth: 20 cm, temperature: 24 ± 2°C) and a circular platform (diameter: 10 cm) for animals to escape. The platform was 1 cm below the water surface. In order to monitor the mice during the

experiment, a camera was installed right above the pool. The MWM was encircled with black and white extra-maze cues on the wall of the pool, which could enable the mice to easily identify the different quadrants. The procedure followed for performing the MWM test was as follows: on the first day, all the mice were allowed to swim freely in order to acclimatize to the new environment. During the next five days, the mice were trained four times a day and were introduced to the four water inlet points with their head facing the wall of the pool on the basis of quadrants I, II, III, and IV, respectively. If the mice found the platform (The platform was quadrant V) before the 60 s cut-off, it was allowed to stay on the platform for 5 s and then it was returned back to the home cage. If the mice didn't find the platform in the pool, it was guided to the platform and assigned a latency of 60 s. After the maze test training, all the mice were dried off. For five consecutive days, each mouse were subjected to the four trials (inter-trial interval: 15–20 min). On the day of the maze test, a spatial probe test was performed to detect the spatial memory of mice. The speed of swimming of the mice in the pool was measured. Then, the platform was removed from the pool. The mice were released from the quadrant opposite to the target quadrant and were allowed to swim freely for 60 s. The number of times the mice crossed the quadrant V (which had earlier housed the platform) was recorded. The time taken for swimming in the target quadrant was recorded.

Reagents

Antibody to Trx-1 (14999-1-AP, 1:1,000), antibody to β-actin (20536-1-AP, 1:1,000), antibody to ATG4B (15131-1-AP, 1:1,000), and antibody to Cathepsin D (21327-1-AP, 1:1,000) were purchased from ProteinTech (Wuhan, China). Antibody to LC3 (4108S, 1:1,000) was purchased from Cell Signaling Technology (Boston, USA). Antibody to ITGAV (ab179475, 1:1,000) and antibody to LAMP2a (ab125068, 1:1,000) were purchased from Abcam (Cambridge, UK). ACR (A501033, purity≥98%) was purchased from Sangon Biotech (Shanghai, China). NR1 (IN0240, purity≥98%) was purchased from Solarbio life sciences (Beijing, China). Trx-1 siRNA and rat Trx-1 (NM_053800.3) plasmid were chemically synthesized by Shanghai GeneChem Corporation, Ltd. (Shanghai, China). RIPA Lysis buffer was purchased from Beyotime Biotechnology (Shanghai, China).

Cell Culture

PC12 cells of the rat pheochromocytoma tumor cell line were purchased from Kunming Institute of Zoology (Kunming, China) and maintained in RPMI1640 medium supplemented with 10% heat-inactivated horse serum, 5% heat-inactivated fetal bovine serum, and antibiotics (100 U/ml penicillin and 100 μg/ml streptomycin) and was maintained at 37°C in a humid atmosphere containing 5% CO_2.

Cell Viability Assay

The Cell viability assay was performed to quantify the proliferation of PC12 cells. It was performed using the Cell Counting Kit-8 (Dojindo Laboratories, Kumamoto, Japan). The neuroprotective effects of low doses of NR1 against ACR-induced cell damage was tested on PC12 cells. PC12 cells were seeded in 96-well plates at a density of 5,000 cells per well. Later, PC12 cells were treated with a wide range of concentrations of NR1 (0 mg/ml, 0.01 mg/ml, 0.02 mg/ml, 0.04 mg/ml, and 0.08 mg/ml) or ACR (0 mM, 1 mM, 2 mM, 4 mM, and 8 mM) for 24 h in the 96-well plates. After incubating it for 24 h, CCK-8 reagent was added to each well and again it was incubated for 1 h. The absorbance of each well was read at 450 nm. Three such independent experiments were performed.

Trx-1 Overexpression Preparation and Cell Transfection

Rat Trx-1 (NM_053800.3) plasmid (4 μg) and lipofectamine™ 2000 (10μl) (per well ratio) were diluted separately in serum-free Opti-MEM to make a final volume of 250 μl. This was gently mixed and incubated for 5 min at room temperature. The diluted plasmid solution and the diluted lipofectamine™ 2000 were mixed together and incubated for 20 min at room temperature. Then, this diluted plasmid/lipofectamine™ 2000 complex was added to the 6-well plates containing PC12 cells. Transfection with the Rat Trx-1 plasmid was allowed to occur for 24 h, and then the cells were stimulated with ACR and NR1. Finally, the cells were harvested for performing different assays.

Trx-1 siRNA Preparation and Cell Transfection

The sequences of Trx-1 siRNA and negative control siRNA that were used in our study were as follows: Trx-1 siRNA sense: 5'-GUCAAAUGCAUGCCAACAUtt-3'; and anti-sense: 5'-AUGUUGGCAUGCAUUUGACtt-3'. The Trx-1 siRNA was diluted to 20 μM with DEPC (diethyl pyrocarbonate) water.

PC12 cells were plated in 6-well plates at a density of 1×10^5 cells/well and were allowed to adhere to the plates for 12 h. By using the proportion of 5 μl siRNA and 5 μl lipofectamine™ 2000 per well, the reagents were diluted separately in serum-free Opti-MEM to acquire a final volume of 250μl. It was gently mixed and incubated for 5 min at room temperature. The diluted siRNA solution and the diluted lipofectamine™ 2000 were gently mixed together and incubated for 20 min at room temperature. Then, the diluted siRNA/lipofectamine™ 2000 complex was added to the 6-well plates containing PC12 cells. Transfection of PC12 cells with siRNA was allowed to take place for 24 h, followed by cell stimulation using ACR and NR1. Finally, the cells were harvested for performing different assays.

Measurement of Intracellular ROS

ROS production was measured using a commercially available intracellular ROS kit (Solarbio, Beijing, China). About 5×10^6 cells were suspended in 1 ml DCFH-DA (10 μmol/L) and were incubated for 20 min at 37°C in the dark. The cells were then washed three times using FBS-free RPMI1640 medium. Finally, the fluorescence found in the cells was measured using a fluorescent microscope (Olympus CKX53, Tokyo, Japan).

Western Blot Analysis

Protein lysates was prepared using a solubilizing solution (20 mM Tris–HCl (pH 7.4), 150 mM NaCl, 1% NP-40, 1 mM

EDTA, 1 mM phenylmethanesulfonyl fluoride, 1 mM EGTA, 1% Triton X-100, 2.5 mM sodium pyrophosphate, 1 mM Na_3VO_4, 1 mM β-glycerol phosphate, and 1 mg/ml leupeptin). The protein concentration found in the cells was determined using a Bio-Rad protein assay reagent (Hercules, CA, USA).

Proteins that were extracted from the cells were separated by using 12% SDS-PAGE (for ITGAV, ATG4B and Cathepsin D, LAMP2a), or 15% SDS-PAGE (for LC3, Trx-1) and were transferred to a polyvinylidene difluoride membrane (Millipore, Billerica, MA, USA). The membrane was then soaked in 10% skimmed milk solution (prepared in phosphate-buffered saline, pH 7.2, containing 0.1% Tween 20) overnight at 4°C. It was then incubated with primary antibody followed by incubation with peroxidase-conjugated anti-mouse or anti-rabbit IgG (KPL, Gaithersburg, MD, USA). The epitope was visualized using an ECL Western blot detection kit (Millipore). Some proteins shared one loading control. Finally, the densitometry analysis was performed using ImageJ software.

Bioinformatics Informatics

We used transcriptome datasets downloaded from NCBI (GSE29004). Microarray data analysis was performed with Affymetrix GeneChip Operating Software v1.1 (GCOS). A Wilcoxon signed rank test were conducted to detect the expressing gene with "Detection-*p*-value" ($P \leq 0.04$). The comparison of gene expression between acrylamide-treated sample and control sample performed with "comparison analysis" tool in GCOS software. The P-value was calculated and used to judge the up-regulated, down-regulated or no-change in gene expression. If $P \leq 0.002$, the expression of this gene is up-regulated or down-regulated. Please find details of RNA preparation and microarray hybridization in (Seale et al., 2012). All genes were annotated to the KEGG database by clusterProfiler and enrichplot functions of R software (version 3.5.1) to find important pathway contained specific genes. Spearman's correlation was computed using cor.test function in R software (version 3.5.1) with gene expression counts to defined genes associated with ITGAV.

Statistical Analysis

Data were expressed as mean ± SE values. Statistical analysis was performed using SPSS software and GraphPad Prism5 software. A one-way or two-way ANOVA followed by a Bonferroni *post hoc* analysis was performed to identify the differences between the treated groups. A P-value of less than 0.05 was considered statistically significant.

RESULTS

NR1 Minimized ACR-Induced Cognitive Dysfunction in Mice

MWM test was performed to evaluate the cognitive dysfunction in mice caused by ACR stimulation. During the spatial acquisition phase, the escape latency for each group had gradually decreased during the five days of training. However, the ACR group was still significantly slower and more sluggish when compared to the control group. It also found that NR1 restored the cognitive dysfunction induced by ACR. From the second day of training, the ACR group spent more amount of time finding the platform when compared to the control group. And, the ACR+NR1 group significantly reduced the escape latency on day 5. Two-way ANOVA revealed a significant NR1 × ACR interaction ($F = 4.4$, $P < 0.05$). The effects of ACR ($F = 12.63$, $P < 0.01$) and NR1 ($F = 13.38$, $P < 0.01$) were considered significant. Bonferroni *post hoc* test showed a significant difference between the control group and the ACR group ($P < 0.01$), but not in the NR1 group and the ACR+NR1 group ($P > 0.05$) (**Figure 1A**).

Probe trial performance was an important method to detect spatial memory. Our results have shown that the number of times the mice from the ACR group crossing the quadrant V was significantly less when compared to the control group. Two-way ANOVA revealed a significant NR1 × ACR interaction ($F = 6.77$, $P < 0.05$). The effects of ACR ($F = 4.74$, $P < 0.05$) and NR1 ($F = 8.70$, $P < 0.01$) were considered significant. Bonferroni *post hoc* test showed a significant difference between the control group and the ACR group ($P < 0.01$), but not in the NR1 group and the ACR+NR1 group ($P > 0.05$) (**Figure 1B**). In addition, the percentage of time spent in the target quadrant of the ACR group was significantly lower compared to the control group. And there was no significant difference between the NR1 group and the ACR+NR1 group. Two-way ANOVA revealed a significant NR1 × ACR interaction ($F = 4.22$, $P < 0.05$). The effects of ACR ($F = 4.90$, $P < 0.05$) and NR1 ($F = 4.28$, $P < 0.05$) were considered significant. Bonferroni *post hoc* test showed a significant difference between the control group and the ACR group ($P < 0.05$), but not in the NR1 group and the ACR+NR1 group ($P > 0.05$) (**Figure 1C**). Besides, we also found that there was no significant difference in the swimming speed between the different experimental groups ($P > 0.05$) (**Figure 1D**). These results suggested that NR1 could restore ACR-induced cognitive and memory impairment, and this aspect needs further exploration.

Bioinformatics Analysis for Gene Transcriptional Expression

We have used transcriptome datasets from Seale et al. (2012). Three-week-old male Wistar rat pups were split into two groups and were treated with either acrylamide or saline solution (30 mg/kg) for 21 days. Later the tissues (cerebellum, spinal cord, and sciatic nerve) were harvested and frozen. Two biological replicate samples, each consisting of pooled tissues from 2 rats, were analyzed for each treatment. It found that Pik3r1 was up-regulated. Nr4a1, Nr4a2, Nr4a3, and Fos were down-regulated in the cerebellum after ACR treatment. Pik3r1 was up-regulated. Itgav, Hspa1a/Hspa1b, Myl1, Mcpt8, Bglap, and Mylpf were down-regulated in the spinal cord after ACR treatment. Pik3r1 and Nr1d1 were up-regulated. Vip and Oprk1 were down-regulated in the sciatic nerve after ACR treatment. It also found that ITGAV was down-regulated after treatment with ACR in the spinal cord.

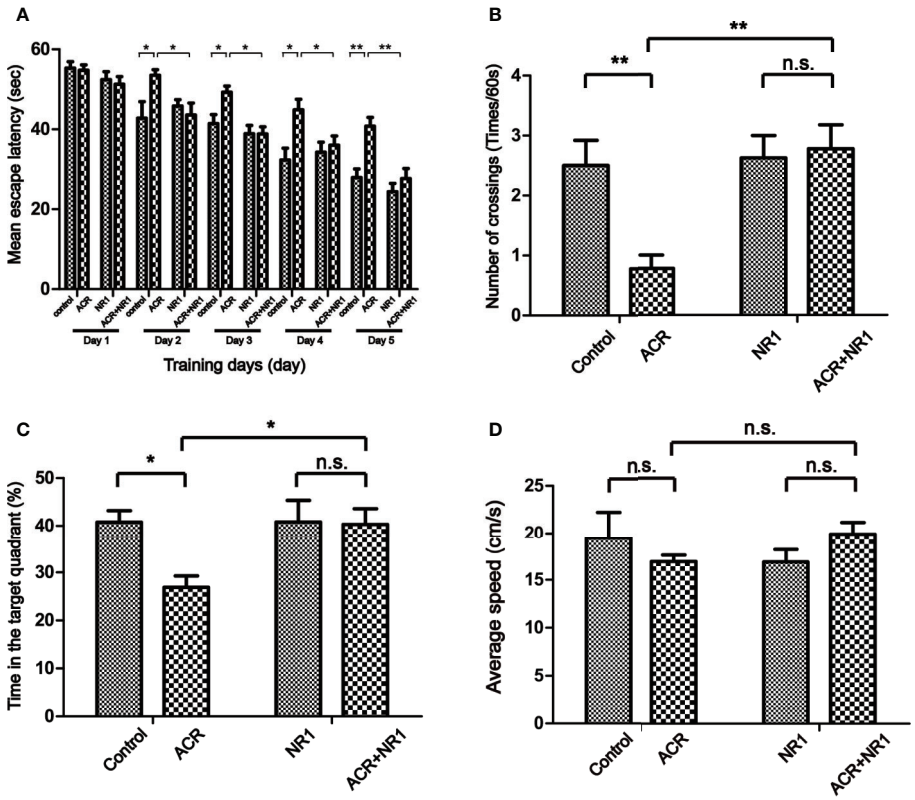

FIGURE 1 | NR1 alleviated ACR-induced cognitive dysfunction in Mice. **(A)** Spatial acquisition phase: the learning curve of escape latency (s) over the five consecutive days of training. Presented was the daily average of four trials (*p < 0.05; **p < 0.01 ACR group compared to control group). **(B)** The number of times the mice crossed the quadrant V. **(C)** The percent of the time each mouse spent in the target quadrant. **(D)** The swimming speed was measured. Each bar represents the mean ± SE (n = 8–9). n.s. (no significance) > 0.05, *P < 0.05, **P < 0.01, statistically significant.

Then, all genes were annotated to the KEGG database by clusterProfiler and enrichplot functions of R software (version 3.5.1). All genes of the autophagy pathway containing TXN1 gene were selected, or genes with a significant difference in expression in both the saline and ACR treated groups were selected. Then, Spearman's correlation of any of the two genes was computed. The gene with a significant correlation ($P < 0.05$) was found to be the coordinated expression. If two genes resulted in a positive correlation, they were concluded to either be up-regulated or down-regulated. If two genes resulted in a negative correlation, one gene was concluded to be up-regulated while the other was down-regulated. We found that the expression of ITGAV was decreased between saline and ACR treatment groups in **Figure 2A**. **Figure 2B** showed that the genes had significant spearman's correlations with ITGAV. Besides, using KEGG pathway analysis, **Figure 2C** showed that the KEGG pathway contained genes that were correlated with ITGAV. These genes were found to be grouped under five pathways: Autophagy-animal pathway, Autophagy-other pathway, Longevity regulating pathway, Shigellosis pathway, and mTOR signaling pathway. We also found that the significant genes were clustered in the Autophagy-animal pathway.

NR1 Suppressed ACR-Induced Autophagy by Regulating ITGAV in the Hippocampus

To reveal the protective mechanism of NR1, Trx-1 had been expressed in the hippocampus of mice. The results also showed that the expression of Trx-1 was lower in the ACR group when compared to the control group. And NR1 was identified to restore the expression of Trx-1 in the ACR+NR1 group. Two-way ANOVA revealed a significant NR1 × ACR interaction ($F = 5.13$, $P < 0.05$). The effects of ACR ($F = 16.48$, $P < 0.001$) and NR1 ($F = 112.2$, $P < 0.001$) were considered significant. Bonferroni *post hoc* test showed a significant difference between the control group and the ACR group ($P < 0.01$), but not in the NR1 group and the ACR+NR1 group ($P > 0.05$) (**Figure 3A**). Besides, we also investigated the expression of ITGAV. Two-way ANOVA revealed a significant NR1 × ACR interaction ($F = 4.77$, $P < 0.05$). The effects of ACR ($F = 10.70$, $P < 0.001$) and NR1 ($F = 8.46$, $P < 0.001$) were considered significant. Bonferroni *post hoc* test showed a significant difference between the control group and the ACR group ($P < 0.01$), but not in the NR1 group and the ACR+NR1 group ($P > 0.05$) (**Figure 3B**). This result was found to be consistent with the results obtained after bioinformatics analysis. We also found that the expression levels of ATG4B,

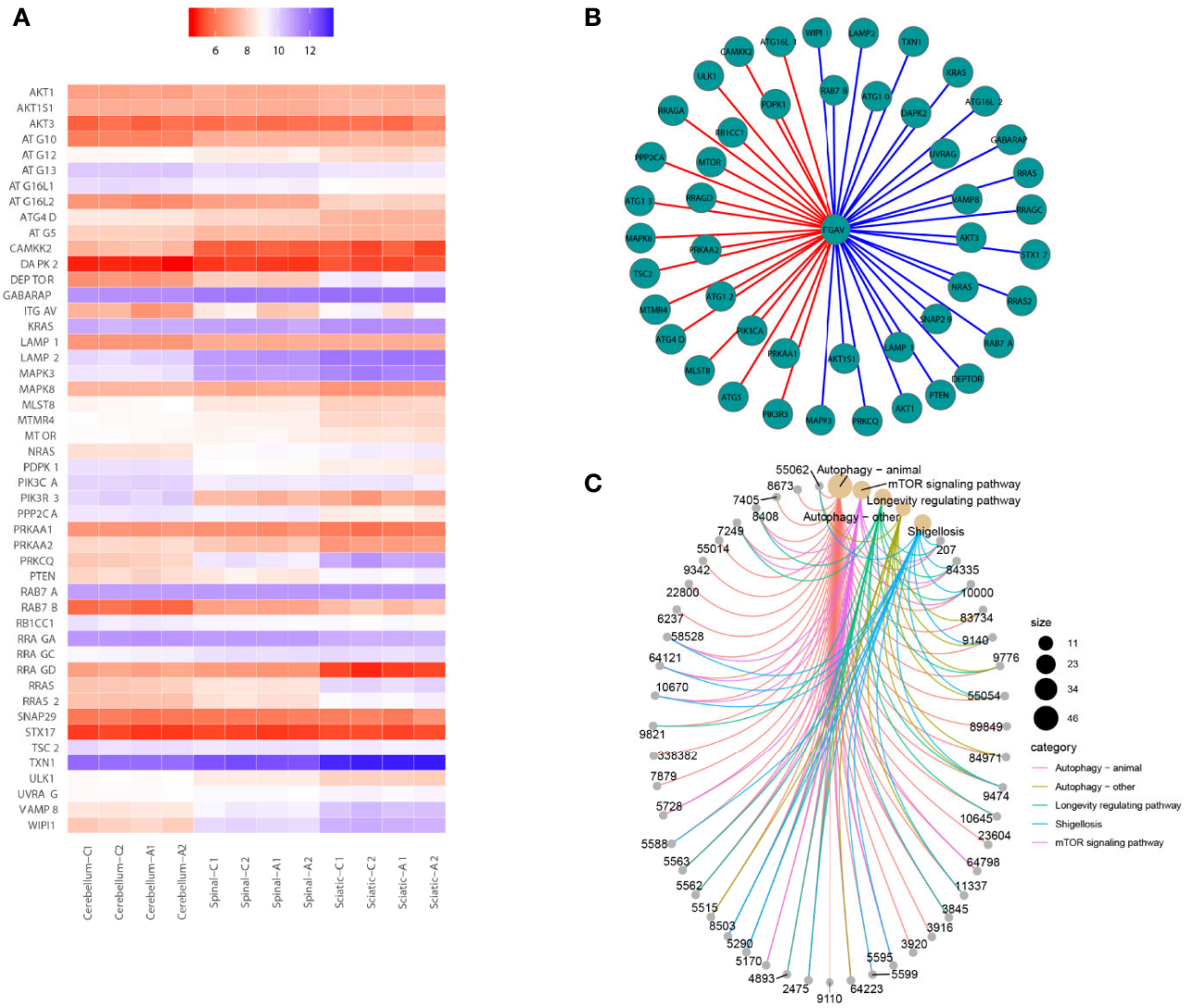

FIGURE 2 | Bioinformatics analysis for gene transcriptional expression. **(A)** Heatmap showed that the expression of genes correlated with ITGAV in 12 samples. **(B)** Correlations between ITGAV and genes in the autophagy pathway or genes in the pathway containing TXN1. **(C)** The genes correlated with ITGAV in the pathway.

LC3II, Cathepsin D, and LAMP2a were elevated, however, NR1 restored the expression of these molecules. Two-way ANOVA revealed a significant NR1 × ACR interaction ($F = 8.39$, $P < 0.01$). The effects of ACR ($F = 6.38$, $P < 0.05$) and NR1 ($F = 4.56$, $P < 0.05$) were considered significant. Bonferroni *post hoc* test showed a significant difference between the control group and the ACR group ($P < 0.01$), but not in the NR1 group and the ACR+NR1 group ($P > 0.05$) (**Figure 3C**). Two-way ANOVA revealed a significant NR1 × ACR interaction ($F = 42.88$, $P < 0.001$). The effects of ACR ($F = 12.12$, $P < 0.01$) and NR1 ($F = 7.92$, $P < 0.05$) were considered significant. Bonferroni *post hoc* test showed a significant difference between the control group and the ACR group ($P < 0.001$), but not in the NR1 group and the ACR+NR1 group ($P > 0.05$) (**Figure 3D**). Two-way ANOVA revealed a significant NR1 × ACR interaction ($F = 13.12$, $P < 0.01$). The effects of ACR ($F = 4.79$, $P < 0.01$) and NR1 ($F = 5.55$, $P < 0.05$) were considered significant. Bonferroni *post hoc* test showed a significant difference between the control group and the ACR group ($P < 0.01$), but not in the NR1 group and the ACR+NR1 group ($P > 0.05$) (**Figure 3E**). Two-way ANOVA revealed a significant NR1 × ACR interaction ($F = 4.37$, $P < 0.05$). The effects of ACR ($F = 12.20$, $P < 0.01$) and NR1 ($F = 5.69$, $P < 0.05$) were considered significant. Bonferroni *post hoc* test showed a significant difference between the control group and the ACR group ($P < 0.01$), but not in the NR1 group and the ACR+NR1 group ($P > 0.05$) (**Figure 3F**).

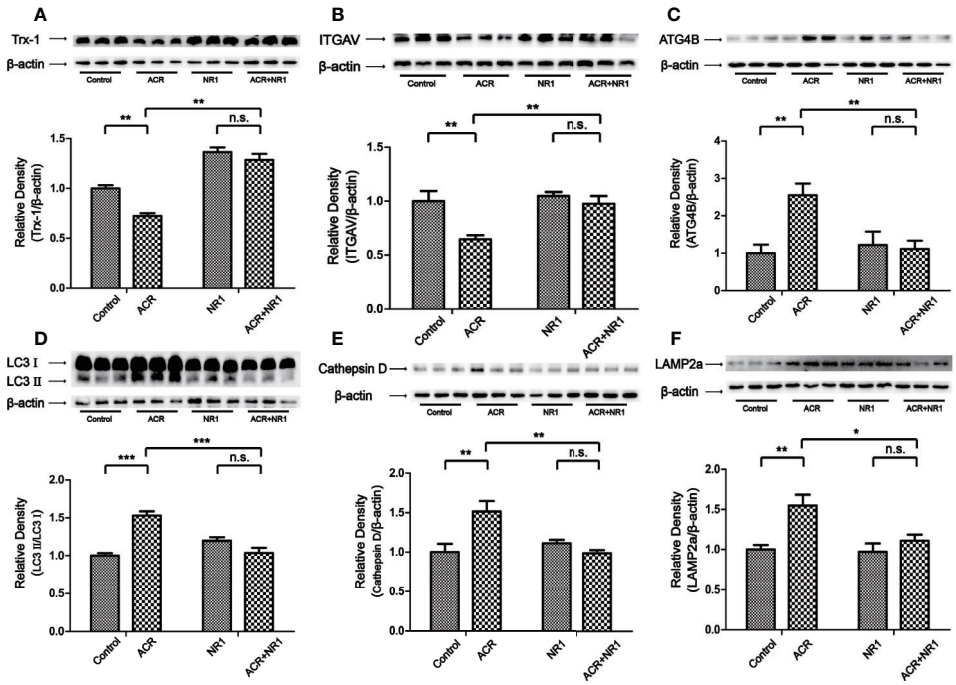

FIGURE 3 | NR1 suppressed ACR-induced autophagy by regulating ITGAV in the hippocampus. **(A)** The expression of Trx-1 in the hippocampus was detected by western blot analysis. NR1 restored the expression of Trx-1. **(B)** The expression of ITGAV in the hippocampus was detected by western blot analysis. NR1 restored the expression of ITGAV. **(C)** The expression of ATG4B in the hippocampus was detected by western blot analysis. NR1 restored the expression of ATG4B. **(D)** The expression of LC3II in the hippocampus was detected by western blot analysis. NR1 restored the expression of LC3II. **(E)** The expression of Cathepsin D in the hippocampus was detected by western blot analysis. NR1 restored the expression of Cathepsin D. **(F)** The expression of LAMP2a in the hippocampus was detected by western blot analysis. NR1 restored the expression of LAMP2a. Each bar represents the mean ± SE (n = 6). n.s. (no significance) >0.05, $^{*}P < 0.05$, $^{**}P < 0.01$, $^{***}P < 0.001$, statistically significant.

Effects of NR1 or ACR on PC12 Cells Viability and Trx-1 Expression

An *in vitro* study was undertaken, to explore the mechanism of action of ACR and NR1 on PC12 cells. Hong et al. proved in their study that ACR induced ROS in BRL-3A cells (Hong et al., 2019). Recent studies have also found that *Panax notoginseng* saponins decreased the level of ROS. However, the mechanism of ACR and NR1 on how it affects the ROS pathway in the nervous system remains unclear. To detect the dose–response, PC12 cells were treated with NR1 at concentrations ranging from 0.01 to 0.08 mg/ml for 24 h. PC12 cells were also treated with ACR at concentrations ranging from 1 to 8 mM for 24 h. The cell viability test was performed using a CCK-8 assay. It was found that both the cell viability as well as the Trx-1 expression levels had increased following the treatment of the cells with increasing concentrations of NR1 (0, 0.01, 0.02, 0.04, and 0.08 mg/ml) (**Figures 4A, B**). And we also found that cell viability and Trx-1 expression levels were decreased by treatment with increasing concentrations of ACR (0, 1, 2, 4, and 8 mM) (**Figures 4C, D**). Here, in this experiment, the concentration levels of NR1 and ACR were optimized and narrowed down to 0.04 mg/ml NR1 and 4 mM ACR.

NR1 Suppressed ACR-Induced ROS in PC12 Cells

The probe DCFH-DA could be oxidized to form a fluorescent compound called DCF. This indirectly indicated the levels of ROS in PC12 cells. As shown in **Figure 5**, the fluorescence intensity of DCFH-DA was evidently strengthened by ACR, indicating an excessive amount of accumulation of ROS. The results have also shown that NR1 could decrease the intracellular ROS levels and halt the oxidative stress triggered by ACR. Two-way ANOVA revealed a significant NR1 × ACR interaction ($F = 37.46$, $P < 0.001$). The effects of ACR ($F = 73.16$, $P < 0.05$) and NR1 ($F = 33.70$, $P < 0.001$) were considered significant. Bonferroni *post hoc* test showed a significant difference between the control group and the ACR group ($P < 0.001$), but not in the NR1 group and the ACR+NR1 group ($P > 0.05$) (**Figure 5**).

NR1 Suppressed ACR-Induced Autophagy by Regulating ITGAV in PC12 Cells

Using bioinformatics analysis, we have established that the mRNA level of ITGAV was reduced after ACR administration when compared to the control group. Mridu had reported that ITGAV plays an important role in regulating autophagy in B-cell

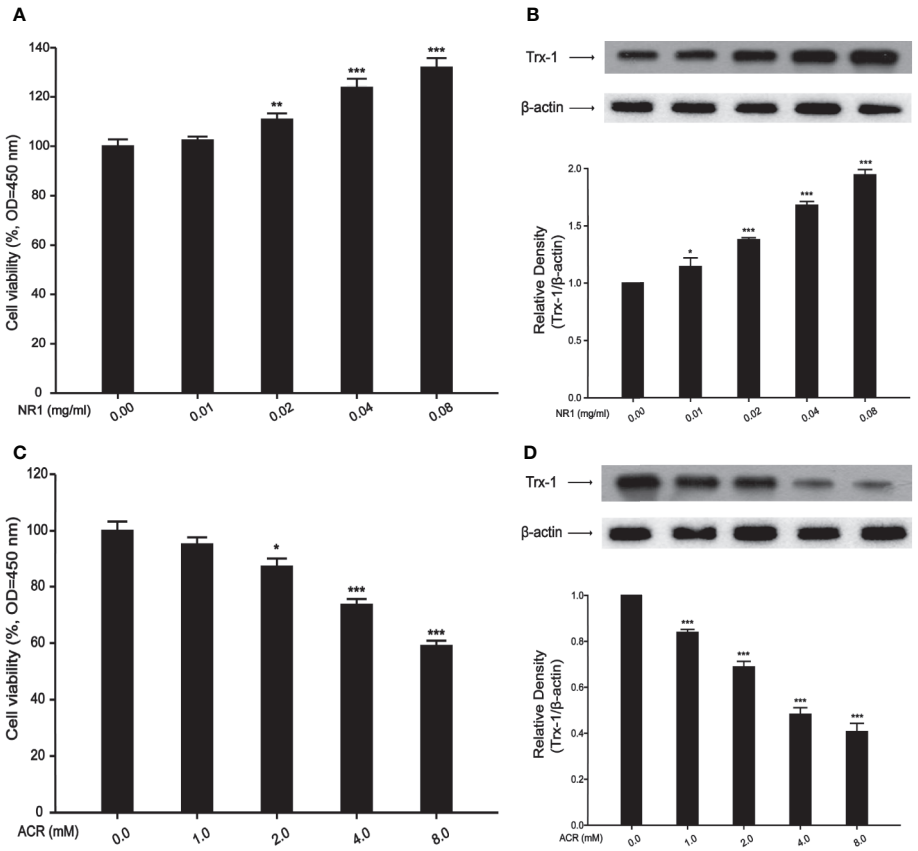

FIGURE 4 | Effects of NR1 or ACR on PC12 cells viability and Trx-1 expression. **(A)** Effects of NR1 on PC12 cells viability. **(B)** Effects of NR1 on PC12 cells Trx-1 expression. **(C)** Effects of ACR on PC12 cells viability. **(D)** Effects of ACR on PC12 cells Trx-1 expression. Each bar represents the mean ± SE (n = 3 independent experiments). n.s. (no significance) > 0.05, *P < 0.05, **P < 0.01, ***P < 0.001, statistically significant.

(Acharya et al., 2016). In our results, we have shown that NR1 inhibited the cytotoxicity triggered by ACR. We have also shown that the decrease in Trx-1 expression triggered by ACR was repressed by NR1. Two-way ANOVA revealed a significant NR1 × ACR interaction ($F = 7.65$, $P < 0.05$). The effects of ACR ($F = 10.52$, $P < 0.05$) and NR1 ($F = 92.52$, $P < 0.001$) were considered significant. Bonferroni *post hoc* test showed a significant difference between the control group and the ACR group ($P < 0.01$), but not in the NR1 group and the ACR+NR1 group ($P > 0.05$) (**Figure 6A**). As described above, the expression of Trx-1 was associated with ITGAV. Therefore, we found that the expression of ITGAV had decreased. NR1 restored the expression levels of ITGAV. Two-way ANOVA revealed a significant NR1 × ACR interaction ($F = 5.32$, $P < 0.05$). The effects of ACR ($F = 7.46$, $P < 0.05$) and NR1 ($F = 13.26$, $P < 0.01$) were considered significant. Bonferroni *post hoc* test showed a significant difference between the control group and the ACR group ($P < 0.05$), but not in the NR1 group and the ACR+NR1 group ($P > 0.05$) (**Figure 6B**). Besides, we investigated the autophagy pathway associated proteins ATG4B, LC3II, Cathepsin D, and LAMP2a. We found that the increase in the levels of ATG4B, LC3II, Cathepsin D, and LAMP2a expression induced by ACR were repressed by NR1. Two-way ANOVA revealed a significant NR1 × ACR interaction ($F = 18.53$, $P < 0.01$). The effects of ACR ($F = 5.80$, $P < 0.05$) and NR1 ($F = 22.72$, $P < 0.01$) were considered significant. Bonferroni *post hoc* test showed a significant difference between the control group and the ACR group ($P < 0.01$), but not in the NR1 group and the ACR+NR1 group ($P > 0.05$) (**Figure 6C**). Two-way ANOVA revealed a significant NR1 × ACR interaction ($F = 6.50$, $P < 0.05$). The effects of ACR ($F = 10.12$, $P < 0.05$) and NR1 ($F = 5.59$, $P < 0.05$) were considered significant. Bonferroni *post hoc* test showed a significant difference between the control group and the ACR group ($P < 0.01$), but not in the NR1 group and the ACR+NR1 group ($P > 0.05$) (**Figure 6D**). Two-way ANOVA revealed a significant NR1 × ACR interaction ($F = 6.02$, $P < 0.05$). The effects of ACR ($F = 5.55$, $P < 0.05$) and NR1 ($F = 6.38$, $P < 0.05$) were considered significant. Bonferroni *post hoc* test showed a significant difference between the control group and the ACR group ($P < 0.05$), but not in the NR1 group and the ACR+NR1 group ($P > 0.05$) (**Figure 6E**). Two-way ANOVA revealed a significant NR1 × ACR interaction ($F = 11.94$, $P < 0.01$). The effects of ACR ($F = 5.38$, $P < 0.05$)

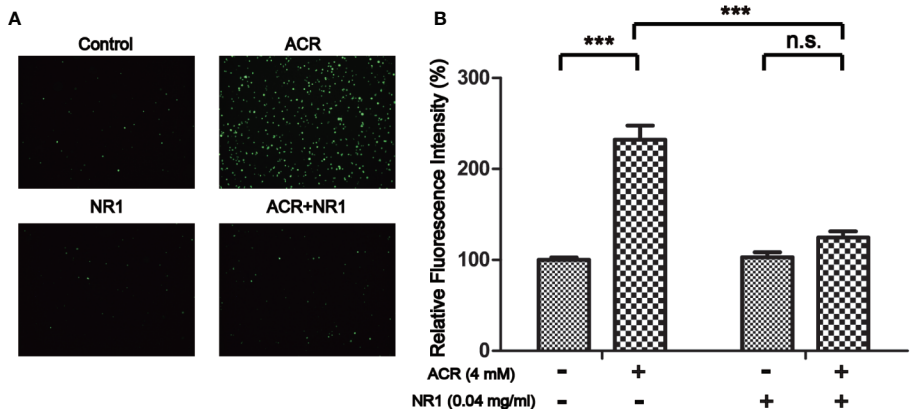

FIGURE 5 | NR1 suppressed ACR-induced ROS in PC12 cells. **(A)** Representative photographs of ROS staining. **(B)** Quantitative analysis of the DCFH-DA fluorescence intensity. Each bar represents the mean ± SE (n = 3 independent experiments). n.s. (no significance) > 0.05, ***P < 0.001, statistically significant (Magnification×100).

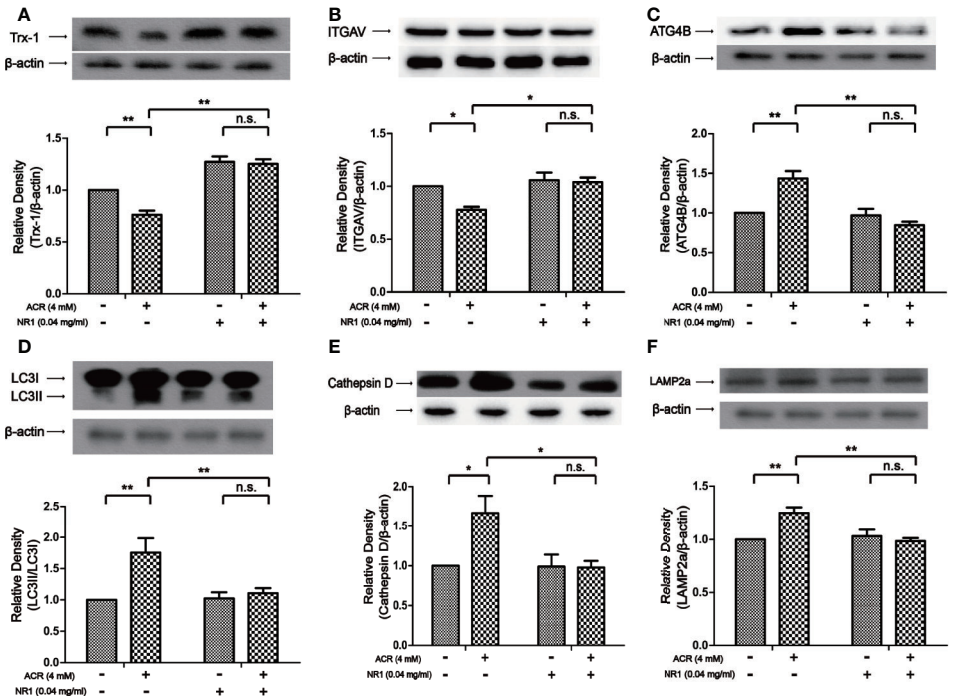

FIGURE 6 | NR1 suppressed ACR-induced autophagy by regulating ITGAV in PC12 cells. **(A)** The expression of Trx-1 in PC12 cells was detected by western blot analysis. NR1 restored the expression of Trx-1. **(B)** The expression of ITGAV in PC12 cells was detected by western blot analysis. NR1 restored the expression of ITGAV. **(C)** The expression of ATG4B in PC12 cells was detected by western blot analysis. NR1 restored the expression of ATG4B. **(D)** The expression of LC3II in PC12 cells was detected by western blot analysis. NR1 restored the expression of LC3II. **(E)** The expression of Cathepsin D in PC12 cells was detected by western blot analysis. NR1 restored the expression of Cathepsin D. **(F)** The expression of LAMP2a in PC12 cells was detected by western blot analysis. NR1 restored the expression of LAMP2a. Each bar represents the mean ± SE (n = 3 independent experiments). n.s. (no significance) > 0.05, *P < 0.05, **P < 0.01, statistically significant. Trx-1 and LAMP2a shared one loading control.

and NR1 ($F = 7.27$, $P < 0.05$) were considered significant. Bonferroni *post hoc* test showed a significant difference between the control group and the ACR group ($P < 0.01$), but not in the NR1 group and the ACR+NR1 group ($P > 0.05$) (**Figure 6F**). These data suggested that NR1 can resist ACR-induced autophagy in PC12 cells.

Trx-1 Overexpression Attenuated ACR-Induced Autophagy by Regulating ITGAV in PC12 Cells

Our results have validated that NR1 can resist ACR-induced cell apoptosis, however, the detailed mechanism is still unknown. Previous studies had proven that NR1 could increase the expression of Trx-1 and thereby protect the neurons (Wang et al., 2014; Zeng et al., 2015). Therefore, we hypothesized that the overexpression of the protein Trx-1 could probably suppress ACR-induced autophagy. Next, we investigated the effects of overexpression of Trx-1 on ACR-induced autophagy in PC12 cells which were transfected with rat Trx-1 plasmid. As shown in **Figure 7A**, Trx-1 was overexpressed in the PC12 cells which was transfected with rat Trx-1 plasmid and it reversed the decline of Trx-1 induced by ACR. Two-way ANOVA revealed a significant Trx-1 overexpression × ACR interaction ($F = 7.18$, $P < 0.01$). The effects of ACR ($F = 50.27$, $P < 0.001$) and Trx-1 overexpression ($F = 95.54$, $P < 0.001$) were considered significant. Bonferroni *post hoc* test showed a significant difference between the control group and the ACR group ($P < 0.01$), but not in the Trx-1 overexpression group and the ACR+Trx-1 overexpression group ($P > 0.05$) (**Figure 7A**). Apart from that, overexpression of Trx-1 restored the expression of ITGAV (**Figure 7B**) and the autophagy pathway associated proteins—ATG4B, LC3II, Cathepsin D, and LAMP2a (**Figures 7C–F**). Two-way ANOVA revealed a significant Trx-1 overexpression × ACR interaction ($F = 7.81$, $P < 0.01$). The effects of ACR ($F = 18.33$, $P < 0.01$) and Trx-1 overexpression ($F = 5.07$, $P < 0.05$) were considered significant. Bonferroni *post hoc* test showed a significant difference between the control group and the ACR group ($P < 0.01$), but not in the Trx-1 overexpression group and the ACR+Trx-1 overexpression group ($P > 0.05$) (**Figure 7B**). Two-way ANOVA revealed a significant Trx-1 overexpression × ACR interaction ($F = 5.24$, $P < 0.05$). The effects of ACR ($F = 20.47$, $P < 0.001$) and Trx-1 overexpression ($F = 4.38$, $P < 0.05$) were considered significant. Bonferroni *post hoc* test showed a significant difference between the control group and the ACR group ($P < 0.01$), but not in the Trx-1 overexpression group and the ACR+Trx-1 overexpression group (**Figure 7C**). Two-way ANOVA revealed a significant Trx-1 overexpression × ACR interaction ($F = 5.29$, $P < 0.05$). The effects of ACR ($F = 14.96$, $P < 0.01$) and Trx-1 overexpression ($F = 4.07$, $P < 0.05$) were considered significant. Bonferroni *post hoc* test showed a significant difference between the control group and the ACR group ($P < 0.05$), but not in the Trx-1 overexpression group and the ACR+Trx-1 overexpression group (**Figure 7D**). Two-way ANOVA revealed a significant Trx-1 overexpression × ACR interaction ($F = 4.96$, $P < 0.05$). The effects of ACR ($F = 13.78$, $P < 0.01$) and Trx-1 overexpression ($F = 3.98$, $P < 0.05$) were considered significant. Bonferroni *post hoc* test showed a

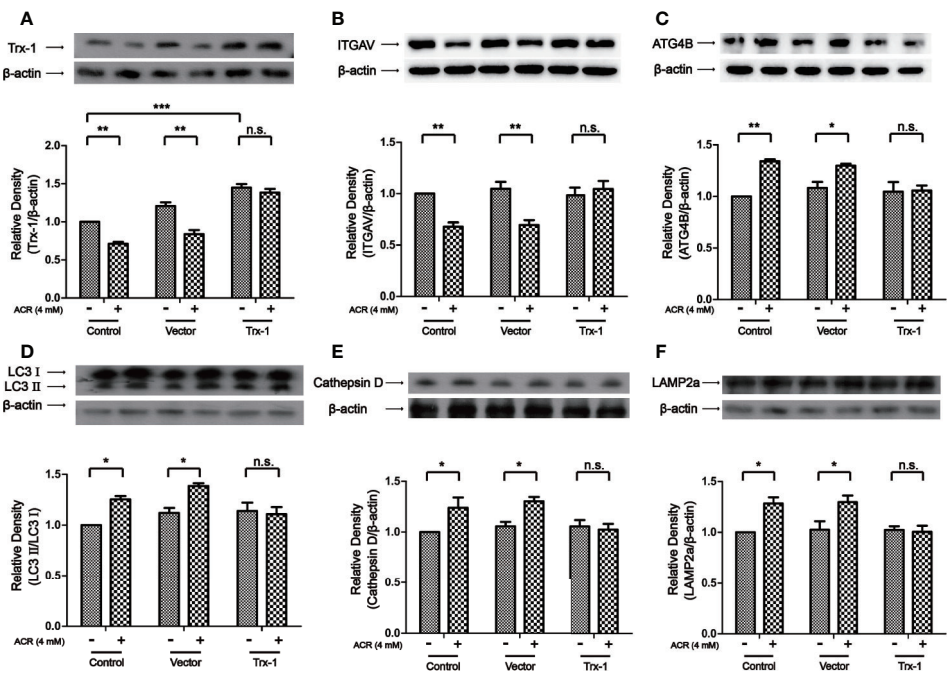

FIGURE 7 | Trx-1 overexpression attenuated ACR-induced autophagy by regulating ITGAV in PC12 cells. **(A)** The expression of Trx-1 in PC12 cells was detected by western blot analysis in PC12 cells. Trx-1 overexpression restored the expression of Trx-1. **(B)** The expression of ITGAV in PC12 cells was detected by western blot analysis. Trx-1 overexpression restored the expression of ITGAV. **(C)** The expression of ATG4B in PC12 cells was detected by western blot analysis. Trx-1 overexpression restored the expression of ATG4B. **(D)** The expression of LC3II in PC12 cells was detected by western blot analysis. Trx-1 overexpression restored the expression of LC3II. **(E)** The expression of Cathepsin D in PC12 cells was detected by western blot analysis. Trx-1 overexpression restored the expression of Cathepsin D. **(F)** The expression of LAMP2a in PC12 cells was detected by western blot analysis. Trx-1 overexpression restored the expression of LAMP2a. Each bar represents the mean ± SE (n = 3 independent experiments). n.s. (no significance) > 0.05, *$P < 0.05$, **$P < 0.01$, ***$P < 0.001$, statistically significant.

significant difference between the control group and the ACR group ($P < 0.05$), but not in the Trx-1 overexpression group and the ACR+Trx-1 overexpression group ($P > 0.05$) (**Figure 7E**). Two-way ANOVA revealed a significant Trx-1 overexpression × ACR interaction ($F = 4.42$, $P < 0.05$). The effects of ACR ($F = 14.51$, $P < 0.01$) and Trx-1 overexpression ($F = 3.89$, $P < 0.05$) were considered significant. Bonferroni *post hoc* test showed a significant difference between the control group and the ACR group ($P < 0.05$), but not in the Trx-1 overexpression group and the ACR+Trx-1 overexpression group ($P > 0.05$) (**Figure 7F**). These results suggested that overexpression of Trx-1 attenuated the ACR-induced autophagy by restoring the expression of ITGAV, ATG4B, LC3II, Cathepsin D, and LAMP2a.

Trx-1 siRNA Aggravated ACR-Induced Autophagy by Regulating ITGAV in PC12 Cells

Then, by using Trx-1 siRNA on ACR-induced autophagy, we examined the effects of downregulation of Trx-1 expression. The results obtained showed that Trx-1 expression had declined due to the presence of Trx-1 siRNA in PC12 cells. Trx-1 expression has further decreased by the presence of ACR along with the presence of Trx-1 siRNA in PC12 cells. Two-way ANOVA revealed a significant Trx-1 siRNA × ACR interaction ($F = 3.90$, $P < 0.05$). The effects of ACR ($F = 121.60$, $P < 0.001$) and Trx-1 siRNA ($F = 46.66$, $P < 0.001$) were considered significant. Bonferroni *post hoc* test showed a significant difference between the control group and the ACR group ($P < 0.001$), and there was also a significant difference between the Trx-1 siRNA group and the ACR+ Trx-1 siRNA group ($P < 0.001$) (**Figure 8A**). Besides, the expression of ITGAV has further declined after Trx-1 siRNA treatment on PC12 cells followed by ACR treatment. Two-way ANOVA revealed a significant Trx-1 siRNA × ACR interaction ($F = 18.81$, $P < 0.001$). The effects of ACR ($F = 92.51$, $P < 0.001$) and Trx-1 siRNA ($F = 7.61$, $P < 0.01$) were considered significant. Bonferroni *post hoc* test showed a significant difference between the control group and the ACR group ($P < 0.05$), and there was also a significant difference between the Trx-1 siRNA group and the ACR+ Trx-1 siRNA group ($P < 0.001$) (**Figure 8B**). More importantly, the expression of ATG4B, LC3II, Cathepsin D, and LAMP2a have further

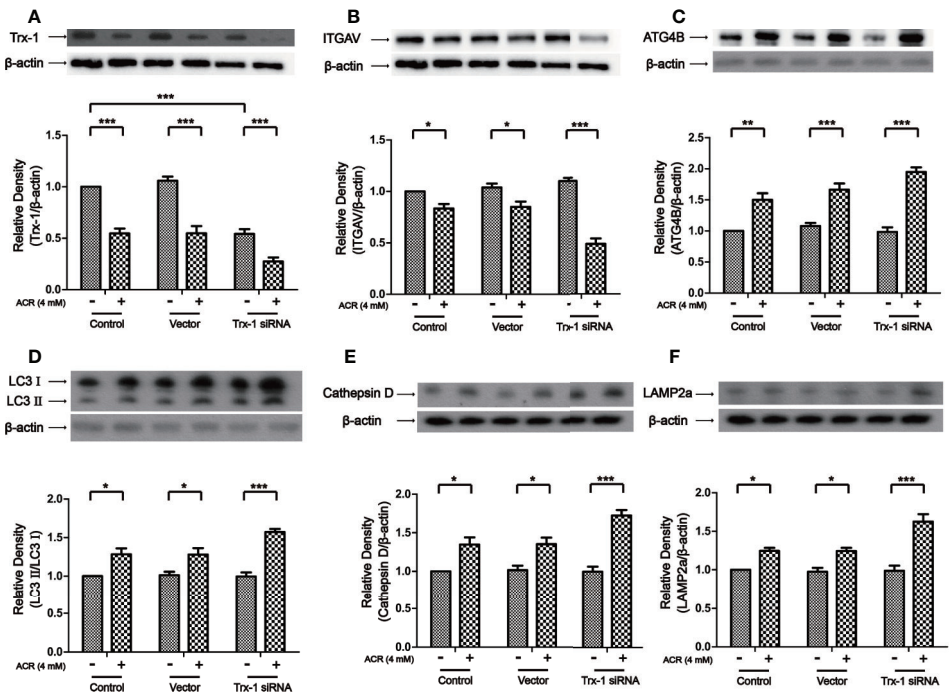

FIGURE 8 | Trx-1 siRNA aggravated ACR-induced autophagy by regulating ITGAV in PC12 cells. **(A)** The expression of Trx-1 in PC12 cells was detected by western blot analysis. Trx-1 expression has further decreased after Trx-1 siRNA treatment on PC12 cells followed by ACR treatment. **(B)** The expression of ITGAV in PC12 cells was detected by western blot analysis. The expression of ITGAV has further decreased after Trx-1 siRNA treatment on PC12 cells followed by ACR treatment. **(C)** The expression of ATG4B in PC12 cells was detected by western blot analysis. The expression of ATG4B has further increased after Trx-1 siRNA treatment on PC12 cells followed by ACR treatment. **(D)** The expression of LC3II in PC12 cells was detected by western blot analysis. The expression of LC3II has further increased after Trx-1 siRNA treatment on PC12 cells followed by ACR treatment. **(E)** The expression of Cathepsin D in PC12 cells was detected by western blot analysis. The expression of Cathepsin D has further increased after Trx-1 siRNA treatment on PC12 cells followed by ACR treatment. **(F)** The expression of LAMP2a in PC12 cells was detected by western blot analysis. The expression of LAMP2a has further increased after Trx-1 siRNA treatment on PC12 cells followed by ACR treatment. Each bar represents the mean ± SE (n = 3 independent experiments). n.s. (no significance) > 0.05, **P* < 0.05, ***P* < 0.01, ****P* < 0.001, statistically significant. Trx-1 and ITGAV shared one loading control. Cathepsin D and LAMP2a shared one loading control.

increased after Trx-1 siRNA treatment on PC12 cells followed by ACR treatment. Two-way ANOVA revealed a significant Trx-1 siRNA × ACR interaction ($F = 5.18$, $P < 0.05$). The effects of ACR ($F = 120.06$, $P < 0.001$) and Trx-1 siRNA ($F = 3.96$, $P < 0.05$) were considered significant. Bonferroni *post hoc* test showed a significant difference between the control group and the ACR group ($P < 0.01$), and there was also a significant difference between the Trx-1 siRNA group and the ACR+ Trx-1 siRNA group ($P < 0.001$) (**Figure 8C**). Two-way ANOVA revealed a significant Trx-1 siRNA × ACR interaction ($F = 4.64$, $P < 0.05$). The effects of ACR ($F = 68.85$, $P < 0.001$) and Trx-1 siRNA ($F = 3.98$, $P < 0.05$) were considered significant. Bonferroni *post hoc* test showed a significant difference between the control group and the ACR group ($P < 0.05$), and there was also a significant difference between the Trx-1 siRNA group and the ACR+ Trx-1 siRNA group ($P < 0.001$) (**Figure 8D**). Two-way ANOVA revealed a significant Trx-1 siRNA × ACR interaction ($F = 5.24$, $P < 0.05$). The effects of ACR ($F = 69.72$, $P < 0.001$) and Trx-1 siRNA ($F = 4.13$, $P < 0.05$) were considered significant. Bonferroni *post hoc* test showed a significant difference between the control group and the ACR group ($P < 0.05$), and there was also a significant difference between the Trx-1 siRNA group and the ACR+ Trx-1 siRNA group ($P < 0.001$) (**Figure 8E**). Two-way ANOVA revealed a significant Trx-1 siRNA × ACR interaction ($F = 7.43$, $P < 0.01$). The effects of ACR ($F = 67.58$, $P < 0.001$) and Trx-1 siRNA ($F = 7.42$, $P < 0.01$) were considered significant. Bonferroni *post hoc* test showed a significant difference between the control group and the ACR group ($P < 0.05$), and there was also a significant difference between the Trx-1 siRNA group and the ACR+ Trx-1 siRNA group ($P < 0.001$) (**Figure 8F**). These data suggested that Trx-1 siRNA treatment promoted ACR-induced autophagy in PC12 cells by inhibiting ITGAV and inducing of ATG4B, LC3II, Cathepsin D, and LAMP2a (**Figures 8B–F**).

DISCUSSION

According to laboratory evidence, ACR has been classified as a possible human carcinogen. It has also been proved that dietary acrylamide intake causes esophageal, gastric, and colorectal cancer (Liu R. et al., 2019). Besides, lots of studies have proved that neurotoxicity of acrylamide in tissues and organs has been confirmed at the animal levels (Song et al., 2008; Tomaszewska et al., 2014). In our present study, using bioinformatics analysis, we have found that the mRNA level of ITGAV was decreased, and there was a correlation between ITGAV and TXN1. Besides, we also found that ITGAV played an important role in autophagy.

Our results have suggested a new mechanism for the regulation of autophagy by regulating ITGAV, which was mediated by Trx-1. Previous studies have proven that integrin was closely involved in the autophagy pathway targeting LC3 and ATG5. Besides, Mridu had already shown that ITGAV promotes the recruitment of the autophagy component LC3 (Acharya et al., 2016). Here, using bioinformatics analysis, we have shown that there was an important link between Trx-1 and ITGAV. Therefore, Trx-1 was an important regulator of autophagy by regulating ITGAV.

Notoginsenoside R1 is a plant extract, purified from *Panax notoginseng* and can be used in the treatment of various types of diseases, such as cerebral ischemia (Xie et al., 2018) and cardiovascular diseases (Yang et al., 2014). Our results have shown that NR1 can induce the expression of Trx-1. Trx-1 played a vital role in various diseases, including ischemic stroke (Qi et al., 2015), morphine addiction (Zeng et al., 2020), and Parkinson's disease (Zeng et al., 2014). Besides, Wang et al. proved that NR1 alleviated ROS which was induced by high glucose present in RSC96 cells (Wang et al., 2019). And Zhang et al. suggested that NR1 inhibited apoptosis in smooth muscle cells through the ROS pathway (Zhang and Wang, 2006). By pretreatment of the cells with H_2O_2, the expression of ITGAV was found to be reduced. Murata et al. (2013) highlighted the relationship between ITGAV and ROS. Previous studies have reported that autophagy exerted a pleiotropic action on multiple cell functions *via* the generation of ROS (Sun et al., 2019; Zhang et al., 2019). It was also possible for NR1 to alter the nerve cell function by regulating Trx-1 expression and thereby the expression of ITGAV was controlled *via* suppression of ROS generation. N-acetylcysteine inhibited ACR-induced ROS in PC12 cells by regulating the mitogen-activated protein kinases (MAPKs) pathway (Pan et al., 2018). Zhang et al. (2017) also proved that the cytotoxicity induced by acrylamide was through the production of ROS. Also, Singh et al. (2017) suggested that ROS-induced activation of autophagy resulted in neurotransmission dysfunction and neurodegeneration in adult rats. Therefore, sum total of these studies have shown that the key mechanism of ACR-induced neurotoxicity was an increase in the levels of ROS. Our results suggested that NR1 inhibited the level of ROS by triggering an increase of Trx-1, and this Trx-1 helped to regulate autophagy by regulating ITGAV. Furthermore, we also found that NR1 resisted ACR-induced spatial and cognitive impairment in mice. In summary, ACR induced oxidative damage *via* ROS generation. ROS production induced the decrease of ITGAV expression, which led to autophagy. Finally, it led to cognitive dysfunction. NR1 could inhibit ROS production by upregulating Trx-1 expression. Although we demonstrated the neuroprotective effects of Trx-1, the specific mechanism of how TRX affected ITGAV needed further study. It was also worth exploring the effects of knockdown or overexpression of ITGAV in PC12 cells after ACR administration. Therefore, NR1 can reduce the accumulation of ROS and represent a promising new avenue for the development of novel treatments for the ACR-induced neurotoxicity.

CONCLUSION

To summarize, ACR aggravates autophagy in PC12 cells by knocking down the expression of Trx-1, on the contrary, overexpression of Trx-1 and NR1 inhibits autophagy induced by ACR. We have also found that ITGAV was an intermediate node linking Trx-1 and the autophagy pathway. Hence, we can conclude by suggesting that NR1 may be a potential drug for the treatment of acrylamide-induced neurotoxicity.

DATA AVAILABILITY STATEMENT

All datasets presented in this study are included in the article/supplementary material.

ETHICS STATEMENT

The animal study was reviewed and approved by animal ethics council of Southwest Medical University.

AUTHOR CONTRIBUTIONS

XL was responsible for the study concept and design. WW, LH, and YH did the experiments. WW and LH drafted the manuscript. XL, FZ, and ET provided a critical revision of the manuscript for important intellectual content. All authors contributed to the article and approved the submitted version.

FUNDING

This study was financially supported by grants from the Science and Technology Strategic Cooperation Project of the Luzhou People's Government and Southwest Medical University (No. 2019LZXNYDJ34) and the undergraduate innovation and entrepreneurship training program (S201910727096). This work was also supported by grants from the Science and Technology Planning Project of Sichuan Province, China (Grant No. 2013SZZ001).

REFERENCES

Acharya, M., Sokolovska, A., Tam, J. M., Conway, K. L., Stefani, C., Raso, F., et al. (2016). Alphav Integrins combine with LC3 and atg5 to regulate Toll-like receptor signalling in B cells. *Nat. Commun.* 7, 10917. doi: 10.1038/ncomms10917

Adewale, O. O., Brimson, J. M., Odunola, O. A., Gbadegesin, M. A., Owumi, S. E., Isidoro, C., et al. (2015). The Potential for Plant Derivatives against Acrylamide Neurotoxicity. *Phytother. Res.* 29 (7), 978–985. doi: 10.1002/ptr.5353

Bai, J., Nakamura, H., Kwon, Y. W., Hattori, I., Yamaguchi, Y., Kim, Y. C., et al. (2003). Critical roles of thioredoxin in nerve growth factor-mediated signal transduction and neurite outgrowth in PC12 cells. *J. Neurosci.* 23 (2), 503–509. doi: 10.1523/JNEUROSCI.23-02-00503.2003

Burkegaffney, A., Callister, M. E. J., and Nakamura, H. (2005). Thioredoxin: friend or foe in human disease? *Trends Pharmacol. Sci.* 26 (8), 398–404. doi: 10.1016/j.tips.2005.06.005

Chan, P., Thomas, G. N., and Tomlinson, B. (2002). Protective effects of trilinolein extracted from panax notoginseng against cardiovascular disease. *Acta Pharmacol. Sin.* 23 (12), 1157–1162.

Chen, X., Zhou, M., Li, Q., Yang, J., Zhang, Y., Zhang, D., et al. (2008). Sanchi for acute ischaemic stroke. *Cochrane Database Syst. Rev.* 4, CD006305. doi: 10.1002/14651858.CD006305.pub2

Chen, S., Liu, J., Liu, X., Fu, Y., Zhang, M., Lin, Q., et al. (2011). Panax notoginseng saponins inhibit ischemia-induced apoptosis by activating PI3K/Akt pathway in cardiomyocytes. *J. Ethnopharmacol.* 137 (1), 263–270. doi: 10.1016/j.jep.2011.05.011

Dou, L., Lu, Y., Shen, T., Huang, X., Man, Y., Wang, S., et al. (2012). Panax notogingseng saponins suppress RAGE/MAPK signaling and NF-kappaB activation in apolipoprotein-E-deficient atherosclerosis-prone mice. *Cell Physiol. Biochem.* 29 (5-6), 875–882. doi: 10.1159/000315061

He, L., Chen, X., Zhou, M., Zhang, D., Yang, J., Yang, M., et al. (2011). Radix/Rhizoma Notoginseng extract (Sanchitongtshu) for ischemic stroke: A randomized controlled study. *Phytomedicine* 18 (6), 437–442. doi: 10.1016/j.phymed.2010.10.004

He, Y., Tan, D., Mi, Y., Bai, B., Jiang, D., Zhou, X., et al. (2017). Effect of epigallocatechin-3-gallate on acrylamide-induced oxidative stress and apoptosis in PC12 cells. *Hum. Exp. Toxicol.* 36 (10), 1087–1099. doi: 10.1177/0960327116681648

Hong, Y., Nan, B., Wu, X., Yan, H., and Yuan, Y. (2019). Allicin alleviates acrylamide-induced oxidative stress in BRL-3A cells. *Life Sci.* 231, 116550. doi: 10.1016/j.lfs.2019.116550

Huynh, K. K., Eskelinen, E. L., Scott, C. C., Malevanets, A., Saftig, P., and Grinstein, S. (2007). LAMP proteins are required for fusion of lysosomes with phagosomes. *EMBO J.* 26 (2), 313–324. doi: 10.1038/sj.emboj.7601511

Lee, Y. S., Lee, C. H., Bae, J. T., Nam, K. T., Moon, D. B., Hwang, O. K., et al. (2018). Inhibition of skin carcinogenesis by suppression of NF-kappa B dependent ITGAV and TIMP-1 expression in IL-32 gamma overexpressed condition. *J. Exp. Clin. Cancer Res.* 37, 293. doi: 10.1186/s13046-018-0943-8

Li, L., Tan, J., Miao, Y., Lei, P., and Zhang, Q. (2015). ROS and Autophagy: Interactions and Molecular Regulatory Mechanisms. *Cell Mol. Neurobiol.* 35 (5), 615–621. doi: 10.1007/s10571-015-0166-x

Liu, R., Sobue, T., Kitamura, T., Kitamura, Y., Ishihara, J., Kotemori, A., et al. (2019). Dietary Acrylamide Intake and Risk of Esophageal, Gastric, and Colorectal Cancer: The Japan Public Health Center-based Prospective Study. *Cancer Epidemiol. Biomarkers Prev.* 28 (9), 1461–1468. doi: 10.1158/1055-9965.EPI-18-1259

Liu, X. W., Lu, M. K., Zhong, H. T., Wang, L. H., and Fu, Y. P. (2019). Panax Notoginseng Saponins Attenuate Myocardial Ischemia-Reperfusion Injury Through the HIF-1alpha/BNIP3 Pathway of Autophagy. *J. Cardiovasc. Pharmacol.* 73 (2), 92–99. doi: 10.1097/FJC.0000000000000640

Luo, F. C., Wang, S. D., Qi, L., Song, J. Y., Lv, T., and Bai, J. (2011). Protective effect of panaxatriol saponins extracted from Panax notoginseng against MPTP-induced neurotoxicity in vivo. *J. Ethnopharmacol.* 133 (2), 448–453. doi: 10.1016/j.jep.2010.10.017

Lv, W., Sui, L., Yan, X., Xie, H., Jiang, L., Geng, C., et al. (2018). ROS-dependent Atg4 upregulation mediated autophagy plays an important role in Cd-induced proliferation and invasion in A549 cells. *Chem. Biol. Interact.* 279, 136–144. doi: 10.1016/j.cbi.2017.11.013

Mondaca-Ruff, D., Riquelme, J. A., Quiroga, C., Norambuena-Soto, I., Sanhueza-Olivares, F., Villar-Fincheira, P., et al. (2018). Angiotensin II-Regulated Autophagy Is Required for Vascular Smooth Muscle Cell Hypertrophy. *Front. Pharmacol.* 9, 1553. doi: 10.3389/fphar.2018.01553

Murata, M., Fukushima, K., Takao, T., Seki, H., Takeda, S., and Wake, N. (2013). Oxidative stress produced by xanthine oxidase induces apoptosis in human extravillous trophoblast cells. *J. Reprod. Dev.* 59 (1), 7–13. doi: 10.1262/jrd.2012-053

Pan, X., Yan, D., Wang, D., Wu, X., Zhao, W., Lu, Q., et al. (2017). Mitochondrion-Mediated Apoptosis Induced by Acrylamide is Regulated by a Balance Between Nrf2 Antioxidant and MAPK Signaling Pathways in PC12 Cells. *Mol. Neurobiol.* 54 (6), 4781–4794. doi: 10.1007/s12035-016-0021-1

Pan, X., Wu, X., Yan, D., Peng, C., Rao, C., and Yan, H. (2018). Acrylamide-induced oxidative stress and inflammatory response are alleviated by N-acetylcysteine in PC12 cells: Involvement of the crosstalk between Nrf2 and NF-kappaB pathways regulated by MAPKs. *Toxicol. Lett.* 288, 55–64. doi: 10.1016/j.toxlet.2018.02.002

Qi, A. Q., Li, Y., Liu, Q., Si, J. Z., Tang, X. M., Zhang, Z. Q., et al. (2015). Thioredoxin is a novel diagnostic and prognostic marker in patients with ischemic stroke. *Free Radic. Biol. Med.* 80, 129–135. doi: 10.1016/j.freeradbiomed.2014.12.021

Santhanasabapathy, R., Vasudevan, S., Anupriya, K., Pabitha, R., and Sudhandiran, G. (2015). Farnesol Quells Oxidative Stress, Reactive Gliosis and Inflammation during Acrylamide-Induced Neurotoxicity: Behavioral and Biochemical Evidence. *Neuroscience* 308, 212–227. doi: 10.1016/j.neuroscience.2015.08.067

Seale, S. M., Feng, Q., Agarwal, A. K., and El-Alfy, A. T. (2012). Neurobehavioral and transcriptional effects of acrylamide in juvenile rats. *Pharmacol. Biochem. Behav.* 101 (1), 77–84. doi: 10.1016/j.pbb.2011.12.006

Sharma, S., Rakoczy, S., and Brown-Borg, H. (2010). Assessment of spatial memory in mice. *Life Sci.* 87 (17-18), 521–536. doi: 10.1016/j.lfs.2010.09.004

Shidal, C., Nagarkatti, M., and Nagarkatti, P. S. (2018). MicroRNA-92 expression in CD133(+) melanoma stem cells regulates immunosuppression in the tumor microenvironment through integrin-dependent TGF-beta activation. *J. Immunol.* 79 (14), 3622–3635. doi: 10.1158/0008-5472.CAN-18-2659

Singh, A. K., Kashyap, M. P., Tripathi, V. K., Singh, S., Garg, G., and Neurobiology, S.I.R.J.M. (2017). Neuroprotection Through Rapamycin-Induced Activation of Autophagy and PI3K/Akt1/mTOR/CREB Signaling Against Amyloid-β-Induced Oxidative Stress, Synaptic/Neurotransmission Dysfunction, and Neurodegeneration in Adult Rats. *Mol. Neurobiol.* 54 (8), 5815–5828. doi: 10.1007/s12035-016-0129-3

Song, H. X., Wang, R., Geng, Z. M., Cao, S. X., and Liu, T. Z. (2008). [Subchronic exposure to acrylamide affects reproduction and testis endocrine function of rats]. *Zhonghua Nan Ke Xue* 14 (5), 406–410.

Sun, X., Wu, A., Kwan Law, B. Y., Liu, C., Zeng, W., Ling Qiu, A. C., et al. (2019). The active components derived from Penthorum chinensePursh protect against oxidative-stress-induced vascular injury via autophagy induction. *Free Radic. Biol. Med.* 146, 160–180. doi: 10.1016/j.freeradbiomed.2019.10.417

Tan, X., Ye, J., Liu, W., Zhao, B., Shi, X., Zhang, C., et al. (2019). Acrylamide aggravates cognitive deficits at night period via the gut-brain axis by reprogramming the brain circadian clock. *Arch. Toxicol.* 93 (2), 467–486. doi: 10.1007/s00204-018-2340-7

Tanaka, Y., Guhde, G., Suter, A., Eskelinen, E. L., Hartmann, D., Lullmann-Rauch, R., et al. (2000). Accumulation of autophagic vacuoles and cardiomyopathy in LAMP-2-deficient mice. *Nature* 406 (6798), 902–906. doi: 10.1038/35022595

Tomaszewska, E., Dobrowolski, P., Puzio, I., Prost, L., Kurlak, P., Sawczuk, P., et al. (2014). Acrylamide-induced prenatal programming of intestine structure in guinea pig. *J. Physiol. Pharmacol.* 65 (1), 107–115.

van der Horst, G., van den Hoogen, C., Buijs, J. T., Cheung, H., Bloys, H., Pelger, R. C. M., et al. (2011). Targeting of alpha(v)-Integrins in Stem/Progenitor Cells and Supportive Microenvironment Impairs Bone Metastasis in Human Prostate Cancer. *Neoplasia* 13 (6), 516–525. doi: 10.1593/neo.11122

Wang, S., Wang, X., Luo, F., Tang, X., Li, K., Hu, X., et al. (2014). Panaxatriol saponin ameliorated liver injury by acetaminophen via restoring thioredoxin-1 and pro-caspase-12. *Liver Int.* 34 (7), 1068–1073. doi: 10.1111/liv.12329

Wang, W., Hao, Y., and Li, F. (2019). Notoginsenoside R1 alleviates high glucose-evoked damage in RSC96 cells through down-regulation of miR-503. *Artif. Cells Nanomed. Biotechnol.* 47 (1), 3947–3954. doi: 10.1080/21691401.2019.1671434

Wang, W., Huang, L., Hu, Y., Thomas, E. R., and Li, X. (2020). Neuroprotective effects of notoginsenoside R1 by upregulating Trx-1 on acrylamide-induced neurotoxicity in PC12. *Hum. Exp. Toxicol.* 39 (6), 797–807. doi: 10.1177/0960327120901586

Xie, W., Zhou, P., Sun, Y., Meng, X., Dai, Z., Sun, G., et al. (2018). Protective Effects and Target Network Analysis of Ginsenoside Rg1 in Cerebral Ischemia and Reperfusion Injury: A Comprehensive Overview of Experimental Studies. *Cells* 7 (12), 270. doi: 10.3390/cells7120270

Yang, X., Xiong, X., Wang, H., and Wang, J. (2014). Protective effects of panax notoginseng saponins on cardiovascular diseases: a comprehensive overview of experimental studies. *Evid. Based Complement. Alternat. Med.* 2014, 204840. doi: 10.1155/2014/204840

Zamani, E., Shaki, F., AbedianKenari, S., and Shokrzadeh, M. (2017). Acrylamide induces immunotoxicity through reactive oxygen species production and caspase-dependent apoptosis in mice splenocytes via the mitochondria-dependent signaling pathways. *BioMed. Pharmacother.* 94, 523–530. doi: 10.1016/j.biopha.2017.07.033

Zeng, X. S., Jia, J. J., Kwon, Y., Wang, S. D., and Bai, J. (2014). The role of thioredoxin-1 in suppression of endoplasmic reticulum stress in Parkinson disease. *Free Radic. Biol. Med.* 67, 10–18. doi: 10.1016/j.freeradbiomed.2013.10.013

Zeng, X. S., Jia, J. J., and Ma, L. F. (2015). Gensenoside Rb1 protects rat PC12 cells from oxidative stress-induced endoplasmic reticulum stress: the involvement of thioredoxin-1. *Mol. Cell Biochem.* 410 (1-2), 239–246. doi: 10.1007/s11010-015-2557-1

Zeng, X. S., Geng, W. S., Wang, Z. Q., and Jia, J. J. (2020). Morphine Addiction and Oxidative Stress: The Potential Effects of Thioredoxin-1. *Front. Pharmacol.* 11, 82. doi: 10.3389/fphar.2020.00082

Zhang, H. S., and Wang, S. Q. (2006). Notoginsenoside R1 inhibits TNF-alpha-induced fibronectin production in smooth muscle cells via the ROS/ERK pathway. *Free Radic. Biol. Med.* 40 (9), 1664–1674. doi: 10.1016/j.freeradbiomed.2006.01.003

Zhang, L., Xu, Y., Li, Y., Bao, T., Gowd, V., and Chen, W. (2017). Protective property of mulberry digest against oxidative stress - A potential approach to ameliorate dietary acrylamide-induced cytotoxicity. *Food Chem.* 230, 306–315. doi: 10.1016/j.foodchem.2017.03.045

Zhang, Z., Yan, J., Bowman, A. B., Bryan, M. R., Singh, R., and Aschner, M. (2019). Dysregulation of TFEB contributes to Manganese-induced Autophagic Failure and Mitochondrial Dysfunction in Astrocytes. *Autophagy* 16 (8), 1506–1523. doi: 10.1080/15548627.2019.1688488

Conflict of Interest: The authors declare that the research was conducted in the absence of any commercial or financial relationships that could be construed as a potential conflict of interest.

frontiers in Integrative Neuroscience

ORIGINAL RESEARCH
published: 04 September 2020
doi: 10.3389/fnint.2020.551676

The Role of Microglial CX3CR1 in Schizophrenia-Related Behaviors Induced by Social Isolation

Hao Zhou[1], *Jiesi Wang*[2], *Yu Zhang*[3], *Feng Shao*[1]* *and Weiwen Wang*[2]*

[1]Beijing Key Laboratory of Behavior and Mental Health, School of Psychological and Cognitive Sciences, Peking University, Beijing, China, [2]Key Laboratory of Mental Health, Institute of Psychology, Chinese Academy of Sciences, Beijing, China, [3]School of Nursing, Binzhou Medical University, Yantai, China

According to the microglial hypothesis of schizophrenia, the hyperactivation of microglia and the release of proinflammatory cytokines lead to neuronal loss, which is highly related to the onset of schizophrenia. Recent studies have demonstrated that fractalkine (CX3CL1) and its receptor CX3CR1 modulate the function of microglia. Thus, the present study aimed to determine whether microglial CX3CR1 plays a role in schizophrenia-related behaviors. A classical animal model of schizophrenia, social isolation (from postnatal days 21–56), was used to induce schizophrenia-related behaviors in C57BL/6J and CX3CR1$^{-/-}$ mice, and the expression of the microglial CX3CR1 protein was examined in several brain areas of the C57BL/6J mice by Western blot analysis. The results revealed that social isolation caused deficits in the prepulse inhibition (PPI) in the C57BL/6J mice but not in the CX3CR1$^{-/-}$ mice and increased locomotor activity in both the C57BL/6J mice and the CX3CR1$^{-/-}$ mice. Moreover, the CX3CR1 protein level was increased in the medial prefrontal cortex, nucleus accumbens, and hippocampus of the isolated C57BL/6J mice. These findings suggested that the function of microglia regulated by CX3CR1 might participate in schizophrenia-related behaviors.

Keywords: CX3CR1, microglia, schizophrenia, social isolation, prepulse inhibition

OPEN ACCESS

Edited by:
Robert N. S. Sachdev, Humboldt University of Berlin, Germany

Reviewed by:
Akira Monji, Saga University, Japan
Marie-Eve Tremblay, University of Victoria, Canada

***Correspondence:**
Feng Shao
shaof@pku.edu.cn
Weiwen Wang
wangww@psych.ac.cn

Received: *14 April 2020*
Accepted: *17 August 2020*
Published: *04 September 2020*

Citation:
Zhou H, Wang J, Zhang Y, Shao F and Wang W (2020) The Role of Microglial CX3CR1 in Schizophrenia-Related Behaviors Induced by Social Isolation. Front. Integr. Neurosci. 14:551676. doi: 10.3389/fnint.2020.551676

INTRODUCTION

Schizophrenia is a complex and severe mental illness that has been predicted to be the second leading factor contributing to the global burden of disease by 2030 together with depression and addiction (Gordon and Dzirasa, 2016). There are three main features of schizophrenia: positive symptoms, negative symptoms, and cognitive deficits. The positive symptoms consist of hallucination and delusion, and the negative symptoms consist of social avoidance and depression (Agnieszka, 2018). Also, cognitive deficits are one of the core features (Lepage et al., 2014). Although the underlying mechanism of schizophrenia remains unclear, evidence has shown that neuroinflammation and immunogenetics might participate in the development of this disease (Keller et al., 2012). In 2009, Monji proposed the microglia hypothesis of schizophrenia in which microglia play an essential role in the development of schizophrenia (Monji et al., 2009). As a core immune component in the central nervous system (CNS), microglia monitor synapses, detect harmful agents and remove dead cells by suppressing or promoting neuroinflammation (Mizuno, 2015). Usually, microglia have a beneficial healing effect towards the damage in the brain, by keeping the balance of suppressing or promoting neuroinflammation.

However, when the damage lasts for a very long period under certain conditions, the production of too many cytokines and the long-term effects of inflammation modulated by microglia may be toxic (Schlegelmilch et al., 2011), which could increase the risk of mental illnesses such as schizophrenia (Monji et al., 2009). For example, Doorduin et al. (2009) found a significantly higher binding potential of ^{11}C-(R)-PK11195 (a peripheral benzodiazepine receptor ligand that can be used for the imaging of microglia cell) in the hippocampus of patients with schizophrenia, which indicated microglia and neuroinflammation might play an important role in schizophrenic patients during psychosis. Moreover, studies have shown that most patients with schizophrenia suffer from an imbalance in their immune function. For example, it was reported that there was a cytokine imbalance in people with schizophrenia, as *in vivo* IL-1RA, soluble IL-2 receptor, and IL-6 were found to be increased (Potvin et al., 2008; Keller et al., 2012). Similarly, Goldsmith et al. (2016) found in a meta-analysis study that levels of IL-6, TNF-α, sIL-2R, and IL-1RA were significantly increased in acutely ill patients with schizophrenia, Boerrigter et al. (2017) found that the anti-inflammatory IL-2 mRNA was decreased and pro-inflammatory cytokines IL-6, TNF-α were increased in the peripheral blood of people with schizophrenia. Consistent results have been found in animal studies. Juckel et al. (2011) reported less branched microglia in the hippocampus and corpus striatum of the offspring induced by the injection of PolyI:C into pregnant rats, which indicated a phagocytic state of microglia in schizophrenia-like animal model. These results have revealed that microglia might participate in the development of schizophrenia.

Thus, researchers have started to focus on a critical target that modulates the function of microglia, the chemokine adhered to the surface of microglia (Ślusarczyk et al., 2015). Among all the chemokines, CX3CR1 and its ligand CX3CL1 directly modulate the function of microglia (Wolf et al., 2013). CX3CL1 localizes in the brain parenchyma to selected neurons, while CX3CR1 exists mostly on the surface of microglia in the CNS (Wolf et al., 2013). CX3CL1 mRNA was found to be highly expressed in the olfactory bulb, cerebral cortex, hippocampus, caudate-putamen, and nucleus accumbens (Nishiyori et al., 1998; Ragozzino, 2002). There are two forms of CX3CL1: the soluble form and the membrane-bound form. The membrane-bound form of CX3CL1 can recognize damaged cells, and the soluble form can attract microglia to damaged cells by binding to CX3CR1 expressed on microglia. Recently, several studies have examined the modulation of CX3CR1 on microglia in patients with schizophrenia. Ishizuka et al. (2017) found that the Ala55Thr mutant downregulates CX3CL1–CX3CR1 signaling, which might be the cause of schizophrenia and autism spectrum disorders. Bergon et al. (2015) also found in a meta-analysis that CX3CR1 expression is dysregulated in the blood and brain of patients with schizophrenia. However, Zhang et al. (2020) found that there was no difference in the CX3CR1 mRNA expression in the anterior cingulate cortex between patients with schizophrenia and controls. There was even increased expression of CX3CR1 mRNA in the anterior cingulate cortex in schizophrenic patients without suicide compared with those who died by suicide (Zhang et al., 2020). These controversial results suggest that further studies are needed to reveal how CX3CR1 and microglia participate in the development of schizophrenia.

CX3CR1$^{-/-}$ mice are a good model to determine whether microglia participate in the development of immune-related diseases. There have been many studies using CX3CR1$^{-/-}$ mice in the field of stress, depression, and other immune-related physical diseases. For example, Winkler et al. (2017) used CX3CR1$^{-/-}$ mice on C57BL/6 background in a stress-related study of microglia and found these mice to be resistant to a typical model of stress, including significantly decreased immobility and increased time of struggling in forced swimming and tail suspension tests. Hellwig et al. (2016) found that CX3CR1 deficient mice showed resistance to depressive-like behaviors and changes in microglia morphology in a particular chronic despair model, compared to wild-type mice. Rimmerman et al. (2016) reported that wild-type mice displayed reduced sucrose preference, impaired novel object recognition memory, and reduced neurogenesis in a chronic unpredictable stress model, while CX3CR1$^{-/-}$ mice were completely resistant to these effects. Schubert et al. (2018) used CX3CR1$^{-/-}$ mice in a study of immunomodulatory mechanisms of post-traumatic stress disorder and found that these mice showed decreased anxiety-like behaviors. Additionally, Yu et al. (2018) used CX3CR1$^{-/-}$ mice and found that the CX3CL1–CX3CR1 axis together with the NF-κB signaling pathway participates in the development of fructose-induced kidney injury. However, until now, there has been a lack of research work to observe schizophrenia-like behaviors, such as prepulse inhibition (PPI), in CX3CR1$^{-/-}$ mice.

Many models, such as maternal interference, early life interference, and social isolation, have been used to observe the schizophrenia-like behaviors of rats (Juckel et al., 2011; Wang et al., 2015). PPI is a typical cognitive function, and impaired PPI function is recognized as one of the most important features of patients with schizophrenia. Thus, impaired PPI is a key characteristic of a good animal model of schizophrenia (Braff et al., 2008; Tapias-Espinosa et al., 2018). In 1993, Geyer et al. (1993) reported that isolation-reared animals showed significantly decreased PPI. Our previous studies also proved that social isolation can efficiently induce deficits in the PPI (Han et al., 2011a; Li et al., 2016, 2019; Sun et al., 2017) and reversal learning (Han et al., 2011b). Hence, social isolation is an appropriate strategy to induce schizophrenia-like behavior.

Thus, in this study, we aimed to test whether CX3CR1 plays a role in the social isolation-induced schizophrenia-like behaviors. First, we investigated the effects of social isolation on the PPI and locomotor activity of C57BL/6J mice, and then, the expression of CX3CR1 in the mPFC, NAc, and HIP was measured. Second, the CX3CR1$^{-/-}$ mice on a C57BL/6J background were used to further demonstrate the impact of impaired modulation of CX3CR1 on microglia in this process. This study might provide further support for the microglial hypothesis of schizophrenia and reveal a new target for future studies.

METHODS

Experiment 1

Animals

Twenty-four specific-pathogen-free (SPF) male C57BL/6J mice were obtained from Vital River Laboratory Animal Technology Company Limited (Beijing, China). All mice were housed at 22 ± 2°C and a humidity of 40–60% in standard cages under a 12 h light/dark cycle (lights on between 7:00 and 19:00); and the cage measured 295 mm long * 190 mm wide * 125 mm high. Water and food were available *ad libitum*. The use of animals and the experimental procedures followed the National Institutes of Health Guide for the Care and Use of Laboratory Animals and were approved by the Institutional Animal Care and Use Committee (IACUC) of Peking University.

Social Isolation

At PND 21, all the mice were divided into two different rearing conditions (social rearing, SR, vs. isolated rearing, IR). All the mice were divided randomly to prevent litter effects. There were 10 mice in the social-rearing (SR) group, while the other 14 mice were in the isolated-rearing (IR) group. For the SR group, there were four mice in one cage, while for the IR group, there was only one mouse per cage. The two groups were reared separately for 5 weeks (PND 21–56). During this period, the mice in the IR group could only interact with others in visual, auditory, and olfactory ways but had no physical interactions. After 5 weeks, there was a handling process for 3 days. During this period, each mouse was put on the hand of the experimenter for 5 min per day. Then, behavioral tests were performed.

Behavioral Tests

Open Field Test for Locomotor Activity in the Animals

At PND 60, an open field test was performed to test the spontaneous locomotion of all the mice. This test was performed in an open, uniformly illuminated square box of 40 cm × 40 cm. The mice were allowed to walk freely for 15 min in the arena. The total distance the mice traveled was recorded by a LabState laboratory animal behavioral analysis system (AniLab ver 4.3, AniLab Scientific Instruments Company Limited).

The Acoustic Startle Response Test and PPI Test

At PND 62, acoustic startle and PPI tests were undertaken with an SR-LAB startle response system apparatus (San Diego Instruments, San Diego, CA, USA). Five of the 10 chambers of the apparatus were used to perform the experiment. Inside each chamber, there is a transparent plexiglass cylinder (interior diameter: 3.5 inches; length: 8 inches) used to keep the mouse still. The size of the cylinder was appropriately adjusted to prevent excessive restraint of the mouse, which could cause further stress. The startle response was quantified by a piezoelectric transducer beneath the cylinder, and the information on each move was displayed on a computer. During the whole session, there was a background noise of 66 dB. After an acclimation period of 5 min, 30 trials were conducted for each mouse. There were three kinds of trials: (1) one 40 ms startle pulse with a 120 dB noise; (2) one 20 ms prepulse with 74 dB and one startle pulse with 120 dB; and (3) one 20 ms prepulse with 82 dB and one startle pulse with 120 dB. All three kinds of trials were presented ten times with random sequences, and the interval between every two trials was also random, ranging from 10 to 30 s with an average of 20 s. The cylinder was cleaned with 75% ethanol between each session. The PPI percent was calculated as follows: %PPI = (1 − startle amplitude in the prepulse trial/startle amplitude in the pulse alone trial) × 100%.

The behavioral tests were designed and performed by two investigators, and the one ran the tests were blind to the experimental conditions. At 24 h after all the behavioral tests, all 24 mice were decapitated without anesthesia. The mPFC, NAc, and HIP tissues were carefully dissected and frozen for Western blot analysis.

Western Blot

The tissues of six mice in the IR group and six mice in the SR group were selected randomly for Western blot. All the tissues were lysed in RIPA buffer containing protease inhibitor cocktail (Roche, USA). After denaturation at 100°C for 10 min in 5* loading buffer (Solarbio, Beijing), total protein (15 μg) was loaded and separated on a 12% gel (Bio-Rad, Hercules, CA, USA) and then transferred to polyvinylidene fluoride (PVDF) membranes (Millipore, Kankakee, IL, USA) using Mini Trans-Blot Electrophoretic Transfer Cell (Bio-Rad, Hercules, CA, USA). For both CX3CR1 and GAPDH, the membranes were blocked at room temperature for 1 h in 5% fat-free milk in TBST buffer (150 mM NaCl, 50 mM Tris-HCl, 0.5% Tween-20, pH = 7.6), after which the membranes were incubated at 4°C overnight with the primary antibody. The primary antibody used for CX3CR1 was rabbit polyclonal anti-CX3CR1 (ab8021, 1:1,500, Abcam), and the one for GAPDH was mouse monoclonal anti-GAPDH (ab8245, 1:2,000, Abcam), and they were both diluted in 5% fat-free milk in TBST buffer. When the incubation ended, the membranes were washed with TBST three times to remove the primary antibody, each of which lasted 15 min. Then, the membranes were incubated with the secondary antibody at room temperature for 1 h. The secondary antibody used were anti-rabbit antibody (1:5,000, Zhongshanjinqiao, China) and anti-mouse antibody (1:5,000, Zhongshanjinqiao, China), which were diluted in 5% fat-free milk in TBST buffer. After incubation, the membranes were again washed with TBST three times. Then, the bands were visualized by ECL Western Blotting Substrate (Solarbio, Beijing), and the images were processed and acquired using ChemiDoc™ XRS + System (Bio-Rad, Hercules, CA, USA). The intensity of the bands was quantified using ImageJ software, and GAPDH was used as a loading control.

Experiment 2

Animals

A total of 12 male CX3CR1$^{GFP/GFP}$ mice in the genetic background of C57BL/6J were obtained from Dr. Bo Peng (The University of Hong Kong, Hong Kong, China), which were firstly imported from The Jackson Laboratory. There were six mice in the SR group, while the other six mice were in the IR group. All the mice were divided randomly to prevent litter

effects. The rearing conditions were the same as those described in Experiment 1.

Social Isolation

At PND 21, the CX3CR1$^{-/-}$ mice were divided into two groups and received the same rearing conditions as in Experiment 1.

Behavioral Tests

The two groups of CX3CR1$^{-/-}$ mice both underwent the two behavioral tests as described in Experiment 1.

Statistical Analysis

All analyses were performed using GraphPad Prism6 software (USA), and data are expressed as the mean ± standard error of the mean. The student's *t*-test was used in the open field test and Western blots. Two-way ANOVA was used in the PPI test. The data which were three-fold standard deviation (SD) above or below the average were regarded as outliers and were dealt with. What's more, two data from the 74 and 82 dB conditions of one control mouse were about 2.8-fold SD below the average in the PPI test. Considering the open field data of the same animal were also outliers, we dealt with these two data as outliers. The significance level was defined as $p < 0.05$.

RESULTS

Social Isolation-Induced Increased Locomotor Activity in the Wild-Type Mice

As shown in **Figure 1A**, in the open field test, the total distance traveled by the IR group was significantly longer than that traveled by the SR group ($t_{(19)} = 3.331$, $p = 0.0035$; If the outliers were included in the analysis, $t_{(22)} = 1.815$, $p = 0.0831$). Social isolation caused significantly increased spontaneous locomotion in the wild-type mice.

Social Isolation Resulted in Impairments in the PPI in the Wild-Type Mice

As shown in **Figure 1B**, there was a significant effect of rearing condition between the SR group and IR group ($F_{(1,22)} = 4.932$, $p = 0.0370$; If the outliers were included in the analysis, $F_{(1,22)} = 0.6050$, $p = 0.4450$) and a significant effect of the startle condition between 74 and 82 dB ($F_{(1,22)} = 66.06$, $p = 0.0001$; If the outliers were included in the analysis, $F_{(1,22)} = 59.97$, $p = 0.0001$). There was no significant interaction between the rearing condition and the startle condition ($F_{(1,22)} = 1.215$, $p = 0.2822$; If the outliers were included in the analysis, $F_{(1,22)} = 0.4099$, $p = 0.5287$). As shown in **Figure 1C**, there was no difference in the pulse-alone trials between the SR group and IR group ($t_{(22)} = 1.071$, $p = 0.2958$). This result showed that social isolation impaired PPI.

Social Isolation Increased the CX3CR1 Expression in the mPFC, NAc, and HIP

Western blot analysis revealed a specific band (≈50 kDa) of CX3CR1. As shown in **Figure 2**, there was a significantly higher expression of CX3CR1 in the mPFC **(A)** of the IR group than in the SR group ($t_{(10)} = 3.932$, $p < 0.01$), and there was a similar trend in the NAc **(B)** ($t_{(10)} = 2.347$, $p = 0.0409$) and HIP **(C)** ($t_{(10)} = 4.862$, $p < 0.01$).

Social Isolation-Induced Increased Locomotor Activity in the CX3CR1$^{-/-}$ Mice

As shown in **Figure 3A**, in the open field test, the IR group of CX3CR1$^{-/-}$ mice also traveled longer than the SR group ($t_{(9)} = 2.594$, $p = 0.0290$). Social isolation could induce increased spontaneous locomotion in the CX3CR1$^{-/-}$ mice.

Social Isolation Did Not Affect the PPI of the CX3CR1$^{-/-}$ Mice

As shown in **Figure 3B**, there was a significant difference between the startle conditions ($F_{(1,9)} = 99.71$, $p < 0.01$), but there was no significant difference between the different rearing conditions of the CX3CR1$^{-/-}$ mice ($F_{(1,9)} = 0.008469$, $p = 0.9287$), and there was no significant interaction effect ($F_{(1,9)} = 0.8609$, $p = 0.3777$). As shown in **Figure 3C**, there was no difference in the pulse-alone trials between the SR group and IR group ($t_{(9)} = 0.8122$, $p = 0.4376$). Social isolation did not cause significant deficits in the PPI of the CX3CR1$^{-/-}$ mice compared to the wild-type mice.

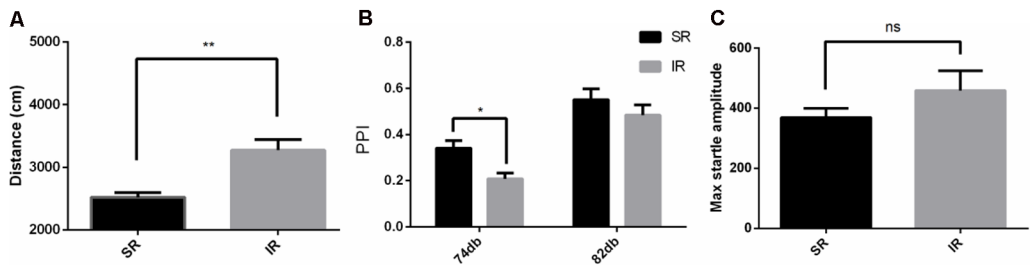

FIGURE 1 | Effects of isolation rearing on the behaviors of the wild-type mice, including the total distance traveled **(A)** in the open field test, the prepulse inhibition (PPI)% **(B)** in the acoustic startle response and the PPI test, and the pulse-alone amplitudes, **(C)** in the acoustic startle response and the PPI test. The results are expressed as the mean ± SEM [$n = 10$ for the social-rearing (SR) group and $n = 14$ for the isolated-rearing (IR) group, $^{*}p < 0.05$, $^{**}p < 0.01$, $^{ns}p > 0.05$, student's *t*-test and two-way ANOVA].

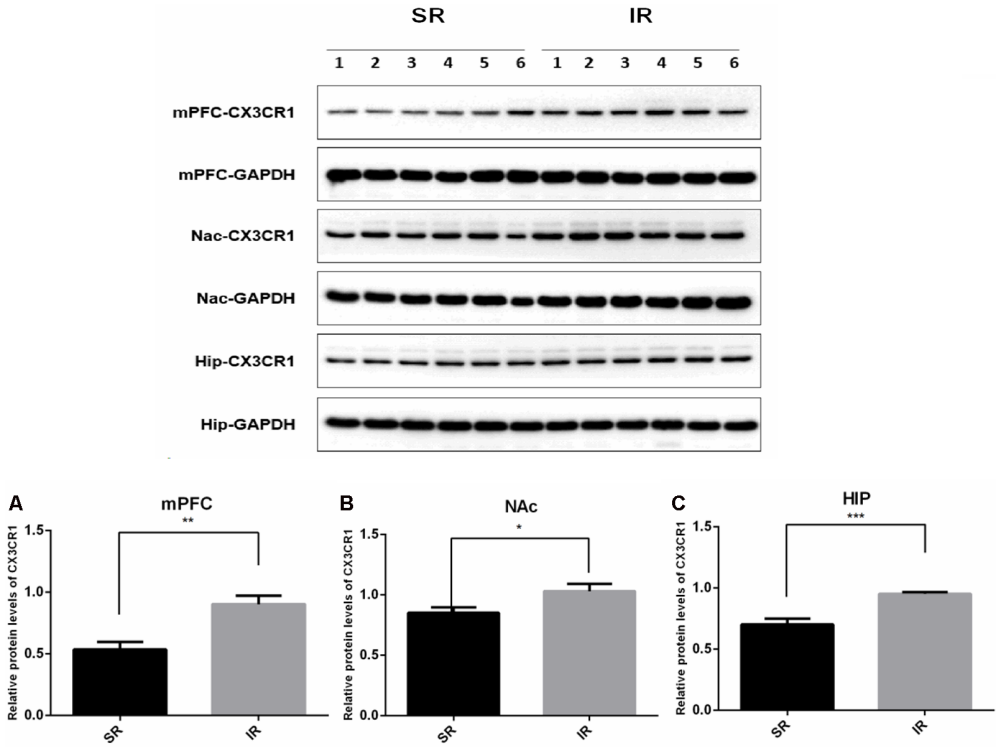

FIGURE 2 | Effects of isolation rearing on the CX3CR1 expression in the wild-type mice. Different regions were tested, including the mPFC **(A)**, NAc **(B)**, and HIP **(C)**. The results are expressed as the mean ± SEM ($n = 6$ for the SR group and $n = 6$ for the IR group. $^{*}p < 0.05$, $^{**}p < 0.01$, $^{***}p < 0.001$, student's *t*-test).

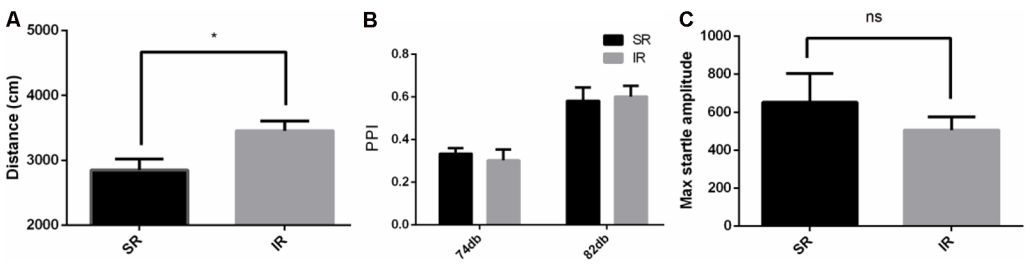

FIGURE 3 | Effects of isolation rearing on the behavior of the CX3CR1$^{-/-}$ mice, including the total distance traveled **(A)** in the open field test, the PPI%, **(B)** in the acoustic startle response and the PPI test, and the pulse-alone amplitudes, **(C)** in the acoustic startle response and the PPI test. The results are expressed as the mean ± SEM ($n = 6$ for the SR group and $n = 6$ for the IR group, $^{*}p < 0.05$, $^{ns}p > 0.05$, student's *t*-test and two-way ANOVA).

DISCUSSION

The current study found that social isolation can induce schizophrenia-like behaviors in mice, similar to the results in rats. After isolated rearing, the C57BL/6J mice showed impaired PPI function and increased locomotor activity, similar to rats. Also, increased CX3CR1 protein levels in the mPFC, NAC, and HIP of the isolated C57BL/6J mice were observed. For the CX3CR1$^{-/-}$ mice, social isolation-induced similarly increased locomotor activity but did not affect the PPI.

In our previous studies, isolation rearing was reported to induce increased locomotor activity and disrupted PPI function in rats (Han et al., 2011a; Li et al., 2016, 2019; Sun et al., 2017). Similar results were shown in experiment 1, where isolated rearing of the wild-type mice resulted in behaviors similar to those in rats. These results are consistent with previous studies using the model of social isolation of rodents (Abramov et al., 2004; Fone and Porkess, 2008; Huang et al., 2017). These findings proved that social isolation is a stable way to induce schizophrenia-like behavior in both rats and mice.

To investigate the effects of CX3CR1 on the schizophrenia-like behaviors induced by social isolation, we assessed the CX3CR1 protein levels within several regions, including the mPFC, NAc, and HIP, which are well-established sites for schizophrenia-like behavior. The results showed that the CX3CR1 protein was upregulated in all three areas of

the wild-type mice. To the best of our knowledge, this is the first study to determine the effects of CX3CR1 in an animal model of PPI-related schizophrenia-like behaviors, and we could not compare the results with related animal studies. However, our results seem to be inconsistent with those of two other clinical studies. Bergon et al. (2015) found abnormal CX3CR1 mRNA expression in the blood and brain of patients with schizophrenia, while Zhang et al. (2020) reported that there was no significant difference between patients with schizophrenia and controls concerning the mRNA level of CX3CR1 in the anterior cingulate cortex. The most likely reasons for these complex and inconsistent results could be as follows. First, the evaluation might occur at a different stage of schizophrenia. As shown in Wynne's study, there indeed was a dynamic change in CX3CR1 surface expression after activation. CX3CR1 expression may decrease first as a response to a stimulus, such as the injection of lipopolysaccharide. However, the reduction disappeared, and CX3CR1 expression returned to the former level in 24 h. Later, this reduction was even reversed, and CX3CR1 expression was found to be significantly increased after 24 h (Wynne et al., 2010). This finding suggested that the expression of CX3CR1 may differ in different stages of schizophrenia. Second, the expression of chemokines might not only be affected by transcriptional regulation but also translational regulation and translocation (Wynne et al., 2010). This phenomenon may explain the opposite results of the CX3CR1 mRNA levels and CX3CR1 expression (Ishizuka et al., 2017). In further studies, we will simultaneously test CX3CR1 mRNA, CX3CR1 protein, and the functional change of microglia to explore the covariation of these three factors. It has been reported that TGFβ might be a key factor that elevates the expression of CX3CR1 after its immediate downregulation and thus could be a new target in the future (Chen et al., 2003; Wynne et al., 2010). Determining the exact changes in both CX3CR1 and microglia may help us better understand the modulation of CX3CR1 on microglia and dynamic neuron-glia crosstalk.

By using CX3CR1$^{-/-}$ mice, we found a similar influence of social isolation on these knock-out mice, where they presented similar increased locomotor activity. However, in contrast to the results in the wild-type mice, there was no significant impairment of the PPI function in the IR group compared to the SR group. Since it was revealed that the basic function of the acoustic response was not affected in CX3CR1$^{-/-}$ mice (Schubert et al., 2018), this difference in isolation rearing-induced PPI deficit between the wild-type and CX3CR1$^{-/-}$ mice could not be a result of the basic acoustic response deficit. The CX3CR1$^{-/-}$ mice were reported to suffer from transiently reduced microglial densities in their first two postnatal weeks (Paolicelli et al., 2011), and this lack of microglia during early age caused microglial dysfunction, which might be related to the resistance to social isolation-induced impairments in the PPI.

Moreover, our results found that the locomotor activity was found to be increased in both genotypes while the PPI deficit was found to be CX3CR1-dependent. It suggested that the schizophrenia-like cognitive deficits such as PPI deficit seemed to be directly related to the function of microglia. This was similar to Rimmerman et al.'s (2016) conclusion that emotional and cognitive stress resilience might be a result of CX3CR1-dependent basal alterations in hippocampal transcription, for the result that the exposure of chronic unexpected stress could alter neuronal gene transcripts (e.g., Arc, Npas4) in both wild-type and CX3CR1$^{-/-}$ mice, while the transcripts downstream of hippocampal estrogen receptor signaling were altered only in CX3CR1$^{-/-}$ mice. While Ieraci et al. (2016) found in a chronic social isolation model of mice that the hyperactivity was correlated with the cortical BDNF-7 levels and metabotropic glutamate receptor mGluR1 in the PFC, Eßlinger et al. (2016) found that PPI deficits were preceded by a strong M1-type microglia polarization pattern in the whole brain during puberty in the model of prenatal Poly(I:C) injection. This might explain the difference between the CX3CR1-independent hyperactivity and CX3CR1-dependent PPI deficit. Further studies are required on the particular signaling pathway related to PPI deficit, CX3CR1, and microglia. Our study first used an animal model of schizophrenia to demonstrate that CX3CR1 might be a necessary factor in the development of schizophrenia-like behaviors, and the blockade of CX3CR1 might be useful in treating schizophrenia.

In conclusion, the present study found that social isolation can induce increased locomotor activity both in the C57BL/6J mice and the CX3CR1$^{-/-}$ mice, and impairments in the PPI in the C57BL/6J mice but not in the CX3CR1$^{-/-}$ mice. Moreover, CX3CR1 was upregulated in the mPFC, NAc, and HIP of the isolated C57BL/6J mice. These findings first demonstrated that CX3CR1 plays a role in the schizophrenia-like behaviors induced by social isolation, providing new directions for studies of microglial function in the development of schizophrenia and treatment strategies for schizophrenia.

DATA AVAILABILITY STATEMENT

The raw data supporting the conclusions of this article will be made available by the authors, without undue reservation.

ETHICS STATEMENT

The animal study was reviewed and approved by Institutional Animal Care and Use Committee (IACUC) of Peking University.

AUTHOR CONTRIBUTIONS

FS and WW designed the study. HZ, JW, and YZ performed the research and obtained the data. HZ and JW interpreted and analyzed the data. HZ, WW, and FS drafted, revised, and wrote the article. All authors contributed to the article and approved the submitted version.

FUNDING

This work was supported by the National Natural Science Foundation of China (Grant numbers 31470988 and 31771217) and the Key Laboratory of Mental Health, Institute of Psychology, Chinese Academy of Sciences.

REFERENCES

Abramov, U., Raud, S., Koks, S., Innos, J., Kurrikoff, K., Matsui, T., et al. (2004). Targeted mutation of CCK_2 receptor gene antagonises behavioural changes induced by social isolation in female, but not in male mice. *Behav. Brain Res.* 155, 1–11. doi: 10.1016/j.bbr.2004.03.027

Agnieszka, N. (2018). Assessment of cognitive functions in animal models of schizophrenia. *Pharmacol. Rep.* 70, 639–649. doi: 10.1016/j.pharep.2018.01.009

Bergon, A., Belzeaux, R., Comte, M., Pelletier, F., Hervé, M., Gardiner, E. J., et al. (2015). CX3CR1 is dysregulated in blood and brain from schizophrenia patients. *Schizophr. Res.* 168, 434–443. doi: 10.1016/j.schres.2015.08.010

Boerrigter, D., Weickert, T. W., Lenroot, R., O'Donnell, M., Galletly, C., Liu, D., et al. (2017). Using blood cytokine measures to define high inflammatory biotype of schizophrenia and schizoaffective disorder. *J. Neuroinflammation* 14:188. doi: 10.1186/s12974-017-0962-y

Braff, D. L., Greenwood, T. A., Swerdlow, N. R., Light, G. A., Schork, N. J., and Investigators of the Consortium on the Genetics of Schizophrenia. (2008). Advances in endophenotyping schizophrenia. *World Psychiatry* 7, 11–18. doi: 10.1002/j.2051-5545.2008.tb00140.x

Chen, S., Luo, D., Streit, W. J., and Harrison, J. K. (2003). TGF-β1 up regulates CX3CR1 expression and inhibits ractalkin stimulated signaling in rat microglia. *J. Neuroimmunol.* 133, 46–55. doi: 10.1016/s0165-5728(02)00354-5

Doorduin, J., de Vries, E. F. J., Willemsen, A. T. M., de Groot, J. C., Dierckx, R. A., and Klein, H. C. (2009). Neuroinflammation in schizophrenia-related psychosis: a PET study. *J. Nuclear Med.* 50, 1801–1807. doi: 10.2967/jnumed.109.066647

Eßlinger, M., Wachholz, S., Manitz, M.-P., Plümper, J., Sommer, R., Juckel, G., et al. (2016). Schizophrenia associated sensory gating deficits develop after adolescent microglia activation. *Brain Behav. Immun.* 58, 99–106. doi: 10.1016/j.bbi.2016.05.018

Fone, K. C., and Porkess, M. V. (2008). Behavioural and neurochemical effects of post-weaning social isolation in rodents-relevance to developmental neuropsychiatric disorders. *Neurosci. Biobehav. Rev.* 32, 1087–1102. doi: 10.1016/j.neubiorev.2008.03.003

Geyer, M. A., Wilkinson, L. S., Humby, T., and Robbins, T. W. (1993). Isolation rearing of rats produces a deficit in prepulse inhibition of acoustic startle similar to that in schizophrenia. *Biol. Psychiatry* 34, 361–372. doi: 10.1016/0006-3223(93)90180-l

Goldsmith, D. R., Rapaport, M. H., and Miller, B. J. (2016). A meta-analysis of blood cytokine network alterations in psychiatric patients: comparisons between schizophrenia, bipolar disorder and depression. *Mol. Psychiatry* 21, 1696–1709. doi: 10.1038/mp.2016.3

Gordon, J. A., and Dzirasa, K. (2016). Animal models of psychiatric disorders. *Neuroscience* 321, 1–2. doi: 10.1016/j.neuroscience.2016.02.004

Han, X., Wang, W., Shao, F., and Li, N. (2011a). Isolation rearing alters social behaviors and monoamine neurotransmission in the medial prefrontal cortex and nucleus accumbens of adult rats. *Brain Res.* 1385, 175–181. doi: 10.1016/j.brainres.2011.02.035

Han, X., Wang, W., Xue, X., Shao, F., and Li, N. (2011b). Brief social isolation in early adolescence affects reversal learning and forebrain BDNF expression in adult rats. *Brain Res. Bull.* 86, 173–178. doi: 10.1016/j.brainresbull.2011.07.008

Hellwig, S., Brioschi, S., Dieni, S., Frings, L., Masuch, A., Blank, T., et al. (2016). Altered microglia morphology and higher resilience to stress-induced depression-like behavior in CX3CR1-deficient mice. *Brain Behav. Immun.* 55, 126–137. doi: 10.1016/j.bbi.2015.11.008

Huang, Q., Zhou, Y., and Liu, L. Y. (2017). Effect of post-weaning isolation on anxiety- and depressive-like behaviors of C57BL/6J mice. *Exp. Brain Res.* 235, 2893–2899. doi: 10.1007/s00221-017-5021-5

Ieraci, A., Mallei, A., and Popoli, M. (2016). Social isolation stress induces anxious-depressive-like behavior and alterations of neuroplasticity-related genes in adult male mice. *Neural Plast.* 2016:6212983. doi: 10.1155/2016/6212983

Ishizuka, K., Fujita, Y., Kawabata, T., Kimura, H., Iwayama, Y., Inada, T., et al. (2017). Rare genetic variants in CX3CR1 and their contribution to the increased risk of schizophrenia and autism spectrum disorders. *Transl. Psychiatry* 7:e1184. doi: 10.1038/tp.2017.173

Juckel, G., Manitz, M. P., Brune, M., Friebe, A., Heneka, M. T., and Wolf, R. J. (2011). Microglial activation in a neuroinflammational animal model of schizophrenia—a pilot study. *Schizophr. Res.* 131, 96–100. doi: 10.1016/j.schres.2011.06.018

Keller, W. R., Kum, L. M., Wehring, H. J., Koola, M. M., and Kelly, D. L. (2012). A review of anti-inflammatory agents for symptoms of schizophrenia. *J. Psychopharmacol.* 27, 337–342. doi: 10.1177/0269881112467089

Lepage, M., Bodnar, M., and Bowie, C. R. (2014). Neurocognition: clinical and functional outcomes in schizophrenia. *Can. J. Psychiatry* 59, 5–12. doi: 10.1177/070674371405900103

Li, M., Du, W., Shao, F., and Wang, W. (2016). Cognitive dysfunction and epigenetic alterations of the BDNF gene are induced by social isolation during early adolescence. *Behav. Brain Res.* 313, 177–183. doi: 10.1016/j.bbr.2016.07.025

Li, M., Wang, W., Sun, L., Du, W., Zhou, H., and Shao, F. (2019). Chronic clozapine treatment improves the alterations of prepulse inhibition and BDNF mRNA expression in the medial prefrontal cortex that are induced by adolescent social isolation. *Behav. Pharmacol.* 30, 311–319. doi: 10.1097/fbp.0000000000000419

Mizuno, T. (2015). Neuron-microglia interactions in neuroinflammation. *Clin. Exp. Neuroimmunol.* 6, 225–231. doi: 10.1111/cen3.12228

Monji, A., Kato, T., and Kanba, S. (2009). Cytokines and schizophrenia: microglia hypothesis of schizophrenia. *Psychiatry Clin. Neurosci.* 63, 257–265. doi: 10.1111/j.1440-1819.2009.01945.x

Nishiyori, A., Minami, M., Ohtani, Y., Takami, S., and Satoh, M. (1998). Localization of fractalkine and CX3CR1 mRNAs in rat brain: does fractalkine play a role in signaling from neuron to microglia? *FEBS Lett.* 429, 167–172. doi: 10.1016/s0014-5793(98)00583-3

Paolicelli, R. C., Bolasco, G., Pagani, F., Maggi, L., Scianni, M., Panzanelli, P., et al. (2011). Synaptic pruning by microglia is necessary for normal brain development. *Science* 333, 1456–1458. doi: 10.1126/science.1202529

Potvin, S., Stip, E., Sepehry, A. A., Gendron, A., Bah, R., and Kouassi, E. (2008). Inflammatory cytokine alterations in schizophrenia: a systematic quantitative review. *Biol. Psychiatry* 63, 801–808. doi: 10.1016/j.biopsych.2007.09.024

Ragozzino, D. (2002). CXC chemokine receptors in the central nervous system: role in cerebellar neuromodulation and development. *J. Neurovirol.* 8, 559–572. doi: 10.1080/13550280290100932

Rimmerman, N., Schottlender, N., Reshef, R., Dan-Goor, N., and Yirmiya, R. (2016). The hippocampal transcriptomic signature of stress resilience in mice with microglial fractalkine receptor (CX3CR1) deficiency. *Brain Behav. Immun.* 61, 184–196. doi: 10.1016/j.bbi.2016.11.023

Schlegelmilch, T., Henke, K., and Peri, F. (2011). Microglia in the developing brain: from immunity to behaviour. *Curr. Opin. Neurobiol.* 21, 5–10. doi: 10.1016/j.conb.2010.08.004

Schubert, I., Ahlbrand, R., Winter, A., Vollmer, L., Lewkowich, I., and Sah, R. (2018). Enhanced fear and altered neuronal activation in forebrain limbic regions of CX3CR1-deficient mice. *Brain Behav. Immun.* 68, 34–43. doi: 10.1016/j.bbi.2017.09.013

Ślusarczyk, J., Trojan, E., Gombik, K., Budziszewska, B., Kubera, M., Lasoń, W., et al. (2015). Prenatal stress is a vulnerability factor for altered morphology and biological activity of microglia cells. *Front. Cell. Neurosci.* 9:82. doi: 10.3389/fncel.2015.00082

Sun, L., Min, L., Zhou, H., Li, M., Shao, F., and Wang, W. (2017). Adolescent social isolation affects schizophrenia-like behavior and astrocyte biomarkers in the PFC of adult rats. *Behav. Brain Res.* 333, 258–266. doi: 10.1016/j.bbr.2017.07.011

Tapias-Espinosa, C., Riò-Álamos, C., Sampedro-Viana, D., Gerbolés, C., Oliveras, I., Sánchez-González, A., et al. (2018). Increased exploratory activity in rats with deficient sensorimotor gating: a study of schizophrenia-relevant symptoms with genetically heterogeneous NIH-HS and Roman rat strains. *Behav. Processes* 151, 96–103. doi: 10.1016/j.beproc.2018.03.019

Wang, Q., Shao, F., and Wang, W. (2015). Maternal separation produces alterations of forebrain brain-derived neurotrophic factor expression in

differently aged rats. *Front. Mol. Neurosci.* 8:49. doi: 10.3389/fnmol.2015.00049

Winkler, Z., Kuti, D., Ferenczi, S., Gulyás, K., Polyák, Á., and Kovács, K. J. (2017). Impaired microglia fractalkine signaling affects stress reaction and coping style in mice. *Behav. Brain Res.* 334, 119–128. doi: 10.1016/j.bbr.2017.07.023

Wolf, Y., Yona, S., Kim, K. W., and Jung, S. (2013). Microglia, seen from the CX3CR1 angle. *Front. Cell. Neurosci.* 7:26. doi: 10.3389/fncel.2013.00026

Wynne, A. M., Henry, C. J., Huang, Y., Cleland, A., and Godbout, J. P. (2010). Protracted downregulation of CX3CR1 on microglia of aged mice after lipopolysaccharide challenge. *Brain Behav. Immun.* 24, 1190–1201. doi: 10.1016/j.bbi.2010.05.011

Yu, Y. W., Li, M. X., Zhang, Z. Y., and Yu, H. (2018). The deficiency of CX3CL1/CX3CR1 system ameliorates high fructose diet-induced kidney injury by regulating NF-kappaB pathways in CX3CR1-knock out mice. *Int. J. Mol. Med.* 41, 3577–3585. doi: 10.3892/ijmm.2018.3573

Zhang, L., Verwer, R. W. H., Lucassen, P. J., Huitinga, I., and Swaab, D. F. (2020). Prefrontal cortex alterations in glia gene expression in schizophrenia with and without suicide. *J. Psychiatr. Res.* 121, 31–38. doi: 10.1016/j.jpsychires.2019.11.002

Conflict of Interest: The authors declare that the research was conducted in the absence of any commercial or financial relationships that could be construed as a potential conflict of interest.

frontiers in Integrative Neuroscience

OPINION
published: 18 September 2020
doi: 10.3389/fnint.2020.00046

Home-Based Transcranial Direct Current Stimulation (tDCS) to Prevent and Treat Symptoms Related to Stress: A Potential Tool to Remediate the Behavioral Consequences of the COVID-19 Isolation Measures?

*Luis Castelo-Branco and Felipe Fregni**

Neuromodulation Center and Center for Clinical Research Learning, Spaulding Rehabilitation Hospital and Harvard Medical School, Boston, MA, United States

Keywords: transcranial direct current stimulation, tDCS, non-invasive brain stimulation, COVID-19, stress, stay-at-home orders, mental health, home therapies

INTRODUCTION

The WHO has recommended self-isolation and social distancing measures for containing the coronavirus 19 (COVID-19) pandemic, and the Centers of Disease Control and Prevention (CDC) and the vast majority of countries have adopted it, with strategies varying in terms of degrees of containment (Wilder-Smith and Freedman, 2020). Despite the worldwide efforts in understanding and combating the disease, many uncertainties remain, including the precise rates of transmission and mortality, not to mention the proper treatment, leading to concerns and confusion regarding the necessary duration of the isolation measures. The possible need to adopt intermittent strategies of social distancing has also been raised, alternating periods of stricter and looser isolation (Kissler et al., 2020) until the discovery of a vaccine or efficient treatment is made.

Social isolation by itself leads to stress and negative mood (Brooks et al., 2020). The uncertainties mentioned above potentiate these effects, particularly in patients with a history of mental health disorders. Social isolation and loneliness are also associated with increased overall mortality (Steptoe et al., 2013), worse cardiovascular, and mental health outcomes (Leigh-Hunt et al., 2017) and cognitive decline (Evans et al., 2019). Furthermore, the recent Covid-19 outbreak has been associated with post-traumatic stress disorder (PTSD) symptoms, which were identified both in medical staff and the general population (Wang et al., 2020).

Numerous studies have demonstrated how non-invasive neuromodulatory techniques such as rTMS and tDCS can help prevent and ameliorate stress, with effects not only on emotion, cognition, and behavior but also on the cardiovascular (Makovac et al., 2017) and autonomic nervous systems (Schestatsky et al., 2013). Although non-invasive, repetitive TMS is expensive and not portable (the only portable option applies a very short train of pulses). Therefore, it is not appropriate during the context of social isolation since patients would have to leave their homes to receive the treatment. On the other hand, tDCS is potentially portable, and its feasibility in home-based settings has been previously studied with promising results regarding its safety and effectiveness (Martens et al., 2018; Brietzke et al., 2020).

Our objective in this short communication is to provide a comment on the potential tDCS application on preventing and treating stress-related symptoms during social isolation, while addressing the feasibility and efficacy of home-based tDCS.

OPEN ACCESS

Edited by:
Weiwen Wang,
Institute of Psychology (CAS), China

Reviewed by:
Philip Tseng,
Taipei Medical University, Taiwan
Ti-Fei Yuan,
Shanghai Jiao Tong University, China

***Correspondence:**
Felipe Fregni
Fregni.Felipe@mgh.harvard.edu

Received: *05 June 2020*
Accepted: *22 July 2020*
Published: *18 September 2020*

Citation:
Castelo-Branco L and Fregni F (2020) Home-Based Transcranial Direct Current Stimulation (tDCS) to Prevent and Treat Symptoms Related to Stress: A Potential Tool to Remediate the Behavioral Consequences of the COVID-19 Isolation Measures? Front. Integr. Neurosci. 14:46. doi: 10.3389/fnint.2020.00046

TDCS AND STRESS: TREATMENT AND PREVENTION OF RELATED SYMPTOMS

There is growing interest and studies investigating the effects of tDCS in animal models of stress and humans with chronic and acute stress. Animal models have shown reversal (Adachi et al., 2012) and prevention (Fregni et al., 2018) of chronic-stress induced pain after tDCS. In addition, tDCS was also able to decrease anxiety-like behaviors in rats submitted to neuropathic pain as a chronic stressor model (Marques Filho et al., 2016).

Interesting results in physiological surrogates of stress, namely heart rate variability (HRV) and salivary cortisol levels after tDCS treatment have been reported. Brunoni et al. (2013) showed that a single session of 1.5 mA anodal tDCS for 3 min targeting the left dorsolateral prefrontal cortex (DLPFC) led to an increase in high-frequency-HRV (HF-HRV) (Cohen's d = 0.77) and a decrease in salivary cortisol level (Cohen's d = 0.78) when compared to sham or cathodal stimulation in healthy individuals, reflecting effects in the autonomic nervous system and the hypothalamic pituitary adrenal (HPA) axis. An increase in parasympathetic and a decrease in sympathetic activity was also demonstrated in athletes by Montenegro et al. (2011) after 2.0 mA anodal stimulation for 20 min targeting the left temporal lobe, with an overall increase in HF-HRV compared to baseline measures (Cohen's d = 0.68).

Direct effects of tDCS on stress symptoms have also been recently published. Individuals such as healthcare workers, which are usually suffering from high levels of stress and even burnout, could benefit from preventive measures. When 1.075 mA tDCS stimulation of the right DLPFC was performed for 6–10 min in healthy individuals exposed to acute stress, there was less impairment of the working memory compared to sham or cathodal stimulation (Cohen's d = 0.62), showing the potential for the prevention of stress-induced mental disorders (Bogdanov and Schwabe, 2016).

On the other hand, patients who already developed psychiatric symptoms related to stress can also benefit from non-invasive brain stimulation. Anodal left DLPFC 1.0 mA tDCS has been shown as well to enhance the working memory when applied for 20 min once a week for 5 weeks in patients with the diagnosis of PTSD undergoing cognitive training programs compared to baseline, although the effects varied between subjects and were dependent on the performance test (Saunders et al., 2015). Another study demonstrated improved extinction-related processes in veterans with warzone-related PTSD when 2.0 mA anodal stimulation for 10 min was combined with fear-extinction therapy. tDCS targeted at the left ventromedial prefrontal cortex (vmPFC) during extinction-consolidation led to lower skin conductance reactivity compared to tDCS applied during extinction-learning (Cohen's d = 0.38) (Van't Wout et al., 2017).

The DLPFC has been the usual cortical target for tDCS to prevent and ameliorate the consequences of psychosocial stress (**Figure 1**). Carnevali et al. (2020) recently postulated that the effects of tDCS may involve both a cognitive control of stress and the autonomic system, involving predominantly parasympathetic (vagal) responses (Carnevali et al., 2020). Further research is needed, however, to determine whether tDCS could prevent the consequences of repeated or persistent exposure to stressful situations such as in the context of social isolation during a pandemic. In addition, the response to anodal 1.0 mA left DLPFC stimulation for 30 min can differ depending on individual anxiety traits (Sarkar et al., 2014), with individuals with high anxiety profiles improving performance in cognitive tests (Cohen's d = 0.82), as well as decreased cortisol levels (Cohen's d = 1.37) compared to sham stimulation, an effect that was not observed in subjects with low anxiety profiles. Therefore, assessing specific psychological traits at baseline could help determine which individuals would benefit more from the effects of tDCS.

Regarding emotional and affective states, tDCS has been well-studied for the treatment of patients with Major Depression, with improvement in depression scores and response rates supported by recent meta-analyses (Cohen's d = 0.74; Odds Ratio 2.44) (Brunoni et al., 2016) and (Hedge's g = 0.37; Odds Ratio 1.63) (Shiozawa et al., 2014). In heathy, non-depressed individuals, one study from Boggio et al. (2009) has shown that 3 min of anodal tDCS to the DLPFC significantly reduced ratings of unpleasantness in subjects exposed to distressing images compared to sham stimulation (Cohen's d = 0.88). Petrocchi et al. (2017) also demonstrated an increase in soothing positive affectivity (Cohen's d = 0.57) and an increase in HRV (Cohen's d = 0.26) after 15 min of 2 mA tDCS over the left temporal lobe compared to sham stimulation. However, other studies found no effect in improving the mood of healthy volunteers. It is worth mentioning that these negative studies explored the effect of a single (Morgan et al., 2014) or less than five sessions (Motohashi et al., 2013) of stimulation, and these very same studies raised the question of whether several consecutive sessions are needed to achieve mood-improving effects in non-depressed subjects. In addition, there have been no studies to our knowledge that applied tDCS as a preventive strategy to prevent future mood reductions.

FEASIBILITY OF HOME-BASED TDCS

It is essential that the home-based tDCS device is specifically designed (Charvet et al., 2015) for this purpose, with safety measures that prevent the incorrect use of the equipment and guarantee the correct placement of the electrodes, since improper use of the device has been associated with skin burns. In order to mitigate such risk, most home-based tDCS devices have pre-programmed the intensity and duration of the stimulation and do not allow the patient to change them (Bikson et al., 2020), while others can be remotely controlled and adjusted by a technician.

Remote supervision using telehealth solutions (Riggs et al., 2018) are paramount to ensure safety and encourage adherence to the stimulation protocols, allowing the researcher to reassure the subject that mild and temporary sensations of tingling, itching, burning, or headache could occur during the stimulation, while also monitoring for unexpected or more severe adverse events, even if unrelated to the stimulation. With the current development of telehealth and ubiquitous use of remote visits, both patients and healthcare providers are becoming increasingly

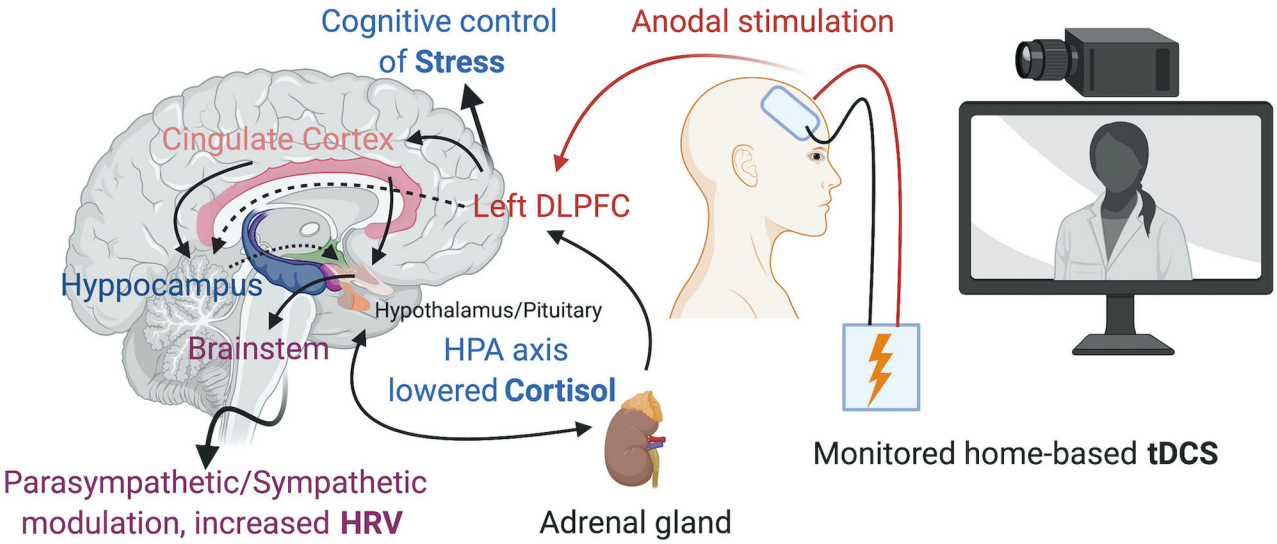

FIGURE 1 | Home-based tDCS over the left DLPFC promoting the cognitive control of Stress, changes in the HPA axis and Parasympathetic/Sympathetic modulation. Created with BioRender.com.

comfortable with this technology. The same data safety and cybersecurity measures used in regular remote clinical work can be used to monitor the use of home-based tDCS, safeguard the patient's privacy, and correct the use of the equipment. In the research setting, the use of electronic informed consent (eIC) is also becoming widely accepted to ensure the proper legal and ethical requirements are met.

Although it is a fairly simple technique with minimal risks associated with the electrical current delivery when done within pre-defined safety parameters, we do not encourage the use of any do-it-yourself stimulation devices. We strongly recommend closely monitoring and supervision, mainly due to the dangers of misuse and overuse.

To date, protocols that have used home-based tDCS have started with an in-person training session, either a home visit from a technician or a visit to the research facility by the subject. This was done to ensure that the individuals understood and properly used it (Kasschau et al., 2016). In the context of stricter social isolation situations such as a quarantine or complete lockdown, future protocols could potentially use solutions with all the instruction and orientation sessions done remotely, but that would require testing for feasibility.

DISCUSSION

Many studies have shown that the effects of tDCS are optimal when combined with behavioral strategies, such as exercise, cognitive training, mindfulness techniques, and Virtual Reality training. In this sense, the remote visit concomitant with the tDCS use would allow both monitoring and the delivery of these other therapies (Wright and Caudill, 2020) through web-based management systems (Chiesa and Serretti, 2009).

Can et al. (2019b) developed an automatic stress detection system that employs machine learning tools and concluded that physiological modalities are more accurate than self-reported perceived stress when analyzing real-world data. With the development of wearable devices and sensors, the assessment of physiological responses to the treatments could become routine (Can et al., 2019a), providing real-world data from patients in their own environment instead of measurements made in the artificial clinical laboratory setting.

It is worth mentioning that other more recent transcranial electrical stimulation techniques, such as alternating current (tACS), pulsed (tPCS), and random-noise (tRNS) use similar devices and therefore could be used at home, although, to the best of our knowledge, they have not been tested in this setting so far. One particular technique with the potential for home-based use that acts on the autonomic nervous system is the vagal nerve stimulation. This neuromodulation modality can be applied non-invasively either by transcutaneous stimulation of the cervical or auricular branches and can be particularly interesting when used in closed-loop systems (Gurel et al., 2020).

Exploring the relationship between non-invasive neuromodulation and the immune system in the context of a viral pandemic, although highly speculative, is also promising. While viral infections often lead to an important dysregulation of immune responses (Qin et al., 2020), neuromodulatory strategies that can down-regulate the excessive inflammation and its detrimental effects (Silverman et al., 2005) could show beneficial effects in the adjuvant treatment and even prevention of infection.

Finally, we believe that, in the context of COVID-19 social isolation, remote supervision could lead to benefits that

are not directly related to the tDCS stimulation, providing support and eventual guidance for the isolated subjects. We understand that, if properly trained to do so, the research personnel, through the screen, could reinforce the importance of maintaining social isolation according to the health authorities.

AUTHOR CONTRIBUTIONS

LC-B: conceptualization and writing—original draft preparation. FF: supervision and writing—reviewing and editing. All authors contributed to the article and approved the submitted version.

REFERENCES

Adachi, L. N. S., Caumo, W., Laste, G., Medeiros, L. F., Rozisky, J. R., De Souza, A., et al. (2012). Reversal of chronic stress-induced pain by transcranial direct current stimulation (tDCS) in an animal model. *Brain Res.* 1489, 17–26. doi: 10.1016/j.brainres.2012.10.009

Bikson, M., Hanlon, C. A., Woods, A. J., Gillick, B. T., Charvet, L., Lamm, C., et al. (2020). Guidelines for TMS/tES clinical services and research through the COVID-19 pandemic. *Brain Stimul.* 13, 1124–1149. doi: 10.1016/j.brs.2020.05.010

Bogdanov, M., and Schwabe, L. (2016). Transcranial stimulation of the dorsolateral prefrontal cortex prevents stress-induced working memory deficits. *J. Neurosci.* 36, 1429–1437. doi: 10.1523/JNEUROSCI.3687-15.2016

Boggio, P. S., Zaghi, S., and Fregni, F. (2009). Modulation of emotions associated with images of human pain using anodal transcranial direct current stimulation (tDCS). *Neuropsychologia* 47, 212–217. doi: 10.1016/j.neuropsychologia.2008.07.022

Brietzke, A. P., Zortea, M., Carvalho, F., Sanches, P. R. S., Silva, D. P. J., Torres, I., et al. (2020). Large treatment effect with extended home-based transcranial direct current stimulation over dorsolateral prefrontal cortex in fibromyalgia: a proof of concept sham-randomized clinical study. *J. Pain* 21, 212–224. doi: 10.1016/j.jpain.2019.06.013

Brooks, S. K., Webster, R. K., Smith, L. E., Woodland, L., Wessely, S., Greenberg, N., et al. (2020). The psychological impact of quarantine and how to reduce it: rapid review of the evidence. *Lancet* 395, 912–920. doi: 10.1016/S0140-6736(20)30460-8

Brunoni, A. R., Moffa, A. H., Fregni, F., Palm, U., Padberg, F., Blumberger, D. M., et al. (2016). Transcranial direct current stimulation for acute major depressive episodes: meta-analysis of individual patient data. *Br. J. Psychiatry* 208, 522–531. doi: 10.1192/bjp.bp.115.164715

Brunoni, A. R., Vanderhasselt, M. A., Boggio, P. S., Fregni, F., Dantas, E. M., Mill, J. G., et al. (2013). Polarity- and valence-dependent effects of prefrontal transcranial direct current stimulation on heart rate variability and salivary cortisol. *Psychoneuroendocrinology* 38, 58–66. doi: 10.1016/j.psyneuen.2012.04.020

Can, Y. S., Arnrich, B., and Ersoy, C. (2019a). Stress detection in daily life scenarios using smart phones and wearable sensors: a survey. *J. Biomed. Inform.* 92:103139. doi: 10.1016/j.jbi.2019.103139

Can, Y. S., Chalabianloo, N., Ekiz, D., and Ersoy, C. (2019b). Continuous stress detection using wearable sensors in real life: algorithmic programming contest case study. *Sensors* 19:1849. doi: 10.3390/s19081849

Carnevali, L., Pattini, E., Sgoifo, A., and Ottaviani, C. (2020). Effects of prefrontal transcranial direct current stimulation on autonomic and neuroendocrine responses to psychosocial stress in healthy humans. *Stress* 23, 26–36. doi: 10.1080/10253890.2019.1625884

Charvet, L. E., Kasschau, M., Datta, A., Knotkova, H., Stevens, M. C., Alonzo, A., et al. (2015). Remotely-supervised transcranial direct current stimulation (tDCS) for clinical trials: guidelines for technology and protocols. *Front. Syst. Neurosci.* 9:26. doi: 10.3389/fnsys.2015.00026

Chiesa, A., and Serretti, A. (2009). Mindfulness-based stress reduction for stress management in healthy people: a review and meta-analysis. *J. Altern. Complem. Med.* 15, 593–600. doi: 10.1089/acm.2008.0495

Evans, I. E., Martyr, A., Collins, R., Brayne, C., and Clare, L. (2019). Social isolation and cognitive function in later life: a systematic review and meta-analysis. *J. Alzheimers Dis.* 70, S119–S144. doi: 10.3233/JAD-180501

Fregni, F., Macedo, I., Spezia-Adachi, L., Scarabelot, V., Laste, G., Souza, A., et al. (2018). Transcranial direct current stimulation (tDCS) prevents chronic stress-induced hyperalgesia in rats. *Brain Stimul.* 11, 299–301. doi: 10.1016/j.brs.2017.11.009

Gurel, N. Z., Wittbrodt, M. T., Jung, H., Ladd, S. L., Shah, A. J., Vaccarino, V., et al. (2020). Automatic detection of target engagement in transcutaneous cervical vagal nerve stimulation for traumatic stress triggers. *IEEE J. Biomed. Health Inform.* 24, 1917–1925. doi: 10.1109/JBHI.2020.2981116

Kasschau, M., Reisner, J., Sherman, K., Bikson, M., Datta, A., and Charvet, L. E. (2016). Transcranial direct current stimulation is feasible for remotely supervised home delivery in multiple sclerosis. *Neuromodulation* 19, 824–831. doi: 10.1111/ner.12430

Kissler, S. M., Tedijanto, C., Goldstein, E., Grad, Y. H., and Lipsitch, M. (2020). Projecting the transmission dynamics of SARS-CoV-2 through the postpandemic period. *Science* 368, 860. doi: 10.1126/science.abb5793

Leigh-Hunt, N., Bagguley, D., Bash, K., Turner, V., Turnbull, S., Valtorta, N., et al. (2017). An overview of systematic reviews on the public health consequences of social isolation and loneliness. *Public Health* 152, 157–171. doi: 10.1016/j.puhe.2017.07.035

Makovac, E., Thayer, J. F., and Ottaviani, C. (2017). A meta-analysis of non-invasive brain stimulation and autonomic functioning: implications for brain-heart pathways to cardiovascular disease. *Neurosci. Biobehav. Rev.* 74, 330–341. doi: 10.1016/j.neubiorev.2016.05.001

Marques Filho, P. R., Vercelino, R., Cioato, S. G., Medeiros, L. F., De Oliveira, C., Scarabelot, V. L., et al. (2016). Transcranial direct current stimulation (tDCS) reverts behavioral alterations and brainstem BDNF level increase induced by neuropathic pain model: Long-lasting effect. *Prog. Neuro Psychopharmacol. Biol. Psychiatry* 64, 44–51. doi: 10.1016/j.pnpbp.2015.06.016

Martens, G., Lejeune, N., O'brien, A. T., Fregni, F., Martial, C., Wannez, S., et al. (2018). Randomized controlled trial of home-based 4-week tDCS in chronic minimally conscious state. *Brain Stimul.* 11, 982–990. doi: 10.1016/j.brs.2018.04.021

Montenegro, R. A., Farinatti, P. D. T. V., Fontes, E. B., Da Silva Soares, P. P., Da Cunha, F. A., Gurgel, J. L., et al. (2011). Transcranial direct current stimulation influences the cardiac autonomic nervous control. *Neurosci. Lett.* 497, 32–36. doi: 10.1016/j.neulet.2011.04.019

Morgan, H. M., Davis, N. J., and Bracewell, R. M. (2014). Does transcranial direct current stimulation to prefrontal cortex affect mood and emotional memory retrieval in healthy individuals? *PLoS ONE* 9:e92162. doi: 10.1371/journal.pone.0092162

Motohashi, N., Yamaguchi, M., Fujii, T., and Kitahara, Y. (2013). Mood and cognitive function following repeated transcranial direct current stimulation in healthy volunteers: a preliminary report. *Neurosci. Res.* 77, 64–69. doi: 10.1016/j.neures.2013.06.001

Petrocchi, N., Piccirillo, G., Fiorucci, C., Moscucci, F., Di Iorio, C., Mastropietri, F., et al. (2017). Transcranial direct current stimulation enhances soothing positive affect and vagal tone. *Neuropsychologia* 96, 256–261. doi: 10.1016/j.neuropsychologia.2017.01.028

Qin, C., Zhou, L., Hu, Z., Zhang, S., Yang, S., Tao, Y., et al. (2020). Dysregulation of immune response in patients with Coronavirus 2019 (COVID-19) in Wuhan, China. *Clin. Infect. Dis.* 71, 762–768. doi: 10.1093/cid/ciaa248

Riggs, A., Patel, V., Paneri, B., Portenoy, R. K., Bikson, M., and Knotkova, H. (2018). At-home transcranial direct current stimulation (tDCS) with telehealth support for symptom control in chronically-ill patients with multiple symptoms. *Front. Behav. Neurosci.* 12:93. doi: 10.3389/fnbeh.2018.00093

Sarkar, A., Dowker, A., and Kadosh, R. C. (2014). Cognitive enhancement or cognitive cost: trait-specific outcomes of brain stimulation in the case of mathematics anxiety. *J. Neurosci.* 34, 16605–16610. doi: 10.1523/JNEUROSCI.3129-14.2014

Saunders, N., Downham, R., Turman, B., Kropotov, J., Clark, R., Yumash, R., et al. (2015). Working memory training with tDCS improves behavioral and neurophysiological symptoms in pilot group with post-traumatic stress disorder (PTSD) and with poor working memory. *Neurocase* 21, 271–278. doi: 10.1080/13554794.2014.890727

Schestatsky, P., Simis, M., Freeman, R., Pascual-Leone, A., and Fregni, F. (2013). Non-invasive brain stimulation and the autonomic nervous system. *Clin. Neurophysiol.* 124, 1716–1728. doi: 10.1016/j.clinph.2013.03.020

Shiozawa, P., Fregni, F., Benseñor, I. M., Lotufo, P. A., Berlim, M. T., Daskalakis, J. Z., et al. (2014). Transcranial direct current stimulation for major depression: an updated systematic review and meta-analysis. *Int. J. Neuropsychopharmacol.* 17, 1443–1452. doi: 10.1017/S1461145714000418

Silverman, M. N., Pearce, B. D., Biron, C. A., and Miller, A. H. (2005). Immune modulation of the hypothalamic-pituitary-adrenal (HPA) axis during viral infection. *Viral Immunol.* 18, 41–78. doi: 10.1089/vim.2005.18.41

Steptoe, A., Shankar, A., Demakakos, P., and Wardle, J. (2013). Social isolation, loneliness, and all-cause mortality in older men and women. *Proc. Natl Acad. Sci.U.S.A.* 110, 5797–5801. doi: 10.1073/pnas.1219686110

Van't Wout, M., Longo, S. M., Reddy, M. K., Philip, N. S., Bowker, M. T., and Greenberg, B. D. (2017). Transcranial direct current stimulation may modulate extinction memory in posttraumatic stress disorder. *Brain Behav.* 7:e00681. doi: 10.1002/brb3.681

Wang, C., Pan, R., Wan, X., Tan, Y., Xu, L., Mcintyre, R. S., et al. (2020). A longitudinal study on the mental health of general population during the COVID-19 epidemic in China. *Brain Behav. Immun.* 87, 40–48. doi: 10.1016/j.bbi.2020.04.028

Wilder-Smith, A., and Freedman, D. O. (2020). Isolation, quarantine, social distancing and community containment: pivotal role for old-style public health measures in the novel coronavirus (2019-nCoV) outbreak. *J. Travel Med.* 27:taaa020. doi: 10.1093/jtm/taaa020

Wright, J. H., and Caudill, R. (2020). Remote treatment delivery in response to the COVID-19 pandemic. *Psychother. Psychosom.* 89:1. doi: 10.1159/000507376

Conflict of Interest: The authors declare that the research was conducted in the absence of any commercial or financial relationships that could be construed as a potential conflict of interest.

frontiers in Psychiatry

STUDY PROTOCOL
published: 03 November 2020
doi: 10.3389/fpsyt.2020.563058

Transcranial Direct Current Stimulation as an Add-on Treatment to Cognitive-Behavior Therapy in First Episode Drug-Naïve Major Depression Patients: The ESAP Study Protocol

Sandra Carvalho[1,2]*, *Óscar F. Gonçalves*[1,2,3], *André R. Brunoni*[4], *Ana Fernandes-Gonçalves*[5], *Felipe Fregni*[2] and *Jorge Leite*[2,6]

[1] Psychological Neuroscience Laboratory, CIPsi, School of Psychology, University of Minho, Braga, Portugal, [2] Department of Physical Medicine and Rehabilitation, Spaulding Neuromodulation Center, Spaulding Rehabilitation Hospital, Massachusetts General Hospital and Harvard Medical School, Boston, MA, United States, [3] Proaction Laboratory, Faculty of Psychology and Educational Sciences, University of Coimbra, Coimbra, Portugal, [4] Department and Institute of Psychiatry, Service of Interdisciplinary Neuromodulation, Laboratory of Neurosciences (LIM-27), Interdisciplinary Center for Applied Neuromodulation University Hospital, University of São Paulo, São Paulo, Brazil, [5] Department of Psychiatry, CUF Porto Hospital, Porto, Portugal, [6] Univ Portucalense, Portucalense Institute for Human Development–INPP, Porto, Portugal

OPEN ACCESS

Edited by:
Bart Ellenbroek,
Victoria University of Wellington, New Zealand

Reviewed by:
Tianmei Si,
Peking University Sixth Hospital, China
Jari Lahti,
University of Helsinki, Finland

***Correspondence:**
Sandra Carvalho
sandrarc@psi.uminho.pt

Specialty section:
This article was submitted to Molecular Psychiatry, a section of the journal Frontiers in Psychiatry

Received: *15 June 2020*
Accepted: *01 October 2020*
Published: *03 November 2020*

Citation:
Carvalho S, Gonçalves ÓF, Brunoni AR, Fernandes-Gonçalves A, Fregni F and Leite J (2020) Transcranial Direct Current Stimulation as an Add-on Treatment to Cognitive-Behavior Therapy in First Episode Drug-Naïve Major Depression Patients: The ESAP Study Protocol. Front. Psychiatry 11:563058. doi: 10.3389/fpsyt.2020.563058

Background: Major Depressive Disorder (MDD) affects more than 264 million people worldwide. Current treatments include the use of psychotherapy and/or drugs, however ∼30% of patients either do not respond to these treatments, or do not tolerate the side effects associated to the use of pharmacological interventions. Thus, it is important to study non-pharmacological interventions targeting mechanisms not directly involved with the regulation of neurotransmitters. Several studies demonstrated that transcranial Direct Current Stimulation (tDCS) can be effective for symptoms relief in MDD. However, tDCS seems to have a better effect when used as an add-on treatment to other interventions.

Methods/Design: This is a study protocol for a parallel, randomized, triple-blind, sham-controlled clinical trial in which a total of 90 drug-naïve, first-episode MDD patients (45 per arm) will be randomized to one of two groups to receive a 6-weeks of CBT combined with either active or sham tDCS to the dorsolateral prefrontal cortex (DLPFC). The primary outcome will depressive symptoms improvement as assessed by the Montgomery-Asberg Depression Rating Scale (MADRS) at 6-weeks. The secondary aim is to test whether CBT combined with tDCS can engage the proposed mechanistic target of restoring the prefrontal imbalance and connectivity through the bilateral modulation of the DLPFC, as assessed by changes over resting-state and emotional task eliciting EEG.

Discussion: This study evaluates the synergetic clinical effects of CBT and tDCS in the first episode, drug-naïve, patients with MDD. First episode MDD patients provide an interesting opportunity, as their brains were not changed by the pharmacological treatments, by the time course, or by the recurrence of MDD episodes (and other comorbidities).

Trial Registration: This study is registered with the United States National Library of Medicine Clinical Trials Registry (NCT03548545). Registered June 7, 2018, clinicaltrials.gov/ct2/show/NCT03548545. Protocol Version 1.

Keywords: MDD (Major Depressive Disorder), study protocol, drug-naïve, tDCS (transcranial direct current stimulation), CBT (cognitive-behavioral therapy)

BACKGROUND

Major Depressive Disorder(MDD) is widely recognized as a staggering global healthcare challenge, as well as a potentially lethal illness (1). The worldwide prevalence of Depression is about 3.4% [2–6%], and mild forms of depression are the most prevalent−13%, as compared to 4% for moderate forms and 5.1 % for severe forms of depression (2). The prevalence in females is about 4.1% and about 2.7% in males (2). Overall, MDD is thought to affect 264 million people worldwide, thus ranking second in the most common causes of disability with prospects of becoming the first by 2040 (3).

The current standard care for MDD involves the use of psychotherapy, antidepressant medication, or a combination of both. Despite the costs involved in these interventions, the efficacy of such treatments may have been overestimated, with recent data suggesting that remission rates can be as low as 23% depending on the self-report scale used (4). Furthermore, 30% of patients suffering from MDD still exhibit depressive symptoms despite the appropriate psychological and pharmacological treatments (5). In order to overcome this, several treatments are frequently combined, usually by the use of drug augmentation and/or combination of different drugs, which often increases the risk of adverse effects (6). Thus, the development of effective treatment alternatives for MDD, which includes non-pharmacological interventions targeting mechanisms not directly involved with the regulation of neurotransmitters, is an urgent research priority. However, in order to do so, it is important to understand the underlying neural mechanisms involved in MDD.

Evidence coming from several electroencephalography (EEG) (7–9), neuroimaging (10, 11), and neuromodulation (12–15) studies showed that the dorsolateral prefrontal cortex (DLPFC) is as an important area of dysfunction in depression, mainly due its left hypo and right hyper-functioning. This inter-hemispheric imbalance over the DLPFC has been shown to be an indicator of lifetime MDD, or in conjunction with depressive self-schema (i.e., an interconnected negative internal representation of the self that has been associated to the onset and maintenance of depressive state (16, 17) to be a predictor of a first prospective MDD episode (18). Nevertheless, some studies failed to show the link between decreased left frontal activation and depression (19).

Transcranial direct current stimulation (tDCS) is a non-invasive method of brain stimulation that is capable of depolarizing or hyperpolarizing the neural membrane and as such, it has been used in people suffering from depression, by placing the anode (excitatory) over the left and the cathode (inhibitory) over the right DLPFC, or by placing the anode over the left DLPFC and the cathode over the right supra-orbital region.

For instance, in one study, 64 MDD patients were randomized to 15 sessions of 2 mA tDCS over 3 weeks, and tDCS was shown to be able to decreased MDD symptoms (20). However, in another study, not only active tDCS was superior to sham but also the combination of tDCS with sertraline was significantly more effective in reducing depressive symptoms than either treatment alone (21). Although tDCS *per se* showed promising results in treating MDD, the previous trial highlights that the effects of tDCS can be enhanced by combining it with other interventions. Overall, tDCS seems to decrease MDD symptoms by a pooled effect size of 0.36 (22). Moreover, according to a recent individual patient data meta-analysis, tDCS seems to be less effective in high-resistant patients, suggesting that tDCS may be a promising add-on therapy to therapies such as the cognitive behavioral therapy (CBT) (23) or cognitive control therapy (24, 25).

CBT is an empirically validated therapy for the treatment of MDD. Several studies have demonstrated the efficacy of CTB alone (26, 27) or as adjuvant to medication (28–30) in acute depression. Another advantage of CBT over anti-depressant drugs is its long-term effects, namely protecting against relapses and recurrences after active treatments has ended (27, 31, 32). Additionally, CBT is a well-established therapy that can restore or normalize abnormal brain activity, namely prefrontal alpha activity (33). Namely, an increase in left frontal brain activity after CBT in individuals with anxiety and depression.

It is important to highlight that MDD seems to induce profound changes in the brain, namely structural alterations in fronto-cingulate-striatal circuits (34–36). However, and somewhat surprisingly, first episode MDD patients have not been extensively studied with tDCS (37, 38). These first episode MDD patients provide an interesting opportunity, as their brains were not changed by the pharmacological treatments, by the time course, or by the recurrence of MDD episodes (and other comorbidities).

PURPOSE, PRIMARY AND SECONDARY OUTCOMES

Therefore, we propose to study the clinical and mechanistic effects of the combination of two well-studied interventions—CBT and tDCS—for the treatment of MDD in drug naïve first episode patients. The primary outcome will be the clinical effects (severity of depression/mood amelioration), as measured by the Montgomery-Asberg Depression Rating Scale (MADRS). Secondary outcomes will be resting state and emotional task eliciting EEG, which will be useful simultaneously to understand

the neural effects of the intervention, as well as potential response predictors for future trials.

RESEARCH QUESTION, AIMS, HYPOTHESIS

By combining two interventions that showed promising results in MDD (CBT and tDCS), we aim to investigate the clinical and underlying neurophysiological effects in first-episode drug naïve MDD patients. The main research question underlying this proposal is whether tDCS as add-on therapy to CBT in drug naïve, first-episode MDD patients could produce greater significant clinical improvements, as measured by the MADRS, when compared to CBT alone. We hypothesize that the combination of these therapies will produce a synergetic effect in the brain, potentiating the effects of CBT and decreasing the depressive symptomatology as assessed by the MADRS.

A secondary aim will be to perform the dose calculation (number of sessions) required to induce a clinically significant effect (50% decrease in the MADRS score). The underlying hypothesis is that the combination of tDCS with CBT will require a lesser number of sessions in order to elicit this clinical meaningful effect.

The second major scientific question is whether these clinical improvements will be correlated with the rebalancing of the inter-hemispheric asymmetry of EEG alpha activity toward the left hemisphere, as assessed by resting-state and emotional task eliciting-EEG. Here, the hypothesis is that both interventions (combined and alone) will reduce the inter-hemispheric alpha imbalance, as indexed by EEG power; however, that reduction will be more pronounced in the group that received the add-on intervention, as compared to CBT alone.

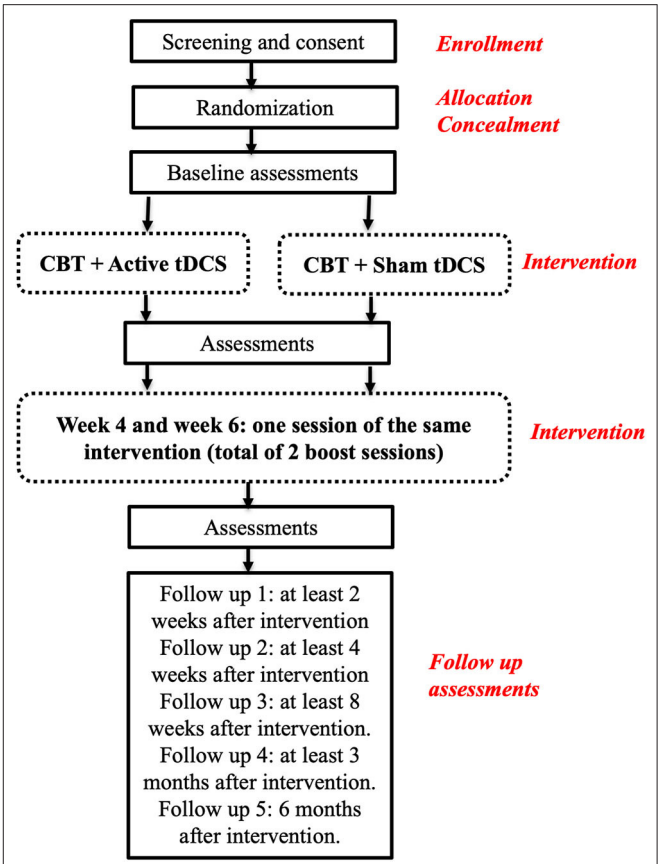

FIGURE 1 | Overview of the Study design (tDCS, transcranial Direct Current Stimulation; CBT, Cognitive Behavioral Therapy).

METHODS

Trial Design, Setting and Registration

This is a parallel, randomized, triple-blind, sham controlled clinical protocol in which a total of 90 drug-naïve, first-episode MDD outpatients (45 per arm) will be randomized to one of two groups: active bilateral tDCS over the DLPFC combined with CBT or sham tDCS combined with CBT (**Figure 1**).

Patients will complete a 6-weeks treatment that involves 18 tDCS sessions (active or sham) and 12 CBT sessions. For the first 2 weeks of intervention, they will receive 10 daily sessions of tDCS (from Monday to Friday) and 4 sessions of CBT (combined at same time with tDCS for the first 30 min, on Monday and on Friday). They will then receive two booster sessions of tDCS combined with CBT will be on weeks 3, 4, 5, and 6 (**Figure 2B**).

This study will then be organized in 3 distinct phases. Phase 1: Recruitment and baseline assessments; Phase 2: Intervention; Phase 3: Post-treatment assessment and 6-month follow-up (**Figure 1**). Once eligibility is determined and consent provided, patients will be randomly assigned to one of the two groups in a 1:1 allocation ratio, by the means of a list generated by an automatic web-based randomization program.

After an initial baseline assessment (visit 1) (for more details see task 1), patients will receive 10 consecutive sessions (in two weeks) of active or sham tDCS (2 mA, 30 min), and 6 sessions of CBT every other day (3 CBT sessions per week). Patients may fail 1 or 2 sessions of tDCS and/or CBT; and in that case, they will have the opportunity to receive the missing session (s) in the following week. The primary outcome will be assessed by week 2, using MADRS. Other assessments will be also performed by week 2, such as EEG, and other clinical measures (see **Table 1**). By week 4 and 6, patients will receive additional booster sessions of the same intervention (active or sham tDCS followed by CBT). Patients will perform the same assessments on week 6 (**Figures 2A,B**). tDCS sessions will follow the same design previously tested by two members of our group, that showed significant clinical effects of tDCS alone, and tDCS combined with sertraline in moderate to severe MDD (21).

Structured CBT sessions will follow the NICE guidelines from the National Institute for Health and Care Excellence (39). Patients will receive a total of 12 CBT sessions administered biweekly for 6 weeks. Mood, will be evaluated at the end of each week, as to perform the dose calculation (i.e., number of sessions) required to induce a clinical significant effect of at least 50% decrease in the MADRS scores.

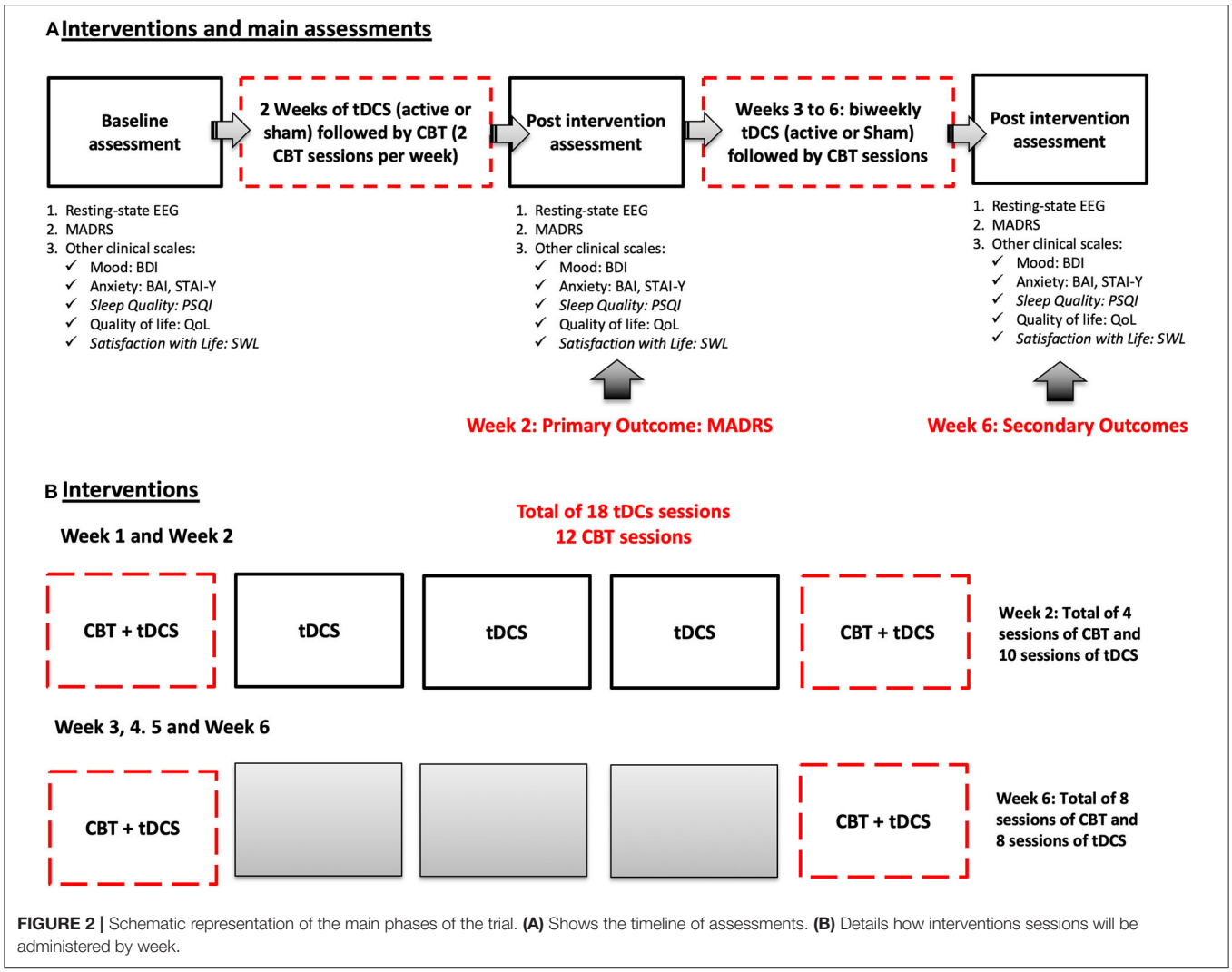

FIGURE 2 | Schematic representation of the main phases of the trial. **(A)** Shows the timeline of assessments. **(B)** Details how interventions sessions will be administered by week.

In addition to the primary outcome measure (MADRS), secondary outcome measures will be clinical response as measured by scores on the 17-item Hamilton Depression Rating Scale, Beck Depression Inventory (BDI), Beck Anxiety Inventory (BAI), clinician-rated Clinical Global Impression–Severity of Illness scale, and quality of life (QoL). These scales will be used at baseline, week 2, 4, 6, and follow-ups (up to 6-month follow up).

Resting-state EGG assessments will be performed on baseline session, on weeks 2 and 6. These assessments will allow us to assess the neural effects of these interventions in the brain.

The Standard Protocol Items: recommendations for Interventional Trials (SPIRIT) statement were used as a framework for developing the study methodology for this trial (40, 41).

Participants

A total of 90 drug-naïve, first-episode MDD outpatients (45 per arm) will be randomized to receive either CBT combined with active bilateral tDCS over the DLPFC or CBT combined with sham tDCS.

Eligibility Criteria

Participants will be included in this study if they meet the following criteria: 1) Aged 18–75 years; 2) Unipolar, nonpsychotic MDD (DSM-V); 3) Score in the MADRS 7 and above (mild, moderate, and severe depression); 4) Low risk of suicide, as evaluated during the clinical interview and through the Scale for Suicidal Ideation [Mild to Moderate SIS; (42)]; and 5) Able to sign informed consent.

Potential participants meeting any of the following criteria will be excluded: 1) any contraindication to receive tDCS (such as metal in the head, implanted brain medical devices); 2) any significant or unstable neurologic or psychiatric disorder other than MDD, such as epilepsy, Parkinson's Disease, Dementias, eating disorders, OCD Spectrum disorders, among others); 3) history of substance abuse within the past 6-months, 4) Any personality disorders; or 5) any severe life-threatening disorders or concurrent medical condition likely to worsen

patient's functional status in next 6-months such as; cancer, or severe heart, kidney, or liver diseases. Participants with reported high risk of suicide will be excluded from the study and will be recommended to receive support from an experience and licensed psychologist/psychiatrist. Information about local and national institutions that provide support to cope with suicidal behaviors and though will be provided.

A screening questionnaire that addresses the specific inclusion and exclusion criteria will be applied to each participant prior to the SCID-5 interview and will help to screen out participants. Diagnosis will be performed using the Structured Clinical Interview for DSM-5 (SCID-5) (43, 44), a widely used semi structured clinical interview designed to evaluate psychopathology, following the categories in the DSM 5 (Diagnostic and Statistical Manual of Mental Disorders, Fifth Edition) for the clinical use and clinical research. Potential participants will also answer the tDCS eligibility questionnaire and the SIS to evaluate the likelihood of suicide attempt. Patients with high likelihood of suicide attempt will be not included in our study and will be recommend for psychological and/or psychiatric intervention.

Description of the Interventions

Cognitive-Behavioral Therapy (CBT)

CBT will be performed following the structure proposed by Beck et al. (17, 45). Each session will last 60 min and will be designed individually for each patient, according to the severity of Depression—including behavioral activation and problem-solving techniques. A licensed and trained practitioner will be responsible for facilitating the self-help programme and for reviewing progresses and outcomes during psychotherapy sessions. A senior clinical psychologist with extensive experience in CBT in patients with depression will supervise the clinical work. A clinical meeting will be hosted weekly in order to perform quality assurance of the therapeutic process.

Transcranial Direct Current Stimulation (tDCS)

tDCS will be delivered by an Eldith DC Stimulator Plus (Neuroconn, Germany), using 25 cm^2 saline-soaked electrode sponges. Anode will be placed over the left (F3) and cathode over the right DLPFC (F4). For the active tDCS, participants will receive 2 mA (current density = 0.80 A/m^2; with 15/15 s ramp/ramp down) for 30 min/d. For sham tDCS, patients will receive 15 s of 2 mA intensity, and 15/15 s ramp in and ramp down, with the same montage of electrodes; however, the device will be turned off after 45 s of active stimulation. Each tDCS session will last about 40 min: 30 min of stimulation and 10-min of set up. tDCS sessions will be performed by a research assistant, not involved in the CBT sessions.

Description of the Assessments

These instruments will be used at baseline, after the first 2 weeks of intervention, at the end of the 5-weeks of biweekly sessions and follow-up visits (up to 2 months after the intervention period) as detailed in the table below. Please see **Table 1** for the complete assessments timetable.

Outcomes

Primary Outcome

For the depression assessment, we will use the Montgomery-Asberg Depression Scale (MADRS) as primary outcomes. Criteria for the use of this clinical scale will be the same as we previously used in Brunoni et al. (21). Secondary outcomes will include also the clinical response (categorical variable, defined as $>$ 50% reduction of the baseline MADRS score), clinical remission (categorical variable, defined as a MADRS scores $\leq$10), and scores on the BDI.

Secondary Outcomes

Resting state EEG and task-elicited prefrontal EEG alpha asymmetry—Resting state EEG screening will be carried out before the intervention (baseline), and in the end of each week of intervention. Each screening will comprise a resting state EEG (3 min eyes open and 3 min eyes closed) and a task-related EEG data collection. The task-related screening will last about 3-min in an open-eyes active state. For this task, we will use a facial emotion task, with approach and avoidance facial expressions, similar to the task used by Stewart and colleagues

EEG will be acquired using 20 channel Starstim (Neuroelectrics, Barcelona, Spain), following the 10/20 system, in a continuous mode at a digitization rate of 500 Hz, with a bandpass filter of 0.01–100 Hz. Electrode impedances will be kept below 5 kΩ and EOG will be recorded from two additional bipolar channels. EEG data will be segmented into 1.5–3 s epochs centered on subject's responses (at least 50 epochs) using EEGlab.

Sample Size Calculation

For the sample size calculation, we assume an effect size(d) of 0.66 [upper limit for the 95% CI of the pooled effect size of tDCS on MDD (22) that for a two-side α of 0.05 and a power of 80%, requires a total of 76 patients (38 per group). We increased the sample size by 15% to 45 per group to account for unexpected factors. This sample size will be adequate to detect this magnitude of effect.

Recruitment

The enrollment of patients will be performed mainly from our Clinical Service at the School of Psychology, and by referral from Primary Care Physicians. After initial referral, potential patients with first episode MDD as primary diagnosis, will undergo the general inclusion and exclusion criteria check list in order to assess their potential eligibility.

We will also use social media (such as the Lab Facebook page), as well as flyers posted in specific spaces such as clinical settings (hospital, clinics), Universities, etc. The first screening will be performed by a research assistant (with a clinical Psychology degree) and the full assessment of the patient will be done by a clinician specialized in MDD (blinded to the study arm).

Randomization

Once eligibility and consent have been approved and obtained, randomization will occur using the randomized list generated by an automatic web-based randomization program. Patients

TABLE 1 | Summary and timeline of assessments.

	Consent and Screening	Assessment pre-intervention	EEG pre-intervention	Interventions Session and tDCS	Assessment 15 days	EEG 15 days	Interventions Session and tDCS	Assessment post-intervention	EEG post-intervention	Follow-ups
				Daily Sessions			*Bi-weekly sessions*			*15 day, 1, 2, 3, and 5 months*
	Email / Visit 1	**Visit 1**	**Visit 2**	**Visit 3-12**	**Visit 13**		**Visit 14-21**	**Visit 22**		**Visit 24 – 27**
Approximate visit time	***1 h 30 min***	***30 min***	***1 h***	***50 min***	***30 min***		***50 min***	***30 min***		***30 min***
PRESCREENING FOR ELIGIBILITY, CONSENTING, AND CLINICAL INTERVIEW										
Pre-screening questionnaires (inclusion and exclusion criteria)	X									
Consent Informed (2 copies)	X									
Questionnaire eligibility for the study	X									
Questionnaire eligibility to tDCS	X									
Questionnaire eligibility to EEG	X									
Demographics and medical questionnaire		X								
The structured clinical interview for DSM-5 (SCID-V)		X								
PRIMARY AND SECONDARY OUTCOME ASSESSMENTS										
The satisfaction with life scale (SWL)		X			X			X		X
The pittsburgh sleep quality index (PSQI)		X			X			X		X
State-trait anxiety inventory (STAI-Y)		X			X			X		X
Beck anxiety inventory (BAI)		X			X			X		X
Beck's depression inventory (BDI)		X			X			X		X
Montgomery-asberg depression rating scale (MADRS)		X			X			X		X
Blinding questionnaire								X		
Visual analog scales (VAS)—pre and post				X			X			

will be randomly assigned to one of the two groups in a 1:1 allocation ratio. Randomization order will be kept in sealed envelopes; therefore, patients will get their assignment according to the order of entrance in the study. This will also ensure that all patients and all other investigators are kept blind to this assignment for the duration of the study (allocation concealment) (see **Figure 1**, for study overview).

The randomization procedures described above will be followed for assignment to treatment groups. Following initial screening, during participant enrollment, a research associate will assign them to their randomly generated treatment group, keeping all patients and all other investigators blind to this assignment for the duration of the study.

Blinding Procedure and Assessment

Participants, the psychologists performing the CBT, the ones performing the assessments, as well the statistician will remain blinded to the tDCS condition up to the end of the clinical trial, ensuring a triple blind design. Researchers applying tDCS will not be blinded. If a serious adverse event occurs, the Principal Investigator (PI) will be responsible for removing the blinding and notify the Ethics Committee within 24 h.

Blinding assessment will be performed to both participants and researchers who assessed the outcomes.

Assessments

Eligibility and tDCS Assessments

Questionnaire to assess eligibility to participate in the study: this questionnaire aims to evaluate inclusion and exclusion criteria to participate in the study. It includes specific questions about neurologic and psychiatric history, history of head injuries, drugs use, and/or abuse, history of treatments, etc.

Side Effects Questionnaire: At each stimulation session, patients will complete a questionnaire to evaluate potential adverse effects of tDCS (tingling, burning sensation, headache, neck pain, mood alterations). If any side effects are reported, the degree of relatedness to the intervention will be assessed on a 5-point scale. This type of adverse events questionnaire has been used frequently in our previous tDCS studies (46–52) including in patients with MDD. In order to further control for changes in suicidal thoughts, we will add a specific question for suicide that can be follow-up with the SSI, if scores are equal to or >3.

The Structured Clinical Interview for DSM 5 (SCID 5): this is a semi-structured clinical interview (the clinician version) that guides the clinician step-by-step through the DSM-5 diagnosis process. This interview will be essential to confirm the diagnosis of first episode MDD and to evaluate for possible comorbid psychiatric disorders (43).

Scale for suicide ideation (SSI): this is a 19-item scale that aims to quantify and assess suicidal intention (42). Patients scoring SSI≥6 will not be enrolled in the study (53).

tDCS blinding questionnaire: After the treatment has ended, patients will complete a questionnaire to determine if our blinding methods were effective. We are using a 30 s sham montage, just as we use in our other trials, keeping the device on the subject for the duration of the session. The tDCS blinding questionnaire is organized in two main questions: 1. Please answer the questions to the best of your ability: 1.1 Did you receive: Sham Stimulation (tDCS) or Active Stimulation (tDCS); 1.2 Please, rate how confident you feel in your answer (please check one), from 1 (not confident at all), 2, 3 (somewhat confident), 4, to 5 (completely confident).

Demographic and Clinical Assessments

Demographics information: We will record information about the demographic characteristics of the study population such as age, gender, race, level of education, and social status.

Medication Use Log: Medication use information will be obtained at enrollment and updated on a weekly basis, by means of a Medication Log. Participants will record their current medications and dosages weekly, until completion of the study. Medication diaries are commonly used to record changes in medication use during the study period. We will also use the Antidepressant History Treatment Form (ATHF) to assess treatment refractoriness.

Montgomery-Asberg Depression Scale (MADRS): For the depression improvement assessments, we will use the MADRS for the primary outcome. This is widely used scale for the measurement of severity of depressive symptoms in patients with MDD. The scale is divided into 10 items, each scored on a 0 to 6-point ordinal scale (54). The MADRS will be administered according to a structured interview procedure that has been empirically found to result in high inter-rater reliability scores.

Beck Depression Inventory (BDI): This self-report inventory consists of 21 multiple-choice questions and is a widely used method to classify depression severity (55). It assesses for the presence of several symptoms related to depression, such as irritability, hopelessness and decreased cognitive performance. Physical symptoms such as weight loss and fatigue are also included. The total time required to complete this inventory is 5 to 10 min.

Quality of Life Assessment (Short version of SF-36): The short version of the SF-36 health survey is used as a measurement of quality of life. It provides a profile of functional health and well-being scores. It is also used as a psychometrical index of physical and mental health (56).

Satisfaction with Life (SWL)—is a short and rapid 7-point Likert scale that measures life satisfaction in the perspective of subjective well-being. Scores in SWL have been positively correlated with measures of mental health and also predictive of future maladaptive behaviors such as suicide attempts (57, 58).

The Pittsburgh Sleep Quality Index (PSQI): a 19-item, self-report measure to evaluate overall sleep quality, primarily designed to evaluate sleep disturbance in patients with psychiatric disorders. The PSQI evaluates sleep quality in 7 categories: subjective sleep quality, sleep latency, sleep duration, habitual sleep efficiency, sleep disturbances, use of sleep medication, and daytime sleep dysfunction (59, 60).

State-Trait Anxiety Inventory (STAI-Y) – a self-report measure is organized in two subscales: State Anxiety Scale (S-Anxiety) wish measures the current ("right now") presence and severity (state) of anxiety; and the Trait Anxiety Scale (T-Anxiety) which measures the general propensity to be anxious (trait). This

measures focus on several domains that characterizes anxiety, such as subjective feelings, and levels of arousal (activations of the autonomic nervous systems). The trait subscale evaluates the more stable aspects of anxiety ("anxiety proneness"), such for instance worry, confidence and security (61).

Beck Anxiety Inventory (BAI): is a 21-item measure of anxiety focusing on somatic symptoms of anxiety. Each item is descriptive of somatic, subjective or panic-related symptoms of anxiety. Administration of BAI takes between 5 to 10 min. Since BAI focus on a "pure" measure of anxiety such as nervousness, dizziness, inability to relax, etc.), it helps discriminating between depression and anxiety (62, 63).

Data Management and Access to Data

Data forms and questionnaires will be coded in a standardized manner, and double-entered in a protected excel sheet. Personal information and all data collect will be kept in locked cabinets that only the principal investigator will have access. A key to access these cabinets will be kept in a safe place with limited access. Only researchers involved in the study and any public health and safety authorities will have access to the data collected in the study. Any information linking data back to the participant will be discarded to ensure that the data are truly anonymous. Data destruction will be conducted 5 years after the study has ended. Data sharing will only be possible after an agreement. The data will be stored and managed following the GDPR in the EU. According to national regulations and the Ethics Committee approval, no Data Monitoring Committee (DMC) will accompany this study.

Statistical Analysis

Primary Outcome

A mixed model ANOVAs will be used to assess the clinical effects for primary outcome measure (MADRS), with intervention as between subject factor (active vs. sham tDCS), and time as within subject factor (weeks 2, 4, 8, 12, and 6 months). If there are significant baseline differences across the groups, those covariates will be included in the analysis (such as severity, anxiety, and quality of life). If significant main effects and/or interactions arise from the main analysis, *post-hoc* analysis corrected for multiple comparisons will be performed. If our hypothesis of prefrontal inter-hemispheric imbalance (as assessed by alpha power EEG) is confirmed, we will then conduct correlation analysis in order to assess whether these brain signatures correlate to long-term clinical effects in MDD.

Secondary Outcomes

EEG Analysis

To evaluate the degree of coupling between electrode pairs, we will use Magnitude Square Coherence as a pairwise connectivity measurement. For power spectrum, band power, and intraband mean and median analysis of the EEG frequency ranges, we will use the Fast Fourier transformation analysis, which will allow us to determine and measure the amplitude of the predominant EEG frequency, and properties in the time and frequency domains. For these two EEG analysis, we will define the following frequency bands: delta (1–4 Hz), theta (4–8 Hz), alpha (8–13 Hz), and beta (13–30 Hz) and four frequency sub-bands: low-alpha (9-10 Hz), high-alpha (10-12 Hz), low-beta (13-20 Hz), and high-beta (20-30 Hz), which can be obtained by decomposing the raw signal being generated in different areas of the brain.

Independent Component Analysis (ICA) will be used for artifact rejection. EEG changes during task will be assessed via task-related power (TRP)–i.e., TRP at a given electrode will be obtained by subtracting (log-transformed) power during a pre-stimulus reference interval from (log-transformed) power during the task. Power estimates will be obtained by squaring filtered EEG signals and then band power values will be averaged for both the pre-stimulus reference period and the task intervals. Degree of coupling between electrode pairs, will be assessed by using Magnitude Square Coherence as a pair-wise connectivity measurement.

Ethics and Dissemination

The trial is registered with the U.S. National Library of Medicine Clinical Trials Registry: NCT03548545 (ClinicalTrials.gov) and is approved by the local ethics committee—*Subcomissão de Ética para as Ciências da Vida e da Saúde (SECVS)* – SECVS 174/2017.

Confidentiality

All participants will be given subject identification codes composed by letters and numbers to which all the data will be linked. The file records that connect each participant to their identification number will be securely kept on University servers during the entire period of the study, and up to 5 years the study has ended.

Dissemination Policy

Results of this study will be published in peer reviewed journals, and will be disseminated in national and international conferences and in social media. In any of the dissemination procedures, subjects will not be identified or notified about the event.

DISCUSSION

The current study describes a protocol for a parallel randomized, triple-blind, sham controlled clinical trial to test the synergetic clinical and electrophysiology effects of combining cognitive-behavioral therapy with transcranial direct current stimulation in drug-naïve, first-episode MDD patients.

By combining two therapies that have shown promising results in patients with MDD, we expect that the group that received CBT combined with active tDCS will have a greater reduction on MADRS scores, and will require lesser number of sessions in order for the clinical outcome to be reached. This result will have a significant impact since major depression is the second most prevalent mental disorder, which is thought to affect 163 million people worldwide (64). Furthermore, in Portugal, 7% of the population is diagnosed with depression every year (65), and suicide is responsible for more than a thousand deaths annually (66).

Despite the fact that tDCS has some promising effects on mood, it seems that it is in the combination of tDCS with other

intervention that the effects are larger. For instance, in the study of Loo et al. (67), which randomized 64 patients to 15 sessions of 2 mA tDCS over 3 weeks and the study of Brunoni et al. (21), which enrolled 120 antidepressant-free patients with moderate and severe depression, tDCS has been shown to be effective in MDD. Moreover, in the study of Brunoni et al. (21), not only active tDCS was superior to sham tDCS but also the combined tDCS/sertraline was significantly more effective than in the other treatment groups in reducing depressive symptoms. Thus, the effects of tDCS seem to be enhanced by the combination with other interventions. This can be particularly important, if patient level data is taken into consideration. In a recent individual patient data meta-analysis (23) tDCS was shown to be less effective in high-resistant patients. This also reinforces the need of improving tDCS techniques so they can be effective in a broader depressed population.

We also propose to study, as secondary aim, whether CBT combined with tDCS can engage the proposed mechanistic target, of restoring the prefrontal imbalance and connectivity, by changes over resting-state and task-eliciting EEG. This trial will help to evaluate the efficacy of this combined treatment as compared to CBT alone and to evaluate bilateral alpha activity over the prefrontal cortex. Thus, we also expect to demonstrate that these interventions are able to reduce the inter-hemispheric asymmetry of alpha EEG activity toward the left hemisphere reported in patients with depression. We expect that the combined intervention will induce greater asymmetry reduction (at least 50% minimum reduction). We also expect that this inter-hemispheric imbalance reduction will be correlated with mood improvement.

Furthermore, this mechanistic approach is one of the main advantages of the current proposal. For instance, the use of EEG as an adjuvant tool to exclude neurological conditions or to help in the diagnosis of psychiatric disorders is a common practice in the clinical setting. Evidence of abnormal findings are obtained in about 64 to 68% of the EEGs performed in psychiatric patients (68). These results suggest that EEG can be a potential technique to be used as a coadjutant for the diagnosis and prognosis of several psychiatric conditions, with potential reliability to guide neural-based interventions. EEG has been shown to differentiate patients with MDD and non-depressed healthy controls. Numerous studies have shown that depressed individuals present an asymmetry of EEG alpha activity toward the left hemisphere, even among previously depressed individuals when compared to those who have never experienced clinically significant depression (7–9). Some studies have nevertheless failed to show the link between decreased left frontal activation and depression (19). It has been suggested that inconsistencies in this literature may be the result of clinical and/or methodological differences between laboratories, such as the inclusion or exclusion of co-morbidities (such as anxiety disorders), gender related differences, or the choice of EEG reference (9, 69, 70). Nonetheless, there is robust evidence suggesting that EEG alpha asymmetry is present among individuals with present or history of clinical depression, or even susceptibility to develop depression in the future (71). Additionally, alpha power asymmetry-based neurofeedback (NFB), which aims to train patients to increase right-to-left ratio by rebalancing the left hemisphere hypoactivation, has shown promising results in MDD (72, 73).

The advantages of EEG in MDD go far beyond its potential to detect differences between depressed vs. non-depressed individuals. Namely, EEG can be used to detect changes in the EEG patterns after interventions, and as such can be used to determine the efficacy of the intervention or if used also in the baseline, as an outcome predictor (74, 75). Furthermore, EEG is a direct measure of neural activity, it allows for chronometric sensitivity, has the potential to assess local and network effects, it is easy to use, cheap, and non-invasive. By using EEG, it is possible to quantify the electrical activity over specify regions of interest (power and coherence analysis) and, therefore, correlate with symptoms severity and response prognostic to specific treatments. Thus, creating brain based interventions.

These changes in EEG patterns have been used to direct several interventions, such as tDCS or TMS, however most study lack in the assessment of the real changes in EEG activity. For instance, based on this neurobiological basis, the main target for treating depressive symptoms using non-invasive brain stimulation (NIBS) techniques, such as tDCS and TMS, have been both the left (hypoactive) and right (hyperactive) DLPFC, by placing anodal (excitatory) over the left and cathodal (inhibitory) over the right DLPFC (76, 77). Using this mechanistic approach of facilitating the activation of the left DLPFC relative to the right, beneficial emotional, and cognitive effects in MDD were shown emotional and cognitive effects in MDD (18, 78, 79). Moreover, we chose to include adults with first episode of MDD only as to increase homogeneity of our study sample and thus increase internal validity of our findings. There are several advantages of studying the combination of these treatments in first episode MD drug-naive patients, as their brains were not changed by the pharmacological treatments, by the time course of the condition, or by the recurrence of MDD episodes (and other comorbidities). Second, combining tDCS and CBT are two therapies that have been shown to improve MDD. Moreover, tDCS is a safe, of easy administration, and not expensive non-invasive brain stimulation technique that has been shown to be effective in neuromodulating our target mechanism (imbalance over the DLPFC). Also, CBT is the golden standard treatment for MDD and has also shown to be able to neuromodulate brain structures involved in MDD. Thus, if we show that tDCS combined with CBT produce greater significant clinical improvements in MDD, this may reduce the global burden of MDD (for instance, by reducing the number of therapy sessions and the number of relapses and by producing larger long-term effects).

Therefore, the results of this project will further provide important insights into the mechanisms underlying MDD. In sum, we will be able to study the mechanistic reason underlying differences between the add-on treatment group vs. CBT combined with sham tDCS. We chose a population that is not very well studied, namely patients drug-naïve, first-episode MDD with mild to moderate symptoms, because several studies failed to show the link between decreased left frontal activation

and depression. By using resting state EEG, it will be possible to simultaneously understand the neural effects of the intervention, as well as potential response predictors for future trials.

TRIALS STATUS

This clinical trial is currently on the recruitment phase.

AUTHOR CONTRIBUTIONS

SC and JL designed and developed the study protocol. ÓFG, AB, AF-G, and FF provided inputs to the design and development of the protocol and contributed equally to this work. All authors read and approved the final manuscript. All authors contributed to the article and approved the submitted version.

FUNDING

This work was partially supported by FEDER funds through the Programa Operacional Factores de Competitividade—COMPETE and by national funds through FCT—Fundação para a Ciência e a Tecnologia through the calls IF/00091/2015 and PTDC/PSI-ESP/29701/2017. The sponsors had no role in the study design, implementation, data analysis or publication.

REFERENCES

1. Murray CJL, Abraham J, Ali MK, Alvarado M, Atkinson C, Baddour LM, et al. The state of uS health, 1990-2010: burden of diseases, injuries, risk factors. *JAMA - J Am Med Assoc.* (2013) 310:591–608. doi: 10.1001/jama.2013.13805
2. Charlson F, van Ommeren M, Flaxman A, Cornett J, Whiteford H, Saxena S. New wHO prevalence estimates of mental disorders in conflict settings: a systematic review and meta-analysis. *Lancet.* (2019) 394:240–8. doi: 10.1016/S0140-6736(19)30934-1
3. World Health Organization. *Depression*. (2020). Available online at: https://www.who.int/news-room/fact-sheets/detail/depression [accessed May 17, 2020].
4. Zimmerman M, Walsh E, Friedman M, Boerescu DA, Attiullah N. Identifying remission from depression on 3 self-Report scales. *J Clin Psychiatry.* (2017) 78:177–83. doi: 10.4088/JCP.16m10641
5. Rush AJ, Trivedi MH, Wisniewski SR, Nierenberg AA, Stewart JW, Warden D, et al. Acute and longer-term outcomes in depressed outpatients requiring one or several treatment steps: a STAR*D report. *Am J Psychiatry.* (2006) 163:1905–17. doi: 10.1176/ajp.2006.163.11.1905
6. Papakostas GI. Tolerability of modern antidepressants. *J Clin Psychiatry.* (2008) 69:8–13.
7. Nusslock R, Shackman AJ, Harmon-Jones E, Alloy LB, Coan JA, Abramson LY. Cognitive vulnerability and frontal brain asymmetry: common predictors of first prospective depressive episode. *J Abnorm Psychol.* (2011) 120:497–503. doi: 10.1037/a0022940
8. Stewart JL, Coan JA, Towers DN, Allen JJB. Frontal eEG asymmetry during emotional challenge differentiates individuals with and without lifetime major depressive disorder. *J Affect Disord.* (2011) 129:167–74. doi: 10.1016/j.jad.2010.08.029
9. Stewart JL, Coan JA, Towers DN, Allen JJB. Resting and task-elicited prefrontal EEG alpha asymmetry in depression: support for the capability model. *Psychophysiology.* (2014) 51:446–55. doi: 10.1111/psyp.12191
10. Fonseka TM, MacQueen GM, Kennedy SH. Neuroimaging biomarkers as predictors of treatment outcome in major depressive disorder. *J Affect Disord.* (2018) 233:21–35. doi: 10.1016/j.jad.2017.10.049
11. Lai CH. Promising neuroimaging biomarkers in depression. *Psychiatry Investig.* (2019) 16:662–70. doi: 10.30773/pi.2019.07.25.2
12. Kaster TS, Daskalakis ZJ, Noda Y, Knyahnytska Y, Downar J, Rajji TK, et al. Efficacy, tolerability, and cognitive effects of deep transcranial magnetic stimulation for late-life depression: a prospective randomized controlled trial. *Neuropsychopharmacology.* (2018) 43:2231–8. doi: 10.1038/s41386-018-0121-x
13. Alexander ML, Alagapan S, Lugo CE, Mellin JM, Lustenberger C, Rubinow DR, et al. Double-blind, randomized pilot clinical trial targeting alpha oscillations with transcranial alternating current stimulation (tACS) for the treatment of major depressive disorder (MDD). *Transl Psychiatry.* (2019) 9:439. doi: 10.1038/s41398-019-0439-0
14. Corlier J, Carpenter LL, Wilson AC, Tirrell E, Gobin AP, Kavanaugh B, et al. The relationship between individual alpha peak frequency and clinical outcome with repetitive transcranial magnetic stimulation (rTMS) treatment of major depressive disorder (MDD). *Brain Stimul.* (2019) 12:1572–8. doi: 10.1016/j.brs.2019.07.018
15. Jog MV, Wang DJJ, Narr KL. A review of transcranial direct current stimulation (tDCS) for the individualized treatment of depressive symptoms. *Pers Med Psychiatry.* (2019) 8:17–22. doi: 10.1016/j.pmip.2019.03.001
16. Evans J, Heron J, Lewis G, Araya R, Wolke D. Negative self-schemas and the onset of depression in women: longitudinal study. *Br J Psychiatry.* (2005) 186:302–7. doi: 10.1192/bjp.186.4.302
17. Beck AT, Dozois DJA. Cognitive therapy: current status and future directions. *Annu Rev Med.* (2011) 62:397–409. doi: 10.1146/annurev-med-052209-100032
18. Wolkenstein L, Plewnia C. Amelioration of cognitive control in depression by transcranial direct current stimulation. *Biol Psychiatry.* (2013) 73:646–51. doi: 10.1016/j.biopsych.2012.10.010
19. Baehr E, Rosenfeld JP, Baehr R. The clinical use of an alpha asymmetry protocol in the neurofeedback treatment of depression: two case studies. *J Neurother.* (1997) 2:10–23. doi: 10.1300/J184v02n03_02
20. Loo CK, Alonzo A, Martin D, Mitchell PB, Galvez V, Sachdev P. Transcranial direct current stimulation for depression: 3-Week, randomised, sham-controlled trial. *Br J Psychiatry.* (2012) 200:52–9. doi: 10.1192/bjp.bp.111.097634
21. Brunoni AR, Valiengo L, Baccaro A, Zanão TA, De Oliveira JF, Goulart A, et al. The sertraline vs electrical current therapy for treating depression clinical study. *JAMA Psychiatry.* (2013) 70:383–91. doi: 10.1001/2013.jamapsychiatry.32
22. Fregni F, El-Hagrassy MM, Pacheco-Barrios K, Carvalho S, Leite J, Simis M, et al. Evidence-based guidelines secondary meta-analysis for the use of transcranial direct current stimulation (tDCS) in neurological psychiatric disorders. *Int J Neuropsychopharmacol.* (2020). doi: 10.1093/ijnp/pyaa051. [Epub ahead of print].
23. Moffa AH, Brunoni AR, Fregni F, Palm U, Padberg F, Blumberger DM, et al. Safety and acceptability of transcranial direct current stimulation for the acute treatment of major depressive episodes: analysis of individual patient data. *J Affect Disord.* (2017) 221:1–5. doi: 10.1016/j.jad.2017.06.021
24. Brunoni AR, Boggio PS, De Raedt R, Bensenor IM, Lotufo PA, Namur V, et al. Cognitive control therapy and transcranial direct current stimulation for depression: a randomized, double-blinded, controlled trial. *J Affect Disord.* (2014) 162:43–9. doi: 10.1016/j.jad.2014.03.026
25. Segrave RA, Arnold S, Hoy K, Fitzgerald PB. Concurrent cognitive control training augments the antidepressant efficacy of tDCS: a pilot study. *Brain Stimul.* (2014) 7:325–31. doi: 10.1016/j.brs.2013.12.008
26. Farb N, Anderson A, Ravindran A, Hawley L, Irving J, Mancuso E, et al. Prevention of relapse/recurrence in major depressive disorder with either mindfulness-based cognitive therapy or cognitive therapy. *J Consult Clin Psychol.* (2018) 86:200–4. doi: 10.1037/ccp0000266
27. Zhang Z, Zhang L, Zhang G, Jin J, Zheng Z. The effect of cBT and its modifications for relapse prevention in major depressive disorder: a systematic review and meta-analysis. *BMC Psychiatry.* (2018) 18:5. doi: 10.1186/s12888-018-1610-5
28. Vitiello B. Combined cognitive-behavioural therapy and pharmacotherapy for adolescent depression: does it improve

outcomes compared with monotherapy? *CNS Drugs.* (2009) 23:271–80. doi: 10.2165/00023210-200923040-00001
29. Peselow ED, Tobia G, Karamians R, Pizano D, IsHak WW. Prophylactic efficacy of fluoxetine, escitalopram, sertraline, paroxetine, and concomitant psychotherapy in major depressive disorder: outcome after long-term follow-up. *Psychiatry Res.* (2015) 225:680–6. doi: 10.1016/j.psychres.2014.11.022
30. Manber R, Buysse DJ, Edinger J, Krystal A, Luther JF, Wisniewski SR, et al. Efficacy of cognitive-behavioral therapy for insomnia combined with antidepressant pharmacotherapy in patients with comorbid depression and insomnia: a randomized controlled trial. *J Clin Psychiatry*. (2016) 2016:e1316–e1323. doi: 10.4088/JCP.15m10244
31. DeRubeis RJ, Siegle GJ, Hollon SD. Cognitive therapy versus medication for depression: treatment outcomes and neural mechanisms. *Nat Rev Neurosci.* (2008) 9:788–96. doi: 10.1038/nrn2345
32. Driessen E, Hollon SD. Cognitive behavioral therapy for mood disorders: efficacy, moderators and mediators. *Psychiatr Clin North Am.* (2010) 33:537–55. doi: 10.1016/j.psc.2010.04.005
33. Yang Z, Oathes D, Linn KA, Bruce SE, Satterthwaite TD, Cook PA, et al. Cognitive behavioral therapy is associated with enhanced cognitive control network activity in major depression and posttraumatic stress disorder. *Biol Psychiatry Cogn Neurosci Neuroimaging.* (2018) 3:311–9. doi: 10.1016/j.bpsc.2017.12.006
34. Wagner G, Schultz CC, Koch K, Schachtzabel C, Sauer H, Schlösser RG. Prefrontal cortical thickness in depressed patients with high-risk for suicidal behavior. *J Psychiatr Res.* (2012) 46:1449–55. doi: 10.1016/j.jpsychires.2012.07.013
35. Goldstein-Piekarski AN, Staveland BR, Ball TM, Yesavage J, Korgaonkar MS, Williams LM. Intrinsic functional connectivity predicts remission on antidepressants: a randomized controlled trial to identify clinically applicable imaging biomarkers. *Transl Psychiatry.* (2018) 8. doi: 10.1038/s41398-018-0100-3
36. Korgaonkar MS, Goldstein-Piekarski AN, Fornito A, Williams LM. Intrinsic connectomes are a predictive biomarker of remission in major depressive disorder. *Mol Psychiatry*. (2019) 25:1537–49. doi: 10.1038/s41380-019-0574-2
37. Jos,é C, Fernando B, Iván C. TMS for major depressive disorder in naïve patients. *Brain Stimul.* (2019) 12:e133. doi: 10.1016/j.brs.2019.03.037
38. Maneeton B, Maneeton N, Woottiluk P, Likhitsathian S. Repetitive transcranial magnetic stimulation combined with antidepressants for first episode of major depressive disorder. *Curr Neuropharmacol.* (2020) 2020:18. doi: 10.2174/1570159x18666200221113134
39. National Institute for Health Care Excellence. *Depression in Adults: Recognition Management*. NICE (2009). Available online at: https://www.nice.org.uk/guidance/cg90/chapter/1-Guidance#treatment-choice-based-on-depression-subtypes-and-personal-characteristics [accessed August 25, 2020].
40. Chan AW, Tetzlaff JM, Gøtzsche PC, Altman DG, Mann H, Berlin JA, et al. SPIRIT 2013 explanation and elaboration: guidance for protocols of clinical trials. *BMJ.* (2013) 346:e7586. doi: 10.1136/bmj.e7586
41. Chan, A.-W., Tetzlaff JM, Altman DG, Laupacis A, Gøtzsche PC, et al. SPIRIT 2013 statement: defining standard protocol items for clinical trials. *Ann Intern Med.* (2013) 158:200. doi: 10.7326/0003-4819-158-3-201302050-00583
42. Beck AT, Kovacs M, Weissman A. Assessment of suicidal intention: the scale for suicide ideation. *J Consult Clin Psychol.* (1979) 47:343–52. doi: 10.1037/0022-006X.47.2.343
43. Shankman SA, Funkhouser CJ, Klein DN, Davila J, Lerner D, Hee D. Reliability and validity of severity dimensions of psychopathology assessed using the Structured Clinical Interview for DSM-5 (SCID). *Int J Methods Psychiatr Res.* (2018) 2018:27. doi: 10.1002/mpr.1590
44. Osório FL, Loureiro SR, Hallak JEC, Machado-de-Sousa JP, Ushirohira JM, Baes CVW, et al. Clinical validity and intrarater and test–retest reliability of the structured clinical interview for dSM-5 – clinician version (SCID-5-CV). *Psychiatry Clin Neurosci.* (2019) 73:754–760. doi: 10.1111/pcn.12931
45. Beck AT, John Rush A, Shaw BF, Emery G. *Cognitive Therapy of Depression, the Guilford Clinical Psychology and Psychopathology Series by Aaron*. New York, NY: Booktopia. (1987). Available online at: https://www.guilford.com/books/Cognitive-Therapy-of-Depression/Beck-Rush-Shaw-Emery/9780898629194 (accessed May 13, 2020).
46. Leite J, Carvalho S, Fregni F, Boggio PS, Gonçalves ÓF. The effects of cross-hemispheric dorsolateral prefrontal cortex transcranial direct current stimulation (tDCS) on task switching. *Brain Stimul.* (2013) 2013:6. doi: 10.1016/j.brs.2012.10.006
47. Carvalho S, Gonçalves OF, Soares JM, Sampaio A, Macedo F, Fregni F, et al. Sustained effects of a neural-based intervention in a refractory case of tourette syndrome. *Brain Stimul.* (2015) 2015:8. doi: 10.1016/j.brs.2014.12.008
48. Carvalho S, Boggio PS, Gonçalves ÓF, Vigário AR, Faria M, Silva S, et al. Transcranial direct current stimulation based metaplasticity protocols in working memory. *Brain Stimul.* (2015) 2015:11. doi: 10.1016/j.brs.2014.11.011
49. Carvalho S, French M, Thibaut A, Lima W, Simis M, Leite J, et al. Median nerve stimulation induced motor learning in healthy adults: a study of timing of stimulation and type of learning. *Eur J Neurosci.* (2018) 48:13990. doi: 10.1111/ejn.13990
50. Carvalho S, Leite J, Jones F, Morse LR, Zafonte R, Fregni F. Study adherence in a tDCS longitudinal clinical trial with people with spinal cord injury. *Spinal Cord.* (2018) 56:5. doi: 10.1038/s41393-017-0023-5
51. Carvalho S, Sampaio A, Mendes AJ, Lema A, Vieira D, Goncalves OF, et al. Polarity specific effects of cross-hemispheric tDCS coupled with approach-avoidance training on chocolate craving. *Front Pharmacol.* (2019) 9:1500. doi: 10.3389/fphar.2018.01500
52. Thibaut A, Carvalho S, Morse LR, Zafonte R, Fregni F. Delayed pain decrease following m1 tDCS in spinal cord injury: a randomized controlled clinical trial. *Neurosci Lett.* (2017) 658:24. doi: 10.1016/j.neulet.2017.08.024
53. De Beurs DP, Fokkema M, O'Connor RC. Optimizing the assessment of suicidal behavior: the application of curtailment techniques. *J Affect Disord.* (2016) 196:218–24. doi: 10.1016/j.jad.2016.02.033
54. Montgomery SA, Asberg M. A new depression scale designed to be sensitive to change. *Br J Psychiatry.* (1979) 134:382–9. doi: 10.1192/bjp.134.4.382
55. Beck AT, Ward CH, Mendelson M, Mock J, Erbaugh J. An inventory for measuring depression. *Arch Gen Psychiatry.* (1961) 4:561–71. doi: 10.1001/archpsyc.1961.01710120031004
56. Jenkinson C, Layte R, Jenkinson D, Lawrence K, Petersen S, Paice C, et al. A shorter form health survey: can the sf-12 replicate results from the sf-36 in longitudinal studies? *J Public Heal.* (1997) 19:179–86. doi: 10.1093/oxfordjournals.pubmed.a024606
57. Diener E, Emmons RA, Larsem RJ, Griffin S. The satisfaction with life scale. *J Pers Assess.* (1985) 49:71–5. doi: 10.1207/s15327752jpa4901_13
58. Pavot W, Diener E, Colvin CR, Sandvik E. Further validation of the satisfaction with life scale; evidence for the cross-Method convergence of well-Being measures. *J Pers Assess.* (1991) 57:149–61. doi: 10.1207/s15327752jpa5701_17
59. Buysse DJ, Reynolds CF, Monk TH, Berman SR, Kupfer DJ. The pittsburgh sleep quality index: a new instrument for psychiatric practice and research. *Psychiatry Res.* (1989) 28:193–213. doi: 10.1016/0165-1781(89)90047-4
60. Del Rio João KA, Becker NB, de Neves Jesus S, Isabel Santos Martins R. Validation of the portuguese version of the pittsburgh sleep quality index (PSQI-PT). *Psychiatry Res.* (2017) 247:225–9. doi: 10.1016/j.psychres.2016.11.042
61. Spielberger CD, Gorsuch RL, Lushene RE. *Manual for the State-Trait Anxiety Inventory*. Palo Alto, CA: Consulting Psychologists Press (1970).
62. Beck AT, Epstein N, Brown G, Steer RA. An inventory for measuring clinical anxiety: psychometric properties. *J Consult Clin Psychol.* (1988) 56:893–7. doi: 10.1037/0022-006X.56.6.893
63. Quintão S, Delgado AR, Prieto G. Validity study of the beck anxiety inventory (Portuguese version) by the rasch rating scale model. *Psicol Reflex e Crit.* (2013) 26:305–10. doi: 10.1590/S0102-79722013000200010
64. James SL, Abate D, Abate KH, Abay SM, Abbafati C, Abbasi N, et al. Global, regional, national incidence. Prevalence, and years lived with disability for 354 Diseases and Injuries for 195 countries and territories, 1990-2017: A systematic analysis for the Global Burden of Disease Study 2017. *Lancet.* (2018) 392:1789–858. doi: 10.1016/S0140-6736(18)32279-7
65. de Almeida JC. Portuguese national mental health plan (2007-2016) executive summary. *Ment Health Fam Med.* (2009) 6:233–44.
66. Alonso J, Angermeyer MC, Bernert S, Bruffaerts R, Brugha TS, Bryson H, et al. Disability and quality of life impact of mental disorders in europe: results from the european study of the epidemiology of mental

disorders (ESEMeD) project. *Acta Psychiatr Scand Suppl.* (2004) 109:38–46. doi: 10.1111/j.1600-0047.2004.00329.x
67. Loo CK, Husain MM, McDonald WM, Aaronson S, O'Reardon JP, Alonzo A, et al. International randomized-controlled trial of transcranial direct current stimulation in depression. *Brain Stimul.* (2018) 11:125–33. doi: 10.1016/j.brs.2017.10.011
68. Newson JJ, Thiagarajan TC. EEG frequency bands in psychiatric disorders: a Review of resting state studies. *Front Hum Neurosci.* (2019) 12:521. doi: 10.3389/fnhum.2018.00521
69. Hagemann D. Individual differences in anterior eEG asymmetry: methodological problems and solutions. *Biol Psychol.* (2004) 67:157–82. doi: 10.1016/j.biopsycho.2004.03.006
70. Stewart JL, Bismark AW, Towers DN, Coan JA, Allen JJB. Resting frontal eEG asymmetry as an endophenotype for depression risk: sex-specific patterns of frontal brain asymmetry. *J Abnorm Psychol.* (2010) 119:502–12. doi: 10.1037/a0019196
71. Allen JJB, Coan JA, Nazarian M. Issues and assumptions on the road from raw signals to metrics of frontal EEG asymmetry in emotion. *Biol Psychol.* (2004) 67:183–18. doi: 10.1016/j.biopsycho.2004.03.007
72. Rosenfeld JP, Cha G, Blair T, Gotlib IH. Operant (biofeedback) control of left-right frontal alpha power differences: potential neurotherapy for affective disorders. *Biofeedback Self Regul.* (1995) 20:241–58. doi: 10.1007/BF014 74516
73. Allen JJB, Harmon-Jones E, Cavender JH. Manipulation of frontal eEG asymmetry through biofeedback alters self-reported emotional responses and facial eMG. *Psychophysiology.* (2001) 38:685–93. doi: 10.1111/1469-8986.3840685
74. Hughes JR, John ER. Conventional and quantitative electroencephalography in psychiatry. *J Neuropsychiatry Clin Neurosci.* (1999) 11:190–208. doi: 10.1176/jnp.11.2.190
75. Badrakalimuthu VR, Swamiraju R, De Waal H. EEG in psychiatric practice: to do or not to do? *Adv Psychiatr Treat.* (2011) 17:114–21. doi: 10.1192/apt.bp.109.006916
76. Berlim MT, Van den Eynde F, Daskalakis ZJ. Clinical utility of transcranial direct current stimulation (tDCS) for treating major depression: a systematic review and meta-analysis of randomized, double-blind and sham-controlled trials. *J Psychiatr Res.* (2013) 47:1–7. doi: 10.1016/j.jpsychires.2012.09.025
77. Shiozawa P, Fregni F, Benseñor IM, Lotufo PA, Berlim MT, Daskalakis JZ, et al. Transcranial direct current stimulation for major depression: an updated systematic review and meta-analysis. *Int J Neuropsychopharmacol.* (2014) 17:1443–52. doi: 10.1017/S1461145714000418
78. Terhune DB, Cohen Kadosh R. Modulating cognitive control in major depression with transcranial electrical stimulation. *Biol Psychiatry.* (2013) 73:595–6. doi: 10.1016/j.biopsych.2013.01.006
79. Moreno ML, Vanderhasselt MA, Carvalho AF, Moffa AH, Lotufo PA, Benseñor IM, et al. Effects of acute transcranial direct current stimulation in hot and cold working memory tasks in healthy and depressed subjects. *Neurosci Lett.* (2015) 591:126–31. doi: 10.1016/j.neulet.2015.02.036

Conflict of Interest: The authors declare that the research was conducted in the absence of any commercial or financial relationships that could be construed as a potential conflict of interest.

frontiers in Integrative Neuroscience

ORIGINAL RESEARCH
published: 05 November 2020
doi: 10.3389/fnint.2020.556839

Deep rTMS Mitigates Behavioral and Neuropathologic Anomalies in Cuprizone-Exposed Mice Through Reducing Microglial Proinflammatory Cytokines

Liu Yang[1], *Yawen Su*[1], *Fannv Guo*[1], *Handi Zhang*[1], *Yinglin Zhao*[1], *Qinjun Huang*[1]* *and Haiyun Xu*[1,2]*

[1]*The Mental Health Center, Shantou University Medical College, Shantou, China,* [2]*The School of Psychiatry, Wenzhou Medical University, Wenzhou, China*

OPEN ACCESS

Edited by:
Amir Shmuel,
McGill University, Canada

Reviewed by:
Aline Miranda,
Federal University of Minas Gerais, Brazil
Nai-Kei Wong,
Chinese Academy of Sciences, China

***Correspondence:**
Qinjun Huang
huangqj@stu.edu.cn
Haiyun Xu
hyxu@stu.edu.cn

Received: *29 April 2020*
Accepted: *05 October 2020*
Published: *05 November 2020*

Citation:
Yang L, Su Y, Guo F, Zhang H, Zhao Y, Huang Q and Xu H (2020) Deep rTMS Mitigates Behavioral and Neuropathologic Anomalies in Cuprizone-Exposed Mice Through Reducing Microglial Proinflammatory Cytokines. Front. Integr. Neurosci. 14:556839. doi: 10.3389/fnint.2020.556839

In comparison to conventional repetitive transcranial magnetic stimulation (rTMS), theta burst stimulation is stronger and more effective as a brain stimulation approach within short periods. Although this deep rTMS technique is being applied in treating neuropsychiatric disorders, few animal studies have attempted to clarify the neurobiological mechanisms underlying its beneficial effects. This animal study examined the effects of deep rTMS on the cuprizone-induced neuropathologic and behavioral anomalies and explored the underlying mechanism. Adolescent male C57BL/6 mice were fed a rodent chow without or with cuprizone (CPZ; 0.2% w/w) for 5 weeks. Another two groups of mice were subjected to deep rTMS or sham rTMS once a day during weeks 2–5 of the CPZ-feeding period. The behaviors of all mice were assessed after the withdrawal of CPZ before neuropathological and immunological analyses. Compared to the CNT group, mice in CPZ and CPZ + Sham groups showed deficits in social recognition and spatial working memory as well as anxiety-like behavior, in addition to myelin breakdown and OL loss in the corpus callosum (CC), caudate putamen, cerebral cortex, and hippocampus of the brain. Deep rTMS effectively reduced behavioral anomalies and blocked myelin breakdown and OL loss in CPZ-fed mice. Besides, it also dampened microglia activation at lesion sites and rectified cytokines levels (IL-1β, IL-6, and IL-10) in CPZ-affected regions. The most significant effect was seen in the cerebral cortex where alleviated neuropathology co-existed with less microglia activation and higher IL-10 level. These data provided experimental evidence for the beneficial effects of deep rTMS in CPZ-fed mice and revealed a neurobiological mechanism of the modality.

Keywords: cuprizone, microglia, oligodendrocyte, rTMS, inflammatory cytokines

INTRODUCTION

Transcranial magnetic stimulation (TMS) is a non-invasive neuromodulation technique. *Via* electromagnetic induction, transient and localized electrical fields are generated in the brain cortex, which in turn affect functions of local neurons such as depolarization and firing (Hallett, 2000). Repetitive TMS (rTMS), as the term implies, delivers multiple TMS pulses at frequencies between 0.5 and 20 Hz over a chosen brain area (Pascual-Leone et al., 1999). Moreover, the theta-burst stimulation (TBS, a newer modality of rTMS) has been developed and applied in humans. TBS delivers relatively greater and more stimulation to the brain in a shorter period (Huang et al., 2005; Chung et al., 2015). This deep rTMS was shown to change cortical excitability that may last longer than with traditional TMS protocols (Ishikawa et al., 2007; Huang et al., 2009). As reported by Levkovitz and colleagues, TBS led to higher response and remission rates in 212 major depressive depression outpatients than in the sham group (Levkovitz et al., 2015). Recent evidence from human studies supports a therapeutic role of TBS in some neuropsychiatric disorders, which implicates certain brain regions important to cognitive functions (Spronk et al., 2011).

In contrast to its growing clinical applications in patients with neuropsychiatric disorders, few animal studies have been done on deep rTMS applications. Of the extant publications, Zhang et al. (2014) reported the beneficial effects of deep rTMS on hippocampal neurogenesis and the development of adult newborn neurons, in addition to its anti-depression effects seen in the learned helplessness mouse model and a mouse model for Rett syndrome. In a more recent study, administration of deep rTMS (gamma Hz) for 6 weeks alleviated schizophrenia-like behaviors in cuprizone (CPZ) exposed mice while promoted the remyelination process and up-regulated the expression of neuregulin-1 and its receptor ErbB4 in the prefrontal cortex (PFC) of the demyelinated mice (Sun et al., 2018).

CPZ is a chemical chelator that is toxic to mitochondria by inhibiting the activity of complexes I-IV in the mitochondrial respiratory chain (Pasquini et al., 2007; Millet et al., 2009; Acs et al., 2013). Feeding C57BL/6 mice with a 0.2% CPZ-supplemented diet for 4–6 weeks was shown to induce acute demyelinating lesions followed by spontaneous remyelination in the brains of subjects (Hiremath et al., 1998; Matsushima and Morell, 2001). In addition to demyelination and loss of mature oligodendrocytes (OLs, the myelin-forming cells in the brain), CPZ-exposed mice also showed astrocyte proliferation and microglia activation in the lesion sites of the brain (Stidworthy et al., 2003; Remington et al., 2007; Zhang L. et al., 2018). These neuropathological features constitute the constructive validity of CPZ-exposed mice being used as an animal model of multiple sclerosis (MS), a major demyelinating disease of the central nervous system.

In 2009, we first proposed to use the CPZ-exposed mice as a novel animal model in biological psychiatry research of schizophrenia based on multiple lines of clinical and experimental evidence (Xu et al., 2009). Not surprisingly, we found that CPZ-exposed mice displayed more climbing behavior and lower prepulse inhibition at weeks 2 and 3 of the CPZ-exposure period along with higher dopamine but lower norepinephrine levels in the PFC. CPZ-exposed mice presented less social interaction in the presence of evident brain demyelination, myelin breakdown, and OL loss at weeks 4 and 6. CPZ-exposed mice spent more time on the open arms of an elevated plus-maze and exhibited spatial working memory impairment at all time points (Xu et al., 2009). Since then, the CPZ-exposed mice have been employed as an animal model of schizophrenia to explore the pathophysiology of this brain disorder and investigate the neurobiological mechanisms underlying the therapeutic effects of antipsychotic treatment (Xu et al., 2010, 2019; Herring and Konradi, 2011; Liu et al., 2017; Sun et al., 2018; Hayakawa et al., 2019).

Unlike the other animal models of schizophrenia, the brain neuropathology of CPZ-exposed mice involves mitochondrial dysfunction, neuroinflammation, and white matter damage, three essential players in the pathogenesis of schizophrenia (Najjar and Pearlman, 2015; Xu et al., 2016; De Picker et al., 2017; Buckley, 2019). With this CPZ mouse model, our recent studies have explored the anti-inflammation and anti-oxidative stress effects of quetiapine, an atypical antipsychotic (Shao et al., 2015; Xuan et al., 2015). On the other hand, the antioxidant *N*-acetylcysteine protected mature OLs against the toxic effects of CPZ through its antioxidant and anti-inflammatory actions (Zhang L. et al., 2018). In line with this animal study, clinical studies reported that atypical antipsychotics clozapine and risperidone decreased serum levels of the cytokines IL-2, IL-6, and TNF-α (Lu et al., 2004) and showed the antipsychotic effect of minocycline, a potent inhibitor of microglial activation in patients with schizophrenia (Miyaoka et al., 2007, 2008). Similarly, Celecoxib, a non-steroidal anti-inflammatory drug, appears to be an efficacious and safe treatment in improving psychotic symptoms, particularly in first-episode schizophrenia (Zheng et al., 2017). These animal models and clinical studies suggest the presence of additional therapeutic actions of the extant antipsychotics and encourage further efforts to explore new antipsychotic medications aside from the existing antipsychotics.

This study aimed to examine the effects of deep rTMS on the neuropathologic changes and behavioral anomalies in CPZ-exposed mice and explore the underlying neurobiological mechanism. In addition to assessing the behaviors relevant to anxiety, spatial working memory, and social interaction symptoms seen in patients with schizophrenia, we emphasized CPZ-induced neuropathological changes in the brain. Specifically, we were interested in the role of neuroinflammation in the pathogenesis of CPZ-induced demyelination and OL loss and wondered if deep rTMS works on cells and molecules relevant to neuroinflammation in the brain. The brain regions of the corpus callosum (CC), caudate putamen, frontal cortex (FC), and hippocampus were closely looked at given that these regions are sensitive to CPZ-intoxication (Yang et al., 2009) and compromised in schizophrenia patients (van Erp et al., 2016; Grazioplene et al., 2018). Administration of the deep rTMS for 4 weeks effectively mitigated the behavioral anomalies, reduced myelin breakdown and OL loss in CPZ-fed mice, inhibited microglia activation in the lesion sites and

rectified levels of IL-1β, IL-6, and IL-10 in the brain regions mentioned above. These results support the application of deep rTMS in clinical practice and help to understand the beneficial or therapeutic effects of this physical modality in treating schizophrenia patients.

MATERIALS AND METHODS

Animals

Five-week-old male C57BL/6 mice were purchased from the Guangdong Medical Laboratory Animal Center (Guangzhou, China). The mice were housed in groups in polypropylene cages and acclimatized for 1 week before the experiment. The vivarium was kept at 50 ± 5% humidity, 22 ± 1°C, 12 h light-dark cycle. In the vivarium, mice had free access to food and water during the experimental period. All experimental procedures applied to this study were approved by the Local Ethical Committee for Animal Experiments, Shantou University Medical College.

Experimental Design

After acclimatization for 7 days, the mice were randomly assigned into one of the following four groups (n = 14/group): control group (CNT), in which mice received a standard rodent chow and tap water during the experimental period; CPZ group, in which mice ate a CPZ-containing (0.2% w/w) chow for 5 weeks as described previously (Xu et al., 2009); CPZ + rTMS group, in which mice consumed the same CPZ-containing chow as those in CPZ group, plus deep rTMS (described later) during weeks 2–5; CPZ + Sham group, in which mice consumed the same CPZ-containing chow as those in CPZ group, plus sham stimulation, i.e., the cage was set up with the same magnetic equipment at working but no magnetic field was outputted. After consumed CPZ-containing chow for 5 weeks, the mice turned to the normal rodent chow (without CPZ) for 3 days during which period they were subjected to the behavioral tests of open-field, social recognition, and Y-maze in the order, one test per day. One day after the last test, mice were euthanized with sodium pentobarbital (50 mg/kg, i.p.). Seven animals in each group were used for enzyme-linked immunosorbent assay (ELISA) analysis (described later). The remaining seven mice in each group were used for immunohistochemical and immunofluorescent staining.

Deep rTMS Procedure

By referring to previous studies (Zhang et al., 2014; Sun et al., 2018), active deep rTMS or sham rTMS was given to mice for successive 4 weeks during which period mice were fed a CPZ-containing diet. The magnetic equipment (Antis Magnetic Stimulation System, Model: Antis-w-180; Tianjin Antis Medical Device Company Limited, Tianjin, China) with two 360 mm-diameter coils was connected to a magnetic field generator which outputted the so-called intermittent gamma burst stimulation (iGBS) at 30–40 Hz. The iGBS consisted of magnetic fields that changed every 4 min (between linear and uniform gradients) and the rhythm gradually increased (30, 32.25, 34.5, 37, or 40 Hz) during the linear gradient. The 2-min linear gradient was composed of several magnetic pulses, each of which lasted for 2 s, followed by a resting interval for 8 s. Each of the 2-s magnetic stimulations was composed of six pulses with 150 μs width at 1,000 Hz frequency.

Behavioral Tests

One day after the 5 weeks of CPZ-exposure, all CPZ-exposed mice and normal controls were subjected to the open-field test, social interaction test, and Y-maze test, once a day in the order (Xu et al., 2009). For the open-field test, the mouse was placed in the central zone of an open-field box (25 × 25 cm) and allowed to move freely for 8 min, of which the first 3 min were defined to be the adaptation period and the data from this period were not included for analysis. The travel path of the animal was recorded by a video camera above the arena. The distances traveled on the whole arena and the central zone (12.5 × 12.5 cm), as well as the time spent at the central zone, were analyzed by a video tracking system (DigBehav System, Yishu Co. Ltd., Shanghai, China). The open field was cleaned with 70% alcohol after each trial.

The social interaction test was performed in the same open-field box. The test consisted of two sessions, each lasted for 150 s. During the first session, an empty wire mesh cage (7 × 7 cm) was placed at one corner of the field while a tested mouse moved there freely. During the second session, the conditions were identical to the first session except that an unfamiliar conspecific had been introduced into the cage. Between the two test sessions, the tested mouse was removed from the arena and placed back into his home cage for approximately 60 s. The unfamiliar conspecific was used one time only. The time spent by the tested mouse at the "interaction zone" (a 5-cm-wide corridor surrounding the cage) under the two conditions of an empty cage (E) and the cage with an unfamiliar conspecific (C) was recorded and analyzed after the test.

In the Y-maze test, each mouse was placed at the junction area of the three equal arms (30 × 8 × 15 cm) of a Y-maze and allowed to move freely through the maze for an 8-min test period. The series of entries and the total number of visiting arms were recorded. An actual entry was defined as all four paws of a mouse entered into an arm. A correct alternation was counted if visits into all three arms are in consecutive order. The theoretical maximal number of correct alternations was the total number of arm entries minus 2. The spontaneous alternation was calculated as the number of correct alternations divided by the theoretical maximal number of correct alternations and expressed as a percentage (%).

Immunohistochemical and Immunofluorescent Staining

Half (n = 7) the mice in each group were deeply anesthetized with sodium phenobarbital (50 mg/kg) and perfused intracardially with sterilized saline, followed by 4% paraformaldehyde in phosphate buffer (0.01 M, pH = 7.4). The mouse brain was removed from the skull and post-fixed in the same fixative at 4°C, overnight, and then cryoprotected in 15, 25 and 30% sucrose solutions for 1 day per concentration. Serial coronal sections (25 μm) were cut using a cryostat microtome (Leica CM1850) and collected in six-well plastic plates.

For immunohistochemical staining, the floating brain sections were washed with 0.01 M PBS for 10 min × 3 and then steeped in PBS with 3.0% hydrogen peroxide at room temperature for 30 min. After rinsed in PBS, the sections were incubated with a blocking solution (5% goat serum, 0.3% Triton X-100 in PBS) for 30 min at room temperature. The primary antibody to myelin basic protein (MBP; 1:200; Abcam, Cambridge, UK) or pi form of glutathione-S-transferase (GST-π; 1:200; Boster Biotechnology, Wuhan, China) was added into the blocking solution and incubated at 4°C overnight. After rinsed in PBS, sections were then incubated with the secondary antibody conjugated with horseradish peroxidase (Zhongshan Gold Bridge Biology Company, Beijing, China) at 37°C for 30 min. Then, the sections were visualized by adding a diaminobenzidine solution (Zhongshan Gold Bridge Biology Company). After rinsed in PBS, the sections were pasted onto the glass slides, dehydrated through gradient ethyl alcohol, and cleared by xylene. After cover-slipped with neutral balsam and dried, the immunohistochemical staining was observed and recorded with a Zeiss microscope (Zeiss Instruments Inc., Oberkochen, Germany). The quantitative analysis of the recorded images was done using the Image-Pro-Plus 6.0 software (Media Cybernetics, Rockville, MD, USA).

For immunofluorescent staining, the free-floating sections were washed with PBST (0.5% Tween 20 in PBS) for 5 min × 3. Then the sections were incubated with the blocking solution (5% BSA in PBST) on a shaker for 60 min at room temperature. Subsequently, the primary rabbit polyclonal anti-IBA-1 (1:1,000; Wako, Osaka, Japan) was added into the blocking solution and the incubation continued overnight at 4°C. After rinsed in PBST for 5 min × 3, the sections were incubated with Cy3-conjugated goat anti-rabbit antibody (Beyotime Biotechnology, Shanghai, China) at room temperature for 60 min. After rinsed in PBST, the sections were pasted and mounted by the Fluor mount (Abcam, Cambridge, UK). The immunofluorescence was observed under a fluorescence microscope (Zeiss Instruments Inc., Germany) and images were recorded with the system. The slides were preserved in a refrigerator at 4°C and shielded from light.

Image Analysis

For quantitative analysis of the immunohistochemical and immunofluorescent staining, all recorded images were read out and analyzed by the Image-Pro Plus 6.0 software (Media Cybernetics, Rockville, MD, USA). The examined brain regions are the CC, caudate-putamen (CPU), FC, and the CA3 of the hippocampus. Three sections were chosen for each brain region. Three images were recorded from each section under the same conditions. The data of MBP-like immunoreactivity were expressed as integrated optical density (IOD), which equals to area × average optical density. The number of GST-π and IBA-1 positive cells was counted and expressed as N/mm^2.

Enzyme-Linked Immunosorbent Assay

The protein levels of the cytokines IL-1β, IL-6, and IL-10 in the brain regions of CPU, FC, and hippocampus were measured using the ELISA kits (Boster, Wuhan, China) by following the procedures recommended by the manufacturer. Briefly, the brain tissue samples were homogenized in PBS (0.01 M, pH = 7.4) at 10% (w/v), followed by centrifugation at 3,000 rpm for 15 min at 4°C. Then, the supernatant was collected and stored at −80°C until use. On the analysis day, the samples were thawed and diluted with the dilute solution (1 volume sample + 9 volumes of dilute solution). Subsequently, the standard and sample solutions were added into the ELISA plates in duplicate (2 wells/solution, 100 μl/well) and incubated for 90 min at 37°C. Then, the liquid was thrown away, and 100 μl of biotin-labeled anti-mouse IL-1β, IL-6, or IL-10 working solution was added into the wells and incubated for 60 min at 37°C. After rinsed with PBS three times, 100 μl ABC (avidin-biotin-peroxidase complex) working solution was added into each well and incubated for 30 min at 37°C. Again, the liquid in wells was thrown away, and the wells were rinsed with PBS three times, followed by the addition of 90 μl TMB (3,3′,5,5′-tetramethylbenzidine) working solution. After incubation for 20–25 min at 37°C in the dark, the reaction was stopped by the addition of 100 μl TMB buffer. The plates were read by the microplate reader (Bio-Rad Laboratories Inc., Hercules, CA, USA) at 450 nm. The protein levels of the cytokines in the tissue samples were calculated by referring to the standard curve and expressed as pg/mg protein.

Statistical Analyses

Excel 2010 and SPSS 20.0 (IBM Corp., Armonk, NY, USA) was used for data analysis. Data were expressed as means ± SD. The Shapiro–Wilk test was used for the normality test of data distribution. The interaction time of the tested mouse in each group under the two conditions of E and C was compared by paired *t*-test. For the data from the other analyses, one-way ANOVA was conducted before the Tukey-post test for comparison of two groups. The significance threshold was set at 0.05.

RESULTS

Deep rTMS Alleviates the CPZ-Induced Anxiety-Like Behavior and Deficits in Social Recognition and Spatial Working Memory

The open-field test was performed with each one of the mice in this study to measure the locomotor activity, exploratory behavior, and anxiety level of the mice. **Table 1** showed the results of the test. For TD, one-way ANOVA showed a significant effect of the treatments ($F_{(3,27)} = 6.880$, $p = 0.002$). The *post hoc* comparisons, however, did not find any significant difference between any two groups. Regarding CD, one-way ANOVA showed no significant effect of the treatments ($F_{(3,27)} = 2.758$, $p = 0.064$). As for CD/TD, one-way ANOVA showed a significant effect of the treatments ($F_{(3,27)} = 3.103$, $p = 0.046$). The results of *post hoc* comparisons indicated that CPZ-feeding decreased the ratio of CD/TD compared to the CNT group ($p < 0.05$); and the difference between groups CPZ + Sham and CPZ + rTMS was also significant ($p < 0.05$), suggesting a protective effect of deep rTMS on the CPZ-induced anxiety-like behavior in mice.

TABLE 1 | Repetitive transcranial magnetic stimulation (rTMS) alleviates cuprizone (CPZ)-induced anxiety behavior in C57BL/6 mice.

Groups	TD (mean ± SD; cm)	CD (mean ± SD; cm)	CD/TD (mean ± SD; %)
CNT	1,723.46 ± 189.15	382.08 ± 59.99	22.17 ± 1.28
CPZ	2,137.64 ± 185.01	365.91 ± 27.60	17.12 ± 1.10*
CPZ + Sham	1,859.21 ± 94.99	332.48 ± 26.14	17.91 ± 1.39*
CPZ + rTMS	1,684.11 ± 103.28	398.25 ± 32.79	23.63 ± 1.20#

*Note: TD, the total distance traveled on the whole arena of the open-field during a 5-min test period. CD, the distance traveled at the central part of the open-field arena during the test period. *$p < 0.05$, compared to CNT group. #$p < 0.05$, compared to CPZ group.*

As for social recognition, mice in the groups CNT and CPZ + rTMS were able to tell an empty mesh cage from the same cage with an unfamiliar conspecific inside as evidenced by much more time spent by the mice under the latter condition relative to that spent under the former condition ($p < 0.05$). However, mice in groups of CPZ and CPZ + Sham were unable to tell the difference between the two different conditions (**Figure 1A**).

The Y-maze test was employed to measure spatial working memory and the exploratory behavior of mice. One-way ANOVA showed no significant effect of the treatments on arm visiting number ($F_{(3,55)} = 1.502$, $p = 0.225$), and no effect on number of correct visiting ($F_{(3,55)} = 1.502$, $p = 0.225$). As for the spontaneous alternation, one-way ANOVA showed a marginal effect of the treatments ($F_{(3,55)} = 1.914$, $p = 0.106$). *Post hoc* comparisons showed significant differences between CNT and CPZ groups, and between CNT and CPZ + Sham groups, but no difference between CNT and CPZ + rTMS groups (**Figure 1B**). The results suggest that rTMS blocked CPZ-induced decrease in spontaneous alternation.

Deep rTMS Attenuates the CPZ-Induced Myelin Breakdown and OL Loss in Mice

We measured and compared the MBP immunoreactivity in the FC and hippocampus of all mice in this study. It seemed that CPZ-feeding led to myelin breakdown in both FC and CA3 of the hippocampus, and this disruption was also seen in the mice of the CPZ + Sham group (**Figures 2A,B**). One-way ANOVA on the quantitative data indicated a significant effect of the treatments on MBP immunoreactivity in FC ($F_{(3,23)} = 3.546$, $p = 0.033$). *Post hoc* comparisons showed a significant difference between CNT and CPZ groups, but no difference between CNT and CPZ + Sham groups and between CNT and CPZ + rTMS groups. The differences between CPZ and CPZ + Sham groups and between CPZ and CPZ + rTMS groups are also significant (**Figure 2C**). As for the IOD of MBP immunoreactivity in CA3, one-way ANOVA indicated a significant effect of the treatments ($F_{(3,23)} = 16.925$, $p < 0.0001$). *Post hoc* comparisons showed significant differences between CNT and each of the other three groups. Also, the differences between the CPZ + rTMS group and CPZ or CPZ + Sham group are significant (**Figure 2C**).

In addition to demyelination and myelin breakdown, CPZ-feeding also led to OL loss in CC, CPU, and FC of the mouse brain. To check if deep rTMS applied in this study can reduce the CPZ-induced OL loss, we labeled mature OLs using the specific antibody to GST-π, a cytosolic isoenzyme used as a marker for mature OLs in the mammalian brain. **Figure 3A** showed many more GST-π positive cells in CC of the mice in the CNT group, whereas the cells were rarely seen in the same region of mice in the other three groups. One-way ANOVA against the quantitative data indicated a significant effect of the treatments on number of GST-π positive cells in the examined brain regions of CC ($F_{(3,27)} = 6.155$, $p = 0.003$), CPU ($F_{(3,27)} = 6.531$, $p = 0.002$), and FC ($F_{(3,27)} = 4.929$, $p = 0.008$). *Post hoc* comparisons indicated: (1) GST-π cells in CC and CPU significantly decreased in all CPZ-feeding mice (CPZ, CPZ + Sham, and CPZ + rTMS groups), but the number in FC of CPZ + rTMS group was comparable to that of CNT group; (2) rTMS significantly alleviated the CPZ-induced

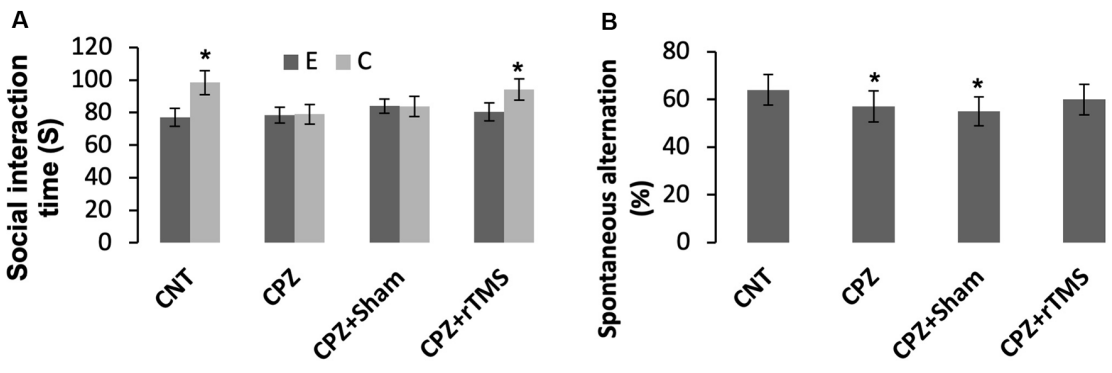

FIGURE 1 | Repetitive transcranial magnetic stimulation (rTMS) improves the behavioral performance of cuprizone (CPZ)-fed mice. **(A)** rTMS improves the performance of CPZ-fed mice in the social interaction test. **(B)** rTMS improves the working memory of CPZ-fed mice. Data are expressed as mean ± SD. *N* = 14/group. *$p < 0.05$, compared to E or compared to CNT.

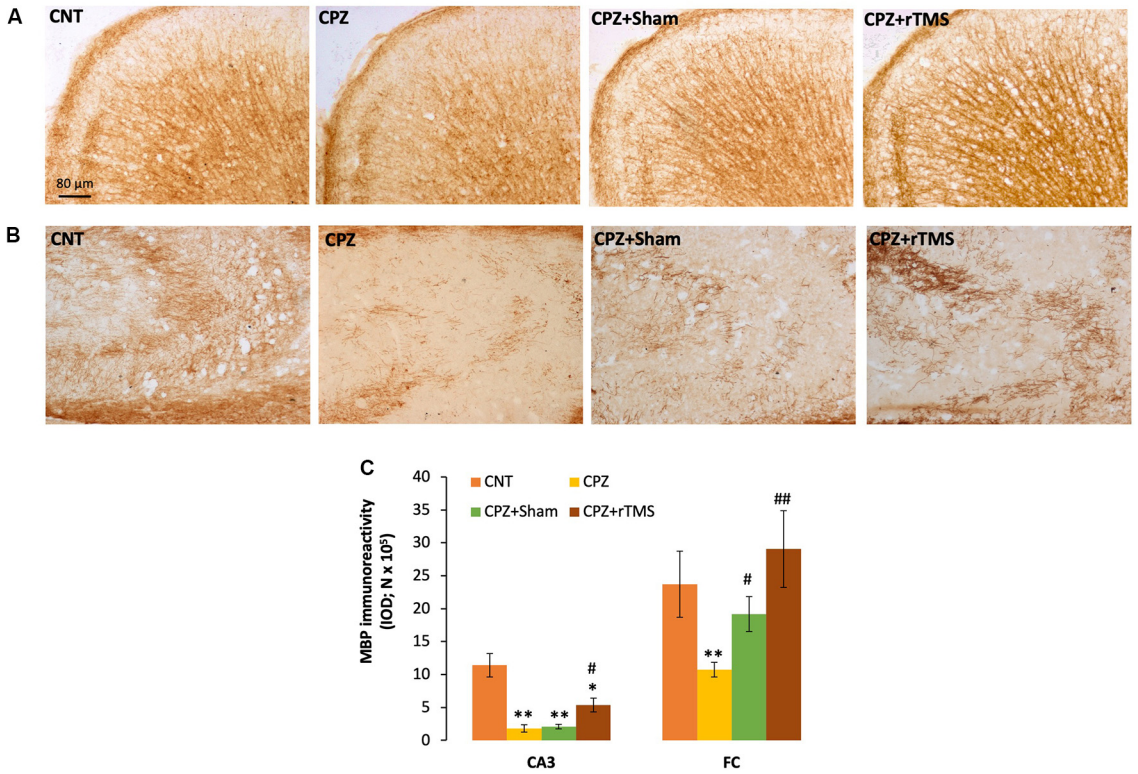

FIGURE 2 | rTMS alleviates the myelin breakdown in CA3 and frontal cortex (FC) of CPZ-fed mice. **(A,B)** Representative images show myelin basic protein (MBP) immunoreactivity in FC and CA3 of the hippocampus of mice from the four groups of CNT, CPZ, CPZ + Sham, and CPZ + rTMS, respectively. **(C)** The bar chart shows the statistical analytic results of quantified MBP immunoreactivity in the two brain regions of mice. Data are expressed as mean ± SD. N = 7/group. $^{*}p < 0.05$, $^{**}p < 0.01$, compared to CNT. $^{\#}p < 0.05$, $^{\#\#}p < 0.01$, compared to CPZ.

decrease in GST-π cells in CC and FC (CPZ + rTMS vs. CPZ), but not in CPU where the number of GST-π cells in CPZ + rTMS was comparable to those in CPZ and CPZ + Sham groups (**Figure 3B**).

Deep rTMS Blocks Microglia Activation and Expression Changes in Inflammatory Cytokines in CPZ-Fed Mice

Previous studies have shown microglia increase and activation along with OL loss in brains of CPZ-exposed mice (Zhang J. et al., 2018; Luo et al., 2020). The microglial activation may exacerbate OLs death and demyelination *via* releasing pro-inflammation cytokines such as IL-1β, IL-6, and TNF-α (Aryanpour et al., 2017; Zhang J. et al., 2018). Therefore, it is plausible to hypothesize that deep rTMS should reduce the CPZ-induced microglia activation and OL loss if it works. We labeled microglia using the antibody to IBA-1, a small protein specifically and constitutively expressed in all microglia (Imai et al., 1996; Ahmed et al., 2007).

Mice in the CPZ group showed many more IBA-1 positive cells in all three brain regions examined, but it was hard to tell differences among the other three groups based on qualitative observation only (**Figure 4A**). As such, we counted the number of IBA-1 positive cells and did comparisons on this parameter across all groups. One-way ANOVA results indicated a significant effect of the treatments on number of IBA-1 positive cells in the examined brain regions of CC ($F_{(3,27)}$ = 8.311, p = 0.001), CPU ($F_{(3,27)}$ = 7.807, p = 0.001), and FC ($F_{(3,27)}$ = 3.112, p = 0.045). *Post hoc* comparisons indicated: (1) CPZ group had many more IBA-1 positive cells (CPZ vs. CNT) in all three regions examined; (2) rTMS significantly alleviated the CPZ-induced increases in IBA-1 positive cells in all the three regions (CPZ + rTMS vs. CPZ); and (3) FC is the only region showing comparable numbers of IBA-1 positive cell between CPZ + Sham and CNT group (**Figure 4B**).

Furthermore, we measured some of the inflammatory cytokines in the brain regions of CPU, FC, and hippocampus of mice. The cytokines assessed in this study included pro-inflammatory ones of IL-1β and IL-6, plus IL-10, an anti-inflammatory one. One-way ANOVA results indicated a significant effect of the treatments on IL-1β levels in the examined brain regions of CPU ($F_{(3,27)}$ = 4.374, p = 0.014), FC ($F_{(3,27)}$ = 4.745, p = 0.01), and Hippocampus ($F_{(3,27)}$ = 10.691, $p < 0.0001$). *Post hoc* comparisons indicated: (1) mice in CPZ and CPZ + Sham groups showed significantly higher IL-1β levels in CPU, FC, and hippocampus compared to CNT group; (2) no

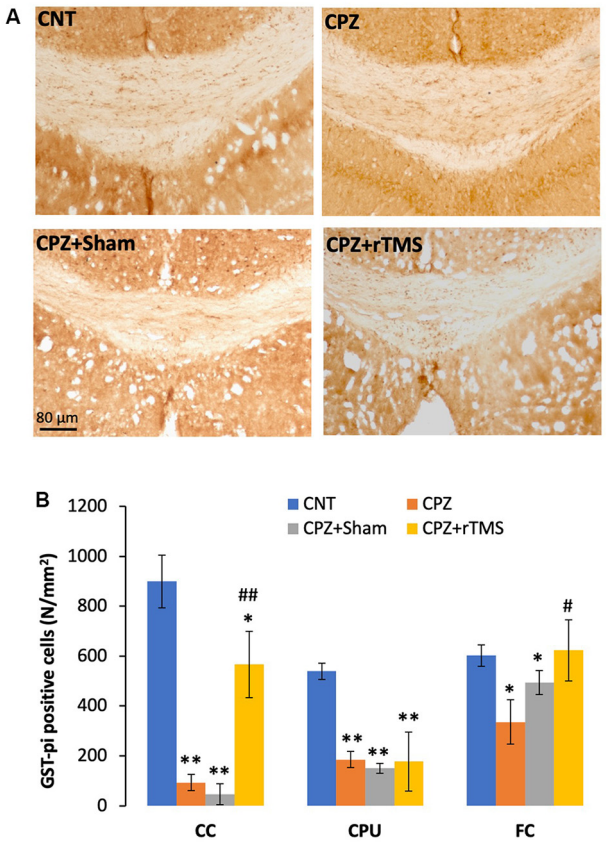

FIGURE 3 | rTMS alleviates OLs loss in corpus callosum (CC), caudate-putamen (CPU), and FC of CPZ-fed mice. **(A)** Representative images show glutathione-S-transferase (GST-π) positive cells in CC of mice from the four groups. **(B)** The bar chart shows the statistical analytic results of GST-π positive cell number in the three brain regions of the mice. Data are expressed as mean ± SD. $N = 7$/group. $^{*}p < 0.05$, $^{**}p < 0.01$, compared to CNT. $^{\#}p < 0.05$, $^{\#\#}p < 0.01$, compared to CPZ.

differences were found between CNT and CPZ + rTMS groups in this parameter in FC and hippocampus (**Figure 5A**).

As for IL-6 levels, one-way ANOVA results indicated a marginal effect of the treatments on this parameter in CPU ($F_{(3,27)} = 2.305$, $p = 0.106$), significant effects in FC ($F_{(3,27)} = 3.833$, $p = 0.025$) and Hippocampus ($F_{(3,27)} = 8.908$, $p < 0.0001$). *Post hoc* comparisons indicated: (1) mice in CPZ and CPZ + Sham groups showed significantly higher IL-6 levels in all the three brain regions compared to CNT group; and (2) no differences were found between CNT and CPZ + rTMS groups in this parameter (**Figure 5B**).

As for IL-10, one-way ANOVA results indicated no significant effect of the treatments on this parameter in CPU ($F_{(3,27)} = 0.820$, $p = 0.496$) and FC ($F_{(3,27)} = 0.054$, $p = 0.983$), but a significant effect in the Hippocampus ($F_{(3,27)} = 11.342$, $p < 0.0001$). *Post hoc* comparisons indicated: (1) all four groups showed comparable IL-10 levels in CPU; (2) the CPZ + rTMS group showed significantly higher IL-10 level than the other three groups; and (3) IL-10 level in the hippocampus was significantly higher in CPZ and CPZ + Sham groups compared to CNT group, but the CPZ + rTMS group was comparable to CNT group in this parameter (**Figure 5C**).

DISCUSSION

Following a recent study (Zhang J. et al., 2018), consuming a CPZ-containing diet for 5 weeks increased the anxiety level of mice in this study as evidenced by a significantly lower ratio of CD/TD in the CPZ group compared to the CNT group. This anxiety-like behavior was also seen in the CPZ + Sham group. However, rTMS treatment completely blocked the CPZ-induced anxiety in mice as the ratio of CD/TD in the CPZ + rTMS group was comparable to that in the CNT group, suggesting a protective effect of deep rTMS on the CPZ-induced anxiety in mice.

We noticed that the CPZ-containing diet did not change the performance of mice in the open-field test in some of the previous studies (Xu et al., 2009; Zhen et al., 2017). We compared the procedure details of the open-field tests performed in the present and previous studies and found that the open-field arena in previous studies was bigger (50 × 50 cm, or 53 × 53 cm) than that in the present study (25 × 25 cm). This difference may partly account for the inconsistency of the results from the present study and previous studies. In support of this speculation, the other two previous studies reported a decreased time and travel distance of CPZ-exposed mice in the central part of an open-field at dimensions of 25 × 25 cm (Zhang J. et al., 2018; Zhang L. et al., 2018). Therefore, the size of an open-field arena is an important factor influencing the performance of mice in this test.

Consuming a CPZ-containing diet for 5 weeks impaired the social recognition and spatial working memory of mice, which are consistent with the findings in previous studies (Xiao et al., 2008; Xu et al., 2009, 2010; Sun et al., 2018; Zhang J. et al., 2018). Moreover, the present study showed that rTMS completely blocked the CPZ-induced deficits in spatial memory and social recognition of mice, but the sham stimulation did not show this protective effect. In line with these results, a recent study reported that administration of high-frequency (gamma Hz) TBS for 6 weeks significantly alleviated schizophrenia-like behaviors in CPZ-fed mice, including improved nesting, social interaction, and sensorimotor gating, while low-frequency TBS only improved sensorimotor gating (Sun et al., 2018). Taken together, the data from the present and previous studies provided experimental evidence that deep rTMS is effective in preventing CPZ-induced behavioral abnormalities relevant to some of the symptoms seen in patients with schizophrenia.

Along with the behavioral improvement in CPZ-exposed mice, rTMS effectively alleviated CPZ-induced myelin breakdown and OL loss in CC, CPU, and hippocampus of mice in this study. These results are in line with a recent study in which both high-frequency and low-frequency TBS repaired the myelin sheath in CPZ-exposed mice (Sun et al., 2018). Relevantly, iGBS effectively enhanced neurogenesis in the dentate gyrus of mice while improved performance of the mice in spatial learning and memory (Zhang et al., 2014). Together, the results of the present study and previous studies suggest that deep rTMS affects a variety of target cells/cell structures in the brain thus improving higher functions of the

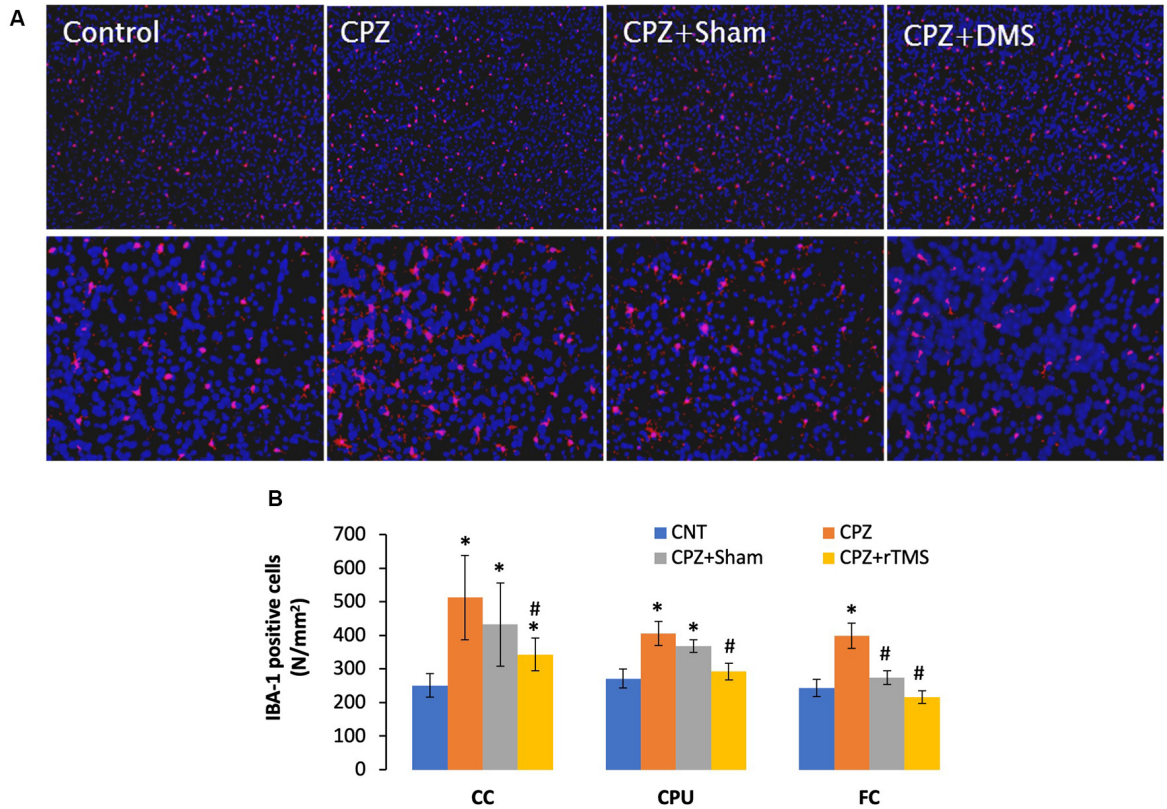

FIGURE 4 | rTMS alleviates microglia increase in CC, CPU, and FC of CPZ-fed mice. **(A)** Representative images show IBA-1 positive cells in FC of mice from the four groups. **(B)** The bar chart shows the statistical analytic results of IBA-1 positive cell numbers in the three brain regions of the mice. Data are expressed as mean ± SD. $N = 7$/group. $^{*}p < 0.05$, compared to CNT. $^{\#}p < 0.05$, compared to CPZ.

brain including cognitive function and emotional function. Therefore, the application of deep rTMS to animal studies has specific relevance to the beneficial effects of this new modality in human patients with neuropsychiatric diseases and may help to reveal the underlying mechanisms for the therapeutic effects of rTMS.

Of the four brain regions examined in this study, we noticed that the CPZ-induced myelin breakdown and OL loss in FC were completely blocked in the CPZ + rTMS group whereas the blockade was incomplete in CPU and hippocampus. This region-specific effect of deep rTMS may be related to the anatomical position of these brain regions, of which CPU and hippocampus are underneath FC. Another possible mechanism may be attributed to a more efficient self-repairing capacity of FC relative to the CPU and hippocampus. This superior self-repairing capacity is associated with the up-regulated levels of IL-10, an anti-inflammatory cytokine, in this region (discussion later).

Previous studies (Zhang et al., 2008; Zhang J. et al., 2018; Zhang et al., 2019; Shao et al., 2015; Zhen et al., 2017; Roboon et al., 2019) have shown that demyelination and OL loss in CPZ-exposed mice are accompanied with astrocyte and microglia activation. The microglial activation appeared even in the absence of demyelination (Roboon et al., 2019) or in the non-myelinolysis regions of the brain (Zhang et al., 2019), suggesting that microglial activation was not initiated by demyelination in the CPZ-exposed mice of these previous studies. On the other hand, activated microglia and inflammatory cytokines released from these cells may induce damage to neighboring neurons and glia, of which OLs are particularly susceptible (Peferoen et al., 2014). For example, intracerebral injection of lipopolysaccharide in young rats invokes activation of microglia and production of pro-inflammatory cytokines that ultimately leads to hypomyelination (Pang et al., 2003; Chew et al., 2013). Moreover, activated microglia arrest oligodendrocyte progenitor cell (OPC) proliferation and induce OPC death as seen in previous *in vitro* studies (Sherwin and Fern, 2005; Li et al., 2008). Considering all these previous findings, it is plausible to claim that deep rTMS alleviates myelin breakdown and OL loss *via* inhibiting microglia activation in the CPZ-exposed mice in the present study. In line with this interpretation, the alleviation of myelin breakdown and OL loss was parallel to the inhibition of microglia activation in the present study. Levels of the pro-inflammatory cytokines IL-1β and IL-6 increased in CPU, CTX, and hippocampus of all mice in CPZ and CPZ + Sham groups relative to the CNT group while these CPZ-exposed mice showed

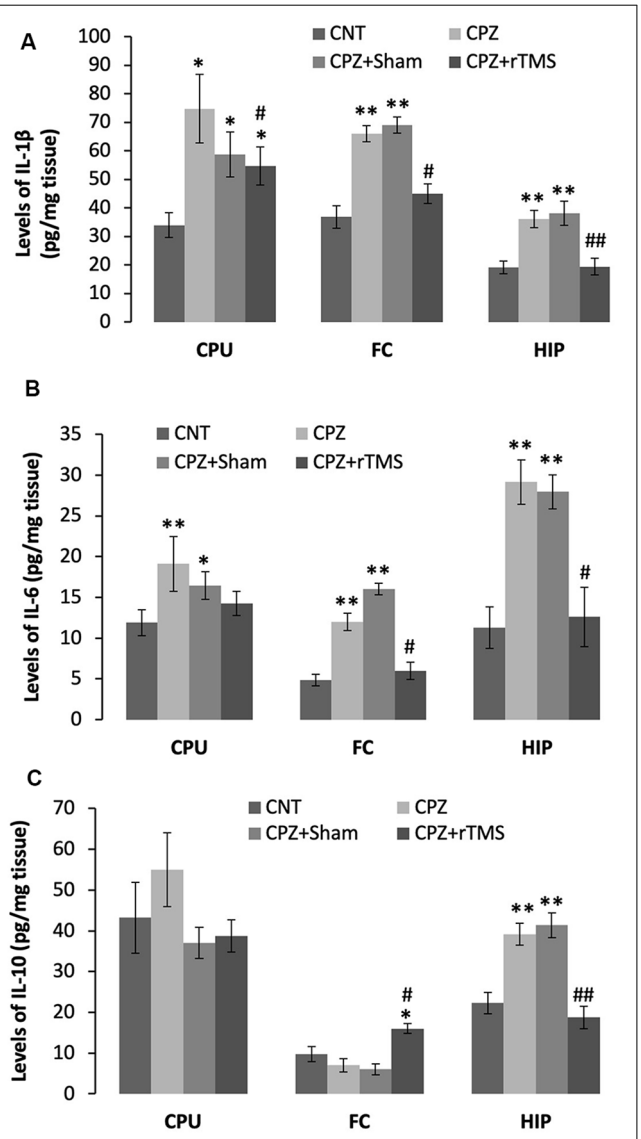

FIGURE 5 | rTMS alleviates the CPZ-induced changes in expression levels of inflammatory cytokines in CPU, FC, and HIP of mice. **(A)** The bar chart shows the statistical analytic results of IL-1β levels in the three brain regions of the mice. **(B)** The bar chart shows the statistical analytic results of IL-6 levels in the three brain regions of the mice. **(C)** The bar chart shows the statistical analytic results of IL-10 levels in the three brain regions of the mice. Data are expressed as mean ± SD. $N = 7$/group. $^{*}p < 0.05$, $^{**}p < 0.01$, compared to CNT. $^{\#}p < 0.05$, $^{\#\#}p < 0.01$, compared to CPZ.

obvious myelin breakdown and OL loss. But, levels of these cytokines in the CPZ + rTMS group were comparable to those in the CNT group, in parallel to alleviated myelin breakdown and OL loss in the examined regions. Relevant to the aforementioned findings in this study, a most recent animal study reported an anti-inflammation action of rTMS as evidenced by reduced levels of TNF-α, iNOS, IL-1β, and IL-6 in the hippocampus, and the decreases were associated with the antidepressant and anxiolytic-like effects in rats (Tian et al., 2020).

IL-10 is a pleiotropic cytokine showing a broad spectrum of anti-inflammatory properties (Moore et al., 2001). Previous human studies have associated lower IL-10 levels with MS severity and with the progressive stage of the disease (van Boxel-Dezaire et al., 1999; Petereit et al., 2003; Soldan et al., 2004). In a recent study, IL-10 suppressed the response of cultured microglia to recombinant granulocyte-macrophage colony-stimulating factor (Mayo et al., 2016). In the present study, consuming CPZ- containing diet for 5 weeks increased IL-10 level in the hippocampus, but not in CPU and FC, compared to the CNT group. Deep rTMS increased IL-10 level in FC, but not in CPU and hippocampus. These results are in line with a recent study, in which CPZ-treated mice showed a higher level of IL-10 in the hippocampus, but lower in CTX. The same study also showed that adenosine (10 mg/kg) increased IL-10 level in CTX but had no effect on IL-10 level in the hippocampus while promoted the remyelination process in the two brain regions of CPZ-treated mice (Zhang J. et al., 2018). Taken together, we may conclude that alleviations of CPZ-induced myelin breakdown and OL loss in FC by deep rTMS (in the present study) and adenosine (in a previous study) were associated with the up-regulation of IL-10 in this region while CPU and hippocampus did not show this up-regulation in response to deep rTMS and adenosine. Further studies are needed to address why these brain regions are different in terms of IL-10 levels in response to CPZ-exposure and rTMS treatment.

We are aware of the limitations of this study. First, it would be best to include two more animal groups of Control-sham and Control-rTMS to examine the possible effects of rTMS on normal healthy controls. Second, depressive-like behaviors could be tested if another batch of animals were included. Third, this study could not determine a causal relationship between microglial activation and levels of IL-1β, IL-6, and IL-10 in the examined regions of the mouse brain. And the role of IL-10 is undetermined. Fourth, there was no significant difference between CPZ + Sham and CPZ + rTMS groups regarding most of the examined indices in CPU, including numbers of GST-π and IBA-1 positive cells, as well as levels of IL-1β, IL-6, and IL-10. This is not surprising given that remyelination occurs spontaneously in demyelinated sites of CPZ-exposed mice. However, this phenomenon cannot be regarded as the argument against the conclusion that the administration of deep rTMS is of help in reducing the CPZ-induced neuropathological changes and/or promoting the recovery process of the subjects from the brain damage thus protecting the brain functions.

In conclusion, consuming a CPZ-containing diet for 5 weeks induced social interaction and spatial memory deficits and increased anxiety level in mice, along with myelin breakdown and OL loss in CC, CPU, FC, and hippocampus of the mouse brain. Deep rTMS for 4 weeks during the CPZ-exposure period effectively blocked the behavioral changes, myelin breakdown, and OL loss in CPZ-fed mice while inhibited microglia activation in the lesion sites and regulated the expression of inflammatory cytokines of IL-1β, IL-6, and IL-10 in the same brain regions. Relative to the other brain regions, FC is one that was protected most effectively by

deep rTMS in terms of neuropathological parameters. This region-specific difference may be related to the anatomical position of FC being over CPU and hippocampus and associated with the upregulated expression of IL-10 in this region. These data added experimental evidence for the beneficial effects of deep rTMS in treating behavioral abnormalities and improving the associated neuropathologic damage to the brain. Moreover, CPZ-exposed mice are a suitable animal model for exploring the neurobiological mechanisms underlying the beneficial effects of this non-invasive physical therapy in treating some of the neuropsychiatric disorders. In such contexts, this study is of particular relevance to the treatment of neuropsychiatric disorders, for which many extant medications are unsatisfactory and new therapeutic modalities are needed.

DATA AVAILABILITY STATEMENT

The raw data supporting the conclusions of this article will be made available by the authors, without undue reservation.

ETHICS STATEMENT

The animal study was reviewed and approved by Shantou University Medical College.

AUTHOR CONTRIBUTIONS

QH, LY, and HX conceived the study idea and designed the experiments. LY, YS, and FG carried out experiments and analyzed the data. YZ and HZ instructed the experiments and data analysis. LY and HX interpreted the results and wrote the manuscript. QH and HX revised the manuscript. All authors contributed to the article and approved the submitted version.

FUNDING

Funding for this research project was supported by a grant to QH from the Department of Science and Technology of Guang Dong Province (Special Fund 190823085553997).

REFERENCES

Acs, P., Selak, M. A., Komoly, S., and Kalman, B. (2013). Distribution of oligodendrocyte loss and mitochondrial toxicity in the cuprizone-induced experimental demyelination model. *J. Neuroimmunol.* 262, 128–131. doi: 10.1016/j.jneuroim.2013.06.012

Ahmed, Z., Shaw, G., Sharma, V. P., Yang, C., McGowan, E., and Dickson, D. W. J. (2007). Actin-binding proteins coronin-1a and IBA-1 are effective microglial markers for immunohistochemistry. *Histochem. Cytochem.* 55, 687–700. doi: 10.1369/jhc.6A7156.2007

Aryanpour, R., Pasbakhsh, P., Zibara, K., Namjoo, Z., Beigi Boroujeni, F., Shahbeigi, S., et al. (2017). Progesterone therapy induces an M1 to M2 switch in microglia phenotype and suppresses NLRP3 inflammasome in a cuprizone-induced demyelination mouse model. *Int. Immunopharmacol.* 51, 131–139. doi: 10.1016/j.intimp.2017.08.007

Buckley, P. F. (2019). Neuroinflammation and schizophrenia. *Curr. Psychiatry Rep.* 21:72. doi: 10.1007/s11920-019-1050-z

Chew, L. J., Fusar-Poli, P., and Schmitz, T. (2013). Oligodendroglial alterations and the role of microglia in white matter injury: relevance to schizophrenia. *Dev. Neurosci.* 35, 120–129. doi: 10.1159/000346157

Chung, S. W., Hoy, K. E., and Fitzgerald, P. B. (2015). Theta-burst stimulation: a new form of TMS treatment for depression? *Depress. Anxiety* 32, 182–192. doi: 10.1002/da.22335

De Picker, L. J., Morrens, M., Chance, S. A., and Boche, D. (2017). Microglia and brain plasticity in acute psychosis and schizophrenia illness course: a meta-review. *Front. Psychiatry* 8:238. doi: 10.3389/fpsyt.2017.00238

Grazioplene, R. G., Bearden, C. E., Subotnik, K. L., Ventura, J., Haut, K., Nuechterlein, K. H., et al. (2018). Connectivity-enhanced diffusion analysis reveals white matter density disruptions in first episode and chronic schizophrenia. *Neuroimage Clin.* 18, 608–616. doi: 10.1016/j.nicl.2018.02.015

Hallett, M. (2000). Transcranial magnetic stimulation and the human brain. *Nature* 406, 147–150. doi: 10.1038/35018000

Hayakawa, E., Ohgidani, M., Fujimura, Y., Kanba, S., Miura, D., and Kato, T. A. (2019). Cuprizone-treated mice, a possible model of schizophrenia, highlighting the simultaneous abnormalities of GABA, serine and glycine in hippocampus. *Schizophr. Res.* 210, 326–328. doi: 10.1016/j.schres.2019.06.010

Herring, N. R., and Konradi, C. (2011). Myelin, copper and the cuprizone model of schizophrenia. *Front. Biosci.* 3, 23–40. doi: 10.2741/s129

Hiremath, M. M., Saito, Y., Knapp, G. W., Ting, J. P., Suzuki, K., and Matsushima, G. K. (1998). Microglial/macrophage accumulation during cuprizone-induced demyelination in C57BL/6 mice. *J. Neuroimmunol.* 92, 38–49. doi: 10.1016/s0165-5728(98)00168-4

Huang, Y. Z., Rothwell, J. C., Lu, C. S., Wang, J., Weng, Y. H., Lai, S. C., et al. (2009). The effect of continuous theta burst stimulation over premotor cortex on circuits in primary motor cortex and spinal cord. *Clin. Neurophysiol.* 120, 796–801. doi: 10.1016/j.clinph.2009.01.003

Huang, Y. Z., Edwards, M. J., Rounis, E., Bhatia, K. P., and Rothwell, J. C. (2005). Theta burst stimulation of the human motor cortex. *Neuron* 45, 201–206. doi: 10.1016/j.neuron.2004.12.033

Imai, Y., Ibata, I., Ito, D., Ohsawa, K., and Kohsaka, S. (1996). A novel gene iba1 in the major histocompatibility complex class III region encoding an EF hand protein expressed in a monocytic lineage. *Biochem. Biophys. Res. Commun.* 224, 855–862. doi: 10.1006/bbrc.1996.1112

Ishikawa, S., Matsunaga, K., Nakanishi, R., Kawahira, K., Murayama, N., Tsuji, S., et al. (2007). Effect of theta burst stimulation over the human sensorimotor cortex on motor and somatosensory evoked potentials. *Clin. Neurophysiol.* 118, 1033–1043. doi: 10.1016/j.clinph.2007.02.003

Levkovitz, Y., Isserles, M., Padberg, F., Lisanby, S. H., Bystritsky, A., Xia, G., et al. (2015). Efficacy and safety of deep transcranial magnetic stimulation for major depression: a prospective multicenter randomized controlled trial. *World Psychiatry* 14, 64–73. doi: 10.1002/wps.20199

Li, J., Ramenaden, E. R., Peng, J., Koito, H., Volpe, J. J., and Rosenberg, P. A. (2008). Tumor necrosis factor α mediates lipopolysaccharide-induced microglial toxicity to developing oligodendrocytes when astrocytes are present. *J. Neurosci.* 28, 521–530. doi: 10.1523/JNEUROSCI.3995-07.2008

Liu, H., Zhai, J., Wang, B., and Fang, M. (2017). Olig2 silence ameliorates cuprizone-induced schizophrenia-like symptoms in mice. *Med. Sci. Monit.* 23, 4834–4840. doi: 10.12659/MSM.903842

Lu, L. X., Guo, S. Q., Chen, W., Li, Q., Cheng, J., and Guo, J. H. (2004). Effect of clozapine and risperidone on serum cytokine levels in patients with first-episode paranoid schizophrenia. *Di Yi Jun Yi Da Xue Xue Bao* 24, 1251–1254.

Luo, M., Deng, M., Yu, Z., Zhang, Y., Xu, S., Hu, S., et al. (2020). Differential susceptibility and vulnerability of brain cells in C57BL/6 mouse to mitochondrial dysfunction induced by short-term cuprizone exposure. *Front. Neuroanat.* 14:30. doi: 10.3389/fnana.2020.00030

Matsushima, G. K., and Morell, P. (2001). The neurotoxicant, cuprizone, as a model to study demyelination and remyelination in the central nervous system. *Brain Pathol.* 11, 107–116. doi: 10.1111/j.1750-3639.2001.tb00385.x

Mayo, L., Cunha, A. P., Madi, A., Beynon, V., Yang, Z., Alvarez, J. I., et al. (2016). IL-10-dependent Tr1 cells attenuate astrocyte activation and ameliorate chronic central nervous system inflammation. *Bain* 139, 1939–1957. doi: 10.1093/brain/aww113

Millet, V., Moiola, C. P., Pasquini, J. M., Soto, E. F., and Pasquini, L. A. (2009). Partial inhibition of proteasome activity enhances remyelination after cuprizone-induced demyelination. *Exp. Neurol.* 217, 282–296. doi: 10.1016/j.expneurol.2009.03.005

Miyaoka, T., Yasukawa, R., Yasuda, H., Hayashida, M., Inagaki, T., and Horiguchi, J. (2007). Possible antipsychotic effects of minocycline in patients with schizophrenia. *Prog. Neuropsychopharmacol. Biol. Psychiatry.* 31, 304–307. doi: 10.1016/j.pnpbp.2006.08.013

Miyaoka, T., Yasukawa, R., Yasuda, H., Hayashida, M., Inagaki, T., and Horiguchi, J. (2008). Minocycline as adjunctive therapy for schizophrenia: an open-label study. *Clin. Neuropharmacol.* 31, 287–292. doi: 10.1097/WNF.0b013e3181593d45

Moore, K. W., de Waal Malefyt, R., Coffman, R. L., and O'Garra, A. (2001). Interleukin-10 and the interleukin-10 receptor. *Ann. Rev. Immunol.* 19, 683–765. doi: 10.1146/annurev.immunol.19.1.683

Najjar, S., and Pearlman, D. M. (2015). Neuroinflammation and white matter pathology in schizophrenia: systematic review. *Schizophr. Res.* 161, 102–112. doi: 10.1016/j.schres.2014.04.041

Pang, Y., Cai, Z., and Rhodes, P. G. (2003). Disturbance of oligodendrocyte development, hypomyelination and white matter injury in the neonatal rat brain after intracerebral injection of lipopolysaccharide. *Brain Res. Dev. Brain Res.* 140, 205–214. doi: 10.1016/s0165-3806(02)00606-5

Pascual-Leone, A., Tarazona, F., Keenan, J., Tormos, J. M., Hamilton, R., and Catala, M. D. (1999). Transcranial magnetic stimulation and neuroplasticity. *Neuropsychologia* 37, 207–217. doi: 10.1016/s0028-3932(98)00095-5

Pasquini, L. A., Calatayud, C. A., Bertone Uña, A. L., Millet, V., Pasquini, J. M., and Soto, E. F. (2007). The neurotoxic effect of cuprizone on oligodendrocytes depends on the presence of pro-inflammatory cytokines secreted by microglia. *Neurochem. Res.* 32, 279–292. doi: 10.1007/s11064-006-9165-0

Peferoen, L., Kipp, M., van der Valk, P., van Noort, J. M., and Amor, S. (2014). Oligodendrocyte-microglia cross talk in the central nervous system. *Immunology* 141, 302–313. doi: 10.1111/imm.12163

Petereit, H. F., Pukrop, R., Fazekas, F., Bamborschke, S. U., Röpele, S., Kölmel, H. W., et al. (2003). Low interleukin-10 production is associated with higher disability and MRI lesion load in secondary progressive multiple sclerosis. *J. Neurol. Sci.* 206, 209–214. doi: 10.1016/s0022-510x(02)00420-3

Remington, L. T., Babcock, A. A., Zehntner, S. P., and Owens, T. (2007). Microglial recruitment, activation and proliferation in response to primary demyelination. *Am. J. Pathol.* 170, 1713–1724. doi: 10.2353/ajpath.2007.060783

Roboon, J., Hattori, T., Ishii, H., Takarada-Iemata, M., Le, T. M., Shiraishi, Y., et al. (2019). Deletion of CD38 suppresses glial activation and neuroinflammation in a mouse model of demyelination. *Front. Cell. Neurosci.* 13:258. doi: 10.3389/fncel.2019.00258

Shao, Y., Peng, H., Huang, Q., Kong, J., and Xu, H. (2015). Quetiapine mitigates the neuro- inflammation and oligodendrocyte loss in the brain of C57BL/6 mouse following cuprizone exposure for 1 week. *Eur. J. Pharmacol.* 765, 249–257. doi: 10.1016/j.ejphar.2015.08.046

Sherwin, C., and Fern, R. (2005). Acute lipopolysaccharide-mediated injury in neonatal white matter glia: role of TNF-a, IL-1b and calcium. *J. Immunol.* 175, 155–161. doi: 10.4049/jimmunol.175.1.155

Soldan, S. S., Alvarez Retuerto, A. I., Sicotte, N. L., and Voskuhl, R. R. (2004). Dysregulation of IL-10 and IL-12p40 in secondary progressive multiple sclerosis. *J. Neuroimmunol.* 146, 209–215. doi: 10.1016/j.jneuroim.2003.10.033

Spronk, D., Arns, M., and Fitzgerald, P. B. (2011). "Repetitive transcranial magnetic stimulation in depression: protocols, mechanisms and new developments," in *Neurofeedback and Neuromodulation Techniques and Applications*, eds R. Coben and J. R. Evans Fitzgerald (San Diego, CA: Elsevier), 257–291.

Stidworthy, M. F., Genoud, S., Suter, U., Mantei, N., and Franklin, R. J. (2003). Quantifying the early stages of remyelination following cuprizone-induced demyelination. *Brain Pathol.* 13, 329–339. doi: 10.1111/j.1750-3639.2003.tb00032.x

Sun, Z., Jiang, T., Wu, Y., Ma, C., He, Y., and Yang, J. (2018). Low field magnetic stimulation ameliorates schizophrenia-like behavior and up-regulates neuregulin-1 expression in a mouse model of cuprizone-induced demyelination. *Front. Psychiatry* 9:675. doi: 10.3389/fpsyt.2018.00675

Tian, L., Sun, S. S., Cui, L. B., Wang, S. Q., Peng, Z. W., Tan, Q. R., et al. (2020). Repetitive transcranial magnetic stimulation elicits antidepressant and anxiolytic-like effect *via* nuclear factor-E2-related factor 2- mediated anti-inflammation mechanism in rats. *Neuroscience* 429, 119–133. doi: 10.1016/j.neuroscience.2019.12.025

van Boxel-Dezaire, A. H., Hoff, S. C., van Oosten, B. W., Verweij, C. L., Dräger, A. M., Adèr, H. J., et al. (1999). Decreased interleukin-10 and increased interleukin-12p40 mRNA are associated with disease activity and characterize different disease stages in multiple sclerosis. *Ann. Neurol.* 45, 695–703. doi: 10.1002/1531-8249(199906)45:6<695::aid-ana3>3.0.co;2-r

van Erp, T. G., Hibar, D. P., Rasmussen, J. M., Glahn, D. C., Pearlson, G. D., Andreassen, O. A., et al. (2016). Subcortical brain volume abnormalities in 2028 individuals with schizophreniaand 2,540 healthy controls *via* the ENIGMA consortium. *Mol. Psychiatry* 21, 547–553. doi: 10.1038/mp.2015.63

Xiao, L., Xu, H., Zhang, Y., Wei, Z., He, J., Jiang, W., et al. (2008). Quetiapine facilitates oligodendrocyte development and prevents mice from myelin breakdown and behavioral changes. *Mol. Psychiatry* 13, 697–708. doi: 10.1038/sj.mp.4002064

Xu, H., Zhang, H., Zhang, J., Huang, Q., Shen, Z., and Wu, R. (2016). Evaluation of neuron-glia integrity by *in vivo* proton magnetic resonance spectroscopy: implications for psychiatric disorders. *Neurosci. Biobehav. Rev.* 71, 563–577. doi: 10.1016/j.neubiorev.2016.09.027

Xu, Z., Adilijiang, A., Wang, W., You, P., Lin, D., Li, X., et al. (2019). Arecoline attenuates memory impairment and demyelination in a cuprizone-induced mouse model of schizophrenia. *Neuroreport* 30, 134–138. doi: 10.1097/WNR.0000000000001172

Xu, H., Yang, H. J., McConomy, B., Browning, R., and Li, X. M. (2010). Behavioral and neurobiological changes in C57BL/6 mouse exposed to cuprizone: effects of antipsychotics. *Front. Behav. Neurosci.* 4:8. doi: 10.3389/fnbeh.2010.00008

Xu, H., Yang, H. J., Zhang, Y., Clough, R., Browning, R., and Li, X. M. (2009). Behavioral and neurobiological changes in C57BL/6 mice exposed to cuprizone. *Behav. Neurosci.* 123, 418–429. doi: 10.1037/a0014477

Xuan, Y., Yan, G., Wu, R., Huang, Q., Li, X., and Xu, H. (2015). The cuprizone-induced changes in ^{1}H-MRS metabolites and oxidative parameters in C57BL/6 mouse brain: effects of quetiapine. *Neurochem. Int.* 90, 185–192. doi: 10.1016/j.neuint.2015.08.015

Yang, H. J., Wang, H., Zhang, Y., Xiao, L., Clough, R. W., Browning, R., et al. (2009). Region-specific susceptibilities to cuprizone- induced lesions in the mouse forebrain: implications for the pathophysiology of schizophrenia. *Brain Res.* 1270, 121–130. doi: 10.1016/j.brainres.2009.03.011

Zhang, J., Yang, L., Fang, Z., Kong, J., Huang, Q., and Xu, H. (2018). Adenosine promotes the recovery of mice from the cuprizone-induced behavioral and morphological changes while effecting on microglia and inflammatory cytokines in the brain. *J. Neuroimmune Pharmacol.* 13, 412–425. doi: 10.1007/s11481-018-9799-0

Zhang, L., Xu, S., Huang, Q., and Xu, H. (2018). *N*-acetylcysteine attenuates the cuprizone-induced behavioral changes and oligodendrocyte loss in male C57BL/7 mice *via* its anti-inflammation actions. *J. Neurosci. Res.* 96, 803–816. doi: 10.1002/jnr.24189

Zhang, Y., Cai, L., Fan, K., Fan, B., Li, N., Gao, W., et al. (2019). The spatial and temporal characters of demyelination and remyelination in the cuprizone animal model. *Anat. Rec.* 302, 2020–2029. doi: 10.1002/ar.24216

Zhang, Y., Xu, H., Jiang, W., Xiao, L., Yan, B., He, J., et al. (2008). Quetiapine alleviates the cuprizone-induced white matter pathology in the brain of C57BL/6 mouse. *Schizophr. Res.* 106, 182–191. doi: 10.1016/j.schres.2008.09.013

Zhang, Y., Mao, R. R., Chen, Z. F., Tian, M., Tong, D. L., Gao, Z. R., et al. (2014). Deep-brain magnetic stimulation promotes adult hippocampal

neuro-genesis and alleviates stress-related behaviors in mouse models for neuropsychiatric disorders. *Mol. Brain* 7:11. doi: 10.1186/1756-6606-7-11

Zhen, J., Qian, Y., Fu, J., Su, R., An, H., Wang, W., et al. (2017). Deep brain magnetic stimulation promotes neurogenesis and restores cholinergic activity in a transgenic mouse model of Alzheimer's disease. *Front. Neural Circuits* 11:48. doi: 10.3389/fncir.2017.00048

Zheng, W., Cai, D. B., Yang, X. H., Ungvari, G. S., Ng, C. H., Müller, N., et al. (2017). Adjunctive celecoxib for schizophrenia: a meta-analysis of randomized, double-blind, placebo-controlled trials. *J. Psychiatr. Res.* 92, 139–146. doi: 10.1016/j.jpsychires.2017.04.004

Conflict of Interest: The authors declare that the research was conducted in the absence of any commercial or financial relationships that could be construed as a potential conflict of interest.

frontiers in Psychiatry

ORIGINAL RESEARCH
published: 23 November 2020
doi: 10.3389/fpsyt.2020.544540

Acute Exposure to the Cold Pressor Stress Impairs Working Memory Functions: An Electrophysiological Study

Zengyou Xin[1,2,3†], *Simeng Gu*[2,4†], *Lei Yi*[5], *Hong Li*[2,5*] *and Fushun Wang*[2*]

[1] *Brain and Cognitive Neuroscience Research Center, Liaoning Normal University, Dalian, China,* [2] *Institute of Brain and Psychological Sciences, Sichuan Normal University, Chengdu, China,* [3] *School of Education Science, Minnan Normal University, Zhangzhou, China,* [4] *Department Medical Psychology, Jiangsu University Medical School, Zhenjiang, China,* [5] *College of Psychology and Sociology, Shenzhen University, Shenzhen, China*

OPEN ACCESS

Edited by:
Haiyun Xu,
Wenzhou Medical University, China

Reviewed by:
Fleur Margaret Howells,
University of Cape Town, South Africa
Kurt Leroy Hoffman,
Autonomous University of Tlaxcala, Mexico

***Correspondence:**
Hong Li
lihongszu@szu.edu.cn
Fushun Wang
13814541138@163.com

† These authors have contributed equally to this work

Specialty section:
This article was submitted to Molecular Psychiatry, a section of the journal Frontiers in Psychiatry

Received: *21 March 2020*
Accepted: *22 October 2020*
Published: *23 November 2020*

Citation:
Xin Z, Gu S, Yi L, Li H and Wang F (2020) Acute Exposure to the Cold Pressor Stress Impairs Working Memory Functions: An Electrophysiological Study. Front. Psychiatry 11:544540. doi: 10.3389/fpsyt.2020.544540

The results of previous literature focusing on the effects of acute stress on human working memory (WM) are equivocal. The present study explored the effects of acute stress on human WM processing using event-related potential (ERP) techniques. Twenty-four healthy participants were submitted to stressful treatments and control treatment at different times. Cold pressor stress (CPS) was used as stressful treatment, while warm water was used as the control treatment before the WM task. Exposure to CPS was associated with a significant increase in blood pressure and salivary cortisol. After the 3-min resting period, systolic blood pressure (SBP) and diastolic blood pressure (DBP) for the CPS session significantly increased relative to the control treatment session (all $p \leq 0.01$), and data also showed a significant increase of 20-min post-treatment cortisol concentration ($p < 0.001$) for CPS. Data from the CPS session showed significantly longer reaction times, lower accuracy, and WM capacity scores than that of the control treatment session. Interestingly, a difference between the two sessions was also found in N_2pc and the late contralateral delay activity (late CDA) components. Specifically, although non-significant main effects of treatment were found for N_2pc amplitudes, there was a significant interaction between treatments and stimuli conditions (processing load) [$F_{(2,46)} = 3.872$, $p = 0.028$, $\eta 2$ $p = 0.14$], which showed a pronounced trend toward equalization of N_2pc amplitude across stimuli conditions during the CPS session clearly different from that of control treatment. As for amplitudes for late CDA, a nearly significant main effect of Treatment was found ($p = 0.069$). That is, the mean amplitude of the late CDA (-2.56 ± 0.27) for CPS treatment was slightly larger than that (-2.27 ± 0.22) for warm water treatment. To summarize, this study not only reported performance impairments in the WM task during CPS trials but also provided high temporal resolution evidence for the detrimental effects of acute stress on processes of information encoding and maintenance.

Keywords: acute stress, working memory (WM), contralateral delay activity (CDA), prefrontal cortex (PFC), N_2pc

INTRODUCTION

The acute stress response is associated with a number of neurochemical responses that trigger the release of various hormones and neurotransmitters, which, acting as neuromodulators, can change cellular properties of large-scale neuronal populations throughout the brain (1). We have shown that a stressful event can induce the release of many stress hormones and neuromodulators (2). In recent years, studies have shown that exposure of humans to acute stressors influences cognitive processing and performance [e.g., (3–5)]. Acute stress used in these studies refers to participants' psychobiological response to a brief laboratory stress induction paradigm, such as cold water pressure [also called cold pressor stress (CPS); e.g., (6)], the Trier Social Stress Test [TSST; (7)], short film clips [e.g., (8, 9)], and so on.

Working memory (WM) is responsible for holding a limited amount of information active for a short time span and is also important for optimal functioning of the executive control involved in filtering out irrelevant information, a function that seems to be particularly important under stressful conditions (3, 9). Up until now, some researchers have focused specifically on the effects of acute stress on human WM and the available data are equivocal. Literature shows that human WM performance after acute stress can be impaired (5, 9–14), as well as improved, not affected, or both improved and impaired (3, 6, 8, 15–20).

These studies suggest that acute stress can affect WM, but the impact direction needs to be further clarified. Thus, the main objective of this study was to investigate how acute stress modulates WM process. Several factors may contribute to the inconsistent findings. Firstly, individual differences, such as the gender and the age of the participant, may moderate the findings because of relevant hormonal fluctuations (9, 20, 21). Secondly, the WM task employed may be attributed to the lack of consistency (5, 14, 22). Thirdly, duration, intensity of exposure, and method used to induce acute stress may mediate the effects on WM (5, 14). Other reasons for these discrepancies may include the time course of stress induction or measurement of WM process (3, 9, 13, 14, 22).

According to the attentional control theory [ACT; (23, 24)], WM function is related to the inhibiting efficiency of task-irrelevant information. Improved (or deficient) inhibition control function mainly promotes (or impairs) processing efficiency, which may not be reflected in task performance explicitly. Thus, the focus of this study should further shift to the effects of acute stress on WM process. In many of the studies exploring the stress–WM relationship mentioned above, reaction time (RT) and performance accuracy have been used as the only indices, which have been criticized broadly, as both measure the outcome of processing rather than processing *per se* (24, 25). As far as we know, at least two studies have shown no effects of acute stress on performance, but significant effects on neuroimaging measures with contradictory findings (17, 18), which suggest that acute stress may influence various neural processes and it is imperative to delineate in detail the underlying mechanisms of stress-related WM performance using a variety of methods. However, studies investigating the neural mechanism of acute stress effect on human WM are relatively limited (6, 8, 9, 17, 18, 20). Most of the findings show that acute stress increases human fronto-parietal activity (20) and the regional oxygen saturation of the frontal lobes (6), or results in larger signal change in PFC from baseline (17), or reduces activity in the medial temporal lobe (8) during WM tasks, which are assumed to support WM processing. However, Qin et al. (18) showed that acute stress resulted in significantly reduced WM-related activity in the dorsolateral prefrontal cortex and less deactivation in DMN, which is assumed to disrupt WM processing. Additionally, there are two electrophysiological studies concerning acute stress effect on WM that report inconsistent findings. Gärtner et al. (9) recorded frontal theta activity (4–8 Hz) during the performance of 2- and 3-back tasks, and showed that WM-related frontal theta activity and task performance were decreased under acute stress. Another study concerned only frontal alpha activity and did not report any acute stress effect on parietal alpha power, but a beneficial effect of stress on RT without decreasing accuracy (6). Interestingly, similar to the results of behavioral and neuroimaging studies, the two experiments provided contradictory findings and were carried out by using frequency-domain features of the EEG signal and not specially designed to investigate stress effects on the whole dynamic course of WM processing. Thus, controlling the potential extraneous factors mentioned earlier, by virtue of the high temporal resolution advantages of EEG, analysis of time-domain features of the event-related potentials (ERPs) was used in the present study to directly explore the time course during which acute stress modulates WM processing.

Vogel and colleagues (26–28) described an ERP component, the contralateral delay activity (CDA), with a 300–900-ms window after the onset of the memory array, which was a sustained negative voltage at posterior electrodes during the maintenance phase of WM. The amplitude of the CDA increases with the number of representations held in WM and reaches an asymptote at an individual's WM capacity. Therefore, the CDA can be used as a neurophysiological marker of the numbers of task-relevant and -irrelevant items held in visual WM during the retention interval and can be used to judge how the subject's WM function is going on by comparing the amplitudes for memory arrays with or without distractors.

The paradigm used by Vogel and colleagues was adopted in this study, and ERP components were analyzed that indexed attentional selection of the stimuli [the N_2pc component; (29)], object identification [the early CDA component; (30)], and the maintenance of WM representations [the late CDA component; (30)].

Studies have revealed a strong relationship between selective attention and visual WM, such that not only attention is biased by what is on our mind, but selective attention determines what is to be recoded, stored, and processed later (31). Representation of task-relevant information at hand is active and within the focus of central executive processes, which means that it was selected by suppressing the irrelevant and gained full access to be further processed. N_2pc, a negative component at the posterior sites, is associated with selective attention, reflecting the top-down guided attentional selection toward the relevant information (32) and object individuation (33, 34). Using visual

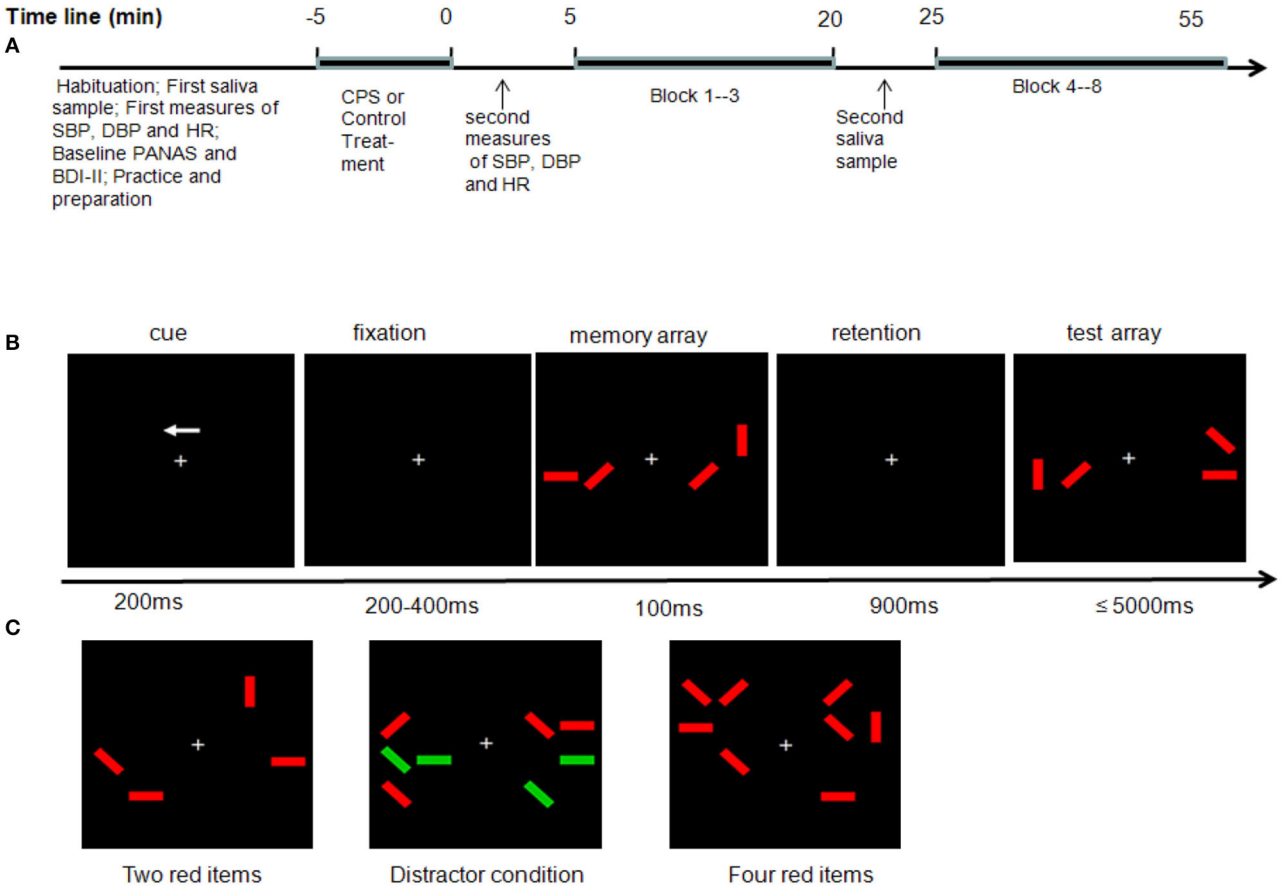

FIGURE 1 | Experimental procedure, stimuli sequence, and array types. **(A)** Timeline of the experimental session. **(B)** Example of two red item conditions in a change trial in which the orientations of the red rectangles in the left hemifield are to be remembered. **(C)** Three task conditions.

search task, Sänger et al. (35) investigated the effects of acute stress on selective attention and showed that acute stress impaired the attentional allocation and resulted in a reduced N_2pc. Because participants had no advanced information about the location of the targets under this paradigm, the orienting of attention involved processing competition between goal-driven and stimulus-driven, of which the former was vulnerable to stress exposure. Thus, according to the authors, N_2pc was decreased significantly for the stressed participants. In the present study, subjects switched their attention to target side in advance (according to cues) and thus N_2pc component reflected more about processing of object individuation. Mather et al. (36) proposed an "NE hot spots" model, according to which acute stress induces high norepinephrine (NE) level, which can induce fear and anger emotions or fight or flight behaviors (37, 38) and can bias perception and WM in favor of more salient information representations, i.e., stimuli-driven process. In the paradigms of Vogel et al. (28) and Qi et al. (30), distractors are highly salient since their luminance is higher than that of the target items (see **Figure 1C**). Thus, in the distractor condition, more objects would be involved in the individuation process, and N_2pc under acute stress would therefore be expected to be greater than under control treatment.

The early and the late CDA components were first proposed by Qi et al. (30), which referred to the early and the late time windows (split at about 450 ms post-stimuli) of the CDA (26–28). Qi et al. (30) proposed that the early CDA might reflect object identification after object individuation, which involved object categorizing in greater detail, and we explored this component as well. The late CDA component in accordance with Vogel et al. (27, 28), was thought to reflect the maintenance of information in WM (30). As reviewed earlier, acute stress improves or impairs WM task performance and the processing of WM-related neural networks. According to the paradigms of Vogel et al. (28) and Qi et al. (30), if it impairs WM processes, an increased amplitude of CDA would be expected because of deficient inhibition control, and as a result, the number of representations would increase due to the coding and storage of task-irrelevant information. However, if the contrary is the case, an intact or slightly smaller amplitude of CDA would be present because of high-efficient inhibition of irrelevant information. According to Luck and Vogel (39), visual WM has a representational limit of about three to four objects. Thus, WM processing in high-load trials

of the present study approaches or reaches the limit, while sufficient resources can be allocated under low-load trials (see **Figure 1**). Therefore, larger CDA amplitude changes would be expected under low-load trials after stress relative to control treatment. Given that behavioral indices reflect the processing outcome rather than processing efficiency, we predict that WM performance would be more prone to be affected by acute stress during the more challenging trials.

METHODS

Participants

Thirty female volunteers participated in the present study. Two participants were excluded because of excessive eye movements in the cue–target interval, and four other participants dropped out. Thus, data from 24 participants between 18 and 23 years (mean age = 20.1, SD = 1.1 years) were included in the analyses. They were all in good physical health, medication-free, non-smokers, right-handed, and with normal or corrected-to-normal vision. Only women during their luteal phase (with regular menstrual cycles, day 18–25) were included to control possible gender and ovarian cycle effects on adrenocortical reactivity (40, 41). None of them had a history of neurological or psychiatric disorders. Moreover, participants were asked to refrain from caffeine and alcohol within 4 h before the experimental sessions. The volunteers were recruited by announcements and received financial compensation. The study was approved by the Ethics Committee of the Sichuan Normal University. All of them gave their written informed consent prior to their inclusion in the study.

Procedure and Stimuli

After a participant's arrival, she was allowed to rest briefly, and then a pre-experimental saliva (cortisol) measurement was taken, and systolic blood pressure (SBP), diastolic blood pressure (DBP), and heart rate (HR) were recorded at the same time. Then, participants filled out the Positive and Negative Affect Schedule [PANAS; (42)] and Beck Depression Inventory-Second Edition [BDI-II; (43)], and all participants also filled out the Trait Anxiety Inventory test (44) during their first experimental session. Then, participants were exposed to either the CPS treatment or the warm water control treatment. Immediately after treatment, all subjects had to rest for 3 min and then SBP, DBP, and HR were measured. Then, subjects were engaged in the WM task. Further saliva samples were taken immediately after the third block was finished, about 20 min after the onset of the treatment (**Figure 1A**).

During the WM task, participants were seated comfortably about 75 cm from a 19-in. screen in an electromagnetically shielded room. They performed a lateralized change detection task, adopted from Qi et al. (30), in which they were cued to remember the visual stimuli on one side of the display and ignore the other side. In each trial (**Figures 1B,C**), the participants were presented with a brief bilateral array of colored rectangles of varying orientations (vertical, horizontal, left 45°, and right 45°). The stimulus positions and orientations were randomized. The numbers of targets and distractors were the same in both hemifields and only the location of the stimuli could differ between hemifields. The task was to remember the orientations only of the red items and to ignore the green ones in either the left or the right hemifield, depending on the cue presented. Green distractors were more physically salient than the red items, as the luminance of green was higher than that of red. There were three types of stimuli arrays (**Figure 1C**). In the two-red-items condition, only two red items were shown on each side of the display. In the four-red-items condition, only four red items were shown on each side. In the distractor condition, two red items along with two green distractors were shown on each side.

Each trial began with a 200-ms arrow presented above a fixation cross (**Figure 1B**). The arrow cued participants to remember the orientations of only red items in either the left or the right side of the memory array. Following a variable interval of 200–400 ms, a memory array was presented for 100 ms. The memory array was removed from the display for 900 ms (retention period). The test array was then displayed for a maximum of 5,000 ms. Participants responded by pressing one of two vertically aligned keys as soon as possible to indicate whether or not a change was present. On one half of the trials, the memory and test arrays were identical, whereas on the other half, the orientation of a single red rectangle within the to-be-remembered side of the memory array was different from its orientation in the test array. Key allocations were counterbalanced between the participants. The instructions emphasized accuracy rather than speed. Moreover, participants were also instructed to keep their eyes fixated throughout the task. The intertrial interval was 2,000 ms. Eight blocks were presented, and each block included 60 trials, in which the three types of memory array were randomly assigned. Overall, participants experienced 160 trials for each type and took ∼45 min.

This experiment was conducted by adopting a within-subject design, in which CPS and control treatment were, respectively, applied to subjects by an interval of at least 24 h, and treatment order was counterbalanced. Subjects were instructed to submerge their feet in ice-cold water (4–7°C) for 5 min for the CPS session while in warm water (37–40°C) during control treatment. To avoid any influence of the circadian profiles of adrenocortical reactivity and cognitive ability, CPS and control treatment were conducted in the same time period of the experiment day, and the other experimental procedures were the very same.

The method of salivary cortisol measurement was described in Yang et al. (45). All salivary samples were stored at −40°C, and analyses were completed within about 1 month.

EEG Recording and Processing

Brain electrical activity was recorded at 64 scalp sites using Ag/AgCl electrodes mounted on an elastic cap (Brain Product, München, Germany), with references on FCz, and a ground electrode on the medial frontal aspect. Vertical electrooculograms (EOGs) were recorded supra- and infra-orbitally at the left eye. The horizontal EOG was recorded from the left vs. right orbital rim. The EEG and EOG were amplified using a 0.05–100-Hz bandpass and were continuously digitized at 1,000 Hz/channel. All interelectrode impedances were maintained below 5 kΩ. Offline, the data were referenced to the

average of the left and right mastoids, low-pass-filtered at 30 Hz and a roll-off of 12 dB/octave, segmented (−200 to 900 ms from the onset of the memory array), and baseline-corrected (200 ms). Trials containing saccades (horizontal EOG exceeding ± 30 μV), blinks (Fpz exceeding ± 60 μV, vertical EOG exceeding ± 75 μV), or muscle artifacts (all other electrodes exceeding ± 75 μV) were removed from further analyses. In addition, we performed extra checks according to the procedures described by Qi et al. (30), to assess the potential effects of the residual horizontal-EOG activity on the target ERP components and the data showed that our N_2pc or CDA results cannot be explained by the residual EOGs. Each correct segment was averaged for each condition separately.

Measures and Analyses

The primary behavioral measure was WM capacity, an estimation of the amount of retrievable objects. Pashler's formula was used because the task in this study used whole-display probes (30, 46). Specifically, K = N × (HR – FA)/(1 – FA), where K is WM capacity, N is the number of to-be-remembered items, HR is the hit rate, and FA is the false alarm rate. We also computed WM capacity for the distractor condition by filling in 2 for N, because of the two target items (47). In addition, the behavioral measures also included (1) RTs for correct detections and (2) response accuracy.

The analysis of the underlying neural mechanisms focused on lateralized ERP components elicited by the memory array. The averaged epoch for the ERPs was 1,100 ms, including 200-ms pre-memory-array and 900-ms post-memory-array onset. Separate averages were computed for each participant in each of the three different conditions and for contralaterality (electrode contralateral vs. ipsilateral to the location of memory arrays). Contralateral waveforms were calculated as the average of the left-sided electrodes to the right-sided items and of the right-sided electrodes to the left-sided items. Ipsilateral waveforms were calculated as the average of the left-sided electrodes to the left-sided objects and of the right-sided electrodes to the right-sided objects (28, 30). The lateralized ERP components were then computed by subtracting the mean amplitudes of the ipsilateral waveform from those of the contralateral waveform. On the basis of previous work (28, 30, 48), mean activity from four pairs of lateral posterior electrode sites (P3/4, P5/6, PO3/4, and PO7/8) were used to calculate the lateralized ERP components. **Figure 2** depicts the lateralized ERP waveforms for the three conditions and the two treatments separately at these electrode pairs. Given the previous studies (28, 30, 48) and our data, three measurement windows were selected: 230–310 ms (N_2pc component), 310–450 ms (early-CDA component), and 450–900 ms (late CDA component) after the onset of the memory array, and the resulting mean amplitudes were calculated for further analysis.

In order to meet the normality assumption according to Shapiro–Wilk test, we conducted logarithmic transformation for data of emotion questionnaires and Box–Cox transformation for all electrophysiological data. Then, all the data were assessed using repeated-measures ANOVA by SPSS version 19.0, and necessary adjustments were made where assumptions were violated (e.g., by using Greenhouse–Geisser degrees of freedom corrections).

RESULTS

Mood, Trait Anxiety, and Physiological Measurements

To evaluate potential differences in mood variables between the CPS and the control sessions, and effects of stress induction, repeated-measures ANOVA was conducted with Treatment (CPS vs. control) as a repeated measure (**Table 1**). The ANOVA showed no difference for mood, basal HR, basal blood pressure, and basal cortisol concentration between the CPS and control sessions. However, results showed significant effect of treatment for post-resting blood pressure. That is, after the 3-min resting period, SBP and DBP for the CPS session significantly increased relative to the control treatment session (all $p = 0.01$). Data also showed significant effect of treatment for 20-min post-treatment cortisol concentration ($p < 0.001$). Moreover, results of anxiety test demonstrated that all participants are of moderate level of trait anxiety (mean = 42.2, SD = 6.2).

Behavioral Results

Repeated-measures ANOVAs were conducted with two within-subject factors: Treatment (CPS vs. control) and Condition (two red items, four red items, and the distractor condition), focusing on WM capacity scores, RT for correct detections, and accuracy. The ANOVA showed significant main effects of Treatment [$F_{(1,23)} = 9.39$, $p = 0.005$, $\eta 2\ p = 0.29$] and Condition [$F_{(2,46)} = 141.97$, $p = 0.000$, $\eta 2\ p = 0.86$], and interaction of Treatment × Condition [$F_{(2,46)} = 3.65$, $p = 0.034$, $\eta 2\ p = 0.14$] for WM capacity. Further analysis showed significant differences between CPS and control treatment only in four red items (2.53 ± 0.09 vs. 2.70 ± 0.09, $p = 0.029$) and distractor condition (1.53 ± 0.03 vs. 1.61 ± 0.02; $p = 0.002$). WM capacity for two red items also decreased after CPS treatment but did not reach statistical significance ($p = 0.818$). Repeated-measures ANOVA showed significant main effects of Treatment [$F_{(1,23)} = 11.34$, $p = 0.003$, $\eta 2\ p = 0.33$] and Condition [$F_{(2,46)} = 252.17$, $p = 0.000$, $\eta 2\ p = 0.92$], and interaction of Treatment × Condition [$F_{(2,46)} = 3.78$, $p = 0.03$, $\eta 2\ p = 0.14$] for accuracy. Further analysis indicated significant differences between CPS and control treatment only in four red items (0.79 ± 0.01 vs. 0.81 ± 0.01, $p = 0.035$) and distractor condition (0.86 ± 0.007 vs. 0.90 ± 0.007; $p = 0.001$). There was no statistical significance ($p = 0.464$) for two red items. As for RTs, the ANOVA showed significant main effects of Treatment [$F_{(1,23)} = 5.28$, $p = 0.031$, $\eta 2\ p = 0.19$] and Condition [$F_{(2,46)} = 66.87$, $p = 0.000$, $\eta 2\ p = 0.74$]. Further analysis indicated that RTs (814 ms) for CPS was significantly longer than that (747 ms) for control treatment. The RTs was shortest for the two red items (742 ms), followed by distractor condition (777 ms), and then four red items (821 ms; for all $p < 0.001$). Further analysis also showed significant differences between CPS and control treatment in all conditions: $p = 0.030$ for four red items (856 vs. 785 ms), $p = 0.049$ for distractor condition (809 vs. 746 ms), and $p = 0.023$ for two red items (776 vs. 708 ms).

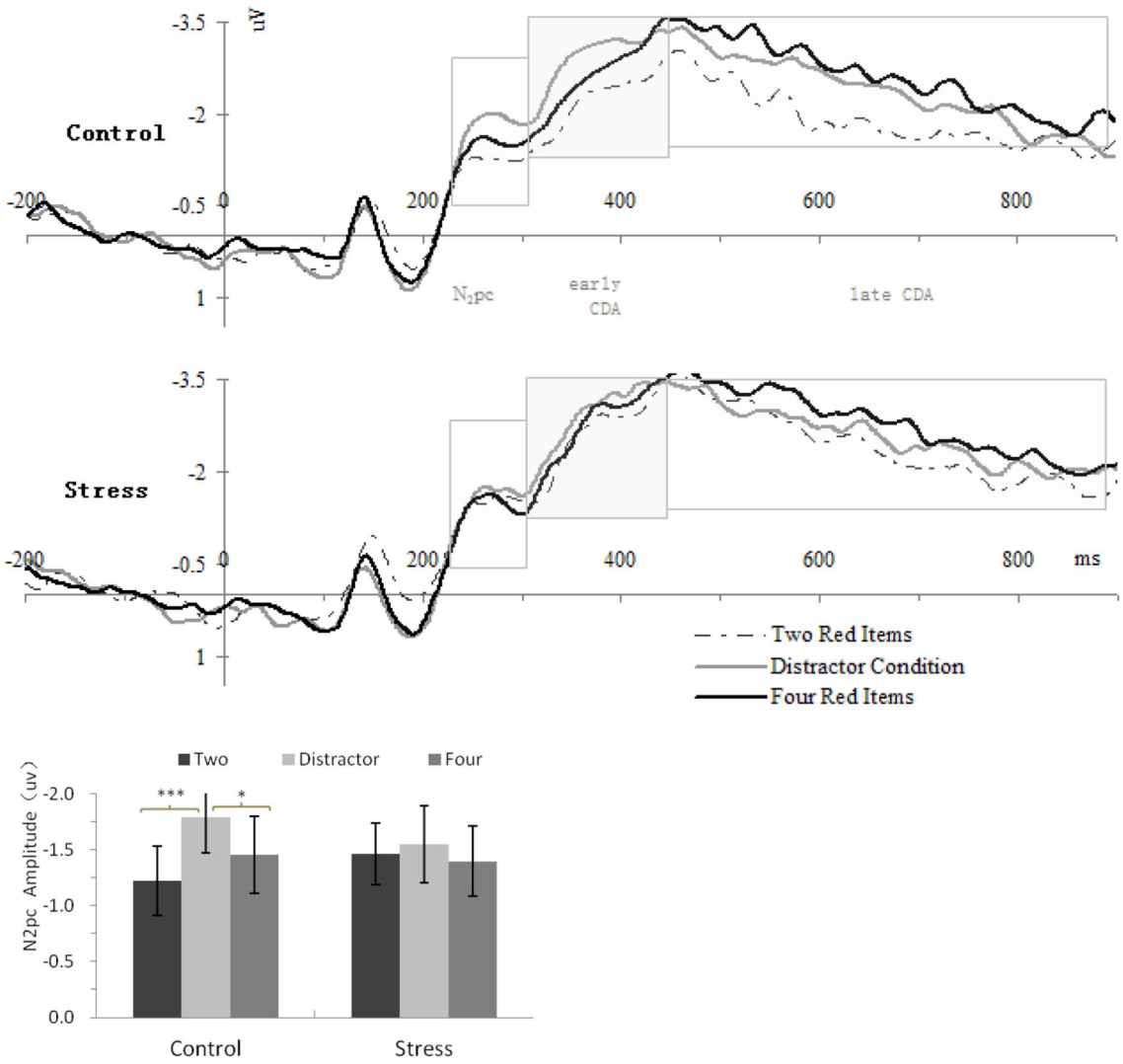

FIGURE 2 | Upper panel, grand-average event-related potential (ERP) waveforms timelocked to memory array onset, showing the contralateral delay activity (CDA) difference waves for each treatment in each condition; Lower panel, mean amplitudes of the N_2pc component. Error bars represent standard errors of the means. Two, two red items; Distractor, the distractor condition; Four, four red items.*$p < 0.05$, ***$p < 0.001$.

Lateralized ERP Results

Repeated-measures ANOVAs were conducted with two within-subject factors: Treatment (CPS vs. control) and Condition (two red items, four red items, and the distractor condition), to evaluate potential differences in ERP amplitudes between treatments and among different stimuli conditions.

N_2pc (230–310 ms)

Figure 2 (lower panel) shows the N_2pc amplitude as a function of Condition and Treatment. Repeated-measures ANOVA showed a significant main effect of Condition [$F_{(2,46)} = 3.725$, $p = 0.032$, $\eta 2\ p = 0.14$] and interaction of Treatment × Condition [$F_{(2,46)} = 4.507$, $p = 0.016$, $\eta 2\ p = 0.164$] for N_2pc. Concerning the interaction of Treatment × Condition, repeated-measures ANOVAs conducted, respectively, within each treatment indicated that the N_2pc amplitudes for control treatment differed significantly across conditions, $F_{(2,46)} = 8.421$, $p = 0.001$, $\eta 2\ p = 0.27$, but there were no significant difference across conditions for CPS, $F_{(2,46)} = 0.38$, $p = 0.61$, $\eta 2\ p = 0.02$. *Post-hoc* analyses for control treatment showed that the N_2pc amplitude for the distractor condition (-1.79 ± 0.316) was larger than that for four red items (-1.45 ± 0.344) ($p = 0.017$) and for two red items (-1.22 ± 0.309) ($p = 0.001$).

Early CDA (310 to 450 ms) (**Table 2**).

Figure 3A shows the mean amplitudes of the early CDA as a function of conditions. Repeated-measures ANOVA only showed a significant main effect of Condition [$F_{(2,46)} = 5.97$, $p = 0.009$, $\eta 2\ p = 0.21$] for the mean amplitudes of the early CDA. Concerning the main effect of condition, larger early CDA amplitudes were found for the distractor condition and four red items with respect to two red items ($p = 0.003$ and 0.019,

TABLE 1 | Pre-experiment mood and physiological measurements before and after control or CPS treatment.

	Positive affect	Negative affect	Depression	Baseline HR	HR after resting 3 min
CON (*M, SD*)	26.2 (9.7)	14.5 (6.4)	6.8 (5.0)	79.6 (8.2)	75.6 (7.5)
CPS (*M, SD*)	27.1 (8.5)	16.0 (6.5)	7.2 (5.3)	80.7 (11.7)	75.2 (9.6)
ANOVA (*F, p*)	0.8 (0.38)	2.6 (0.12)	0.2 (0.67)	0.2 (0.64)	0.1 (0.81)
Baseline SBP	**SBP after resting 3 min**	**Baseline DBP**	**DBP after resting 3 min**	**Baseline Cortisol (nmol/L)**	**Cortisol after 20 min (nmol/L)**
101.2 (6.4)	98.7 (9.0)	63.5 (7.5)	62.3 (6.1)	3.1 (1.1)	3.1 (1.2)
102.8 (5.4)	105.2 (6.3)	64.0 (6.0)	66.0 (7.0)	3.1 (1.1)	6.7 (2.0)
2.5 (0.13)	7.0(0.01)	0.1 (0.73)	7.4 (0.01)	0.1 (0.75)	75.1 (0.00)

Values represent means (M) and standard deviations (SD); CON, control treatment; CPS, cold pressor stress; HR, heart rate (beats per minute); DBP, diastolic blood pressure (mmHg); SBP, systolic blood pressure (mmHg); CORT, cortisol (nmol/L).

TABLE 2 | Early and late CDA amplitudes for cold pressor stress (CPS) treatment and control treatment across three conditions (M ± SD).

	Two red items		Distractor condition		Four red items	
	Stress	**Control**	**Stress**	**Control**	**Stress**	**Control**
Early CDA	−2.65 (1.48)	−2.24 (1.56)	−2.95 (2.04)	−2.96 (1.67)	−2.78 (1.72)	−2.65 (1.77)
Late CDA	−2.38 (1.26)	−1.89 (1.00)	−2.54 (1.62)	−2.34 (1.18)	−2.77 (1.42)	−2.58 (1.30)

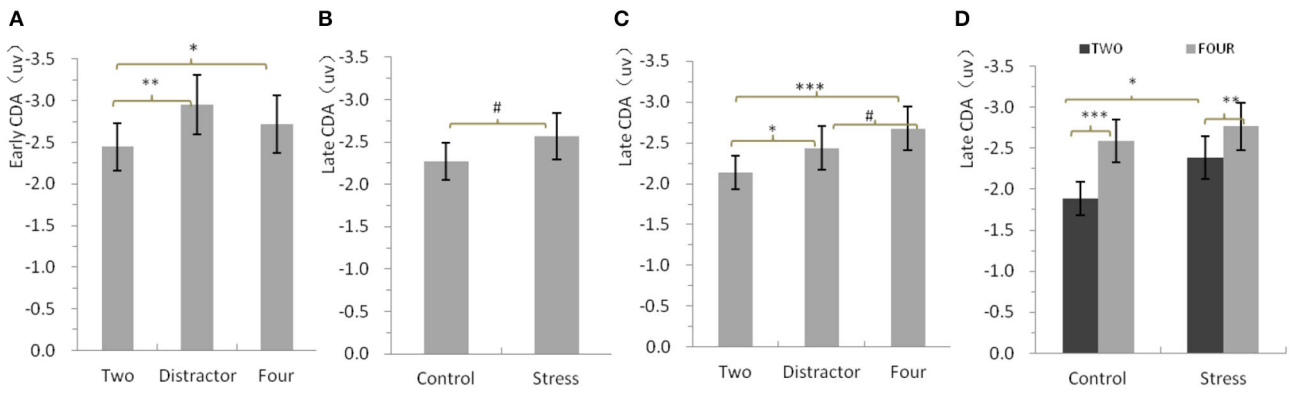

FIGURE 3 | (A) Mean amplitudes of the early contralateral delay activity (CDA) potential, between 310 and 450 ms after memory array onset. **(B–D)** Mean amplitude of the late CDA, between 450 and 900 ms after memory array onset. Error bars represent standard errors of the means.*$p < 0.05$, **$p < 0.01$, ***$p < 0.001$, #$p = 0.069$ for b, #$p = 0.052$ for c.

respectively), while there was no significant difference between the distractor condition and the four red items ($p = 0.186$).

Late CDA (450 to 900 ms) (**Table 2**).

Figures 3B–D show the mean amplitudes of the late CDA as a function of all conditions. Repeated-measures ANOVA showed a significant main effect of Condition [$F_{(2,46)}$ =11.44, $p = 0.000$, η2 $p = 0.332$] and a nearly significant main effect of Treatment [$F_{(1,23)} = 3.63$, $p = 0.069$, η2 $p = 0.136$] for the mean amplitudes of the late CDA. Further analysis indicated that the mean amplitudes of the late CDA of all three types of stimuli arrays (-2.56 ± 0.27) for CPS treatment were nearly significantly larger than that (-2.27 ± 0.22) for control treatment (**Figure 3B**). Concerning the main effect of condition, larger late CDA amplitudes were found for the four red items and the distractor condition with respect to two red items ($p = 0.000$ and 0.027, respectively), while larger late CDA amplitudes were also found for four red items with respect to the distractor, but the difference was borderline significant ($p = 0.052$; **Figure 3C**). Given the concerns of this study and the attempts to make clear how stress affects the maintenance in visual–spatial WM, we conducted repeated-measures ANOVAs with two red items and four red items as one factor and Treatment as another one. The results showed that CPS significantly increased the amplitudes of late CDA [$F_{(1,23)} = 4.38$, $p = 0.047$, η2 $p = 0.16$], especially for

the two items ($p = 0.026$), and the same as mentioned above, the amplitudes for four red items were much larger than those for two red items [$F_{(1,23)} = 43.07$, $p = 0.00$, $\eta 2$ $p = 0.65$], with no interaction (**Figure 3D**).

DISCUSSION

The main objective of this study was to investigate the effect of acute stress on WM processing. In the present study, we used a well-validated neural measure of visual–spatial WM storage to investigate how acute stress influences human WM functions. The main findings were that the subjects after control treatment performed the visual WM task better than after the CPS treatment, and as expected, subjects showed a late CDA amplitude in the two-red-items condition after the CPS treatment, which was significantly larger than that after the control treatment, but no significant difference in the four-red-items condition and distractor condition between the treatments. More importantly, as for the ERP waves, it was statistically proven that the N_2pc components showed significant disparity across three types of stimuli arrays after control treatment, which disappeared in the CPS session. These results demonstrate that acute stress impaired individuals' cognition processes of object individuation (as reflected in alterations in N_2pc amplitude) and maintenance in visual–spatial WM (as reflected in alterations in Late CDA amplitude), as well as in task performance. Therefore, the findings of the present study extend the recent literature investigating the effects of acute stress on human WM processing by providing evidences of detrimental effects of acute stress on WM task performance and the temporal course of the detrimental effects at least as early as the N_2pc time window using the ERP technique.

To characterize the response to the CPS, salivary cortisol, blood pressure, and HR were assessed. The results revealed significantly higher ratings of blood pressures in the CPS treatment session, as well as an increased activity of the HPA, compared to the control treatment session. These findings are well in line with previous studies [e.g., (6, 14, 17, 49)] and indicate the successful induction of a neuroendocrine stress response.

The findings of longer RTs and accuracy decrement clearly observed in high cognitive load trials under acute stress treatment are in line with our hypothesis and some previous studies [e.g., (5, 9, 11, 14)]. The behavioral data also showed larger WM capacity in high cognitive load trials during the control treatment session with respect to the CPS session. Importantly, our experimental design controlled for a number of extraneous variables, such as individual differences, circadian profiles of adrenocortical reactivity and cognitive ability, and so on, by use of within-subject design and only women during their luteal phase participating in the experiment, and the CPS or control treatment assigned at the same timing of different experimental days, which proved that acute stress impaired individuals' task performance.

Attentional selection was quantified as the magnitude of the N_2pc component, a well-established ERP component that reflects the focusing of attention onto multistimulus arrays (30, 33, 34). The data of the control session in this study showed clear N_2pc components for the three conditions, and the mean amplitude of the N_2pc for the distractor condition was the largest, followed by four red items, and then two red items, which was in accordance with a recent study using the same experimental protocol (30) and supported the proposition that the N_2pc increased as a function of target numerosity, reflecting a process of object individuation (30, 33, 34). However, the data of the CPS session in this study showed a very different N_2pc response pattern, which is a pronounced trend of increased amplitude for the two-item condition relative to control treatment, while amplitude was decreased in the distractor condition. Given that Qi et al. (30) using University students as subjects in normal conditions, which was the same as the control treatment condition in this study, reported the same N_2pc response pattern, CPS treatment substantially impaired subjects' attentional selection and the object individuation process.

However, contrary to our hypothesis, no significantly larger N_2pc amplitude was shown after CPS. According to Mather et al. (36), acute stress should affect attentive selection, which involved the mechanisms of amplified activation of the irrelevant information representations. Therefore, though no competition between goal-driven and stimulus-driven processes existed, much more task-irrelevant information would be expected to be encoded, leading to a larger N_2pc component. Some evidence suggests that the N_2pc can be decomposed into two functionally distinct lateralized subcomponents: the target negativity (Nt), reflecting target selection and object individuation, and the distractor positivity (Pd), associated with distractor suppression [e.g., (50)]. Thus, the outcome pattern under CPS in the present study might result from the increasing input of task-irrelevant information and the disproportionate allocation of resources in the suppression of task-irrelevant information. According to the "NE hot spots" model (36), acute stress triggers locus coeruleus and induces increased NE (2, 51), which biases perception and memory in favor of more salient information representations at the expense of less salient representations. At the same time, acute stress also affects PFC network by the induction of catecholamines and cortisol (1, 52–55), which is an important regulator of locus coeruleus output and an important area of appraising sensory information based on goal relevance (36). Thus, acute stress might lead to inputting information more based on bottom-up salience, instead of top-down goals. In the case of the present study, acute stress resulted in representations of more task-irrelevant information (i.e., Nt increases significantly), and for the two-red-items condition, there was no need to recruit much resources to suppress irrelevant information (i.e., Pd, would not show a significant change) to perform successfully due to low processing load. Thus, the overlaying of the two subcomponents resulted in N_2pc amplitude increasing. For the same reasons, during the CPS session, much more resource must be recruited to suppress the task-irrelevant information (i.e., Pd increases significantly) in order to achieve good performance in four-red-item trials and the distractor condition trials in which too much resources are devoted to the object individuation process, and thus, the overlaying of the two subcomponents resulted in N_2pc amplitude decreasing or no significant change, and in the end, there is no

difference in N_2pc amplitudes across the three types of stimuli arrays in CPS trials. Studies have shown that not only attention is biased by representations in WM, but selective attention determines what is to be stored and processed later (31). Thus, CPS might make more additional task-irrelevant information be encoded during the N_2pc time window and further processed in WM.

As for the early CDA component, Qi et al. (30) proposed it as a measure of the amount of processing resources required to perform object identification after object individuation, in order to categorize objects in greater detail. Our results showed only the main effect of condition in the early CDA during the time interval of 310–450 ms. Specifically, subjects showed more consumption of processing resources for object identification for the distractor condition and the four red items than that for the two red items, mostly because of identification or categorizing process involving more details in the distractor and the four-red-items conditions, as reflected by their larger early CDA for the distractor condition and the four red items than for the two red items, which is in line with the findings of Qi et al. (30). Our data also showed no main effect of treatment and no interaction of Treatment × Condition, and one possible explanation for this finding is that, in contrast to the control treatment session, more task-irrelevant information was encoded and represented but the classification and identification process might be relatively more difficult during the CPS session. Given the limitations of processing capacity during stimulus classification and identification, and finer processing involved in the control treatment session, no main effect of treatment and interaction was found in the end. If this were true, information maintained in WM during the CPS session were overload and low accuracy. Further studies would be necessary to determine the cognitive correlates and the stress effect on this component, and examination of the early CDA was exploratory in this study.

During the subsequent WM maintenance phase, as expected, the results showed that larger late CDA amplitudes were found for the four red items and the distractor condition with respect to two red items in the control treatment session, which is similar to former studies (28, 30, 47). Analyses of data from CPS and control treatments showed that there was a borderline significant main effect of treatment, in which although significantly larger late CDA amplitudes were found only for two red items during the CPS session with respect to the control treatment session, there was a clear trend of increased late CDA amplitude across all other conditions in the CPS session compared to the control treatment session. These findings supported our hypothesis that larger CDA amplitude changes would appear mostly under low-load trials. Given that there were significant main effects of Treatment in behavioral data and the discussions about N_2pc and early CDA mentioned earlier, these late CDA findings indicated that acute stress impaired the encoding of information into WM and disrupted the inhibition of irrelevant information in WM via intricate mechanisms, which probably involved the interaction of NE and cortisol and the dysfunction of top-down appraisal of inputting information [see (36)] and PFC network [see (1, 53, 54)]. Thus, more task-irrelevant information got stored in WM due to low-efficient inhibition of irrelevant information, and late CDA amplitudes increased markedly for two red items during the CPS session relative to that of the control session, while only showing an increasing trend for four-red-items and the distractors condition mostly because of the limitation of WM capacity, which was thought to be approximately three to four objects (39).

The finding of detrimental effects of acute stress on WM was in line with some aforementioned studies (5, 9–14). Gärtner et al. (9) investigated the frequency-domain features of the EEG while subjects performed WM tasks, and the results showed impairment effects of acute stress only on the late time window, that is, WM maintenance processing. Although they distinguished two separate time windows (0–800 ms and 1,000–1,800 ms) to calculate the frontal theta power, which was thought to be related to attentional and maintenance processes during WM, respectively, the research design was far from direct observation of the dynamic course of the WM process. However, in this study, we used time-domain features of the ERPs, which could provide the direct observation of the dynamic course of WM processing, by which we discerned that the effects of acute stress emerged about 200 ms after the onset of memory array, and determined that the acute stress effect appeared as early as the end of the N_2pc time window, which would be difficult to distinguish in studies using frequency-domain feature analysis (6, 9). As far as we know, this study was among the first ones that used time-domain analysis of the ERPs to investigate the effects of acute stress on human WM process and not only reported performance impairments but also provided high temporal resolution evidence for the detrimental effects of acute stress on WM processes.

However other studies reported inconsistent results in the WM task performance, some of which found no or improved effects of stress treatment on WM [e.g., (16–19)]. As mentioned earlier, major explanations for this contradiction might include the following:

1. The different load placed on WM. Three of the aforementioned studies reported acute stress impaired WM at high loads or involving more cognitive operations, but not at low loads (9, 11, 14), and studies reporting no detrimental effects were usually low load, such as the 0-back and 2-back task (8, 18). Sufficient resources can be reallocated in low-load tasks, when additional irrelevant information was represented in WM for exposure to stressor, while in case of high-load tasks, process resources were easily exhausted, as was proved in our study that significant acute stress effects for WM capacity and accuracy for four red items and the distractor conditions were reported, but not for two red items, and the electrophysiological evidence that reflected the employment of resources seemed to be the opposite, that significantly larger late CDA amplitudes were found only for two red items during the CPS session relative to the control session due to limitations of resources.

2. The time interval between assessing WM process and stressor offset. In the aforementioned studies showing harmless stress effects on WM, the cortisol peak was already exceeded when subjects performed the WM task 20 or 30 min after stress procedure [e.g., (3, 6, 15, 16)] and the catecholamine (NE and dopamine) concentration, which is the marker of the

activation of the sympathetic nervous system (SNS), had by then returned to baseline, while in studies reporting harmful effects, the WM was tested in < 10 min after the stress exposure [5 min in our experiment; (5, 9–14)] when cortisol levels were rising and SNS might still be activated. Given evidence from animal studies showing that corticosteroid actions interact with catecholaminergic activity and potentiate the negative effects of stress hormones on PFC (56, 57), the detrimental effects of acute stress might be also stronger during concurrent SNS and HPA activation for humans.

3. The intensity or the methods of inducing acute stress. In studies reporting beneficial effects on performance or WM-related networks, subjects were exposed to CPS only for 1 or 2 min (6, 17), or other milder stressors, such as negative movie clips (8), so that the levels of stress hormones secreting might be relatively low. Pharmacological studies in animals have revealed that catecholamines exert an inverted U influence on PFC in which sub- or supra-optimal levels of catecholamine impaired the prefrontal network processing (58, 59), and on the cellular level, a study using intracellular recordings indicated that catecholamine also showed such inverted U relationships with neural firing activities of the dlPFC (60). Similar results were also reported for corticosterone in animals (61). Therefore, the relatively low levels of cortisol or catecholamines might have just reached an optimal point or returned to baseline (in case of the second explanation), resulting in enhanced or normal WM-related neural network activities and performance.

However, as there were no manipulations of stress severity and time interval between WM test and stressor offset in this study, additional studies are required to test the last two hypotheses.

LIMITATIONS

Several limitations of the present study should be noted. In the current experiment, we only use self-reported information to choose participants in the luteal phase, which is characterized by high estradiol and progesterone concentrations. These self-reported measures are problematic, since they might not match rigorous neuroendocrine measurements (21). Future studies should use physiological measures to choose subjects of specific menstrual cycle phase to replicate the present findings and investigate possible differences between different cycle phases, since, for the long-term memory, evidence has been reported that beneficial effects on memory consolidation only occur in the luteal phase (62). Moreover, our study did not consider the influence of other factors (personality traits, intelligence, socioeconomic status, etc.) that may influence WM function, and it will be important to control these factors in future studies.

CONCLUSIONS

To summarize, this study indicates that acute stress has substantial and detrimental effects on WM processing and can lead to large amounts of task-irrelevant information encoded and stored in WM, and the detrimental effects emerge at least as early as the N_2pc time window.

DATA AVAILABILITY STATEMENT

The raw data supporting the conclusions of this article will be made available by the authors, without undue reservation.

ETHICS STATEMENT

The studies involving human participants were reviewed and approved by Ethics Committee of the Sichuan Normal University. The patients/participants provided their written informed consent to participate in this study.

AUTHOR CONTRIBUTIONS

ZX, LY, and HL planned the study. ZX, SG, and FW analyzed the data. ZX and HL did the writing. All authors contributed to the article and approved the submitted version.

FUNDING

This study was supported by National Science Foundation of China (31571153 and 31671150).

REFERENCES

1. Hermans EJ, van Marle HJ, Ossewaarde L, Henckens MJ, Qin S, van Kesteren MT, et al. Stress-related noradrenergic activity prompts large-scale neural network reconfiguration. *Science.* (2011) 334:1151–3. doi: 10.1126/science.1209603
2. Gu S, Wang W, Wang F, Huang JH. Neuromodulator and emotion biomarker for stress induced mental disorders *Neural Plasticity.* (2016) 2016:2609128. doi: 10.1155/2016/2609128
3. Duncko R, Johnson L, Merikangas K, Grillon C. Working memory performance after acute exposure to the cold pressor stress in healthy volunteers. *Neurobiol Learn Mem.* (2009) 91:377–81. doi: 10.1016/j.nlm.2009.01.006
4. Hidalgo V, Pulopulos MM, Puig-Perez S, Espin L, Gomez-Amor J, Salvador A. Acute stress affects free recall and recognition of pictures differently depending on age and sex. *Behav Brain Res.* (2015) 292:393–402. doi: 10.1016/j.bbr.2015.07.011
5. Paulauskas, H., Brazaitis M, Mickevičiene D, Pukenas K, Eimantas N. Acute cold stress and mild hypothermia impact on short-term, working memory and attention. *Biologija.* (2015) 61:1–5. doi: 10.6001/biologija.v61 i1.3106
6. Lai V, Theppitak C, Makizuka T, Higuchi Y, Movahed M, Kumudini G, et al. A normal intensity level of psycho-physiological stress can benefit working memory performance at high load. *Int J Ind Ergon.* (2014) 44:362–7. doi: 10.1016/j.ergon.2013.11.015
7. Kirschbaum C, Pirke K-M, Hellhammer DH. The 'Trier social stress test'–a tool for investigating psychobiological stress responses in a laboratory setting. *Neuropsychobiology.* (1993) 28:76–81. doi: 10.1159/000119004
8. Cousijn H, Rijpkema M, Qin S, van Wingen GA, Fernández G. Phasic deactivation of the medial temporal lobe enables working memory processing under stress. *Neuroimage.* (2012) 59:1161–7. doi: 10.1016/j.neuroimage.2011.09.027
9. Gärtner M, Rohde-Liebenau L, Grimm S, Bajbouj M. Working memory-related frontal theta activity is decreased under

acute stress. *Psychoneuroendocrinology.* (2014) 43:105–13. doi: 10.1016/j.psyneuen.2014.02.009
10. Elzinga BM, Roelofs K. Cortisol-induced impairments of working memory require acute sympathetic activation. *Behav Neurosci.* (2005) 119:98. doi: 10.1037/0735-7044.119.1.98
11. Oei N, Everaerd W, Elzinga B, van Well S, Bermond B. Psychosocial stress impairs working memory at high loads: an association with cortisol levels and memory retrieval. *Stress.* (2006) 9:133–41. doi: 10.1080/10253890600965773
12. Robinson SJ, Sünram-Lea S, Leach J, Owen-Lynch P. The effects of exposure to an acute naturalistic stressor on working memory, state anxiety and salivary cortisol concentrations. *Stress.* (2008) 11:115–24. doi: 10.1080/10253890701559970
13. Schoofs D, Preuß D, Wolf OT. Psychosocial stress induces working memory impairments in an n-back paradigm. *Psychoneuroendocrinology.* (2008) 33:643–53. doi: 10.1016/j.psyneuen.2008.02.004
14. Schoofs D, Wolf OT, Smeets T. Cold pressor stress impairs performance on working memory tasks requiring executive functions in healthy young men. *Behav Neurosci.* (2009) 123:1066. doi: 10.1037/a0016980
15. Cornelisse S, van Stegeren AH, Joëls M. Implications of psychosocial stress on memory formation in a typical male vs. female student sample. *Psychoneuroendocrinology.* (2011) 36:569–78. doi: 10.1016/j.psyneuen.2010.09.002
16. Hoffman R, al'Absi M. The effect of acute stress on subsequent neuropsychological test performance (2003). *Arch Clin Neuropsychol.* (2004) 19:497–506. doi: 10.1016/j.acn.2003.07.005
17. Porcelli AJ, Cruz D, Wenberg K, Patterson MD, Biswal BB, Rypma B. The effects of acute stress on human prefrontal working memory systems. *Physiol Behav.* (2008) 95:282–9. doi: 10.1016/j.physbeh.2008.04.027
18. Qin S, Hermans EJ, van Marle HJ, Luo J, Fernández G. Acute psychological stress reduces working memory-related activity in the dorsolateral prefrontal cortex. *Biol Psychiatr.* (2009) 66:25–32. doi: 10.1016/j.biopsych.2009.03.006
19. Smeets T, Jelicic M, Merckelbach H. The effect of acute stress on memory depends on word valence. *Int J Psychophysiol.* (2006) 62:30–7. doi: 10.1016/j.ijpsycho.2005.11.007
20. Weerda R, Muehlhan M, Wolf OT, Thiel CM. Effects of acute psychosocial stress on working memory related brain activity in men. *Hum Brain Mapp.* (2010) 31:1418–29. doi: 10.1002/hbm.20945
21. Schoofs D, Pabst S, Brand M, Wolf OT. Working memory is differentially affected by stress in men and women. *Behav Brain Res.* (2013) 241:144–53. doi: 10.1016/j.bbr.2012.12.004
22. Meeks JT, Rosnick CB, Blackhurst J, Overton A. Does sex matter? *Curr Psychol.* (2014) 33:199–218. doi: 10.1007/s12144-014-9206-9
23. Berggren N, Derakshan N. Attentional control deficits in trait anxiety: why you see them and why you don't. *Biol Psychol.* (2013) 92:440–6. doi: 10.1016/j.biopsycho.2012.03.007
24. Eysenck MW, Derakshan N. New perspectives in attentional control theory. *Personal Ind Differ.* (2011) 50:955–60. doi: 10.1016/j.paid.2010.08.019
25. Basten U, Stelzel C, Fiebach CJ. Trait anxiety and the neural efficiency of manipulation in working memory. *Cogn Affect Behav Neurosci.* (2012) 12:571–88. doi: 10.3758/s13415-012-0100-3
26. McCollough AW, Machizawa MG, Vogel EK. Electrophysiological measures of maintaining representations in visual working memory. *Cortex.* (2007) 43:77–94. doi: 10.1016/S0010-9452(08)70447-7
27. Vogel EK, Machizawa MG. Neural activity predicts individual differences in visual working memory capacity. *Nature.* (2004) 428:748–51. doi: 10.1038/nature02447
28. Vogel EK, McCollough AW, Machizawa MG. Neural measures reveal individual differences in controlling access to working memory. *Nature.* (2005) 438:500–3. doi: 10.1038/nature04171
29. Mazza V, Turatto M, Caramazza A. Attention selection, distractor suppression and N_2pc. *Cortex.* (2009) 45:879–90. doi: 10.1016/j.cortex.2008.10.009
30. Qi S, Ding C, Li H. Neural correlates of inefficient filtering of emotionally neutral distractors from working memory in trait anxiety. *Cogn Affect Behav Neurosci.* (2014) 14:253–65. doi: 10.3758/s13415-013-0203-5
31. Olivers CN, Peters J, Houtkamp R, Roelfsema PR. Different states in visual working memory: when it guides attention and when it does not. *Trends Cogn Sci.* (2011) 15:327–34. doi: 10.1016/j.tics.2011.05.004
32. Hickey C, Di Lollo V, McDonald JJ. Electrophysiological indices of target and distractor processing in visual search. *J Cogn. Neurosci.* (2009) 21:760–75. doi: 10.1162/jocn.2009.21039
33. Ester EF, Drew T, Klee D, Vogel EK, Awh E. Neural measures reveal a fixed item limit in subitizing. *J Neurosci.* (2012) 32:7169–77. doi: 10.1523/JNEUROSCI.1218-12.2012
34. Mazza V, Caramazza A. Temporal brain dynamics of multiple object processing: the flexibility of individuation. *PLoS ONE.* (2011) 6:e17453. doi: 10.1371/journal.pone.0017453
35. Sänger J, Bechtold L, Schoofs D, Blaszkewicz M, Wascher E. The influence of acute stress on attention mechanisms and its electrophysiological correlates. *Front Behav Neurosci.* (2014) 8:353. doi: 10.3389/fnbeh.2014.00353
36. Mather M, Clewett D, Sakaki M, Harley CW. Norepinephrine ignites local hot spots of neuronal excitation: How arousal amplifies selectivity in perception and memory. *Behav. Brain Sci.* (2015) 1:e200. doi: 10.1017/S0140525X15000667
37. Wang F, Pan F, Shapiro LA, Huang JH. Stress induced neuroplasticity and mental disorders. *Neural Plas.* (2017) 2017:9634501. doi: 10.1155/2017/9634501
38. Zheng Z, Gu S, Lei Y, Lu S, Wang W, Li Y, et al. Safety needs mediate stressful events induced mental disorders. *Neural Plast.* (2016) 2016:8058093. doi: 10.1155/2016/8058093
39. Luck SJ, Vogel EK. The capacity of visual working memory for features and conjunctions. *Nature.* (1997) 390:279–81. doi: 10.1038/36846
40. Kirschbaum C, Kudielka BM, Gaab J, Schommer NC, Hellhammer DH. Impact of gender, menstrual cycle phase, and oral contraceptives on the activity of the hypothalamus-pituitary-adrenal axis. *Psychosom Med.* (1999) 61:154–62. doi: 10.1097/00006842-199903000-00006
41. Kudielka BM, Kirschbaum C. Sex differences in HPA axis responses to stress: a review. *Biol Psychol.* (2005) 69:113–32. doi: 10.1016/j.biopsycho.2004.11.009
42. Watson D, Clark LA, Tellegen A. Development and validation of brief measures of positive and negative affect: the PANAS scales. *J Pers Soc Psychol.* (1988) 54:1063–70. doi: 10.1037/0022-3514.54.6.1063
43. Beck A, Steer R, Brown G. *Beck Depression Inventory-II*. Toronto, ON (1996). doi: 10.1037/t00742-000
44. Shek DTL. The Chinese version of the state-trait anxiety inventory: its relationship to different measures of psychological well-being. *J Clin Psychol.* (1993) 49:349–58. doi: 10.1002/1097-4679(199305)49:3<349::AID-JCLP2270490308>3.0.CO;2-J
45. Yang Y, Koh D, Ng V, Lee C, Chan G, Dong F, et al. Self perceived work related stress and the relation with salivary IgA and lysozyme among emergency department nurses. *Occup Environ Med.* (2002) 59:836–41. doi: 10.1136/oem.59.12.836
46. Rouder JN, Morey RD, Morey CC, Cowan N. How to measure working memory capacity in the change detection paradigm. *Psychon Bull Rev.* (2011) 18:324–30. doi: 10.3758/s13423-011-0055-3
47. Lee EY, Cowan N, Vogel EK, Rolan T, Valle-Inclan F, Hackley SA. Visual working memory deficits in patients with Parkinson's disease are due to both reduced storage capacity and impaired ability to filter out irrelevant information. *Brain.* (2010) 133:2677–89. doi: 10.1093/brain/awq197
48. Störmer VS, Li S-C, Heekeren HR, Lindenberger U. Normative shifts of cortical mechanisms of encoding contribute to adult age differences in visual–spatial working memory. *Neuroimage.* (2013) 73:167–75. doi: 10.1016/j.neuroimage.2013.02.004
49. Zoladz PR, Peters DM, Cadle CE, Kalchik AE, Aufdenkampe RL, Dailey AM, et al. Post-learning stress enhances long-term memory and differentially influences memory in females depending on menstrual stage. *Acta Psychol.* (2015) 160:127–33. doi: 10.1016/j.actpsy.2015.07.008
50. Munneke J, Fait E, Mazza V. Attentional processing of multiple targets and distractors. *Psychophysiology.* (2013) 50:1104–8. doi: 10.1111/psyp.12123
51. Gu S, Wang F, Patel NP, Bourgeois JA, Huang JH. A model for basic emotions using observations of behavior in Drosophila. *Front Psychol.* (2019) 10:781. doi: 10.3389/fpsyg.2019.00781
52. de Kloet ER, Joëls M, Holsboer F. Stress and the brain: from adaptation to disease. *Nat Rev Neurosci.* (2005) 6:463–75. doi: 10.1038/nrn1683
53. Herman JP, Figueiredo H, Mueller NK, Ulrich-Lai Y, Ostrander MM, Choi DC, et al. Central mechanisms of stress integration: hierarchical

circuitry controlling hypothalamo–pituitary–adrenocortical responsiveness. *Front Neuroendocrinol.* (2003) 24:151–80. doi: 10.1016/j.yfrne.2003.07.001
54. Hermans EJ, Henckens MJ, Joëls M, Fernández G. Dynamic adaptation of large-scale brain networks in response to acute stressors. *Trends Neurosci.* (2014) 37:304–14. doi: 10.1016/j.tins.2014.03.006
55. McEwen BS, Morrison JH. The brain on stress: vulnerability and plasticity of the prefrontal cortex over the life course. *Neuron.* (2013) 79:16–29. doi: 10.1016/j.neuron.2013.06.028
56. Butts KA, Weinberg J, Young AH, Phillips AG. Glucocorticoid receptors in the prefrontal cortex regulate stress-evoked dopamine efflux and aspects of executive function. *Proc Natl Acad Sci USA.* (2011) 108:18459–64. doi: 10.1073/pnas.1111746108
57. McReynolds JR, Donowho K, Abdi A, McGaugh JL, Roozendaal B, McIntyre CK. Memory-enhancing corticosterone treatment increases amygdala norepinephrine and Arc protein expression in hippocampal synaptic fractions. *Neurobiol Learn Memory.* (2010) 93:312–21. doi: 10.1016/j.nlm.2009.11.005
58. Arnsten AF. Catecholamine and second messenger influences on prefrontal cortical networks of representational knowledge: a rational bridge between genetics and the symptoms of mental illness. *Cereb Cortex.* (2007) 17(Suppl. 1):i6. doi: 10.1093/cercor/bhm033
59. Arnsten AF, Li BM. Neurobiology of executive functions: catecholamine influences on prefrontal cortical functions. *Biol Psychiatr.* (2005) 57:1377–84. doi: 10.1016/j.biopsych.2004.08.019
60. Vijayraghavan S, Wang M, Birnbaum SG, Williams GV, Arnsten AF. Inverted-U dopamine D1 receptor actions on prefrontal neurons engaged in working memory. *Nat Neurosci.* (2007) 10:376–84. doi: 10.1038/nn1846
61. Akirav I, Kozenicky M, Tal D, Sandi C, Venero C, Richterlevin G. A facilitative role for corticosterone in the acquisition of a spatial task under moderate stress. *Learn Mem.* (2004) 11:188–95. doi: 10.1101/lm.61704
62. Andreano JM, Arjomandi H, Cahill L. Menstrual cycle modulation of the relationship between cortisol and long-term memory. *Psychoneuroendocrinology.* (2008) 33:874–82. doi: 10.1016/j.psyneuen.2008.03.009

Conflict of Interest: The authors declare that the research was conducted in the absence of any commercial or financial relationships that could be construed as a potential conflict of interest.

frontiers in Psychiatry

ORIGINAL RESEARCH
published: 07 December 2020
doi: 10.3389/fpsyt.2020.555133

Decreased Plasma Levels of Growth Differentiation Factor 11 in Patients With Schizophrenia: Correlation With Psychopathology and Cognition

Zhao-xi Yang[1,2†], Jin-qiong Zhan[2†], Jian-wen Xiong[3,4†], Bo Wei[2,3,4], Yong-hui Fu[3], Zhi-peng Liu[3], Ya-ting Tu[3], Yuan-jian Yang[2,3,4] and Ai-lan Wan[1*]*

[1] Department of Psychosomatic Medicine, The First Affiliated Hospital of Nanchang University, Nanchang, China, [2] Biological Psychiatry Laboratory, Jiangxi Mental Hospital/Affiliated Mental Hospital of Nanchang University, Nanchang, China, [3] Department of Psychiatry, Jiangxi Mental Hospital/Affiliated Mental Hospital of Nanchang University, Nanchang, China, [4] Jiangxi Provincial Clinical Research Center on Mental Disorders, Nanchang, China

OPEN ACCESS

Edited by:
Bart Ellenbroek,
Victoria University of Wellington,
New Zealand

Reviewed by:
Yanling Zhou,
Guangzhou Medical University, China
Tianhua Niu,
Tulane University, United States

***Correspondence:**
Ai-lan Wan
waljm699@sina.com
Yuan-jian Yang
yuanjimyang@yeah.net

[†] These authors have contributed equally to this work

Specialty section:
This article was submitted to Molecular Psychiatry, a section of the journal Frontiers in Psychiatry

Received: 13 May 2020
Accepted: 17 November 2020
Published: 07 December 2020

Citation:
Yang Z-x, Zhan J-q, Xiong J-w, Wei B, Fu Y-h, Liu Z-p, Tu Y-t, Yang Y-j and Wan A-l (2020) Decreased Plasma Levels of Growth Differentiation Factor 11 in Patients With Schizophrenia: Correlation With Psychopathology and Cognition. Front. Psychiatry 11:555133. doi: 10.3389/fpsyt.2020.555133

Schizophrenia is linked with abnormal neurodevelopment, on which growth differentiation factor 11 (GDF-11) has a great impact. However, a direct evidence linking GDF-11 to the pathophysiology of schizophrenia is still lacking. The current study aimed to investigate the relationship between plasma GDF-11 levels and both psychopathological symptoms and cognitive function in schizophrenia. Eighty-seven schizophrenia patients and 76 healthy controls were enrolled in the present study. The symptomatology of schizophrenia was evaluated using the Positive and Negative Syndrome Scale (PANSS). Cognitive function was assessed by Repeatable Battery for the Assessment of Neuropsychological Status (RBANS) including twelve neurocognitive tests in five aspects of cognitive function. Plasma GDF-11 levels were determined by enzyme-linked immunosorbent assay (ELISA). We found that plasma levels of GDF-11 were significantly lower in schizophrenia patients relative to healthy controls. Correlation analysis showed significant negative correlations between the GDF-11 levels and the PANSS total score, the positive symptoms score, the negative symptoms score or the general score. Additionally, positive associations were observed between plasma GDF-11 levels and the visuospatial/constructional, attention, immediate memory, or delayed memory in patients. Partial correlation analysis showed that these correlations were still significant after adjusting for age, gender, education years, body mass index, duration of illness, and age of onset except for the visuospatial/constructional and attention index. Multiple regression analysis revealed that GDF-11 was an independent contributor to the immediate memory, delayed memory and RBANS total score in patients. Collectively, the correlations between plasma GDF-11 and psychopathological and cognitive symptoms suggest that abnormal GDF-11 signaling might contribute to schizophrenic psychopathology and cognitive impairments and GDF-11 could be a potential and promising biomarker for schizophrenia.

Keywords: schizophrenia, psychopathology, cognition, growth differentiation factor 11 (GDF-11), correlation

INTRODUCTION

The neurodevelopmental hypothesis has proposed that the abnormalities of brain development are involved in the etiology and pathogenesis in schizophrenia (1, 2). Clinical, epidemiological, genetic and neuropathological studies performed in schizophrenia have provided numerous evidence for supporting this hypothesis (3, 4). For example, the brain gray matter and volume of children with schizophrenia are smaller than those of healthy children, and the decrease of gray matter density is earlier than that of schizophrenia (5). The abnormal brain development of patients with schizophrenia has occurred in the fetal stage, and this pathological change persists through childhood (6). A 45-year demographic follow-up survey in Denmark also reveals that patients with schizophrenia tend to lag behind their peers in its growth and development, even in the first year after birth (7).

Growth differentiation factor 11 (GDF-11) is a secretory protein of the transforming growth factor beta (TGF-β) superfamily that regulates diverse cellular processes. GDF-11 has a critical impact on development, including anterior/posterior patterning (8), kidney formation, spleen, stomach and endocrine pancreas (9, 10). Recent studies have demonstrated that GDF-11 has a regulatory role in the formation of the central nervous system (CNS). GDF-11 is intensely expressed in astrocytes, ependymal cells, neurons and their axons (11). During the development period, GDF-11 is able to modulate the patterning of CNS and the genesis, differentiation, maturation, and activity of new brain cells (8, 12). In addition, high content of plasma GDF-11 is observed when the body is young and it decreases gradually with aging (13, 14). Systemic GDF-11 treatment in rodents could improve vasculature in the cortex and hippocampus (15).

Recent studies have suggested that GDF-11 might be implicated in the pathogenesis of schizophrenia. Glutamate imbalance is an important cause of neuroinflammation (16, 17). Activation of astrocytes can directly affect the glutamate concentration in the synaptic gap (18), thus the changes in neuroinflammation caused by activation of astrocytes might contribute to the pathogenesis of schizophrenia. Furthermore, GDF-11 can modulate the function of astrocytes by regulating the expression of glutamate dehydrogenase (11). Lander et al. showed that mice lacking glutamate dehydrogenase (GDH), a glutamate-metabolizing enzyme, displayed schizophrenia-like psychotic symptoms and cognitive disorders, as well as hippocampal dysfunction (19). Cognitive impairments are considered as a core characteristic of schizophrenia. Treatment with GDF-11 in aging mice improved olfactory discrimination via promoting the cerebral vasculature and enhancing neurogenesis (20). A single dose of recombinant GDF-11 increased hippocampal transcription factor Sox2 expression and promoted short-term spatial and visual memory in mice at middle age (21). However, a direct evidence linking GDF-11 to the pathophysiology of schizophrenia is still lacking.

In view of the vital regulatory role of GDF-11 in normal brain neural development and disrupted brain development in schizophrenia, we hypothesized that abnormal GDF-11 signaling might be implicated with the pathophysiology of schizophrenia. In this study, we verified this hypothesis by examining whether (i) plasma GDF-11 level was changed in schizophrenia patients and (ii) there was any association between GDF-11 level and both psychopathological and cognitive symptoms in these patients.

MATERIALS AND METHODS

Study Subjects

Eighty-seven schizophrenia patients (male/female = 52/35) were enrolled from Jiangxi Mental Hospital, a Nanchang city-owned psychiatric hospital. Two psychiatrists confirmed their diagnosis of schizophrenia based on the Structured Clinical Interviews for DSM-IV Axis I Disorders (SCID). The inclusion criteria included the compliance with DSM-IV diagnostic criteria for schizophrenia, the Positive and Negative Syndrome Scale (PANSS) score $\geq$ 60, age 18–50 years old, and patients or their families agreed to take part in the research and sign informed consent. Only patients with PANSS total score > 60 were recruited in current study because previous study has demonstrated that being considered "mildly ill" according to the Clinical Global Impressions (CGI) approximately corresponded to a PANSS total score of 61 (22). Furthermore, schizophrenia tends to show up in people around late adolescence or early adulthood (23) and psychosis rarely starts to appear in older aged adults (>50 years of age), thus we recruited patients with age between 18 and 50 years old in this study. The exclusion criteria included patients with severe physical diseases (such as cardiovascular, liver, kidney, gastrointestinal diseases, etc.), infectious diseases and immune system diseases, patients with severe nervous system diseases and mental retardation, patients with other mental illness or drug dependence, and women during pregnancy or lactation. All enrolled patients in this study had not received any antipsychotic medication for at least 3 months before participating in the research. Seventy-six healthy subjects (male/female = 49/27), who were matched with the patients by gender, age, years of education, and body mass index (BMI), were enrolled as control group. Those subjects who presented either a personal or a family history of psychiatric disorders were ruled out from the control group.

The study was conducted in accordance with the Declaration of Helsinki (24) and was approved by the Institutional Review Board at Jiangxi Mental Hospital. All participants or their legal guardians were informed with the content of this study and signed a written informed consent.

Clinical Assessments

The PANSS (25) was used to evaluate the severity of psychopathology of patients. To ensure consistency and reliability of rating across the study, three psychiatrists participating in this study simultaneously attended a uniform training session in the use of the PANSS prior to the study. After unified training, the correlation analysis showed that the correlation coefficient for the PANSS total score between observers was higher than 0.80.

The Repeatable Battery for the Assessment of Neuropsychological Status (RBANS) (26) was adopted to

examine participants' cognitive ability. The scale has good clinical reliability and validity in Chinese population (27). The RBANS consists of 12 subtests that are used to calculate a total score and five age-adjusted index scores. The cognitive domains include Immediate memory (List Learning, Story Memory), Visuospatial/constructional (Figure Copy, Line Orientation), Language (Picture Naming, Semantic Fluency), Attention (Digit Span, Coding), and delayed memory (List Recognition, List Recall, Story Recall, Figure Recall). In this study, the total score and five index scores of RBANS were reported by standard score.

Plasma GDF-11 Detection

Blood samples were collected from the antecubital vein of patients who were fasted overnight. Whole blood was collected into tubes with EDTA and the tubes were centrifuged at 3,000 rpm for 5 min at temperature of 4°C. The plasma was carefully separated, aliquoted, and stored at −80°C before measurement.

The concentration of GDF-11 was determined by enzyme-linked immunosorbent assay (ELISA). The microplate provided in this kit has been pre-coated with an antibody specific to GDF-11 standards or samples are then added to the appropriate wells with a biotin-conjugated antibody specific to GDF-11. Next, avidin conjugated to Horeradish Peroxidase (HRP) is added to each microplate well and incubated. After tetramethylbenzydine (TMB) substrate solution is added, only those wells that contain GDF-11, biotin-conjugated antibody an enzyme-conjugated avidin will exhibit a change in color. The enzyme-conjugate reaction is terminated by the addition of sulphuric acid solution and the color change is determined by spectrophotometry at a wavelength of 450 ± 10 nm. The detecting O.D. is then compared with the standard curve to determine the concentration of GDF-11 in the sample. The minimum detectable concentration of this method is 6.2 pg/mL. The coefficients of variation for within and between batches are 8 and 11%, respectively.

Statistical Analysis

Multiple statistical methods were used to compare demographic and clinical variables. Student's t test or analysis of variance (ANOVA) were used to statistically analyze continuous variables, and chi-square test were adopted to statistically analyze categorical variables. Since the GDF-11 variables were normally distributed in control and patient groups (the Kolmogorov-Smirnov one-sample test, both $p > 0.05$), one-way ANOVA was adopted to examine where there was a difference in GDF-11 level between two groups. If the ANOVA test displayed a significant result, we continued to use age, gender, years of education, and BMI as covariates to perform the analysis of covariance (ANCOVA) to evaluate the effects of these variables. The Pearson correlation analysis was used to investigate the correlation between variables. Then we conducted partial correlation analysis to determine the associations of GDF-11 levels with psychotic symptoms or cognitive function by adjusting for clinical variables such as gender, age, education years, BMI, duration of illness, as well as age of onset. Bonferroni corrections were conducted to control for multiple testing. Finally, multivariate regression analyses (stepwise regression model) were used to examine the degree of association among independent variables in both patient and control groups. Statistical Product and Service Solutions (SPSS) 22.0 software was used to perform all statistical analyses. Data are presented as mean ± SD. All reported p-values are 2-tailed and $p < 0.05$ was considered statistically significant.

TABLE 1 | Demographic and clinical characteristics between schizophrenia patient group and normal control group.

	Healthy controls ($n = 76$)	Patients with schizophrenia ($n = 87$)	F or χ^2	p
Sex, M/F	49/27	52/35	0.381	0.537
Age (years)	35.50 ± 8.19	32.98 ± 10.74	2.856	0.093
Education (years)	11.05 ± 2.24	10.74 ± 4.07	0.364	0.547
BMI (kg/m^2)	22.29 ± 3.9	22.92 ± 3.75	1.315	0.253
Age of onset (years)	–	24.68 ± 6.85	–	–
Duration of illness (years)	–	8.49 ± 7.93	–	–
PANSS total score	–	102.76 ± 8.93	–	–
Positive subscale	–	27.59 ± 6.60	–	–
Negative subscale	–	25.19 ± 6.77	–	–
General psychopathology subscale	–	48.88 ± 11.9	–	–

M/F, Male/Female; BMI, body mass index; PANSS, Positive and Negative Syndrome Scale.

RESULTS

Demographic and Clinical Characteristics and Cognitive Performance

Table 1 presents the clinical demographic data of healthy controls and schizophrenia patients. There was no significant difference in age, gender, education years, and BMI between two groups (all $p > 0.05$). **Table 2** shows the cognitive performances of healthy controls and schizophrenia patients. Patients with schizophrenia performed more poorly in all these cognitive tasks compared to healthy controls (all $p < 0.05$). Significant differences remained after adjusting for age, gender, education years and BMI (all $p < 0.05$).

Plasma GDF-11 Levels in Healthy Controls and Schizophrenia Patients

Plasma GDF-11 levels in control and patient groups are presented in **Figure 1**. The content of plasma GDF-11 in the patients ranged from 9.91 to 101.94 pg/mL and plasma GDF-11 in the controls ranged from 10.26 to 119.42 pg/mL. Plasma GDF-11 levels were significantly different between patients and controls (32.30 ± 18.25 vs. 45.64 ± 24.41 pg/mL; $F = 15.87$, $p < 0.001$). When age, gender and BMI were used as potentially confounding covariates, the difference between the patient and control groups was still significant ($F = 4.247$, $p = 0.003$).

In the healthy control group, there were no significant correlations between plasma GDF-11 level and age, gender, or BMI, respectively. In the patients, there were no significant correlations between the level of GDF-11 and any demographic

TABLE 2 | Comparisons of RBANS cognitive function measurements between schizophrenia patient group and normal control group.

	Healthy controls ($n = 76$)	Patients with schizophrenia ($n = 87$)	F	p	Adjusted F^*	P^{**}
Immediate memory	77.28 ± 16.623	59.67 ± 12.753	48.506	<0.001	38.819	<0.001
Visuospatial/ constructional	79.13 ± 16.324	69.88 ± 14.765	11.693	0.001	9.386	<0.001
Language	81.30 ± 17.390	67.77 ± 17.140	19.931	<0.001	14.725	<0.001
Attention	92.38 ± 15.232	77.18 ± 17.880	26.149	<0.001	10.535	<0.001
Delayed memory	19.83 ± 21.789	65.06 ±16.598	19.999	<0.001	21.102	<0.001
Total score	409.92 ± 69.367	339.57 ± 54.679	43.313	<0.001	33.224	<0.001

**Adjusted F indicates the F value controlled for age, gender, years of education, and BMI.*
***p for Adjusted F test.*
BMI, body mass index; RBANS, Repeatable Battery for the Assessment of Neuropsychological Status.

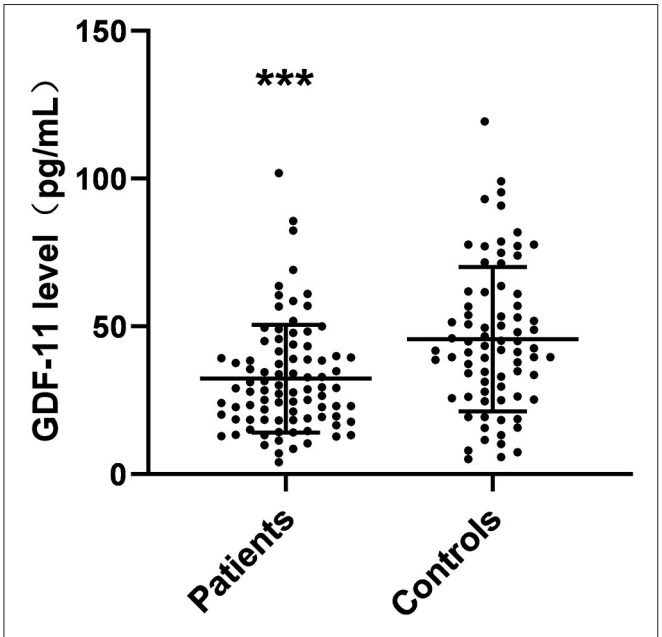

FIGURE 1 | Scattergrams of plasma GDF-11 levels from patients with schizophrenia ($n = 87$) and from normal control subjects ($n = 76$). The sample means are indicated by the black bars. ***$p < 0.001$.

variables, including age, gender, BMI, age of psychosis onset, and duration of the illness (all $p > 0.05$).

Association of GDF-11 Level With Psychopathology in Schizophrenia

Correlation analysis showed significant negative associations of plasma levels of GDF-11 with the PANSS total score ($r = -0.475$, $p < 0.001$), the positive symptoms score ($r = -0.357$, $p = 0.002$), the negative symptoms score ($r = -0.310$, $p = 0.006$), or the general psychopathological score ($r = -0.388$, $p = 0.001$) in patients with schizophrenia. Partial correlation analysis demonstrated that the correlations between GDF-11 levels and the PANSS total score ($r = -0.458$, $p = 0.001$), the positive symptoms score ($r = -0.333$, $p = 0.004$), the negative symptoms score ($r = -0.328$, $p = 0.005$), or the general psychopathological score ($r = -0.373$, $p = 0.001$) remained significant after adjusting for gender, age, education years, BMI, duration of illness, and age of onset (**Figure 2**). Given 9 tests [3 PANSS tests: (i) PANSS positive symptoms score, (ii) PANSS negative symptoms score, (iii) PANSS general psychopathology score, and 6 RBANS tests: (i) RBANS total score, (ii) immediate memory score, (iii) visuospatial/constructional score; (iv) language score; (v) attention score, and (vi) delayed memory score] were performed, multiplicity-adjusted p-value threshold based on Bonferroni method is 0.05/9 = 0.005556, and these correlation tests' p values remained significant after Bonferroni correction for multiple testing.

Correlations Between GDF-11 Level and Cognitive Function in Schizophrenia

The RBANS cognitive tests were classified into five domains: immediate memory (List Learning, Story Memory), visuospatial/constructional (Figure Copy, Line Orientation), language (Picture Naming, Semantic Fluency), attention (Digit Span, Coding), and delayed memory (List Recognition, List Recall, Story Recall, Figure Recall). Then the correlations between plasma GDF-11 level and cognitive function in both healthy control and patients were investigated.

No significant association was observed between plasma GDF-11 levels and cognitive performances in healthy controls (all $p > 0.05$). For patients, correlation analysis showed significant positive associations of plasma GDF-11 level with the RBANS total score ($r = 0.383$, $p = 0.001$), the immediate memory ($r = 0.348$, $p = 0.001$), the visuospatial/constructional ($r = 0.249$, $p = 0.023$), the attention ($r = 0.250$, $p = 0.023$), or the delayed memory ($r = 0.383$, $p = 0.001$). No significant association was found between plasma GDF-11 level and the language index ($r = 0.159$, $p = 0.152$). Partial correlation analysis showed that the correlations between GDF-11 level and the total score ($r = 0.350$, $p = 0.002$), the immediate memory ($r = 0.294$, $p = 0.011$) or the delayed memory ($r = 0.307$, $p = 0.008$) were still significant after adjusting for

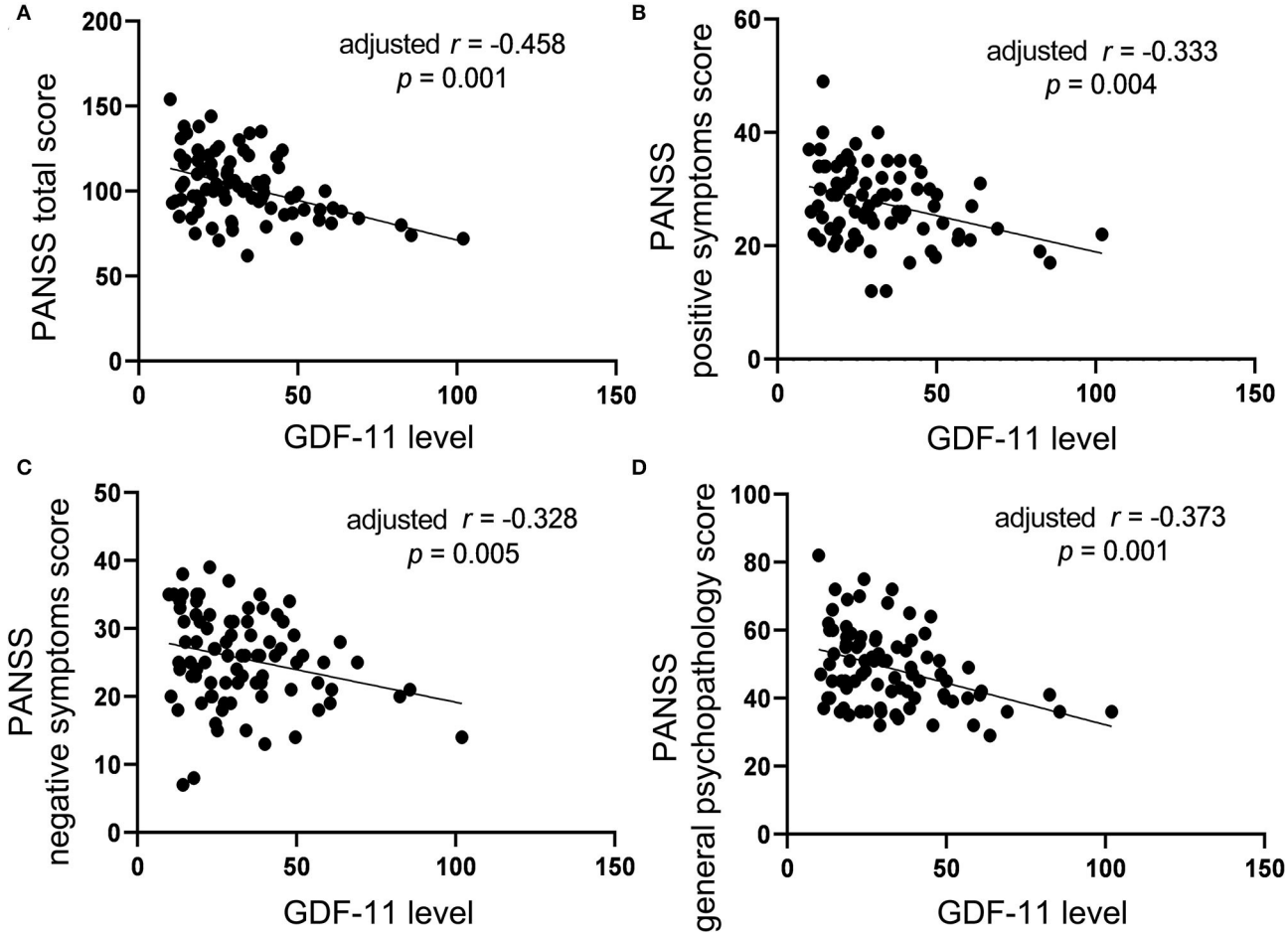

FIGURE 2 | The correlations between plasma GDF-11 level and the PANSS total score **(A)**, the positive symptoms score **(B)**, the negative symptoms score **(C)** or the general psychopathology score **(D)** in patients with schizophrenia. The *r* value in the panel is actually partial correlation coefficient after adjustment for the covariates including age, gender, years of education, BMI, duration of illness, and age of onset.

gender, age, education years, BMI, duration of illness, and age of onset (**Figure 3**). Given 9 tests [3 PANSS tests: (i) PANSS positive symptoms score, (ii) PANSS negative symptoms score, (iii) PANSS general psychopathology score, and 6 RBANS tests: (i) RBANS total score, (ii) immediate memory score, (iii) visuospatial/constructional score; (iv) language score; (v) attention score, and (vi) delayed memory score] were performed, multiplicity-adjusted p-value threshold based on Bonferroni method is $0.05/9 = 0.005556$, and these correlation tests' p values remained significant after Bonferroni correction for multiple testing.

Then we performed multiple regression analysis to examine independent determinants of RBANS and its indexes. For the healthy controls, GDF-11 was not a contributor to any of the total or sub-index score of RBANS (all $p > 0.05$). For the patients, GDF-11 was an independent contributor to the immediate memory ($t = 3.334$, $p = 0.001$), delayed memory ($t = 3.036$, $p = 0.003$) and RBANS total score ($t = 3.371$, $p < 0.001$). PANSS negative symptoms score was an independent contributor to the visuospatial/constructional ($t = -2.552$, $p = 0.013$), and PANSS total score was an independent contributor to the attention index of RBANS ($t = -3.524$, $p = 0.001$).

DISCUSSION

Our study revealed that (i) plasma GDF-11 levels were significantly lower in schizophrenia patients than those in healthy controls; (ii) there were significant negative correlations between GDF-11 level and the PANSS total score, positive symptoms score, negative symptoms score or general psychopathological score in patients; and (iii) plasma GDF-11 level was positively associated with the immediate memory and delayed memory in patients. For all we know, this study is the first to show that GDF-11 is associated with the psychopathology and cognition in schizophrenia.

GDF-11 is a member of the transforming growth factor β superfamily (28). It is widely expressed in adult CNS and has a crucial impact on brain development (11). Previous study has shown that GDF-11 can enhance neurogenesis in the brain,

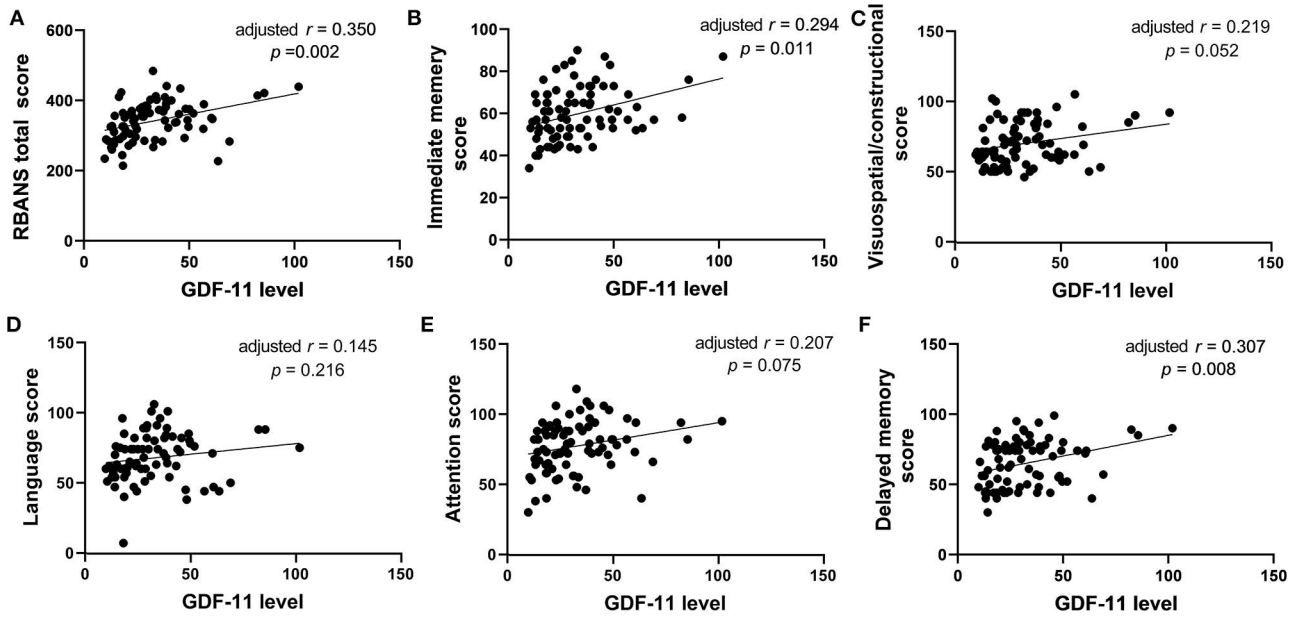

FIGURE 3 | The correlations between plasma GDF-11 level and the RBANS total score **(A)**, immediate memory score **(B)**, visuospatial/constructional score **(C)**, language score **(D)**, attention score **(E)** or delayed memory score **(F)** in patients with schizophrenia. The *r* value in the panel is actually partial correlation coefficient after adjustment for the covariates including age, gender, years of education, BMI, duration of illness, and age of onset.

especially in the hippocampus, helping remodeling the synapses and repairing the injured neurons (15, 29, 30). It can also regulate the function of astrocytes, whose activation are shown to contribute to the pathogenesis of schizophrenia (11). Our present findings show a significant decrease in plasma GDF-11 levels in schizophrenia patients, and GDF-11 level was related to the psychopathological symptoms and cognitive impairments. In combination with the roles of GDF-11 in neurogenesis and brain function (15, 29, 31) and the effects of GDF-11 on nerve development and cell regulations (32–34), it is indicated that GDF-11 may be related to the pathophysiology of schizophrenia. However, it should be noted that the difference in plasma GDF-11 levels between the patient and control groups could result from schizophrenia itself or other potential influence factors, such as the effect of antipsychotics. In this study, we enrolled patients who had not received any antipsychotic medication at least for 3 months before participating in the research. Combined with the findings that the decrease of plasma GDF-11 level was correlated to the severity of psychotic symptoms and cognitive impairments, we speculate that the population difference of plasma GDF-11 is more likely to be from to the disease itself, rather than to the secondary influence of drug therapy.

There were significantly negative relationships between GDF-11 level and the PANSS total score, or the positive, negative, and general psychopathological subscore, suggesting that patient with lower GDF-11 level would have a more severer psychopathological symptoms. Many studies could support the presumption that decrease of GDF-11 in schizophrenia might not be just an incidental phenomenon, but be associated to the pathological mechanisms of schizophrenia. Specifically, patients with abnormal brain function and structure such as Alzheimer's disease (35), Parkinson's syndrome (36) or craniocerebral trauma (37) show psychotic symptoms such as delusions and emotional disorders. Treatment with GDF-11 can effectively improve the symptoms of Alzheimer's and stroke patients (29, 38). The study of Katsimpardi et al. has also demonstrated that GDF-11 can improve the cerebral vasculature and enhance the neurogenesis (20). Systemic GDF-11 treatment significantly improved the vasculature in the cortex and hippocampus of old mice (15). However, this presumption is still required to be tested by using animal experiments. Furthermore, the exact mechanism of the decrease in GDF-11 levels in patients with schizophrenia is unclear, requiring further study.

Cognitive impairments are generally deemed as a core symptom of schizophrenia (39). A large number of studies have reported that patients with schizophrenia have cognitive impairments in many aspects, including speech learning, visual memory, attention, processing speed, working memory, and executive function (40, 41). Our results showed that the performances of immediate memory, language, attention, visuospatial/constructional and delayed memory in patients with schizophrenia were much poorer than those in the normal control group, and GDF-11 was positively associated with immediate memory and delayed memory in schizophrenia patients. GDF-11 can regulate the neuronal neurodevelopment process, including induction, proliferation, migration and survival of cells (15, 33, 34). Furthermore, GDF-11 is shown to have novel roles in neuronal plasticity and cognition (15), in which GDF-11 promotes synaptic remodeling in the

hippocampus (20). Thus, the finding that decreased plasma GDF-11 levels were correlated with cognitive impairments in patients with schizophrenia suggests that abnormal GDF-11 signaling is implicated with the pathogenesis of schizophrenia-associated cognitive impairments. However, it is uncertain whether the decline in GDF-11 levels in patients with schizophrenia is accidental or related to the pathogenesis of schizophrenia, as this is a cross-sectional study at which other factors, including the secondary influences of drug therapy and chronic diseases, cannot be completely excluded. More researches including animal experiments or longitudinal and prospective studies are required to further test these hypotheses.

The neurodevelopmental hypothesis of schizophrenia holds that the function state of the nervous system would be disturbed by genetic and early environmental factors during postnatal development, leading to abnormal neuronal proliferation and differentiation, excessive pruning, abnormal synaptic connection (4, 42). GDF-11 can enhance neurogenesis in the brain, helping remodeling the synapses and repairing the injured neurons (43). It also regulates the function of astrocytes and brain activity such as the dopamine neural loop (44), whose dysfunctions would cause schizophrenia-associated behavioral and cognitive symptoms. In this study, we showed a significant decrease in plasma GDF-11 level in schizophrenia, and decreased GDF-11 was correlated with the psychopathology and cognitive function of patients. Therefore, we postulate that disrupted GDF-11 signaling results in abnormalities of neurogenesis, astrocyte function and brain activity during early development, leading to the emergence of psychotic symptoms and cognitive disorders in late adolescence and young adulthood.

Our research has some limitations. First of all, although we found that decreased plasma GDF-11 was closely related to the severities of psychopathology and cognitive impairments in schizophrenia patients, the exact mechanism of GDF-11 affecting schizophrenia-related behaviors is not clear. It is necessary to conduct animal experiments to further reveal the mechanism of GDF-11 and its signaling pathway. Second, we only measured the level of GDF-11 in plasma, not the level of GDF-11 in the cerebrospinal fluid. This is not enough to infer similar changes in GDF-11 in the CNS and peripheral nervous system. Third, the number of schizophrenia subjects was relatively small in the present study. Larger-scale clinical research is necessary to confirm this finding in the future. Finally, all study subjects were of Chinese ancestry, which could limit the generalizability of the findings to other ethnic groups.

Taken together, our study revealed that decreased plasma GDF-11 in Chinese patients with schizophrenia was significantly correlated with the patients' psychopathological and cognitive symptoms, suggesting that altered GDF-11 signaling might contribute to the psychopathology and cognitive deficits in schizophrenia.

DATA AVAILABILITY STATEMENT

The raw data supporting the conclusions of this article will be made available by the authors, without undue reservation.

ETHICS STATEMENT

The studies involving human participants were reviewed and approved by Institutional Review Board at Jiangxi Mental Hospital. The patients/participants provided their written informed consent to participate in this study.

AUTHOR CONTRIBUTIONS

Z-xY, J-qZ, J-wX, BW, Y-hF, Z-pL, Y-tT, and A-lW participated in clinical data collection and lab data analysis. Y-jY and Z-xY designed the study, analyzed data, and prepared the manuscript. All authors contributed to the article and approved the submitted version.

FUNDING

This research was supported by grants from the National Natural Science Foundation of China (Nos. 82060258 and 81760254) and the Jiangxi Provincial Natural Science Foundation (Nos. 2020BCG74002, 20202BBG73022, and 20202BAB206026).

REFERENCES

1. Insel TR. Rethinking schizophrenia. *Nature.* (2010) 468:187–93. doi: 10.1038/nature09552
2. Rapoport JL, Giedd JN, Gogtay N. Neurodevelopmental model of schizophrenia: update 2012. *Mol Psychiatry.* (2012) 17:1228–38. doi: 10.1038/mp.2012.23
3. Van Winkel R, Stefanis NC, Myin-Germeys I. Psychosocial Stress and Psychosis. A review of the neurobiological mechanisms and the evidence for gene-stress interaction. *Schizophr Bull.* (2008) 34:1095–105. doi: 10.1093/schbul/sbn101
4. Lu L, Mamiya T, Koseki T, Mouri A, Nabeshima T. Genetic animal models of schizophrenia related with the hypothesis of abnormal neurodevelopment. *Biol Pharm Bull.* (2011) 34:1358–63. doi: 10.1248/bpb.34.1358
5. Sporn AL, Greenstein DK, Gogtay N, Jeffries NO, Lenane M, Gochman P, et al. Progressive brain volume loss during adolescence in childhood-onset schizophrenia. *Am J Psychiatry.* (2003) 160:2181–89. doi: 10.1176/appi.ajp.160.12.2181
6. Lieberman JA. Pathophysiologic mechanisms in the pathogenesis and clinical course of schizophrenia. *J Clin Psychiatry.* (1999) 60:9–12.
7. Bullmore ET, Frangou S. The dysplastic net hypothesis: an integration of developmental and dysconnectivity theories of schizophrenia. *Schizophr Res.* (1997) 28:143–56. doi: 10.1016/S0920-9964(97)00114-X
8. Kim J, Wu HH, Lander AD, Lyons KM, Matzuk MM, Calof AL. GDF11 controls the timing of progenitor cell competence in developing retina. *Science.* (2005) 308:1927–30. doi: 10.1126/science.1110175
9. Harmon EB, Apelqvist AA, Smart NG, Gu X, Kim S. GDF11 modulates NGN3+ islet progenitor cell number and promotes -cell differentiation in pancreas development. *Development.* (2005) 131:6163–74. doi: 10.1242/dev.01535
10. Mcpherron AC, Huynh TV, Lee SJ. Redundancy of myostatin and growth/differentiation factor 11 function. *BMC Dev Biol.* (2009) 9:1–9. doi: 10.1186/1471-213X-9-24
11. Hayashi Y, Mikawa S, Masumoto K, Katou F, Sato K. GDF11 expression in the adult rat central nervous system. *J Chem Neuroanat.* (2018) 89:21–36. doi: 10.1016/j.jchemneu.2018.02.003

12. Shi Y, Liu JP. Gdf11 facilitates temporal progression of neurogenesis in the developing spinal cord. *J Neurosci.* (2011) 31:883–93. doi: 10.1523/JNEUROSCI.2394-10.2011
13. Brun CE, Rudnicki M. GDF11 and the mythical fountain of youth. *Cell Metab.* (2015) 22:54–6. doi: 10.1016/j.cmet.2015.05.009
14. Poggioli T, Vujic A, Yang P, Maciastrevino C, Uygur A, Loffredo FS, et al. Circulating growth differentiation factor 11/8 levels decline with age. *Circ Res.* (2016) 118:29–37. doi: 10.1161/CIRCRESAHA.115.307521
15. Ozek C, Krolewski RC, Buchanan SM, Rubin LL. Growth differentiation factor 11 treatment leads to neuronal and vascular improvements in the hippocampus of aged mice. *Sci Rep.* (2018) 8:17293. doi: 10.1038/s41598-018-35716-6
16. Takaki J, Fujimori K, Miura M, Suzuki T. L-glutamate released from activated microglia downregulates astrocytic L-glutamate transporter expression in neuroinflammation: the 'collusion' hypothesis for increased extracellular L-glutamate concentration in neuroinflammation. *J Neuroinflam.* (2012) 9:275. doi: 10.1186/1742-2094-9-275
17. Cai, K. Magnetic resonance imaging of glutamate. *Nat Med.* (2012) 18:302–6. doi: 10.1038/nm.2615
18. Al Awabdh S, Gupta-Agarwal S, Sheehan DF, Muir J, Norkett R, Twelvetrees AE, et al. Neuronal activity mediated regulation of glutamate transporter GLT-1 surface diffusion in rat astrocytes in dissociated and slice cultures. *Glia.* (2016) 64:1252–64. doi: 10.1002/glia.22997
19. Lander SS, Khan U, Lewandowski N, Chakraborty D, Provenzano FA, Mingote S, et al. Glutamate dehydrogenase-deficient mice display schizophrenia-like behavioral abnormalities and CA1-specific hippocampal dysfunction. *Schizophr Bull.* (2019) 45:127–37. doi: 10.1093/schbul/sby011
20. Katsimpardi L, Litterman NK, Schein PA, Miller CM, Loffredo FS, Wojtkiewicz GR, et al. Vascular and neurogenic rejuvenation of the aging mouse brain by young systemic factors. *Science.* (2014) 344:630–4. doi: 10.1126/science.1251141
21. Zhang M, Jadavji NM, Yoo HS, Smith PD. Recombinant growth differentiation factor 11 influences short-term memory and enhances Sox2 expression in middle-aged mice. *Behav Brain Res.* (2018) 341:45–9. doi: 10.1016/j.bbr.2017.12.019
22. Leucht S, Kane JM, Kissling W, Hamann J, Etschel E, Engel RR. What does the PANSS mean? *Schizophr Res.* (2005) 79:231–8. doi: 10.1016/j.schres.2005.04.008
23. Celso A, Carmen M, Salvador M, Mara P, Manuel D, Dolores M, et al. Longitudinal brain changes in early-onset psychosis. *Schizophr Bull.* (2008) 34:341–53. doi: 10.1093/schbul/sbm157
24. World Medical Association. World Medical Association Declaration of Helsinki: ethical principles for medical research involving human subjects. *JAMA*. (2013) 310:2191–4. doi: 10.1001/jama.2013.281053
25. Kay SR, Fiszbein A, Opler LA. The positive and negative syndrome scale (PANSS) for schizophrenia. *Schizophr Bull.* (1987) 13:261–76. doi: 10.1093/schbul/13.2.261
26. Randolph C, Tierney MC, Mohr E, Chase TN. The repeatable battery for the assessment of neuropsychological status (RBANS): preliminary clinical validity. *J Clin Exp Neuropsychol.* (1998) 20:310–9. doi: 10.1076/jcen.20.3.310.823
27. Cheng Y, Wu W, Wang J, Feng W, Wu X, Li C. Reliability and validity of the repeatable battery for the assessment of neuropsychological status in community-dwelling elderly. *Arch Med Sci.* (2011) 7:850–7. doi: 10.5114/aoms.2011.25561
28. Egerman M A, Glass DJ. The role of GDF11 in aging and skeletal muscle, cardiac and bone homeostasis. *Crit Rev Biochem Mol Biol.* (2019) 54:174–83. doi: 10.1080/10409238.2019.1610722
29. Ma J, Zhang L, Niu T, Ai C, Jia G, Jin X, et al. Growth differentiation factor 11 improves neurobehavioral recovery and stimulates angiogenesis in rats subjected to cerebral ischemia/reperfusion. *Brain Res Bull.* (2018) 139:38–47. doi: 10.1016/j.brainresbull.2018.02.011
30. Rochette L, Malka G. Neuroprotective Potential of GDF11: myth or reality? *Int J Mol Sci.* (2019) 20:356. doi: 10.3390/ijms20143563
31. Hudobenko J, Ganesh BP, Jiang J, Mohan EC, Lee S, Sheth S, et al. Growth differentiation factor-11 supplementation improves survival and promotes recovery after ischemic stroke in aged mice. *Aging.* (2020) 12:8049–66. doi: 10.18632/aging.103122
32. Williams G, Zentar MP, Gajendra S, Sonego M, Doherty P, Lalli G. Transcriptional basis for the inhibition of neural stem cell proliferation and migration by the TGFβ-family member GDF11. *PLoS ONE.* (2013) 8:e78478. doi: 10.1371/journal.pone.0078478
33. Zhang Y, Wei Y, Liu D, Liu F, Chen D. Role of growth differentiation factor 11 in development, physiology and disease. *Oncotarget.* (2017) 8:81604–16. doi: 10.18632/oncotarget.20258
34. Schafer MJ, Lebrasseur NK. The influence of GDF11 on brain fate and function. *Geroence.* (2019) 41:1–11. doi: 10.1007/s11357-019-00054-6
35. Matsuoka T, Jin N, Shibata K, Taga C, Fukui K. Jealous delusions and dysfunction of the right parietal lobe in early-onset Alzheimer's disease. *J Neuropsychiatry Clin Neurosci.* (2011) 23:E29–30. doi: 10.1176/jnp.23.4.jnpe29
36. Rongve A, Auning E, Ehrt U, Arsland D. Psychosis in Parkinson's disease. *Tidsskr Nor Laegeforen.* (2012) 132:155–8. doi: 10.4045/tidsskr.11.0723
37. Molloy C, Conroy RM, Cotter DR., Cannon M. Is traumatic brain injury A risk factor for schizophrenia? A meta-analysis of case-controlled population-based studies. *Schizophr Bull.* (2011) 37:1104–10. doi: 10.1093/schbul/sbr091
38. Zhang W, Guo Y, Li B, Zhang Q, Xu JR. GDF11 rejuvenates cerebrovascular structure and function in an animal model of Alzheimer's disease. *J Alzheimers Dis.* (2018) 62:807–19. doi: 10.3233/JAD-170474
39. Lencz T, Smith CW, Mclaughlin D, Auther A, Nakayama E, Hovey L, et al. Generalized and specific neurocognitive deficits in prodromal schizophrenia. *Biol Psychiatry.* (2006) 59:863–71. doi: 10.1016/j.biopsych.2005.09.005
40. Van OJ, Kapur S. Schizophrenia. *Lancet.* (2009) 374:635–45. doi: 10.1016/S0140-6736(09)60995-8
41. Mcintosh BJ, Zhang XY, Kosten T, Tan SP, Xiu MH, Rakofsky J, et al. Performance-based assessment of functional skills in severe mental illness: results of a large-scale study in China. *J Psychiatr Res.* (2011) 45:1089–94. doi: 10.1016/j.jpsychires.2011.01.012
42. Rapoport JL, Addington A, Frangou S. The neurodevelopmental model of schizophrenia: update 2005. *Mol Psychiatry.* (2005) 10:434–49. doi: 10.1038/sj.mp.4001642
43. Zhang YH, Cheng F, Du XT, Gao JL, Xiao XL, Li N, et al. GDF11/BMP11 activates both smad1/5/8 and smad2/3 signals but shows no significant effect on proliferation and migration of human umbilical vein endothelial cells. *Oncotarget.* (2016) 7:12063–74. doi: 10.18632/oncotarget.7642
44. Sun YY, Zhang Y, Sun XP, Liu TY, Liu ZH, Chen G, et al. Fasciculation and elongation protein zeta-1 (FEZ1) expression in reactive astrocytes in a rat model of Parkinson's disease. *Neuropathol Appl Neurobiol.* (2014) 40:164–76. doi: 10.1111/nan.12077

Conflict of Interest: The authors declare that the research was conducted in the absence of any commercial or financial relationships that could be construed as a potential conflict of interest.

frontiers in Pharmacology

ORIGINAL RESEARCH
published: 09 December 2020
doi: 10.3389/fphar.2020.568423

Salidroside Attenuates Cognitive Dysfunction in Senescence-Accelerated Mouse Prone 8 (SAMP8) Mice and Modulates Inflammation of the Gut-Brain Axis

*Zeping Xie[1], Hui Lu[2], Sixia Yang[1], Yi Zeng[2], Wei Li[3], Linlin Wang[2], Guanfeng Luo[2], Fang Fang[1], Ting Zeng[2] and Weidong Cheng[2]**

[1]Traditional Chinese Pharmacological Laboratory, School of Traditional Chinese Medicine, Southern Medical University, Guangzhou, China, [2]School of Traditional Chinese Medicine, Southern Medical University, Guangzhou, China, [3]Institute of Chinese Materia Medica, Shanghai University of Traditional Chinese Medicine, Shanghai, China

Background: Alzheimer's disease (AD) is a fatal neurodegenerative disease characterized by progressive cognitive decline and memory loss. However, several therapeutic approaches have shown unsatisfactory outcomes in the clinical setting. Thus, developing alternative therapies for the prevention and treatment of AD is critical. Salidroside (SAL) is critical, an herb-derived phenylpropanoid glycoside compound, has been shown to attenuate lipopolysaccharide (LPS)-induced cognitive impairment. However, the mechanism underlying its neuroprotective effects remains unclear. Here, we show that SAL has a therapeutic effect in the senescence-accelerated mouse prone 8 (SAMP8) strain, a reliable and stable mouse model of AD.

Methods: SAMP8 mice were treated with SAL, donepezil (DNP) or saline, and cognitive behavioral impairments were assessed using the Morris water maze (MWM), Y maze, and open field test (OFT). Fecal samples were collected and analyzed by 16S rRNA sequencing on an Illumina MiSeq system. Brain samples were analyzed to detect beta-amyloid (Aβ) 1–42 (Aβ1-42) deposition by immunohistochemistry (IHC) and western blotting. The activation of microglia and neuroinflammatory cytokines was detected by immunofluorescence (IF), western blotting and qPCR. Serum was analyzed by a Mouse High Sensitivity T Cell Magnetic Bead Panel on a Luminex-MAGPIX multiplex immunoassay system.

Results: Our results suggest that SAL effectively alleviated hippocampus-dependent memory impairment in the SAMP8 mice. SAL significantly 1) reduced toxic Aβ1-42 deposition; 2) reduced microglial activation and attenuated the levels of the proinflammatory factors IL-1β, IL-6, and TNF-α in the brain; 3) improved the gut barrier integrity and modified the gut microbiota

OPEN ACCESS

Edited by:
Zili You,
University of Electronic Science and Technology of China, China

Reviewed by:
Gustavo Provensi,
University of Florence, Italy
Villers Agnes,
University of Mons, Belgium

***Correspondence:**
Weidong Cheng
chengweidong888@sina.com

Specialty section:
This article was submitted to Neuropharmacology, a section of the journal Frontiers in Pharmacology

Received: *01 June 2020*
Accepted: *21 October 2020*
Published: *09 December 2020*

Citation:
Xie Z, Lu H, Yang S, Zeng Y, Li W, Wang L, Luo G, Fang F, Zeng T and Cheng W (2020) Salidroside Attenuates Cognitive Dysfunction in Senescence-Accelerated Mouse Prone 8 (SAMP8) Mice and Modulates Inflammation of the Gut-Brain Axis. Front. Pharmacol. 11:568423. doi: 10.3389/fphar.2020.568423

Abbreviations AD Alzheimer's disease, SAL salidroside, SAMP8 senescence-accelerated mouse prone eight, Aβ beta-amyloid, NFTs neurofibrillary tangles, CNS central nervous system, SCFAs short-chain fatty acids, SAMR1 senescence-accelerated mouse resistant 1, OFT open field test, MWM Morris water maze, HE hematoxylin-eosin, IHC immunohistochemistry, IF immunofluorescence, IBA-1 ionized calcium binding adaptor molecule 1, APP amyloid precursor protein, IL interleukin, PCoA principal coordinate analysis, Th helper T cell, GM-CSF granulocyte-macrophage colony stimulating factor.

(reversed the ratio of Bacteroidetes to Firmicutes and eliminated Clostridiales and Streptococcaceae, which may be associated with cognitive deficits); and 4) decreased the levels of proinflammatory cytokines, particularly IL-1α, IL-6, IL-17A and IL-12, in the peripheral circulation, as determined by a multiplex immunoassay.

Conclusion: In summary, SAL reversed AD-related changes in SAMP8 mice, potentially by regulating the microbiota-gut-brain axis and modulating inflammation in both the peripheral circulation and central nervous system. Our results strongly suggest that SAL has a preventive effect on cognition-related changes in SAMP8 mice and highlight its value as a potential agent for drug development.

Keywords: microbiota, inflammation, microglia, SAMP8, cognition, salidroside

INTRODUCTION

A prevalence-based study reported that the worldwide cost of dementia in 2015 was an enormous sum of US $818 bn, an increase of 35.4% compared to that in 2010 that was related to an increasing number of patients and rising costs per person (Wimo et al., 2017). The latest data from the United States show that the total costs for health care and hospice care for elderly people (≥65 years) with dementia in 2020 are estimated to be up to $305 billion (Alzheimer's disease facts and figures. Alzheimer's & dementia, 2020). Alzheimer's disease (AD), as the primary cause of dementia, is a fatal neurodegenerative disease characterized by progressive cognitive decline and memory loss. The amyloid cascade hypothesis has been considered the main pathogenic concept in AD research for the past few decades. This hypothesis suggests that the accumulation of amyloid-β (Aβ) peptide in brain tissue is the primary event in AD, followed by the formation of neurofibrillary tangles (NFTs) containing tau protein (Hardy and Selkoe, 2002).

A number of recent studies have revealed the significance of the gut microbiota in AD. The microbiota-gut-brain axis has emerged as a potential key player that can have marked effects on AD pathology (Cryan et al., 2019). It has been confirmed that germ-free mice exhibit deficits in nonspatial and working memory, indicating that a commensal microbiota is required for cognition (Thion et al., 2018). It is widely accepted that the microbiota has a direct impact on the immune system, which is one of the various routes through which the microbiota communicates with the central nervous system (CNS). In addition, the microbiota has a profound impact on the maturation of microglial cells and effectively promotes the steady-state condition of microglia via secretion of short-chain fatty acids (SCFAs), highlighting the importance of the microbiota-gut-brain axis (Erny et al., 2015; Thion et al., 2018). On the other hand, there has been a growing number of recent studies investigating immune system-related events in AD, which have been shown to have strong pathogenic and therapeutic relevance (Heppner et al., 2015). Indeed, the inflammatory reaction that occurs in AD is driven mainly by CNS-resident immune cells, particularly microglia, which exert a dual influence in AD. It has been reported that disruption of the defense function of microglia leads to injury and even neuronal death (Hickman et al., 2018). Recent evidence strongly suggest that both the innate and adaptive immune systems are involved in AD, and it has been shown that proinflammatory mediators, including cytokines and chemokines, are increased in the peripheral circulation in individuals with AD (Cao and Zheng, 2019).

Animal models are paramount in AD research, especially for linking pathological changes, such as Aβ and tau accumulation. The senescence-accelerated mouse prone 8 (SAMP8) mouse strain, a spontaneous model of dementia, exhibits deficits in learning and memory abilities as well as pathological alterations in the brain, including increased oxidative stress, inflammation, Aβ accumulation and tau hyperphosphorylation (Currais et al., 2015). In contrast, its control, the senescence-accelerated mouse resistant 1 (SAMR1) line, ages normally. Salidroside (SAL), an herb-derived phenylpropanoid glycoside compound, has been shown to attenuate cognitive impairment in both lipopolysaccharide (LPS)-induced and d-gal-induced cognitive deficit models (Gao et al., 2015; Xu et al., 2019). Recent evidence has revealed that SAL provides neuroprotection by modulating mitochondrial biogenesis and microglial polarization (Barhwal et al., 2015; Liu et al., 2018). Notably, SAL exhibits significant anti-inflammatory effects in multiple diseases, such as osteoarthritis (Chen et al., 2019), colitis (Liu et al., 2019), skeletal muscle atrophy (Huang et al., 2019), renal interstitial fibrosis, (Li et al., 2019) and CNS diseases (Liu et al., 2018; Wang et al., 2018). Furthermore, recent findings have suggested that SAL alleviates liver injury by maintaining the balance of the gut microbiota (Yuan et al., 2019). Thus, it is reasonable to speculate that SAL exerts its neuroprotective function by regulating the gut microbiota, systemic inflammation, and subsequently neuropathologic changes. This study reports that SAL ameliorates cognitive decline in a reliable AD model, the SAMP8 mouse strain, and has beneficial effects on the inflammation-related microbiota-gut-brain axis.

MATERIALS AND METHODS

Animals

A total of 10 male SAMR1 mice and 30 male SAMP8 mice weighing 27–32 g were used. The mice were obtained from the

First Affiliated Hospital of Tianjin Traditional Chinese Medicine University (Tianjin, China). They were housed in a specific pathogen-free (SPF) level laboratory at Southern Medical University (Guangzhou, China) under standard conditions (22–23°C, 12-h light/dark cycle, and 60 ± 10% humidity) and provided with water and food ad libitum. They were adapted to their environmental conditions for 7 days before the experiments. All experimental protocols and animal handling procedures were conducted in strict accordance with the Guide for the Care and Use of Laboratory Animals published by the National Institutes of Health (NIH Publications No. 8023, revised in 1978). This study was approved by the Ethical Committee on Animal Experimentation of Southern Medical University.

Experimental Designs

After being acclimatized to the laboratory conditions for 1 week, the 10 male SAMR1 mice were assigned to the control group (R1-Ct, treated with saline), and the 30 SAMP8 mice were randomly divided into the following three groups (10 mice/group): the model group (P8-Ct , treated with saline), the SALgroup (P8-SAL, treated with 50 mg kg^{-1} d^{-1} SAL) and donepezil (DNP) group (P8-DNP , treated with 1 mg kg^{-1} d^{-1} DNP). SAL ($C_{14}H_{20}O_7$, purity >98%) was obtained from Macklin Biochemical Co., Ltd. (Shanghai, China). DNP was supplied by Eisai Pharmaceutical Co., Ltd. (Tokyo, Japan). All mice were treated by daily gavage for 3 months, and tissues were then removed for other experiments. Every effort to minimize suffering was made **Figure 1**.

Y-Maze

Spontaneous spatial working memory was assessed with a Y maze apparatus, which consisted of three identical arms (30 cm long, 8 cm wide, and 15 cm high). Each mouse was allowed to freely explore the three arms from the center of the maze for 5 min. The sequence of arm entries was recorded by a camera above the apparatus. A spontaneous alternation was defined as arm choices differing from the previous two choices (e.g., ABC, BCA, CAB, etc.). The alternation percentage (%) was calculated as the proportion of total spontaneous alternations relative to possible alternations (total arm entries −2) × 100%.

Morris Water Maze (MWM)

To assess the hippocampus-dependent learning and memory abilities of the mice, the MWM test was performed after the Y maze. The MWM apparatus consisted of a blue circular pool with a diameter of 120 cm filled *2/3* with water (25°C ± 1) containing nontoxic ink and a circular platform (14 cm in diameter) submerged 1.5 cm below the water surface. The MWM test was performed as described previously (O'Neal-Moffitt et al., 2015). Briefly, during the acquisition trial (days 1–5), each mouse was trained to find the hidden platform within 60 s. The search trajectories were recorded with a camera, and the escape latencies were measured using DigBehv-Morris software (Shanghai, China). The time each mouse needed to find the platform within 60 s was defined as the escape latency. If a mouse did not find the platform successfully, the latency was recorded as 60 s, and the mouse was gently guided to the platform and allowed to stay on it for 10 s. A probe trial, in which the platform was removed, was performed on day 6. The number of target platform crossings and the time spent in each quadrant were recorded.

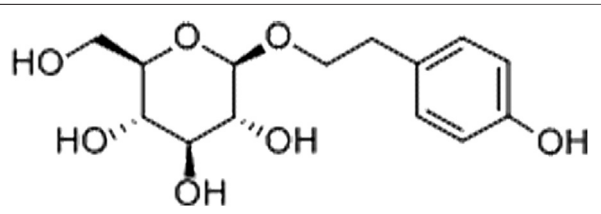

FIGURE 1 | Molecular structure of Salidroside.

Histological Analysis

Mice were anesthetized and intracardially perfused with cold PBS. Brain and intestinal tissues were carefully dissected and immersed in 4% paraformaldehyde at 4°C overnight. After being embedded in paraffin, the tissues were cut into sections (3 μm). Intestinal tissues were subjected to hematoxylin-eosin (HE) staining. Immunohistochemistry (IHC) analysis with a beta-amyloid 1–42 ($A\beta_{1\text{-}42}$) antibody (ab201060-10, 1:1,000; Abcam) was performed on the brain sections following the standard IHC-paraffin protocol from Abcam. Pictures were taken with an MVX10 microscope (Olympus). For immunofluorescence (IF) analysis, brain sections were blocked with 5% BSA for 1 h and incubated with a primary antibody against CD68 (1:500; Servicebio) overnight at 4°C followed by an anti-rabbit Cy3-labeled secondary antibody for 1 h at room temperature. The nuclei were stained with DAPI reagent (Servicebio). For IF imaging, confocal microscopy (Zeiss, LSM800) was used, and images were taken and processed with ZEN software and Microsoft PowerPoint.

Flow Cytometry

Flow cytometry was performed to detect the proportion of $CD4^+$ or $CD8^+$ lymphocytes in the spleen. Following sacrifice, the spleens were removed under sterile conditions, weighed, and processed into single cell suspensions, which then stained simultaneously with the following antibodies: PerCP-Cy™5.5 Rat Anti-Mouse CD3 (BD Biosciences, 560527), BV421 Rat Anti-Mouse CD4 (BD Biosciences, 562891), and FITC Rat Anti-Mouse CD8a (BD Biosciences, 553030), protected from light for 30 min. Labeled cells were fixed with 1% PFA and analyzed with a LSRFortessa X-20 flow cytometer (BD Biosciences, MA, United States) on FACSDiva 8.0.1 software (BD Biosciences). For each sample, corresponding isotype control antibodies were used. $CD3^+$ cells were gated as T lymphocytes, and then the $CD4^+$ and $CD8^+$ populations were analyzed.

Western Blot

Protein was extracted using the Whole Cell Lysis Assay (KeyGEN, Nanjing, China) according to the manufacturer's instructions.

The proteins were separated using SDS-PAGE and transferred to PVDF membranes (Millipore, Bedford, MA, United States). The membranes were blocked in 5% BSA for 1.5 h and then incubated with the following primary antibodies: anti-Aβ_{1-42} (ab201060-10, 1:1,000; Abcam), occludin (DF7504, 1:1,000; Affinity), ZO-1 (AF5145; 1:1,000; Affinity), β-actin (4,970; 1:1,000; CST), and GAPDH-HRP (HRP-60004, 1:8,000; Proteintech). After being washed with TBS-T, the membranes were incubated with secondary antibodies (SA00001-2, 1:8,000; Proteintech) for 2 h at 4°C except when the GAPDH-HRP antibody was used. The protein signals were detected using an ECL system (Affinity, Jiangsu, China).

Polymerase Chain Reaction

Total RNA was extracted from brain tissues using TRIzol reagent (Vazyme Biotech Co., Ltd) and converted to cDNA using the HiScript® III RT SuperMix for qPCR (+gDNA wiper) kit (Vazyme Biotech Co., Ltd.). qPCR was performed with ChamQ Universal SYBR qPCR Master Mix (Vazyme Biotech Co., Ltd.). All primers used are shown in **Supplementary Table S1**. Relative mRNA levels were calculated by normalization to the level of GAPDH (B661304, Sangon Biotech, Shanghai, China). Relative gene expression was analyzed based on the fold change (the $2^{-\Delta\Delta Ct}$ method) **Table 1**.

16S rRNA Sequencing and Data Analysis of Fecal Samples

Fecal samples were collected by using standardized collection procedures and were chosen at random. Five samples per group were used for 16S rRNA sequencing. The DNA samples were quantified, and then the V3-V4 hypervariable region was amplified using 338F (5′ACTCCTACGGGAGGCAGCAG 3′) and 806R (5′GGACTACHVGGGTWTCTAAT 3′) primers. All PCR amplicons were concentrated and purified by gel electrophoresis and 3 μg of each amplicon was subsequently extracted. Sequencing was performed on the Illumina MiSeq system. The raw data were quality-filtered using QIIME (version 1.9.1). Operational taxonomic units (OTUs) were clustered by UPARSE (version 7.0.1090 http://www.drive5.com/uparse) with 97% similarity cut-off. The taxonomy of each 16S rRNA gene sequence was analysed using the RDP Classifier (https://sourceforge.net/projects/rdp-classifier) against the SILVA rRNA database (https://www.arb-silva.de) with 70% confidence threshold. PCoA were conducted according to the distance matrices. LEfSe analysis (linear discriminant analysis [LDA]) was conducted to calculate significant changes in relative abundance of microbial taxa between the groups.

TABLE 1 | Primers used for qPCR.

QPCR Timers	Sequence(5'-3')
CD68-F	GAAATGTCACAGTTCACACCAG
CD68-R	GGATCTTGGACTAGTAGCAGTG
AIF1-F	ATTATGTCTTTGAAGCGAATGC
AIF1-R	TCTGAAGATGGCAGATCTCTTG
TNFα-F	ATGTCTCAGCCTCTTCTCATTC
TNFα-R	GCTTGTCACTCGAATTTTGAGA
IL6-F	CTCCCAACAGACCTGTCTATAC
IL6-R	CCATTGCAGAATGGAAAGTG
APP-F	TGAATGTGCAGAATGGAAAGTG
APP-R	AACTAGGCAACGGTAAGGAATC
IL-1β-F	TCGCAGCACATCAACAAGAG
IL-1β-F	AGGTCCACGGGAAAGACAGG
TREM2-F	TCATGTACTTATGAACGCCTGA
TREM2-R	GAGGTTCTTCAGAGTGATGGTG
TNF-F	ATGTCTCAAGCCTCTTCTCATTC
TNF-R	GCTTGTCAACTCGAATTTTGAGA

Multiplex Cytokine Assay

Serum was collected by centrifugation at 1000 *g* for 15 min at 4°C, aliquoted, and stored at −80°C until analysis. A Mouse High Sensitivity T Cell Magnetic Bead Panel (EMD Millipore, Billerica, MA, Unites States) was performed on the Luminex-MAGPIX multiplex immunoassay system according to the manufacturer's instructions. The data were analyzed using Milliplex Analyst 5.1 software (EMD Millipore, Billerica, MA, United States).

Statistical Analyses

Statistical analyses were performed with SPSS (IBM SPSS Statistics for Windows, version 20; IBM Corp., Armonk, NY, United States). Comparisons between groups were performed using one-way ANOVA for groups with one independent variables, and using two-way ANOVA for groups with two independent variables, followed by the least significant difference (LSD) test post hoc test. The following significance levels were used for comparisons between independent groups: #$p < 0.05$, ##$p < 0.01$, and ###$p < 0.001$ versus the R1-Ct group and *$p < 0.05$, **$p < 0.01$, and ***$p < 0.001$ versus the P8-Ct group. "ns" indicates no significant difference.

RESULTS

Effect of SAL on the Behavioral Performance of SAMP8 Mice

We treated mice with 50 mg kg^{-1} d^{-1} SAL, 1 mg kg^{-1} d^{-1} DNP or saline for 3 months, as described in the *Materials and Methods*. Treatment was started when the mice were 5 months of age, which is when AD pathological changes begin to emerge in this mouse strain (Pallas et al., 2008). To evaluate the effect of salidroside on the behavioral performance of SAMP8 mice, the Y maze test was conducted on day 78. Afterward, the MWM was performed for six consecutive days. Subsequently, the mice were sacrificed by euthanasia for histological and biochemical analyses (**Figure 2A**). The learning trials of the MWM revealed that SAMP8 required more time than SAMR1 mice to find the hidden platform and that escape latency was shortened by treatment with SAL or DNP (**Figures 2B–D**). Moreover, SAL treatment resulted in significant improvements in the percentage of time spent in the target quadrant and the number of target platform crossings, which represent memory recall, during the 60-s probe trial on the last day of the MWM (**Figures 2E,F**). Although the

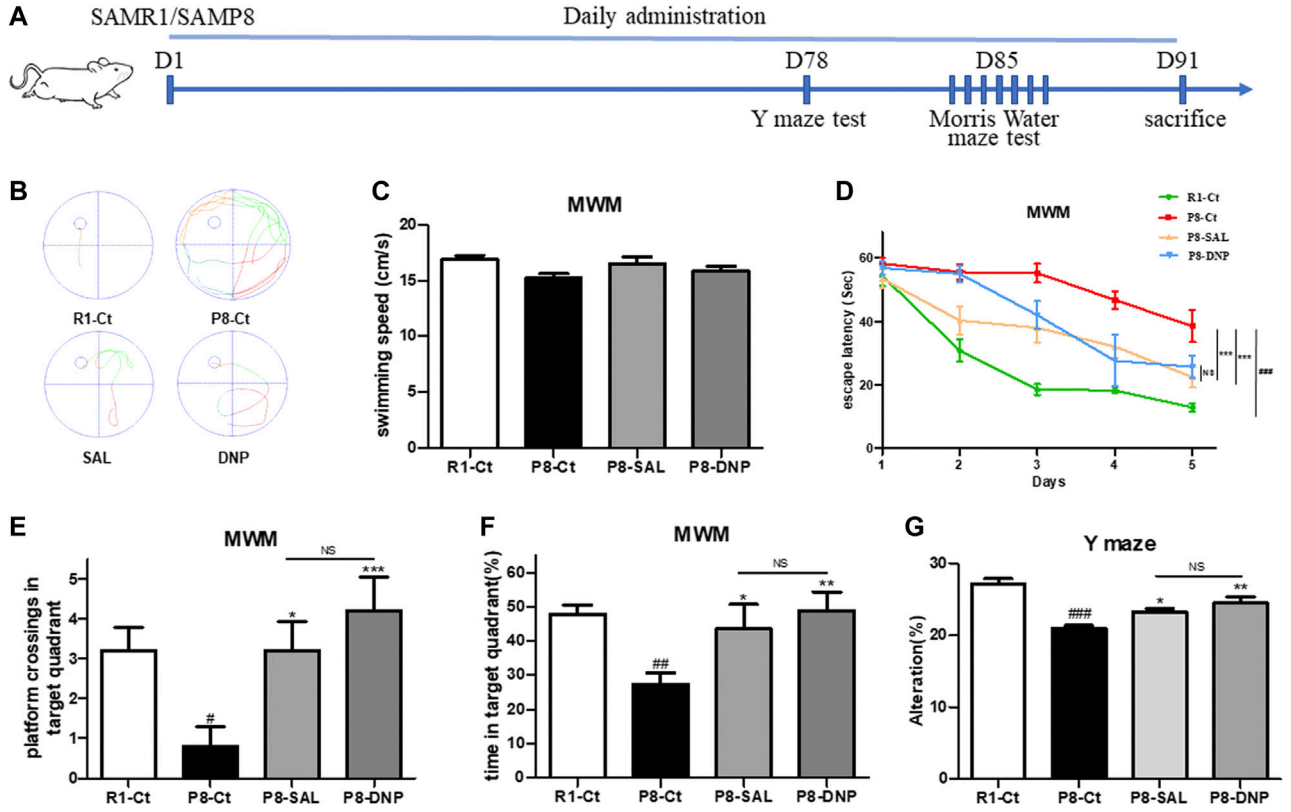

FIGURE 2 | Effect of SAL on the behavioral performance of SAMP8 mice. **(A)** Schematic of the experimental design. **(B)** Representative automated traces from day 5 of the MMW are shown for each group. **(C)** The average swimming speed. **(D)** The escape latency to reach the hidden platform was measured during the 5-day training period. **(E,F)** In the probe trial, the number of platform crossings and the percentage of time that the mice spent in the target quadrant were analyzed (n = 5 for each group). **(G)** The percentage of correct alternations (alternation rate) in the Y maze test was calculated (n = 8 for each group). All data are shown as the mean ± SEM. One way ANOVA for **(D–F)**, two way ANOVA for **(C)**. #$p < 0.05$, ##$p < 0.01$, and ###$p < 0.001$ versus the R1-Ct group and *$p < 0.05$, **$p < 0.01$, and ***$p < 0.001$ versus the P8-Ct group. "ns" indicates no significant difference.

performances of P8-DNP mice were slightly better than those of P8-SAL mice, the difference was not significant ($p > 0.05$). In the Y maze test, the correct alternation rates of the SAL- and DNP-treated SAMP8 mice were significantly higher than the correct alternation rate of the model group (**Figures 2G**).

Effect of SAL on Neurodegeneration and Neuroinflammation in SAMP8 Mice

The immunohistochemical results showed that A$\beta_{1\text{-}42}$ was highly expressed in the hippocampi (CA1 and CA3 regions) and cortices of SAMP8 mice but showed almost no expression in SAMR1 mice. Due to their exposed hydrophobic surfaces, Aβ_{1-42} monomers and oligomers tend to interact with the neuronal membrane and cause toxicity (Narayan et al., 2013). However, SAL administration induced a reduction in neuronal damage resulting from Aβ_{1-42}, which is thought to lead to an improvement in cognitive function, in SAMP8 mice (**Figures 3A,B**). The western blot analysis yielded results consistent with those of Aβ_{1-42} IHC (**Figures 3C,D**), and the mRNA expression of the amyloid precursor protein (APP) was also prevented by SAL (**Figure 3E**).

We observed strong CD68 immunoreactivity in the P8-Ct group and fewer CD68-positive cells in the P8-SAL group than in the P8-Ct group, indicating that SAL reduced microglial activation in SAMP8 mice (**Figures 4A, B**). Consistently, the mRNA expression of CD68 and ionized calcium binding adaptor molecule 1 (IBA-1) was also prevented by SAL (**Figures 4C,D**). Moreover, the production of proinflammatory cytokines (interleukin (IL)-1β, IL-6, and TNF-α) was decreased in the SAL-treated group compared to the saline-treated group (**Figures 4E–G**). Our data revealed that SAL administration significantly reduced toxic Aβ peptide deposition in SAMP8 mice and that this effect was accompanied by a reduction in microglial neuroinflammation.

Effect of SAL on the Intestinal Barrier and Gut Microbiota in SAMP8 Mice

Histological analysis and western blot analysis demonstrated that the integrity and tight junctions of the intestine were destroyed in SAMP8 mice. The HE staining of intestine showed that cells in the SAMP8 group were arranged irregularly, and edema was noted in villi (width of the villi). The intestinal mucosa of the P8-

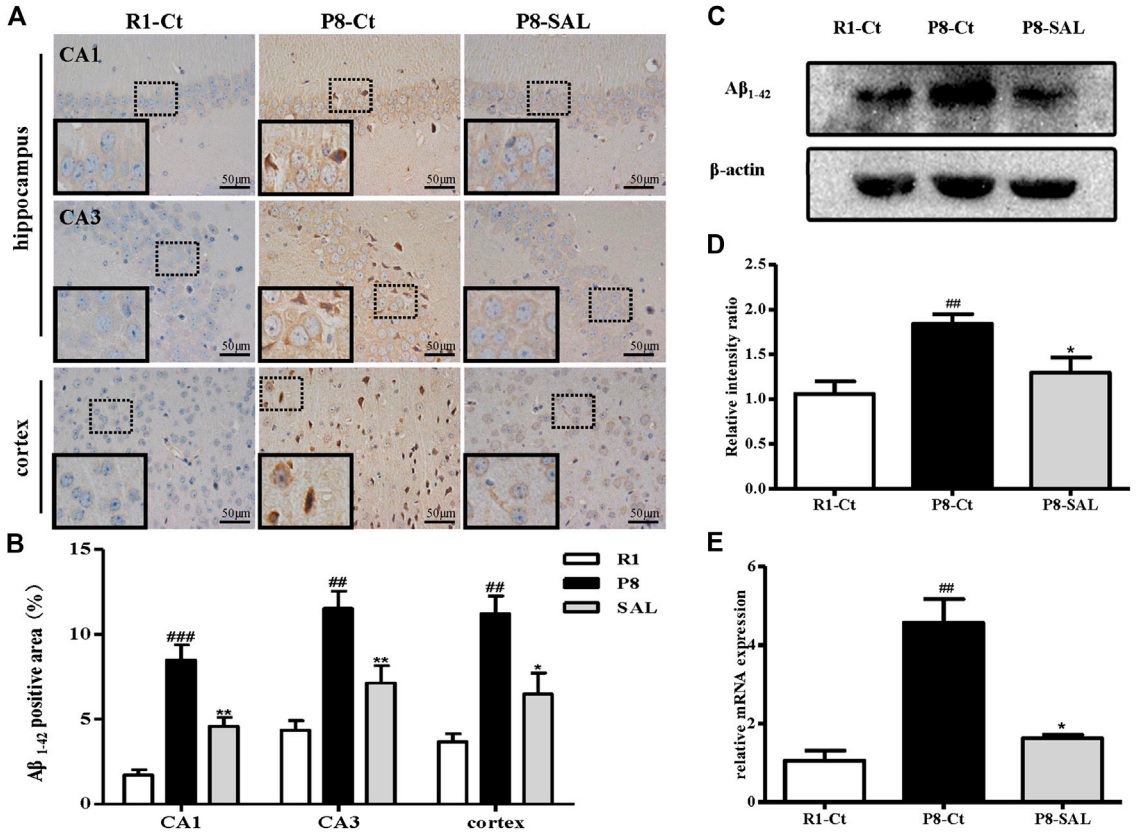

FIGURE 3 | Effect of SAL on neurodegeneration in SAMP8 mice. **(A,B)** Immunohistochemical staining and quantification of Aβ1-42 in the hippocampus and cortex in each group (magnification ×400). The dotted box presents an enlarged image of the inset. **(C)** Western blot analysis of Aβ1-42 expression and quantification in the hippocampus. **(D)** mRNA levels of APP determined by qPCR. All data are shown as the mean ± SEM (n = 3 for each group). $^{\#\#}p < 0.01$, versus the R1-Ct group and $^{*}p < 0.05$ versus the P8-Ct group.

SAL group exhibited a more complete structure, less inflammatory infiltration in crypts, and less swelling of villi than the intestinal mucosa of the P8-Ct group (**Figure 5 A**), and the ZO-1 and occludin protein levels were higher in the P8-SAL group (**Figures 5B,C**).

The sequence of the variable region of the 16S rRNA gene V3/V4 in fecal samples was analyzed. Fecal metagenomic sequencing data is available in the National Center for Biotechnology Information (NCBI) database with accession code PRJNA637826. To evaluate alterations in the microbial alpha diversity, we measured Chao, Shannon, Simpson, sob and ace diversity indices, which were not significantly different among groups (**Supplemental Figure S1**). Neither improvement in the total species diversity nor adverse effects was observed after SAL administration. Principal coordinate analysis (PCoA) revealed that the cluster from P8-SAL samples was more similar to that from R1-Ct samples, whereas the cluster from P8-Ct samples was more distinct (**Figure 6A**). To illustrate the differences in the microbiota composition, we conducted bar plot (**Figure 6B**), Circos (**Supplemental Figure S2**), and heatmap (**Figure 6C**) analyses. At the phylum level, there was a decrease in the *Bacteroidetes* phyla (R1-Ct, P8-Ct, and P8-SAL = 34, 30, and 36%, respectively) and an increase in the Firmicutes phyla (30, 40, and 29%, respectively), which are considered age-related differences that may also be associated with altered immune system function, in P8-Ct group (Nicholson et al., 2012). Interestingly, SAL treatment reversed the ratio of *Bacteroidetes* to *Firmicutes* to a level that was more similar to that observed in the R1-Ct group. Community barplot analysis at genus level showed that SAL administration increased the median abundance of *Norank_f_Muribaculaceae* (R1-Ct, P8-Ct, and P8-SAL = 37, 26, and 37%, respectively), *Alloprevotella* (70, 0.0, and 30%, respectively) and *Parasutterella* (48, 6.3, and 46%, respectively), and decreased the median abundance of *Prevotellaceae* (32, 37, and 31%, respectively), *Lachnospiraceae_NK4A136_group* (30, 46, 24%, respectively), *Unclassified_f_Lachnospiraceae* (35, 42, and 23%, respectively), *Alistipes* (28, 38, and 34%, respectively), *Norank_f_Lachnospiraceae* (26, 44, and 29%, respectively), *Odoribacter* (17, 55, and 28%, respectively), *Rikenellaceae_RC9_gut_group* (14, 61, and 25%, respectively), *Ruminococcaceae_UCG-014* (5.1, 78, and 17%, respectively) and *Ruminiclostridium_9* (28, 47, and 25%, respectively) in SAMP8 mice. A Circos diagram was used to visualize the associations between the abundance relationship between samples and bacterial communities at the genus level, which were consistent with the bar plot analysis results.

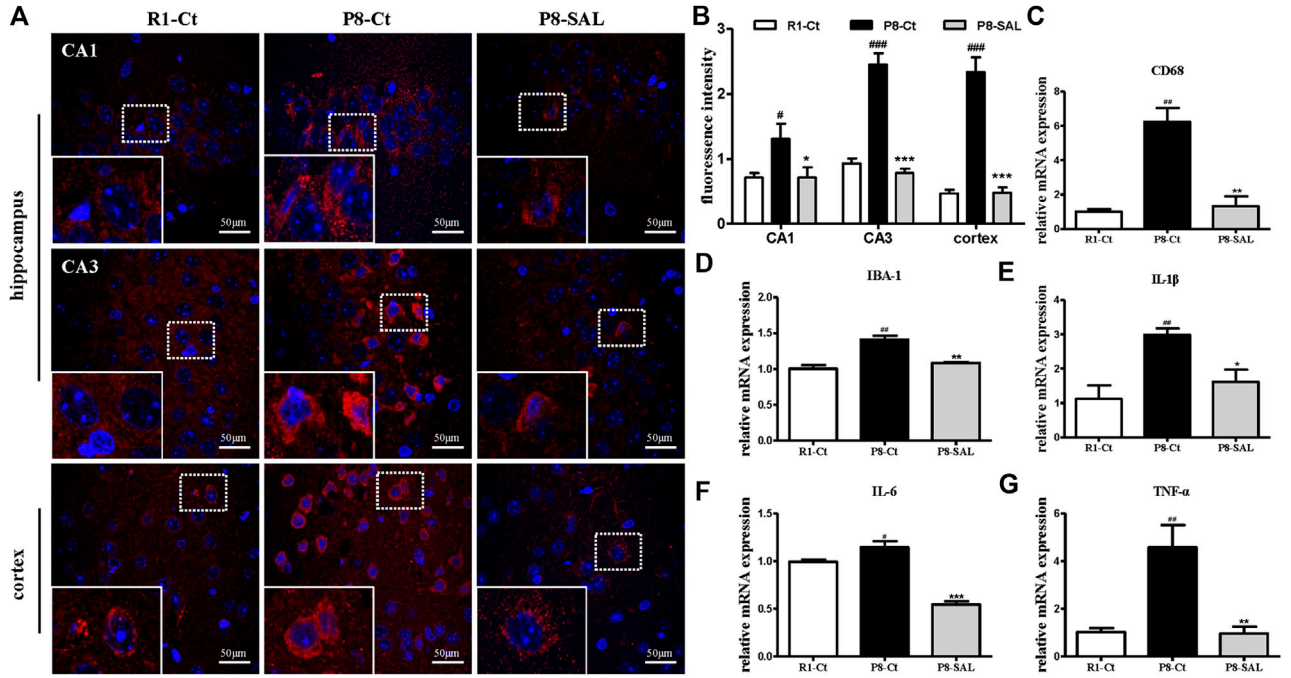

FIGURE 4 | Effect of SAL on neuroinflammation in SAMP8 mice. **(A,B)** Representative images and quantification of immunofluorescence analysis using antibodies against CD68 (red) and DAPI staining (blue) in the hippocampus (CA1 and CA3 regions) and cortex (magnification ×400). The dotted box presents an enlarged image of the inset. The mRNA levels of **(C)** CD68, **(D)** IBA-1, **(E)** IL-1β, **(F)** IL-6 and **(G)** TNF-α,were determined by qPCR. All data are shown as the mean ± SEM (n = 3 for each group). $^{\#}p < 0.05$, and $^{\#\#}p < 0.01$ versus the R1-Ct group and $^{*}p < 0.05$, $^{**}p < 0.01$, and $^{***}p < 0.001$ versus the P8-Ct group.

To further identify specific individual bacterial taxa that were differentially enriched among groups, we applied LEfSe analysis (**Supplemental Figure S3**). As shown above, significant enrichments in two families (*Clostridiales_vadinBB60* and *Streptococcaceae*), four genera (*norank_f_Clostridiales_vadinBB60*, *Peptococcus*, *Streptococcus*, and *Ruminococcaceae_UCG_009*) and seven species that were abolished by the SAL administration were identified in the SAMP8 mice, and five newborn species were present only in the P8-SAL group (**Figure 6D**). Venn diagram at the phylum, family, and genus levels. The analysis of the species in the Venn plots showed that salidroside basically eliminated the Chloroflexi phylum and five families and seven genera in SAMP8, and Corynebacterium was confirmed to be associated with AD-related pathological development (**Supplemental Figure S4**).

Effect of SAL on Systematic Inflammation in SAMP8

To assess the effects of SAL on peripheral cytokine secretion, a magnetic bead analysis approach was used to detect the concentration of 18 cytokines/chemokines in the plasma. The results showed that granulocyte-macrophage colony stimulating factor (GM-CSF), IL-1α, IL-6, IL-12, IL-13, and IL-17A were increased in SAMP8 mice compared to SAMR1 mice (**Supplemental Figure S5**) and that the levels of IL-1α (**Figure 7B**), IL-6 (**Figure 7C**), IL-17A (**Figure 7D**) and IL-12 (**Figure 7E**) were decreased after SAL administration compared to after saline administration. These data suggest that there is chronic inflammation in the circulation of SAMP8 mice and that SAL has significant anti-inflammatory properties in SAMP8 mice. In addition, the flow cytometry results demonstrated that the number of $CD3^{+}CD4^{+}$ lymphocytes and the $CD4^{+}/CD8^{+}$ ratio were significantly decreased in the spleens of SAMP8 mice compared to the spleens of SAMR1 mice. However, there were no significant changes in these measures after SAL administration compared to after saline administration (**Figure 7F**).

DISCUSSION

The senescence-accelerated prone mouse 8 (SAMP8) mouse strain is considered a reliable experimental model for studying the pathogenesis of and developing preventive and therapeutic strategies for age-related AD (Cheng et al., 2014). SAMP8 mice develop early deficits in learning and memory (at 5 months of age) accompanied by a number of AD-related brain alterations, including increased oxidative stress and tau phosphorylation (Pallas et al., 2008). Here, we treated 5-month-old SAMP8 with SAL for 3 months. At 8 months of age, the mice presented a stronger AD-related phenotype than SAMR1 mice, and the preventive effect of SAL was prominent. Our results suggest that SAL effectively alleviated hippocampus-dependent memory impairment in SAMP8 mice and did not have significantly different effects from those of DNP. Although DNP exerts a neuroprotective

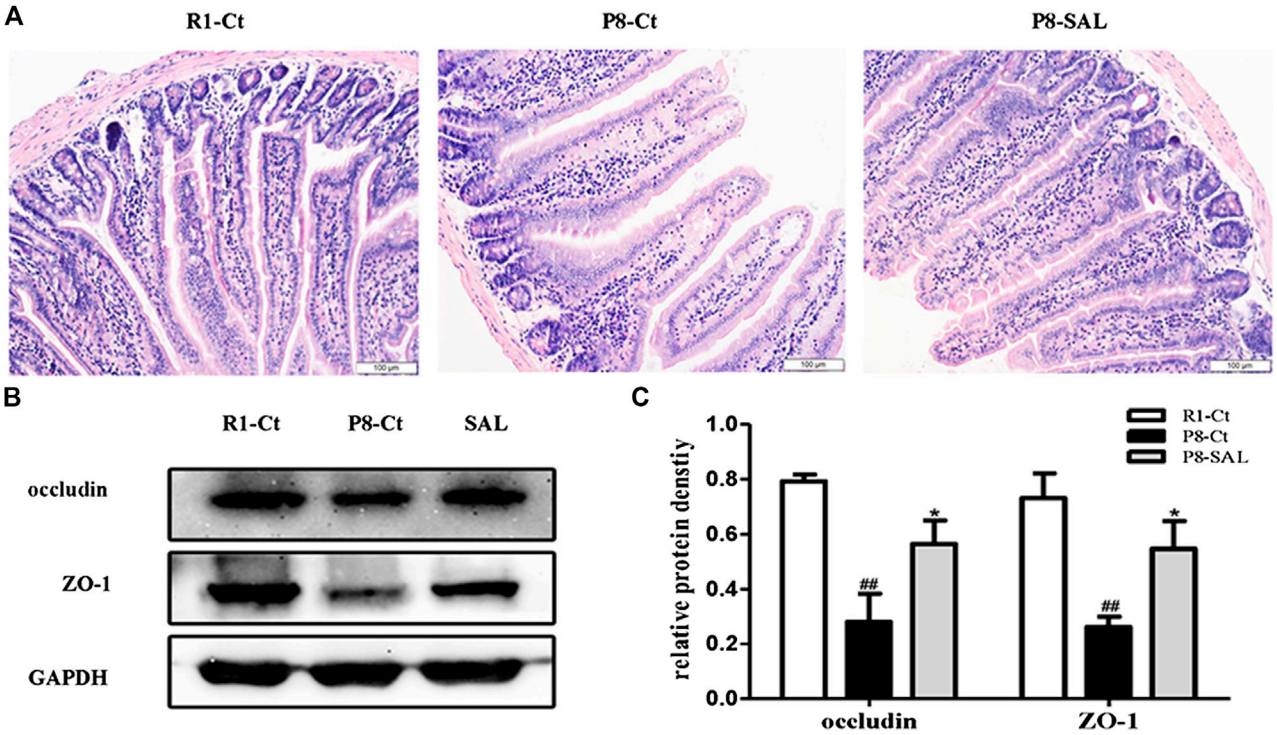

FIGURE 5 | Effect of SAL on the intestinal barrier in SAMP8 mice. **(A)** HE staining of mouse intestinal tissues (scale bar = 100 μm). **(B)** Western blot analysis of ZO-1 and occludin in the intestine. **(C)** Protein quantification by western blotting. All data are shown as the mean ± SEM (n = 3 for each group). $^{\#\#}p < 0.01$ versus the R1-Ct group and $^{*}p < 0.05$ versus the P8-Ct group.

effect and is widely used in the treatment of AD, numerous studies have demonstrated that it causes adverse effects, including symptoms such as hostility, somnolence, fecal incontinence, nausea and rhinitis (Birks and Harvey, 2006; Lee et al., 2017; Adlimoghaddam et al., 2018). Previous studies have shown that SAL exerts neuroprotection, and no significant adverse effects have been reported yet (Zhang et al., 2010; Zhang et al., 2016; Zhong et al., 2018). Thus, SAL has the potential to be developed into an alternative treatment for AD.

In this study, SAL was shown to effectively attenuate both $A\beta_{1-42}$ deposition and neuroinflammation in the brains of SAMP8 mice. Recent research in on a 3D noncell-autonomous cell culture model showed that a high Aβ42/40 ratio drives robust tau phosphorylation in human neurons, suggesting that selectively reducing the Aβ42/40 ratio could be a novel therapeutic approach (Kwak et al., 2020). In the present study, less $A\beta_{1-42}$ deposition were observed in the hippocampi (CA1 and CA3 regions) and cortices of SAMP8 mice after SAL treatment compared to after saline treatment, confirming its therapeutic efficacy. Indeed, $A\beta_{1-42}$ oligomers have a high tendency to attach to the membrane and have been implicated in neuronal injury and cognitive impairment associated with AD (Guglielmotto et al., 2014). Proinflammatory microglial activities are believed to have various detrimental effects on the brain and contribute to neurodegeneration. In particular, the activation of microglia increases the formation of Aβ oligomers and further aggregation (Narayan et al., 2013; Venegas et al., 2017). We showed here that the number of activated microglial cells, as determined by CD68 immunofluorescence, was significantly reduced in SAL-treated SAMP8 mice compared to saline-treated SAMP8 mice. Moreover, the mRNA levels of the proinflammatory cytokines IL-1β, IL-6, and TNF-α were decreased by varying degrees in SAMP8 mouse brains after SAL administration compared to after saline administration. These results therefore illustrate a novel effect of SAL involving attenuation of neuroinflammation in the AD brain **Figure 8**.

Multiple studies have indicated that microbial colonization of the gut is linked to dementia pathogenesis via detrimental effects on metabolic disorders or low-grade inflammatory progression, leading to brain damage (Alkasir et al., 2017). Consistent with previous studies (Peng et al., 2018), our findings provide further evidence that the microbiota-gut-brain axis may be involved in AD-like pathogenesis in SAMP8 mice. PCoA and microbiota composition analysis revealed that the cluster from salidroside-treated SAMP8 mice was more similar to that from SAMR1 mice, whereas the cluster from untreated SAMP8 mice was the most distinct. In our study, a shift in the ratio of *Bacteroidetes* to *Firmicutes*, which is one of the classic age-related changes in microbiota composition that is associated with increased inflammation, was observed in SAMP8 mice (Nicholson et al., 2012; Cowan et al., 2014). The

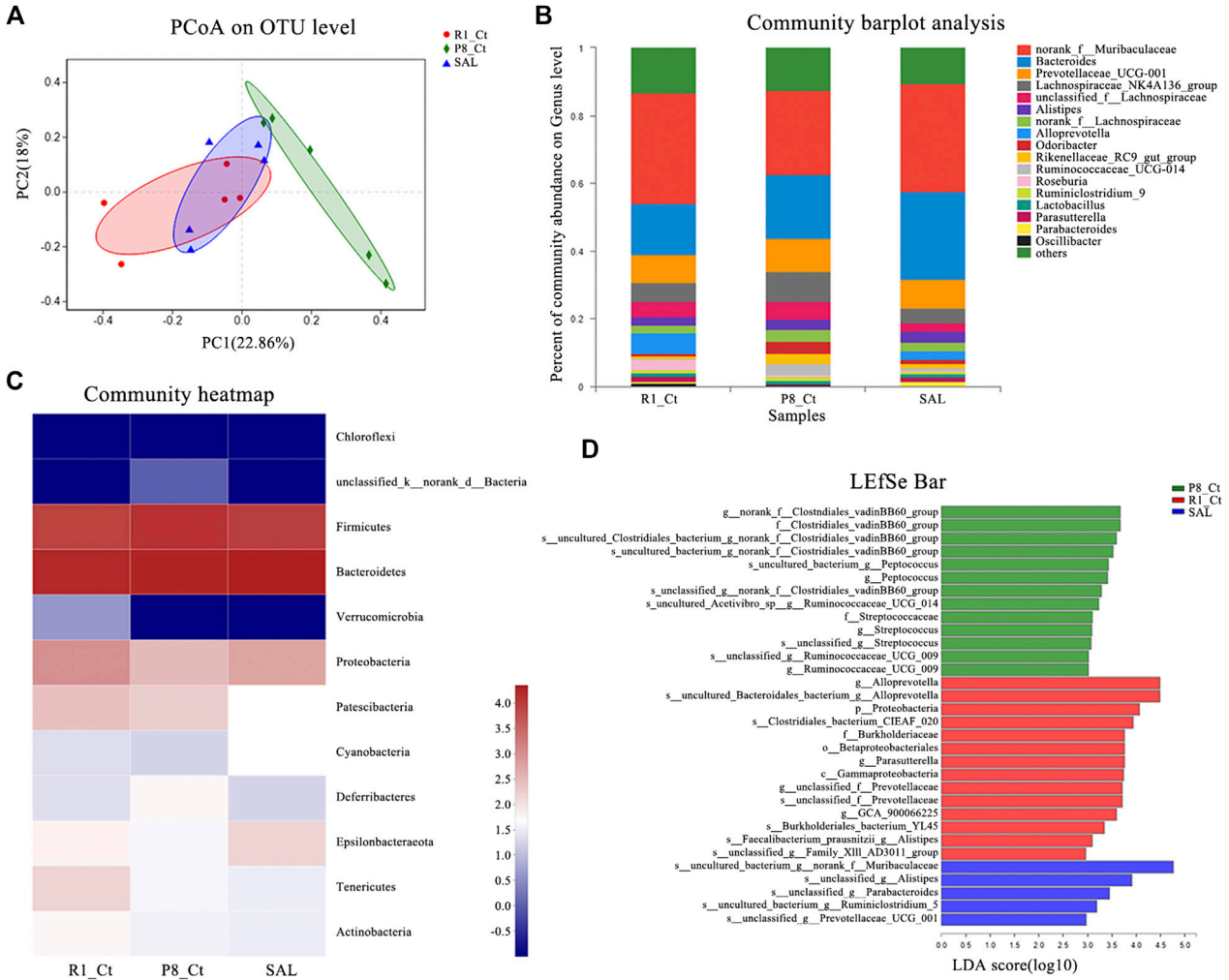

FIGURE 6 | Effect of SAL on the gut microbiota in SAMP8 mice. **(A)** PCoA plots of the Bray-Curtis distance at the operational taxonomic unit (OTU) level. **(B)** Barplot analysis of the relative abundance in the community at the genus level. Genera with abundances less than 0.01 (1%) are summed in the category "others". **(C)** Heatmap of microbial community abundance profiles at the phylum level. Top 50 species by total abundance. **(D)** Results of the LEfSe analysis (LDA > 2) at the phylum to the species level.

reversal effect of SAL indicated its potential to delay senescence and reduce inflammation. Significant enrichments in two families (*Clostridiales_vadinBB60* and *Streptococcaceae*), four genera (*norank_f_Clostridiales_vadinBB60*, *Peptococcus*, *Streptococcus*, and *Ruminococcaceae_UCG_009*) and seven species, which were abolished by SAL administration, were identified in SAMP8 mice,. These results suggest that SAL normalizes alterations in the intestinal microbiota. It should be noted that *Clostridiales* and *Streptococcaceae* are part of the phylum *Firmicutes* and may be associated with cognition (Bajaj et al., 2019). In addition, five newborn species were present only in the P8-SAL group, but whether they are beneficial requires further study.

Given the importance of microglial functions in the promotion of neurodegenerative processes, it is reasonable to speculate that changes in the gut microbiota, which are capable of inducing inflammation via some cell components or metabolites, may influence these inflammatory and degenerative alterations in the AD brain. In our study, SAL was able to restore intestinal barrier integrity, which may result in less accumulation of microbial products in the periphery as well as a reduction in chronic inflammation. As immune-related effects on bacteria are important steps toward understanding bacterial contributions to cognition, we estimated alterations in the circulating levels of proinflammatory and anti-inflammatory cytokines/chemokines, which directly affect brain function. Low-grade systemic inflammation was observed in the serum of SAMP8 mice, whereas SAL decreased the levels of the proinflammatory cytokines IL-1α, IL-6, IL-17A and IL-12. Notably, elevated levels of these four proinflammatory cytokines are reported to be involved in cognitive decline or AD pathology (Veerhuis et al., 2003; Vom Berg et al., 2012; Fragoulis et al., 2017; Italiani et al., 2018). Th1 cells significantly accelerate markers of AD, as demonstrated primarily in murine models (Lambracht-Washington et al., 2011), and *in vivo* imaging experiments have shown that Th17 cells induce severe

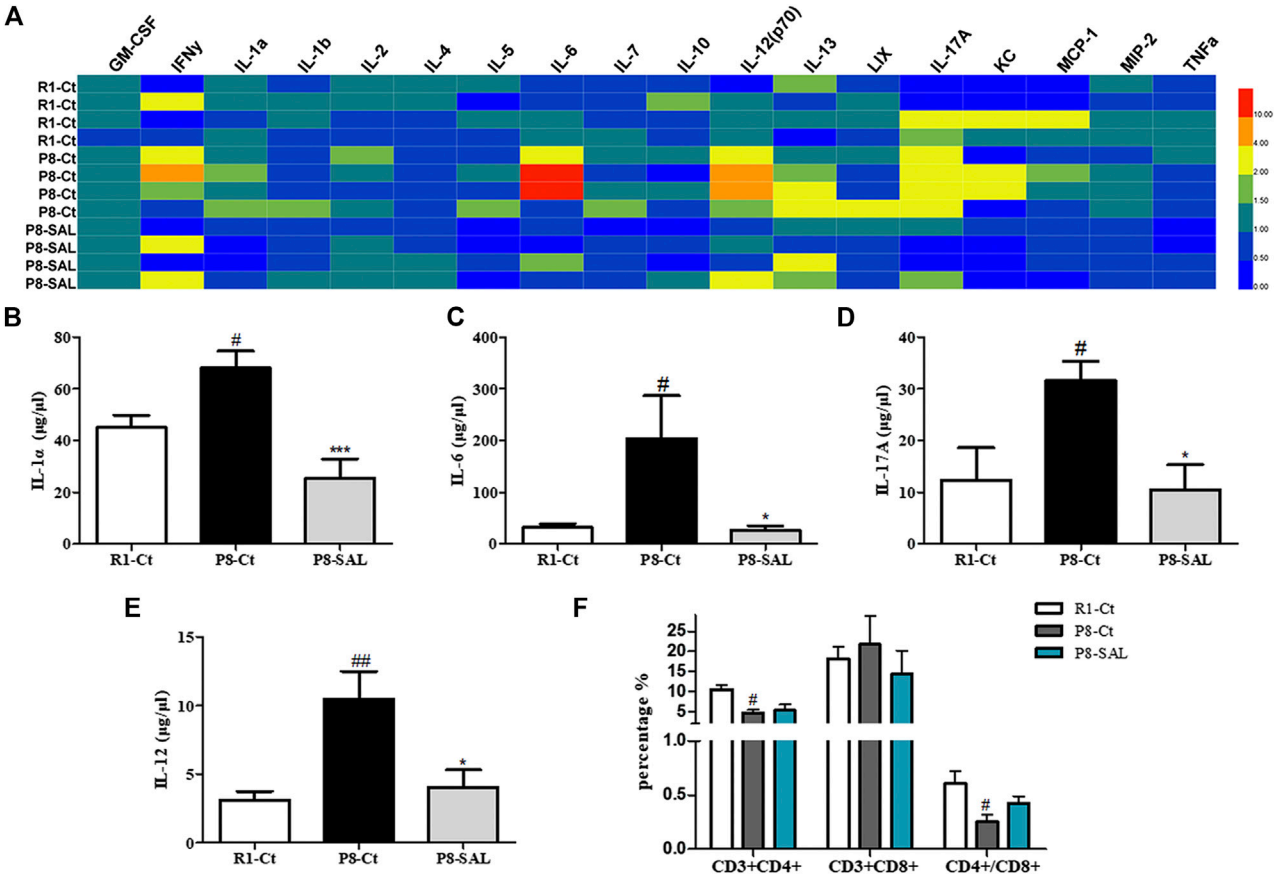

FIGURE 7 | Effect of SAL on peripheral inflammation in SAMP8 mice. **(A)** Heatmap of 18 serum cytokine/chemokine levels, as detected by the Mouse High Sensitivity T Cell Magnetic Bead Panel. Quantitation of **(B)** IL-1α, **(C)** IL-6, **(D)** IL-12 and **(E)** IL-17A levels. **(F)** The spleen index was calculated as spleen weight **(G)**/mouse weight **(G)**. **(G)** Flow cytometry results, including the proportions of $CD3^+CD4^+$ and $CD3^+CD8^+$ cells and the ratio of $CD4^+/CD8^+$ spleen lymphocytes. The bars represent the mean ± SE of each group (n = 3). $^{\#}p < 0.05$, and $^{\#\#}p < 0.01$ versus the R1-Ct group and $^{*}p < 0.05$ and $^{***}p < 0.001$ versus the P8-Ct group.

fluctuations in the neuronal intracellular Ca (2+) concentration, causing neuronal damage and neuroinflammation (Siffrin et al., 2010). It is known that IL-12 induces T lymphocytes to differentiate into Th1 cells and that IL-17A is a Th17-specific cytokine. Additionally, the pleiotropic cytokine IL-6 is crucial for the differentiation of Th17 cells. Indeed, there are associations between serum profiles of inflammatory factors and gut microbiomes. One study suggested that variability of the microbiota, especially the phylum *Proteobacteria*, is positively correlated with IL-6 (Biagi et al., 2010). Moreover, it has been reported that blocking IL-1α leads to a modification in the gut microbiome and effectively reduces inflammation and damage in a mouse model of Crohn's-like ileitis (Menghini et al., 2019). Microbial products have direct effects on the immune system, which affects brain function through circulating cytokines (Cryan and Dinan, 2012). It has been reported that many of the beneficial effectual of bacteria on learning and memory occur alongside reductions in proinflammatory cytokines (Wang et al., 2015; Allen et al., 2016; Burokas et al., 2017). One study showed that systemic immune alterations trigger and drive the development of AD-related neuropathology, specifically Aβ accumulation and tau phosphorylation, as well as microglia and gliosis activation in wild-type mice, suggesting that immune reactions can precede AD-related pathology and may even be sufficient to cause it (Krstic et al., 2012). Thus, the effect of SAL on cognition may be associated with recovery of the gut microbiota composition, which is crucial for reducing peripheral low-grade inflammation thus improving of brain-blood barrier function and suppressing neuroinflammatory stimuli.

In summary, SAL reversed the AD-related changes in the SAMP8 mice potentially by regulating the microbiota-gut-brain axis and modulating inflammation in both the peripheral circulation and central nervous system. Our results strongly suggest that SAL has a therapeutic effect on cognition-related changes in SAMP8 mice and highlight its value as a potential agent for drug development.

DATA AVAILABILITY STATEMENT

The datasets presented in this study can be found in online repositories. The names of the repository/repositories and accession

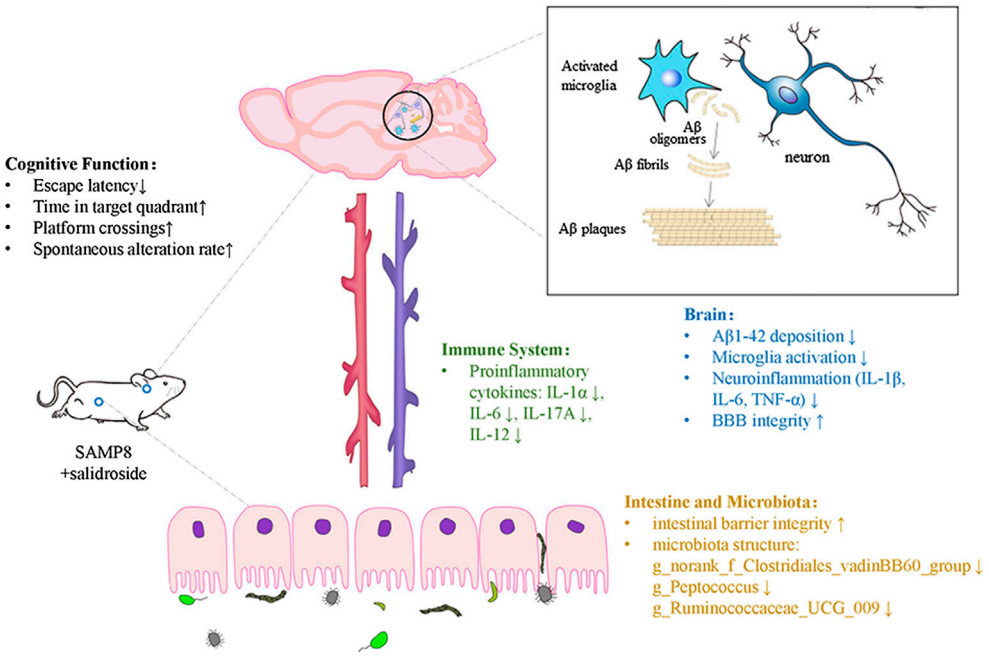

FIGURE 8 | Salidroside modulates the Gut-brain Axis in SAMP8 mice.

number(s) can be found below: https://www.ncbi.nlm.nih.gov/, PRJNA637826.

ETHICS STATEMENT

The animal study was reviewed and approved by the Ethical Committee on Animal Experimentation of Southern Medical University.

AUTHOR CONTRIBUTIONS

ZX designed and performed the experiments, analyzed the data, and drafted the manuscript. HL collected the fecal samples and assisted with the 16S rRNA sequencing analysis. SY, YZ, FF, and TZ assisted with the histological staining and qPCR. LW designed the flow cytometry experiment and assisted with the flow cytometry data acquisition and analysis. LW and GL assisted with the behavioral tests and western blot analysis. FF assisted with the multiplex immunoassay experiments. WC provided study supervision and manuscript revision. All authors read and approved the final manuscript. All authors contributed to the article and approved the submitted version.

FUNDING

This research was funded by the Guangzhou Municipal Science and Technology Project (grant number 201904010168), the National Natural Science Foundation of China (grant number 81973641), and the National Key Research and Development Program of China (grant number 2018YFC1704400).

ACKNOWLEDGMENTS

This manuscript has been released as a pre-print at https://doi.org/10.21203/rs.3.rs-24799/v1 (Xie et al., 2020). We sincerely thank Prof. Xingmei Zhang, Prof. Yuyao Chen and the Department of Neurobiology, Southern Medical University for their assistance.

SUPPLEMENTARY MATERIAL

The Supplementary Material for this article can be found online at: https://www.frontiersin.org/articles/10.3389/fphar.2020.568423/full#supplementary-material.

REFERENCES

Adlimoghaddam, A., Neuendorff, M., Roy, B., and Albensi, B. C. (2018). A review of clinical treatment considerations of donepezil in severe Alzheimer's disease. *CNS Neurosci. Ther.* 24 (10), 876–888. doi:10.1111/cns.13035

Alkasir, R., Li, J., Li, X., Jin, M., and Zhu, B. (2017). Human gut microbiota: the links with dementia development. *Protein Cell* 8 (2), 90–102. doi:10.1007/s13238-016-0338-6

Allen, A. P., Hutch, W., Borre, Y. E., Kennedy, P. J., Temko, A., Boylan, G., et al. (2016). Bifidobacterium longum 1714 as a translational psychobiotic: modulation of stress, electrophysiology and neurocognition in healthy volunteers. *Transl. Psychiatry*. 6 (11), e939. doi:10.1038/tp.2016.191

2020 Alzheimer's disease facts and figures. *Alzheimer's & Dementia*.

Bajaj, J. S., Salzman, N. H., Acharya, C., Sterling, R. K., White, M. B., Gavis, E. A., et al. (2019). Fecal microbial transplant capsules are safe in hepatic encephalopathy: a phase 1, randomized, placebo-controlled trial. *Hepatology*, 70 (5), 1690–1703. doi:10.1002/hep.30690

Barhwal, K., Das, S. K., Kumar, A., Hota, S. K., and Srivastava, R. B. (2015). Insulin receptor A and Sirtuin 1 synergistically improve learning and spatial memory following chronic salidroside treatment during hypoxia. *J. Neurochem.* 135 (2), 332–346. doi:10.1111/jnc.13225

Biagi, E., Nylund, L., Candela, M., Ostan, R., Bucci, L., Pini, E., et al. (2010). Through ageing, and beyond: gut microbiota and inflammatory status in seniors and centenarians. *PloS One*, 5 (5), e10667. doi:10.1371/journal.pone.0010667

Birks, J., and Harvey, R. J. (2006). Donepezil for dementia due to Alzheimer's disease. *Cochrane Database Syst. Rev.* 2018 (6), CD001190.

Burokas, A., Arboleya, S., Moloney, R. D., Peterson, V. L., Murphy, K., Clarke, G., et al. (2017). Targeting the microbiota-gut-brain Axis: prebiotics have anxiolytic and antidepressant-like effects and reverse the impact of chronic stress in mice. *Biol. Psychiatr.*, 82 (7), 472–487. doi:10.1016/j.biopsych.2016.12.031

Cao, W., and Zheng, H. (2019). Peripheral immune system in aging and Alzheimer's disease. *Mol. Neurodegener.* 13 (1), 51. doi:10.1186/s13024-018-0284-2

Chen, D., Lu, D., Liu, H., Xue, E., Zhang, Y., Shang, P., et al. (2019). Pharmacological blockade of PCAF ameliorates osteoarthritis development via dual inhibition of TNF-α-driven inflammation and ER stress. *EBioMedicine* 50, 395–407. doi:10.1016/j.ebiom.2019.10.054

Cheng, X.-R., Zhou, W.-X., and Zhang, Y.-X. (2014). The behavioral, pathological and therapeutic features of the senescence-accelerated mouse prone 8 strain as an Alzheimer's disease animal model. *Ageing Research Reviews* 13, 13–37. doi:10.1016/j.arr.2013.10.002

Cowan, T. E., Palmnäs, M. S. A., Yang, J., Bomhof, M. R., Ardell, K. L., Reimer, R. A., et al. (2014). Chronic coffee consumption in the diet-induced obese rat: impact on gut microbiota and serum metabolomics. *J. Nutr. Biochem.*, 25 (4), 489–495. doi:10.1016/j.jnutbio.2013.12.009

Cryan, J. F., and Dinan, T. G. (2012). Mind-altering microorganisms: the impact of the gut microbiota on brain and behaviour. *Nat. Rev. Neurosci.* 13 (10), 701–712. doi:10.1038/nrn3346

Cryan, J. F., O'Riordan, K. J., Cowan, C. S. M., Sandhu, K. V., Bastiaanssen, T. F. S., Boehme, M., et al. (2019). The microbiota-gut-brain Axis. *Physiol. Rev.* 99 (4), 1877–2013.

Currais, A., Goldberg, J., Farrokhi, C., Chang, M., Prior, M., Dargusch, R., et al. (2015). A comprehensive multiomics approach toward understanding the relationship between aging and dementia. *Aging* 7 (11), 937–955. doi:10.18632/aging.100838

Erny, D., Hrabě de Angelis, A. L., Jaitin, D., Wieghofer, P., Staszewski, O., David, E., et al. (2015). Host microbiota constantly control maturation and function of microglia in the CNS. *Nat. Neurosci.* 18 (7), 965–977. doi:10.1038/nn.4030

Fragoulis, A., Siegl, S., Fendt, M., Jansen, S., Soppa, U., Brandenburg, L.-O., et al. (2017). Oral administration of methysticin improves cognitive deficits in a mouse model of Alzheimer's disease. *Redox Biology* 12, 843–853. doi:10.1016/j.redox.2017.04.024

Gao, J., He, H., Jiang, W., Chang, X., Zhu, L., Luo, F., et al. (2015). Salidroside ameliorates cognitive impairment in a d-galactose-induced rat model of Alzheimer's disease. *Behav. Brain Res.* 293, 27–33. doi:10.1016/j.bbr.2015.06.045

Guglielmotto, M., Monteleone, D., Piras, A., Valsecchi, V., Tropiano, M., Ariano, S., et al. (2014). Aβ1-42 monomers or oligomers have different effects on autophagy and apoptosis. *Autophagy*, 10 (10), 1827–1843. doi:10.4161/auto.30001

Hardy, J., and Selkoe, D. J. (2002). The amyloid hypothesis of Alzheimer's disease: progress and problems on the road to therapeutics. *Science* 297 (5580), 353–356. doi:10.1126/science.1072994

Heppner, F. L., Ransohoff, R. M., and Becher, B. (2015). Immune attack: the role of inflammation in Alzheimer disease. *Nat. Rev. Neurosci.*, 16 (6), 358–372. doi:10.1038/nrn3880

Hickman, S., Izzy, S., Sen, P., Morsett, L., and El Khoury, J. (2018). Microglia in neurodegeneration. *Nat. Neurosci.* 21 (10), 1359–1369. doi:10.1038/s41593-018-0242-x

Huang, Z., Fang, Q., Ma, W., Zhang, Q., Qiu, J., Gu, X., et al. (2019). Skeletal muscle atrophy was alleviated by salidroside through suppressing oxidative stress and inflammation during denervation. *Front. Pharmacol.* 10, 997. doi:10.3389/fphar.2019.00997

Italiani, P., Puxeddu, I., Napoletano, S., Scala, E., Daniela, M., Manocchio, S., et al. (2018). Circulating levels of IL-1 family cytokines and receptors in Alzheimer's disease: new markers of disease progression?. *J. Neuroinflammation* 15 (1), 342. doi:10.1186/s12974-018-1376-1

Krstic, D., Madhusudan, A., Doehner, J., Vogel, P., Notter, T., Imhof, C., et al. (2012). Systemic immune challenges trigger and drive Alzheimer-like neuropathology in mice. *J. Neuroinflammation* 9, 151. doi:10.1186/1742-2094-9-151

Kwak, S. S., Washicosky, K. J., Brand, E., Maydell, D. V., Aronson, J., Kim, S., et al. (2020). Amyloid-beta42/40 ratio drives tau pathology in 3D human neural cell culture models of Alzheimer's disease. *Nat. Commun.* 11 (1), 1377. doi:10.1038/s41467-020-15120-3

Lambracht-Washington, D., Qu, B. X., Stüve, O., Eagar, T. N., and Rosenberg, N. (2011). DNA immunization against amyloid beta 42 has high potential as safe therapy for Alzheimer's disease as it diminishes antigen-specific Th1 and Th17 cell proliferation. *Cell. Mol. Neurobiol.* 31 (6), 867–874. doi:10.1007/s10571-011-9680-7

Lee, C., Lee, K., Yu, H., Ryu, S.-H., Moon, S. W., Han, C., et al. (2017). Adverse events with sustained-release donepezil in alzheimer disease. *J. Clin. Psychopharmacol.* 37 (4), 401–404. doi:10.1097/jcp.0000000000000726

Li, R., Guo, Y., Zhang, Y., Zhu, L., and Yan, T. (2019). Salidroside ameliorates renal interstitial fibrosis by inhibiting the TLR4/NF-kappaB and MAPK signaling pathways. *Int. J. Mol. Sci.* 20(5),1103. doi:10.3390/ijms20051103

Liu, X., Wen, S., Yan, F., Liu, K., Wang, L., Zhao, S., et al. (2018). Salidroside provides neuroprotection by modulating microglial polarization after cerebral ischemia. *J. Neuroinflammation* 15 (1), 39. doi:10.1186/s12974-018-1081-0

Liu, J., Cai, J., Fan, P., Zhang, N., and Cao, Y. (2019). The abilities of salidroside on ameliorating inflammation, skewing the imbalanced nucleotide oligomerization domain-like receptor family pyrin domain containing 3/autophagy, and maintaining intestinal barrier are profitable in colitis. *Front. Pharmacol.* 10, 1385. doi:10.3389/fphar.2019.01385

Menghini, P., Corridoni, D., Butto, L. F., Osme, A., Shivaswamy, S., Lam, M., et al. (2019). Neutralization of IL-1alpha ameliorates Crohn's disease-like ileitis by functional alterations of the gut microbiome. *Proc. Natl. Acad. Sci. USA* 116, 26717–26726.

Narayan, P., Ganzinger, K. A., Mccoll, J., Weimann, L., Meehan, S., Qamar, S., et al. (2013). Single molecule characterization of the interactions between amyloid-β peptides and the membranes of hippocampal cells. *J. Am. Chem. Soc.* 135 (4), 1491–1498. doi:10.1021/ja3103567

Nicholson, J. K., Holmes, E., Kinross, J., Burcelin, R., Gibson, G., Jia, W., et al. (2012). Host-gut microbiota metabolic interactions. *Science*, 336 (6086), 1262–1267. doi:10.1126/science.1223813

O'Neal-Moffitt, G., Delic, V., Bradshaw, P. C., and Olcese, J. (2015). Prophylactic melatonin significantly reduces Alzheimer's neuropathology and associated cognitive deficits independent of antioxidant pathways in AβPP(swe)/PS1 mice. *Mol. Neurodegener.* 10, 27. doi:10.1186/s13024-015-0027-6

Pallas, M., Camins, A., Smith, M. A., Perry, G., Lee, H.-G., and Casadesus, G. (2008). From aging to alzheimer's disease: unveiling "the switch" with the senescence-accelerated mouse model (SAMP8). *J. Alzheimers Dis.* 15 (4), 615–624. doi:10.3233/jad-2008-15408

Peng, W., Yi, P., Yang, J., Xu, P., Wang, Y., Zhang, Z., et al. (2018). Association of gut microbiota composition and function with a senescence-accelerated mouse model of Alzheimer's Disease using 16S rRNA gene and metagenomic sequencing analysis. *Aging* 10 (12), 4054–4065. doi:10.18632/aging.101693

Siffrin, V., Radbruch, H., Glumm, R., Niesner, R., Paterka, M., Herz, J., et al. (2010). *In vivo* imaging of partially reversible th17 cell-induced neuronal dysfunction in the course of encephalomyelitis. *Immunity* 33 (3), 424–436. doi:10.1016/j.immuni.2010.08.018

Thion, M. S., Low, D., Silvin, A., Chen, J., Grisel, P., Schulte-Schrepping, J., et al. (2018). Microbiome influences prenatal and adult microglia in a sex-specific manner. *Cell* 172 (3), 500–516.e16. doi:10.1016/j.cell.2017.11.042

Veerhuis, R., Van Breemen, M. J., Morbin, M., Ouladhadj, J., Tagliavini, F., et al. (2003). Amyloid β plaque-associated proteins C1q and SAP enhance the Aβ1-42 peptide-induced cytokine secretion by adult human microglia *in vitro*. *Acta Neuropathol.* 105 (2), 135–144. doi:10.1007/s00401-002-0624-7

Venegas, C., Kumar, S., Franklin, B. S., Dierkes, T., Brinkschulte, R., Tejera, D., et al. (2017). Microglia-derived ASC specks cross-seed amyloid-β in Alzheimer's disease. *Nature* 552 (7685), 355–361. doi:10.1038/nature25158

Vom Berg, J., Prokop, S., Miller, K. R., Obst, J., Kälin, R. E., Lopategui-Cabezas, I., et al. (2012). Inhibition of IL-12/IL-23 signaling reduces Alzheimer's disease-like pathology and cognitive decline. *Nat. Med.* 18 (12), 1812–1819. doi:10.1038/nm.2965

Wang, T., Hu, X., Liang, S., Li, W., Wu, X., Wang, L., et al. (2015). Lactobacillus fermentum NS9 restores the antibiotic induced physiological and psychological abnormalities in rats. *Beneficial Microbes* 6 (5), 707–717. doi:10.3920/bm2014.0177

Wang, C., Wang, Q., Lou, Y., Xu, J., Feng, Z., Chen, Y., et al. (2018). Salidroside attenuates neuroinflammation and improves functional recovery after spinal cord injury through microglia polarization regulation. *J. Cell Mol. Med.* 22 (2), 1148–1166. doi:10.1111/jcmm.13368

Wimo, A., Guerchet, M., Ali, G.-C., Wu, Y.-T., Prina, A. M., Winblad, B., et al. (2017). The worldwide costs of dementia 2015 and comparisons with 2010. *Alzheimer's & Dementia* 13 (1), 1–7. doi:10.1016/j.jalz.2016.07.150

Xie, Z., Lu, H., Yang, S., Li, W., Wang, L., Luo, G., et al. (2020). Salidroside attenuates cognitive dysfunction in senescence-accelerated mouse prone 8 (SAMP8) and modulating inflammation on the gut-brain Axis. doi:10.21203/rs.3.rs-24799/v1

Xu, N., Huang, F., Jian, C., Qin, L., Lu, F., Wang, Y., et al. (2019). Neuroprotective effect of salidroside against central nervous system inflammation-induced cognitive deficits: a pivotal role of sirtuin 1-dependent N rf-2/HO -1/NF -κ B pathway. *Phytother Res.*

Yuan, Y., Wu, X., Zhang, X., Hong, Y., and Yan, H. (2019). Ameliorative effect of salidroside from Rhodiola Rosea L. on the gut microbiota subject to furan-induced liver injury in a mouse model. *Food Chem. Toxicol.* 125, 333–340. doi:10.1016/j.fct.2019.01.007

Zhang, L., Yu, H., Zhao, X., Lin, X., Tan, C., Cao, G., et al. (2010). Neuroprotective effects of salidroside against beta-amyloid-induced oxidative stress in SH-SY5Y human neuroblastoma cells. *Neurochem. Int.* 57 (5), 547–555. doi:10.1016/j.neuint.2010.06.021

Zhang, B., Li, Q., Chu, X., Sun, S., and Chen, S. (2016). Salidroside reduces tau hyperphosphorylation via up-regulating GSK-3β phosphorylation in a tau transgenic Drosophila model of Alzheimer's disease. *Transl. Neurodegener.* 5, 21. doi:10.1186/s40035-016-0068-y

Zhong, Z., Han, J., Zhang, J., Xiao, Q., Hu, J., and Chen, L. (2018). Pharmacological activities, mechanisms of action, and safety of salidroside in the central nervous system. *Drug Des. Devel. Ther.* 12, 1479–1489. doi:10.2147/dddt.s160776

Conflict of Interest: The authors declare that the research was conducted in the absence of any commercial or financial relationships that could be construed as a potential conflict of interest.

Advantages of publishing in Frontiers

OPEN ACCESS
Articles are free to read for greatest visibility and readership

FAST PUBLICATION
Around 90 days from submission to decision

HIGH QUALITY PEER-REVIEW
Rigorous, collaborative, and constructive peer-review

TRANSPARENT PEER-REVIEW
Editors and reviewers acknowledged by name on published articles

Frontiers
Avenue du Tribunal-Fédéral 34
1005 Lausanne | Switzerland

Visit us: www.frontiersin.org
Contact us: frontiersin.org/about/contact

REPRODUCIBILITY OF RESEARCH
Support open data and methods to enhance research reproducibility

DIGITAL PUBLISHING
Articles designed for optimal readership across devices

FOLLOW US
@frontiersin

IMPACT METRICS
Advanced article metrics track visibility across digital media

EXTENSIVE PROMOTION
Marketing and promotion of impactful research

LOOP RESEARCH NETWORK
Our network increases your article's readership